University of Huddersfield

University of Huddersfield Repository

Ibraheem, K.

The role of CD40 in regulating renal cell carcinoma cell fate

Original Citation

Ibraheem, K. (2018) The role of CD40 in regulating renal cell carcinoma cell fate. Doctoral thesis, University of Huddersfield.

This version is available at http://eprints.hud.ac.uk/id/eprint/34515/

The University Repository is a digital collection of the research output of the University, available on Open Access. Copyright and Moral Rights for the items on this site are retained by the individual author and/or other copyright owners. Users may access full items free of charge; copies of full text items generally can be reproduced, displayed or performed and given to third parties in any format or medium for personal research or study, educational or not-for-profit purposes without prior permission or charge, provided:

- The authors, title and full bibliographic details is credited in any copy;
- A hyperlink and/or URL is included for the original metadata page; and
- The content is not changed in any way.

For more information, including our policy and submission procedure, please contact the Repository Team at: E.mailbox@hud.ac.uk.

http://eprints.hud.ac.uk/

The role of CD40 in regulating renal cell carcinoma cell fate

Khalidah A Ibraheem

A thesis submitted to the University of Huddersfield in partial fulfilment of the requirements for the degree of Doctor of Philosophy

The University of Huddersfield
School of Applied Science

June 2017

Abstract

CD40 is a member of the TNF receptor (TNFR) superfamily and its expression by a variety of cell types including tumour cells has suggested a possible role for CD40 in epithelial homeostasis and potentially in the pathogenesis of cancer. CD40 ligation by membrane-presented CD40L (mCD40L), but not soluble agonists, causes extensive apoptosis in malignant epithelial cells, including bladder and colorectal cancer cells, while sparing their normal counterparts. However, the role of CD40 in renal cell carcinoma (RCC) is relatively unknown and the effect of CD40 ligation in RCC cells has not been studied previously. This thesis aimed to investigate the effect of CD40 ligation in RCC cells, compare this to their normal counterparts (HRPT cells), and identify the mechanisms of CD40-mediated effects.

The experimental work described in this thesis involved optimisation of assays for the detection of cell death (based on loss of plasma membrane integrity, DNA fragmentation and caspase activation) and for the detection of pro-inflammatory cytokine secretion. Immunoblotting techniques were adapted for a co-culture system to deliver mCD40L for detection of key intracellular CD40 signalling-associated mediators. Optimisation was also carried out for functional experiments using pharmacological inhibitors of intracellular mediators and caspases and for the detection of reactive oxygen species (ROS).

Expression of CD40 by RCC cells was detected in RCC lines and in their normal counterparts HRPT cells and treatment with IFN-ɣ up-regulated CD40 expression in RCC cells. Cytotoxicity assays showed for the first time that mCD40L induced massive apoptosis in human RCC cells which further increased in the presence of IFN-ɣ, whereas it caused no cytotoxic effect in their normal counterparts (HRPT cells). By contrast, the G28-5 mAb did not cause death in RCC cells, and combination of IFN-ɣ with cross-linked G28-5 antibody did not render the G28-5 antibody significantly pro-apoptotic. Moreover, induction of cell death by mCD40L was accompanied by caspase-3/7 activation and DNA fragmentation in RCC cells, while mCD40L did not induce detectable DNA fragmentation in normal HRPT cells indicating that mCD40L triggered “apoptotic” cell death in RCC cells and in a tumour cell-specific fashion.

ELISA assays showed that mCD40L induced marked secretion of IL-8 and IL-6 in RCC cells, which was stronger than that triggered by soluble agonist. More importantly, mCD40L induced GM-CSF secretion in RCC cells, but soluble agonist caused little GM-CSF release. In normal HRPT cells mCD40L caused secretion of IL-8 and IL-6 and a more pronounced secretion of GM-CSF, when it was compared to agonistic G28-5 mAb, confirming that CD40 on HRPT cells was functional despite being non-apoptotic.

mCD40L triggered rapid induction of TRAFs 1, 2, 3 and 6 as early as 1.5h post CD40 ligation in RCC cells. By contrast, despite up-regulation of TRAF1 at 6h post CD40 ligation, in normal HRPT cells mCD40L down-regulated TRAF2 expression and caused no induction in TRAF3 expression. In addition, CD40-mCD40L interactions in RCC cells triggered MKK4/7 activation and downstream phosphorylation of both JNK and p38. Functional inhibition experiments demonstrated that JNK and p38 phosphorylation was essential in CD40-mediated apoptosis in RCC cells, and suggested that activation of p38 may be dependent on JNK activity. By contrast, inhibition of MEK1/2 and NF-κB did not alter CD40-mediated apoptosis in RCC cells, whilst inhibition of AP-1 caused moderate (not complete) reduction in apoptosis.

This study demonstrated that induction of Bak and Bax occurred by 6h post CD40 ligation in RCC cells. Inhibition of caspase-9 significantly attenuated CD40-mediated apoptosis in RCC cells, while caspase-8 and 10 inhibition caused non-significant effects whilst no induction of death ligands was detectable, suggesting that CD40-induced apoptosis in RCC cells occurs via a direct, intrinsic apoptotic pathway. mCD40L triggered ROS production in RCC cells within 1h post CD40 ligation and ROS production were critical in the induction of death, as apoptosis was inhibited by the antioxidant NAC. Moreover, mCD40L triggered phosphorylation of the NOX subunit $p40^{phox}$ and the NOX inhibitor DPI attenuated apoptosis suggesting that a ROS-dependent NOX-triggered pathway may occur in RCC cells. By contrast, non-apoptotic CD40 agonist (G28-5 mAb) did not induce ROS production in RCC cells. Equally importantly, mCD40L caused rapid ASK-1 phosphorylation and down-regulated Trx-1 expression in all RCC lines.

Collectively**,** this study has for the first time reported that mCD40L induced extensive apoptosis in RCC cells while sparing their normal cell counterparts. However, agonistic anti-CD40 antibody G28-5 did not cause cell death in RCC cells. Although additional functional experiments would be necessary to fully elucidate the functional mechanisms of apoptosis, it appears that CD40-mediated killing in RCC cells occurs via a TRAF3-p40phox-ASK-1-MKK4/7-p38/JNK pathway leading to caspase-9 and effector caspase-3/7 activation and intrinsic apoptosis. Importantly, whilst increasing ROS levels in RCC cells, mCD40L actively down-regulated Trx-1 expression. These findings have provided novel observations on the role of CD40 in regulating human RCC cell fate, and have also reinforced the importance of the quality of CD40 signal in determining functional outcome. Equally importantly, the findings have also assisted in the formulation of novel therapeutic avenues that may exploit CD40 for anticancer therapy and specifically for renal cell carcinoma.

Contents

CHAPTER 1 ..... **2**

1.1 APOPTOSIS 3
1.1.1 GENERAL 3
1.1.2 THE DIFFERENCES BETWEEN APOPTOTIC AND NECROTIC CELL DEATH 4
1.2 MOLECULAR COMPONENTS OF APOPTOSIS 6
1.2.1 CASPASES 6
1.2.1.1 STRUCTURE AND ACTIVATION OF CASPASES 7
1.3 THE BCL-2 PROTEIN FAMILY 9
1.3.1 STRUCTURE 9
1.3.2 REGULATION 11
1.3.3 MECHANISM OF ACTION 11
1.4 ROLE OF MITOCHONDRIA IN APOPTOSIS 13
1.4.1 GENERAL 13
1.4.2 THE RUPTURE OF THE OUTER MITOCHONDRIAL MEMBRANE 13
1.4.3 THE MITOCHONDRIAL PERMEABILITY TRANSITION PORE 14
1.4.4 PORE FORMATION BY MEMBERS OF THE BCL-2 FAMILY 14
1.5 APOPTOSIS PATHWAYS 17
1.5.1 THE EXTRINSIC (DEATH RECEPTOR-MEDIATED) APOPTOTIC PATHWAY 19
1.5.1.1 THE TNFR SUPERFAMILY 19
1.5.1.2 THE TNF/TNF-R PATHWAY 22
1.5.2 THE MITOCHONDRIAL (INTRINSIC) APOPTOTIC PATHWAY 24
1.5.2.1 THE CASPASE-DEPENDENT MITOCHONDRIAL PATHWAY 24
1.5.2.2 CYTOCHROME C 24
1.5.2.3 THE APAF-1 PROTEIN 27
1.5.2.4 APOPTOSOME FORMATION 27
1.5.3 REGULATION OF CASPASE-DEPENDENT PATHWAYS 30
1.5.3.1 THE INHIBITORS OF APOPTOSIS PROTEINS (IAPS) 30
1.5.3.2. INHIBITORS OF IAPS 30
1.5.3.3 OTHER REGULATORY PROTEINS 31
1.5.4 THE CASPASE-INDEPENDENT MITOCHONDRIAL PATHWAY 34
1.5.4.1 THE AIF 34
1.5.4.2 ENDONUCLEASE G 35
1.6 REACTIVE OXYGEN SPECIES (ROS) 36
1.6.1 THE MAIN SOURCES OF CELLULAR ROS 39
1.6.2 ROLE OF ROS IN APOPTOSIS 41
1.7 CD40 AND ITS COGNATE LIGAND CD154 (CD40L) 43
1.7.1 BACKGROUND 43
1.7.2 STRUCTURE OF CD40 44
1.7.2.1 EXTRACELLULAR DOMAIN 44
1.7.2.2 INTRACELLULAR DOMAIN **45**
1.7.3 EXPRESSION OF CD40 47

1.7.4 CD40 LIGAND (CD40L) CD154 48
1.7.5 ROLE OF CD40 IN THE IMMUNE SYSTEM **48**
1.7.5.1 B CELLS **48**
1.7.5.3 MONOCYTES AND MACROPHAGES 51
1.7.5.4 DENDRITIC CELLS (DCS) 51
1.7.5.5 EPITHELIAL CELLS 52
1.7.6 CD40 CELL SIGNALLING 52
1.7.6.1 TRAF PROTEINS IN CD40 SIGNALLING 55
1.7.6.1.1 TRAF1 57
1.7.6.1.2 TRAF2 57
1.7.6.1.3 TRAF3 58
1.7.6.1.4 TRAF4 59
1.7.6.1.5 TRAF5 59
1.7.6.1.6 TRAF6 59
1.8 THE MITOGEN ACTIVATED PROTEIN KINASES (MAPKS) 60
1.8.1 GENERAL STRUCTURE 60
1.8.2 ERK 1/2 61
1.8.3 JNK 1/2 (SAPK) 61
1.8.4 THE P38/MAPK 62
1.9 THE EFFECT OF CD40 LIGATION IN CANCER CELLS 62
1.10 MECHANISMS OF CD40-MEDIATED APOPTOSIS IN CARCINOMA CELLS 63
1.11 THE IMPORTANCE OF SIGNAL QUALITY IN CD40-MEDIATED APOPTOSIS 64
1.12 MALIGNANT TRANSFORMATION AND SUSCEPTIBILITY TO CD40 LIGATION 65
1.13 TARGETING CD40 FOR IMMUNOTHERAPY 66
1.15 KIDNEY CANCER 69
1.15.1 KIDNEYS 69
1.15.2 CANCER 69
1.15.3 KIDNEY CANCER 70
1.16 AIMS OF STUDY 72
CHAPTER 2 ..... **74**
2. MATERIALS AND METHODS 75
2.1 GENERAL 75
2.2 DISPOSABLE PLASTICWARE 75
2.3 STOCK SOLUTIONS 75
2.4 REAGENTS 75
2.4.1 PRIMARY ANTIBODIES 75
2.5.2 SECONDARY ANTIBODIES 78
2.5.3 AGONISTS & ANTAGONISTS 78
2.6 TISSUE CULTURE 80
2.6.1 GENERAL 80
2.6.2 MAINTENANCE AND PASSAGE 80

2.6.3 Cryo-preservation and recovery of cell lines 81
2.6.4 Primary cell culture 81
2.6.5 Carcinoma cell culture 82
2.6.6 Murine fibroblast (3T3) cell culture 83
2.6.7 Mycoplasma testing 83
2.7 Methods for CD40 ligation 84
2.8 Detection of cell viability, cell death (apoptosis) and reactive oxygen species (ROS) generation 85
2.8.1 General 85
2.8.2 Detection of cell growth (viability) 85
2.8.3 Detection of cell death using caspase3/7 assays 87
2.8.3.1 SensoLyte® Homogenous AFC Capase-3/7 assay kit 87
2.8.4 Estimation of cell death using the CytoTox-Glo™ assay 89
2.8.5 DNA fragmentation ELISA for the detection of apoptosis 91
2.8.6 Detection of Reactive oxygen species (ROS) using H_2DCFDA 93
2.9 Western Blotting - SDS-PAGE and Immunoblotting 95
2.9.1 General 95
2.9.2 Treatment with mCD40L to investigate CD40-mediated intracellular signalling 95
2.9.3 Protein extraction 96
2.9.4 Protein Quantification 97
2.9.6 Electrophoretic membrane transfer 97
2.9.7 The immunolabelling and visualisation of the membrane using the Li-Cor Odyssey™ system 98
2.10 Flow cytometry 99
2.10.1 Background 99
2.10.2 Detection of CD40 expression by Flow cytometer 100
2.11 Cell treatment with INF-ɣ and TNF-a 101
2.12 Detection of the secretion of cytokines by RCC cells following CD40 ligation 101
2.12.1 GM-CSF detection 102
2.12.2 IL-8 and IL-6 detection 102
The human CXCL8/IL-8 and IL-6 detection kits 102
2.12.3 The Human Cytokine Array panel A 104
The R&D Systems/Proteome profiler antibody arrays kit was used for the quantification of a panel of cytokines. 104
2.14 Arithmetical investigation 106

CHAPTER 3 107

3. Background 108
3.1 CD40 ligation using different methodologies and investigations into its biological effects in RCC cells 110
3.3 Objectives 111
3.4 Confirmation of CD40 and CD40L expression 112

3.5 THE EFFECT OF PRO-INFLAMMATORY CYTOKINES ON CD40 EXPRESSION ON RCC CELLS.....115
3.6 OPTIMISATION OF APOPTOSIS (CYTOTOX-GLO) ASSAYS FOR DETECTION OF MCD40L-MEDIATED CELL DEATH.....117
3.7 THE ROLE OF CD40 SIGNAL 'QUALITY' (DEGREE OF RECEPTOR CROSS-LINKING) IN APOPTOSIS: EFFECT OF AGONISTIC ANTI-CD40 ANTIBODY G28-5 IN RCC CELLS.....125
3.8 DETECTION OF CASPASE-3/7 ACTIVITY FOLLOWING CD40 LIGATION IN RCC CELLS (SENSOLYTE ASSAY).....131
3.9 DETECTION OF DNA FRAGMENTATION FOLLOWING CD40 LIGATION.....135
3.10 OPTIMISATION OF IMMUNOBLOTTING (WESTERN BLOTTING) FOR THE DETECTION OF EPITHELIAL CELL PROTEINS IN CO-CULTURES.....140
3.11 SUMMARY.....150

CHAPTER 4.....152

4. BACKGROUND.....153
4.1 OBJECTIVES.....155
4.2 DETECTION OF CYTOKINE SECRETION IN CO-CULTURE SUPERNATANTS OF RCC CELLS 786-O USING A CYTOKINE ARRAY APPROACH.....156
4.2.1 DETECTION OF IL-8 SECRETION IN RCC CELLS FOLLOWING CD40 LIGATION BY MCD40L .158
4.2.2 DETECTION OF IL-6 SECRETION IN RCC CELLS FOLLOWING CD40 LIGATION BY MCD40L .161
4.2.3 DETECTION OF GM-CSF SECRETION IN RCC CELLS FOLLOWING CD40 LIGATION BY MCD40L.....164
4.3 THE ROLE OF THE MODE OF CD40 LIGATION IN GM-CSF SECRETION.....167
4.4 SUMMARY.....169

CHAPTER 5.....171

5 BACKGROUND.....172
5.1 OBJECTIVES.....174
5.2 REGULATION OF TRAF -1, -2, -3 AND -6 EXPRESSION.....175
5.3 DETECTION OF ACTIVATION OF MKK4 AND MKK7 MAPKS.....180
5.4 ACTIVATION OF JNK AND P38 MAPKS.....184
5.5THE FUNCTIONAL ROLE OF MAPKS AND TRANSCRIPTION FACTORS IN CD40 MEDIATED APOPTOSIS IN RCC CELLS.....188
5.6 ACTIVATION OF THE INTRINSIC (MITOCHONDRIAL) PATHWAY DURING MCD40L-MEDIATED APOPTOSIS IN RCC CELLS.....195
5.7 EXPRESSION OF JNK AND P38 IN RCC CELLS IN THE PRESENCE OF JNK AND P38 INHIBITORS 200
5.8 THE EFFECT OF JNK AND P38 INHIBITION ON THE EXPRESSION BAK AND BAX (ANTI-APOPTOTIC PROTEINS).....200
5.9 INVESTIGATIONS ON THE ROLE OF REACTIVE OXYGEN SPECIES (ROS) AND NADPH OXIDASE (NOX) IN CD40-MEDIATED APOPTOSIS IN RCC CELLS.....203
5.9.1 RATIONALE.....203
5.9.2 INDUCTION OF ROS GENERATION IN RCC CELLS BY MCD40L.....204
5.9.3 CD40-MEDIATED APOPTOSIS IN RCC CELLS WAS ROS DEPENDENT.....210
5.9.4 THE ROLE OF NADPH IN CD40-MEDIATED APOPTOSIS IN RCC CELLS.....215

5.9.5 ASK-1 REGULATION DURING CD40-MEDIATED APOPTOSIS 221
5.9.6 THIOREDOXIN-1 (TRX) EXPRESSION FOLLOWING CD40 LIGATION.....221
5.10 SUMMARY.....224

CHAPTER 6.....226

6. BACKGROUND 227
6.1 OBJECTIVES 229
6.2 CD40 EXPRESSION BY PRIMARY HRPT CELLS.....230
6.3 DETECTION OF CELL DEATH IN NORMAL HRPT FOLLOWING CD40 LIGATION BY MCD40L.....233
6.3.1 DETERMINATION OF CELL DEATH BY THE CYTOTOX-GLO ASSAY 233
6.3.2 DETERMINATION OF CELL DEATH BY THE DNA FRAGMENTATION ASSAY 237
6.4 DETECTION OF CYTOKINE SECRETION FOLLOWING CD40 LIGATION IN NORMAL HRPT CELLS 241
6.5 REGULATION OF TRAF PROTEINS IN NORMAL PRIMARY HRPT FOLLOWING CD40 LIGATION.246
6.6 SUMMARY 250

CHAPTER 7.....252

7.1 GENERAL CONCEPT 253
7.2 EXPRESSION OF CD40 ON HUMAN RCC CELLS AND THEIR NORMAL COUNTERPARTS (HRPT CELLS) AND ITS CYTOKINE-MEDIATED REGULATION 254
7.3 THE INFLUENCE OF CD40 LIGATION ON RCC CELLS.....256
7.3.1 SOLUBLE CD40 AGONIST IS A NOT A PRO-APOPTOTIC SIGNAL IN RCC CELLS.....256
7.3.2 MEMBRANE CD40L INDUCES EXTENSIVE APOPTOSIS IN RCC CELLS.....258
7.3.3 REGULATION OF CYTOKINE SECRETION BY CD40.....259
7.4 REGULATION OF TRAF PROTEINS AND MAPKS BY MCD40L IN RCC CELLS.....261
7.5 CD40-MEDIATED APOPTOSIS VIA THE INTRINSIC PATHWAY IN RCC CELLS 264
7.6 THE ROLE OF ROS AND NOX IN CD40-MEDIATED APOPTOSIS IN RCC CELLS.....265
7.7 THE ROLE OF ASK-1 AND TRX IN MCD40L-MEDIATED APOPTOSIS IN RCC CELLS.....267
7.8 FUTURE DIRECTIONS 268
7.9 CONCLUDING REMARKS.....269

APPENDIX.....270

APPENDIX I.....271
APPENDIX II 274
APPENDIX III 279
APPENDIX IIII 282

REFERENCES 285

List of figures

Figure 1.1 Morphological differences between apoptosis and necrosis 5
Figure 1.2 Caspase activation mechanisms 8
Figure 1.3 Structure of the Bcl-2 family proteins 10
Figure 1. 4 The role of BCL2 family in the mitochondrial permeability transition pore 16
Figure 1.5 The extrinsic and intrinsic pathways of apoptosis 18
Figure 1.6 The division of TNFRs 21
Figure 1.7 The death receptor (extrinsic) pathway and cross-talk 23
Figure 1.8 The mitochondrial pathway of apoptosis 26
Figure 1.9 The apoptosome formation and its inactivation 29
Figure 1.10 Events in the mitochondrial apoptotic pathway regulated by Heat shock proteins (Hsp) 33
Figure 1.11 Production and interconversion of reactive oxygen species 38
Figure 1.12 Main sources of ROS inside the cell 40
Figure 1.13 Structure of CD40 46
Table 1.1 Expression of CD40 and CD40L on different cell types 47
Figure 1.14 CD40 functions in B cell homeostasis 50
Figure 1.15 CD40 signalling pathways 54
Figure 1. 16 Structures of the TRAF proteins 56
Figure 1.17 Signalling through CD40 in carcinoma cells 68
Table 2.1 Primary antibodies 76
Table 2.3 Agonists & antagonists 79
Figure 2.1 The principle of MTS tetrazolium assay 86
Figure 2.2 The opinion of SensoLyte® Homogenous AFC Capase-3/7 assay kit 88
Figure 2.3 The opinion of the CytoTox-Glo™ assay 90
Figure 2.4 Opinion of DNA fragmentation kit 92
Figure 2.5 The opinion of ROS detection using H2DCFDA 94
Figure 2.6 Co-culture of RCCs cells with 3T3 fibroblasts; 3T3-CD40L (A) and 3T3Neo (B) ..96
Figure 2. 7 Immunoblotting module 98
Figure 2.8 The principle of flow cytometry 99
Table 2.4 Flow Cytometry antibodies 100
Table 2.5 Cytokine detection kits 102
Figure 2.9 Illustrate the organization of cytokines spots for easy identification 105
Figure 2.10 Principle of the membrane cytokine array kit 105
Figure 3.1 Detection of CD40 expression in RCC cells by Western blotting 113
Figure 3. 2 Detection of CD40 expression by flow cytometry 114
Figure 3.3 Flow cytometric analysis of CD40L expression by effector cells 115
Figure 3.4 Effect of IFN-ɣ and TNF-α on CD40 expression by RCC cells 116
Figure 3.5 Determination of optimal cell density and time-point for apoptosis detection assays in ACHN cells 119
Figure 3.6 Determination of optimal cell density and time-point for apoptosis detection assays in 786-O cells 120
Figure 3.7 Determination of optimal cell density and time-point for apoptosis detection assays in A-704 cells 121
Figure 3.8 Optimal detection of mCD40L-mediated apoptosis in RCC cells 123

Figure 3.9 Regulation of mCD40L-induced death in RCC cells by IFN-γ 124
Figure 3.10 Effect of agonistic G28-5 mAb in ACHN cells 127
Figure 3.11 Effect of agonistic G28-5 mAb in 786-O cells.....128
Figure 3.12 Effect of agonistic G28-5 mAb in A-704 cells.....129
Figure 3.13 Treatment of RCC cells with G28-5 mAb in the presence of IFN-γ 130
Figure 3.14 Detection of caspase 3/7 activity at 24 h post CD40 ligation.....132
Figure 3.15 Detection of caspase 3/7 activity at 48 h post CD40 ligation.....133
Figure 3.16 Detection of caspase 3/7 activity at 72 h post CD40 ligation.....134
Figure 3.17 Detection of DNA fragmentation in ACHN cells following co-culture 137
Figure 3.18 Detection of DNA fragmentation in 786-O cells following co-culture 138
Figure 3.19 Detection of DNA fragmentation in A-704 cells following co-culture.....139
Figure 3.20 Detection of Cytokeratin 8 (CK8) and 18 (CK18) expression in epithelial cells and fibroblasts.....142
Figure 3.21 Detection of CK18 in ACHN cell co-cultures with effector cells 143
Figure 3.22 Detection of CK18 in 786-O cell co-cultures with effector cells 144
Figure 3.23 Detection of CK18 in A-704 cell co-cultures with effector cells.....145
Figure 3.24 protein expression was corrected according to the CK18 band intensity values by using densitometry analysis 146
Figure 3.25 Confirmation of equal loading in ACHN cell co-cultures following CK-based normalisation.....147
Figure 3.26 Confirmation of equal loading in 786-O cell co-cultures following CK-based normalisation.....148
Figure 3.27 Confirmation of equal loading in A-704 cell co-cultures following CK-based normalisation.....149
Figure 4.1 Detection of cytokine secretion in RCC cells 786-O using a human cytokine array approach.....157
Figure 4.2 mCD40L-mediated IL-8 secretion in RCC cells.....160
Figure 4.3 mCD40L-mediated IL-6 secretion in RCC cells.....163
Figure 4.4 mCD40L-mediated GM-CSF secretion in RCC cells.....166
Figure 4.5 GM-CSF secretion in 786-O cells following CD40 activation by soluble versus membrane-presented agonist.....168
Figure 5.1The regulation of TRAF1 expression by CD40 ligation in RCC cells.....176
Figure 5.2 The regulation of TRAF2 expression by CD40 ligation in RCC cells.....177
Figure 5.3The regulation of TRAF3 expression by CD40 ligation in RCC cells.....178
Figure 5.4The regulation of TRAF6 expression by CD40 ligation in RCC cells.....179
Figure 5.5 CD40 ligation induces MKK7 protein phosphorylation in RCC cells.....182
Figure 5.6 CD40 ligation induces MKK4 phosphorylation in RCC cells.....183
Figure 5.7 JNK activation after CD40 ligation in RCC cells.....186
Figure 5.8 p38 activation post CD40 ligation in RCC cells.....187
Figure 5.9 Effect of pharmacological inhibition of JNK on CD40-mediated apoptosis in RCC cells.....190
Figure 5.10 Effect of pharmacological inhibition of p38 on CD40-mediated cell death in RCC cells.....191
Figure 5.11 Effect of pharmacological inhibition of AP-1 on CD40-mediated cell death in RCC cells.....192

Figure 5.12 Effect of pharmacological inhibition of MEK/ERK on CD40-mediated cell death in RCC cells 193
Figure 5.13 Effect of pharmacological inhibition of NF-κB on CD40-mediated cell death in RCC cells 194
Figure 5.14 Effect of caspase inhibitors on mCD40L-mediated cell death 197
Figure 5.15 Induction of Bak following CD40 ligation by mCD40L 198
Figure 5.16 Induction of Bax following CD40 ligation by mCD40L 199
Figure 5.17 Effect of JNK and p38 pharmacological inhibitors on JNK and p38 phosphorylation post CD40 ligation 201
Figure 5.18 Effect of JNK and p38 pharmacological inhibitors on Bak and Bax expression post CD40 ligation 202
Figure 5.19 mCD40L-mediated ROS generation in ACHN cells 206
Figure 5.20 mCD40L-mediated ROS generation in 786-O cells 207
Figure 5.21 mCD40L-mediated ROS generation in A-704 cells 208
Figure 5.22 ROS generation in ACHN cells treated with soluble agonist 209
Figure 5.23 NAC titration experiments 211
Figure 5.24 Effect of NAC on CD40-mediated apoptosis in ACHN cells 212
Figure 5.25 Effect of NAC on CD40-mediated apoptosis in 786-O cells 213
Figure 5.26 Effect of NAC on CD40-mediated apoptosis in A-704 cells 214
Figure 5.27 DPI titration experiments 216
Figure 5.28 Effect of Nox inhibitor DPI on CD40-mediated death in ACHN cells 217
Figure 5.29 Effect of Nox inhibitor DPI on CD40-mediated death in 786-O cells 218
Figure 5.30 Effect of Nox inhibitor DPI on CD40-mediated death in A-704 cells 219
Figure 5.31 Induction of p^{40phox} phosphorylation following CD40 ligation in RCC cells 220
Figure 5.32 Induction of ASK-1 phosphorylation following CD40 ligation 222
Figure 5.33 Thioredoxin-1 expression in RCC cells following CD40 ligation 223
Figure 6.1 Detection of CD40 expression in HRPT cells by Western blotting 231
Figure 6.2 Detection of CD40 expression on HRPT cells by flow cytometry 232
Figure 6.3 Detection of cell death in HRPT cells following 24h of CD40 ligation by mCD40L 234
Figure 6.4 Detection of cell death in HRPT cells following 48h of CD40 ligation by mCD40L 235
Figure 6.5 Detection of cell death in HRPT cells following 72h of CD40 ligation by mCD40L 236
Figure 6.6 Detection of DNA fragmentation in normal HRPT cells following 24h of CD40 ligation by membrane-presented ligand and soluble agonist 238
Figure 6.7 Detection of DNA fragmentation in normal HRPT cells following 48h of CD40 ligation by membrane-presented ligand and soluble agonist 239
Figure 6.8 Detection of DNA fragmentation in normal HRPT cells following 72h of CD40 ligation by membrane-presented ligand and soluble agonist 240
Figure 6.9 Detection of IL-8 secretion by HRPT following CD40 ligation 243
Figure 6.10 Detection of IL-6 secretion by HRPT following CD40 ligation 244
Figure 6.11 Detection of GM-CSF secretion by HRPT following CD40 ligation 245
Figure 6.12 TRAF1 protein expression by HRPT cells following CD40 ligation by mCD40L 247

Figure 6.13 TRAF2 protein expression by HRPT cells following CD40 ligation by mCD40L 248
Figure 6.14 TRAF3 protein expression by HRPT cells following CD40 ligation by mCD40L 249
Human Cytokine Array coordinates 282

List of Tables

Table 1.1 Expression of CD40 and CD40L on different cell types……..……47
Table 2.1 Primary antibodies……..76
Table 2.2 Agonists & antagonists 79
Table 2.3 Flow Cytometry antibodies 100
Table 2.5 Cytokine detection kits 102

Acknowledgement

This PhD has been a truly life-changing experience for me and it would not have been achievable without the continuous support that I received from my supervisor **Dr. Nikolaos Georgopoulos** who has been and still a great mentor and faithful friend. His patience, generous, gentleness, motivation and enthusiasm build my self-confidence and helped me not only during my difficult times of research and writing of this thesis but also in all my life as international student. His guidance, advice, familiarity, and immense knowledge carried me to the glory and highness. **Dr. Georgopoulos** has demonstrated a fantastic level of academic quality. He has been a bright candle in his research group who are surrounded him as his family. I have been extremely lucky and delighted to have worked with him. I would like to express my warmest feelings of appreciation, admiration, thanks and gratitude that come from the bottom of my heart. Thank you for giving me a helping hand. I can never really thank you enough.

Besides my supervisor, there was **Dr. Christopher Dunnill**, the chief of the team who is always available to help and advise. I would like to give him a huge thanks and appreciation for his continuous collaboration.

My thanks to every member in NTG group, and everyone in the laboratories for the cooperation during my study.

My gratitude and appreciation to my country Iraq for providing the financial support. My deepest thanks must also go to the university of Huddersfield, particularly, school of applied science for support and advice.

Dedication

This thesis is dedicated to my father who encouraged me to continue with my study, but sadly he passed away in 2012.

And to my mother who left the life in 2005

Khalidah Ibraheem

List of Abbreviations

ACD	Accidental cell death
AIF	Apoptosis inducing factor
IAP	Inhibitor of apoptosis protein
AML	Acute myeloid leukaemia
ANT	Adenine nucleotide translocator
AP-1	Activator protein 1
Apaf-1	Apoptosis protease-activating factor 1
APC	Antigen presenting cell
ASK	Apoptosis signalling kinase 1
Bad	Bcl2 associated death promoter
BAFF	B cell activating factor belonging to the TNF family
Bak	Bcl2 antagonist killer
BAX	BCL2-associated X protein
BCL-2	B-cell lymphoma 2
Bcl-w	Bcl2 like 2 proteins (Apoptosis regulator Bcl-w)
Bcl-xL	B-cell lymphoma-extra large
Bcl-XS	Bcl2 related protein (short isoform)
bFGF	basic Fibroblast Growth factor
Bid	BH3 interacting domain
BIK.	Bcl-2 Interacting Killer
BIM (BOD)	BCL-2 interacting mediator of cell death
BLyS	B-lymphocyte Stimulation protein
BOK/MTD	Bcl-2 related ovarian killer/ Matador
BOO/DIVA	Bcl-2 homolog of Ovary
BrdU.	5-bromo-2-dedoxyuridine
BSA.	Bovine Serum Albumine
CAD.	Caspase activated DNase
CARD	Caspase activation and recruitment domain

Caspase	Cysteinyl Aspartic acid-protease
CD154	Cluster of Differentiation 154
CD28	Cluster of Differentiation 28
CD40R	CD40 receptor (Cluster of differentiation 40)
CDK	Cyclin dependant kinase
cDNA	Complementary DNA
cFLIP	Cellular Flice-Like inhibitory protein
CMV	Cytomegalovirus
CN	Calcinneurin
CO_2	Carbone dioxide
Cox-2	Cyclooxygenase-2
CRC	Colorectal cancer
Cyto-c	Cytochrome C
dATP	2'-deoxyadenosine triphosphate
DC	Dendritic cell
DD	Death domain
DED	Death effector domain
DEDAF	Death effector domain- Associated Factor
DEM	Diethyl Maleate
DFF40	DNA Fragmentation Factor 40/CAD
DFF45	DNA Fragmentation Factor 45/ICAD
DISC	Death inducing signalling complex
DIABLO	Direct IAP binding protein with low PI
DMEM	Dulbecco's modified Eagle's medium
DMSO	Dimethyl Sulphoxide
DNA	Deoxyribonucleic acid
DNase	Deoxyribonuclease
DPI	Diphenylene iodonium
DR	Death receptor

DR4	Death receptor 4
DR5	Death receptor 5
EDTA.	Ethylenediamine Tetra-Acetic Acid
ELISA.	Enzyme-linked immunosorbent assay
Endo G	Endonuclease G
ERK1, 2	Extracellular signal regulated Kinase1, 2
EpiCM	Epithelial Cell Medium
EpiCGS	Epithelial Cell Growth Supplement
FAD	Flavine adinine dinucleotide
FADD	Fas-associated death domain
FBS	Foetal Bovine Serum
GM-CSF	Granulocyte Macrophage – Colony Stimulating Factor
H2DCFDA.	6-carboxy-2,7 dichloro dihydrofluorescin diacetate
H_2SO_4	Sulphuric acid
HIGM	Hyper IgM syndrome
HSP27, 70, 90	Heat shock proteins 27, 70, 90
hTERT	Human telomerase reverse transcriptase
Htr A2	High temperature requirement protein-A2
IAP	Inhibitor of Apoptosis Proteins
ICAM-1	Intracellular adhesion molecule-1
ICD	Intracellular domain
IFN	Interferon
Ig	Immunoglobulin
IgA.	Immunoglobulin A
IgE	Immunoglobulin E
IgG.	Immunoglobulin G
IKK	I-κB kinase
IL	Interleukin
IL-2,4,6,8,8,12	Interleukin-2,4,6,8,10,12

IκB	Inhibitor of NF-κB
JAK3	Janus Kinase 3
JNK	C-jun N-terminal kinase
kDa	Kilo Dalton
KGD domain	Lysine - Aspartic acid - Glycine domain
LFA-1	Lymphocyte function Antigen-1
LG	L-glutamine
LMP1	Latent membrane protein-1
Mac-1	Macrophage-1 antigen
MAPK	Mitogen activated Protein kinase
mCD40L	Membrane CD40 ligand
MCL-1	Myeloid cell leukaemia-1
MCP-1	Monocyte Chemo-attractant protein-1
MEKK-1	MAP Kinase kinase-1
MHC-1	Major Histocompatibility Complex-1
MHC-2	Major Histocompatibility Complex-2
mM	Millimolar
MM	Malignant melanoma
MMC	Mitomycine C
MMP	Matrix Metalloproteinase
MOMP	Mitochondrial outer membrane permeabilisation
mRNA	Messenger Ribonucleic acid
NAC	N-acetyl cysteine
NF-kB	nuclear factor kappa-B
NIK.	NF-κB-inducing kinase
NK	Natural killer
NO	Nitric Oxide
Nox	NADPH oxidase
NR	Near infrared

NGF	Nerve growth factor
NHU	Normal human urothelial cells
OMM	Outer mitochondrial membrane
PBS	Phosphate buffer saline
PCD	Programmed cell death
PVDF	Poly Vinylidine difluoride membrane
RCC	Renal Cell Carcinoma
Redox	Reduction-oxidation
RFU	Relative Fluorescent unit
RIP	Receptor-interacting protein
RLU	Relative Luminescence Unit
RNA	Ribonucleic acid
RNase	Ribonuclease
ROS	Reactive oxygen Species
RPMI Medium	Roswell Park Memorial Institute medium
RT	Room Temperature
SAPK	Stress Activated Protein Kinase
sCD40L	Soluble CD40 ligand
shRNA	Short hairpin RNA
Smac	Second mitochondrial activator of caspases
TC	T-cells (T-lymphocyte)
TCR	T-cell receptor
TGF-β	Transforming Growth factor-β
TIM	TRAF interacting motif
TNF	Tumour necrosis factor
TNFR	Tumour necrosis factor receptor
TNFR-I	Tumour necrosis factor receptor I
TNFRSF	Tumour necrosis factor receptor superfamily
TNF-α	Tumour necrosis factor alpha

TRADD	Tumour necrosis factor receptor associated death domain
TRAF	Tumour necrosis factor receptor associated factor
TRAP	Tumour Necrosis Factor-related Activation Protein
UV	Ultra violet
VDAC	Voltage Dependent Anion Channel
XAF-1	XIAP- associated factor-1
xIAP	X-linked inhibitor of apoptosis protein

Chapter 1

Introduction

1.1 Apoptosis

1.1.1 General

Apoptosis is a biological form of cell death that preserves the balance between cell passing and cell existence by selectively eradicating any undesirable cells such as injured, transformed or old cells. Apoptosis is frequently identical to programmed cell death (PCD) that refers to the cell death taking place at specific times and places (tissues) during the development of multi-cellular organisms. PCD was observed for the first time in the 19th century in the toad embryo's nervous system by German researchers. As a Professor of Greek language, James Cormack first introduced the term of apoptosis with the suffix "ptosis" referring to the "falling off" of leaves from trees or falling of the petals of flowers (Duque-Parra, 2005).

PCD is the first description used since the 1960s, and in 1973 arrangement of cell death depending on its morphological structures was anticipated, including Type 1: heterophagy (compatible to apoptosis), Type 2 autophagy (identical to autophagic cell death) and Type 3: necrosis (which was not related to any type of (cell 'digestion'). More recently, the classification of cell death has moved on to better-demarcated biochemical characteristics to encompass programmed physiological cell death (caspase dependent) as different to more 'pathological' cell death (caspase-independent) for instance. Classification based on biochemical organisation methods permits cell death researchers to determine superiority and amount grounded on biochemical analyses that describe modalities of death including caspase activity, DNA fragmentation, and the generation of reactive oxygen species (ROS) and phosphatidylserine translocation. Because recent detections have established that there are many types of cell death with different as well as overlapping characteristics, there is no uniform classification of cell death and several biochemical characteristics are simultaneously required to better define the different types of cell death as discussed by the Nomenclature Committee on Cell Death (NCCD) (Galluzzi et al., 2011).

Cellular death occurs in different ways due to distinct stimuli but the main processes are apoptosis and necrosis and here only apoptosis and how we can distinguish between apoptosis and necrosis will be discussed (Adrain et al., 2002).

1.1.2 The differences between apoptotic and necrotic cell death

Apoptotic cell death can be induced either intracellularly due to cellular stresses, such as heat, radiation, viral infection, genotoxic damage, hypoxia and increase in calcium levels, or extracellularly as a response to toxins, hormones and cytokines or death receptor activation. Generally, a main biochemical feature of apoptosis is DNA fragmentation and it is also characterized by nuclear and cytoplasmic condensation, nuclear fragmentation and cell shrinkage, formation of apoptotic bodies (membrane associated with cytoplasmic and nuclear debris). Apoptotic cells are phagocytosed without (or little) detectable immunological (inflammatory) response or release of cellular content to surrounding tissues (Gewies, 2003).

By contrast, necrotic cell death is mainly triggered by external stresses such as trauma or loss of blood supply, often occurs without specific biochemical markers and is characterized by cell swelling, severe loss of plasma membrane integrity, release of cellular contents into the surrounding tissue, cell degradation and unorganized cell death that causes inflammation (Rath and Aggarwal, 1999). (Figure 1.1).

It should, however, be noted that there is accumulating evidence that necrotic cell death is not always accidental and it can be regulated by specific cellular proteins and enzymes; for instance the RIP (receptor interacting protein) kinases RIP1/RIP3 are essential in TNF-induced necrosis. Programmed necrosis (or necroptosis) leads to mitochondrial dysfunction and necrotic cell death and is a significant driver of inflammation and pathology in both animal models and human disease (Kroemer et al., 2007).

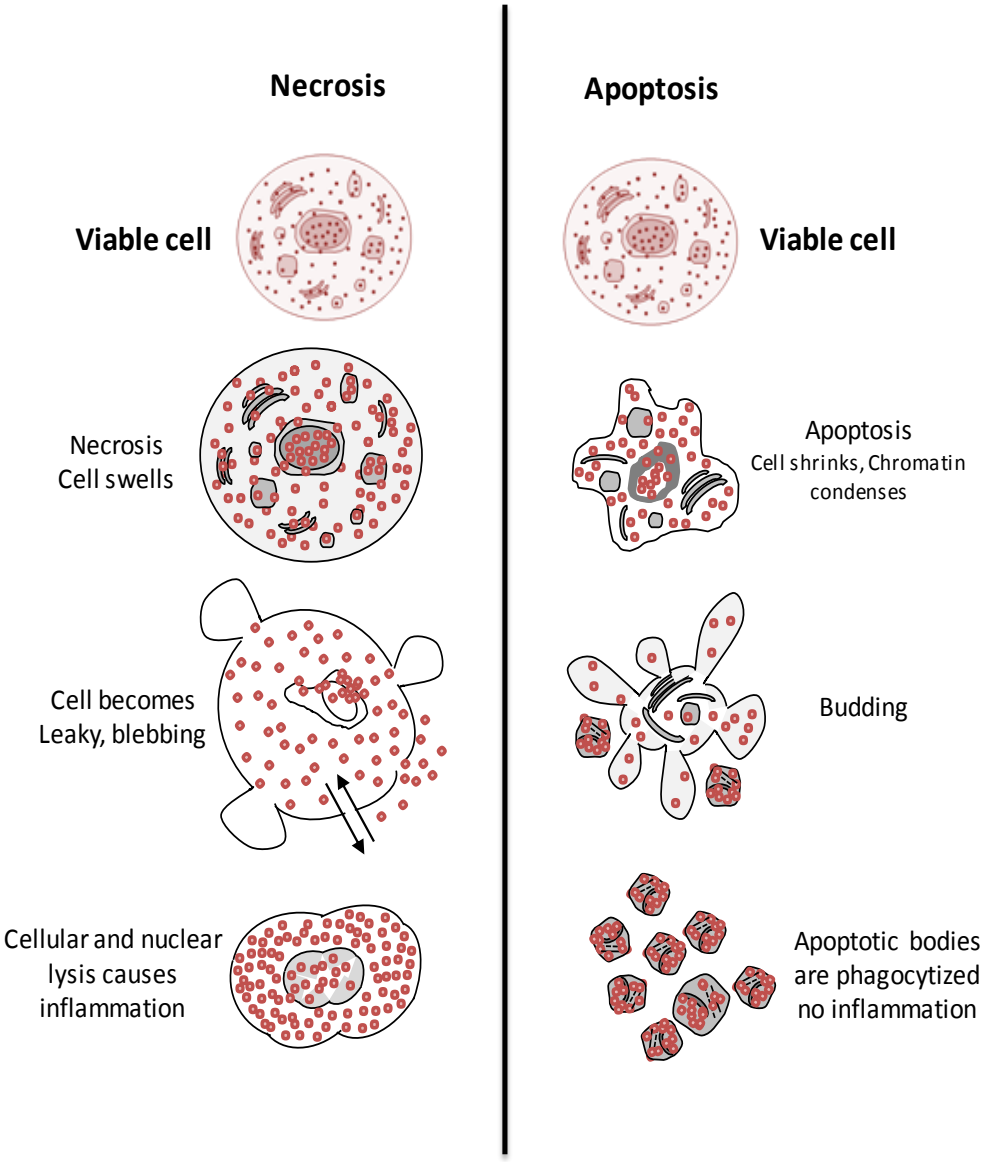

Figure 1.1 Morphological differences between apoptosis and necrosis

Apoptosis characterised by cellular shrinking, condensation of the chromatin, nucleus margination and the formation of apoptotic body (contain organelles, cytosol and nuclear fragments) and cells are phagocytosed without causing inflammatory responses. A necrosis involves cell swells, becomes leaky and finally is ruptured and releases its contents into the surrounding tissue causing inflammation. **Drawn by K. Ibraheem.**

1.2 Molecular components of apoptosis

1.2.1 Caspases

The term caspases refers to Cysteine-dependent Aspartate-Specific Proteases. There are 7 members of caspases identified in Drosophila, a further 14 members are found in mammals, plus caspase-11 and -12 which have been discovered only in mice (Denault and Salvesen, 2002, Richardson and Kumar, 2002).

Caspases are highly distinguished by the catalytic activity which is based on a critical cysteine residue in their active-site pentapeptide QACRG. Therefore caspases have two main features: their cysteine amino acid in their active site and the remarkable specificity for Aspartic acid residues (Pop and Salvesen, 2009). The family has been divided into two subfamilies, the interleukin-1β converting enzyme (ICE)-like and Caenorhabditis elegans protein-3 (CED-3)-like. Caspase-1 and CED-3 have been identified as the prototypic members of the subfamilies, respectively (Grütter, 2000). Other classification is based on their major functions that divides caspases into two subfamilies, pro-apoptotic and pro-inflammatory. Caspase-2, -3, -6, -7, -8, -9, -10 are pro-apoptotic caspases and mostly contribute in cell death signalling, while Caspases -1, -4, -5, -11, -12 are recognized as pro-inflammatory caspases that adjust cytokine secretion during the inflammatory process. However, there is indication suggesting participation in several cellular progressions not only pro-apoptotic and pro-inflammatory roles. Moreover, the pro-inflammatory caspases can also induce apoptosis.

The most common, current classification is based on prodomains lengths, and thus caspases are divided into initiator and executioner caspases. Caspases-1, -2, -4, -5, -8, -9, -10, -11, -12 are identified as initiator caspases that hold long prodomains. Caspases-3, -6, -7 are executioner caspases and they possess short prodomains, and also known as effector caspases that control the implementation of last stages of apoptosis via cleavage of numerous cellular substrates and are themselves stimulated by the initiator caspases (Lakhani et al., 2006).

1.2.1.1 Structure and activation of caspases

All caspases are synthesised as inactive structures (zymogens) (Parrish et al., 2013) and are single proteins consisting of three major parts. The amino terminal side includes a pro-domain variable in size and a sequence that contains either a death effector domain (DED) or caspase recruitment domain (CARD), which are protein-protein interaction motifs to permit the interaction of initiator caspases with adaptor molecules; the large subunit p20 is in the middle of the protein and comprises the active site; finally, the carboxy terminal part contains the small subunit p10. A binding domain between large and small subunit has been also identified in some caspases (Li and Yuan, 2008) (Figure 1.2). Active caspases are usually homodimers, with each monomer consisting of large and small subunit. The six anti-parallel β-strands of each of the monomer represent a continuous twelve strand β-sheet present in the native active enzyme. The sites which are found to be active are created by the four outstanding loops (L1 to L4) and these are found in the two obverse ends of the β-sheet.

Zymogens are generally activated by proteolytic cleavage; this occurs usually at two sites and this eliminates the pro-domain and detaches the p20 and p10 domains. Active caspases can then also activate other caspases or substrates, which triggers an enzymatic cascade in order to amplify and integrate pro-apoptotic signals (Thornberry, 1998). The cleavage takes place after the Asp-X bond. The combination of two heterodimers holding two independent catalytic sites enables the formation of active tetrameric forms of caspases (Wilson et al., 1994) (Figure 1.2). Caspases have different abilities to cleave cellular substrates. Initiator caspases seems to cleave specific substrates and other caspases downstream as part of their role in apoptosis. The majority of substrate proteolysis during the destructive stage of apoptosis is the responsibility of the effector caspases.

The activation of caspases has been observed during the early stage of apoptosis and the use of specific caspases inhibitors (caspase-specific peptide substrates) can block the appearance of apoptosis. Inversely, insertion of recombinant caspases can induce apoptosis (Thornberry et al., 2000).

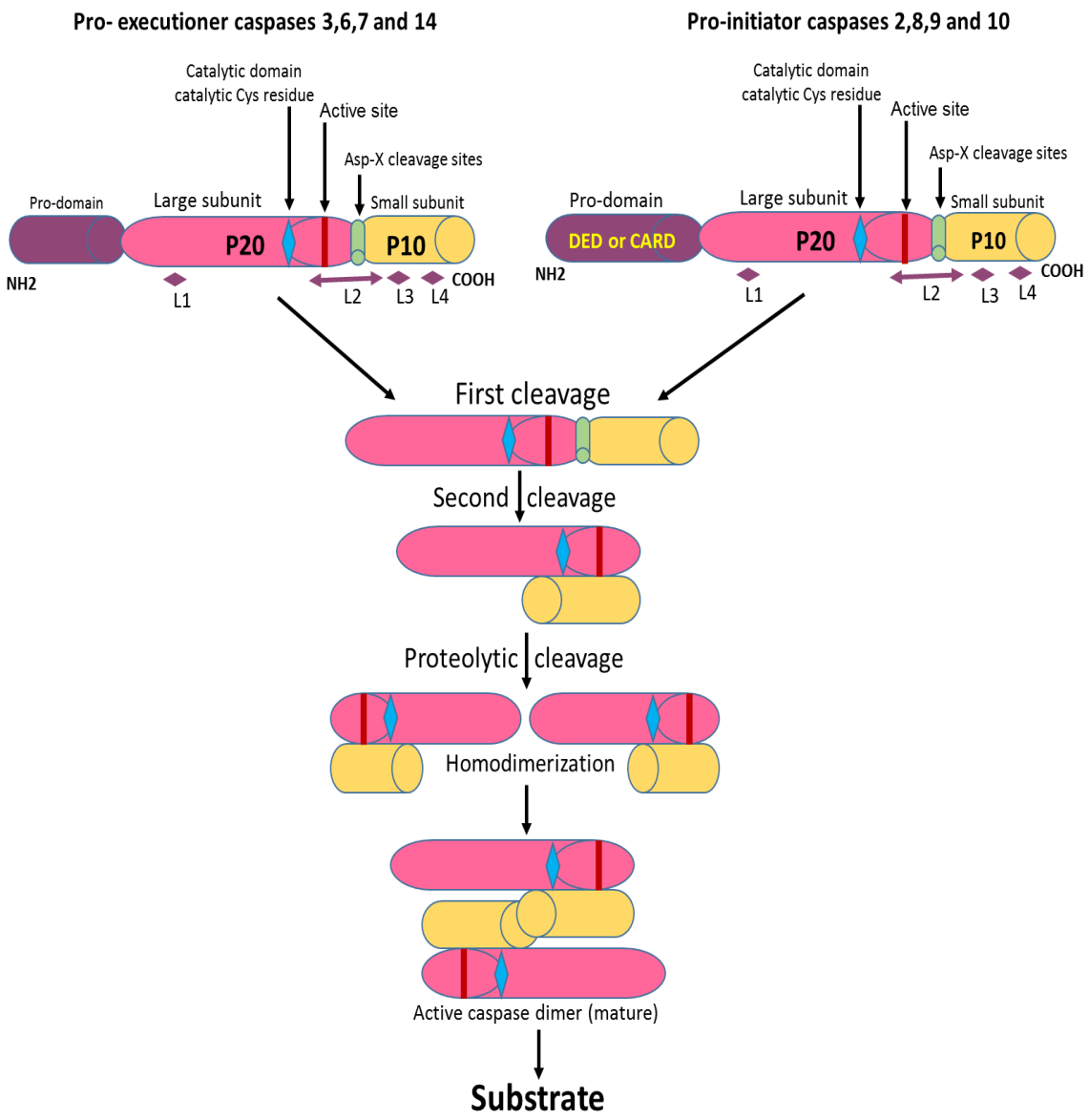

Figure 1.2 Caspase activation mechanisms

Caspases are synthesised as inactive single chain proteins consisting of a pro-domain (which is longer in pro-initiator caspases) and contain either death effector domain (DED) or caspase recruitment domain (CARD) that are essential for interaction with adaptor molecules. They comprise a large subunit p20 that possesses the active site and a small subunit p10, as well as a binding domain located between large and small subunit. After subsequent cleavage of pro-caspases, the subunits bind together to form the active structure, having two active sites (Li and Yuan, 2008). **Drawn by K. Ibraheem.**

1.3 The Bcl-2 protein family

1.3.1 Structure

The Bcl-2 (B-cell leukaemia/lymphoma 2-like protein) family play a significant role in the regulation of apoptosis. The Bcl-2 family comprises 15 members which can be classified into two separate categories in accordance to the role they perform; i.e. anti-apoptotic and pro-apoptotic proteins. These two distinct groups vary in their physical structure but they consist of four common and conserved areas, the BH domains (which stands for "Bcl-2 homology") (Figure 1.3). The areas BH1, BH2 and BH3 form the hydrophobic pocket which has the ability of bringing together a BH3 domain from a different protein; the BH3 domain is an amphipathic α-helix (Petros, 2004 pp390).

The anti-apoptotic members of the Bcl-2 family (Bcl-2, Bcl-xL, Bcl-w, Mcl-1, A1/BFL-1 and BOO/DIVA) contain domains BH1, 2, 3 and 4. The pro-apoptotic members are divided into two subgroups: one contains three domains (BH1, 2 and 3) such as Bax, Bak, Bok/MTD, whereas the other contains proteins with only the BH3-domain such as Bid, Bad, Bik/NKB, BLK, HRK and BIM (BOD), also referred to as "BH3-only" proteins. The BH3 region appears to be critical for pro-apoptotic activity; the BH4 domain can exist in both anti- and pro-apoptotic proteins and can be phosphorylated. The existence of such domain allows complex formation with other proteins, for example calcineurin (CN), and connections with other apoptosis pathways can be initiated (Shibasaki et al., 1997). All members of the Bcl-2 family possess a hydrophobic carboxyl-terminal domain of 20 amino acids for their attachment to intracellular membranes, primarily those of the mitochondria but also the endoplasmic reticulum (Krajewski et al., 1993) (Figure 1.3).

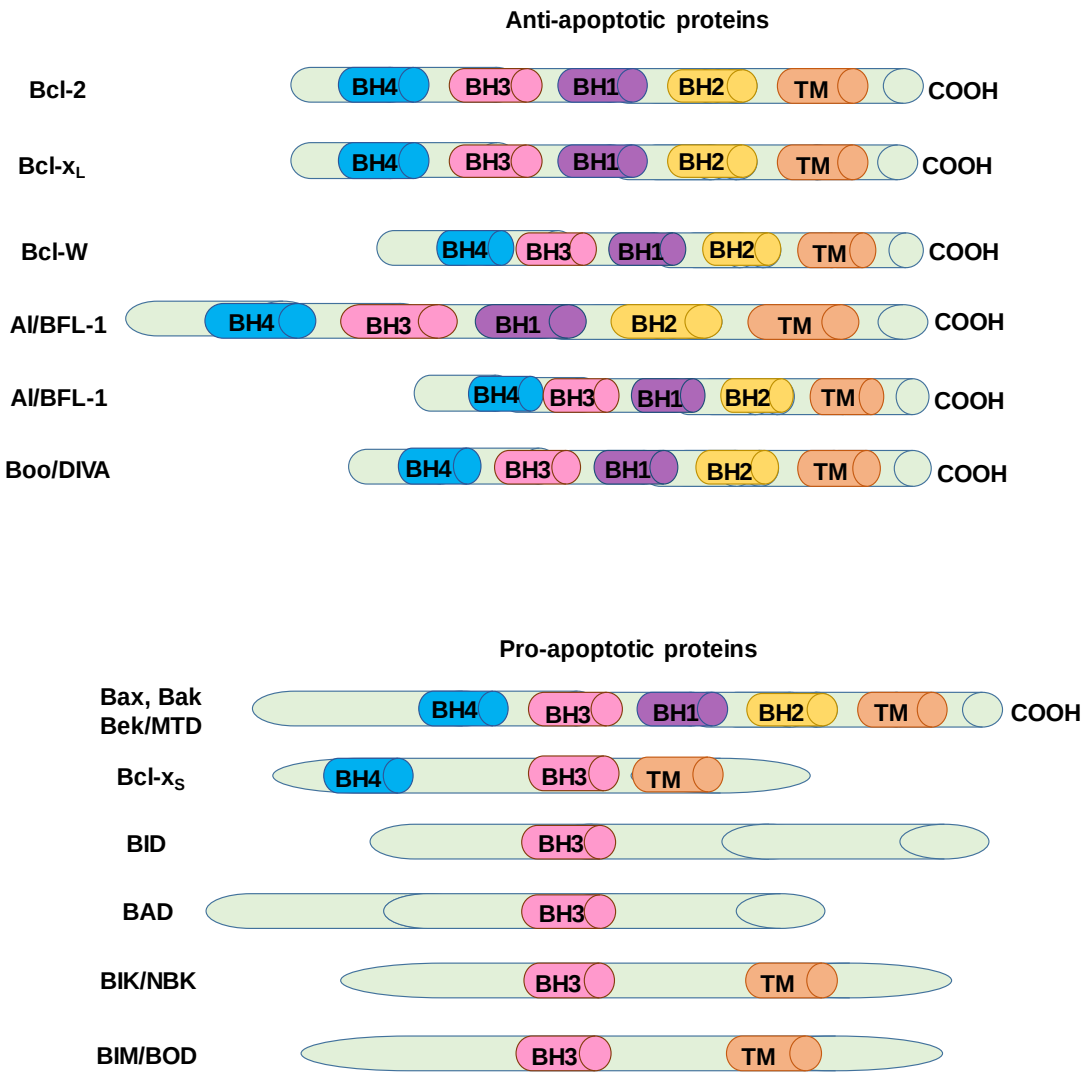

Figure 1.3 Structure of the Bcl-2 family proteins

Representative members of the Bcl-2 family are diagrammatically presented for comparison. Their categorisation depends on their function in mammals. BH domains are also indicated. Re-drawn based on diagram from (Petros et al., 2004). **Drawn by K. Ibraheem.**

1.3.2 Regulation

Bcl-2 family members are controlled transcriptionally and post-translationally by cytokines as well as proliferation- and death-inducing factors. In addition to dimerisation that enables proteins to activate (homodimerisation) or to inhibit (heterodimerisation) apoptosis, post-translational modifications (phosphorylation or proteolysis) are also able to influence the activity of some members of this family. Hyper-phosphorylation of Bcl-2 seems to modify its anti-apoptotic activity in certain cells, for instance the c-Jun N-terminal kinase (JNK), which is activated by stress and pro-apoptotic signalling, can phosphorylate Bcl-2 (Chang et al., 1997).

Bad is a protein that has the ability to bind to Bcl-xL and inhibit its anti-apoptotic activity. This relationship is conditional provided the binding site of Bad is dephosphorylated, as Bad can be phosphorylated by several kinases, such as Akt/PKB, a Ser/Thr kinase acting upstream kinase of the phosphatidylinositol triphosphate (PIP_3) pathway(Zha et al., 1996), and cAMP dependent kinase (PKA) (Harada et al., 1999).

It has been well demonstrated that the Bid protein (22 kDa) is a substrate of both caspase-8 and caspase-10. To be activated, Bid has to be cleaved by proteolysis which produces the C-terminal (15 kDa) fragment called truncated Bid (tBid). Then tBid can be inserted into the mitochondrial membrane and enables the activation of the mitochondrial pathway, thus subsequently amplifying the apoptotic signal initiated by death receptors (Luo et al., 1998, Milhas et al., 2005).

BH3-only proteins Bim and Bmf are located in distinct cytoskeletal structures such as microtubules and actin filaments, respectively. In response to certain cell death stimuli, Bim and/or Bmf are released from the cytoskeleton and translocate to mitochondria, where they bind to and inactivate Bcl-2 and its pro-survival homologues such as Bcl-xL. Bim moves to the mitochondria without being cleaved (Puthalakath et al., 1999).

1.3.3 Mechanism of action

Because of their dual role as pro- and anti-apoptotic proteins, the regulation of apoptosis by the Bcl-2 proteins can be the result of the precise balance in the expression level of pro- *versus* anti-apoptotic proteins; cells expressing more pro-

apoptotic proteins are susceptible to death, while cells that do not are more resistant (Hengartner, 2000).

The main role of these regulators is to control the release of pro-apoptotic mediators, e.g. cytochrome c, from the mitochondrial intermembrane space to the cytosol, as part of the process referred to as mitochondrial outer membrane permeabilisation (MOMP). The release of cytochrome c can be induced by pro-apoptotic proteins and is prevented by anti-apoptotic Bcl-2 proteins. Caspases are not strictly involved in this process, as the inhibition of caspase activity does not alter cytochrome c release. Bcl-2 is predominantly linked to the mitochondrial membrane, whereas the translocation from the cytosolic areas to the mitochondria during apoptosis is the mode of action of the pro-apoptotic proteins such as Bax, Bid, Bak, Bad and Bim. These are significant in transducing the signal from the cytosol to the mitochondria and their translocation can be regulated by post-translational modifications, e.g. Bad de-phosphorylation or cleavage of Bid (Antonsson and Martinou, 2000, Gross et al., 1999).

Bak is predominantly found in the mitochondria, while Bax primarily exists in the cytosol and stabilized by its interaction with the pro-survival Bcl-2 proteins in the outer mitochondrion membrane (OMM), but Bak and Bax share a common regulation of localization and activity. Both pro-apoptotic proteins are retro-translocated by pro-survival Bcl-2 proteins from mitochondria to cytosol of healthy cells. Bax is constantly translocating to the OMM, establishing an equilibrium between cytosolic and mitochondrial Bax (Edlich et al., 2011, Schellenberg et al., 2013). However, activated Bax is not retrotranslocated, as Bax activation blocks shuttling back to the cytosol. Reduction of Bax retrotranslocation initiates full Bax toxicity and if the Bax shuttling rate is reduced sufficiently, mitochondrial Bax ‘obliges’ the cell to apoptosis even in the absence of an apoptotic stress. Therefore, fast Bax retrotranslocation from the mitochondria is important in regulating cell fate. Interestingly, despite its predominantly mitochondrial localization, Bak commits the cell to apoptosis only in the existence of apoptotic inducements (Todt et al., 2013) and mitochondrial Bax activation adds to the differential regulation of both redundant proteins (Sarosiek et al., 2013). Bax activation could differ among different mitochondria, resulting in different organelle fates under stress conditions (Tait et al., 2010). Of note, there is no correlation between Bax

accumulation and Bax activation (Todt et al., 2013). Therefore, to prevent Bax activation in the absence of apoptosis signalling, cells must accelerate Bax shuttling into cytosol and minimizing the time Bax molecules spend on the OMM (Todt et al., 2015).

1.4 Role of mitochondria in apoptosis

1.4.1 General

The mitochondrion has an essential role in cell physiology, being the organelle that produces cellular energy, whilst protecting both the redox potential and the intracellular pH, and also playing an active role in the modulation of calcium homeostasis and oxidative stress. Programmed cell death can be a result of major dysfunction in mitochondria. The production of oxygen free radicals and acidification of the cytoplasm may be caused by the alteration in electron exchange. In these circumstances, insufficient production of electrons and ATP synthesis reduction leads to the lactate accumulation by glycolysis stimulation. In addition, the superoxide ions can be released from mitochondria and they are highly reactive oxygen free radicals (Adams, 2003).

1.4.2 The rupture of the outer mitochondrial membrane

Initially, this entails hyperpolarisation of the internal membrane before the release of cytochrome c in some systems. This hyperpolarisation stems from the failure of the exchange between cytoplasmic ADP and mitochondrial ATP. It is normal practice for the exchange to occur by the voltage-dependent anion channels (VDAC) which are situated in the outer membrane of the mitochondria and the carrier of adenylic nucleotide (ANT) that is located in the inner membrane. The absence of exchange seems to inhibit the activity of the F1F0–ATPase that would stop the return of H^+ ions to the matrix and then contributes to the hyperpolarisation. The extensive increase in mitochondrial membrane potential results in osmotic puffiness of the matrix and subsequent destruction of the external mitochondrial membrane (Vander Heiden et al., 1999).

1.4.3 The mitochondrial permeability transition pore

In this instance, a second mega-channel, which is the mitochondrial permeability transition pore (or MPTP), is involved. The MPTP is a non-selective channel with "high conductance" that is possibly created by transmembrane proteins that are found in the inner membrane and the outer membrane of the mitochondrion. Evidence suggests that the pore is primarily formed by the assembly of ANT of VDAC and cyclophilin D. Different physiological effectors can induce the opening of the pore, these effectors include calcium and a reduction in the concentration of adenine nucleotide or inorganic phosphate, the production of oxygen free radicals or a change in pH and the presence of Bax protein (Crompton, 1999, Rasola and Bernardi, 2007).

The permeability of the inner membrane of the mitochondria is increased by opening of the pore. As a result, it cause the dissipation of the mitochondrial membrane potential (proton-dependent), the chemical imbalance between the cytoplasm and the mitochondrial matrix and an uncoupling of oxidative phosphorylation, consequently causing an osmotic swelling which leads to the rupture of the outer membrane. Significantly, it has been suggested that the amount of the ATP present after the opening of the pore is one of the main reasons in the induction of death by necrosis or apoptosis. Furthermore, the Bcl-2 family are able to regulate the opening of the pore. Bcl-2 can also block pore opening (Kroemer et al., 2007, Shimizu et al., 1998).

1.4.4 Pore formation by members of the Bcl-2 family

The Bcl-2 proteins Bax and Bak are involved in MOMP (Mitochondrial outer membrane permeability) by their oligomerization and translocation from cytosol to mitochondria to promote pore formation in mitochondria membrane and cytochrome c release (Edlich et al., 2011). It remains unclear, however, what the chronology of events is, i.e. whether the pore opening is the cause or the consequence of the release of cytochrome c. Indeed, several studies have shown that the release of cytochrome c can occur in the absence or before the collapse of mitochondrial membrane potential (Bossy-Wetzel et al., 1998, Goldstein et al., 2000).

One explanation of this phenomenon is that the reversible (transient) MPTP opening may affect the permeability of the mitochondrial outer membrane, while allowing

restoration of the mitochondrial membrane potential. In addition, the opening of the pore may be a consequence of the inhibition of electron transport due to the release of cytochrome c, resulting in a fall of the mitochondrial membrane potential and the level of ATP, or the consequence of the activation of caspases (Kim et al., 2006, Kuwana et al., 2005). Indeed, caspase inhibitors can prevent the collapse of mitochondrial membrane potential without blocking the release of cytochrome c. Opening caspase-dependent MPTP could amplify the loop through which the early release of cytochrome c induces changes at the mitochondrial level. This model would seem to reinforce the observations made, i.e. the release of cytochrome c followed by a drop in mitochondrial membrane potential. Rupture of the outer mitochondrial membrane explains the massive release of pro-apoptotic factors or soluble inner mitochondrial membrane proteins (SIMP) contained in the mitochondria (Bossy-Wetzel et al., 1998).

Nevertheless, many studies indicate that these changes would be a consequence rather than a cause of the release of cytochrome c. Therefore, another mechanism must allow the release of cytochrome c. The assumption of a channel capable of passing the protein has been studied. It could be formed by some members of the Bcl-2 in view of the strong homology of Bcl-xL with the subunit of diphtheria toxin capable of forming a membrane pore. It has been suggested that of the Bcl-2 family such as Bax can insert themselves, following appropriate conformational change, in the outer mitochondrial membrane. Whether these proteins, consisting of a hydrophobic region and a helix alpha (α) surrounded by five amphipathic helices (Schendel et al., 1998), can be inserted into the lipid bilayer and oligomerised to form a channel that is large enough to pass small proteins remains to be demonstrated. It has been shown that these proteins could form a functional ion channel in synthetic lipid vesicles. These channels are pH-dependent, have voltage and show low ionic selectivity. The properties of the channels formed by proteins, pro-or anti-apoptotic, differ significantly (Figure 1.4) (Schlesinger et al., 1997).

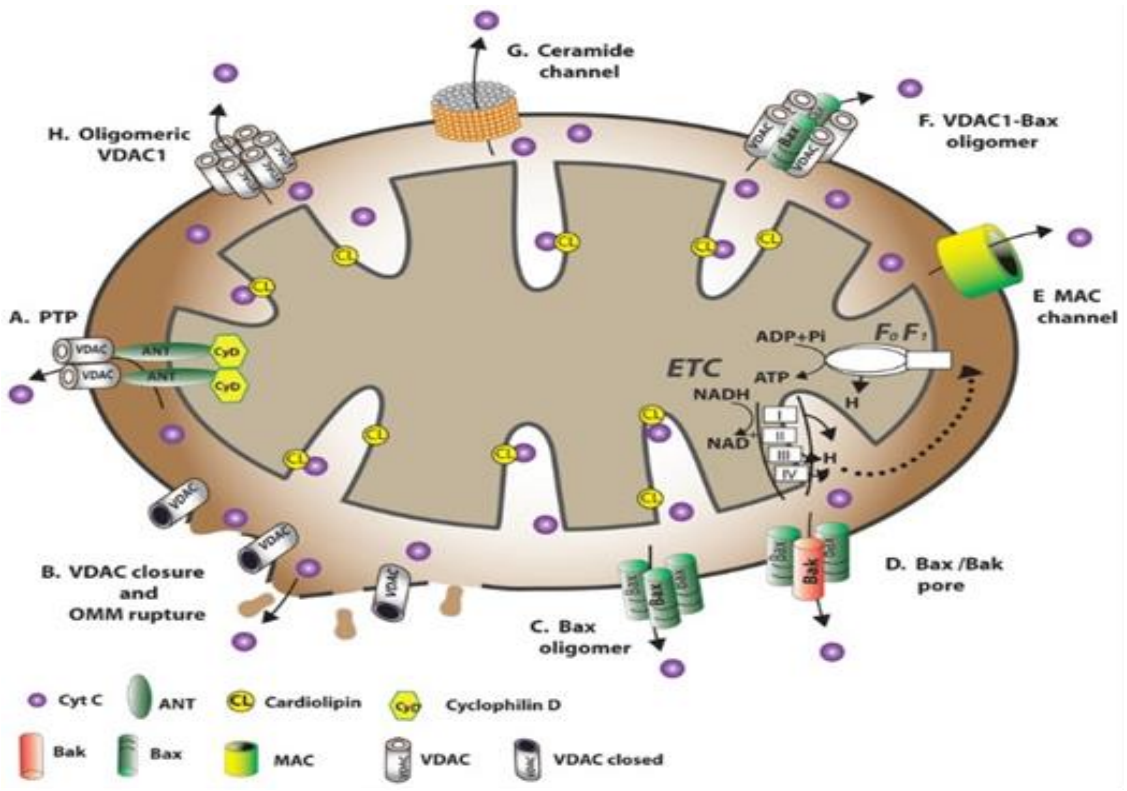

Figure 1. 4 The role of BCL2 family in the mitochondrial permeability transition pore

The diagram explain how BCL2 family involved in OMM permeability that occur during the induction of apoptosis, which permit the release of many apoptotic factors, such as Cyto c. The dynamic show the balance between the monomeric and oligomeric VDAC. Different factors can be involved in regulation of this, including Ca2+, oxidative stress and cytochrome c. Adapted from **www.frontiersin.org**

1.5 Apoptosis pathways

Apoptosis usually operates in cells via three pathways, 1) the extrinsic (death receptor-mediated) pathway 2) the intrinsic (mitochondrial) pathway and 3) the perforin/granzyme pathway (that relates to cytotoxic T lymphocytes and NK cells) (Elmore, 2007). The following sections will focus on the two main pathways (intrinsic and extrinsic). Both of these pathways often involve caspase activity following recruitment of adaptor molecules (Reed, 2000) (Figure 1.5). Although the two pathways are distinct, pathway cross-talk between the extrinsic and the intrinsic pathways can take place via the involvement (cleavage and subsequent activation) of Bid. Additional apoptotic pathways have been demonstrated involving caspase-dependent and caspase-independent pathways, e.g. mediated by apoptotic-inducing factors (AIF) released from mitochondria (Elmore, 2007).

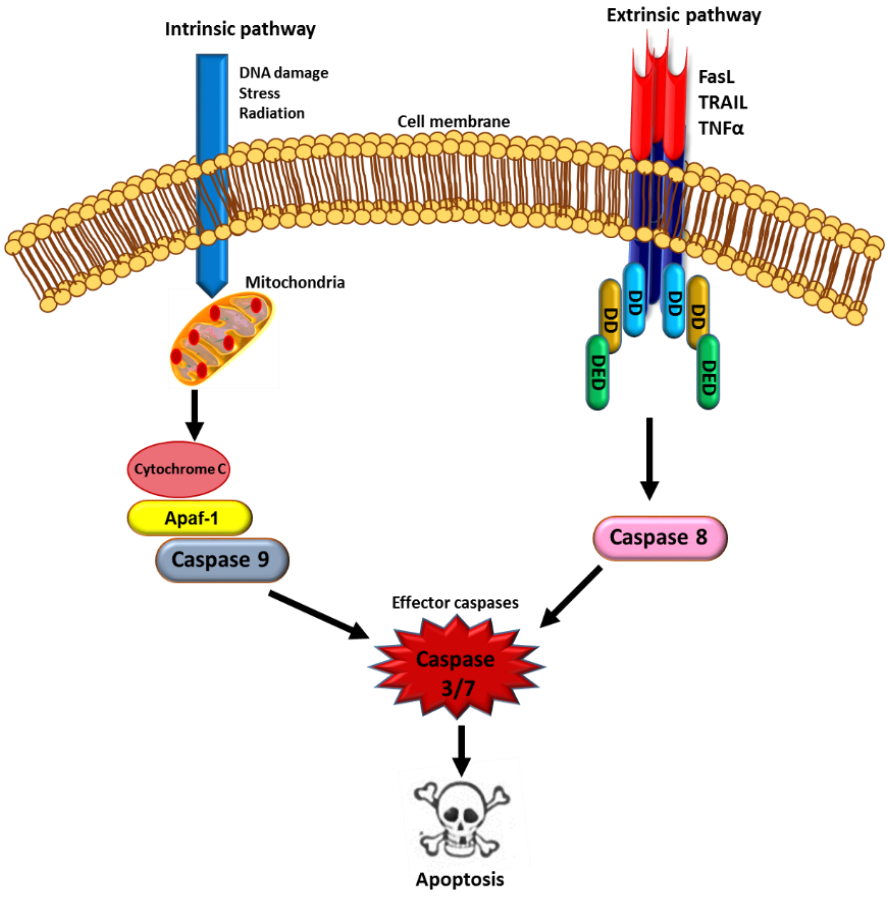

Figure 1.5 The extrinsic and intrinsic pathways of apoptosis

Members of the TNFR family activate the extrinsic pathway. Receptor aggregation (cross-linking) triggered by specific ligands leads to DISC (death inducing signalling complex) formation that involves pro-caspases (e.g. pro-caspase-8) via receptor associated proteins, which are adaptor proteins (not shown) containing DD and DED domains (see text). Stress signals, such as DNA damage, trigger the mitochondrial pathway which involves activation of anti- apoptotic Bcl-2 family members, cytochrome c release and pro-caspase-9 recruitment. Effector caspases are subsequently activated and specific cellular substrates are cleaved resulting in cell death. **Drawn by K. Ibraheem**.

1.5.1 The Extrinsic (death receptor-mediated) apoptotic pathway

The extrinsic pathway is initiated by engagement primarily of the Death Receptors (DRs) which are transmembrane proteins that belong to the Tumour Necrosis Factor (TNF) Receptor (TNFR) superfamily including TNFR-1, Fas (CD95), and TRAIL receptors (DR4 and DR5). Ligation of these receptors by their cognate ligands mediates extrinsic apoptotic signalling pathways and this is triggered by a variety of signals (Ashkenazi, 2002). These include toxins, hormones and cytokines that are found outside the cells or released in response to other stimuli (Figure 1.7) (Adams and Cory, 2007, Pai et al., 2006).

The ligands of the TNFRs such as TNFα, FasL, TRAIL (APO-2L), lymphotoxin α, lymphotoxin β, CD27L, CD30L, CD40L, CD137L, OX40L, RANKL, LIGHT, TWEAK, APRIL, and BAFF are members of the TNF family, they are organised in in trimeric form and are responsible for receptor activation. These ligands are initially synthesised as transmembrane precursors before the extracellular domain is cleaved by the action of metalloproteinases to form soluble ligands. Some of these ligands such as CD27L, CD30L and CD40L can also induce cell survival, whilst ligands such as TNFα, FasL and TRAIL mainly induce cell death (Albarbar et al., 2015).

1.5.1.1 The TNFR superfamily

There are three sub-groups of TNFRs which are divided according to the features of their intracellular domain ICD (Dempsey et al., 2003). The function of extracellular section of TNFR superfamily members is to recognise and bind to their specific ligand via the cysteine-rich domains, such binding induce receptor activation. First group: the essential contents in the ICD is the death domain (DD), e.g. TNFRI, Fas and TRAIL-Rs. These cytoplasmic sequences are important for the recruitment and binding of TNFR-associated DD (TRADD) for TNFR-I and Fas-associated DD (FADD) for Fas and TRAIL-Rs which act as adapter proteins that bind to the receptor via there DDs, while the other end of the adapter proteins triggers the binding with the caspases via the DED which are existed in both (adapter proteins and caspases mainly caspase-8 and caspase-10). Subsequently, such binding resulted in the formation Death-Inducing Signalling Complex (DISC). (Engels et al., 2005, Dempsey et al., 2003). Therefore, the

active initiator caspases that are released from the DISC complex mediates the activation of the executioner caspases (-3, -6, -7) which subsequently induce apoptosis (reviewed in (Albarbar et al., 2015)).

Second group: contain different type of domain known as the TRAF-interacting motif (TIM). Activation of the receptor induce the recruitment of TNFR-associated factors (TRAFs), these adaptor proteins are characterised by zinc RING finger proteins with a C-terminal region responsible for receptor binding, and subsequently trigger the activation of downstream signalling pathways, specifically, the Mitogen Activated Protein Kinases (MAPKs), such as p38 and JNK, resulting in activation of transcription factors (TFs) such as NF-κB and AP-1. At present, seven TRAF proteins have been specified and various TNFRs count on distinct signalling pathways triggered by different TRAFs after the activation of the receptor (Wajant et al., 2001).

Third group: Has no ICD in their cytoplasmic part. As a result of this group of TNFRs lack the ability to induce intracellular signalling function and binding of these receptors to TNFLs reduce the binding of other TNFRs and decay their signalling. The preferable examples are the TRAIL decoy receptors TRAIL-R3 (DcR1) and TRAIL-R4 (DcR2) (Ashkenazi, 2002, Hehlgans and Pfeffer, 2005) (Figure1.6).

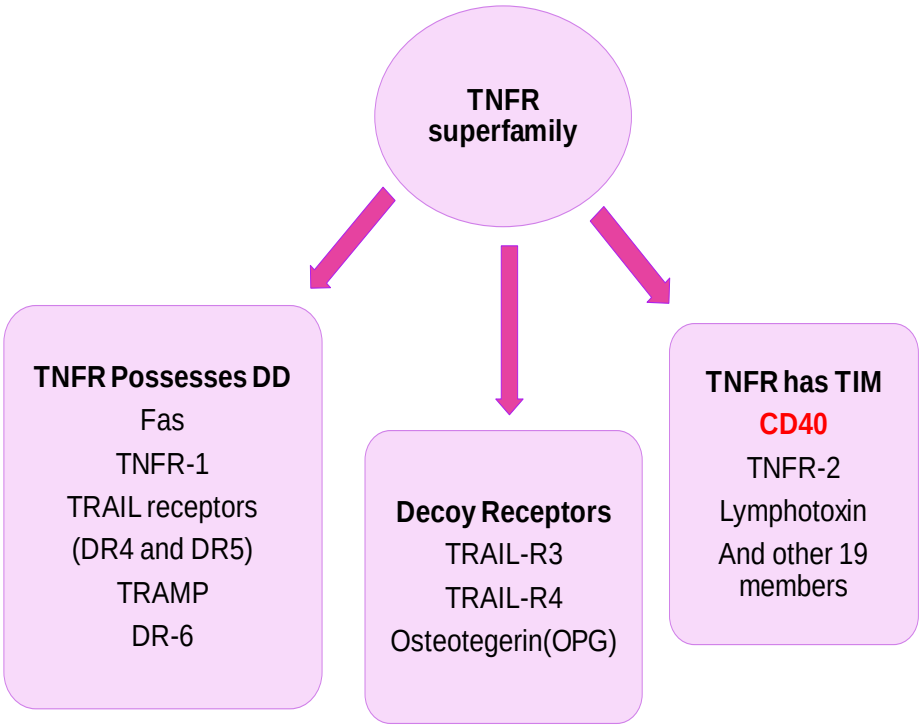

Figure 1.6 The division of TNFRs

TNFR superfamily divided into three sub-groups based on the specific structural features that they contain within their intracellular domains. **Drawn by K. Ibraheem**.

1.5.1.2 The TNF/TNF-R pathway

The prototypical member of the TNF family is TNF-α. Following binding to its cognate receptors TNF-R1 and TNF-R2, TNF-α can activate several signalling pathways. TNF-R1 and TNF-R2 differ in their cytoplasmic domains and as result are able to induce cell survival and death signals, the latter mainly by TNF-R1 via its DD. Activation of the transcription factors NF-κB (anti-apoptotic) and AP-1 (pro-apoptotic) represent downstream events of TNF-α mediated signalling. Interaction between TNFα and TNF-R1 causes TNF-R1 trimerisation and recruitment of adaptor protein TRADD, which in turn binds to FADD via its DD, leading to DISC formation which is complete after formation of a complex containing TNF-R1/TRADD/FADD and pro-caspase-8 or -10 which in turn activates effector caspases -3, -6 and -7 (Ermolaeva, 2008, Boldin et al., 1996).

However, cell survival can also induced by TNFα through either TRAF-2 (TNFR-associated factor-2) or RIP. Cell survival can be induced either by the activation of MAP Kinase pathway which is mediated by TRAF-2 or via NF-κB activation which is triggered by RIP. The interaction between TNFα and TNF-R2 results in the recruitment of TRAF-1 and -2 to the cytoplasmic tail of TNF-R2 (Declercq et al., 1998).

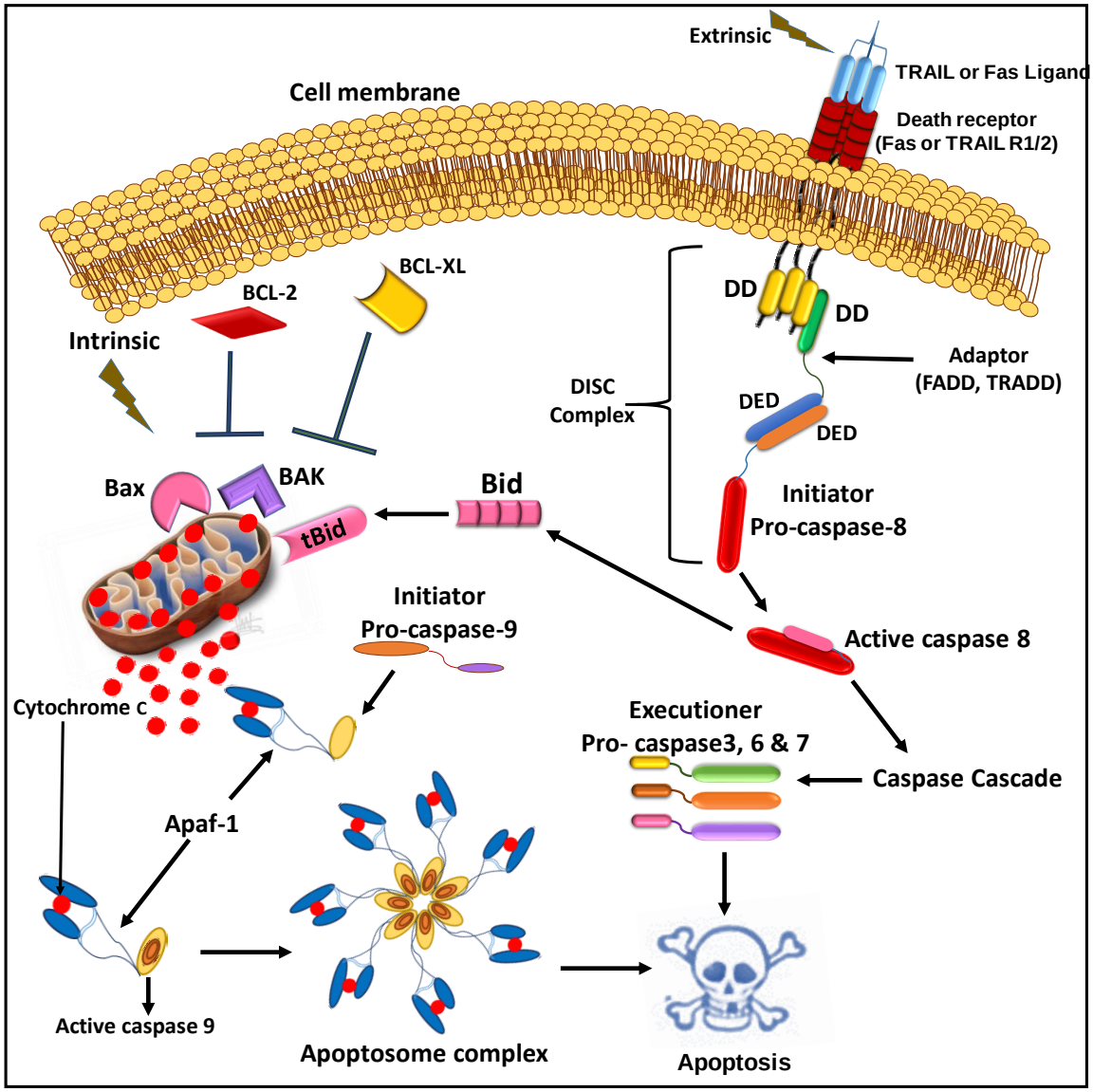

Figure 1.7 The death receptor (extrinsic) pathway and cross-talk

The schematic provides the main molecular components of death receptor (e.g. Fas, TRAIL-R1/R2)-induced apoptosis pathways. In the presence of ligand (FasL, TRAIL), the DR trimerises which recruits adapter FADD (Fas Associated Death Domain) via the cytoplasmic DD (death domain) (an interaction between DD of the adapter with DD of the receptor). FADD also contains a DED (Death Effector Domain) and in turn recruits pro-caspases-8 (or -10) as the latter comprises a homologous DED. This activates pro-caspase-8 by means of induced proximity and leads to the release of active caspase-8. Active caspase-8 in turn triggers a caspase cascade and apoptosis or cleaves Bid to active truncated Bid (tBid) then mediates cross-talk with the mitochondrial pathway. **Drawn by K. Ibraheem.**

1.5.2 The mitochondrial (intrinsic) apoptotic pathway

As discussed above, due to various types of stress, or as a result of TNFR signalling and cross-talk mediated by Bid activation, the mitochondrial pathway can be activated to mediate apoptosis. Pro-apoptotic proteins such as Bax and Bak can insert themselves into the mitochondrial outer membrane and stimulate the release of cytochrome c which trigger the establishment of apoptosome complex by its binding to the apoptotic protein activating factor 1 (Apaf-1) in the cytoplasm and initiator procaspase 9, facilitated by the presence of ATP. Active caspase-9 cleaves executioner caspases (-3,-6,-7) which leads to cell degradation and death. As mentioned above, other Bcl-2 family members, such as Bcl-2, Bcl-xL, Mcl-1 and IAP are anti-apoptotic proteins and act as inhibitors (Figure 1.8) (Kroemer et al., 2007).

1.5.2.1 The caspase-dependent mitochondrial pathway

The mitochondrion contains an outer membrane (MOM), a transmembrane area, an inner membrane and a matrix. In normal physiological conditions, the formation of an electrochemical gradient (membrane potential) by the respiratory chain is allowed by three proteins that exist in the inner membrane: the ATP synthase, the electron transport chain and the Adenylic Nucleotide Transporter (ANT) (Zoratti and Szabò, 1995). Cytochrome c, the Smac/Diablo protein, Apoptosis-Inducing Factor protein (AIF) and endonuclease G (Endo G) are components of the inner membrane space (Shoshan-Barmatz and Gincel, 2003). Permeabilisation of the inner membrane causes alteration in the mitochondrial membrane potential followed by the release of these proteins into the cytoplasm, with cytochrome c release in particular representing a main step in the mitochondrial pathway of apoptosis (Ravagnan et al., 2001).

1.5.2.2 Cytochrome c

The physiological function of Cytochrome c relates to electron transport between complex III and IV of the respiratory chain in the mitochondrial intermembrane space (Ravagnan et al., 2001). According to study by Liu and colleagues in 1996,(Liu et al., 1996). Cytochrome c is necessary for caspase-3 activation. This has been confirmed by other studies demonstrating that anti-apoptotic Bcl-2 can block both cytochrome c release and the activation of caspase-3 (Li et al., 2000). (Kluck et al., 1997, Yang et

al., 1997). Formation of the apoptosome complex is completely dependent on cytochrome c, as shown by the effects of gene knockout (Vempati et al., 2007), and cytochrome c is the only protein responsible for oligomerisation of Apaf-1 (Apoptotic protease activating factor-1) and caspase-9 activation induced by cellular stress agents or agents targeting the mitochondria (Li et al., 2000).

As mentioned above, there has been some lack of consensus in the mechanism by which cytochrome c is released but to a lesser extent the kinetics of its release. The presence of Bax or Bak in the outer mitochondrial membrane appears to be essential for cytochrome c release. Concerning the kinetics of cytochrome c release, it appears to occur rapidly (Goldstein et al., 2000). To reach the threshold required for the release of cytochrome c, various signals have to merge in the mitochondrion then in one step release of the entire cytochrome c can occur. It has been suggested that there is a link between the collapse of mitochondrial membrane potential (MMP) and the release of cytochrome c. It was observed that when even a few mitochondria partially release cytochrome c, the amount is adequate to induce caspase activation, and that the release of cytochrome c occurred before the collapse of MMP (Goldstein et al., 2000). By contrast, other studies reported that these incidents happened at the same time (Heiskanen et al., 1999). The observation of release of cytochrome c before the collapse of MMP reveals that the mitochondrion can retain its MMP with some of the cytochrome c continuing to operate within the respiratory chain. Therefore, the existence of two possible groups of cytochrome c in mitochondria would permit triggering the mitochondrial apoptotic pathway whilst maintaining a population to drive production of ATP that is required for apoptosome complex formation (Martinou et al., 2000).

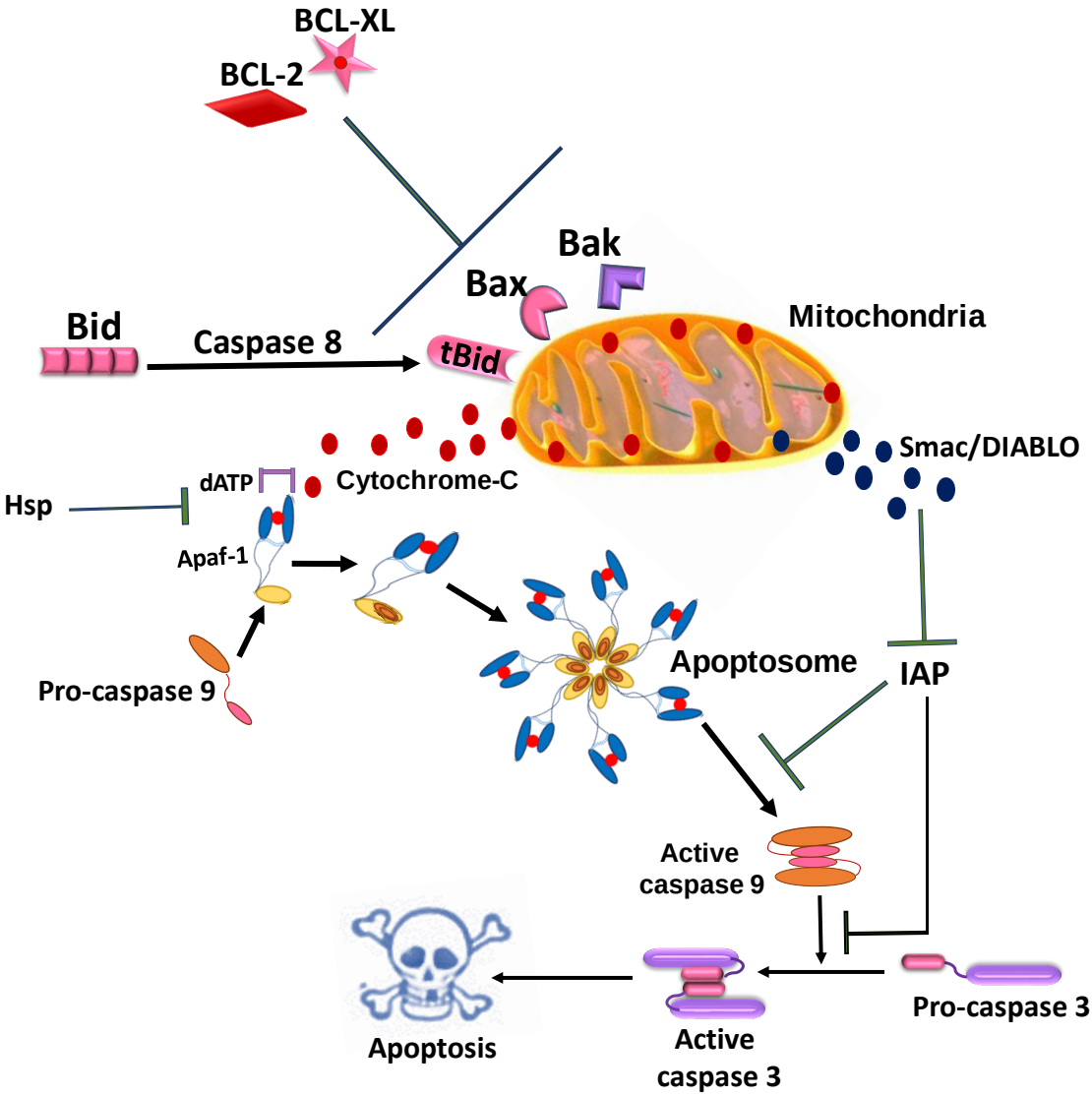

Figure 1.8 The mitochondrial pathway of apoptosis

Many of mitochondrial intermembrane space proteins are released under the control of pro-apoptotic proteins of the Bcl-2 family. Binding of cytochrome c to Apaf-1 is controlled by dATP which can be inhibited by Hsp. Formation of the apoptosome complex leads to executioner caspases 3&7 activation and cell death. IAP (inhibitor of apoptosis protein) family members mediate caspase inhibition which can be blocked by Smac/Diablo. **Drawn by K. Ibraheem.**

1.5.2.3 The Apaf-1 protein

The Apoptotic protease activating factor-1 (Apaf-1) is a protein of approximately 130 kDa. Its N-terminal possesses a caspase recruitment domain (CARD), the region which characterised by high homology to Ced-4, while there are several WD40 domains repeats located in the C-terminal region; these are implicated in protein-protein interactions (Cain et al., 2002). These domains are required for binding to cytochrome c and recruitment of caspase-3. Under normal conditions the CARD domain of Apaf-1 is unavailable thus there is no interaction with caspase-9; following a conformation change the CARD domain of Apaf-1 is exposed and can interact with caspase-9, which requires ATP and triggered by cytochrome c as shown in Figure 1.8. It has been reported by many studies that there are at least six splice variants of Apaf-1 in human cells and some of them (Apaf-1XL and Apaf-1L) are able to engage with cytochrome c and cleave pro-caspase-9 (Delivoria-Papadopoulos et al., 2007).

1.5.2.4 Apoptosome formation

As explained above, a key step in mitochondrial apoptosis is the formation of the apoptosome protein complex, a large ~700 kDa structure that consists of Apaf-1, cytochrome c and procaspase-9. In the cytoplasm, the first interaction that occurs is between cytochrome c and the carboxyl terminal of Apaf-1 which reveals the WD40 domains and CARD domains, key domains of Apaf-1. The multimerization of Apaf-1 is mediated by the WD40 domains while the recruitment of the initiator pro-caspase-9 is via the CARD domain of Apaf-1 and the CARD domain of caspase-9 (Cain et al., 2002, Hu et al., 1998). Cryo-electron microscopy has been used to solve the structure of the apoptosome which is a three-dimensional structure (Acehan et al., 2002, Yuan et al., 2010), in which seven Apaf-1 molecules at their N-terminus can form the apoptosome in a wheel-like structure (the “wheel of death”). At the center of the apoptosome, the exposed CARD domains of Apaf-1 gather pro-caspase-9 locally. The formation of the holoenzyme complex activates caspase-9 by self-dimerization and proteolytic cleavage and causes elevation in its enzymatic activity (Rodriguez and Lazebnik, 1999, Shi, 2002a) (Figure 1.9). It has been shown that caspase-9 can be cleaved in both apoptosome and in the cytoplasm, but the active caspase-9 form is the apoptosome-associated one(Shi, 2002a) (Shi, 2002a). The residue D315 of caspase-

9 is the point of its auto-proteolytic cleavage, but this cleavage is only indicative of its activation and is not necessary for its activity (Rodriguez and Lazebnik, 1999, Shi, 2002a). Once caspase-9 been activated, then it will be able to cleave the executioner caspases, such as caspase-3 and -7 (Acehan et al., 2002).

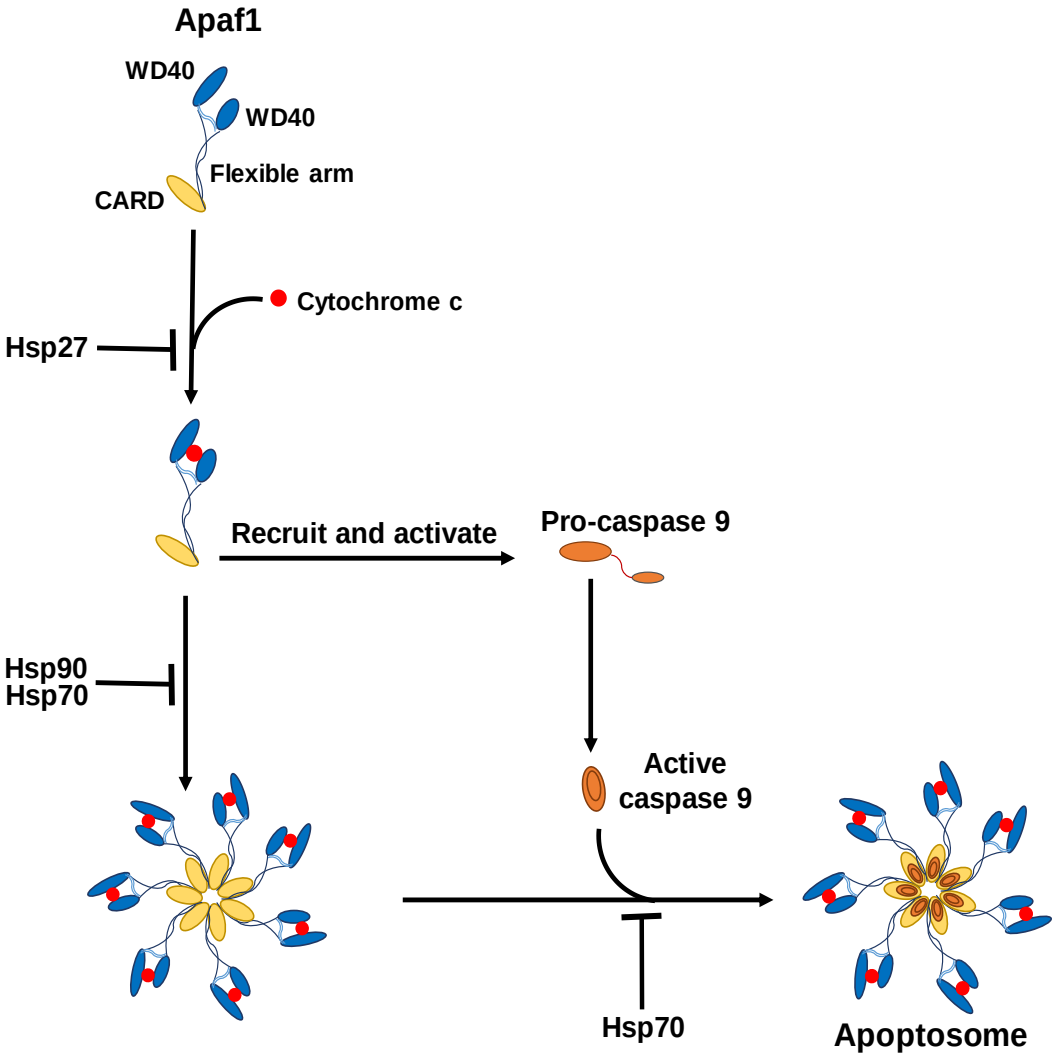

Figure 1.9 The apoptosome formation and its inactivation

Cytochrome c released into the cytoplasm intreacts with the WD40 domain of the Apaf1, resulting in the formation of heptameric wheel structure. The center of this consists of CARD domains of Apaf1 able to amplify recruitment of pro-caspase 9 and trigger caspase 9 activation. Some antiapoptotic proteins control the apoptosome formation steps. Binding of cytochrome c to Apaf1 is inhibited by HSP27, the multimerization of Apaf1 is inhibited by Hsp70 and Hsp90 and the recruitment of caspase 9 inhibited by Hsp70. **Drawn by K. Ibraheem.**

1.5.3 Regulation of caspase-dependent pathways

1.5.3.1 The inhibitors of apoptosis proteins (IAPs)

Cell death can be inhibited by the ability of IAPs to prevent the cleavage of caspases and stop their activity (Fesik and Shi, 2001). Initially, IAPs were described as viral (baculovirus expressed) inhibitors, but cellular homologues (c-IAPs) were soon identified. The BIR domains (baculoviral IAP repeat) are required for the anti-apoptotic activity of IAPs and enable their binding to caspases. There are specific functions for each BIR domain, also each BIR domain has its own binding specificity to caspases (Verhagen et al., 2001). For example, inhibition of caspases-3 and -7 is the function of BIR2 domain whereas inhibition of caspase-9 is the responsibility of BIR3 domain (Ekert et al., 2001). One of the well-known members of IAPs family is the X-linked inhibitor-of-apoptosis (xIAP) which can bind to and inhibit the activation of both the initiator caspase-9 and the executioner caspases -3 and -7 (Deveraux et al., 1999, Wei et al., 2008).

1.5.3.2. Inhibitors of IAPs

There are some blocking proteins that act to inhibit the activity of the IAPs such as Smac (Second Mitochondria-derived Activator of Caspase) and its analogue DIABLO (Direct IAP Binding protein with Low pI), which have also some resemblance with Grim Reaper and HID Drosophila proteins (Verhagen et al., 2001, Du et al., 2000). Smac/DIABLO is highly-expressed in many cell types such as heart, kidney, liver, spleen and also in several cancer cell lines, it was the first protein that identified to directly block the inhibition action of IAPs, and is also able to join the death receptor pathway (Srinivasula et al., 2001, Shi, 2002b). Smac/DIABLO is synthesised in the cytoplasm as a 239 amino acid precursor then translocates to the mitochondrion by its MLS (55 amino acid N-terminal mitochondrion localisation signal), which is subsequently cleaved, whilst it is activated by homo-dimerisation (Chai et al., 2000). Several pro-apoptotic stimuli can induce the release of Smac/DIABLO protein from mitochondria, this release appears to be caspase-dependent and members of Bcl-2 family also control its release (Adrain et al., 2002). The mechanism by which Smac/DIABLO can inhibit the action of IAPs is by physical interaction with the third BIR

domain (BIR3), as shown by X-ray crystallography studies on XIAP (Liu et al., 2000), and this interaction inhibits IAP binding to caspase-3, -7 and -9.

Another protein, XAF-1 (XIAP associated factor 1), also has the ability to activate caspases by inhibiting IAPs. XAF-1 is a nuclear protein which found continuously active, in contrast to Smac/DIABLO which is active only after stimulation, XAF-1 interact directly with XIAP via its zinc finger domain (Liston, 2001 pp478).

Moreover, the Omi/HtrA2 (high temperature requirement protein A2) can also regulate IAPs. Its precursor is a 50 kDa protein that contains an MLS in its N-terminus. Once HrtA2 is imported to mitochondria the MLS is cleaved and a 36 kDa protein produced. HtrA2 is a serine protease which in normal cells is located in the mitochondrial intermembrane space, but after induction of apoptosis by different stimuli, like TRAIL, staurosporine or UV irradiation, HtrA2 is released to the cytosol and binds to XIAP and IAPs similarly to Smac/DIABLO and promotes activation of caspases. There are two different mechanisms by which HtrA2 can induce apoptosis, one is by targeting the ability of IAPs to inhibit caspase activation, and the second by the serine protease activity independent of caspase (Suzuki et al., 2001, Hegde et al., 2002).

1.5.3.3 Other regulatory proteins

Other ‘strategic’ sites within cells, such as the endoplasmic reticulum, the Golgi apparatus, the lysosomes or the nucleus, contain proteins that can be involved in the regulation of apoptosis signalling (Ferri and Kroemer, 2001, Galluzzi et al., 2014). The role of the nucleus in the regulation of apoptosis is newly characterised. In addition to the nuclear protein XAF-1 above, the DED-containing DNA-binding protein (DESD) is another nuclear protein able to inhibit caspase-6 activation or block the transcription and has anti-apoptotic activity. The DED-associated factor (DEDAF) is another protein that appears to be responsible for the modulation of DESD protein; the DEDAF promotes DISC formation by its ability to bind to FADD and caspase-8 or -10 (Zheng et al., 2001).

Interestingly, the Hsp (heat shock protein) family can act as regulators of the apoptotic pathway; in fact they can simultaneously be inducers and inhibiting factors of apoptosis

(Figure 1.10). Oligomerisation and activation of pro-caspase-9 can be prevented by binding of Hsp70 and Hsp90 to the CARD domain of Apaf-1 (Pandey et al., 2000, Saleh et al., 2000). The oligomerisation of Apaf-1 can also be blocked by binding of Hsp-27 to the cytochrome c (Bruey et al., 2000).

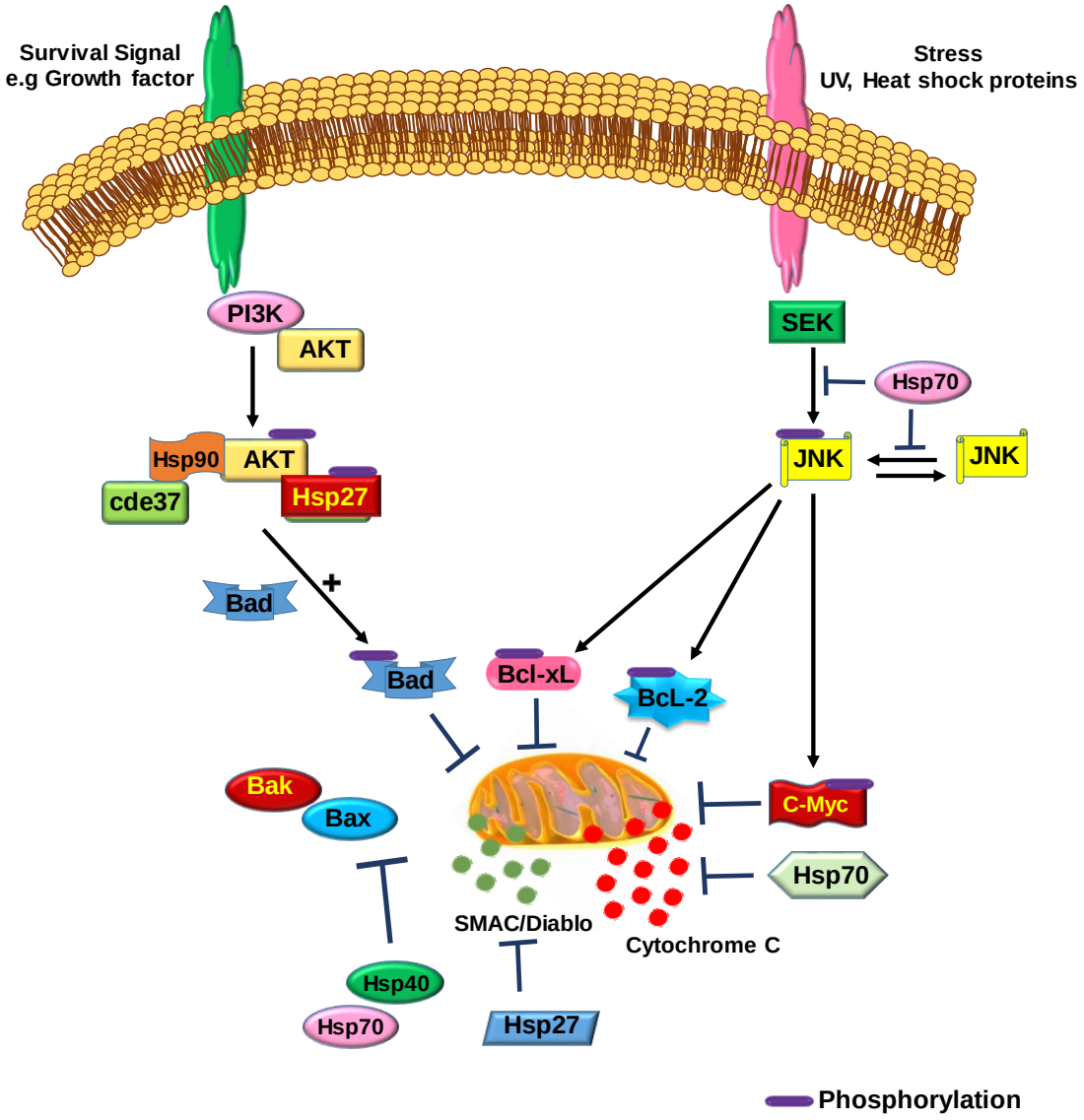

Figure 1.10 Events in the mitochondrial apoptotic pathway regulated by Heat shock proteins (Hsp)

The mitochondrial pathway of apoptosis and subsequent caspase activation can be controlled by either extracellular signals (survival signals) or stresses (death signals). The interaction of Hsps with their targets at several points of these pathways mediates either inhibition of apoptosis (indicated as (T)), or potentiation of a signalling pathway of apoptosis (depicted as "+"). **Drawn by K. Ibraheem.**

1.5.4 The caspase-independent mitochondrial pathway

The mitochondrial intermembrane space contains additional proteins, such as apoptotic inducing factors and Endonuclease G, which are able to induce apoptosis directly without caspase activation. When these proteins are released from mitochondria, they translocate to the nucleus and cause chromatin condensation plus cleavage of DNA which leads to DNA fragmentation (Candé et al., 2002).

1.5.4.1 The AIF

The identification of Apoptosis-inducing factor (AIF) was performed by Guido Kroemer's team (Candé, 2002;Susin, 1999). The AIF gene encodes a 57 kDa protein and is located on chromosome X. The flavoprotein AIF comprises an amino terminal side that has the MLS sequence which is a sequence of 27 amino acids, while the carboxyl terminal contains a domain of 485 amino acids with oxidoreductase activity (Candé et al., 2002). AIF is synthesised as a 67 kDa precursor and then imported into the mitochondrial intermembrane space (Susin et al., 1999), where the MLS sequence is cleaved and the conformation of the protein alters whilst it combines with the prosthetic group FAD (Flavin-adenine dinucleotide). AIF may thus have a dual action, one being oxidoreductase activity and the second its pro-apoptotic role (Ye et al., 2002).

Following cell exposure to pro-apoptotic stimuli, the first translocation of AIF is from the intermembrane space into the cytosol and then from the cytosol to the nucleus (Susin et al., 1999). How AIF translocates to the cytosol is not understood yet, but its transportation to the nucleus is due to the sequence of a nuclear localisation signal. *In vivo* and *in vitro* studies have been conducted to show the effect of the AIF as an apoptotic molecule. *In vitro* studies have shown that after translocation through the cytoplasm to the nucleus, AIF causes condensation of the chromatin and degradation of the DNA into large fragments (50kb). This interaction is direct, without sequence specificity and is mediated by its carboxy-terminal domain. The extent of its translocation to the nucleus can modulate its activity and appears to be maximal during the condensation phase at the late phase of apoptotic body formation (Ye et al., 2002).

Interestingly, over-expression of Bcl-2 can attenuate the effects of AIF, and this is independently of caspase activation. Furthermore, as mentioned above, Hsp70 can exert anti-apoptotic activity by preventing the formation of apoptosome by its binding to Apaf-1. But in cells without caspase expression, overexpression of Hsp70 can also block cell death and this appears to be via its ability to bind AIF. The ATP domain of Hsp70 seems to be its binding site for Apaf-1 and AIF interaction, and is independent of Hsp70's chaperone activity (Ravagnan et al., 2001).

The precise mechanism of function of AIF, including its mode of action on the DNA, its oxidoreductase activity and its signal transduction are still unclear. The direct interaction between DNA and AIF may be the cause of DNA condensation observed during apoptosis (Ye et al., 2002). In fact, chromatin structure could be modified by this interaction and AIF may cause elevation in nucleases such as topoisomerase II, as the fragments produced by these nucleases (50kb) are similar in size to those generated by AIF (Widlak and Garrard, 2009, Samejima et al., 2001).

1.5.4.2 Endonuclease G

Endonuclease G (Endo G) is non-specific nuclease and it is a highly conserved enzyme. It is encoded by a nuclear gene but it may also be involved in the mitochondrial genome replication. During the process of apoptosis, Endo G goes through the outer membrane of the mitochondria and translocates to the nucleus (Li et al., 2001). Endo G has the ability to cooperate with exo-nuclease and the DNase I in the nucleus to produce DNA fragments of higher molecular weight (Widlak and Garrard, 2009). However, its action can also generate oligonucleosomal fragments (Samejima et al., 2001).

1.6 Reactive oxygen species (ROS)

Although ROS have long been considered as mere by-products of cellular metabolism, they appear to play important roles in several Aspects of cellular physiology particularly as signalling molecules. Accumulating evidence suggests a role of ROS in normal cell signal transduction as a second messenger. Studies in the 1990s first showed that hydrogen peroxide (an extremely diffusible ROS) is an important molecule in signalling pathways induced by cytokines, hormones, growth factors, and the AP-1 and NF-κB pathways (Finkel, 1998). Moreover, ROS are key molecules in immune cell activation and overall immune responses.

Reactive oxygen species (ROS) is a term used to describe the molecules or ions that are characterized by a single unpaired electron in their outward shell of electrons. This property makes ROS highly reactive, as ROS are able to oxidize other molecules. There are two types of ROS recognised (Liou and Storz, 2010):

a) The free oxygen radicals include one or more unpaired electron in their outer molecular orbital such as superoxide ($O_2^{\bullet-}$), hydroxyl radical (•OH), nitric oxide (NO•), organic radicals (R•), peroxyl radicals (ROO•), alkoxyl radicals (RO•), thiyl radicals (RS•), sulfonyl radicals (ROS•), thiyl peroxyl radicals (RSOO•), and disulfides (RSSR).

b) The non-radical ROS lack unpaired electrons but are chemically reactive and can be converted to radical ROS; they include hydrogen peroxide (H_2O_2), singlet oxygen ($^1O_2$), ozone/trioxygen (O_3), organic hydroperoxides (ROOH), hypochloride (HOCl), peroxynitrite (ONO−), nitrosoperoxycarbonate anion ($O{=}NOOCO_2^-$), nitrocarbonate anion ($O_2NOCO_2^-$), dinitrogen dioxide (N_2O_2), nitronium (NO_2^+) and highly reactive lipid-or carbohydrate derived carbonyl compounds.

Superoxide dismutases (SODs) can convert radical superoxide to one H_2O_2 molecule (non-radical ROS) and one water molecule. Then by Fenton reaction, one more electron from free Fe^{2+} can be accepted by H_2O_2 and converted to hydroxyl radical (HO) which is excessively reactive and has cellular damage effect. Glutathione

peroxidase (GPXs), peroxiredoxins (PRXs) and catalase can reduce H_2O_2 to water (H_2O) (Figure 1.11). Cellular physiology can be differentially affected by the reactivity of these ROS forms (Cross et al., 1987, Sundaresan et al., 1995).

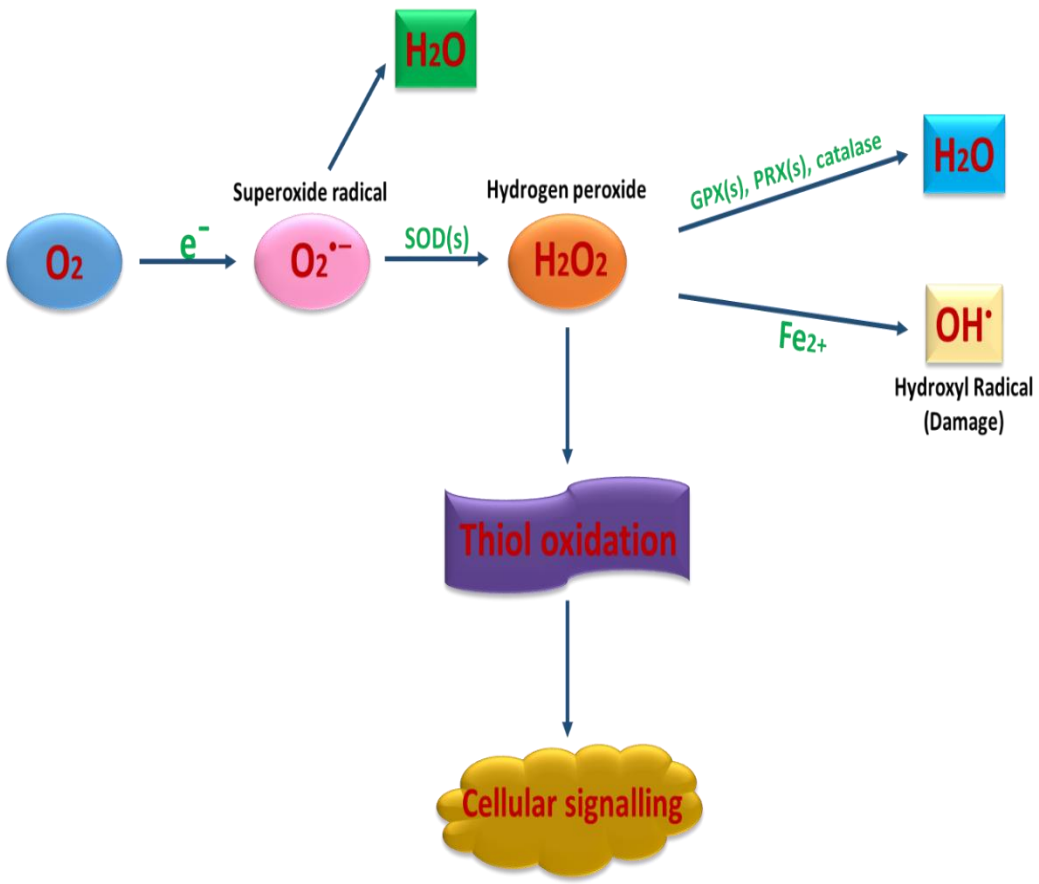

Figure 1.11 Production and interconversion of reactive oxygen species

$O_2^{\bullet-}$ is generally derived from molecular O_2, using one electron from a NADPH oxidase (NOX) enzyme or from the electron transport chain of the mitochondria. Superoxide dismutase (SOD) enzymes transform two superoxide molecules into a H_2O_2 and a water (H2O) molecule. H_2O_2 can undergo Fenton chemistry with Fe2+ to form HO which is highly reactive and can cause cellular damage. H_2O_2 can also alter redox-sensitive cysteine residues to modulate cellular signalling. Alternatively, H_2O_2 can be reduced to water by glutathione peroxidases (GPXs), peroxiredoxins (PRXs) or catalase. **Drawn by K. Ibraheem.**

1.6.1 The main sources of cellular ROS

Production of ROS was initially thought to be only via phagocytic cells as part of the host defence mechanisms. ROS can be produced by either extracellular or intracellular triggers. Pollutants, tobacco, smoke, drugs, xenobiotics and radiation are responsible for 'extracellular' ROS. The majority of intracellular ROS originates from the mitochondria, peroxisomes, endoplasmic reticulum and the NADPH oxidase (NOX) complex in cell membranes (Inoue et al., 2003, Luis et al., 1992).

The NOX complex is a major source of intracellular ROS by catalysing the superoxide production from O_2 and NADPH. NOX can be found in different sites in the cell membrane and include subunits NOX1, NOX2, NOX4, NOX5, and more regulatory components such as $p22^{phox}$, $p40^{phox}$, $p47^{phox}$ and the small G protein Rac1. (Babior, 1999, Brown and Griendling, 2009, Jiang et al., 2011).

The other major ROS source is the mitochondrial electron transport chain, which removes electrons from NADPH during aerobic respiratory reactions and ATP synthesis. This leads to reduction of molecular oxygen to superoxide, which then infiltrates to the cytoplasm through the MPTP (described in section 1.6). Superoxide is dismutated to H_2O_2 either in the mitochondrial matrix by Mn-SOD or in the cytosol by Cu-ZnSOD (Gogvadze et al., 2008, Murphy, 2009). Catalase activity can convert H_2O_2 to water or H_2O_2 can also convert to highly reactive hydroxyl radicals in the presence of transition metals (Mishina et al., 2011). The superoxide can interact with reactive nitric oxide ($NO^{\bullet}$) and form peroxynitrite ($ONOO^{-}$) (Szabó et al., 2007).

The endoplasmic reticulum can also produce ROS through the protein folding process and the formation of disulphide bonds. The major sources of ROS in the endoplasmic reticulum are the glycoprotein endoplasmic reticulum oxidoredutin 1 (ERO1), the protein disulfide isomerase and NOX4 (Gupta et al., 2012) (Figure 1.12).

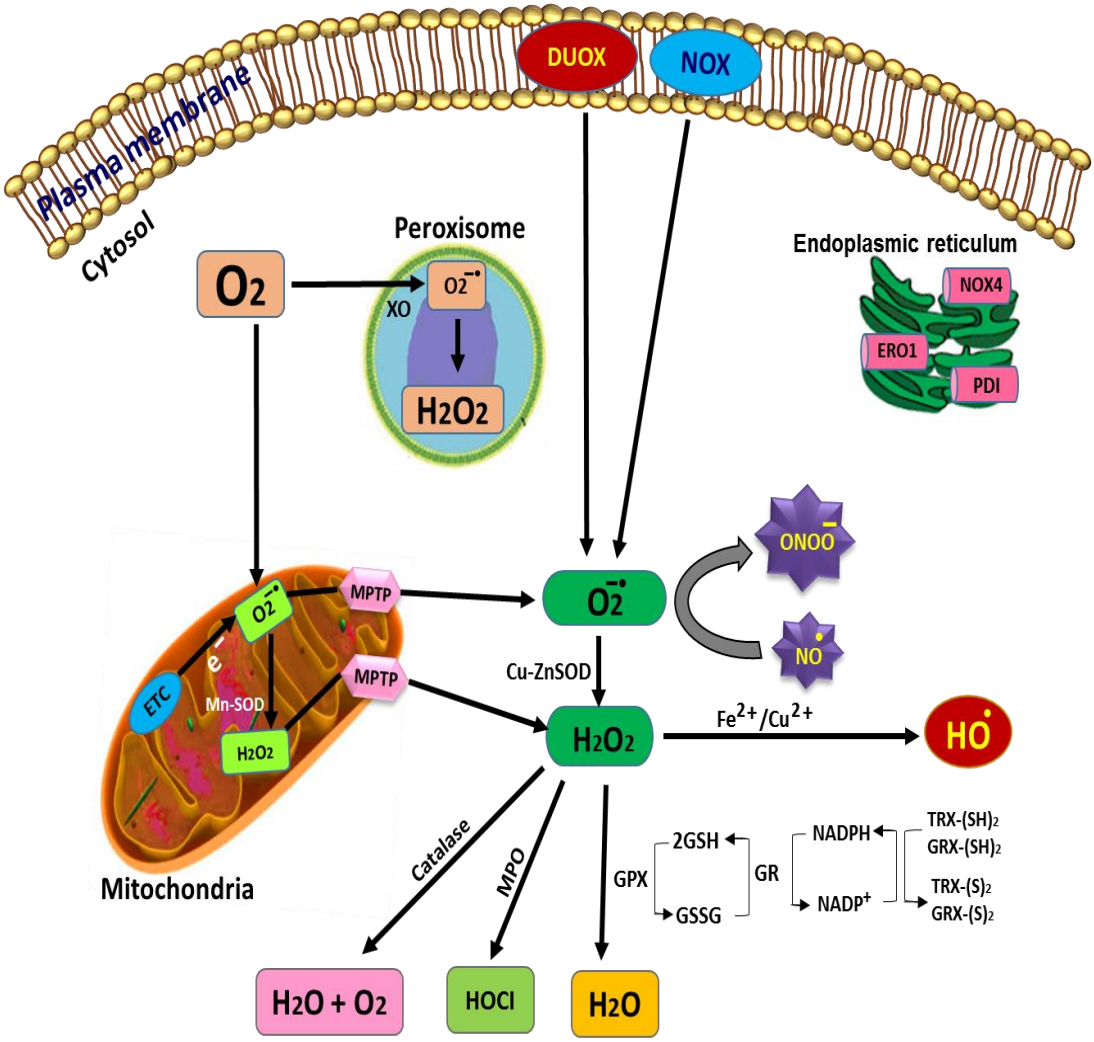

Figure 1.12 Main sources of ROS inside the cell

The origins of ROS are mitochondria, peroxisomes, endoplasmic reticulum, and the NOX complex in cell membranes. Under normal conditions, excess ROS is scavenged by the antioxidant defence systems of the cell. DUOX, dual oxidase; ERO1, endoplasmic reticulum oxidoreductin 1; ETC, electron transport chain; GPx, glutathione peroxidase; GR, glutathione reductase; GRX-(S)2, glutaredoxin oxidized; GRX-(SH)2, glutaredoxin reduced; GSH, glutathione; GSSG, glutathione oxidized; H2O2, hydrogen peroxide HO, hydroxyl radical; HOCl, hypochlorous acid; MPO, myeloperoxidase; MPTP, mitochondrial permeability transition pore; NADP+ , nicotinamide adenine dinucleotide phosphate oxidized; NADPH, nicotinamide adenine dinucleotide phosphate reduced; NO, nitric oxide; NOX, NADPH oxidase; O2 -, superoxide radical; ONOO- , peroxynitrite; PDI, protein disulfide isomerase; SOD, superoxide dismutase; TRX-(S)2, thioredoxin oxidized; TRX-(SH)2, thioredoxin reduced; XO, xanthine oxidase. **Drawn by K. Ibraheem.**

1.6.2 Role of ROS in apoptosis

It is well-established that basal (physiological) levels of ROS are capable of acting as "redox messengers" in cell signalling and its regulation, whereas excessive ROS levels can induce oxidative damage to cellular macromolecules, can inhibit protein function, and directly and efficiently promote cell death.

One main pathway by which ROS can activate apoptosis, whether the trigger is extrinsic or intrinsic apoptotic signalling is via ROS-mediated activation of JNK signalling (Shen and Liu, 2006). Importantly, upstream of JNK is the redox-sensitive MAP3K ASK1 (Apoptosis signal-regulating kinase 1), the activity of which is inhibited by interactions with redox protein Thioredoxin-1 (Trx1). Transient and modest JNK activation is associated with cell survival, whereas sustained and marked JNK activation induces cell apoptosis via ASK1 signalling (Circu and Aw, 2010). Under low basal ROS conditions, Trx1 interacts with the N-terminal domain of ASK1, preventing activation and downstream pro-apoptotic signalling. Elevated cellular ROS cause Trx1 reduction and inactivation thus releasing Trx-1 from the "ASK1 signalosome" – this complex is believed to act as a "redox sensor" that is activated under oxidizing conditions. Dissociation of Trx1 from the complex then permits ASK1 oligomerization and promotes full ASK1 kinase activity and apoptosis (Fujino et al., 2006).

ROS are known triggers of the intrinsic apoptotic cascade via interactions with proteins of the mitochondrial permeability transition (PTP) complex. Components of the PTP and VDACs represent ROS targets, whilst oxidative modifications of PTP proteins significantly impact mitochondrial ion transport. For instance, enforced transient increase in mitochondrial membrane hyperpolarization by exposure to H_2O_2 can initiate the collapse of the mitochondrial membrane potential ($\Delta\Psi m$) and is followed by mitochondrial translocation of Bax and cytochrome c release (Circu and Aw, 2010). Moreover, direct ROS-mediated effects on caspase activity have been documented, with ROS capable of inducing intra-mitochondrial auto-activation of caspase-9, which can take place during the "pre-apoptotic phase" and before cytochrome c release can be detectable (Katoh et al., 2004).

1.6.3 Role of ROS in cellular transformation and tumorigenesis

A direct role for ROS in gene expression, activation of cell signalling cascades and cell apoptosis is supported by a growing number of reports (Hancock et al., 2001). Moreover, the relationship between ROS and malignant transformation has been reported previously by many studies (Jackson and Loeb, 2001, Valko et al., 2006, Wang and Yi, 2008). The mechanism by which ROS is triggered by oncogene activation remains unclear, but DNA damage has been shown to play a role in this process. The oncogenic transformation of ovarian epithelial cells with H-RasV12 or the oncogenic effect of tyrosine kinase Bcr-Abl in hematopoietic cells was associated with an increase in ROS. In another study, transformation of fibroblasts with constitutively active isoforms of Rac and Ras was associated with production of superoxide (Gupta et al., 2012).

ROS is a by-product of cell growth, and the key hallmark of cancer cells is the unrestricted growth (Hanahan and Weinberg, 2000), thus cancer cells produce much higher level of ROS than normal cells. However, this is “proliferation at a cost”, as high level of ROS generate an oxidative stress on the cell which can essentially lead to cell senescence or death (Trachootham et al., 2006, Dunnill et al., 2016).

As a result of malignant transformation, the Carcinoma cells operate under the oxidative stress status (Gupta et al., 2012). It has been suggested that the potential function of basal cellular ROS in defining whether cytotoxic agents can induce apoptosis in malignant cells by ‘pushing’ them past a critical ‘lethal threshold’ (Trachootham et al., 2009, Wang et al., 2011). Previous evidence also showed that during the malignant transformation process, the basal oxidative stress can be augmented by the genetic deviations that mediate carcinogenesis (such as the activation of oncogenes (Höll et al., 2014, Benhar et al., 2001). Recently, some studies have revealed that, control on the effect of ROS can conclude the capability to metastasise or not (Piskounova et al., 2015), Collectively, malignant cells (a) are accommodated to control the redox balance by adjust a system of antioxidant defence (Harris et al., 2015, Young et al., 2004), and this clarifies the high expression of endogenous antioxidants such as Trx in cancer (Baker et al., 2006), and (b) become gradually more susceptible to ROS-associated invectives that subsequently enhances

ROS generation and/or deteriorate antioxidant defences in cells (Gupta et al., 2012, Wang et al., 2011). Therefore, tumour cells may operate in a ‘ primed’ state (Chonghaile et al., 2011), that can more readily ‘push’ them past such a lethal threshold (Dunnill et al., 2016). Recent studies using tumour xenografts models showed that antioxidant pathways such as Glutathione (GSH) and Trx pathways are central in carcinogenesis, and that non-significant reduction in tumour development has been observed after inhibition of GSH (one of the major antioxidant agents in cells). moreover, synergism between GSH inhibitor and Thioredoxin (Trx) inhibitor, mediated cancer cells death and delayed carcinogenesis (Harris et al., 2015).

1.7 CD40 and its cognate ligand CD154 (CD40L)

1.7.1 Background

CD40 is associate to the TNFR superfamily (TNFRS) and is essential immune co-stimulatory molecule. Interestingly, the CD40 antigen was identified for the first time in 1984 during immunohistochemistry-based studies using an antibody raised against urinary bladder carcinoma (UCC), yet the same antibody reacted with antigen expressed on lymphocytic B cells (Paulie et al., 1985, Eliopoulos and Young, 2004). Following this, in 1989, CD40 was cloned and characterized as a Type I transmembrane protein. Its cognate ligand, CD40L (or CD154), was identified in 1992 on the surface of activated T lymphocytes (Armitage et al., 1992).

Isolated from the Burkitt lymphoma Raji cell line in 1989 (Schönbeck and Libby, 2001), the human CD40 gene is located on chromosome 20 (q12-q13.5) and encodes a single 1.5-kb mRNA species (Anand et al., 2003). By contrast, the murine CD40 gene is located on chromosome 2. The amino acid sequence of human CD40 shows homology with the receptors of nerve growth factor (NGF), TNF-RI and Fas, whilst showing a 62% homology with murine CD40 (Ramesh et al., 1993).

Deferent sizes of CD40 have been reported. Originally, CD40 was described as a 50 kDa superficial receptor on B cells (Clark and Ledbetter, 1986, Ramesh et al., 1993). Other reports showed that the translation of the 1.5-kb CD40 mRNA produces a superficial glycoprotein that comprises 277 amino acid with a molecular weight of 43-

48 kDa (Braesch-Andersen et al., 1989, Schönbeck and Libby, 2001). Yet, some reports referred to it as a 45-50 kDa receptor (Grammer and Lipsky, 2001).

1.7.2 Structure of CD40

1.7.2.1 Extracellular domain

The extracellular region of CD40 has a 20 repetitive amino acid sequence pattern rich in cysteine residues and divided into four domains, each domain consisting of two modules with each module established by one or two disulfide bonds (Singh et al., 1998, van Kooten and Banchereau, 2000). The second and third domains have been identified as containing the CD40L binding sites which are important for CD40 ligation (Figure 1.13).

With regards to the presence of CD40 on the cell surface and its valency, some studies have described CD40 as a dimer, with the initial observation of CD40 as homodimer being in normal human B cells, human Burkitt lymphoma cell lines and UCC cell lines, but the biological function of this homodimer was unclear. Later studies have reported that CD40 is a trimer receptor that expressed on the surface of the cells and CD40L binding does not oligomerize CD40 into trimeric receptor, but CD40 is an already pre-formed trimeric complex via its PLAD domain (pre-ligand binding assembly domain), which is important for biological activities including atherogenesis, thrombosis, inflammation and extracellular membrane (ECM) degradation compared to the monomeric form (Anand et al., 2003, Chan et al., 2000). Aggregation of the monomeric receptor to form CD40 oligomers enhances the formation of disulphide-links and the PLAD domain may be important in signalling via CD40/CD40L interactions, for instance, the engagement of monomeric CD40 provides a weak signal for MAPKs and p38 activation (Reyes-Moreno et al., 2004, Antoniades et al., 2009). Moreover, different CD40 epitopes have been observed to be expressed on different type of cells, and it has been suggested that epithelial cells may express a monomeric CD40 whereas dendritic cells express oligomeric CD40 and only B-cells express both CD40 modules (BERG et al., 1996, Clark and Ledbetter, 1986).

1.7.2.2 Intracellular domain

The intracellular domain of CD40 unlike other member of the TNFR family has no death domain but displays recognition sites for TNF Receptor Associated Factors (TRAFs) (Ellmark, 2002). The cytoplasmic tail of CD40 lacks motifs usually found in other immunologic receptors such as signalling motifs and tyrosine kinase activity-containing or phosphatase-binding motifs. The location of functional residues was investigated using large and point mutations of specific amino acids in both human B cell lines and mouse T cell lines transfected with CD40 mutants. Initial results indicated that Threonine at 234 in the cytoplasmic domain of CD40 in mice mediated growth inhibition, yet T234 stimulates normal B cells instead of growth inhibition. Later studies performed in a variety of B cell lines found that up-regulation of B cell homotypic adhesion, CD80, CD95 and CD23, and JNK activation are mediated by determinant A which consist of 22 amino acids, while the designated determinant B (contains 10 amino acids) is required for CD40-mediated activation of NF-κB, IgM production and isotype Ab switching. The remaining are involved in the determinant B as individual motif called determinant C. (Bishop and Hostager, 2001, Inui et al., 1990) (Figure 1.13).

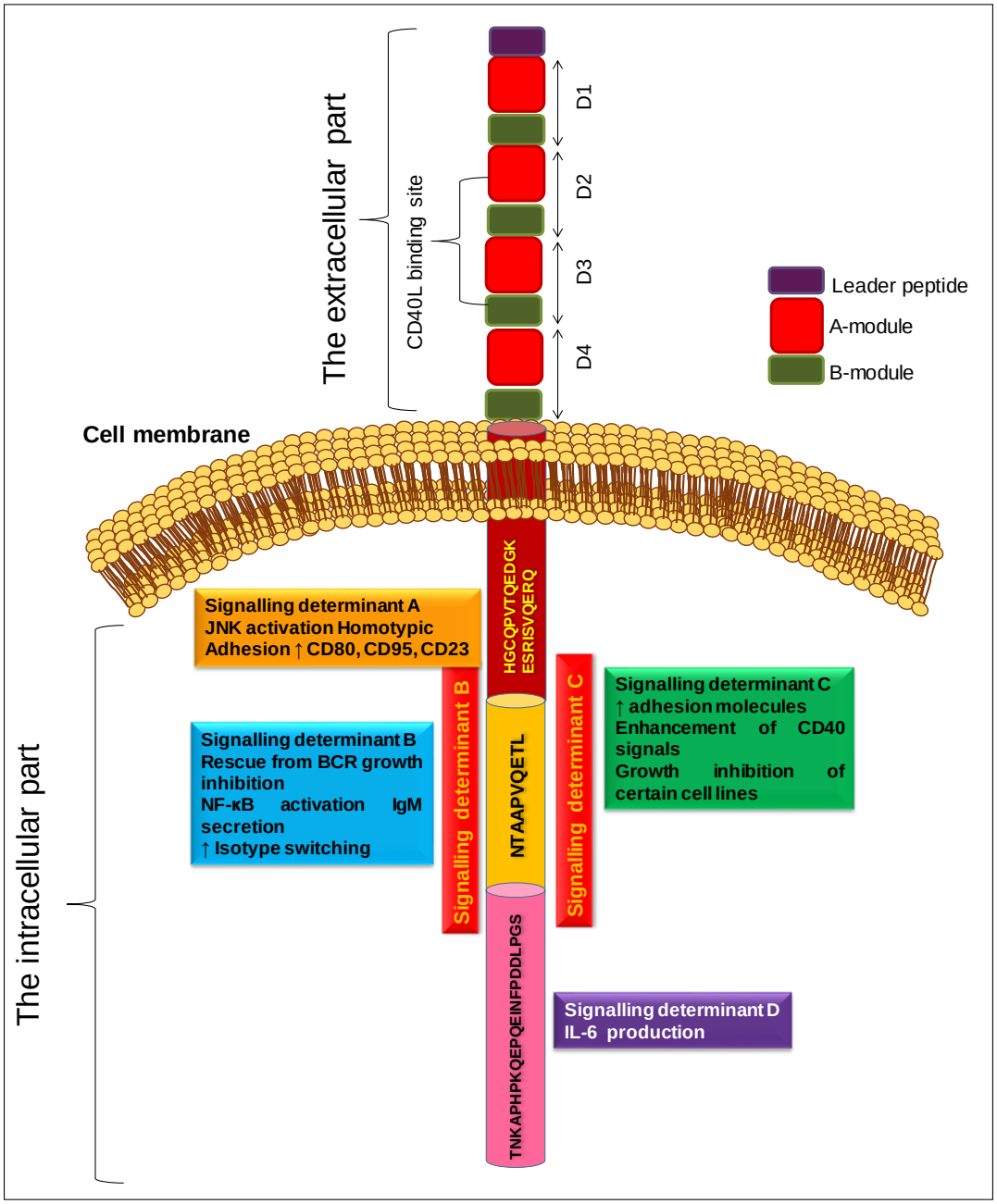

Figure 1.13 Structure of CD40

Schematic representation of the domains of the CD40 receptor. The cytoplasmic part contains Individual structural motifs of the cytoplasmic tail that play roles in B cell function. Determinant A consists of 22 amino acid, while the following 10 amino acids are designated determinant B. The remaining T234 is involved in determinant B is referred to as individual motif called determinant C. The extracellular part of CD40 consists of four domains (denoted “D”), each composed of two modules. The 2nd & 3rd domain are the specific binding sites for CD40 ligand. **Drawn by K. Ibraheem.**

1.7.3 Expression of CD40

Although initially characterised as an antigen present on immune cells, such as B and T cells, expression of CD40 is constitutive in various cell types, such as epithelial cells, keratinocytes, fibroblasts, endothelial cells, smooth muscle cells and DCs (Kaykas et al., 2001, Pham et al., 2002) (Table 1.1). CD40 expression can be stimulated by pro-inflammatory cytokines, such as tumor necrosis factor alpha (TNF-α) and interferon gamma (IFN-γ) (Schönbeck and Libby, 2001), while transforming growth factor-β (TGF-β) inhibits CD40 expression by mediating an increase in the degradation of CD40 mRNA (Nguyen et al., 1998).

CD40	CD40L
T-Cells and B-Cells	T-Cells and B-Cells
Macrophages	Macrophages
Eosinophils	Eosinophils
Basophils	Basophils
Dendritic cells	Dendritic cells
Endothelial cells	NK Cells
Fibroblasts	Platelets
Keratinocytes	Mast cells
Smooth muscle cells	Smooth muscle cells
Epithelial cells	Epithelial cells

Table 1.1 Expression of CD40 and CD40L on different cell types

CD40 is expressed on a variety of cell types, both hematopoietic and non-hematopoietic cells.

1.7.4 CD40 ligand (CD40L) CD154

CD40 ligand (CD40L) or CD154, is a Type II transmembrane protein of 39 kDa related to the TNF ligand family. The CD40L gene is located at the (q26.3-q27.1) region of chromosome X, a fragment with a length of 13 kb (Chakrabarti et al., 2005). It consists mainly of five exons; exon I encrypts the transmembrane and intracellular region of CD40L, whereas exons II -V encode the extracellular region of the molecule (Carbone et al., 1997, Blossom et al., 1997, Schönbeck et al., 2002, Schönbeck and Libby, 2001).

CD40L has a double-decker extracellular construction which consists of β-sheet, α-helix and β-sheet. These properties facilitate the homo-trimerization of CD40L on the cell surface (Xia et al., 2010). Besides the membrane form, there is also a form of soluble CD40L (sCD40L) circulating in the blood. This form is almost exclusively an enzymatic cleavage at the membrane following platelet activation and remains a functional trimer of 18 kDa (Li et al., 2008). Membrane-bound CD40L is mainly expressed on stimulated T cells, B cells and platelets, it is also expressed on monocyte cells, dendritic cells (DCs), natural killer cells and basophils.

1.7.5 Role of CD40 in the immune system

1.7.5.1 B cells

B cells constitutively express CD40 which interacts with CD40L on T cells activated in the existence of antigens during infection. This interaction induces proliferation and differentiation of B lymphocytes into plasma cells and antibody production in the presence of cytokines (IL-4, IL-2 and IL-10) secreted by T cells, (Aruffo et al., 1993). CD40/CD40L interaction seems sufficient by itself to induce the production of IgG and IgA antibodies, while a co-stimulation in the presence of IL-4 is necessary particularly for the production of antibody IgE (Armitage et al., 1993, Bishop and Gail, 2009).

In the absence of CD40/CD40L interaction, B cells produce only IgM, as observed in patients suffering from syndrome HIGM (X-linked, hyper-IgM syndrome) (Hill and Chapel, 1993). Furthermore, in activated B cells, the CD40/CD40L interaction induces release of cytokines IL-6, IL-10 and TNF-α (Boussiotis et al., 1994), an increase in the

intercellular adhesion molecule-1 (ICAM-1), Lymphocyte function-associated antigen - 1 (LFA-1), vascular cell adhesion molecule-1 (VCAM-1) (Rousset et al., 1991) and increased major histocompatibility protein class I and II (MHC-I and MHC-II), (Khanna et al., 1997), all of which facilitate the proliferation and differentiation of these cells into plasma cells. Interestingly, B lymphocyte expression of CD40L also appears to be involved in a positive feedback loop, since CD40L expressed on one B cells can in turn interact with CD40 of another B cell, thereby facilitating activation and differentiation of B lymphocytes (Clodi et al., 1998). Collectively, these CD40 activation-associated mechanisms play critical roles in the differentiation of B cells into memory B cells (Figure 1.14) (Xu et al., 1994, Castigli et al., Hu et al., 1997, Eliopoulos and Young, 2004, van Kooten and Banchereau, 2000, Morimoto et al., 2000).

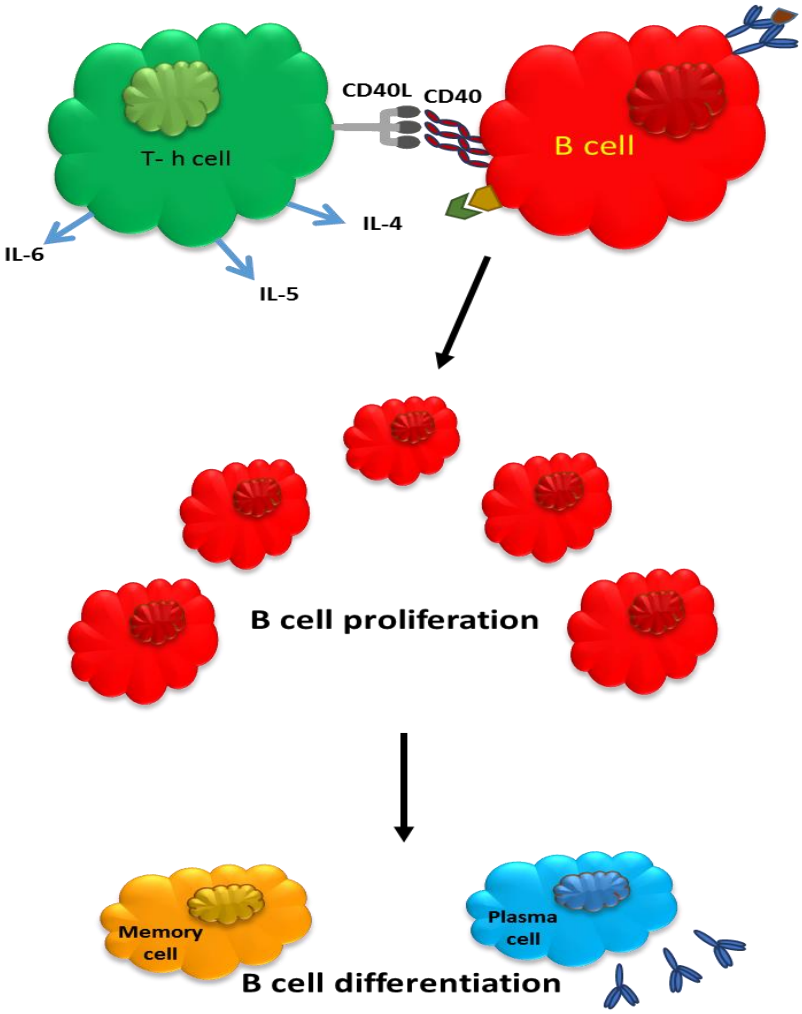

Figure 1.14 CD40 functions in B cell homeostasis

Activation of CD40 on normal B cells by CD40 ligand (CD40L) expressed on T-helper cells as part of an immune response provides B cell survival and proliferative signals as well as cytokine production. CD40 ligation on normal B cells can also mediate B cell differentiation into plasma cell which produce immunoglobulin and memory cells for Ab production following secondary infection. **Drawn by K. Ibraheem**

1.7.5.3 Monocytes and Macrophages

The role of the CD40/CD40L dyad in monocytes is well documented. Monocytes constitutively express CD40 and, as APCs, they are able to interact with the CD40L of T cells (Schönbeck and Libby, 2001). This interaction is bidirectional, so that the monocyte promotes activation of T cells which, in turn, induce monocyte activation (Suttles and Stout, 2009, Buhtoiarov et al., 2005, Lum et al., 2006) and monocyte differentiation into macrophages. Binding of CD40L on T lymphocytes to CD40 of monocytes and macrophages leads to release of several cytokines (IL-12, IL-1β, IL-6, IL-8 and TNF-α (Wagner et al., 2002), matrix metalloproteinases (MMPs) (MMP-1 MMP-2, MMP-3 and MMP-9), an increase of co-stimulatory molecules (ICAM-1, LFA-3, B7-1 and B7-2) and secretion of nitric oxide (NO) (Mach et al., 1997). These biological effects are essential to the immunity-related, inflammatory and angiogenic function of these cells.

Most biological effects of CD40L on monocytes are due to its interaction with CD40, although other receptors on the surface of these cells are able to induce various cellular responses, especially Mac-1. It was recently demonstrated that CD40L/Mac-1 interaction promotes adhesion and migration of monocytes to the endothelium, and release of myelo-peroxidases during the inflammatory response (Zirlik et al., 2007).

1.7.5.4 Dendritic cells (DCs)

DCs occupy a central place in the immune system and binding of CD40 by CD40L on DC promotes T lymphocytes activation. DC activation, such as that observed in the presence of pathogens, causes a significant increase in CD40 on the surface of DC cell. This receptor is able to interact with the CD40L on activated T cells, increasing the expression of co-stimulatory molecules CD80/CD86 and B7-1/B7-2, and it promotes the release of the IL-12 by DCs (Banchereau et al., 2000).Binding of T cell-CD40L to DC-CD40 promotes DCs to become active antigen presenting cells (APC) via the up-regulation of MHC class II and CD80/CD86 (Ma and Clark, 2009) and CD40-CD40L co-simulation is essential for the activation of DC in response to pathogen associated molecular patterns (PAMPs) (Kawai and Akira, 2007, Ip and Lau, 2004). CD40L can also be expressed on DCs but at a lower level compared to CD40. Although

the exact function of CD40L on DC remains to be fully verified, it appears to be involved in bidirectional interaction between dendritic cells and B lymphocytes (Bergtold et al., 2005).

Interestingly, previous work by our research group, has demonstrated that CD40L expressed on DCs may serve additional roles. Stimulation of DCs by strongly pro-inflammatory bacterial products induced membrane CD40L (mCD40L) expression and, in vitro, mCD40L on activated DCs mediated direct, T cell-independent cytotoxic effects towards carcinoma cells (such as UCC and CRC). Therefore, cell surface CD40L expressed by DCs may be important in the ability of DCs to have direct cytotoxic effects on tumour cells by inducing CD40-mediated carcinoma cell apoptosis (Hill et al., 2008).

1.7.5.5 Epithelial cells

In addition to its identification as a UCC associated antigen, CD40 expression on epithelial cells was originally demonstrated on human nasopharynx, tonsil and ectocervical tissue by immunohistochemical analysis (Young et al., 1998), while CD40 ligand (CD154) expression has been observed on epithelial cells of the glomerulus as well as the proximal tubule. CD40 expression has been also observed on normal kidney, and parietal epithelial cells (Yellin et al., 1995). Other reports have demonstrated that intestinal epithelial cells, which encounter enteric antigens, express CD40 together with other co-stimulatory molecules (Yellin et al., 1995).

1.7.6 CD40 cell signalling

As mentioned above, CD40 lacks intrinsic kinase activity and related intracellular signalling motifs, however adapter molecules TNF receptor associated factors (TRAFs) are the mediators of signal transduction by CD40-CD154 interactions (Schönbeck and Libby, 2001). The TRAF family consists of six members, five of which (TRAF 1, 2, 3, 5, 6) have been identified to bind CD40 in both a context- and cell type-dependent fashion (Zapata et al., 2001). Activation of pro-inflammatory signalling pathways in endothelial cells has been shown to be induced by the association of TRAF2 and CD40 (Mukundan et al., 2005). TRAF4 is a more enigmatic TRAF member that seems to have interesting roles in inflammation; however no interactions with

CD40 have been reported (Rousseau et al., 2011). Finally, an additional TRAF molecule TRAF7 has been identified, although TRAF7 does not comprise a TRAF domain (Napolitano and Karin, 2010).

The specificity of CD40 signal transduction pathways is influenced not simply by the interaction with the different TRAFs. Rather, the topology and localisation of the receptor plays an important role. CD40 is located in special membrane micro-domains called “lipid rafts“. After initial CD40/CD154 interaction, the majority of CD40 translocates to lipid rafts , where the receptor then associates with various TRAFs (Arron et al., 2002). This relocation is critical, for instance lipid raft-dependent association of TRAF2 with CD40 leads to the formation of pro-inflammatory cytokines (such as MCP-1) (Chen et al., 2006, Arron et al., 2002).

CD40 signalling has mainly been characterised in the context of B cell function and comparatively less is known about the precise signalling pathways triggered following activation by CD40L in epithelial cells (Eliopoulos and Young, 2004, Albarbar et al., 2015). One common feature, nevertheless, is that cellular responses to CD40 signalling, whether in B cells or epithelial cells, are exquisitely context-specific. The engagement of CD40 with CD40L causes the recruitment of adapter TRAFs to the intracellular end of the CD40 molecule (Bishop et al., 2007). Cellular relocation of TRAFs and their interaction with CD40 triggers the activation of several signalling pathways, which include NF-κB, the MAPK pathways p38 and JNK/AP-1, and the PI3-K/Akt pathway (Davies et al., 2005, Elgueta et al., 2009). Any intracellular signalling induced by CD40 depends almost exclusively on TRAFs, but can be independent of TRAFs, such as the pathway of STAT5 resulting from the direct association of Janus kinase 3 (JAK3) with CD40 (Säemann et al., 2003, Säemann et al., 2002) (Figure 1.15).

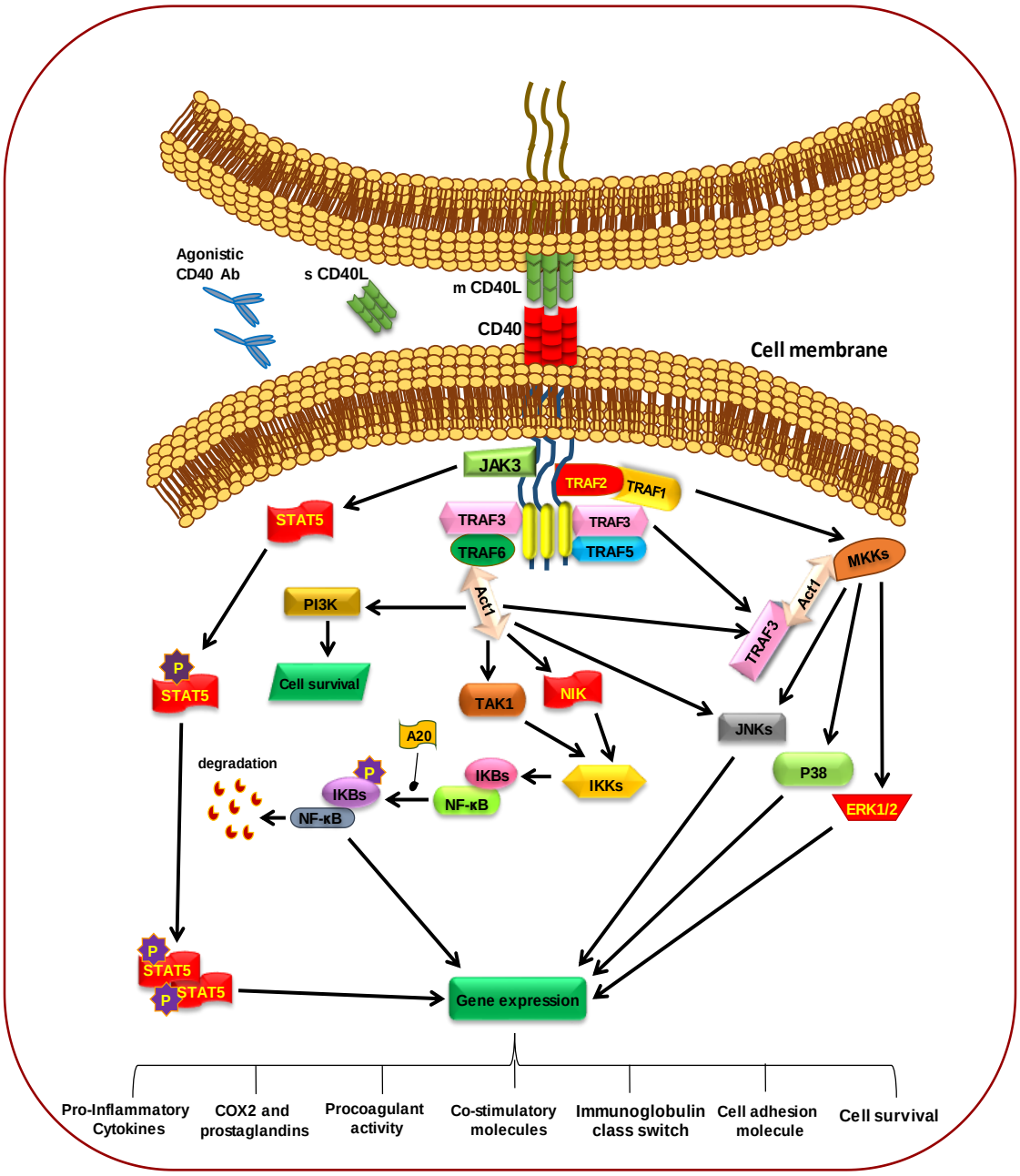

Figure 1.15 CD40 signalling pathways

Signalling pathways of CD40 can be stimulated by membrane CD40L (CD154) or soluble agonists (sCD40L) and agonistic antibodies and result in different patterns of gene expression depending on the cell type. CD40 ligation induce the recruitment of TRAF proteins to the cytoplasmic tail of CD40 which subsequently activate either MKKs pathway via TRAF3 or activation of Act1 and NF-κB degradation. CD40 stimulation can also recruit JAC3 which cause phosphorylation of STAT5. **Drawn by K. Ibraheem.**

1.7.6.1 TRAF proteins in CD40 signalling

TRAFs are characterized by a C-terminal domain called TRAF-C domain which is involved in the binding of TRAFs to CD40, two areas of zinc motifs (zinc ring and zinc fingers) are involved in the recruitment of additional proteins, such as kinases for activation of downstream transcriptional factors. The other main domain in the C-terminus is referred to as N-terminal domain (TRAF-N domain) which is responsible for homo- and hetero-dimerisation interactions of TRAFs (for instance TRAF2/TRAF interaction) (Arch et al., 1998) (Figure 1.16).

Following CD40 engagement by its ligand CD40L, TRAFs are engaged to specific motifs in the intracellular domain of CD40 (see Figure 1.13). The protein sequence involved in the interaction of TRAFs with CD40 differs from one member to another; thus, there is no consensus on the sequence responsible for this interaction, although some sequences have been found to overlap between some members, such as TRAF2 and TRAF3 (McWhirter et al., 1999, Ni et al., 2000). The consensus binding sites identified for TRAF1, TRAF2, and TRAF3 are located at the membrane distal area of the cytoplasmic end of CD40 (Figure 1.13) with the aa sequence PxQxT representing the binding site.

Finally, the zinc finger domain is important for CD40 signalling. The importance of this domain has been reported by studies showing that CD40 signalling induction via TRAFs proteins was inhibited upon ‘knockout’ of the zinc finger domain (Gail A Bishop and Kraus, 2007).

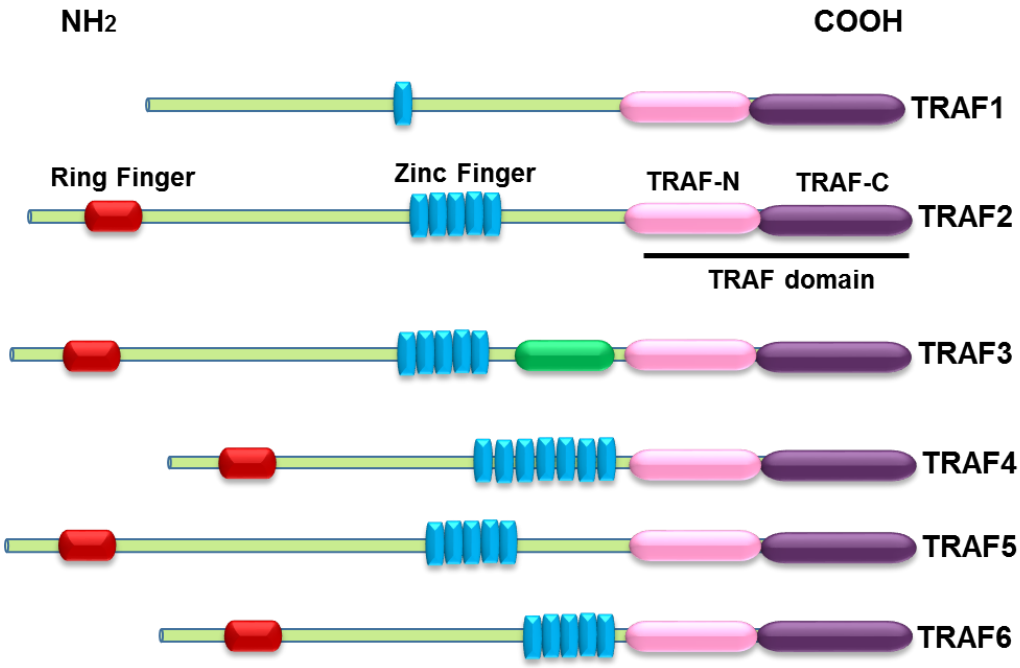

Figure 1. 16 Structures of the TRAF proteins

The diagram displays the structure of the main TRAF proteins identified and characterised to date, all characterized by having a TRAF domain at their C-terminus which represents the binding site of TRAFs to the receptor and can interact with other TRAFs via TRAF-N domain; also all TRAFs contain Zinc area (Zinc finger and Zinc ring) with the exception of TRAF1. **Drawn by K. Ibraheem.**

1.7.6.1.1 TRAF1

TRAF1 expression is significantly increased following CD40 activation (Zapata et al., 2001), including following CD40 ligation in carcinoma cells (Georgopoulos et al., 2006). Since TRAF1 lacks an N-terminal RING finger domain, it seems to be involved in regulating the signalling of other members of TRAFs, particularly TRAF2 (Arch et al., 1998, Bishop et al., 2007). The binding site of TRAF1 on CD40 overlaps with that of TRAF2 and TRAF3, and it appears that TRAF1 is only able to interact weakly with CD40, in the absence of the involvement of TRAF2 (Pullen et al., 1999). TRAF1 deficiency causes a decrease in TRAF2 recruitment to CD40 and an increase in the enzymatic degradation of the receptor in B lymphocytes and APCs (Arron et al., 2002, Xie et al., 2006). Moreover, the NF-κB pathway seems to be dependent on the recruitment of TRAF1 and TRAF2, since the dual genetic deletion of both members strongly attenuated NF-κB activation, in comparison to individual gene deletion of one of these members (Xie et al., 2006).

1.7.6.1.2 TRAF2

The main role of TRAF2 is the activation of p38 MAPK, Akt, JNK and ERK1/2. In embryonic fibroblasts and B cells from TRAF2-deficient mice, following the engagement of CD40L to CD40 the activation of these signalling pathways was significantly inhibited (Hostager et al., 2000, Brown et al., 2002). Moreover, after CD40 ligation, the recruitment of TRAF2 triggers recruitment of protein kinase mitogen-activated kinase-1 (MEKK1) to the intracellular end of CD40, which is an essential step in the activation of ERK1/2 proteins and activation of kinases JNK and p38 (Gallagher et al., 2007). In B lymphocytes, TRAF2 also appears to participate in the activation of NF-κB, in collaboration with TRAF6. Notably, however, the interaction of one or the other with CD40 seems sufficient to induce activation of NF-κB, which was confirmed by results showing that TRAF2 or TRAF6 deficiency does not cause abnormality in the activation of NF-κB, but the double deletion of these two members caused severe inhibition of this pathway (Hsing et al., 1997, Rothe et al., 1995, Yeh et al., 1997).

Despite its important role in the activation of signalling pathways induced by CD40, in B cell signalling, TRAF2 also appears to have a negative regulatory function (Gardam

et al., 2008) via its interaction with TRAF3. The interaction of TRAF2/TRAF3 allows proteins cIAP1 and cIAP2 to degrade NIK protein, which inhibits activation of NF-κB and promotes apoptosis (Vallabhapurapu et al., 2008). Moreover, the removal of an accumulation of TRAF2 generates NIK in B cells (Vince et al., 2007). Following stimulation with CD40L, this protein complex is destabilized and TRAF2/TRAF3 is recruited to the CD40, which allows TRAF2 to activate NF-κB. Self-degradation of TRAF2 and TRAF3 (via cIAP1 / 2), has a role in releasing NF-κB and allow NIK to activate NF-κB. In short, cIAP1/2 play a dual role, that of degradation of NIK in the basal conditions and degradation of TRAF3 upon binding of CD40L. Meanwhile, TRAF2 also performs a dual function, i.e. that of its inhibitory role of NF-κB activation via its interaction with TRAF3, and its activator role of NF-κB following its interaction with CD40 and its subsequent degradation (Bishop et al., 2007, Brown et al., 2002, Zarnegar et al., 2008).

1.7.6.1.3 TRAF3

TRAF3 was initially identified as an adaptor molecule that interacts with intracellular end of CD40 and the Latent membrane protein 1 (LMP1) of EBV (Cheng et al., 1995, Mosialos et al., 1995). Additionally, TRAF3 associates with other TNF-Receptor superfamily proteins such as CD27, CD30, Lymphotoxin-β receptor, OX40, 4-IBB, RNK, HVEM, GITR, EDAR, XEDAR, BCMA, TACL and BAFF-R (Wajant et al., 2001, Xu and Shu, 2002, Inoue et al., 2000).

It has been shown that TRAF3 has the ability to block the activation of NF-κB induced by CD40 and TRAF2 overexpression (Rothe et al., 1995). TRAF3 negatively regulates CD40-stimulated antibody secretion, but it is not clear if this response mediated by NF-κB inhibition (Hostager and Bishop, 1999). This implication is supported by experiments showing that removal of this protein in B cells increases the activation of NF-κB and JNK following stimulation by CD40L (Xie et al., 2004, He et al., 2004). Furthermore, a study on mice deficient in TRAF3 showed an intracellular accumulation of the NIK protein (Xie et al., 2004, Vallabhapurapu et al., 2008, Zarnegar et al., 2008). However, activation of the NF-κB pathway in epithelial cells has been shown to be promoted by overexpression of TRAF3, contrary to B cells (Propst et al., 2002), while

Urbich et al. suggest that TRAF3 has dual functions depending on the cell type (Urbich et al., 2001).

1.7.6.1.4 TRAF4

The first identification of TRAF4 protein was in the nuclei of breast cancer cells, and it has also been detected in the cytoplasm of cells (Régnier et al., 1995, Glauner et al., 2002). Little expression of TRAF4 has been observed by vascular cells. It is more important in neuronal cell physiology and during embryogenesis (Régnier et al., 1995, Masson et al., 1998). As mentioned above, TRAF4 seems unable to interact with CD40 (Krajewski et al., 1993). Paradoxically, TRAF4 has been implicated in promoting apoptotic pathways mediated by p53, yet has been observed to inhibit Fas-mediated cell death (Fleckenstein et al., 2003, Sax and El-Deiry, 2003). Expression of TRAF4 in T cells is dependent on stimulators of the NF-kB pathway (Glauner et al., 2002).

1.7.6.1.5 TRAF5

The role of TRAF5 in CD40 signalling still unclear. It has been reported that TRAF5 unable to directly bind the cytoplasmic tail of CD40, but it seems to form a heterodimer with TRAF3 and facilitates NF-KB activation (Gail A Bishop and Kraus, 2007). Moreover, RNAi-mediated TRAF5 knockdown in B-cells significantly reduces the activation of NF-κB, resulting in the reduction of co-stimulatory molecule expression and antibody production by these cells (Bishop, 2004, Hauer et al., 2005, Nakano et al., 1999).

1.7.6.1.6 TRAF6

TRAF6 has been shown to play an central role in CD40 signalling pathway via its specific binding site on the cytoplasmic tail of CD40 (Bishop et al., 2007). TRAF6 can induce apoptosis via interaction with caspases and its activation by a RING domain-dependent mechanism (He et al., 2006). However, inhibition of caspase activation via TRAF6 and the PI3K/Akt pathway permits CD40 to protect B cells from Fas-mediated (Benson et al., 2006).

Blocking of TRAF6 in human epithelial cells by RNAi meaningfully abridged the activation of NF-κB pathways, p38, JNK and Akt following CD40 stimulation with

CD40L, showing the importance of this TRAF member (Davies et al., 2005). TRAF6 interacts directly with TRAF2 to regulate the activation of NF-κB. This close collaboration between TRAF2 and TRAF6 does not seem to necessarily depend on the direct interaction with CD40 since, even in the presence of the deletion of the binding domain of TRAF6 to CD40, TRAF6 is still able to interact indirectly with CD40 through its direct interaction with TRAF2 and activate several important signalling pathways (Rowland et al., 2007). Under these conditions (where the binding domain is removed from CD40), activation of CD40 leads to expression of CD80 receptor and initiation of the JNK pathway (Rowland et al., 2007). One of the other important functions of TRAF6 lies in PI3K pathway activation and subsequent activation of Akt, which protects against apoptosis particularly in epithelial cells (Arron et al., 2002, Davies et al., 2004).

1.8 The mitogen activated protein kinases (MAPKs)

Mitogen-activated protein kinases (MAPKs) are a preserved group of protein kinases involved in an assortment of fundamental cellular progressions extending from motility, multiplying and existence to stress responses and apoptosis. MAPKs are serine/threonine kinase activated by phosphorylation at specific Ser and Thr residues. These kinases are part of phosphorylation cascades that have been well-characterised in many species including mammals (Jin et al., 2013, L'Allemain, 1994). MAPK cascades are involved in signalling pathways leading to mitosis, proliferation, differentiation, cell growth, and cell death in response to intracellular and extracellular signals (Johnson and Lapadat, 2002, Zhang and Liu, 2002).

1.8.1 General structure

Overall the MAPK family comprises five groups of kinases. Three main groups have been widely studied: the extracellular signal controlled kinases 1 and 2 (ERK1/2), the c-Jun N-terminal kinases (JNK) 1, 2 and 3 (also mentioned to as stress-activated protein kinase, SAPK)) and the p38MAPK α, β, γ and δ. The other two groups include Extracellular signal regulated kinases 3 and 4 and Extracellular signal regulated kinase 5 are less well known and their roles in cell signalling remains unclear (Coulombe and Meloche, 2007). Downstream, the phosphorylated MAPK activate transcription factors

such as c-myc, c-Jun, AP-1 and ATF2 but can also activate other kinases upstream and downstream of the MAPK cascade, thus refining the regulation of signalling pathways (Whitmarsh, 2007).

1.8.2 ERK 1/2

Extracellular signal regulated kinases (ERK) 1 and 2 were the first MAPKs identified as 42 and 44 kDa in size, respectively, and are the most studied. They are activated by several factors such as growth factors, hormones, osmotic shock, cytokines, GPCR (G-protein coupled receptors). They perform a main function particularly in cell propagation and differentiation (Kang and Sucov, 2005, Kim et al., 2007).

The ERK pathway is composed of a multi-module complex where the protein kinases Raf, MEK and ERK1/2 are activated in a cascade by sequential phosphorylation. ERK/12 transmit the signal generated by the receptor by phosphorylating a variety of substrates in different subcellular compartments, which leads to the execution of various biological functions such as cell propagation, cell differentiation and cell movement (Katz et al., 2007). Although ERK1/2 mainly promote cell survival, under certain conditions, they can also demonstrate pro-apoptotic functions (Lu and Xu, 2006).

1.8.3 JNK 1/2 (SAPK)

The c-Jun N-terminal kinase (JNK) or stress-activated MAP kinase (SAPK) has three isoforms. These can be stimulated by several factors such as physical anxiety (heat, UV, osmotic shock), chemical factors (pH, ROS), metabolic factors, biological factors (bacterial proteins, cytokines). The typical pattern of MAPK activation is that MAP3K (MEK1-4) activate MAP2K (MKK4 and MKK7) to then activate MAPK. JNK activation causes phosphorylation of transcription factors including c-Jun, ATF2, EIk-1, MEF-2 leading to the induction of expression of several genes. The JNKs are closely involved in activation of apoptosis for instance following induction of ROS (as described in previous sections 1.6.2). In addition to their action as pro-apoptotic proteins, they also play anti-apoptotic functions according to the type of the cells and the quality of the stimulation. As described in previous sections (1.6.2), transient JNK activation is related to the cell existence, whereas continued JNK activation induces apoptosis

signalling (Circu and Aw, 2010). JNK pathways predominate in cellular responses initiated by adrenergic G-protein coupled receptors and tyrosine kinase receptors and growth factors. They are also involved in several functions in cells physiology including development of nervous system, regulation of insulin and obesity, hypertrophy and heart failure (Brancho et al., 2003, Derijard et al., 1995).

1.8.4 The p38/MAPK

MAPK signaling pathways have been reported to activate four isoforms of p38 Ser/Thr kinases p38α/Mpk2/CSBP, p38β, p38γ/SAPK3 and p38δ/SAPK4. Stimulation of p38 shows similarities to JNK activation. Firstly, those two MAPKs were grouped under the term SAPK. The cascade of p38 phosphorylation can be activated by many stimuli such as osmotic shock, or UV irradiation, oxidative stress and anticancer agents. Different stimuli can activate MAP3K (ASK, TAK, PTKs), which activate MAP2K (MKK3, MKK6) but also other cascades (such as MEK4, MEKK1, 2 and 5, ASK), allowing them to phosphorylate p38. The p38 pathway displays an central function in the induction of genes involved in the inflammatory response (Kontoyiannis et al., 2001) . The p38 pathway is also involved in apoptosis induced by signals including Fas (Juo et al., 1997), by loss of cell anchorage (Cardone et al., 1997) and also plays a synergistic role with the JNK pathway in the induction of apoptosis (Xia et al., 1995).

1.9 The effect of CD40 ligation in cancer cells

It has been demonstrated that soluble CD40 ligand (sCD40L) can be cytotoxic to CD40-transfected cervical and lung carcinoma cells only if protein synthesis is blocked, mostly by using cycloheximide (CHX), and in combination with IFN-γ. However, membrane-presented CD40 ligand (mCD40L) is highly cytotoxic independently of pharmacological intervention (Bugajska et al., 2002, Hess and Engelmann, 1996b). Furthermore, ovarian cell lines show both apoptotic and non-apoptotic responses demonstrating the context specificity of CD40 killing (Eliopoulos et al., 2000). Soluble CD40 agonists without pharmacological intervention also trigger growth inhibition in UCC, ovarian, cervical, squamous epithelial cells, transformed keratinocytes, ectocervical epithelial cells and rat fibroblastic cell lines. Moreover, the toxicity of cisplatin, TNF-α, Fas and ceramide in UCC cells can be enhanced by sCD40L

(Eliopoulos et al., 1996), and of 5-Flurouracil and Mitomycin C in cervical and ovarian cell models (Vardouli et al., 2009). sCD40L has also shown to have direct anti-tumour effects in ovarian cell lines, ovarian cells obtained from ascites fluid and ovarian adenocarcinomas transplanted into severe combined immunodeficient mice (Ghamande et al., 2001), and still remains a promising tool for this type of cancer (Scarlett et al., 2009). It has been suggested that CD40 binding may cause the paracrine expression of TNF Fas and TRAIL, which mediate apoptosis via the extrinsic cell death pathway (Eliopoulos et al., 2000). By contrast, more recent reports have challenged this, implying CD40-mediated apoptosis is regulated by direct signalling pathways involving the activation of the intrinsic pathway of apoptosis (Georgopoulos et al., 2006, Elmetwali et al., 2010b).

CD40 engagement growth inhibits lymphoma cells and multiple myeloma (MM) cells (Baker et al., 1998), however it can induce both proliferation and apoptosis among MM cells (Qi et al., 2004). MM cells during transformation can demonstrate the ability to down-regulate CD40 expression possibly allowing evasion of CD40L-induced T-cell mediated apoptosis (von Leoprechting et al., 1999). Furthermore, in vitro, an equal amount of CD40 engagement causes B-cell proliferation, whilst it growth-inhibits carcinoma cells (Eliopoulos et al., 1996). Angiogenesis and proliferative state of some cancers can also induced by CD40 ligation (Qi et al., 2004), confirming that CD40 responses are highly context-specific; a finding that is particularly exemplified by the most unique feature of CD40, which appears to be its ability to kill malignant cells whilst sparing normal human epithelial cells (NHU) (Bugajska et al., 2002) (also see subsequent sections).

1.10 Mechanisms of CD40-mediated apoptosis in carcinoma cells

In vitro studies using cervical and ovarian carcinoma lines implied that the isoleucine zipper sCD40L (in the presence of protein synthesis inhibitors) causes paracrine expression of Fas, TRAIL and TNF to induce apoptosis. These classical “death receptors‟ were shown to induce cell apoptosis via the extrinsic pathway, and inhibition of caspase-8 attenuated CD40-mediated cytotoxicity (Eliopoulos et al., 2000). Yet, CD40 ligation by mCD40L in UCC cells stabilizes and recruits TRAF3, triggers JNK and AP-1 activation and subsequent cell death. However, there is discrepancy over

whether this is mediated via extrinsic or intrinsic pathways of apoptosis, or their cross-talk(Georgopoulos et al., 2006, Elmetwali et al., 2010b). At least in part, there has been a consistent implication for Bak and Bax expression and caspase-9 dependency; therefore, it is likely that intrinsic pathways play a key role in the overall event, due to their ability to create MOMP (Bugajska et al., 2002, Georgopoulos et al., 2006). Furthermore, there is a report that TRAF6 attenuation is essential for mCD40L to mediate its full apoptotic potential (Elmetwali et al., 2010b). Perhaps some discrepancy over the signalling mechanism underlying CD40-mediated cell death is attributed to the mechanism of mCD40L delivery. Some studies utilise a co-culture method, which involves the culturing of carcinoma cell with mCD40L expressing third party cells(Bugajska et al., 2002), whereas others utilised paracrine expression of mCD40L by transfection with a replication defective recombinant adenovirus(Elmetwali et al., 2010b). Either way, the signalling events leading to JNK activation via TRAF3 are a pre-requisite for the further understanding of the CD40-mediated pathway of cell death.

1.11 The importance of signal quality in CD40-mediated apoptosis

The susceptibility of carcinoma cells to CD40-mediated death was first demonstrated by Hess and Engelmann (1996) and since there has been a number of investigations into the capability of CD40 to prompt malignant cell death, particularly by Young and colleagues. The response of carcinoma cell lines is highly affected by the type of CD40 agonist and mode of delivery, i.e. the “quality” of the CD40 signal, reflected by the degree of receptor cross-linking which has a dramatic influence on the functional outcome of CD40 ligation. The significance of receptor cross-linking was also observed in other members of the TNFRSF, such as Fas, which requires a minimum of a hexameric ligand (Schneider et al., 1998). Similar observations have been reported for TRAIL receptor activation (Steele et al., 2006). Yet, although in the case of other TNFRs more cross-linking corresponds to more apoptosis, in the case of CD40 the strength of the signal is often the difference between detectable apoptosis or not: extensive cross-linking corresponds to high level of apoptosis, whilst treatment with weakly cross-linked agonistic anti-CD40 antibodies causes little (in many cases, if any apoptosis) and mainly growth-inhibition without pharmacological intervention (Tong et al., 2001, Hirano et al., 1999). In addition to agonistic anti-CD40 antibodies, the main

soluble recombinant CD40L preparations previously used are the leucine zipper-based cross-linked CD40L (Morris et al., 1999) (by Immunex) and less cross-linked preparations, such as the FLAG-tagged CD40L(available by various commercial suppliers). Although sCD40L biologically mimics the action of mCD40L in some cell models, particularly in the case of B cells, it appears that more extensive cross-linking is required for biological activity in the induction of carcinoma cell apoptosis (Bugajska et al., 2002, Elmetwali et al., 2010b, Georgopoulos et al., 2006, Dunnill et al., 2016).

1.12 Malignant transformation and susceptibility to CD40 ligation

The lack of consistency with regards to the use of cell models and ligand delivery strategies has made the full understanding of CD40-mediated apoptosis difficult. Using the robust and well-characterised urothelial cell model, Georgopoulos and colleagues however have delivered understandings into biological aspects that underlie the effects of CD40-killing. The model utilises normal urothelial cells (NHU) and well-characterised, established malignant urothelial cell carcinoma (UCC) lines, as well as normal cell derivatives with defined genetic alterations, referred to as “para-malignant" cells (Crallan et al., 2006). The use of this system has permitted studies that have attempted to address 1) the significance of the amount of receptor cross-linking on efficient consequence, 2) the important intracellular signalling events that regulate CD40-mediated apoptosis and 3) the influence of malignant transformation on CD40-mediated effects on epithelial cells (Dunnill et al., 2016). (Figure 1.17). Fundamental was the observation that without pharmacological intervention soluble CD40 agonists are growth inhibitory and non-toxic to carcinoma cells, whereas mCD40L is highly apoptotic and in a tumour cell-specific fashion (Bugajska et al., 2002, Eliopoulos et al., 1996). However, it appears that the precise mechanism of apoptosis might show some differences between different carcinoma cells types (Mohamed et al, manuscript in preparation) (Figure 1.17). Thus it was of interest to apply this system on other types of carcinoma cells including RCCs.

Further exploration has shown that the differential susceptibility between normal and malignant urothelial cells may be attributed to events relating to changes observed during malignant transformation (Shaw et al., 2005). In this context, the human papillomamovirus-16 (HPV-16) E6 oncoprotein immortalises NHU cells *in vitro* and

renders them susceptible to CD40 and to the same extent observed with UCC cell lines. It has been suggested that this may be most likely attributed to the ability of E6 to abrogate p53 function (Bugajska et al., 2002) and cause the activation of human telomerase, which consequently disrupts p16 expression and allows constitutive stimulation of the Retinoblastoma (Rb) pathway (Kiyono et al., 1998, Dickson et al., 2000).

Using paramalignant NHU cell derivatives with inactivated p53 and p16 function the effects of mCD40L-CD40 ligation were studied. Interestingly, p53 loss-of-function cells did not show CD40 susceptibility, however loss of p16 function rendered urothelial cells partially susceptible to CD40 in comparison to HPV 16 E6 over-expressers and fully-malignant UCC cells. These findings suggested that loss of p16 and thus possibly over-activation of the Rb pathway is a contributory factor in the sensitivity of cells to CD40 killing (Shaw et al., 2005). The reasons underlying the partial susceptibility remained until recently unknown and it has been important to understand what the other determinants of susceptibility are. For instance, as HPV E6 affects telomerase activity (Reznikoff et al., 1996), it is of interest to recognise the function of telomerase over-activation in CD40 susceptibility. More recent studies have shed light into these possibilities as it has been shown that over-expression of the catalytic subunit of telomerase (hTERT) not only immortalises NHU cells but also renders them highly susceptible to CD40 ligation via mCD40L (Dunnill et al., 2016).

1.13 Targeting CD40 for immunotherapy

The great capacity of CD40 to activate the immune response permits the possibility of using agonistic CD40-targeting humanised mAbs for the treatment of cancer. Such mAb preparations can enhance the immune response against tumours via activating APC and DC and supporting an effective cytotoxic T-cell response (Khong et al., 2012). In phase I and II clinical trials for cancer treatment, the anti-CD40 CP-870,893 humanised mAb showed improvement in the response of T-cells against tumour antigen (Fonsatti et al., 2010). The most promising results reported are when CD40 is delivered with chemotherapy which poses an interesting concept as this type of treatment normally depletes immunocytes The results were achieved without blocking for the cytotoxicity of agonistic Ab (Khong et al., 2012). Several clinical trials have been

performed for testing The synergism between chemotherapy (as a promoter for tumour antigen release) and CD40 agonists (as APC activator), and the results were promising, but many challenges remain to be resolved including a proper combinations, mode of administration and optimal dose reviewed in (Vonderheide and Glennie, 2013).

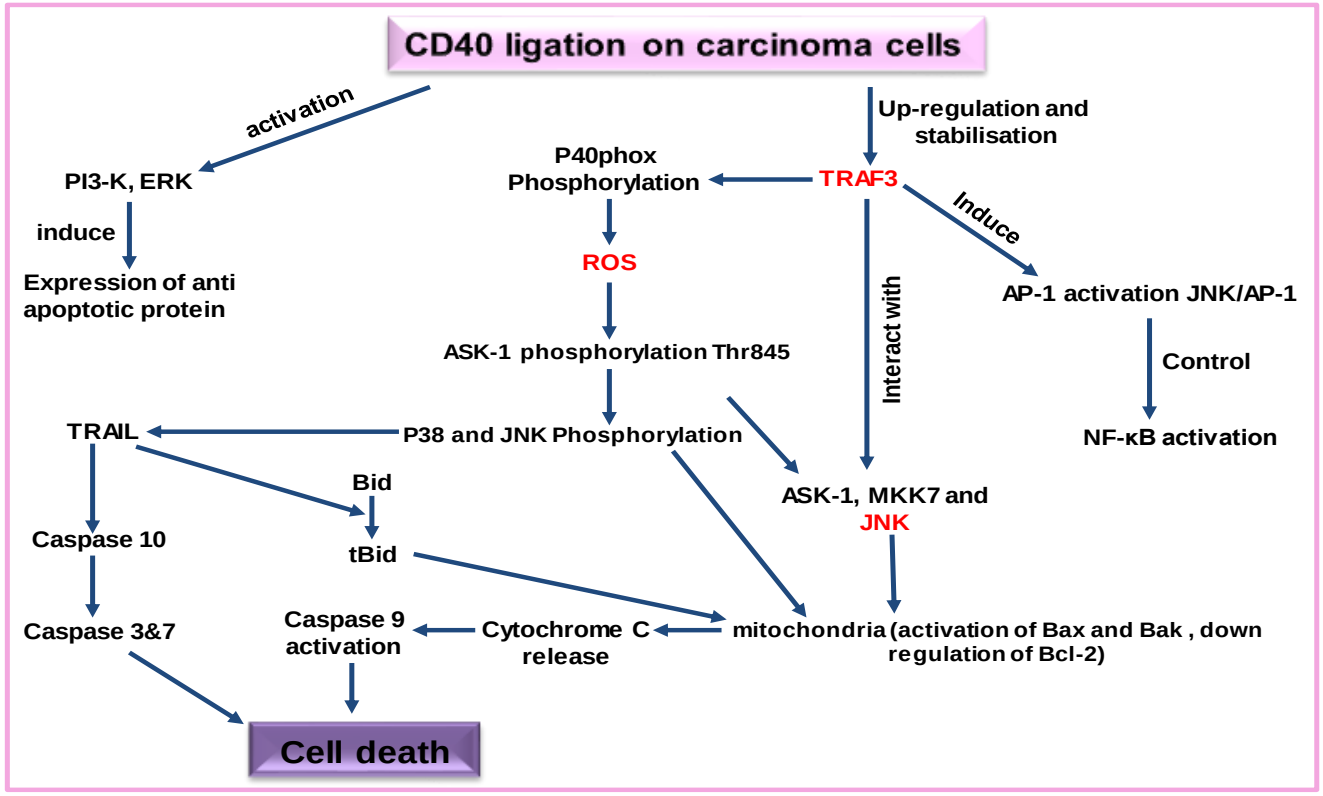

Figure 1.17 Signalling through CD40 in carcinoma cells

Diagrammatic representation of our current knowledge of signaling events triggered by CD40 in carcinoma cells based on findings from our laboratory. CD40 ligation in carcinoma activates (stabilizes) TRAF3 and TRAF3 can either activate ASK-1, MKK7, MKK4 and JNK/AP-1 which induces expression of components of the mitochondrial pathway. TRAF3 may help phosphorylate the NOX-2 component p40phox that is responsible for ROS production which then permits phosphorylation of ASK-1, JNK activation and apoptosis (Georgopoulos 2006; Dunnill 2016). Alternatively, CD40 can trigger p38 and JNK which may induce cross-talk with the extrinsic pathway and up regulate TRAIL to induce apoptosis via caspase 10 (Mohamed et al, manuscript in preparation). **Drawn by K. Ibraheem.**

1.15 Kidney cancer

1.15.1 Kidneys

Kidneys are important organs of the urinary system located one on either side of the spine. The processes by which kidneys regulate the composition of blood include: maintaining ions and other blood components at constant concentration, by removal of waste and unwanted water from the body and maintaining the acid/base balance in the body. These maintenance processes are controlled by three processes: A) Filtration of blood into the nephron's lumen; B) Reabsorption of required components from the lumen and by return to the blood; and C) secretion of some toxic products from the blood to the nephron and then outside of the body in the form of urine (Gland, 2012).

1.15.2 Cancer

Cancer in general is a disease characterized by out-of-control cell growth. There are many types of cancer, each classified by the type of the cell that is affected. Cancer harms the body when aberrant cells divide uncontrollably to form lumps (masses) of tissue (tumours), except in the case of leukaemia where cancer involves abnormal cell division in blood cells. Tumours can grow and interfere with vital systems such as the digestive, nervous, and circulatory system. Tumours that stay in their tissue of origin and demonstrate tissue-limited growth are generally considered to be benign. Malignant tumours form when cancerous cells manage to move escape the tissue using the blood or lymph systems, destroying healthy tissue in a process called invasion. When a tumour spreads to other parts of the body, invading and destroying other healthy tissues, this process is called metastasis (Kenny, 2012).

Tumourigenesis in humans is the result of a multistep process which often involves genetic (and epigenetic) alterations that lead to the progressive conversion of normal human cells into malignant cells and mainly involve activation of oncogenes and inactivation of tumour suppressors. Genetic predisposition can be a critical factor, as is age, an important risk factor for cancer. Several viruses have also been linked to cancer such as papillomavirus and hepatitis B and C as well as some carcinogenic

substances are directly responsible for DNA damage and causing cancer, for example tobacco and radiation (Hanahan and Weinberg, 2000).

The progression of tumour arising from epithelial tissue to high pathological grades and stages indicates a topical invasion and metastasis. A key stage of this progression is often the loss of E-cadherin by carcinoma cells as part of the important phenomenon of epithelial-mesenchymal transition (EMT) during which E-cadherin is down-regulated. E-cadherin is a major cell-to-cell adhesion molecule that forms the adherence junctions with neighbouring epithelial cells to provide epithelial cell sheets. Therefore, the decreased in expression of E-cadherin result in highly invading cancer cells. On the contrary, N-cadherin that expressed normally in migrating neurons and mesenchymal cells during organogenesis is up-regulated in many invasive carcinoma cells (Hanahan and Weinberg, 2011).

1.15.3 Kidney cancer

Kidney cancer represents approximately 3% of all cancers. It can occur either in the kidney center in which the urine is collected (renal pelvis carcinoma) or in the lining tissues of the proximal tubules of the kidney's nephrons in which blood filtration from toxic products takes place. The incidence of kidney cancer has increased steadily, and it has been estimated that in the United States more than 38,000 people developed RCC and more than 12,000 were dead from the disease (Jemal et al., 2006). While 58,000 persons were affected with kidney cancer and around 13000 out of them died in 2010 (Jemal et al., 2010). In comparison, in 2013 around 65,150 cases were diagnosed with kidney cancer (de Moor et al., 2013). RCC affects more men than women (approximately 2-3 times) and it increases with age. Kidney cancer is more common in people over 60 and rarely affects people under 40 and children (Vogelzang and Stadler, 1998).

There are several types of kidney cancer. Based on histological examination, clear cell carcinoma (renal cell carcinoma, RCC) is the most common subtype of renal cell cancer and it accounts for more than 75% of cases. The tumour usually arises from the proximal renal tubule and patients have inactivated von Hippel-Lindau (VHL) gene. The second most common type of kidney cancer is known as papillary tumour,

estimated to occur in about 10% of cases. The tumour also arises from proximal tubules but without inactivation of VHL gene. Other tumours of the proximal tubule include Sarcomatoid which is related to p53 inactivation (Vogelzang and Stadler, 1998). Chromophobe renal cell carcinoma subtype occurs in few cases. A very rare subtype is duct renal cell carcinoma. Cancer that develops in the lining of the pelvis called transitional cell carcinoma occurs in about 5%-10% of kidney cancer. The children kidney cancer Wilms tumour (or nephroblastomas) account for ~5% of kidney cancer (Cancer research UK http://www.cruk.org/cancerhelp; and NHS www.nhs.uk).

1.16 Aims of study

This study was aimed for the first time to investigate the CD40 expression on human RCC cells and explore the efficient outcome of its stimulation in human RCC by unravelling the signalling events and the capability of membrane CD40 ligand to stimulate CD40-mediated apoptosis in RCC cells. Overall aim is to determine the potential of CD40 as a therapeutic target in RCCs.

More specifically:

Chapter 3:

To characterise the expression and functional activity of CD40in RCCs.

- Using different techniques (Western blot/ Flow cytometry) to investigate the expression of CD40 on a panel of well –characterised RCC cells
- To activate CD40 on RCC, different modes of CD40 ligation were used including a co-culture system for delivery of mCD40L versus treatment with agonistic anti-CD40 antibody.
- A series of assays based on characterisation of different features of apoptosis were optimised for the detection of CD40-mediated apoptosis in RCC cells

Chapter 4:

- Investigate the stimulation of pro-inflammatory cytokine (IL-8, IL-6 and GM-CSF) secretion following CD40 ligation

Chapter 5:

Determine the physiological response to the activation of CD40in RCCs, using in vitro cell model.

- Apoptosis detection assays, immunoblotting, and pharmacological inhibitors were used to study for the first time the regulation of key intracellular components involved in CD40-mediated apoptosis in RCC cells

- Studies were carried out for the first time to identify the involvement of the ROS pathway in CD40-mediated apoptosis by examining the ROS generation, involvement of NADPH oxidase (NOX) during CD40-mediated apoptosis

Chapter 6:

Using normal human renal proximal tubule (HPRT) cells and utilise apoptosis assays and immunoblotting to for the first time

- Examine the expression of CD40 on normal HRPT cells by different techniques (immunoblotting and Flow cytometry)
- Examine the outcome of CD40 ligation in normal cells and investigate the tumour specificity of CD40-mediated killing

Chapter 2

Materials and Methods

2. Materials and Methods

2.1 General

All laboratory work was performed in the School of Applied Sciences, at the University of Huddersfield in the JP2/70 and JP1/68 laboratories.

2.2 Disposable plasticware

Sterile and non-sterile plasticware was purchased from different suppliers (Sarstedt, Fisher Scientific, Greiner Bio-One or Alpha Laboratories). Non-sterile, disposable plasticware was decontaminated by autoclaving in a Prior Clave/London Autoclave at 121°C under pressure (2 Bar) for 15 min and then left to dry at room temperature.

2.3 Stock solutions

The chemical reagents were either of methodical or tissue culture grade as suitable for the experiments and were supplied by Sigma Aldrich unless otherwise stated. General laboratory stock solutions were made in the laboratories with deionised water (dH_2O). The solutions which were used in tissue culture were made with ultra-pure water from a LabStar Ultra Violet purification unit and sterilised as previously {Dunnill, 2013 #608}.

2.4 Reagents

2.4.1 Primary antibodies

A list of the primary antibodies that used in this study are presented in Table 2.1, the Antibodies were stored according to the manufacturer's instructions until required. TBS-Tween buffer (0.1% Tween20) was used to dilute the stock antibodies and made the Working antibody solutions. The dilution factor was dependent on the manufacturer's instructions.

Table 2.1 Primary antibodies

Antigen	Catalogue no/ Clone	Host	Supplier (product of)	Dilution	Application	Molecular weight (kDa)
Human CD40L	AF617	Rabbit	R&D systems	1:500 in TBS Tween20 0.1%	FC, WB	37
TRAF3	sc-949 / c20	Rabbit	Insight Bio (Santa Cruz)	1:500 in TBS Tween20 0.1%	WB, IP, IF, FCM and ELISA	65
TRAF1	sc-7186 / h-186	Rabbit	Insight Bio (Santa Cruz)	1:1000 in TBS Tween20 0.1%	WB, IP, IF and ELISA	52
TRAF2	SC-876/c-20	Rabbit	Insight Bio (Santa Cruz)	1:1000 in TBS Tween20 0.1%	WB, IP, IF and ELISA	50
TRAF5	7220/H-257	Rabbit	Insight Bio (Santa Cruz)	1:1000 in TBS Tween20 0.1%	WB, IP, IF and ELISA	55
TRAF6	sc-8409	Mouse	Insight Bio (Santa Cruz)	1:500 in TBS Tween20 0.1%	WB, IP, IF, IHC(P) and ELISA	60
Phospho-SEK1/MKK4 (Ser457)	#4514 (C36C11)	Rabbit	New England Biolabs (NEB)/Cell Signalling Technology (CST)	1:1000 in TBS, 5% w/v BSA, 0.1% Tween20	WB, FC	44
Phospho-MKK7 (Ser271/Thr275)	#4171	Rabbit	NEB (CST)	1:1000 in TBS, 5% w/v BSA, 0.1% Tween20	WB	48
JNK/SAPK	#9258	Rabbit	NEB (CST)	1:1000 in TBS, 5% w/v BSA, 0.1% Tween20	WB	46, 54
Phospho-ASK1 (Ser967)	#3794	Rabbit	NEB (CST)	1:1000 in TBS, 5% w/v BSA, 0.1% Tween20	WB	155

Phospho-JNK/SAPK (Thr183/Tyr185)	255 (G9)	Mouse	NEB (CST)	1:500 in TBS, 5% w/v non-fat dry milk, 0.1% Tween20	WB, IP IF, FC	46 (phospho-JNK1) 54 (Phospho-JNK2/3)
ASK1	#3762	Rabbit	NEB (CST)	1:1000 in TBS, 5% w/v BSA, 0.1% Tween20	WB	155
BAX	2282-MC-100 (YTH-2D2)	Mouse	R&D systems (Trevigen)	1:500 in TBS 0.1% Tween20	WB, IP	23
BAK	AF816	Rabbit	R&D systems	1:500 in TBS 0.1% Tween20	WB	28
Phospho-p40phox (Thr154)	#4311	Rabbit	NEB (CST)	1:500 5% w/v BSA, 0.1% Tween20	WB	40
Human Thioredoxin	#2285S	Rabbit	NEB (CST)	1:500 5% w/v BSA, 0.1% Tween20	WB	12
β-actin Clone AC15	A5441 - 2ML	Mouse	Sigma	1:20,000 in0.1% Tween20	WB	42
CD40	Sc-13128/ (H	Mouse	NEB(CST)	1:500 in0.1% Tween20	WB	43
CK18	C8541	Mouse	Sigma-Aldrich	1:2000 in0.1% Tween20	WB	45
CK8	081213	Mouse	Invitrogen	1:1000 in 0.1% Tween20	WB	45
CK8/18	889257A	Mouse	Invitrogen	1.1000 in 0.1% Tween 20	WB	52/48
Phospho-P38	4511	Rabbit	NEB (CST)	1.500 in 0.1% Tween 20	WB	40

The table illustrate full information about all primary antibodies that used in this study.

2.5.2 Secondary antibodies

Monoclonal antibodies were detected by the addition of the Molecular probes Alexa Fluor® 680 Goat anti-mouse IgG (H+L) antibody (Invitrogen). Goat anti-Rabbit IgG IRDYE800 antibody (Tebu-bio) was used for the detection of all polyclonal antibodies. Fluorochrome conjugated secondary antibodies were diluted freshly just before use.

2.5.3 Agonists & antagonists

Table 2.3 illustrate the Pharmalogical agonists and antagonists as well as agonistic antibodies. Either tissue culture grade dimethyl sulphoxide (DMSO) or sterile dH_2O were used for re-formation according to the manufacturer's instructions. These were aliquoted in small Eppendorf tubes and stored for single use at -20°C according to the provider recommendation. Earlier to use, the cell viability assay (CellTiter 96® AQ_{ueous} One Solution Cell Proliferation Assay; Promega, UK) was used to titrate all these agents to determine the highest effective and non-toxic amount. At the first mention of all such reagents used in this study, the suppliers were indicated as appropriate.

Table 2.2 Agonists & antagonists

Compound	Target	Supplier	Stock concentration	Effective concentration
N-acetyl L-cysteine (NAC)	ROS	Sigma	30mM (culture media)	30mM
DPI	NADPH Oxidase	Sigma	10mM (DMSO)	0.5µM
SP600125	JNK	Enzo	20mM (DMSO)	5µM
NDGA	AP-1	Sigma	20mM (DMSO)	5µM
SB202190	p38	Sigma	20mM (DMSO)	5µM
PX-12	Thioredoxin	Sigma	20mM (DMSO)	1-3µM
Diethyl Maleate	Gluthathione	Sigma	6.45 Molar	75µM
Staurosporine	Protein Kinases	Sigma	100µM	1-10µM
Caspase-8 Inhibitor	Caspase-8	R&D systems	20mM	25µM
Caspase-9 Inhibitor	Caspase-9	R&D systems	20mM	100µM
Caspase-10 Inhibitor	Caspase-10	R&D systems	20mM	100µM
General caspase Inhibitor (Z-VAD)	Caspases	R&D systems	20mM	100µM
Hydrogen peroxide	N/A	Sigma	9.79M	100µM-3200µM
G28-5 mAb	CD40	N/A	1.1mg/ml	10µg/ml
IFN-ɣ Human recombinant	Human	Tebu-bio	$20x10^6$ u/ml	1000 & 100 U/ml
TNF-α Human recombinant	Human	Tebu-bio	$20x10^6$ u/ml	1000 & 100 u/ml

The table show a list of agonists and antagonists employed in this work, with their objective molecule, the provider, and the standard and working applications.

2.6 Tissue culture

2.6.1 General

All tissue/cell culture work was carried out using hygienic strategies within a HEPA filtration CellGard class II biological safety cabinet (NUAIRE). Erlier to and after use, 70% (w/v) ethanol, (99% Ethanol solution (Fisher) was diluted properly (150ml: 350ml) with purified autoclaved dH_20) and used to sterilised the internal working areas inside the cabinet. Mikrozid® (Gompel Healthcare) was used to disinfect the internal hood discharges and this was also used for a monthly routine sterilisation. A large conical flask containing 10% (w/v) Virkon was used to remove any annoying cells, drained media or solutions. The flask then left for about 30 min before being poured and washed into sewage.

The cell culture reagents were of tissue culture rank, and were a purchased from Sigma. Hettich Zentrifugen Universal 320 bench top centrifuge was used for cells centrifugation for 5 min at 1500 RPM (210 RCF) and to isolate cells from solution. Marienfield Neubauer improved bright line haemocytometer was used for cell counts which were completed from cell suspensions prior cells were cultured at appropriate cell number.

2.6.2 Maintenance and passage

Iso class 5 Nuaire Autoflow direct heat CO_2 incubator with a HEPA filtration system at 37°C in a 5% CO_2 humidified atmosphere was used for cells maintenance. For humidification, the incubators contained a tray with sterile (autoclaved) dH_2O, supplemented with Sigma clean (Sigma) or AQUAGUARD-1 Geneflow Limited), as recommended by the respective suppliers.

Phase contrast microscopy using an EVOS XL (PeqLab, and now Fisher Scientific) inverted microscope at x100 (or x200) magnification was used for daily observation of seeded cells. For cells culture, T75 flasks with 12-14ml medium or T25 flasks in 5ml medium were used and incubated at 37ºC under 5% CO_2. When cells being confluent in about 85-90%, Sub-cultured was performed for all cell lines.

For repetitive passaging, cells were washed with with 0.1% (w/v) EDTA in phosphate buffered saline (PBS) (Ca2+ and Mg2+ free) (Invitrogen) for 2 min, then trypsin-EDTA (Sigma) in Ca2+ and Mg2+ free Hanks-balanced salt solution (HBSS, Sigma) was added, when cells lifted, Trypsin was inactivated by the re-addition of the respective serum-supplemented culture medium when cells were re-suspended. For long term storage, following growth and appropriate passage, cell 'banks' and 'sub-banks' were cryo-preserved as described in section 2.6.3 (below).

2.6.3 Cryo-preservation and recovery of cell lines

A Statebourne storage dewar containing liquid nitrogen at -196°C was used for cryopreservation of cell lines, cultured cells were lifted as for normal passaging (as described in section 2.6.2) and centrifuged. Then cell re-suspended in the proper ice-cold growth medium complemented with 10% (v/v) FBS and 10% (v/v) dimethylsulphoxide (DMSO) at a cell density not less than $1x10^6$ cells/ml. polypropylene cryovials (Sarstedt was used for cells aliquote in a total volume 1-1.5 ml/vial, cooling rate 1°C per minute was achieved by transferring the vials to an ice-cold Nalgene "Mr Frosty" (Fisher) containing 250ml of isopropanol (Fisher). Cells were then located in a -80°C freezer for 4-6 h earlier to allocation in liquid nitrogen.

Fast thawing at 37°C was carried out, and 5-10 ml of culture medium was added. Then centrifuged at 1500 RPM (210g) for 5 min. Cells were then cultured in a tissue culture flasks as necessary.

2.6.4 Primary cell culture

Primary Human Renal Proximal Tubule Epithelial Cells (HRPTEpiC), purchased from Caltag Medsystems Ltd) were isolated from human kidney (and henceforth referred to as HRPT cells). HRPT were cryopreserved at passage one and delivered frozen.

According to the supplier's instructions, HRPT were maintained in Epithelial Cell Medium (EpiCM) supplemented with 10 ml of FB, 5 ml of Epithelial Cell Growth Supplement and 5 ml of penicillin/streptomycin solution (P/S) (Caltag Medsystems). At all times, cells were cultured in T25 flasks with 5 ml medium and incubated at 37°C under 5% CO2, then sub-cultured when they were ~80-90% confluent. HRPT cells

were harvested by initial washing with 0.1% (w/v) EDTA in PBS solution for 3 min, followed by addition of Trypsin-EDTA solution until cells lifted. Trypsin was inactivated by the re-addition of 5 ml of complete medium. Any traces of trypsin were excluded by centrifugation and re-suspension in 5 ml of fresh complete medium. This technique was used for routine passage and HRPT cells used in this study were only between passages 1-4.

For cell death detection (CytoTox-Glo) assays only, these cells were adapted in DR5% medium to avoid high background interference from the effector (3T3-CD40L and 3T3-Neo) cells (see section 2.6.6), as effectors were highly sensitive to any changes in the normal culture medium (DR5%).

2.6.5 Carcinoma cell culture

Three Renal Cell Carcinoma (RCC) cell lines were used in this study: ACHN, 786-0 and A-704 (Brodaczewska et al., 2016). The cell surface (membrane) and total expression of CD40 receptor in these lines is described in Chapter 3.The malignant bladder carcinoma cell line (EJ) and the colorectal adenocarcinoma cell line (HCT116) were also used as positive controls as previously (Georgopoulos et al., 2007, Georgopoulos et al., 2006).

As recommended by the cell suppliers, ACHN (Fibroblast phenotype, purchased from Sigma) was initially cultured in complete DMEM 10% FBS; 786-0 (epithelial phenotype, purchased from ATCC) was initially grown in RPMI 10% FBS and A-704 (epithelial phenotype, purchased from Sigma) was initially maintained in EMEM 10% FBS.

For ease of maintenance as well as experimentation purposes, all three cell lines were gradually adapted for culture in ‘DR medium’ by following a sequential adaptation methodology. Once adapted, all RCC lines were conserved in a 50:50 (v/v) combination of Dulbecco’s modified eagle medium (DMEM Sigma) and Roswell Park Memorial Institute 1640 (RPMI Sigma) (referred to as D:R medium). 5% fetal calf serum (FCS Biosera or Sigma) and 1% L-Glutamine (Sigma) were added to this medium.

More specifically, adaptation into DR5% FBS medium performed by culturing and passaging through gradual reducing in the amount of standard (recommended) culture medium. Briefly, this involved: medium-change of cells following healthy growth from standard culture medium to 9:1 (v/v) standard medium:DR5% (i.e. 10% DR5%) (step 1); medium change to 3:1 (v/v) standard medium:DR5% (i.e. 25% DR5%) and passage (step 2); medium-change to 1:1 (v/v) standard medium:DR5% (i.e. 50% DR5%) followed by passage (step 3); medium-change to 1:3 (v/v) standard medium:DR5% (i.e. 75% DR5%) and passage in this medium (step 4); medium-change to 1:9 (v/v) standard medium:DR5% (i.e. 90% DR5%) and passage (step 5); final medium-change to DR5% only and subsequent passage (step 6).

2.6.6 Murine fibroblast (3T3) cell culture

The NIH3T3 fibroblast cell line has been isolated from mouse and two expression plasmids were used for the transfection, one of them with the sequences coding for CD40L and Neomycin resistance gene (3T3-CD40L cells) and the other one was for Neomycin resistance only (3T3-Neo cells), as described by Bugajska et al. (2002). DR medium supplemented with 10% FCS, 1% L-Glutamine and 0.5µg/ml G418 (Invivogen supplied by Source BioScience LifeSciences) was used for the maintenance of these derivatives 3T3s, and to ensure cells maintained transgene expression. Continuously, 3T3s cell lines were maintained in the mentioned medium and incubated at 37°C in 5% CO_2 or collected and passaged similar to carcinoma cells but with the diminutive time of treatment with 0.1% (w/v) EDTA in PBS as prolonged periods risked quick cell dissociation.

2.6.7 Mycoplasma testing

It has been documented that *Mycoplasma spp.* infection is a substantial problem in eukaryotic cell culture which cause variable experimental outcomes (Capes-Davis et al., 2010). The intracellular bacterial infection with Mycoplasma spp were investigated regularly for all cell lines in our lab. The MycoProbe™ Mycoplasma detection assay (R&D systems) which is designed for the screening of cultured cells was used for the detection of Mycoplasma 16S ribosomal RNA (rRNA) depending on the intensification system for colorimetric signal. The sensitivity of this kit is similar to PCR. The test was

achieved according to the manufacturer instructions that included preparation of samples in 96 well plates, and the recognition of 16S Ribosomal RNA by ELISA technique. FLUOstar OPTIMA (BMG Labtech) plate reader at 492nm absorbance was used for the detection of the signal. The kit was provided with positive control samples which used to compare the results.

2.7 Methods for CD40 ligation

The ligation of CD40 receptor for the experiments defined in this study was achieved by either membrane CD40L or soluble agonist.

Membrane-presented CD40L (mCD40L) was achieved by co-culture of 3T3CD40L cells (mCD40L) with CD40-positive target RCC cells. As a negative control RCC cells were also co-cultured with equal number of 3T3Neo cells (Controls).

Both CD40L positive and negative 3T3s were growth arrested by treatment with 10µg/ml of Mitomycine C (Santa Cruz) for 2 h in DR medium then washed 3 times with 1X PBS, harvested and seeded either in 96 well plates at $1x10^4$ cells/well for apoptosis detection assays, in $10cm^2$ culture dishes at $3x10^6$/dish for protein lysates preparation or in 24 well plates at $6x10^4$ for supernatant collection. Following overnight incubation, culture medium was removed and epithelial cell suspensions were added at $8x10^3$ cells/well in 96 well plates, $3x10^6$ in 10cm dishes or $5x10^4$ in 24 well plates (as optimised in this study).

Receptor ligation by soluble CD40 agonist was performed by treatment of RCC cells (at density of $8x10^3$ cells/well in 96 well plates and $5x10^4$ in 24 well plates) with 10µg/ml of well-characterised agonistic monoclonal antibody (mAb) G28-5 that purified from cultured supernatant of the hybridoma line HB9110 (Bugajska et al., 2002, Georgopoulos et al., 2006).. For most experiments the G28-5 antibody was cross-linked with Goat anti-mouse IgG cross linking secondary antibody (Sigma).

2.8 Detection of cell viability, cell death (apoptosis) and reactive oxygen species (ROS) generation

2.8.1 General

For most assays, epithelial cells were co-cultured with either 3T3-CD40L (mCD40L) or 3T3-Neo (Control) cells. To calculate cell death, background fluorescence and luminescence readings were subtracted pairwise as appropriately, (e.g. “mCD40L/ACHN – mCD40L” and “Control/ACHN – Control” readings). The exemption was DNA fragmentation as this was unnecessary due to the pre-labelling of target epithelial cells. Finally, in all experiments blank controls were included as appropriate.

2.8.2 Detection of cell growth (viability)

RCC cells were cultured into 96 well, and 5 wells were used as technical replicates. Plates then incubated overnight, after cells adherence, cells were treated with either pharmacological agonists or inhibitors. Following a proper incubation. Cells viability was determined by using the cellTiter 96® AQueous One Solution according to manufacturer’s instructions. FLUOstar OPTIMA (BMG Labtech) plate reader was used at a wavelength of 492nm and data was acquired using MARS software (BMG Labtech). Microsoft Excel was used to analysed the data and the percentage of cells viability was compared with the controls and the following formula was used

(T/C) x100, where T= treated cells and C= controls non treated cells.

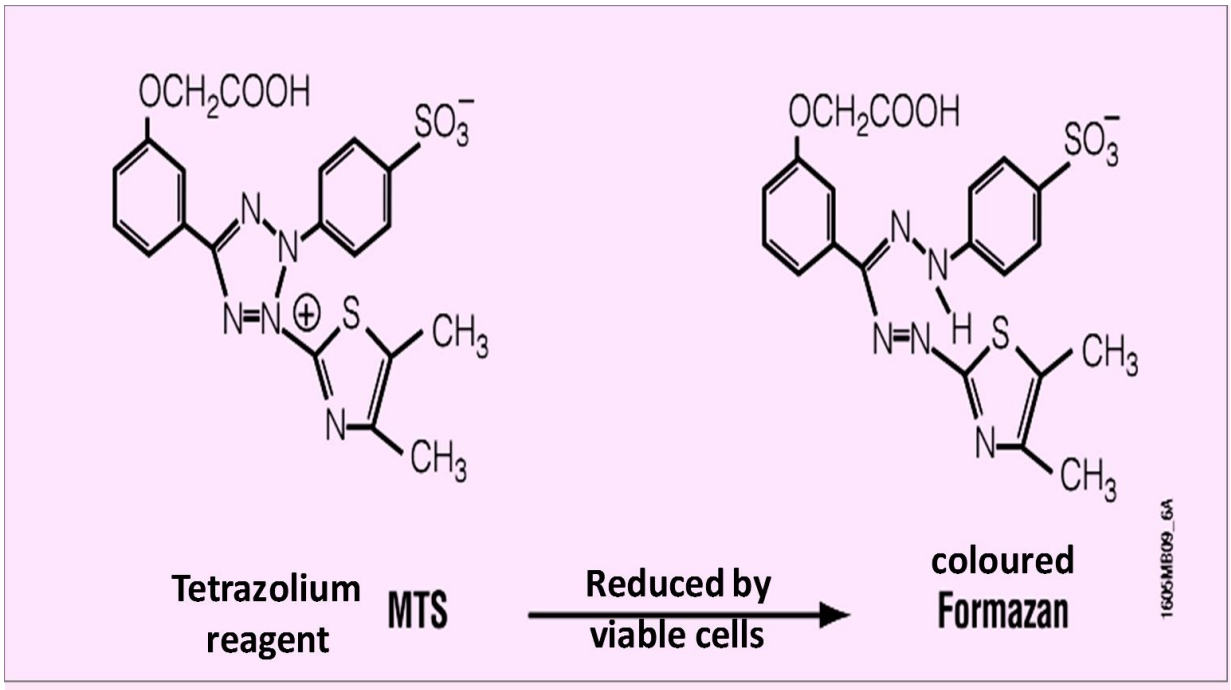

Figure 2.1 The principle of MTS tetrazolium assay

The MTS solution contains tetrazolium compound 3-(4,5-dimethythiazol-2-yl)-5-(3-carboxymethoxyphenyl)-2-(4-sulfophenyle)-2H-tetrazolium and the reagent phenazine ethosufate (PES), which customs as an electron connecter reagent that can bind with MTS to form a constant solution. Viable cells reduce this regent to form coloured solution (Formazan) which is soluble in the medium. The density of the colour is directly proportional with the number of viable cells. The figure is adapted from the manufacturer's webpage (www.promega.com).

2.8.3 Detection of cell death using caspase3/7 assays

One of the well-recognised feature of cell apoptotic cell death is the Caspases 3 and 7 activation, which are objective a definite amino acid sequence established on several proteins which eventually cause programed cell death (apoptosis). The activation of Caspases 3/7 was estimated by SensoLyte® Homogenous AFC Caspase-3/7 substrate (supplied by Cambridge Bioscience).

2.8.3.1 SensoLyte® Homogenous AFC Capase-3/7 assay kit

RCC cells were co-cultured with membrane CD40L in 96 well plates as described in section 2.8. Following an appropriate incubation time. The Caspase3/7 activity was determined using the above kit according to the manufacturer's instructions (Figure 2.2). The measurement using FLUOstar OPTIMA (BMG Labtech) plate reader was performed as previously {Dunnill, 2013 #608}. Fibroblasts cells were cultured alone and the calculation was carried out as explained in Section 2.8.1.

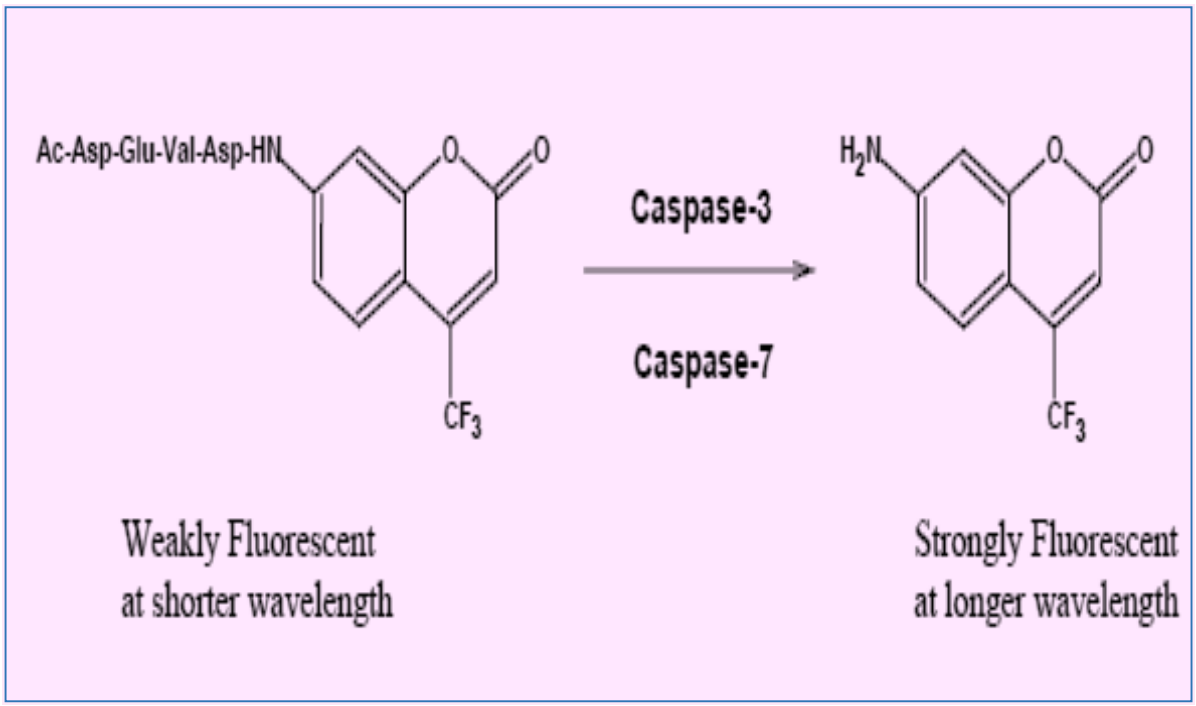

Figure 2.2 The opinion of SensoLyte® Homogenous AFC Capase-3/7 assay kit

The caspase-3/7 Ac-DEVD-AFC substrate is weak fluorescent compound which cleaved by the action of caspase 3/7 and converted to highly fluorescent complex. The intensely of fluorescent is related to the cleavage activity of caspase 3/7. **The diagram adapted from manufacturer's website.**

2.8.4 Estimation of cell death using the CytoTox-Glo™ assay

The CytoTox-Glo kit was designed to detect the protease activity which is usually exist inside the cells, the disintegration of the cell membrane during apoptosis process resulted in the release of the protease which ultimately cleave AAF-Glo™ substrate and cause the generation of luminescence signal which increased depending on the amount of cell death (Figure 2.3).

RCC cells were co-cultured with mCD40L as described in section 2.8.1. Following an appropriate incubation at 37°C in 5% CO_2. The estimation of cell death was performed according to the manufacturer's instructions. FLUOstar OPTIMA (BMG Labtech) plate reader was used to detect the Luminescence, using the Gain adjustment on the MARS software to guarantee the estimations were engaged within the dynamic range of the machine. Readings were taken and Microsoft Excel was used to analyse the data. Fibroblasts cells were cultured alone and the calculation was carried out as explained in Section 2.8.1.

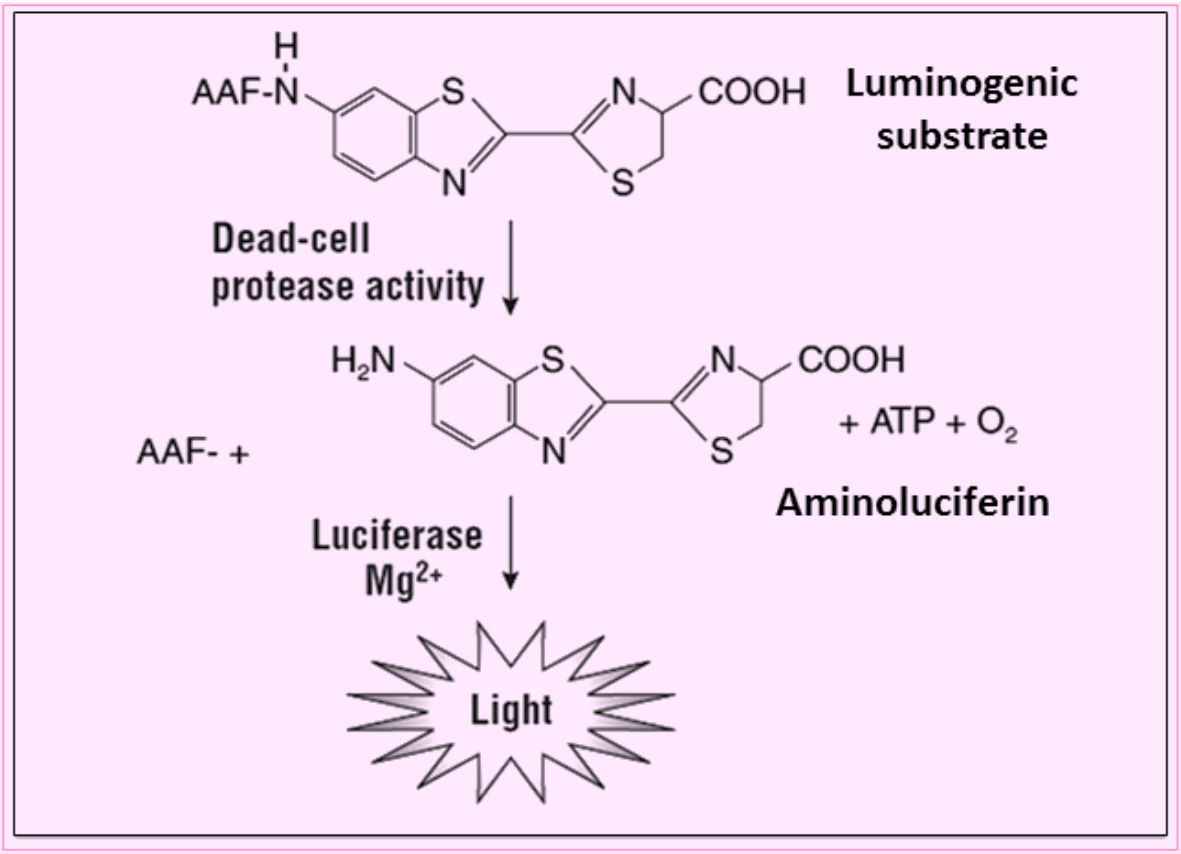

Figure 2.3 The opinion of the CytoTox-Glo^{TM} assay

The Aminoluciferin is released by the action of protease and act as substrate for the luciferase that present in the solution resulting in light production. **The diagram adapted from manufactures website.**

2.8.5 DNA fragmentation ELISA for the detection of apoptosis

Following labelling with DNA labelling agent according to the manufacturer's instructions. 1x PBS was used for RCC cells washing one time, then cells were harvested, counted and then co-cultured with mCD40L as described in section 2.8.1. The DNA fragments were determined in culture supernatants by DNA fragmentation ELISA kit according to the manufacturer's instructions (Figure 2.4). FLUOstar OPTIMA (BMG Labtech) plate reader was used to measure the absorbance at 455-10nm filter. Readings were picked up and Microsoft Excel was used to analyse the data. Brdu was used to labile only the RCC cells. Therefore, the background of 3T3s was excluded. For positive control 5µM of Staurosporine was used and the percentage of apoptosis was estimated using the following equation.

$$\%\ \text{of apoptotic cells} = \frac{(\text{Target cells} + \text{Killer cells})}{(\text{Target cells} + \text{Staurosporine})}\ \text{x}\ 100$$

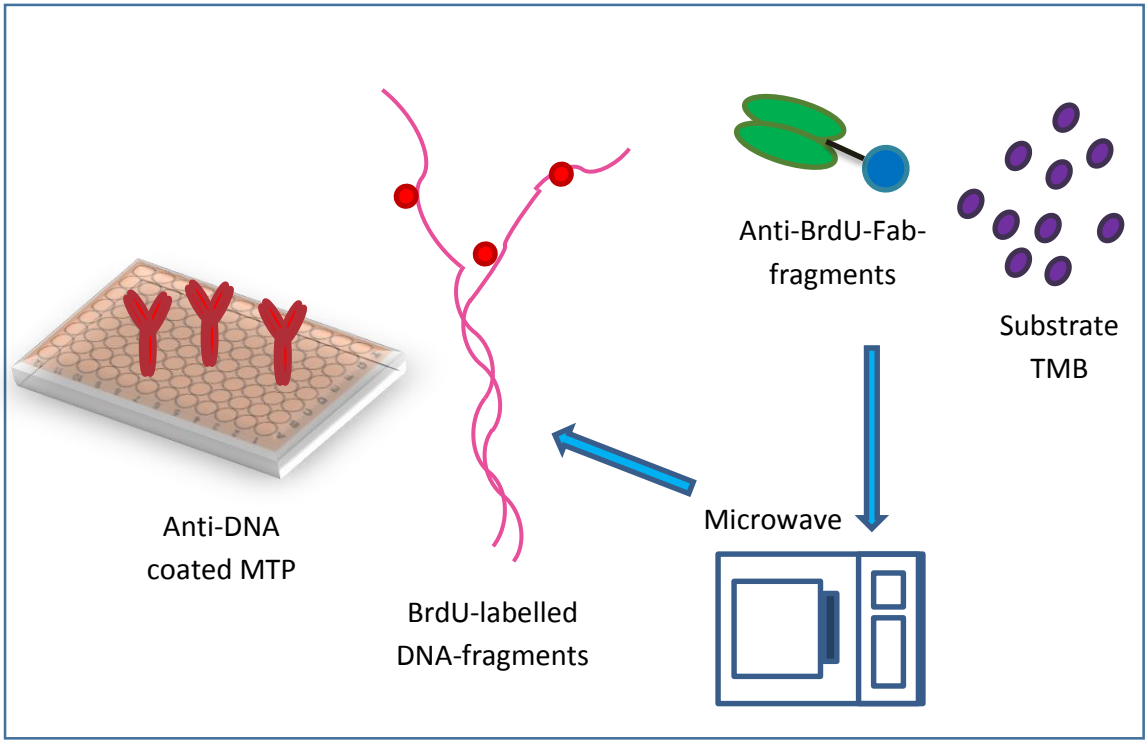

Figure 2.4 Opinion of DNA fragmentation kit

BrdU-labelled fragments of DNA from co-culture supernatants are caught by the antibody that coat the ELISA plate. Microwave was used at 500 Watt for 5 min for denaturation then secondary antibody (anti-BrdU-Fab) was added and the plate was incubated for 1.5h at room temperature. Finally, substrate was added. A blue colour was developed, and the reaction was stopped by adding sulphuric acid. **Drawn by K. Ibraheem.**

2.8.6 Detection of Reactive oxygen species (ROS) using H_2DCFDA

The H2DCFDA (6-carboxy-2', 7'-dichlorodihydrofluorescein diacetate) (Invitrogen Cat # c2938) was reconstituted and used for the detection of ROS generation according to the manufacturer's instructions. Figure 2.5 explain the principle of the test.

RCC cells were co-cultured with mCD40L as described in section 2.8. Taking in consideration 3T3s were not treated with MMC. After incubation for the specified time points, one time wash was performed with PBS and 1µM of H_2DCFDA in pre warmed (37°C) PBS was added and cells were incubated for 30 min at 37°C in 5% CO_2. Following treatment with H2DCFDA, FLUOstar OPTIMA (BMG Labtech) plate reader was used at Excitation 485nm/Emission 520nm to measure the fluorescence by using Gain adjustment on the MARS software to guarantee the readings were engaged at the dynamic assortment of the machine.

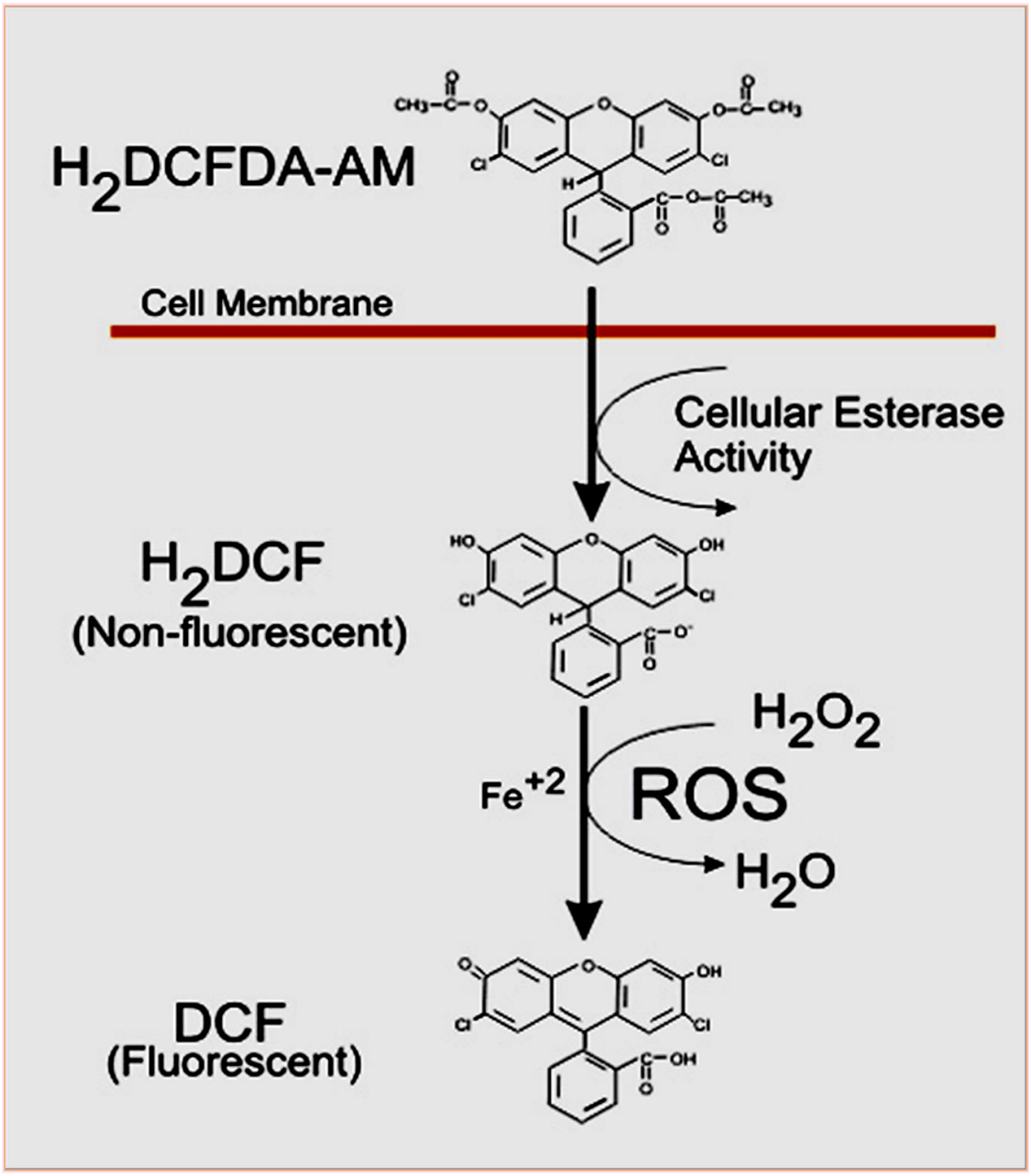

Figure 2.5 The opinion of ROS detection using H2DCFDA

The (H2DCFDA) in its reduced form is a non-fluorescein reagent and has cell penetrability. When acetyl groups are detached by the activity of intracellular esterase(s) which cause oxidation inside the cells. The molecules become more established due to the changing in their charge and start to produce fluorescence signal. The strength of the fluorescence indicate the amount of the intracellular ROS. **Adapted from (Held, 2010).**

2.9 Western Blotting - SDS-PAGE and Immunoblotting

2.9.1 General

Western bolting is an influential method extensively used in various fields in biological research to detect exact proteins in a cell lysate. Proteins from cell lysate can be take out and preserved in buffers to guarantee their reliability. Under denaturing situations numerous proteins are sectioned based on their dimension using SDS-PAGE, a form of gel electrophoresis.

SDS (sodium dodecyl sulfate) was used for denaturation during the SDS-PAGE separation procedure. The SDS buffer have a hydrophobic hydrocarbon extremity and a negatively charged end by which it bind the proteins and communicates the negative charge triggered migration towards the anode. The function of SDS buffer is to prevent the folding of the proteins.

Therefore, proteins travel towards the anode because their negative charge due to the presence of SDS, The proteins having a small molecular weight will be retained within the pores of the polyacrylamide gel and therefore will migrate farther than larger proteins. The detached proteins then transferred onto a membrane as described previously {Dunnill, 2013 #608}.

2.9.2 Treatment with mCD40L to investigate CD40-mediated intracellular signalling

3T3-Neo and 3T3-CD40L cells were treated with MMC as explained in section 2.8. Cells were cultured in $10cm^2$ dishes at $3x10^6$ cells/dish (duplicate dishes were prepared for every cell line and 3T3 cells were seeded in a 5ml volume) (see Figure 2.6). All dishes were incubated at 37ºC and 5% CO_2 overnight.

Following overnight attachment, the medium was replaced by RCC cell containing suspension (10 ml volume added to provide 30 $x10^5$cells/dish) and dishes were incubated at 37ºC and 5% CO_2 for the required times (1.5, 3, 6, 12 and 24h). Upon completion of the incubation period, lysates were prepared as explained in section 2.10.3. Protein concentration was measured in all lysates as detailed in section 2.12.3.

Lysates were used for immunoblotting to detect intracellular protein expression in target RCC cells.

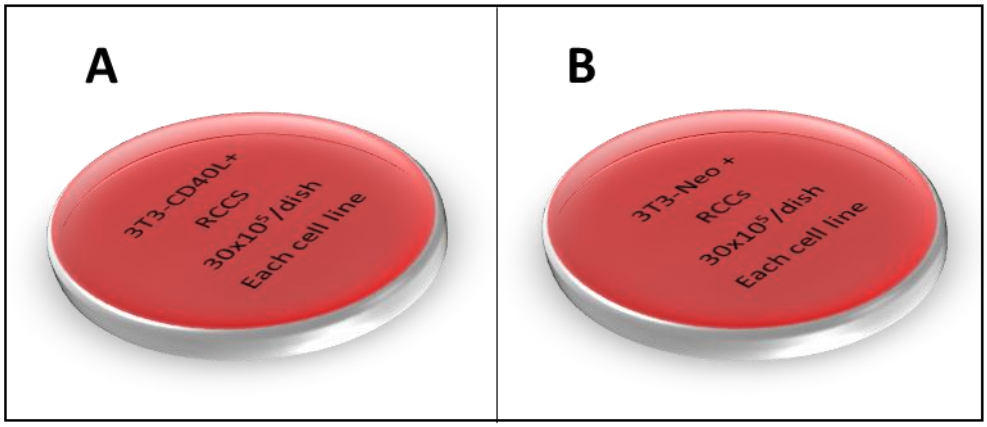

Figure 2.6 Co-culture of RCCs cells with 3T3 fibroblasts; 3T3-CD40L (A) and 3T3Neo (B)

2.9.3 Protein extraction

RCC cells were co-cultured with mCD40L-expressing (3T3CD40L) and Control (3T3Neo) as described above, the co-culture were carried out either for cells alone or in presence of pharmacological agonist/antagonists as indicated. Following incubation at 37°C and 5% CO_2, then two times wash was performed with ice-cold PBS and 50 µl of lysis buffer was added on top of the cells monolayer (Lysis buffer: 2x sodium dodecyl sulphate (SDS) buffer (Appendix I) having 2mg/ml DTT and 0.2% (v/v) protease inhibitor mixture set III (Calbiochem)). Cell scraper (Fisher) was used for cells robbing. Cells laysate was then collected in a micro-centrifuge tube (placed on ice). ultrasonic probe (Sonics Vibra cell) was used for cells sonication at 10 second bursts. After forth established, the tubes were placed on ice for 30 min then centrifuged at 12,000-14000g, 4°C for 30 min. The supernatant was collected, aliquoted and stored at -20°C.

2.9.4 Protein Quantification

Coomassie protein reagent assay kit (Pierce) was used to estimate the protein concentration in each lysate. dH_2O was used to dilute each lysate at v/v 2:23 (Dilution factor 12.5). In a transparent 96-well plate, 10µl of lysate was added in duplicate. The plate was also contain a protein standard solution at seven points 0-1mg/ml (0, 25, 125, 250, 500, 750 100µg/ml) BSA (Pierce). (200µl) of Coomassie reagent was added to each well and mixed quietly. A FLUOstar OPTIMA (BMG Labtech) plate reader was used to quantity the absorbance at 595nm.Data were analysed using MARS analysis software 2.0 (BMG Labtech) and standard curve based on the BSA standards was planned to evaluation the concentration of proteins in each lysate (Appendix I). The samples then subject for SDS-Polyacrylamide gel Electrophoresis (SDS-PAGE) according to Invitrogen protocol as previously {Dunnill, 2013 #608}.

2.9.6 Electrophoretic membrane transfer

X*cell* II™ blot module (Invitrogen) was used for transferring the proteins onto immobilon membrane (Immobilon-FL™ polyvinylidine difluoride membrane PVDF; Millipore Fisher Scientific). The membrane was first immersed in methanol, second washed with dH_2O and third steeped in transfer buffer (Appendix I). A sandwich immunoblotting was made up with Whatman™ filter paper (Fisher) and essential number of blotting pads. The sandwich was then gathered in configuration as three blot pads, filter paper, gel, membrane, filter paper and three blot pads. (As shown in Figure 2.7). X*cell* SureLock™ Mini-Cell was used to fortify the blot components and complete the inside with transfer buffer and ice-cold dH_2O was used to fill the outer space around the module. The tank then placed on ice and the transfer was carried at 25V for 2 h.

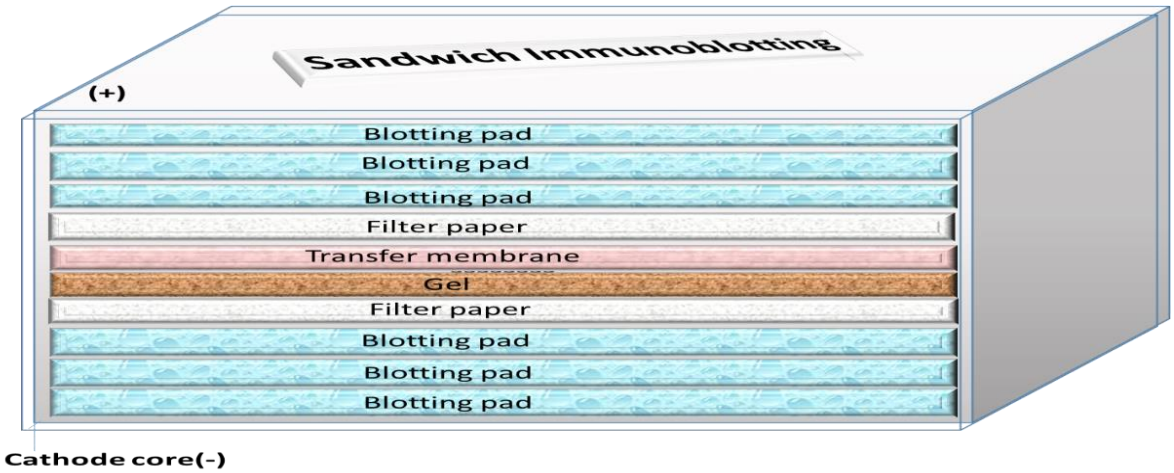

Figure 2. 7 Immunoblotting module

The diagram illustrates the individual components of the 'sandwich' system for protein relocation during immunoblotting.

2.9.7 The immunolabelling and visualisation of the membrane using the Li-Cor Odyssey™ system

Blocking buffer 50:50 (v/v Odyssey blocking (Li-Cor) buffer/TBS (Appendix I)) was used on rocking platform for 1h at room temperature to reduce the non-specific binding. Then diluted primary antibody was added and the membrane was incubated on rocking platform overnight at 4°C (Dilution depend on the manufacturer's instructions). Three times wash for 5 min were performed with TBS-T (Appendix I) and 10 ml of infra-red secondary antibody was added and incubated on rocking platform in dark at room temperature for 1h. Repeat the 3 times wash as for Primary antibody. Odyssey™ Infra-red imaging system (Li-Cor) was used to visualize the membrane. Cytokeratin 18 was used as housekeeping genes to confirm the equal loading of target cells, and normalisation (Densitometry) according to Cytokeratin 18 was achieved by using Odyssey V3.1 software (Li-Cor).

2.10 Flow cytometry

2.10.1 Background

Flow cytometry is widely used to examine the chemical and physical features of elements and cells, and mainly used in immunology and cell biology to count cells, detect protein expression or determine numbers of dead or alive cells. The particles or cells move at high speed in front of a laser beam and a computer acquires the data and permits analysis of their physical and molecular characteristics (in addition to detecting cell numbers). Flow cytometry can also permit detection of cell morphology changes and to highlight any cell defects.

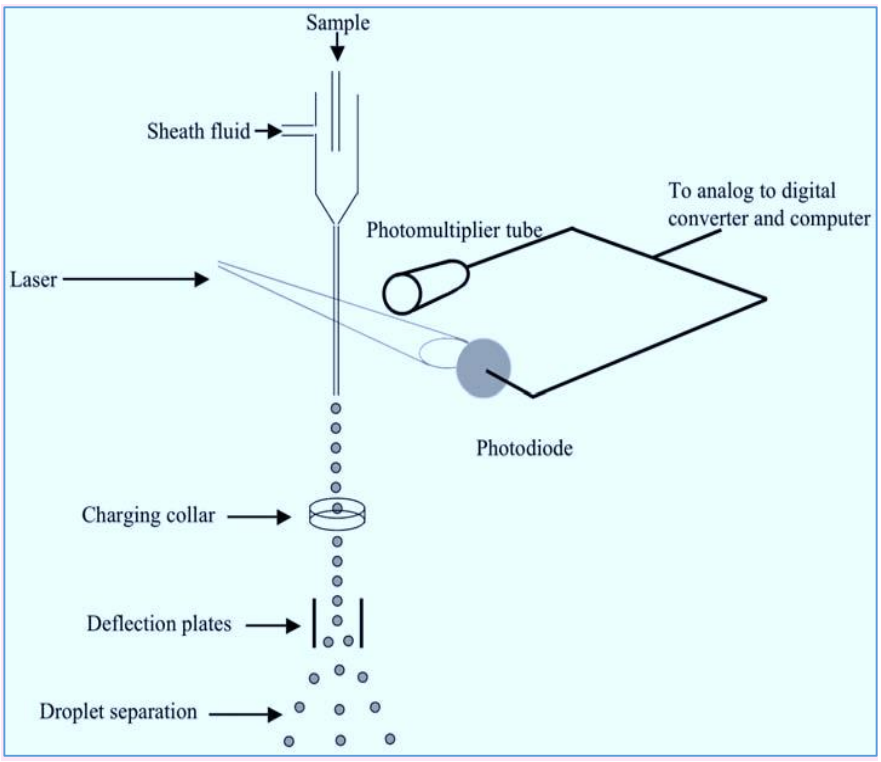

Figure 2.8 The principle of flow cytometry

Flow cytometry is a method depend on using a laser (light beam past a detecting area) for investigating cells or particles as they passage in a liquid runlet. The sprinkling of the light and the distinguishing of the colour are qualified to measure the fluorescence of the particles. The granularity, the dimensions of the cells and the antibody use for cells marking are essential for the fluorescence and analysis.

2.10.2 Detection of CD40 expression by Flow cytometer

To detect CD40 receptor expression on RCC cell surface, RCC cells were picked from flasks by trypsinisation when they were in about of 80-85% confluent, then centrifuged and resuspend in culture medium. 400µl of FACS buffer (1X PBS/1% v/v FBS) was added to $1x10^6$ cells, mixed and then aliquoted into 4 Eppendorf tubes (100µl each) that labelled as CA (cells alone), PE control (isotype control Ab conjugated with PE) and two tubes for CD40-PE test (PE-conjugated anti-CD40 antibody). Then 10 µl of pre-diluted (1/10 in FACS buffer) PE-conjugated Ab was added to the PE tube (control) and 10 µl of CD40-PE antibody (ready to use according to the manufacturer instructions) to each test tube. Control cells (CA) were used to establish the health of the culture and set up the flow cytometer. Incubation was performed for 25-30 min at 4ºC for. After that, all suspensions were washed by addition of 700µl of FACS buffer and centrifuged at 1500 rpm for 5 min at room temperature, then 400µl of FACS buffer was added to the pellets and then all tubes were mixed properly and cells acquired on a EasyCyte Guava flow cytometer and results analysed using EasyCyte software (Millipore).

Table 2.3 Flow Cytometry antibodies

List of antagonists that used for Flow cytometry assay in this study, with their target molecule (where appropriate), the supplier, as well as the stock and effective concentrations being shown

Compound	Cat	Host	Target	Supplier	Stock concentration	Effective concentr--ation
CD40-PE	555589/5C3	Mouse	Human	BD Bioscience	Pre-diluted by manufacturer	Ready to use
Isotype control IgG1 PE	556650/MOPC-21	Mouse	N/A	BD Bioscience	Pre-diluted by manufacturer	Ready to use

2.11 Cell treatment with INF-ɣ and TNF-α

RCC cells were cultured in 24-well plates ($5x10^4$ cells/well) in duplicate. Following incubation overnight at 37^0C with 5% $CO_{2..}$ Cells were medium-changed with fresh medium containing 1000U/ml of INF-ɣ or TNF-α and incubated for 48 h at 37ºC / 5% CO_2. Cells were harvested and centrifuged, then 400µl of FACS buffer was added to each pellet, mixed properly and divided into 4 Eppendorfs tubes labelled as CA (cells alone), PE (isotype control) and two tubes for CD40-PE. Then 10 µl of control PE (pre-diluted by manufacturer) and 10 µl of CD40-PE Ab (ready to use according to the manufacturer instructions) were added, mixed and incubated at 4°C for 25-30 min. This was followed by the addition of 700 µl of FACS buffer to each tube and centrifugation for 5 min at 1500 rpm at room temperature. The supernatants were then removed and 400 µl of FACS buffer was added then were acquired by flow cytometry as above (section 2.10.2).

2.12 Detection of the secretion of cytokines by RCC cells following CD40 ligation

To detect cytokine secretion following CD40 ligation by a) mCD40L or b) soluble agonist, both RCC and HRPT cells were a) co-cultured at density of $5x10^4$cells/well with $6x10^4$cells/well of growth-arrested 3T3-CD40L and 3T3-Neo in 24 well plates as described in section 2.8.1 or b) treated with 10µg/ml of cross-linked agonistic anti-CD40 antibody G28-5 ($5x10^4$ cells/well were seeded in 24 well plates) as described in section 2.7.

Cell culture supernatants were collected at specified time points post receptor ligation (1.5, 3, 6, 12, 24, 36 and 48 h). Supernatants were, centrifuged to remove any debris and 100µl was added to each Eppendorf tube and kept in -80°C. The concentration of IL-6, IL-8 and granulocyte-macrophage colony stimulating factor (GM-CSF) following receptor engagement was determined by ELISA-based or membrane-array techniques as described in the following sections. Table 2.5 lists all cytokine detection kits (both ELISA- and filter array-based).

Table 2.4 Cytokine detection kits

List of ELISA kits and human cytokine array that used in this study, with their the supplier and catalogue number

Cytokines	Cat. No.	Supplier
Human cytokine array panel A	ARY005	R&D Systems
Quantikine ELISA Human GM-CSF	DGM00	R&D Systems
Human CXCL8/IL-8 ELISA	DY208-05	R&D Systems
Human IL-6	DY206-05	R&D Systems

2.12.1 GM-CSF detection

The human Granulocyte Macrophage Colony Stimulating Factor (GM-CSF) detection kit (Table 2.5) was used to measure GM-CSF released in culture supernatants prepared as above (section 2.12).

The assay was performed according to the manufacturer's instructions, optical density was measured spectrophotometrically at 450 nm. For cytokine quantification, a stock standard solution was used to construct an 8-point standard curve with a 0-500pg/ml range (0, 7.8, 15.6, 31.3, 62.5, 125 and 500pg/ml) by 2-fold serial dilutions in calibrator diluent. The concentrated standard functioned as the highest standard (500 pg/ml) and the diluent reagent used as zero standard (0 pg/ml). The standard curve was created either on the FLUOstar plate reader software (MARS) that generated 4-parameter logistic (4-PL) curve fit or manually by using Microsoft Excel and plotting the mean absorbance for each standard on the x-axis against the concentrations on the y-axis. The concentration of cytokine in each sample then calculated by using a specific equation provided with the curve by Microsoft Excel (Appendix IIII).

2.12.2 IL-8 and IL-6 detection

The human CXCL8/IL-8 and IL-6 detection kits (Table 2.5) were used to measure release of the respective cytokines in culture supernatants prepared as above (section 2.12). Each well in microtiter plates was coated with 100 µl of diluted capture antibody for both IL-8 and IL-6 and incubated overnight at room temperature. Capture antibody was discharged and 3x wash with washing buffer were performed then 300 µl of

blocking buffer was added to each well and 1h incubation at room temperature was carried out. After the second wash, a 100 µl of samples, standards and control were added to the appropriate wells in the microtiter plates, plates then covered and incubated for 2 h. A third wash was performed, followed by the addition of 100 µl of diluted detection antibody, plates covered and 2h incubation was performed at room temperature. Washing was repeated for the fourth time and 100 µl of diluted secondary antibody (streptavidin-HRP) was added, followed by 20min incubation at room temperature away from light. A fifth wash then took place followed by the addition of 100 µl of substrate solution, 20 min incubation protected from light at room temperature was carried out. 50 µl of stop solution was added to stop the reaction. FLUOstar plate reader at 450 nm was used to estimate the optical density. For cytokine quantification, a stock standard solution was used to construct an 8-point standard curve with a, 0-600pg/ml range (0, 9.38, 18.8, 37.5, 75, 150, 300 and 600pg/ml) for IL-6 and 0-2000pg/ml (0, 31.3, 62.5, 125, 250, 500, 1000 and 2000pg/ml) for IL-8 by 2-fold serial dilutions in reagent diluent. Undiluted standard served as the highest standard (600pg/ml) for IL-6 and (2000pg/ml) for IL-8 and diluent only served as zero standard (0pg/ml). The standard curve was created either on the FLUOstar plate reader software (MARS) that generated 4-parameter logistic (4-PL) curve fit or manually by using Microsoft Excel and plotting the mean absorbance for each standard on the x-axis against the concentrations on the y-axis. The concentration of cytokine in each sample then calculated by using a specific equation provided with the curve by Microsoft Excel (Appendix IIII).

2.12.3 The Human Cytokine Array panel A

The R&D Systems/Proteome profiler antibody arrays kit was used for the quantification of a panel of cytokines.

For washes and incubations of the nitrocellulose membranes (arrays) 4-well multi-dishes were used. 2 ml of Array buffer 4 (serves as a blocking buffer) was added to each well. Using forceps, membranes were removed from the protective sheets and the stamped identification number was cut using scissors. Membranes were placed in individual wells in the 4-well dishes containing array buffer and incubated for 1h on a rocking platform. Meanwhile, each culture supernatant sample was prepared by mixing 1 ml of supernatant with 0.5 ml of array buffer 4 and 15 µl of re-formed human cytokine array panel A detection antibody cocktail in separate tubes. The combination was incubated at room temperature for 1h. The array buffer 4 in the 4-well plates was replaced by sample/antibody mixtures and plates were incubated overnight at 2-8oC on a rocking platform. Then the membranes were washed 3x with 20 ml of 1x wash buffer in individual dish on a rocking platform for 10 min. The membranes were removed from the dish and the excess wash buffer drained by contact with filter paper. Membrane were then returned to the 4-well dishes containing diluted IRDye 800CW Streptavidin Ab diluted at 1/2000 in array buffer 5 (secondary Ab). The dish was incubated at room temperature on a rocking platform for 30 min. Another 3 time wash was carried out as described above, then each membrane was kept in separated dishes containing 1x wash buffer. Finally, visualisation was performed using an OdysseyTM Infra-red Imaging system (Li-Cor). Results were analysed by densitometry using image studio software and cytokine spot intensity readings were normalised according to the reference spots indicated by the human cytokine array coordinates (Appendix IIII).

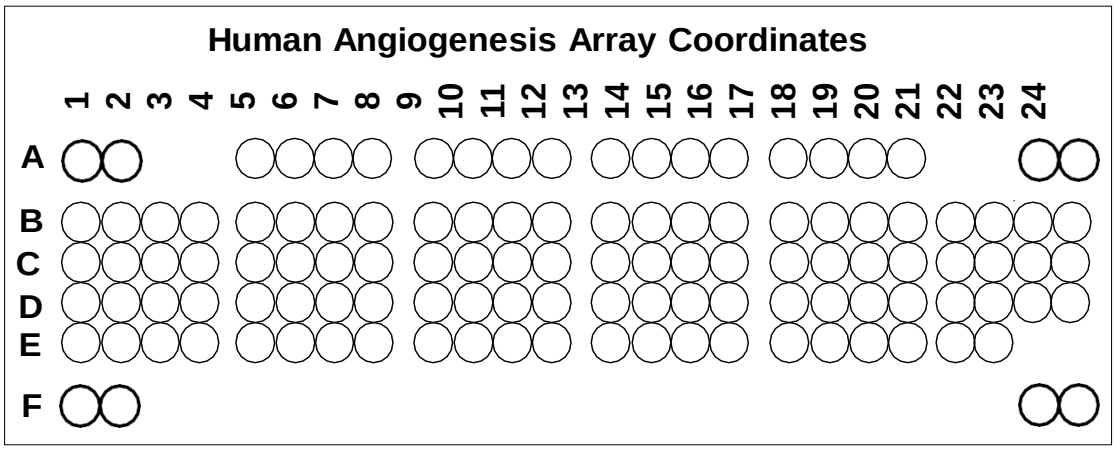

Figure 2.9 Illustrate the organization of cytokines spots for easy identification

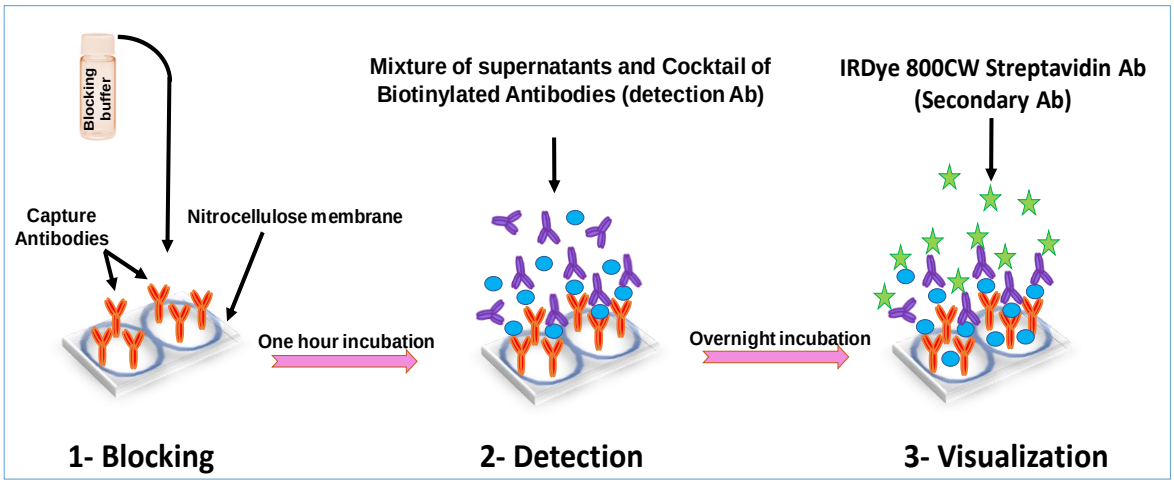

Figure 2.10 Principle of the membrane cytokine array kit

Nitrocellulose membranes contain a panel of cytokine detection 'spots' containing cytokine specific capture antibodies (two replicates for each cytokine). Membranes were incubated with diluted cell culture supernatants and a cocktail of biotinylated detection antibodies (sample/antibody mixture) overnight on rocking platform at 4**ºc**. Cytokines were captured (bound) by their cognate capture Abs on the membrane. Unbound materials were removed by washing (3x), after that the membranes were drained, and the streptavidin IRDye 800CW Ab (secondary Ab) was added. Following 30 min incubation on rocking platform at room temperature in dark, a second series of washes was performed and membranes were then visualized using an Odyssey™ Infra-red Imaging system (Li-Cor), to measure the amount of fluorescence released from each spot, the more fluorescence indicates the more cytokine intensity. Results were analysed by densitometry using either Li-Cor itself or by using the Image Studio software and the cytokine intensity were normalised according to the reference spots on each array.

2.14 Arithmetical investigation

Results analysis was carried out using Excel® (Microsoft) software. The standard error of mean (S.E.M.) was used for bar charts with error bars demonstrating ± the mean values of all repeats (minimum 5-6 practical repeats) are provided, Minitab 17 statistical software was used for statistical analysis. For comparison between two samples, Two-tailed, paired or unpaired T-tests were used and the means with levels of significance cited in the text (figure captions). Associations were expected to be biologically significant where $p<0.05$.

Chapter 3

Optimization of experimental techniques to investigate CD40-mediated apoptosis in RCC cells

3. Background

CD40 is a member of the TNFR superfamily identified initially as B cell specific receptor and as a bladder cancer-specific antigen (Albarbar et al., 2015). Later studies have shown that CD40 is expressed on a variety of cells hematopoietic and non-hematopoietic, normal and cancer cells including epithelial cells, endothelial cells, keratinocytes, smooth muscle cells and fibroblasts. The expression of CD40 can be stimulated by proinflammatory cytokines such as interleukin (IL) 1, 3 and 4, and particularly tumor necrosis factor alpha (TNF-α) and interferon gamma (IFN-ɣ). Its cognate ligand, CD40L (also known as CD154) is mainly presented on activated T-cells, but also on eosinophils, basophils, macrophages, dendritic cells, Natural Killer (NK) cells, B lymphocytes, platelets, mast cells, endothelial cells, smooth muscle cells and in some cases epithelial cells (Schönbeck and Libby, 2001).

It has been demonstrated that CD40 stimulation (ligation) can regulate tumour cell growth (Eliopoulos and Young, 2004, Tong and Stone, 2003). Furthermore, various studies have shown that growth inhibition can be mediated by soluble CD40 agonists in variety of carcinoma cells, reviewed in (Vonderheide, 2007, Tong and Stone, 2003). In general, soluble agonists produce weak pro-apoptotic or mainly growth inhibitory signals (Albarbar et al., 2015), but efficient pro-apoptotic signals can be triggered only in combination with pharmacological inhibitors or other cytotoxic compounds (Bugajska et al., 2002, Hess and Engelmann, 1996b, Afford et al., 2001, Dallman et al., 2003). Previous findings in our laboratory showed that the quality of the CD40 signal plays an important role in the functional outcome of CD40 ligation as mCD40L is a highly pro-apoptotic signal that induces extensive apoptosis in malignant cells but has no effect on their normal epithelial counterparts (Bugajska et al., 2002, Georgopoulos et al., 2006, Georgopoulos et al., 2007, Shaw et al., 2005, Hill et al., 2008, Dunnill et al., 2016).

The role of CD40 in renal cell carcinoma remains essentially unexplored. CD40 expression has been demonstrated in RCC tumours in vivo (Weiss et al., 2014) et al 2014) and CD40 expression by mouse and human RCC lines in vitro has been shown previously in two studies (Shorts et al., 2006, Lee et al., 2005). Expression of CD40 in RCC appears to be strongly associated with prolonged patient survival, although no relation was observed between CD40 expression and tumour stage (Weiss et al., 2014). In vitro induction of CD40 on mouse and human RCC cells triggered cytokine secretion, such as GM-CSF and IL-8, upregulation of costimulatory molecules, such as ICAM-1, and also up-regulated Fas expression (Lee et al., 2005). Furthermore, activation of CD40 in human RCC cells resulted in recruitment of monocytes and T cells into the tumour in vivo and increased the number of DC and caused reduction in tumour size (Shorts et al., 2006).

To date no systematic investigation on the effect of CD40 ligation on human RCC cells has been performed. The aim of this work was to provide for the first time detailed investigations into the role of CD40 stimulation in RCC cells by using different mode of CD40 ligation on RCC cells and to compare the effects of CD40 ligation in RCC cells versus their normal cell counterparts.

3.1 CD40 ligation using different methodologies and investigations into its biological effects in RCC cells

To understand the efficient role of CD40 ligation in RCC cells, a co-culture system was used where target (epithelial) cells were cultured with effector cells (fibroblasts expressing CD40L) in order to deliver membrane presented CD40L. These co-cultures were performed in 96-well plates for death assays, in 24-well plates for detection of cytokine secretion and in 10cm dishes for preparation of whole cell lysates and immunoblotting experiments.

Growth arrested effector cells (see section 2.7) were used to deliver the membrane CD40L (mCD40L) signal by co-culture with target RCC cells. The effector cells are murine fibroblasts (NIH3T3) derivatives previously characterised (Bugajska et al., 2002). Throughout this thesis effector cells displaying CD40L on their membrane are termed “3T3CD40L” cells or “mCD40L”. To ensure that 3T3CD40L cells retained CD40L expression (due to possible culture-related genetic drift) continuous culture in the presence of G418 antibiotic (0.5mg/ml) was performed (they expressed the neomycin resistance gene that was co-transfected as a part of the CD40L gene expression construct). Homologous NIH3T3 cells with a gene cassette conferring G418 resistance only were used as negative (background) controls and therefore from this point will be termed “3T3Neo” cells (or “Control” to compare with “mCD40L”) throughout this study. Finally, to investigate the importance of the role of CD40 signal quality on the functional outcome of CD40 ligation, receptor activation was also triggered using soluble agonist, the well characterised agonistic antibody G28-5 mAb (Bugajska et al., 2002).

3.3 Objectives

The objectives of this chapter were:

- To demonstrate detectable expression of CD40 receptor on the RCC cell lines employed in this study.
- To optimise and use a co-culture system for the detection of mCD40L-mediated apoptosis in renal cancer cells (RCCs) for a variety of experimental techniques.
- To optimise the co-culture system for CD40-mediated apoptosis detection using assays detecting loss of membrane integrity during apoptotic cell death (Cytotox-Glo), DNA fragmentation (DNA fragmentation ELISA) and effector caspase (3/7) detection (Sensolyte assay).
- To examine the effect of agonistic anti-CD40 antibody G28-5 mAb in RCC cells versus mCD40L.
- To investigate the effect of proinflammatory cytokines INF-ɣ and TNF-α on CD40 expression and also to test the ability of these cytokines to modulate CD40-mediated apoptosis.
- To carry out optimisation of immunoblotting techniques for epithelial cell protein detection using the co-culture system.

3.4 Confirmation of CD40 and CD40L expression

For this study, the well characterised RCC lines ACHN, 786-O and A-704 were used. Expression of CD40 was investigated by immunoblotting and flow cytometry (Figure 3.1 and Figure 3.2 respectively). CD40-positive colorectal cancer (CRC) HCT116 cells were used as positive control and CD40-negative SW480 cells were used as negative controls, respectively, for CD40 expression (Georgopoulos et al., 2006) in immunoblotting experiments (Figure 3.1). Another positive control used was the UCC line EJ when CD40 expression was detected by flow cytometry (Figure 3.2). Results using both techniques confirmed constitutive CD40 expression on the RCC cell lines. Moreover, adaptation from the original culture medium to DR5% medium (see section 2.6.5) did not affect the expression of CD40 on all RCC lines (Figure 3.1). These findings are in agreement with previous reports that showed expression of CD40 on ACHN, 786-O and A-704 cell lines (Shorts et al., 2006, Lee et al., 2005). Finally, flow cytometry confirmed expression of membrane CD40L on 3T3-CD40L effector cell surface while 3T3-Neo cells showed no CD40L expression (Figure 3.3) as previously (Bugajska et al., 2002, Georgopoulos et al., 2006, Dunnill et al., 2016).

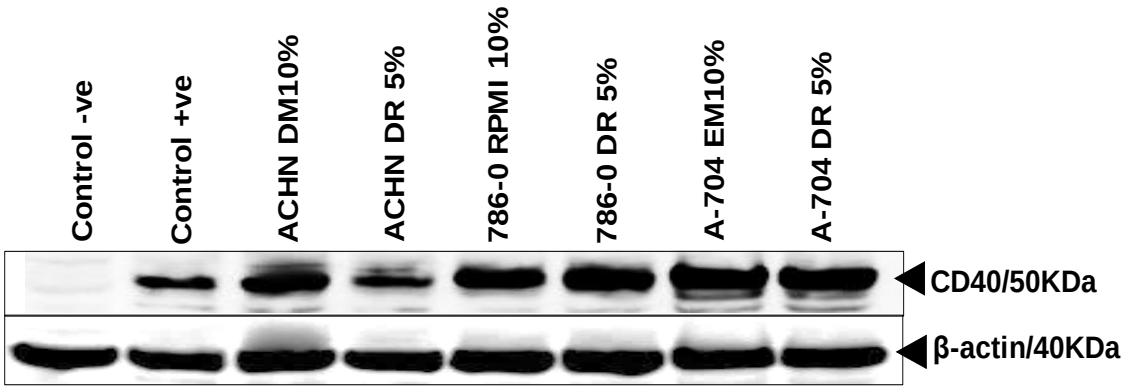

Figure 3.1 Detection of CD40 expression in RCC cells by Western blotting

RCC lines ACHN, 786-O and A-704 were cultured either in original medium and (after adaptation) in DR5% medium. Whole cell lysates were m as described in the Methods (Section 2.9.3) and 20µg of protein/well was analysed by immunoblotting (Section 2.9.5). After overnight incubation at 4ºC by rocking with primary antibody (CD40 H-10 mouse monoclonal IgG diluted 1:500), secondary antibody (goat-anti mouse IgG Alexa 680 dilution 1:10,000) was added and the membrane was incubated in the dark for 1h. For specifity and as a loading control, β-actin antibody was used (at 1:10,000 dilution) and incubation overnight at 4ºC, then the membrane was incubated with secondary antibody goat-anti mouse IgG Alexa 680 (diluted 1:10000) in the dark for 1h. Antibody binding was visualised at 700nm using a LI-COR Odyssey Infra-Red Imaging System and the image is shown in black and white. Lysates from HCT116 cell cultures were used as positive controls ('Control +ve') and from SW480 cell cultures as negative controls ('Control –ve').

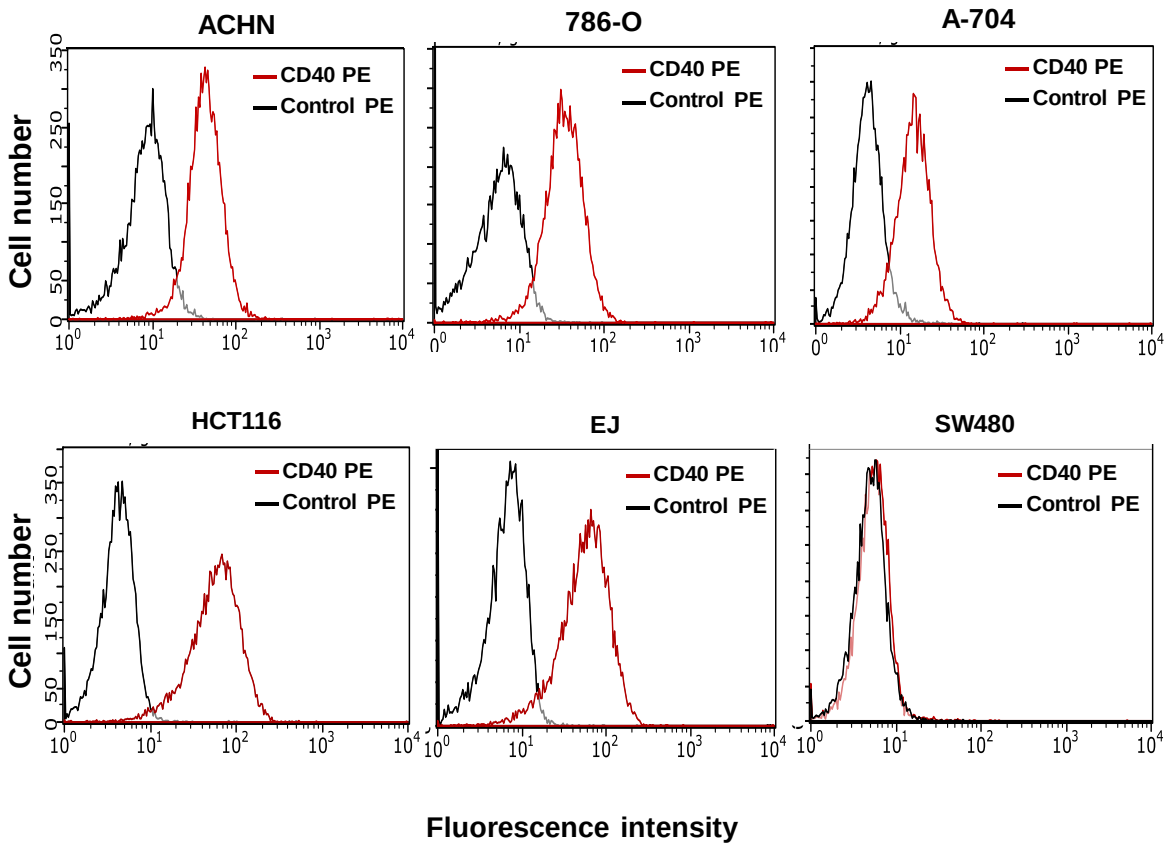

Figure 3. 1 Detection of CD40 expression by flow cytometry

Surface expression of CD40 on RCC lines (ACHN, 786-O and A-704), CRC HCT116 (positive control), SW480 (negative control) and UCC line EJ (positive control) was detected by flow cytometry (section 2.10.2). Cells were cultured until approximately 80% confluent, lifted, counted, washed and re-suspended in FACS buffer (0.25×10^5 cells/100µl), then cells were incubated for 30 min at 4ºC with PE-conjugated mouse anti-human CD40 Ab (CD40 PE), and a control PE-conjugated isotype-matched control Ab (Control PE). Cells were adjusted on a Guava EasyCyte flow cytometer and results interpreted using GuavaSoft software. Overlay histograms indicate the level of CD40 expression on all RCC cell lines (ACHN, 786-O and A-704), in comparison with the positive controls HCT116 and EJ, and the negative control SW480.

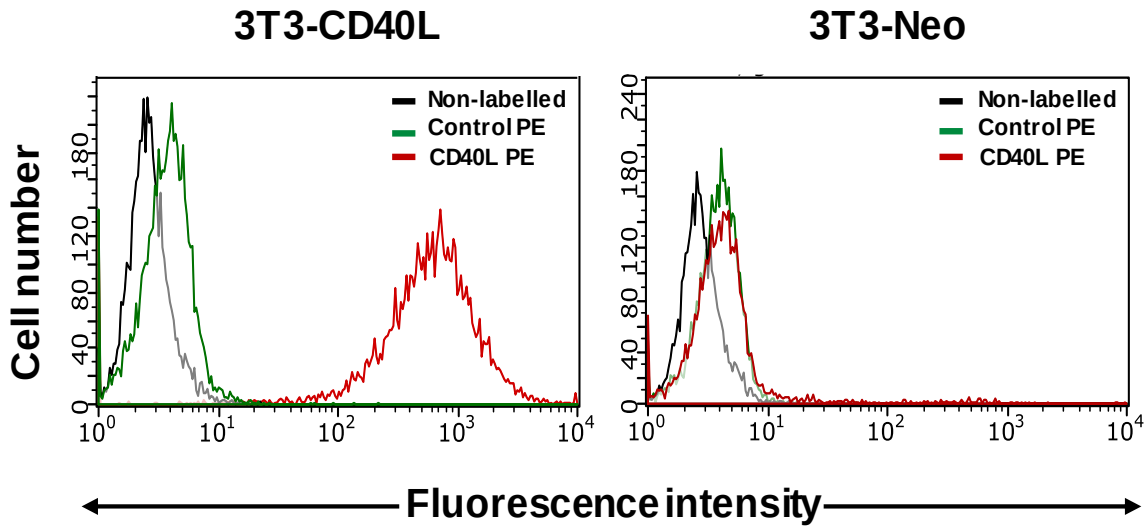

Figure 3.2 Flow cytometric analysis of CD40L expression by effector cells

Expression of CD40L on the surface of effector cells (3T3-Neo and 3T3-CD40L) was detected by flow cytometry (section 2.10). Following routine culture in DR10% medium until ~80% confluent, cells were lifted, counted, washed and re-suspended in FACS buffer (0.25×10^5 cells/100µl), then cells were incubated for 30 min at 4ºC with PE-conjugated mouse anti-human CD40L (CD40L PE), and a PE-conjugated isotype-matched control Ab (Control PE). Cells were adjusted on a Guava EasyCyte flow cytometer and results interpreted using GuavaSoft software. Unlabelled cells that were not incubated with antibody ('Non-labelled') were also acquired as additional controls.

3.5 The effect of pro-inflammatory cytokines on CD40 expression on RCC cells

In order to investigate the effect of INF-ɣ and TNF-α on CD40 expression, RCC cells were treated with INF-ɣ and TNF-α at concentrations of 10^2 and 10^3 units/ml for 48 h and were then examined for CD40 expression using flow cytometry. Treatment with 10^3 unit/ml of INF-ɣ showed more significant effect on CD40 expression than treatment with 10^3 unit/ml of TNF-α (Figure 3.4), while treatment with 10^2 unit/ml of both cytokines (IFN-ɣ and TNF-α) had either no or very little effect on CD40 expression (data not shown).

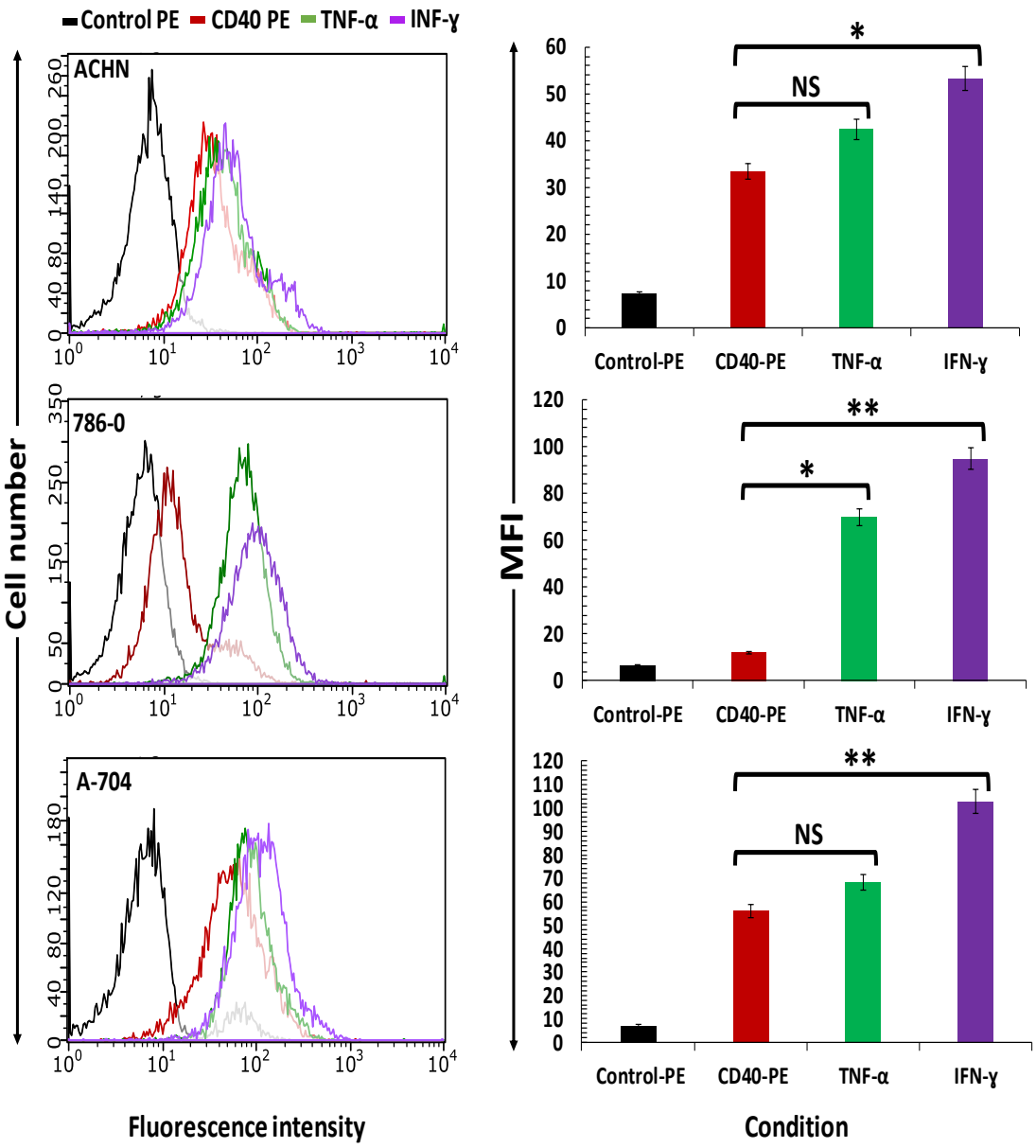

Figure 3.3 Effect of IFN-ɣ and TNF-α on CD40 expression by RCC cells

$5x10^4$ cells/well of RCC cells were cultured in 24-well plates in duplicate and incubated overnight before the culture medium was replaced with fresh medium containing 10^3 units/ml of INF-ɣ or TNFα. After cytokine treatment for 48 h, cells were harvested, counted, washed and re-suspended in FACS buffer ($0.25x10^5$ cells/100µl), followed by 30 min incubation at 4ºC with PE-conjugated mouse anti-human CD40 Ab (CD40 PE) and a control PE-conjugated isotype-matched control Ab (Control-PE). Cells were adjusted on a Guava EasyCyte flow cytometer and results interpreted using GuavaSoft software. Representative fluorescence histograms are shown on the left and median fluorescence intensity (MFI) also presented as bar graphs on the right. Bars represent mean values (MFI) ± SEM. Stats: ***, $p < 0.001$; **, $p<0.01$; *, $p<0.05$ and NS. non-significant, paired Student T-test.

3.6 Optimisation of apoptosis (Cytotox-Glo) assays for detection of mCD40L-mediated cell death

Based on previously published guidelines regarding the use of cell death assays for biological investigations (Galluzzi et al., 2009a), it is mentioned that minimum two independent analyses are used for the detection and demonstration of apoptotic cell death. The Georgopoulos group has previously used assays that a) involved use of radioactive precursors (e.g. JAM test of DNA fragmentation), b) did not permit high-throughput 96-well plate-based analysis (e.g. Annexin V/PI assays), or c) were not very sensitive (had a narrow dynamic range) (Bugajska et al., 2002, Georgopoulos et al., 2006, Shaw et al., 2005, Georgopoulos et al., 2007, Hill et al., 2008). One of the aims of this study was to employ assays that would address these issues and permit high throughput analysis. The assays optimised for the detection of CD40-mediated death were the CytoTox-Glo™ cytotoxicity assay and the Sensolyte™ Homogenous Caspase-3/7 assay (see Materials and Methods). In addition, a DNA fragmentation ELISA assay was also investigated for its sensitivity and practicality in this study.

The CytoTox-Glo assay, which can quantify cytotoxicity due to loss of membrane integrity, was carried out using the co-culture system and as described in section 2.8.4. An important consideration when using Cytotox-Glo for the co-culture system was that the relative luminescence (RLU) detected represents readings for both epithelial (target) cells and effector (3T3) cells. Therefore, 3T3-CD40L and 3T3-Neo cultures alone were included alongside (in addition to the experimental replicates of co-cultured cell populations) and any background attributed to the effector cells was accounted for by pair wise subtraction of RLU for cells cultured alone (3T3Neo and 3T3CD40L) from the RLU detected for the respective co-cultures. For example: RLU values from replicate 3T3-CD40L cultures were subtracted from the RLU of '3T3-CD40L/ACHN' (i.e. co-cultures of ACHN cells with 3T3-CD40L effectors) in a pairwise fashion, thus allowing the deduction of 'background-corrected' RLU. Similarly, '3T3-Neo/ACHN' co-culture RLU readings minus '3T3-Neo' RLU readings allowed background subtraction in control co-cultures. Finally, as the assay was extremely sensitive at detecting loss of cell viability, both effector and particularly target cells were harvested only during log phase growth to reduce any background death 'noise' (not shown).

Our group has demonstrated previously that mCD40L efficiently induces apoptotic death in carcinoma cells specially in UCC and CRC cells (Bugajska et al., 2002, Georgopoulos et al., 2006, Georgopoulos et al., 2007, Dunnill et al., 2016, Hill et al., 2008). This study was designed to investigate for the first time whether human RCCs are susceptible to mCD40L-mediated apoptosis. In order to determine the optimal cell density and apropriate time point to be used for RCC cell death detection using Cytotox-Glo, different numbers of RCC cells ($0.6x10^4$, $0.8x10^4$ and $1x10^4$ cells/well) were co-cultured with 3T3Neo and 3T3CD40L effectors for different time periods (24, 48 and 72 h). The effector cells were growth-arrested by treatment with Mitomycin C (MMC), to avoid artifacts of cell overgrowth, ; the effector cells were MMC-treated as optimised previously by our group (Georgopoulos et al., 2006, Georgopoulos et al., 2007) and seeded (at $1x10^4$ cells/well) first in multi-well plates before target cells were added (as detailed in the Methods – section 2.7).

Results shown in Figures 3.5, 3.6 and 3.7 demonstrate for the first time that mCD40L induced cell death in all 3 RCC cell lines. Although little detectable death was seen at 24 h, extensive cell death was detected by 48 h. No further increase in CD40 killing were detectable at 72 h. Moreover, these optimisation experiements demonstrated that the $0.8x10^4$ (cells/well) density was optimal for co-culture with $1x10^4$ (cells/well) effector cells for all RCC lines, thus the 1:0.8 ratio (effector:target) was adopted for further studies.

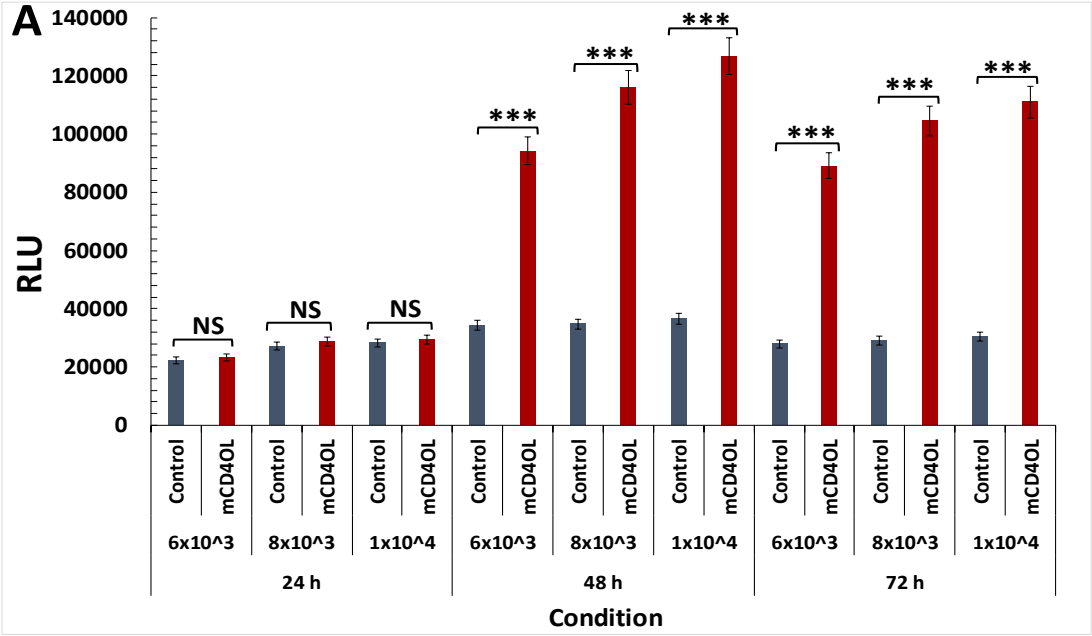

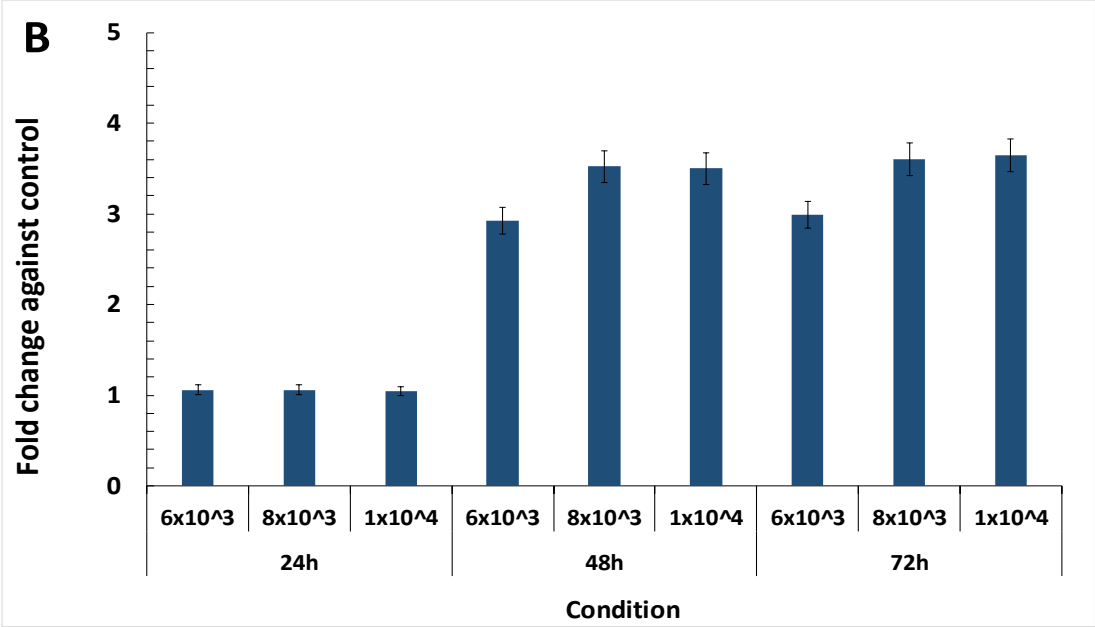

Figure 3.4 Determination of optimal cell density and time-point for apoptosis detection assays in ACHN cells

RCC cells ACHN were co-cultured at 0.6x10^4, 0.8x10^4 and 1x10^4 cells/well with 1x10^4 cells/well MMC-treated fibroblasts 3T3-CD40L and 3T3-Neo in white 96-well plates (as detailed in the Methods). Plates were incubated for 24, 48, and 72h and apoptosis was assessed by the Cytotox-Glo assay. 50µl of substrate was added to each well followed by 10 min incubation at room temperature. Luminescence was measured on a FLUOStar Optima plate reader and background-corrected relative luminescence units (RLU) were deduced by pair-wise subtraction of mCD40L and Control RLU from the respective co-cultures as described in Materials and Methods (and the text). **A)** Background corrected RLU readings for ACHN/3T3-CD40L (mCD40L) and ACHN/3T3-Neo (Control). Bars show mean of 4-6 technical replicates (RLU) ± SEM .Stats:. NS, non-significant; ***, $p<0.001$ paired student T-test. **B)** Results from graphs in A are also presented as fold change (mCD40L relative to control).

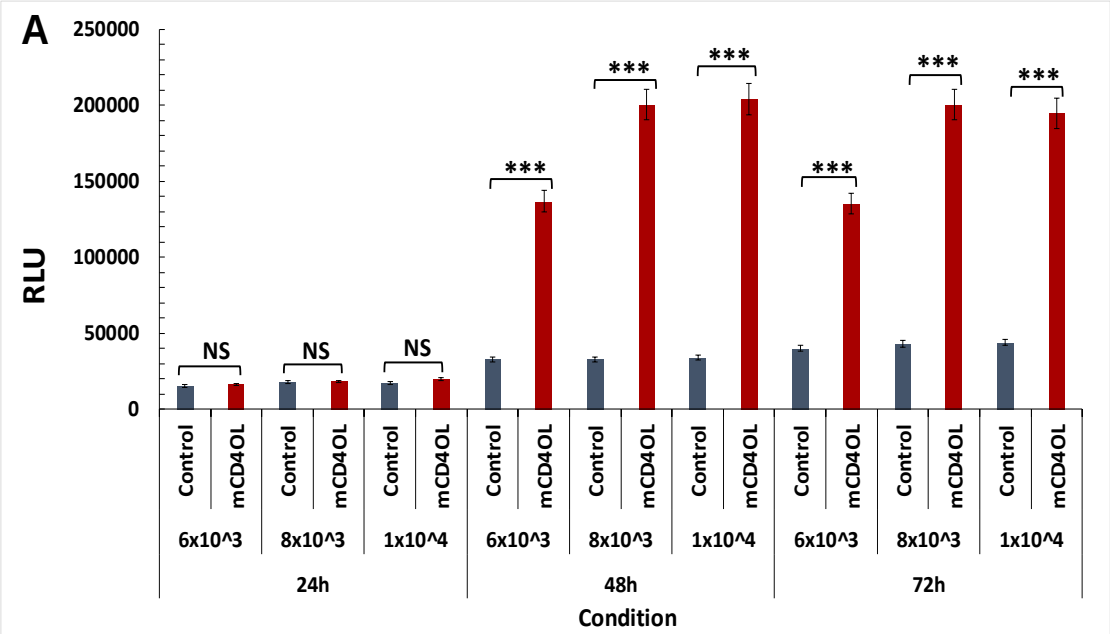

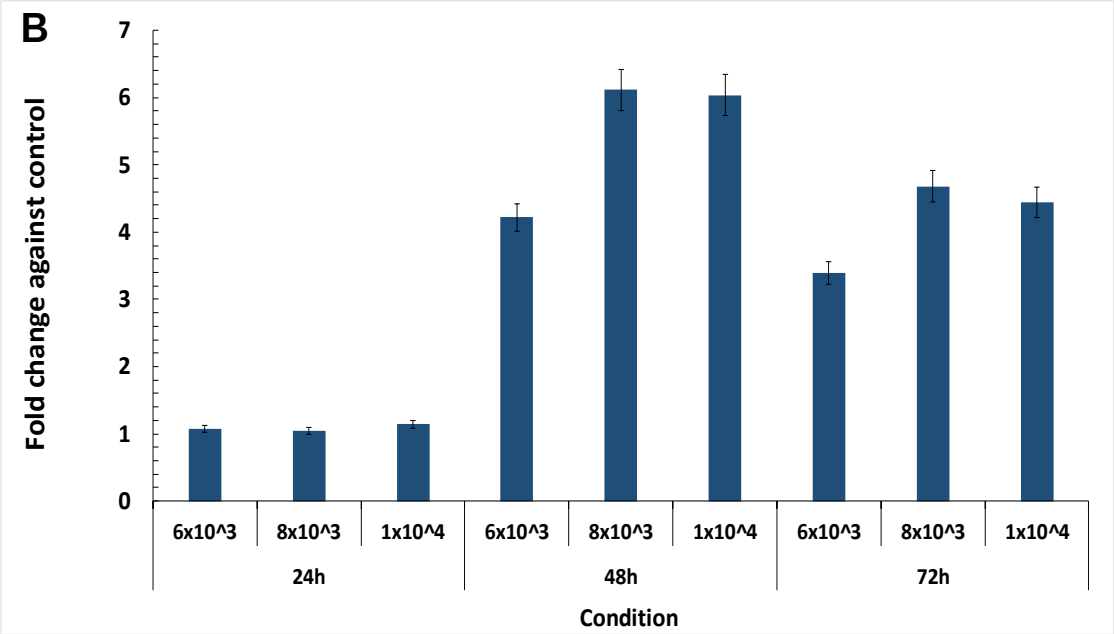

Figure 3.5 Determination of optimal cell density and time-point for apoptosis detection assays in 786-O cells

RCC cells 786-O were co-cultured at $0.6x10^4$, $0.8x10^4$ and $1x10^4$ cells/well with $1x10^4$ cells/well MMC-treated fibroblasts 3T3-CD40L and 3T3-Neo in white 96-well plates (as detailed in the Methods). Plates were incubated for 24, 48, and 72h and apoptosis was assessed by the Cytotox-Glo assay. 50µl of substrate was added to each well followed by 10 min incubation at room temperature. Luminescence was measured on a FLUOStar Optima plate reader and background-corrected relative luminescence units (RLU) were deduced by pair-wise subtraction of mCD40L and Control RLU from the respective co-cultures as described in Materials and Methods (and the text). **A)** Background corrected RLU readings for 786-O/3T3-CD40L (mCD40L) and 786-O/3T3-Neo (Control). Bars show mean of 4-6 technical replicates (RLU) ± SEM. Stats: NS. non-significant; ***, $p<0.001$ paired student T-test. **B)** Results from graphs in A are also presented as fold change (mCD40L relative to control).

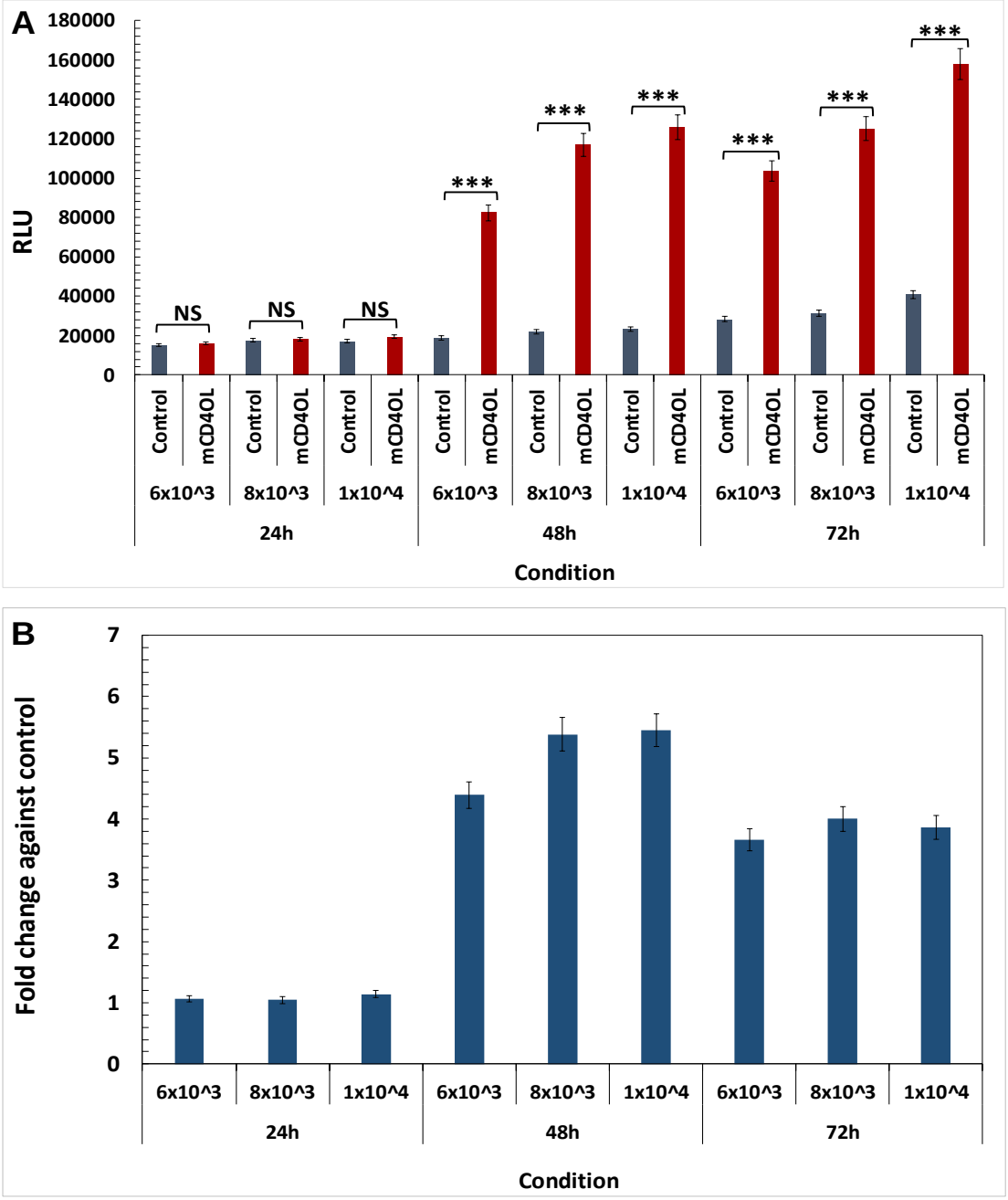

Figure 3.6 Determination of optimal cell density and time-point for apoptosis detection assays in A-704 cells

RCC cells A-704 were co-cultured at $0.6x10^4$, $0.8x10^4$ and $1x10^4$ cells/well with $1x10^4$ cells/well MMC-treated fibroblasts 3T3-CD40L and 3T3-Neo in white 96-well plates (as detailed in the Methods). Plates were incubated for 24, 48, and 72h and apoptosis was assessed by the Cytotox-Glo assay. 50µl of substrate was added to each well followed by 10 min incubation at room temperature. Luminescence was measured on a FLUOStar Optima plate reader and background-corrected relative luminescence units (RLU) were deduced by pair-wise subtraction of mCD40L and Control RLU from the respective co-cultures as described in Materials and Methods (and the text). **A)** Background corrected RLU readings for A-704/3T3-CD40L (mCD40L) and A-704/3T3-Neo (Control). Bars show mean of 4-6 technical replicates (RLU) ± SEM. Stats: NS. non-significant; ***, $p<0.001$ paired student T-test. **B)** Results from graphs in A are also presented as fold change (mCD40L relative to control).

As these Cytotox-Glo assays were being optimised, it became apparent that at times high background RLU arose from low level death of either target (epithelial) cells or the effector cells (particularly after MMC treatment), which at times interfered with the assay results and thus its sensitivity. Further experiments were performed that demonstrated that no such background interference was obtained when a) target cells were harvested in their log phase of growth, and b) effector cells (3T3-Neo and 3T3-CD40L) were MMC-treated to induce cell growth arrest only when they were at ~70% confluency. Such experimental modifications provided extremely consistent assay results indicating maximal induction of death at at 48h post-ligation. Moreover, it was found that the degree of cell death detected for RCC cells (particualrly 786-O) using this assay was closely comparable with the extent of apoptosis (for the same effector:target ratio and time-point) detected using the UCC line EJ, which has been extensively characterised in our laboratory for its response to CD40 ligation (Bugajska et al., 2002, Georgopoulos et al., 2006, Georgopoulos et al., 2007, Dunnill et al., 2016); EJ cells therefore served as a valuable positive control (Figure 3.8).

As shown in Figure 3.4, treatment of RCC cells with IFN-ɣ caused an increase in CD40 expression, therefore experiments were carried out to investigate whether this enhancement may affect (increase) the susceptibility of RCC cells to mCD40L-death. The presence of IFN-ɣ in co-cultures consistently caused a clear increase in cell death in all RCC cell lines, although the increase in cell death only reached statistical significance in A-704 and ACHN cells (not in 786-O cells) (Figure 3.9). These results are in agreement with previous findings in our laboratory on CRC cells, where an increase in mCD40L-mediated apoptosis by co-treatment with IFN-ɣ in some CRC cells was reported (Georgopoulos et al., 2007).

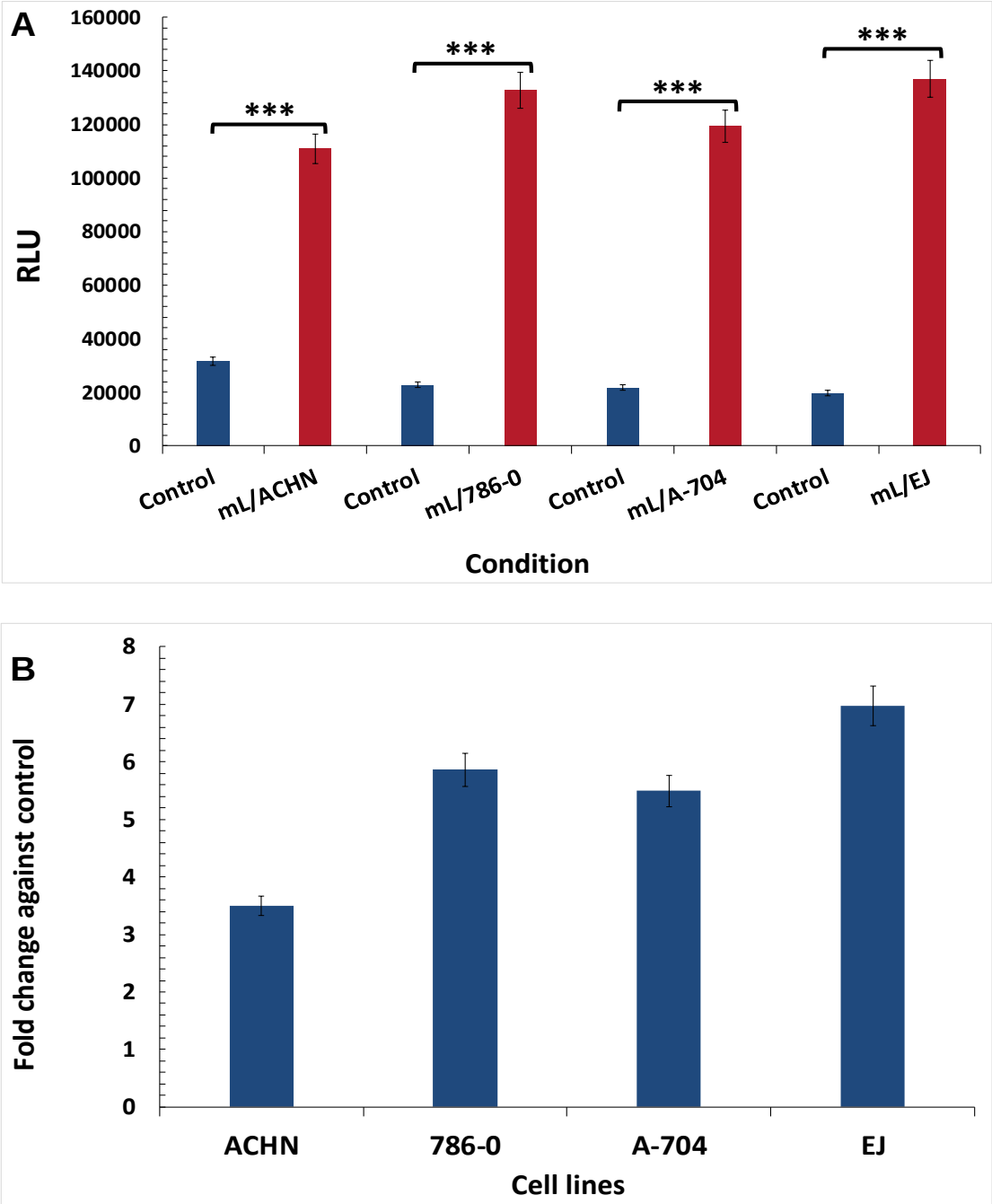

Figure 3.7 Optimal detection of mCD40L-mediated apoptosis in RCC cells

RCC (ACHN, 786-O and A-704) and UCC (EJ) cells were co-cultured at $0.8x10^4$ cells/well with $1x10^4$ cells/well MMC-treated fibroblasts 3T3-CD40L ('mL') and 3T3-Neo ('Control') in white 96-well plates. Plates were incubated for 48 h and cell death was assessed by the Cytotox-Glo assay. 50µl of substrate was added to each well followed by 10 min incubation at room temperature. Luminescence was measured on a FLUOStar Optima plate reader and background-corrected relative luminescence units (RLU) were deduced by pair-wise subtraction of mL and Control RLU from the respective co-cultures (as described in the Methods). **A)** Background corrected RLU readings for co-cultures ACHN, 786-O, A-704 and EJ/3T3-CD40L (mL) and respective 3T3-Neo co-cultures (Control). Bars show mean of 4-6 technical replicates (RLU) ± SEM. Stats: ***, $p<0.001$ paired Student T-test. **B)** Results from graphs in A are also presented as fold change of mCD40L treatment (mL) relative to Control).

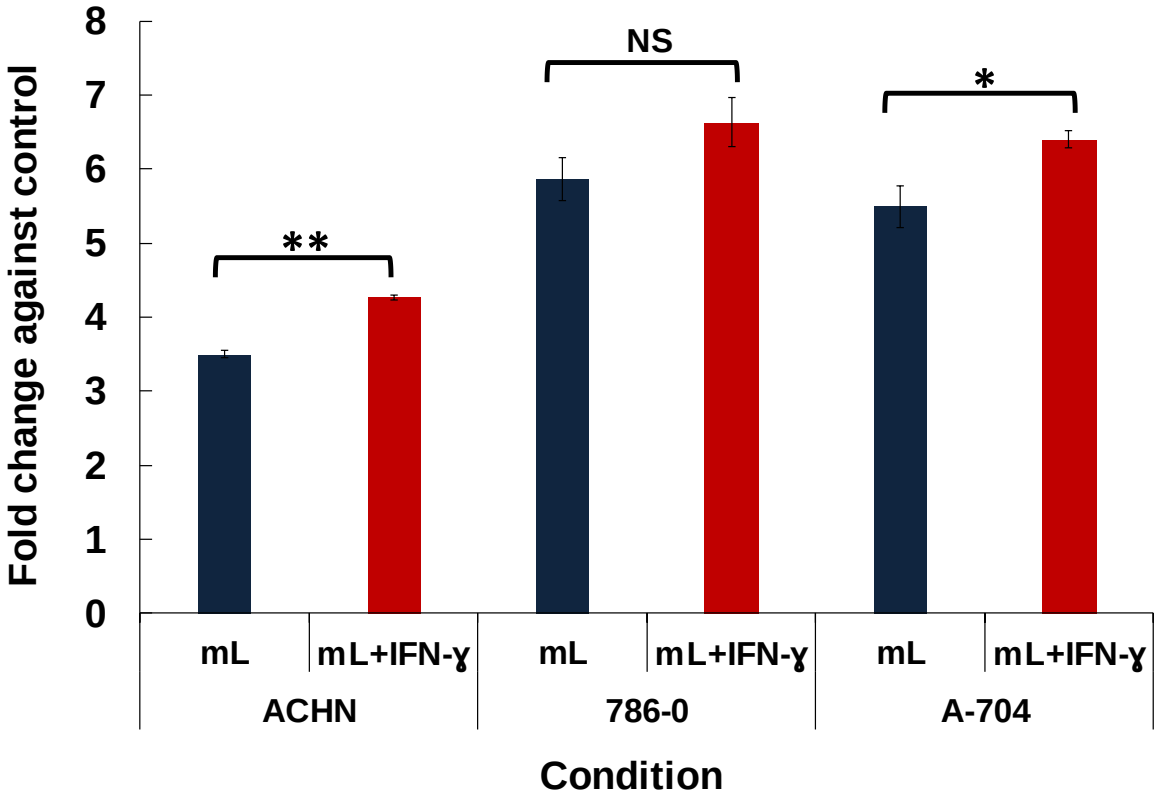

Figure 3.8 Regulation of mCD40L-induced death in RCC cells by IFN-ɣ

RCC cells (ACHN, 786-O and A-704) were co-cultured at $0.8x10^4$ cells/well with$1x10^4$ cells/well MMC treated fibroblasts 3T3-CD40L and 3T3-Neo in whit 96 well plates ± 10^3 U/ml of IFN-ɣ . Plates were incubated for 48h at and apoptosis was assessed by Cytotox-Glo assay. 50µl of substrate was added to each well followed by 10 min incubation at room temperature. FLUOSar Optoma plate reader was used to measure the luminescence and background-corrected relative luminescence units (RLU) were deduced by pair-wise subtraction of mCD40L and Control RLU from the respective co-cultures as described in Materials and Methods (and the text). . Bars show mean fold change of RLU of 4-5 technical replicates ± SEM . Stats: NS. Non-significant; **, P<0.01, and *, p<0.05 paired Student T-test, co-culture for each cell line (mL) compared with its co-culture plus IFN-ɣ (mL+IFN-ɣ).

3.7 The role of CD40 signal 'quality' (degree of receptor cross-linking) in apoptosis: effect of agonistic anti-CD40 antibody G28-5 in RCC cells

It has previously been shown that the degree of receptor cross-linking determines the functional outcome of CD40 ligation in carcinoma cells (Albarbar et al., 2015). Previous reports have demonstrated that agonistic anti-CD40 antibody can inhibit tumour growth (Sotomayor EM1, 1999, Diehl et al., 1999, French et al., 1999), whilst clinical use of CD40 agonists such as the mAb CP-870,893 and SGN-40 were associated with partial responses in melanoma and multiple myeloma patients (Khalil and Vonderheide, 2007, Vonderheide et al., 2006). In vitro, CD40 agonists such as anti-human CD40 Ab ChiLob7/4 can cause growth inhibition in epithelial lines and human malignant lymphoma, and activity was associated with up-regulation of co-stimulatory molecules in a culture system of dendritic cells (Chowdhury et al., 2014, Geldart et al., 2004). A much better characterised agonistic anti-CD40 antibody is the G28-5 mAb. This can induce growth inhibition in carcinoma cells but little apoptosis can be observed even when protein synthesis is inhibited by cycloheximide; Ab cross-linking by secondary antibody (goat anti mouse IgG) did not significantly enhance the capacity of G28-5 to induce apoptosis in UCC or CRC cells (Georgopoulos et al., 2006, Afford et al., 1999). Even though G28-5 mAb can induce cytokine secretion, the repertoire of cytokines released differs from that triggered by membrane presented agonist as shown by ourselves in carcinoma cells (Georgopoulos et al., 2007) and by others in B cells (Baccam and Bishop, 1999). The importance of receptor cross-linking in rendering the CD40 signal apoptotic was demonstrated when it was shown that an efficient apoptotic signal was induced in carcinoma cells (UCC line EJ) when the G28-5 agonist was presented on the surface of mouse L fibroblasts transfected to express the Fcɣ receptor CD32 (Bugajska et al., 2002, Georgopoulos et al., 2006).

To investigate whether the signal 'quality' (extent of receptor cross-linking) was critical in RCC cell apoptosis, too, G28-5 mAb was used in this study and compared for its ability to induce cell death in comparison with membrane presented CD40L (mCD40L). Therefore, RCC cells were either treated with mCD40L (co-culture) or treated with G28-5 mAb. Results showed that agonistic anti CD40 antibody G28-5 did not induce

apoptosis in all cell lines at 3 time-points tested in comparison to mCD40L which consistently induced extensive cell death at 48h and 72h. (Figures 3.10, 3.11 and 3.12). Moreover, the presence of 10^3 U/ml of IFN-ɣ in cultures of RCC cells treated with G28-5 mAb did not significantly alter (enhance) the ability of the agonist to induce apoptosis in RCC cells after 48h (Figure 3.13).

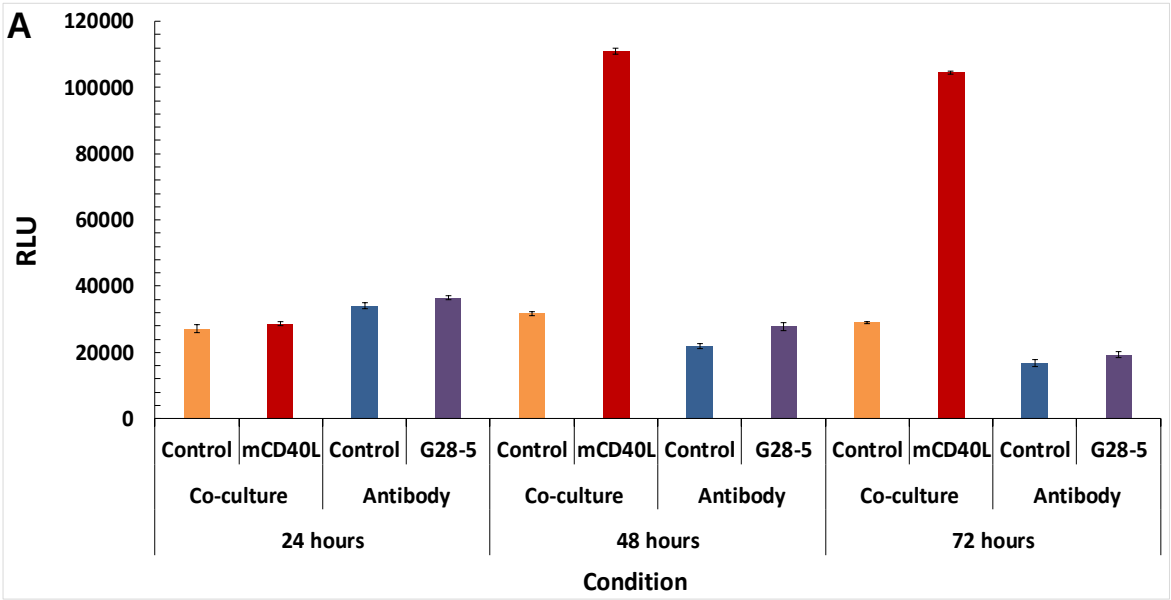

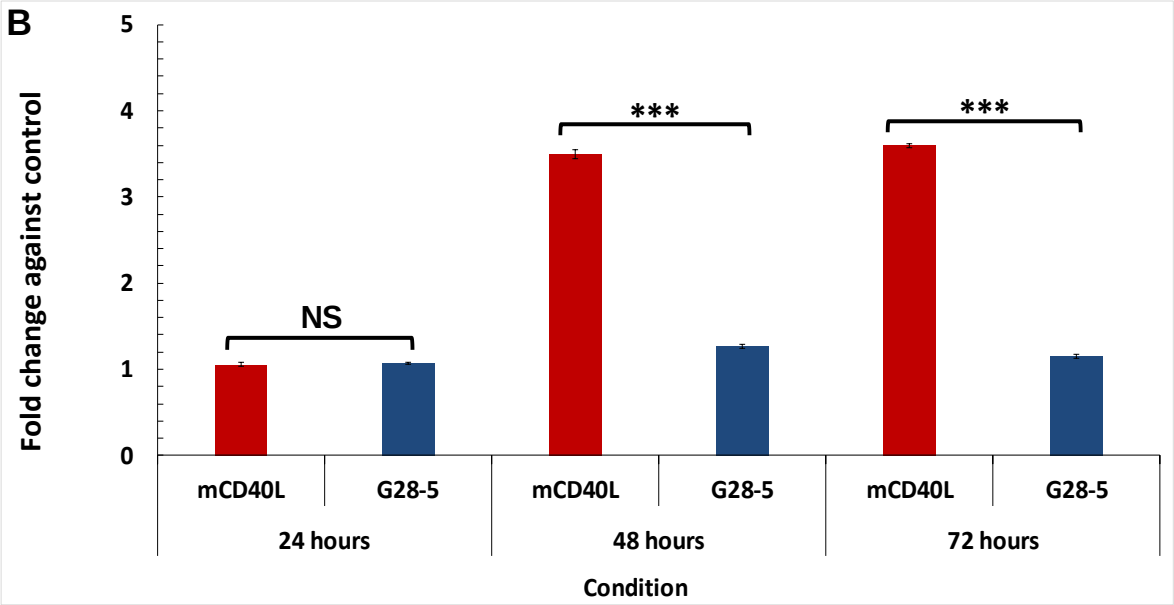

Figure 3.9 Effect of agonistic G28-5 mAb in ACHN cells

ACHN cells at a density of $0.8x10^4$ cells/well were either co-cultured with $1x10^4$ cells/well 3T3Neo (Control) or 3T3CD40L (mCD40L) or treated with 10µg/ml of G28-5 mAb cross-linked with 2.5µg/ml goat anti-mouse Ig in white 96-well plates (untreated cells served as non-treated Controls). The plates were incubated for 24h, 48h and 72h before cell death was assessed by adding 50µl of CytoTox-Glo assay substrate to each well followed by 10 min incubation at room temperature. FLUOStar Optima plate reader was used to measure the luminescence and for co-cultures background-corrected relative luminescence units (RLU) were deduced by pair-wise subtraction of mCD40L and Control RLU from the respective co-cultures (see Methods). **A)** Background corrected RLU readings for ACHN/3T3-CD40L (mCD40L) and ACHN/3T3-Neo (Control) are indicated as 'Co-culture' and treatment with G28-5 as 'Antibody'. Bars show mean of 4-6 technical replicates (RLU) ± SEM. **B)** Results from graphs in A are also presented as fold increase (mCD40L relative to control for co-cultures and G28-5 relative to untreated cells). Bars show mean fold change Stats: ***, $p<0.001$; NS, non-significant ($p>0.05$).

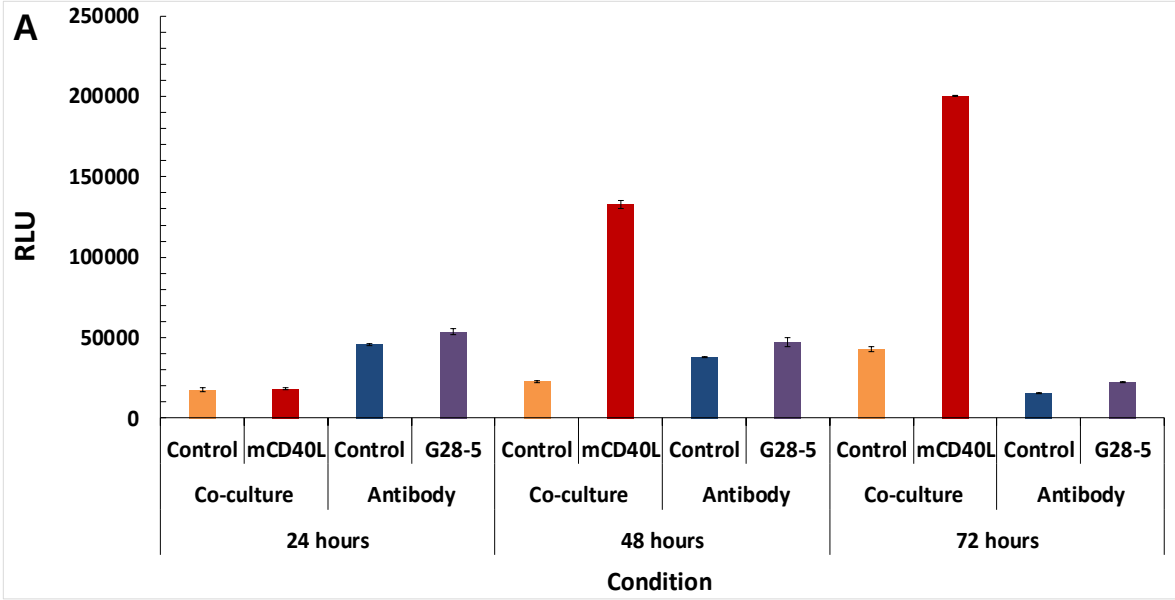

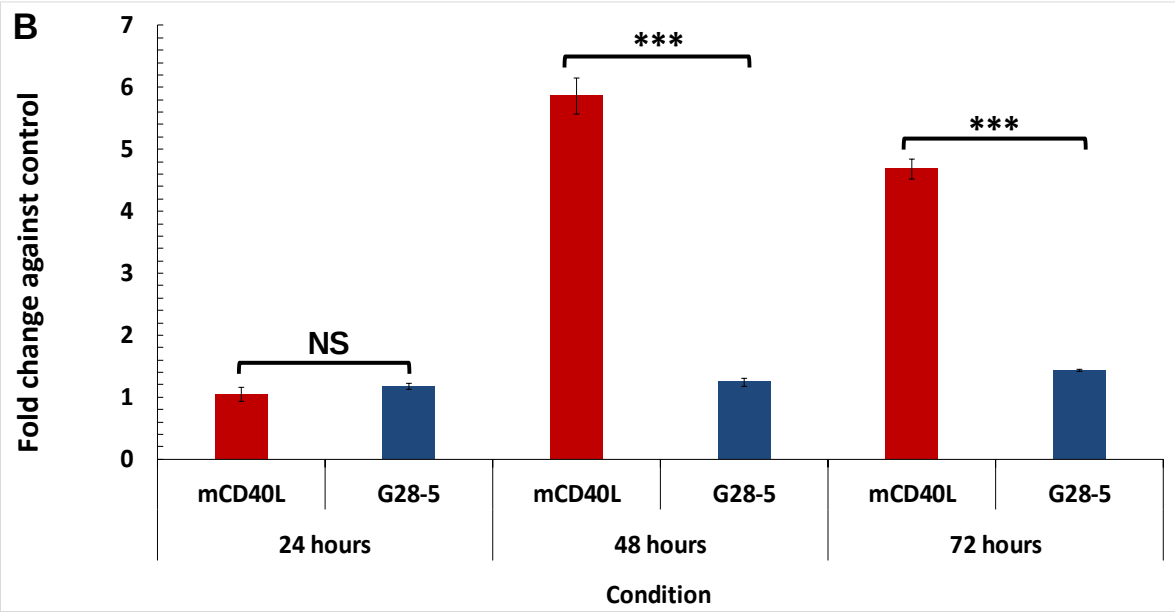

Figure 3.10 Effect of agonistic G28-5 mAb in 786-O cells

786-O cells at a density of $0.8x10^4$ cells/well were either co-cultured with $1x10^4$ cells/well 3T3Neo (Control) or 3T3CD40L (mCD40L) or treated with 10µg/ml of G28-5 mAb cross-linked with 2.5µg/ml goat anti-mouse Ig in white 96-well plates (untreated cells served as non-treated Controls). The plates were incubated for 24h, 48h and 72h before cell death was assessed by adding 50µl of CytoTox-Glo assay substrate to each well followed by 10 min incubation at room temperature. Luminescence was measured on a FLUOStar Optima plate reader and for co-cultures background-corrected relative luminescence units (RLU) were deduced by pair-wise subtraction of mCD40L and Control RLU from the respective co-cultures (see Methods). **A)** Background corrected RLU readings for 786-O/3T3-CD40L (mCD40L) and 786-O/3T3-Neo (Control) are indicated as 'Co-culture' and treatment with G28-5 as 'Antibody'. Bars show mean of 4-6 technical replicates (RLU) ± SEM. **B)** Results from graphs in A are also presented as fold increase (mCD40L relative to control for co-cultures and G28-5 relative to untreated cells). Bars show mean fold change Stats: ***, $p<0.001$; NS, non-significant ($p>0.05$).

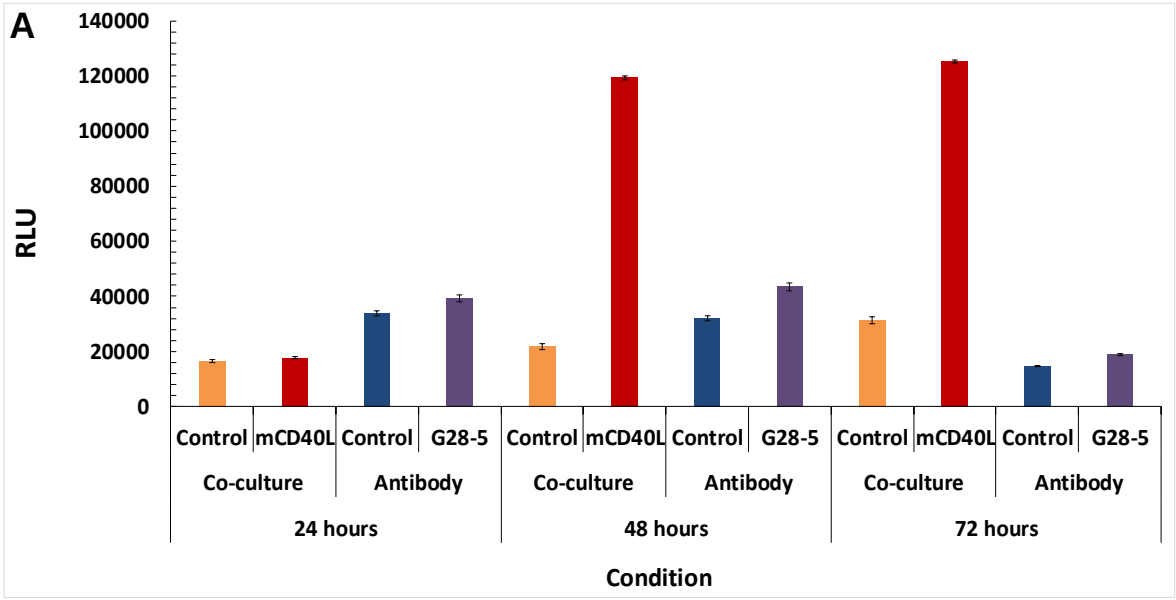

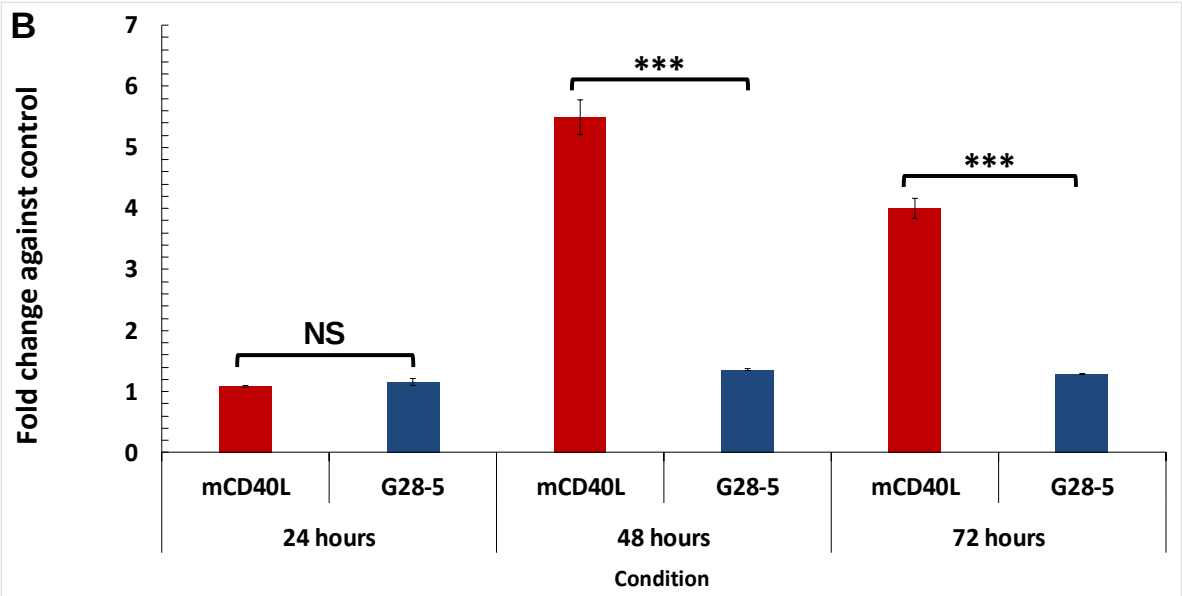

Figure 3.11 Effect of agonistic G28-5 mAb in A-704 cells

A-704 cells at a density of $0.8x10^4$ cells/well were either co-cultured with $1x10^4$ cells/well 3T3Neo (Control) or 3T3CD40L (mCD40L) or treated with 10µg/ml of G28-5 mAb cross-linked with 2.5µg/ml goat anti-mouse Ig in white 96-well plates (untreated cells served as non-treated Controls). The plates were incubated for 24h, 48h and 72h before cell death was assessed by adding 50µl of CytoTox-Glo assay substrate to each well followed by 10 min incubation at room temperature. FLUOStar Optima plate reader was used to measure the luminescence and for co-cultures background-corrected relative luminescence units (RLU) were deduced by pair-wise subtraction of mCD40L and Control RLU from the respective co-cultures (see Methods). **A)** Background corrected RLU readings for A-704/3T3-CD40L (mCD40L) and A-704/3T3-Neo (Control) are indicated as 'Co-culture' and treatment with G28-5 as 'Antibody'. Bars show mean of 4-6 technical replicates (RLU) ± SEM. **B)** Results from graphs in A are also presented as fold increase (mCD40L relative to control for co-cultures and G28-5 relative to untreated cells). Bars show mean fold change Stats: ***, $p<0.001$; NS, non-significant ($p>0.05$).

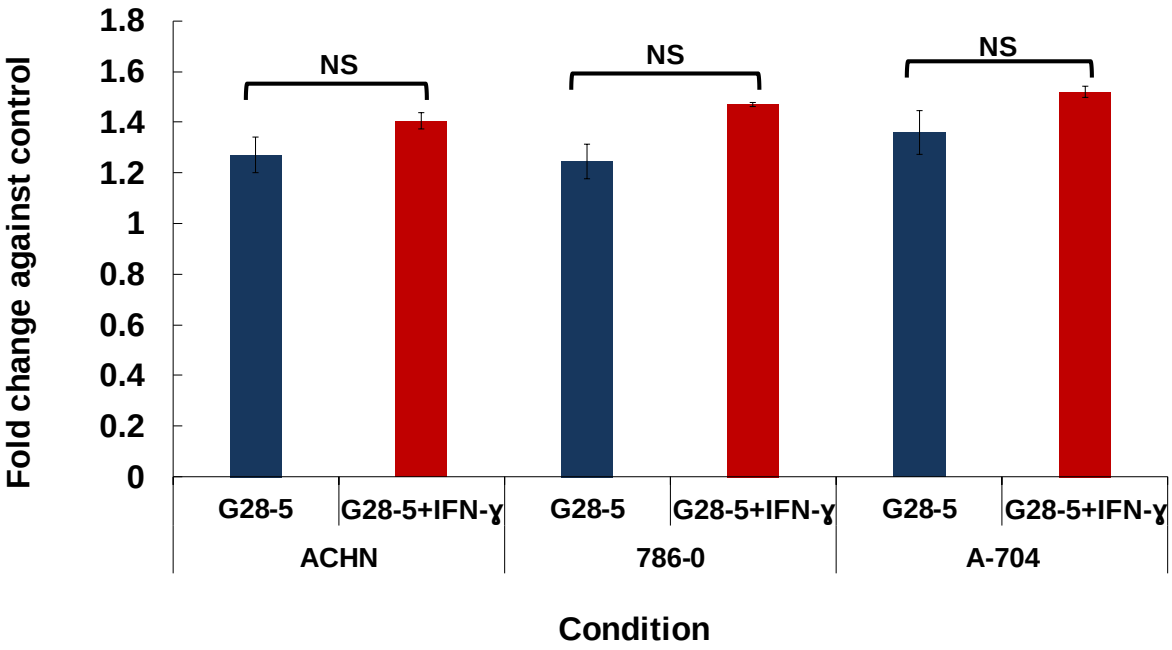

Figure 3.12 Treatment of RCC cells with G28-5 mAb in the presence of IFN-ɣ

ACHN, 786-O and A-704 cell lines were seeded at a density of $0.8x10^4$ cells/well and treated with 10µg/ml of G28-5 mAb cross-linked with 2.5µg/ml goat anti-mouse Ig ± 103 U/ml of IFN-ɣ in white 96-well plates. The plates were incubated for 48h before cell death was assessed by adding 50µl of CytoTox-Glo assay substrate to each well followed by 10 min incubation at room temperature. Luminescence was measured on a FLUOStar Optima plate reader. Bars show mean fold change of 4-5 technical replicates ± SEM. Stats: NS. Non-significant paired student T-test. Culture of each cell line treated with G28-5 indicated (G28-5) and compared with compared with its corresponding culture in presence of IFN-ɣ (mL + IFN-ɣ).

-

3.8 Detection of caspase-3/7 activity following CD40 ligation in RCC cells (SensoLyte assay)

Although caspases -3 and -7 are both effector caspases and demonstrate structural similarities, they exhibit slightly different functionalities. Caspase-3 is involved in the process of DNA fragmentation as well as in morphological changes of apoptosis, while a minor role has been shown for caspase-7 in this process (Saquib A. Lakhani and Booth, 2006). Moreover, although caspases -3 and -7 do exhibit some overlapping substrate preferences, these proteases are non-redundant and do show distinct activity towards certain substrates (Cullen and Martin, 2009). Previous studies in our laboratory have reported activation of caspase-3/-7 in UCC and CRC cells within 48h after CD40 ligation (Georgopoulos et al., 2006, Dunnill et al., 2016). Interestingly, in CRC cells the activation of caspases 3/7 was sustained and was even slightly higher at 72h of co-culture (Mohamed, 2014).

To determine caspase-3/7 activity following CD40 ligation by mCD40L in RCC cells, ACHN, 786-O and A-704 cells were co-cultured with effector cells (as above) for 24, 48 and 72h and caspase activity determined using the SensoLyte® Assay (Methods section 2.8.3.1). For the calculation of results from these fluorescence-based assays, the same principle as in the CytoTox-Glo assays was followed (Section 3.4.1), which involved a) appropriate calculations for background 3T3 cell-related fluorescence readings and b) the optimisation of target cell ‘health’ and effector cell MMC treatment (detailed in Sections 3.6).

Results from such experiments demonstrated for the first time that mCD40L triggered rapid activation of caspase 3/7 activity as early as 24h post-ligation (Figure 3.14), which was more marked and extensive at 48h (Figure 3.15) and further elevated at 72h (Figure 3.16) post CD40 ligation by mCD40L. Therefore, the results from these caspase detection experiments not only corroborated the Cytotox-Glo assay data (above) which demonstrated that CD40 ligation induces extensive cell death in RCC cells, but also provided evidence that mCD40L-mediated RCC cell death is apoptotic.

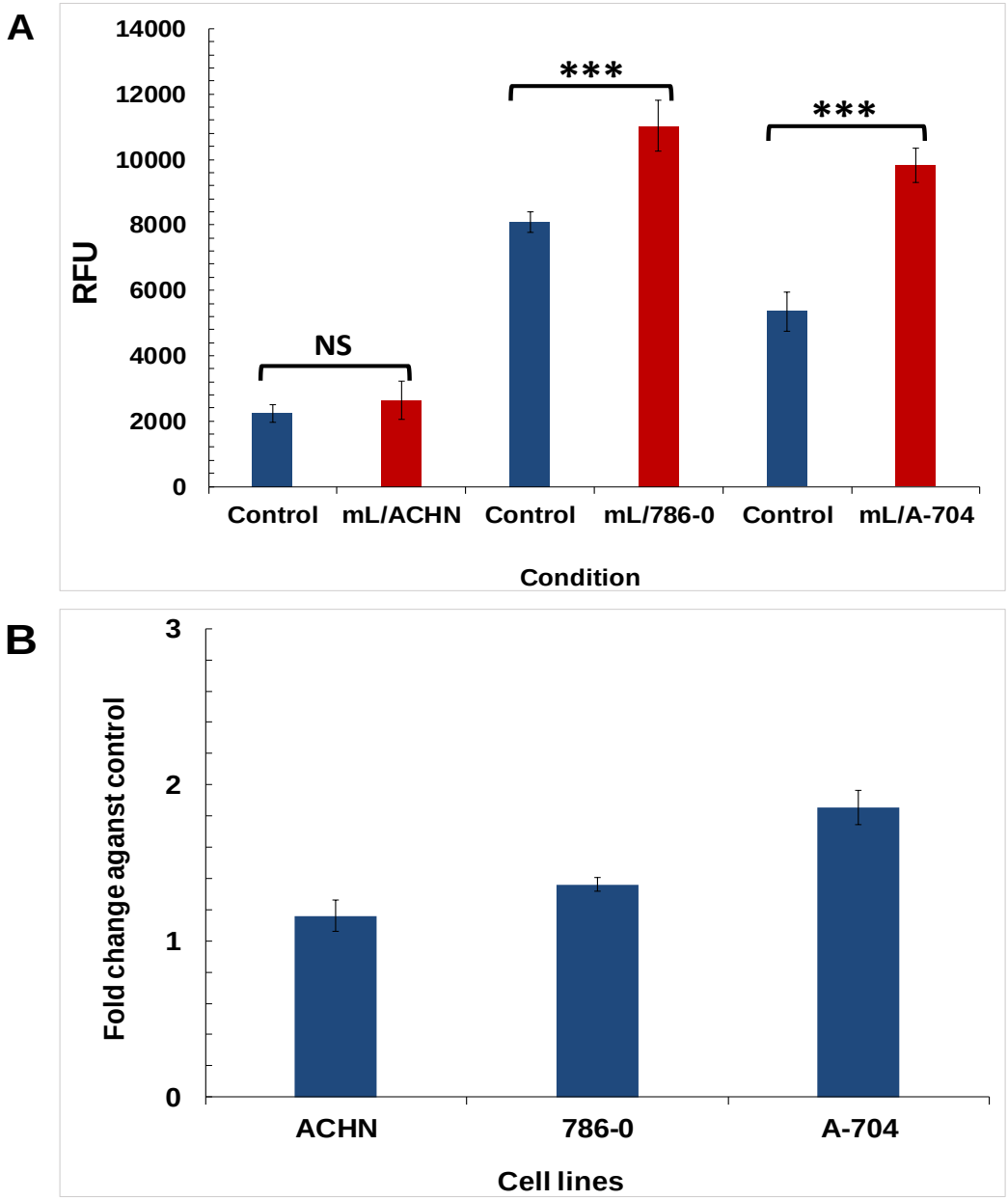

Figure 3.13 Detection of caspase 3/7 activity at 24 h post CD40 ligation

ACHN, 786-O and A-704 were co-cultured at $0.8x10^4$ cells/well with 1x104 cells/well MMC-treated fibroblasts 3T3-CD40L (mL) and 3T3-Neo (Control) in white 96-well plates. Plates were incubated for 24h and caspase activity assessed by the SensoLyte® Assay. 50µl of assay substrate was added to each well followed by 90 min incubation at room temperature in the dark. Fluorescence was measured on a FLUOStar Optima plate reader (as detailed in the Methods) and background-corrected relative fluorescence units (RFU) were deduced by pair-wise subtraction of mCD40L and Control RFU from the respective co-cultures (as described in the text). A) Background corrected RFU readings for co-cultures ACHN, 786-O and A-704/3T3-CD40L (mL) and respective 3T3-Neo co-cultures (Control). Bars show mean RFU of 4-6 technical replicates ± SEM and results are representative of three experiments. Stats: ***, $p<0.001$; NS, non-significant ($p>0.05$) paired student T-test. B) Results from graphs in A are also presented as fold change (mCD40L relative to control).

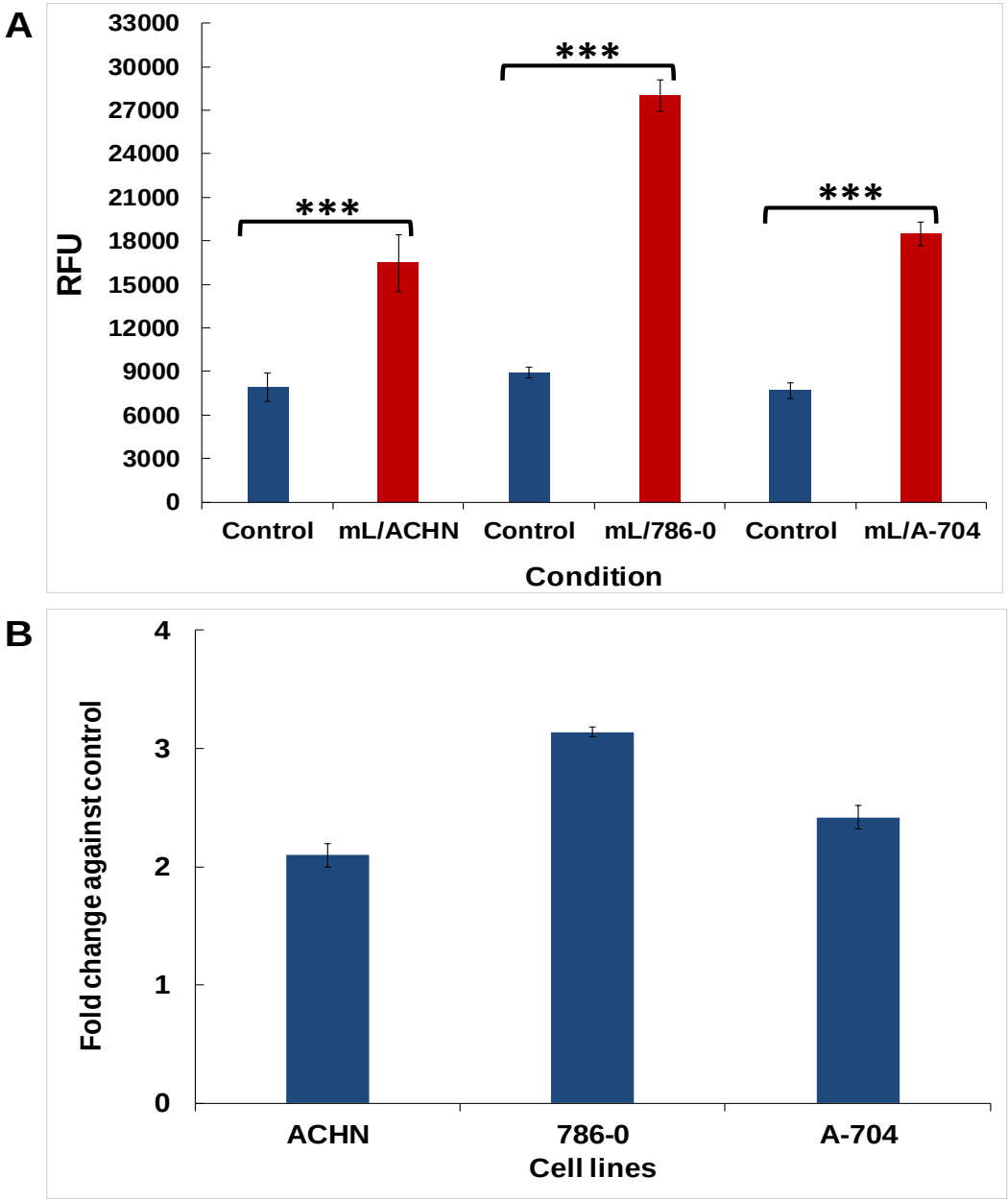

Figure 3.14 Detection of caspase 3/7 activity at 48 h post CD40 ligation

ACHN, 786-O and A-704 were co-cultured at $0.8x10^4$ cells/well with 1x104 cells/well MMC-treated fibroblasts 3T3-CD40L (mL) and 3T3-Neo (Control) in white 96-well plates. Plates were incubated for 48h and caspase activity assessed by the SensoLyte® Assay. 50µl of assay substrate was added to each well followed by 90 min incubation at room temperature in the dark. Fluorescence was measured on a FLUOStar Optima plate reader (as detailed in the Methods) and background-corrected relative fluorescence units (RFU) were deduced by pair-wise subtraction of mCD40L and Control RFU from the respective co-cultures (as described in the text). **A)** Background corrected RFU readings for co-cultures ACHN, 786-O and A-704/3T3-CD40L (mL) and respective 3T3-Neo co-cultures (Control). Bars show mean RFU of 4-6 technical replicates ± SEM and results are representative of three experiments. Stats: ***, $p<0.001$ paired student T-test. **B)** Results from graphs in A are also presented as fold change (mCD40L relative to control).

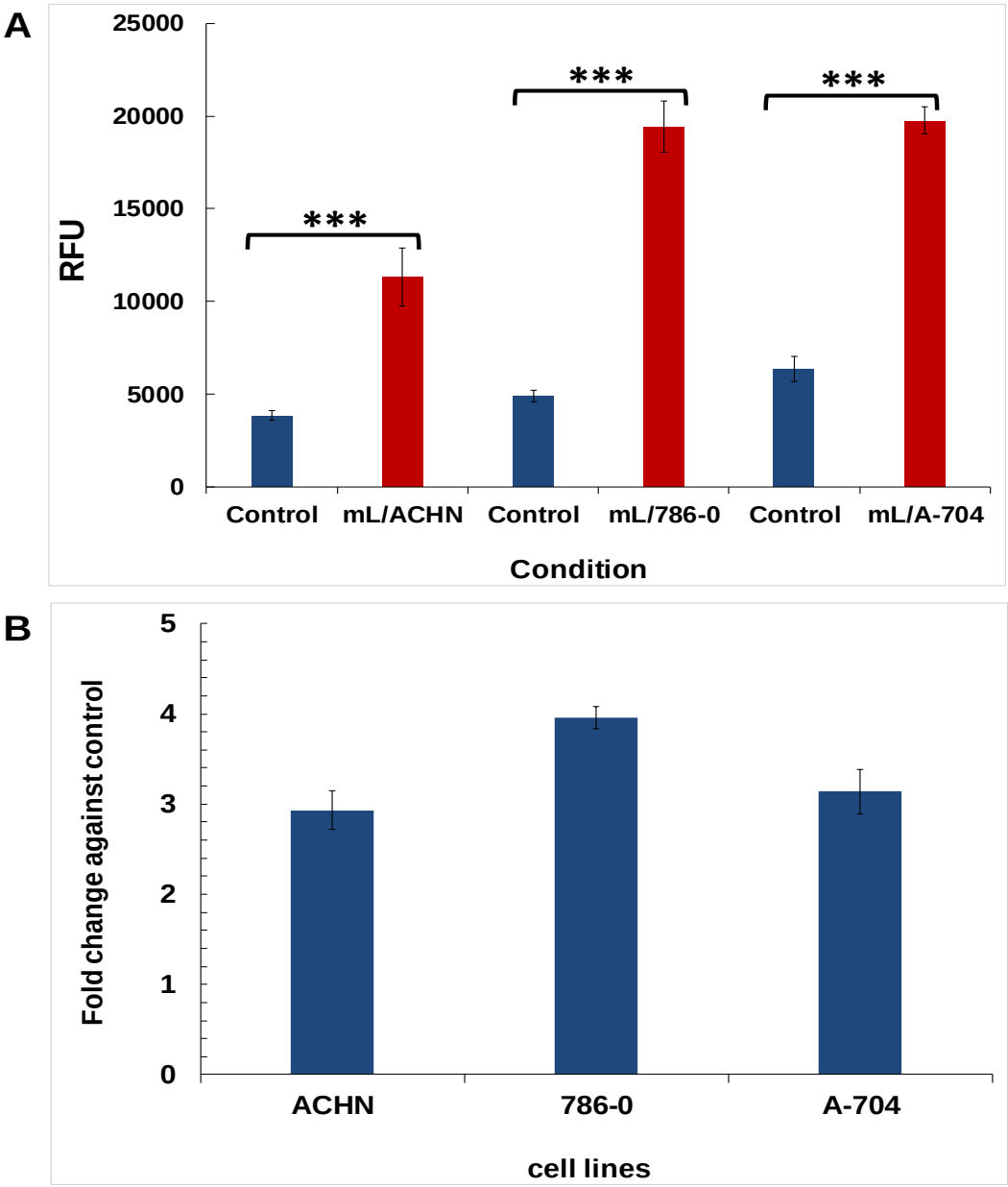

Figure 3.15 Detection of caspase 3/7 activity at 72 h post CD40 ligation

ACHN, 786-O and A-704 were co-cultured at $0.8x10^4$ cells/well with 1x104 cells/well MMC-treated fibroblasts 3T3-CD40L (mL) and 3T3-Neo (Control) in white 96-well plates. Plates were incubated for 72h and caspase activity assessed by the SensoLyte® Assay. 50µl of assay substrate was added to each well followed by 90 min incubation at room temperature in the dark. Fluorescence was measured on a FLUOStar Optima plate reader (as detailed in the Methods) and background-corrected relative fluorescence units (RFU) were deduced by pair-wise subtraction of mCD40L and Control RFU from the respective co-cultures (as described in the text). **A)** Background corrected RFU readings for co-cultures ACHN, 786-O and A-704/3T3-CD40L (mL) and respective 3T3-Neo co-cultures (Control). Bars show mean RFU of 4-6 technical replicates ± SEM and results are representative of three experiments. Stats: ***, $p<0.001$ paired student T-test. **B)** Results from graphs in A are also presented as fold change (mCD40L relative to control).

3.9 Detection of DNA fragmentation following CD40 ligation

DNA fragmentation represents one of the hallmarks of apoptosis (Saraste and Pulkki, 2000). Previous work in our laboratory established a DNA fragmentation detection assay ('JAM test') for the detection of TNFR-mediated epithelial cell apoptosis and determination of '% DNA fragmentation' (by sample normalisation using appropriate controls) (Bugajska et al., 2002). Based on this assay, it was shown that mCD40L induced extensive apoptosis in both UCC cells (60-70%) (Bugajska et al., 2002, Georgopoulos et al., 2006, Shaw et al., 2005) and CRC cells (80-85%) (Georgopoulos et al., 2007). More recently, these findings have been confirmed using an ELISA method-based DNA fragmentation assay that has allowed the determination of '% cell death' using normalisation based on staurosporine-mediated DNA fragmentation (Mohamed, 2014). The ability of staurosporine to induce apoptosis via the intrinsic pathway has been described by ourselves (Chopra et al., 2009) and others (Zhang et al., 2004).

Of note, DNA fragmentation is a reliable and well characterised method to determine cell death, however not all apoptosis mediated by members of the TNFR superfamily is associated with DNA fragmentation (Steele et al., 2006). Yet, when TNFR-mediated apoptosis is accompanied by DNA fragmentation, its detection permits robust determination of % cell death. An important advantage of the ELISA-based method is that, because it involves pre-labelling (BrdU-based 'pulsing') of target epithelial cells, effector 3T3 cells do not interfere with the assay and no background subtraction is necessary (as also detailed in Section 2.8.5).

Using the DNA fragmentation ELISA assay (section 2.8.5), following CD40 ligation by mCD40L, RCC cells demonstrated high levels of DNA fragmentation at 48 h post-ligation. Following normalisation against staurosporine-induced DNA fragmentation, it was possible to deduce % cell death (calculated as detailed in Section 2.8.5). High levels of cell death were detected in all RCC lines: 83% in 786-O (compared with control 16%) (Figure 3.18), 80% in ACHN cells (compared with control 31%) (Figure 3.17), and 73% in A-704 cells (compared with control 13%) (Figure 3.19). These findings are in agreement with the Cytotox-Glo and Caspase-detection assays and

confirmed activation of apoptosis by mCD40L. Collectively, the results from all three independent assays (Cytotox-Glo, SensoLyte and DNA fragmentation ELISA) also provided strong evidence that CD40 induces cell death by activating an apoptotic (not necrotic) death programme.

Although the DNA fragmentation assay negates the need to include ‘3T3 effector cell alone’ controls to account for any effector cell-related background, it nevertheless represents a more laborious experimental assay (it requires 2 days for completion). Therefore, following the completion of all the experiments described in the sections above, the CytoTox-Glo assay (as a surrogate marker of loss of membrane integrity) was mainly used in this study as a standard apoptosis detection assay and confirmation of apoptosis using DNA fragmentation ELISA was performed, where appropriate, for specific experiments.

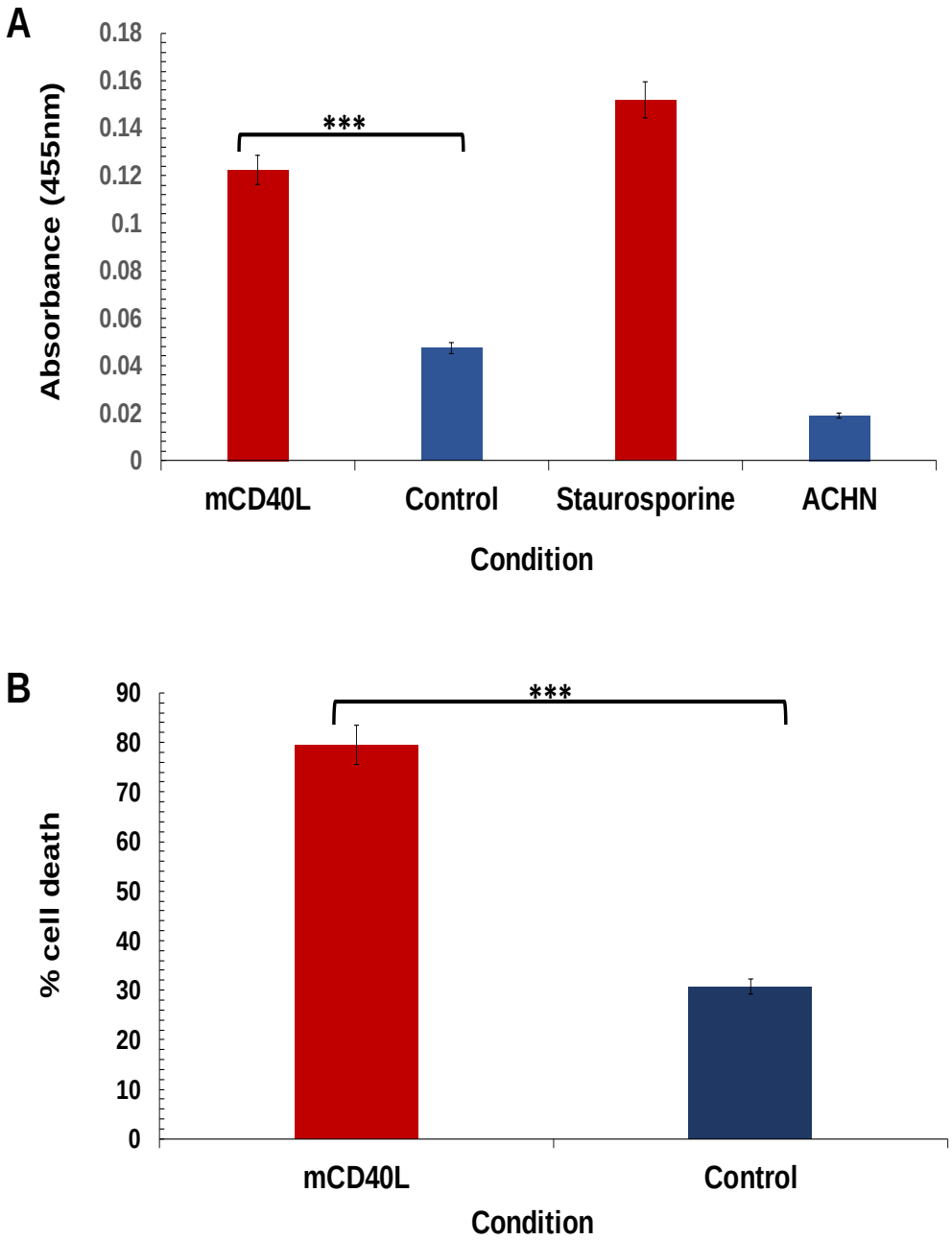

Figure 3.16 Detection of DNA fragmentation in ACHN cells following co-culture

ACHN cells were pre-labelled with 10µM of DNA labelling agent BrdU for 2h. Then ACHN cells were co-cultured at a density of $0.8x10^4$cells/well with $1x10^4$ cells/well MMC-treated fibroblasts 3T3-CD40L (mCD40L) and 3T3-Neo (Control) in 96-well plates. Treatment with 5µM of staurosporine was used as positive control and untreated cells were also included (ACHN). The plates were then incubated for 48h and supernatants were collected. Supernatants (150µl) from each of 6 replicate wells were collected and used to determine DNA fragmentation by ELISA. Absorbance (at 455nm) was measured on a FLUOStar Optima plate reader and % cell death calculated as described in the Methods. **A)** Bars represent mean Absorbance units of 6 technical replicates ± SEM and results are representative of two experiments. **B)** Results from A are also presented as % cell death. Stats: ***, $p<0.001$ paired student T-test.

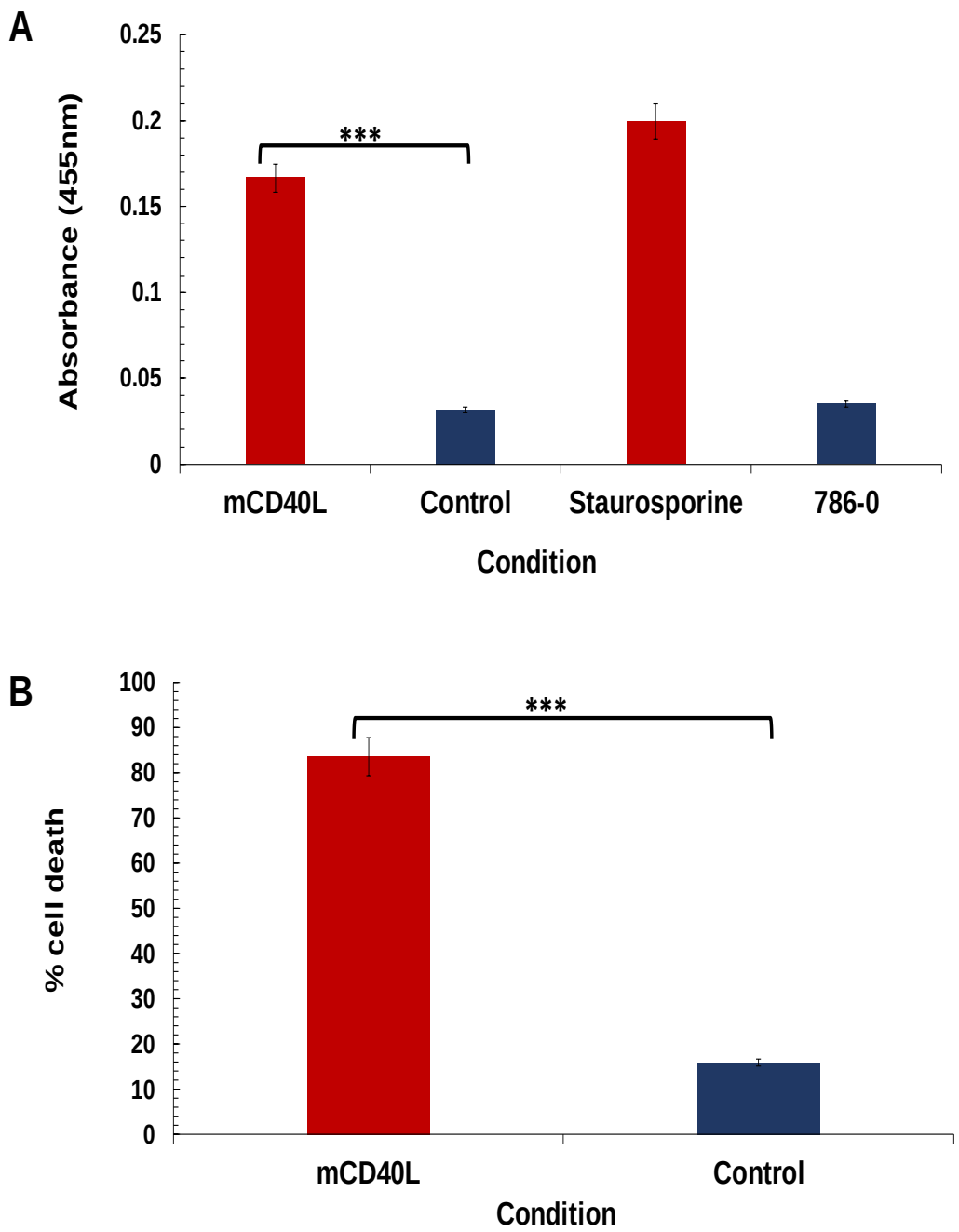

Figure 3.17 Detection of DNA fragmentation in 786-O cells following co-culture

786-O cells were pre-labelled with 10µM of DNA labelling agent BrdU for 2h. Then ACHN cells were co-cultured at a density of $0.8x10^4$cells/well with $1x10^4$ cells/well MMC-treated fibroblasts 3T3-CD40L (mCD40L) and 3T3-Neo (Control) in 96-well plates. Treatment with 5µM of staurosporine was used as positive control and untreated cells were also included (786-O). The plates were then incubated for 48h and supernatants were collected. Supernatants (150µl) from each of 6 replicate wells were collected and used to determine DNA fragmentation by ELISA. Absorbance (at 455nm) was measured on a FLUOStar Optima plate reader and % cell death calculated as described in the Methods. **A)** Bars represent mean Absorbance units of 6 technical replicates ± SEM and results are representative of two experiments. **B)** Results from A are also presented as % cell death. Stats: ***, $p<0.001$ paired student T-test.

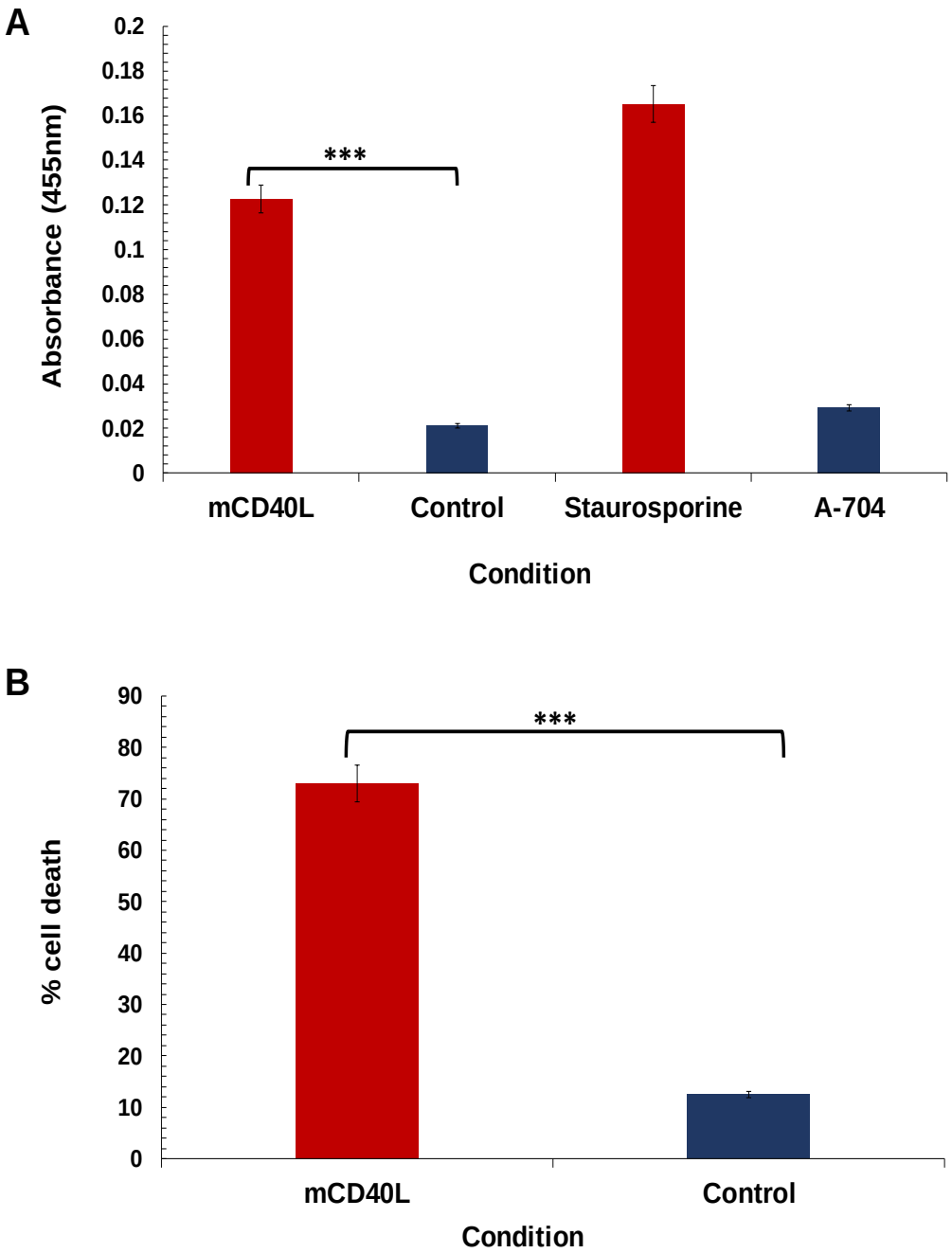

Figure 3.18 Detection of DNA fragmentation in A-704 cells following co-culture

A-704 cells were pre-labelled with 10µM of DNA labelling agent BrdU for 2h. Then ACHN cells were co-cultured at a density of $0.8x10^4$cells/well with $1x10^4$ cells/well MMC-treated fibroblasts 3T3-CD40L (mCD40L) and 3T3-Neo (Control) in 96-well plates. Treatment with 5µM of staurosporine was used as positive control and untreated cells were also included (A-704). The plates were then incubated for 48h and supernatants were collected. Supernatants (150µl) from each of 6 replicate wells were collected and used to determine DNA fragmentation by ELISA. Absorbance (at 455nm) was measured on a FLUOStar Optima plate reader and % cell death calculated as described in the Methods. **A)** Bars represent mean Absorbance units of 6 technical replicates ± SEM and results are representative of two experiments. **B)** Results from A are also presented as % cell death. Stats: ***, $p<0.001$ paired student T-test.

3.10 Optimisation of immunoblotting (Western blotting) for the detection of epithelial cell proteins in co-cultures

Preparation of whole cell lysates from co-cultures and performing Western blotting required epithelial cell lysate-specific controls, as the whole cell lysates from co-cultures contains a mixture of proteins from both effectors (fibroblasts) and target (epithelial) cells. For this purpose, and as detailed previously (Georgopoulos et al., 2006, Mohamed, 2014, Dunnill, 2013), expression of epithelial-specific markers (cytokeratins) has been employed to ensure equal loading based on cytokeratin (CK) expression.

It was thus necessary, for the present study, that optimisation experiments were carried out to establish procedures for the recognition of total protein (based on β-actin expression detection) and RCC cell-specific indicators. CK8 and CK18 expression was investigated with the aim to use it as control for the adjustment of immunoblotting and densitometry-based normalisation..

Figure 3.20 shows representative Western blotting experiments where lysates from a panel of carcinoma cell lines were analysed for expression of cytokeratins CK8 and CK18 alongside lysates from effector (3T3-Neo and 3T3-CD40L) fibroblasts. The panel of epithelial cells included, in addition to the RCC lines (ACHN, 786-O and A-704), the UCC cell lines RT4, RT112 and EJ, and the CRC cell line SW480-CD40 which is an SW480-derivative engineered to express CD40 (Georgopoulos et al., 2007). The results in Figure 3.20 show that the carcinoma cell lines expressed detectable (though variable and cell line-dependent) CK8 and/or CK18 protein levels, whilst confirming that effector cells (3T3 fibroblasts) did not express such epithelial markers and thus were, as expected, CK8/18-negative.

When lysates from co-cultures of RCC lines ACHN, 786-O and A-704 with 3T3-Neo and 3T3CD40L effector cells were analysed by immunoblotting, CK18 expression could be detected consistently in all cell lines for time points ranging from 1.5h to 36 h (Figures 3.21, 3.22 and 3.23, respectively). Lysates from co-cultures of 3T3-Neo and 3T3CD40L effectors with the CRC line HCT116 were used as positive controls (here and in subsequent chapters for CD40 signalling pathway analysis – Chapter 4). Yet,

as co-cultures progress, there is an increasing risk that, due to RCC cell apoptosis triggered by mCD40L, there will be progressive loss of epithelial lysate relatively to fibroblast lysate in co-culture protein extracts as has been observed previously in our laboratory (Mohamed, 2014). In fact, upon careful inspection, a slight reduction in epithelial marker CK18 expression was visible at the 36h time-point, e.g. in 786-O co-cultures (Figure 3.22); this time points coincides with the start of physical changes in cells and apoptotic cell death initiation (see results above, particularly for 786-O cells).

Hence, to ensure that equal loading could be achieved for both 3T3-Neo and 3T3-CD40L co-cultures, densitometry was carried out in order to quantify band intensity for CK18 for RCC cell lines (using the Li-Cor Odyssey analysis software or Image Studio freeware) and 'lysate loading correction' based on CK18 band intensity was performed (for an example see Figure 3.24). Following band intensity-based normalisation (correction) of lysates in the original membranes ('first run'), new Western blotting experiments were carried out with equal protein from target cells guaranteed ('second run'), as shown in Figures 3.25, 3.26 and 3.27, where representative such data are provided. Once a set of lysates, created for specific co-cultures, has been 'corrected' by this type of normalisation and similar CK expression was detectable for all conditions and time points, the set of lysates could then be used reproducibly for immunoblotting analyses to detect intracellular mediators involved in CD40 signalling in RCC cells (Chapter 4).

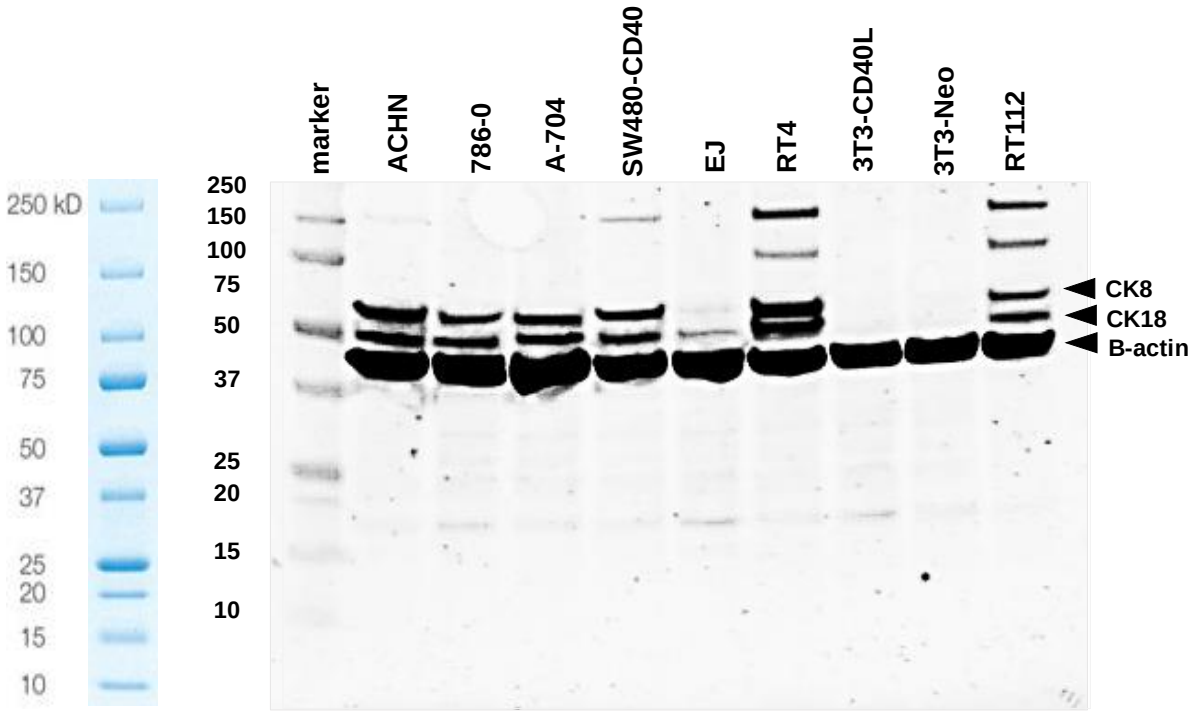

Figure 3.19 Detection of Cytokeratin 8 (CK8) and 18 (CK18) expression in epithelial cells and fibroblasts

Carcinoma cell lines and fibroblast cells (3T3-CD40L and 3T3-Neo) were cultured and a complete cell lysates were made as described in the Methods (Section 2.9.3) and 20µg of protein/well was analysed by immunoblotting (Section 2.9.5). After overnight incubation at 4ºC by rocking with primary antibody anti CK8 and CK18 mouse monoclonal IgG diluted 1:1000), secondary antibody (goat-anti mouse IgG Alexa 680 dilution 1:10000) was added and the membrane was incubated in the dark for 1h. For specificity and as a loading control, β-actin antibody was used (at 1:10,000 dilution) and incubation overnight at 4ºC, then the membrane was incubated with secondary antibody goat-anti mouse IgG Alexa 680 (diluted 1:10000) in the dark for 1h. Antibody binding was visualised at 700nm using a LI-COR Odyssey Infra-Red Imaging System and the image is shown in black and white.

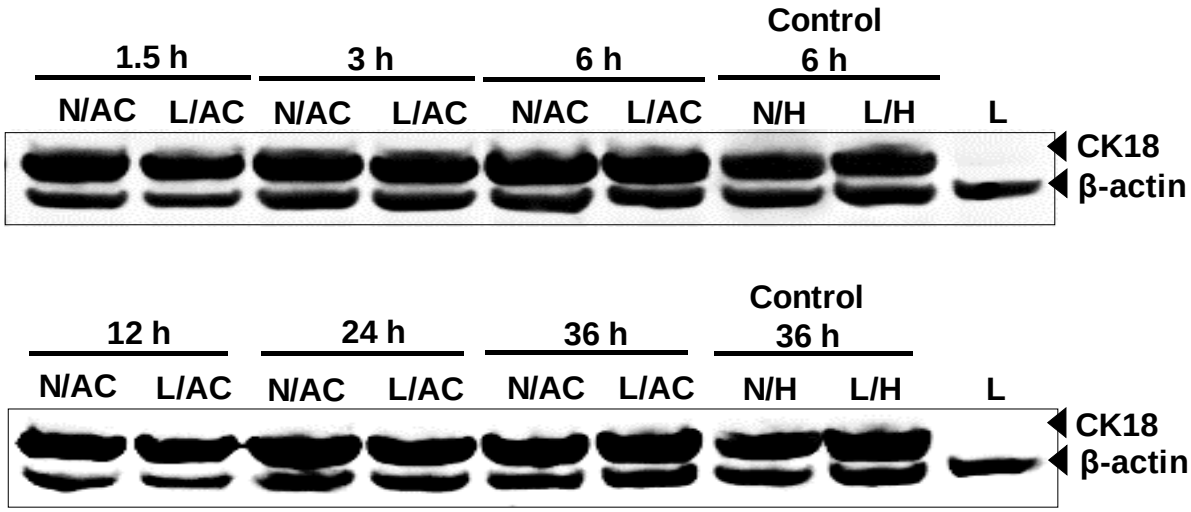

Figure 3.20 Detection of CK18 in ACHN cell co-cultures with effector cells

ACHN cells were co-cultured in 10cm dishes at density of $3x10^6$ with MMC treated fibroblast (3T3-Neo and 3T3-CD40L) and incubated for (1.5, 3, 6, 12, 24 and 36h). Whole cell lysate were prepared as described in the Methods (Section 2.9.3) and 40µg of protein/well was analysed by immunoblotting (Section 2.9.5). After overnight incubation at 4ºC by rocking with primary antibody anti CK18 mouse monoclonal IgG diluted 1:1000), secondary antibody (goat-anti mouse IgG Alexa 680 dilution 1:10000) was added and the membranes were incubated in the dark for 1h. For specificity and as a loading control, β-actin antibody was used (at 1:10,000 dilution) and incubation overnight at 4ºC, then 1h incubation with secondary antibody goat-anti mouse IgG Alexa 680 (diluted 1:10000) away from light. Antibody binding was visualised at 700nm using a LI-COR Odyssey Infra-Red Imaging System and the images are presented in black and white. Lysates from co-culture of CRC were used as control.

Key:
N/AC: 3T3Neo co-cultured with ACHN
L/AC : 3T3CD40L co-cultured with ACHN
NH : 3T3Neo co-cultured with HCT116
L/H : 3T3CD40L co-cultured with HCT116
L : 3T3-CD40L fibroblasts alone

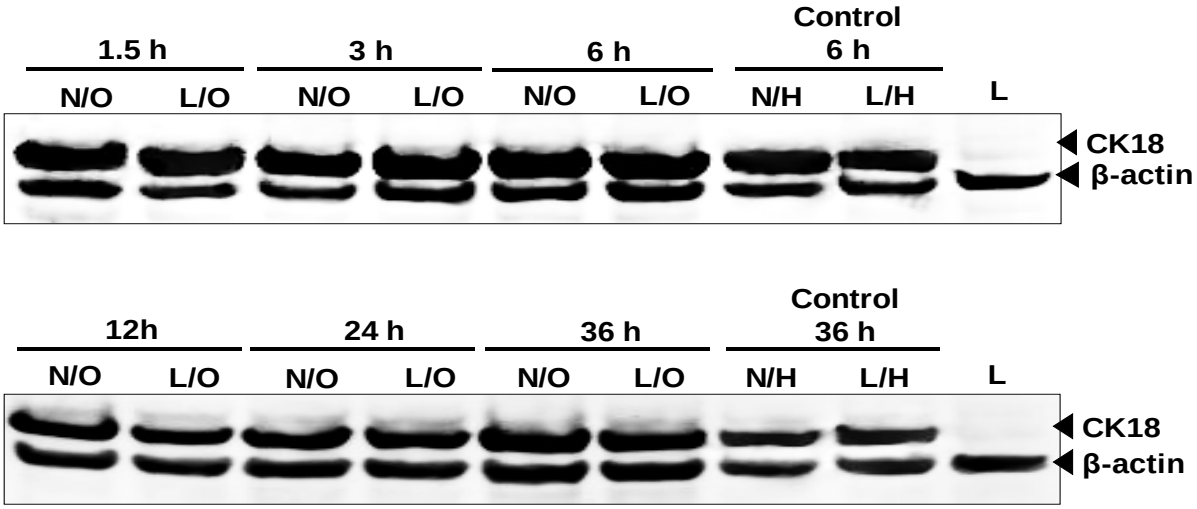

Figure 3.21 Detection of CK18 in 786-O cell co-cultures with effector cells

786-O cells were co-cultured in 10cm dishes at density of $3x10^6$ with MMC treated fibroblast (3T3-Neo and 3T3-CD40L) and incubated for (1.5, 3, 6, 12, 24 and 36h). Whole cell lysate were prepared as described in the Methods (Section 2.9.3) and 40µg of protein/well was analysed by immunoblotting (Section 2.9.5). After overnight incubation at 4ºC by rocking with primary antibody anti CK18 mouse monoclonal IgG diluted 1:1000), secondary antibody (goat-anti mouse IgG Alexa 680 dilution 1:10000) was added and the membranes were incubated in the dark for 1h. For specificity and as a loading control, β-actin antibody was used (at 1:10,000 dilution) and incubation overnight at 4ºC, then the membranes were incubated with secondary antibody goat-anti mouse IgG Alexa 680 (diluted 1:10000) in the dark for 1h. Antibody binding was visualised at 700nm using a LI-COR Odyssey Infra-Red Imaging System and the images are shown in black and white. Lysates from co-culture of CRC were used as control.

Key:

N/O : 3T3Neo co-cultured with 786-O
L/O : 3T3CD40L co-cultured with 786-O
NH : 3T3Neo co-cultured with HCT116
L/H : 3T3CD40L co-cultured with HCT116
L : 3T3-CD40L fibroblasts alone

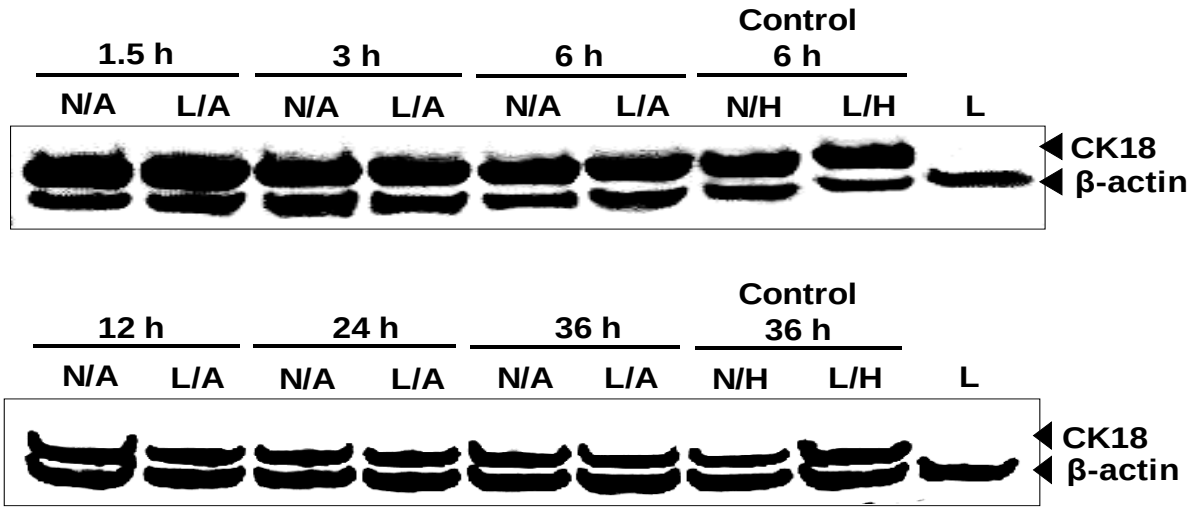

Figure 3.22 Detection of CK18 in A-704 cell co-cultures with effector cells

A-704 cells were co-cultured in 10cm dishes at density of $3x10^6$ with MMC treated fibroblast (3T3-Neo and 3T3-CD40L) and incubated for (1.5, 3, 6, 12, 24 and 36h). Whole cell lysate were prepared as described in the Methods (Section 2.9.3) and 40µg of protein/well was analysed by immunoblotting (Section 2.9.5). After overnight incubation at 4ºC by rocking with primary antibody anti CK18 mouse monoclonal IgG diluted 1:1000), secondary antibody (goat-anti mouse IgG Alexa 680 dilution 1:10000) was added and the membranes were incubated in the dark for 1h. For specificity and as a loading control, β-actin antibody was used (at 1:10,000 dilution) and incubation overnight at 4ºC, then the membranes were incubated with secondary antibody goat-anti mouse IgG Alexa 680 (diluted 1:10000) in the dark for 1h. Antibody binding was visualised at 700nm using a LI-COR Odyssey Infra-Red Imaging System and the images are shown in black and white. Lysates from co-culture of CRC were used as control.

Key:
N/A : 3T3Neo co-cultured with A-704
L/A: 3T3CD40L co-cultured with A-704
NH : 3T3Neo co-cultured with HCT116
L/H : 3T3CD40L co-cultured with HCT116
L : 3T3-CD40L fibroblasts alone

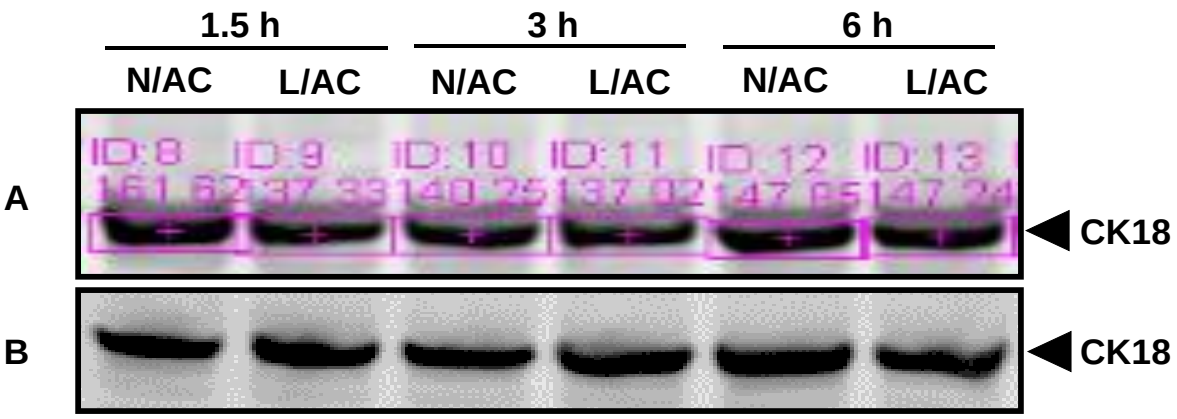

Figure 3.23 protein expression was corrected according to the CK18 band intensity values by using densitometry analysis

Co-culture for $3x10^6$ ACHN cells in 10cm dishes with MMC-treated fibroblast (3T3-Neo and 3T3-CD40L) and incubated for (1.5, 3 and 6h). Whole cell lysate were prepared as described in the Methods (Section 2.9.3) and 40µg of protein/well was analysed by immunoblotting (Section 2.9.5). After overnight incubation at 4ºC by rocking with primary antibody anti CK18 mouse monoclonal IgG (diluted 1:1000), secondary antibody (goat-anti mouse IgG Alexa 680 dilution 1:10,000) was added and the membranes were incubated in the dark on rocking platform for 1h. Antibody binding was visualised at 700nm using a LI-COR Odyssey Infra-Red Imaging System and the images are presented in black and white. **A)** Bands from first experiment with estimation of band intensities for CK8 expression. **B)** "Second experiment" after normalisation analysis.

Key:
N/AC : 3T3Neo co-cultured with ACHN L/AC : 3T3CD40L co-cultured with ACHN

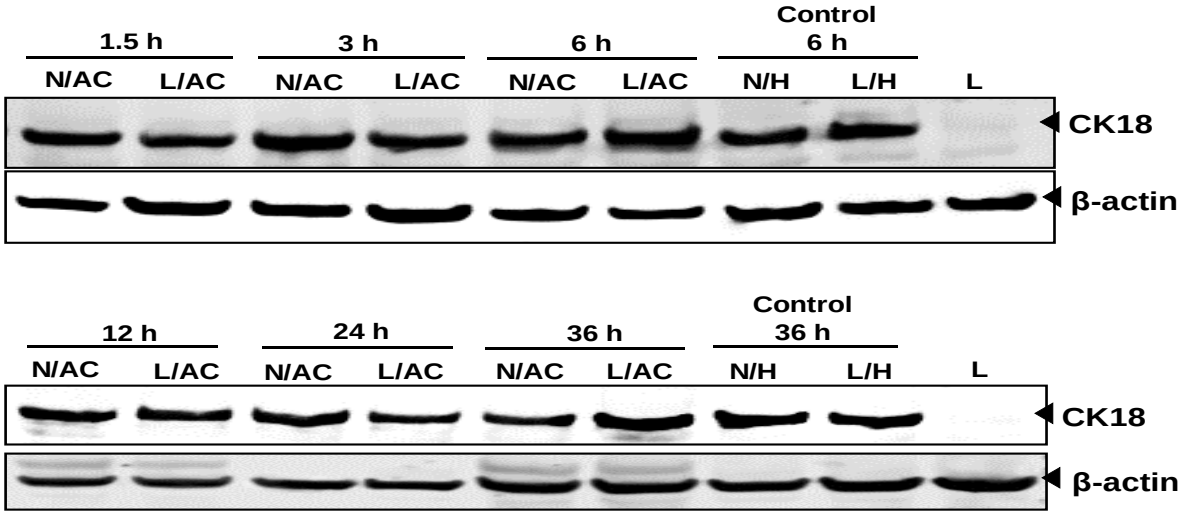

Figure 3.24 Confirmation of equal loading in ACHN cell co-cultures following CK-based normalisation

40µg of normalized lysates were analysed by immunoblotting (Section 2.9.5). After overnight incubation at 4ºC by rocking with primary antibody anti CK18 mouse monoclonal IgG diluted 1:1000), secondary antibody (goat-anti mouse IgG Alexa 680 dilution 1:10000) was added and the membranes were incubated in the dark for 1h. For specificity and as a loading control, β-actin antibody was used (at 1:10,000 dilution) and incubation overnight at 4ºC, then the membranes were incubated with secondary antibody goat-anti mouse IgG Alexa 680 (diluted 1:10000) in the dark for 1h. Antibody binding was visualised at 700nm using a LI-COR Odyssey Infra-Red Imaging System and the images are pesented in black and white. Lysates from co-culture of CRC were used as control.

Key:
N/AC: 3T3Neo co-cultured with ACHN
NH : 3T3Neo co-cultured with HCT116
L : 3T3-CD40L fibroblasts alone
L/AC : 3T3CD40L co-cultured with ACHN
L/H : 3T3CD40L co-cultured with HCT116

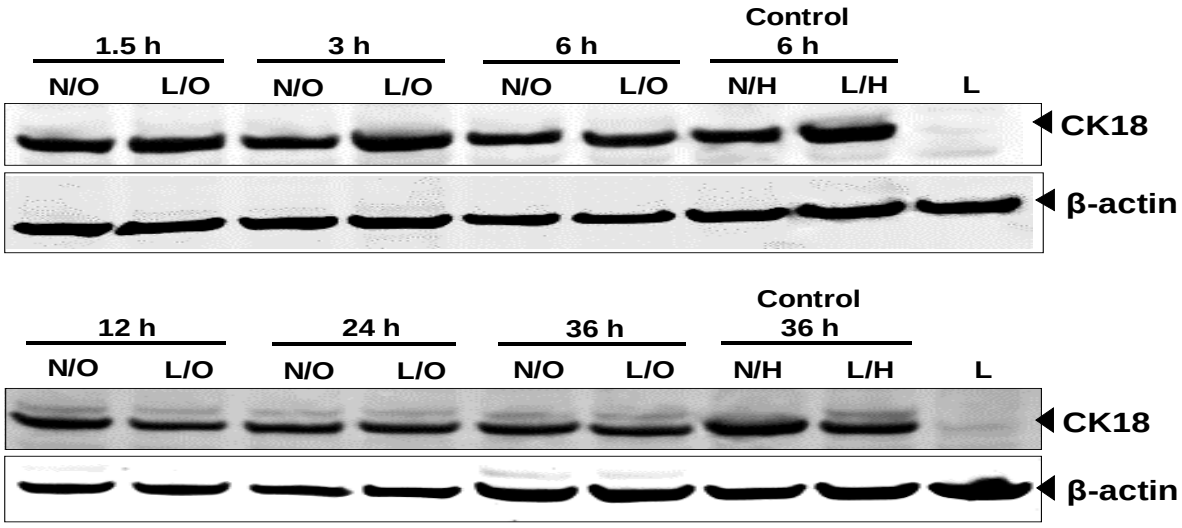

Figure 3.25 Confirmation of equal loading in 786-O cell co-cultures following CK-based normalisation

40µg of normalized lysates were analysed by immunoblotting (Section 2.9.5). After overnight incubation at 4ºC by rocking with primary antibody anti CK18 mouse monoclonal IgG diluted 1:1000), secondary antibody (goat-anti mouse IgG Alexa 680 dilution 1:10000) was added and the membranes were incubated in the dark for 1h. For specificity and as a loading control, β-actin antibody was used (at 1:10,000 dilution) and incubation overnight at 4ºC, then the membranes were incubated with secondary antibody goat-anti mouse IgG Alexa 680 (diluted 1:10000) in the dark for 1h. Antibody binding was visualised at 700nm using a LI-COR Odyssey Infra-Red Imaging System and the images are shown in black and white. Lysates from co-culture of CRC were used as control.

Key:
N/O : 3T3Neo co-cultured with 786-O
L/O : 3T3CD40L co-cultured with 786-O
NH : 3T3Neo co-cultured with HCT116
L/H : 3T3CD40L co-cultured with HCT116
L : 3T3-CD40L fibroblasts alone

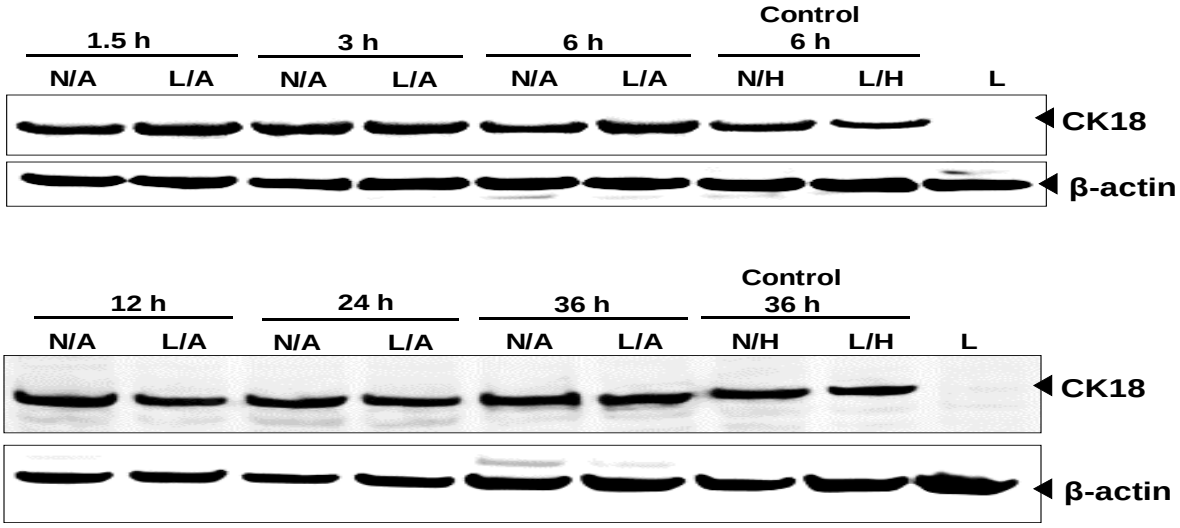

Figure 3.26 Confirmation of equal loading in A-704 cell co-cultures following CK-based normalisation

40µg of normalized lysates were analysed by immunoblotting (Section 2.9.5). After overnight incubation at 4ºC by rocking with primary antibody anti CK18 mouse monoclonal IgG diluted 1:1000), secondary antibody (goat-anti mouse IgG Alexa 680 dilution 1:10000) was added and the membranes were incubated in the dark for 1h. For specificity and as a loading control, β-actin antibody was used (at 1:10,000 dilution) and incubation overnight at 4ºC, then the membranes were incubated with secondary antibody goat-anti mouse IgG Alexa 680 (diluted 1:10000) in the dark for 1h. Antibody binding was visualised at 700nm using a LI-COR Odyssey Infra-Red Imaging System and the images are shown in black and white. Lysates from co-culture of CRC were used as control.

Key:
N/A : 3T3Neo co-cultured with A-704
L/A: 3T3CD40L co-cultured with A-704
NH : 3T3Neo co-cultured with HCT116
L/H : 3T3CD40L co-cultured with HCT116
L : 3T3-CD40L fibroblasts alone

3.11 Summary

- Immunoblotting and Flow cytometry confirmed high expression of CD40 on human RCC cell lines. In addition, flow cytometry definite the expression of mCD40L on 3T3-CD40L effector cell surface in comparison to 3T3-Neo cells that showed no CD40L expression.

- Treatment with pro-inflammatory cytokines increased CD40 expression with IFN-ɣ showing more significant induction in CD40 expression than treatment with TNF-α.

- Using Cytotox-Glo death assays, results demonstrated for the first time that CD40 ligation by mCD40L triggered cell death in all 3 human RCC cell lines, with massive cell death detected particularly at 48 h post-ligation. No further increase in CD40 killing was detectable at 72 h.

- Treatment of all RCC cell lines with G28-5 agonistic anti-CD40 antibody did not induce cell death at the time-points tested.

- The presence of IFN-ɣ in co-cultures of RCC cells with mCD40L consistently caused a clear increase in cell death in all RCC cell lines, although the increase in cell death only reached statistical significance in A-704 and ACHN cells (but not in 786-O cells). However, presence of IFN-ɣ in cultures of RCC cells treated with G28-5 mAb did not significantly enhance the ability of the agonist to induce cell death in RCC cells after 48h.

- Results from the SensoLyte assay demonstrated for the first time that CD40 ligation by mCD40L in RCC cells induced activation of effector caspases 3/7 at 24h post-ligation, which was more extensive at 48h and further elevated at 72h. These results corroborated the Cytotox-Glo assay findings.

- DNA fragmentation ELISA assays showed for the first time induction of DNA fragmentation at 48h following CD40 ligation by mCD40L, which confirmed the induction of mCD40L-mediated apoptotic cell death in RCC cells.

- The experiments described in this chapter also confirmed the optimisation of immunoblotting techniques for the detection of epithelial lysate in whole cell lysates from epithelial and effector (fibroblast) co-cultures. CK8 and 18 expression was detected by only epithelial cells and densitometric analysis (based on CK18 bands intensity) allowed lysate normalisation, to ensure that equal amount of RCCs protein were analysed by the technique.

- The experiments in this chapter therefore allowed the establishment of the methodologies required to systematically study the mechanisms of CD40-mediated cell death as well as investigations of CD40-mediated intracellular signalling in RCC cells (in the following chapters).

.

Chapter 4

Investigation of the induction of proinflammatory cytokine secretion following CD40 ligation

4. Background

It has been reported that receptor ligation of members of TNFR family can induce cytokine secretion in epithelial cells. Previous studies showed that treatment with Fas and TNF-α triggered IL-8 secretion in HT29 cells (Abreu-Martin et al., 1995). IL-8 secretion has also been observed in primary epithelial cells and in carcinoma cell lines in response to TNF-α treatment (Sharma et al., 1998). Other studies performed on A375 cells showed that stimulation of other TNFRs (LTβR) either by agonistic anti-LTβR monoclonal antibody (M12) or by membrane bound LTβ and LTαβ ligands induced IL-8 and RANTES secretion (Degli-Esposti et al., 1997). Recent studies in our laboratory demonstrated that stimulation of LTβR by membrane bound ligand triggered IL-6, IL-8 and GM-CSF secretion in a variety of carcinoma cells (Albarbar, et al, manuscript in preparation).

Ligation of CD40 on monocytes, dendritic cells and other APC cells by membrane bound CD40L expressed on activated T-cells in vitro enhanced multiple cytokines secretion such as IL-1, IL-6, IL-8, IL10, IL-12 and TNF-α (van Kooten and Banchereau, 2000, Kooten and Banchereau, 1997). While in B-cells, CD40 ligation in vitro led to production of IL-6, IL-10, TNF-α and LT-α (van Kooten and Banchereau, 2000).

CD40 is functionally expressed on adherent cells such as primary lines of endothelial cells, keratinocytes and synovial fibroblasts and its ligation on these cells induced cytokines secretion (Kooten and Banchereau, 1997). Secretion of cytokines such as IL-8 and IL-6 has also been observed in response to CD40 ligation by recombinant soluble CD40 ligand (rsCD40L) in human epithelial cells including ovarian carcinoma cells and epidermal keratinocytes (Gallagher et al., 2002b), whilst other studies showed that treatment of some carcinoma cells including bladder, pancreatic and breast cancer cells, with either rhCD40L or agonistic antibody induced secretion of various cytokines such as IL-8, IL-6, GM-CSF, GRO-α and TNF-α (Alexandroff et al., 2000).

The effect of membrane-bound CD40 ligand on cytokine secretion in epithelial cells has provided some interesting observations. CD40 ligation by membrane-presented CD40L (mCD40L) can mediate cytokine secretion in different types of carcinoma cells

particularly bladder, pancreatic and breast cancer cells (Grammer and Lipsky, 2000, van Kooten and Banchereau, 2000). More importantly, while mCD40L mediate secretion of cytokines IL-6, IL-8 and GM-CSF in CRC and UCC (Georgopoulos et al., 2007), interestingly, IL-8 secretion and to a smaller extent IL-6 secretion could be induced by soluble CD40 agonist, but GM-CSF secretion was induced only by mCD40L (Georgopoulos et al., 2007). This observation is in covenant with findings in B cells, where the degree of CD40 cross-linking determines the ability of the receptor to induce IL-6 secretion (Baccam and Bishop, 1999).

More recent studies showed that ligation of CD40 in mouse and human RCC cells triggered cytokine gene expression and cytokine protein secretion. In particular, CD40 ligation by soluble agonists induced GM-CSF and MCP-1 protein secretion and up-regulated gene expression of GM-CSF, MCP-1, IL-23, IP-10 and ITAC (Lee et al., 2005). Another study has confirmed this and reported that treatment of mouse RCC cells with agonistic anti-CD40 antibody induced GM-CSF and MCP-1 gene expression and mediated substantial GM-CSF and MCP-1 secretion in a dose-dependent manner (Shorts et al., 2006).

Having demonstrated the effects of CD40 ligation in RCC cell fate, the work in this chapter focused on human RCC cells and investigate the secretion of cytokines in response to CD40 ligation. Initially, a cytokine array approach was employed to investigate secretion of a large panel of cytokines in culture supernatants in the 786-O cell line following CD40 ligation at 48h, which was the time point where maximal CD40-mediated killing was observed in human RCC cells (see Chapter 3). Following this initial screening, cytokine-specific ELISA assays were performed for all cell lines ACHN, 786-O and A-704 and detailed investigations at different time points for the selected cytokines IL-8, IL6 and GM-CSF.

4.1 Objectives

The aims of this chapter were to

- Investigate whether CD40-CD40L interaction induce cytokine secretion in RCC cells

  - Use a cytokine array approach to screen for a large panel of cytokines following CD40 ligation in 786-O cells
  - Determine IL-6, IL-8 and GM-CSF secretion in culture supernatants of a panel of RCC cells

- Examine whether the mode of CD40 ligation (soluble versus membrane agonist) can modulate the secretion of cytokines in RCC cells

  - Determine GM-CSF secretion levels in culture supernatants of RCC cells after treatment with agonistic anti-CD40 antibody G28-5 and compare findings with its concentration in co-culture supernatants

4.2 Detection of cytokine secretion in co-culture supernatants of RCC cells 786-O using a cytokine array approach

In order to obtain a preliminary idea of what types of cytokine were secreted post CD40 ligation in human RCC cells, a human cytokine array kit was used for quantification of cytokine secretion in culture supernatants collected at 48h post CD40 ligation by mCD40L for the human RCC cells line 786-O. For these initial screening experiments, similar co-cultures of the UCC cell line EJ were also used as controls, as secretion of cytokines following CD40 ligation in EJ cells has been reported previously by our laboratory (Georgopoulos et al., 2007).

As shown in Figure 4.1, the cytokine array experiments showed that mCD40L induced marked secretion of a number of cytokines, as demonstrated by comparison of test (786-O/mCD40L) versus control (786-O/Neo) supernatants. Figure 4.1 panel A illustrates the whole arrays for all conditions tested for both 786-O and EJ cells. The most highly induced cytokines specifically associated with CD40 signalling (IL-8, IL-6, GM-CSF, GROa, sICAM-1 and MCP-1) were plotted for both cell lines in panel B, whilst presentation of data as “fold change” allowed a better side-by-side comparison of 786-O and EJ cells (as the basal levels of cytokine secretion differed between the two cell lines).

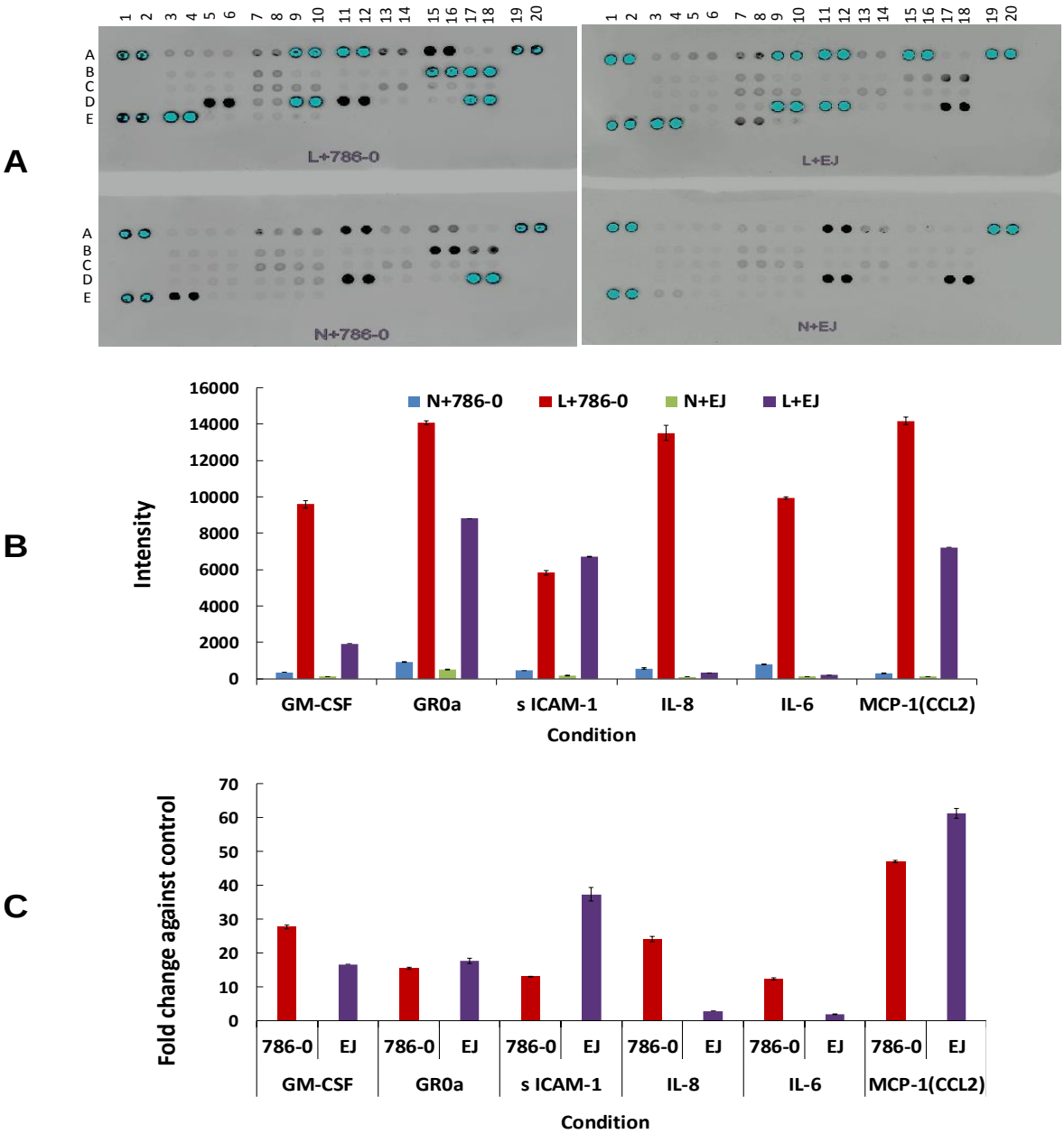

Figure 4.1 Detection of cytokine secretion in RCC cells 786-O using a human cytokine array approach

RCC cells 786-O were co-cultured at a density of $5x10^4$ cells/well with $6x10^4$ cells/well of MMC-treated fibroblasts 3T3-CD40L and 3T3-Neo in 24 well plates (as detailed in section 2.7) for 48h. Supernatants were collected and cytokines secretion was determined using the human cytokine array kit (as described in materials and methods section 2.12.3). A) Image for scanned nitrocellulose membranes using an Odyssey™ Infra-red Imaging system. B) Bars represent mean fluorescence intensity of the 2 replicates spots on the arrays for the selected cytokines. C) Results from graphs in A are presented as fold change of mCD40L treatment (L+786-O and L+EJ) relative to (N+786-O and N+EJ).

Key:

N+786-O : 3T3-Neo co-cultured with 786-O
L+786-O : 3T3-CD40L co-cultured with 786-O
N+EJ : 3T3-Neo co-cultured with EJ
L+EJ : 3T3-CD40L co-cultured with EJ

4.2.1 Detection of IL-8 secretion in RCC cells following CD40 ligation by mCD40L

IL-8 is a well-characterised proinflammatory cytokine/chemokine that is secreted by many types of cells including epithelial cells and fibroblast, but the main sources of IL-8 secretion are monocytes and macrophages. (Zhu and Woll, 2005). IL-8 stimulates neutrophils and enhances their migration, through the activation of (phosphatidylinositol-3 kinase) PI-3K to induce chemotaxis and chemokinesis (Knall et al., 1997). The action of PI-3K links IL-8 receptors to MAPK signalling in neutrophils. The biological activity of IL-8 is mediated by its interaction with the two specific cell-surface G protein-coupled chemokine receptors CXCR1 and CXCR2 (Waugh and Wilson, 2008). IL-8 secretion can be induced by various stimuli involving inflammatory signals including TNF-α, chemotherapy, hypoxia etc (Brat et al., 2005).

This activity of IL-8 has been observed in several cancer cell lines. In lung and ovarian cancer cells, IL-8 signalling enhances the activation of mitogen activated protein kinase (MAPK) p42/44 signalling (Waugh and Wilson, 2008), whilst, IL-8 signalling caused activation of the pro-apoptotic MAPK pathway p38 via down regulation of ERK1/2 in both neutrophils and carcinoma cells (MacManus et al., 2007, Knall et al., 1996, Venkatakrishnan et al., 2000, Luppi et al., 2007).

Treatment of intestinal epithelial cells (IEC) with TNF-α resulted in IL-8 secretion in an ERK and p38 dependent-manner, as inhibition of ERK or p38 by PD98059 and SB203580 inhibitors, respectively, alone or in combination caused reduction in IL-8 secretion (Jijon et al., 2002). CD40-CD40L signalling induced IL-8 secretion in ovarian carcinoma cell lines, when cells were treated with recombinant human CD40L (Toutirais et al., 2007). Whilst previous findings in our laboratory showed that ligation of CD40 by either mCD40L or agonistic anti-CD40 antibody G28-5 triggered IL-8 secretion in CRC and UCC cells (Georgopoulos et al., 2007).

Having demonstrated marked induction of IL-8 secretion in the preliminary cytokine detection experiments in Figure 4.1, IL-8 secretion in response to CD40 ligation by mCD40L in human RCC cells was systematically investigated following co-culture of RCC cells with 3T3-CD40L and 3T3-Neo effectors. Co-cultures were performed and

cell culture supernatants collected at different time points: 1.5h, 3h, 6h, 12h, 24h, 36h and 48h, and then the concentration of secreted IL-8 was determined by ELISA assay (as described in the Methods sections 2.7, 2.12 and 2.12.2).

Results presented in Figure 4.2 showed marked induction of secretion of IL-8 in response to CD40 ligation in all three RCC lines in a time-dependant manner, consistent with the observations with control EJ cells. This induction was observed as early as 1.5h following CD40 ligation. It should be noted that during the course of the experiments the relative increase in IL-8 secretion subsided, which was clearly due to the basal IL-8 secretion by all RCC cell lines (Figure 4.2. left panels), which resulted in progressive accumulation of cytokine in the control supernatants. Of note also, no detectable secretion of IL-8 was observed in culture supernatants from 3T3-CD40L and 3T3-Neo fibroblast alone as shown in this study (chapter 6) and as previously reported (Georgopoulos et al., 2007).

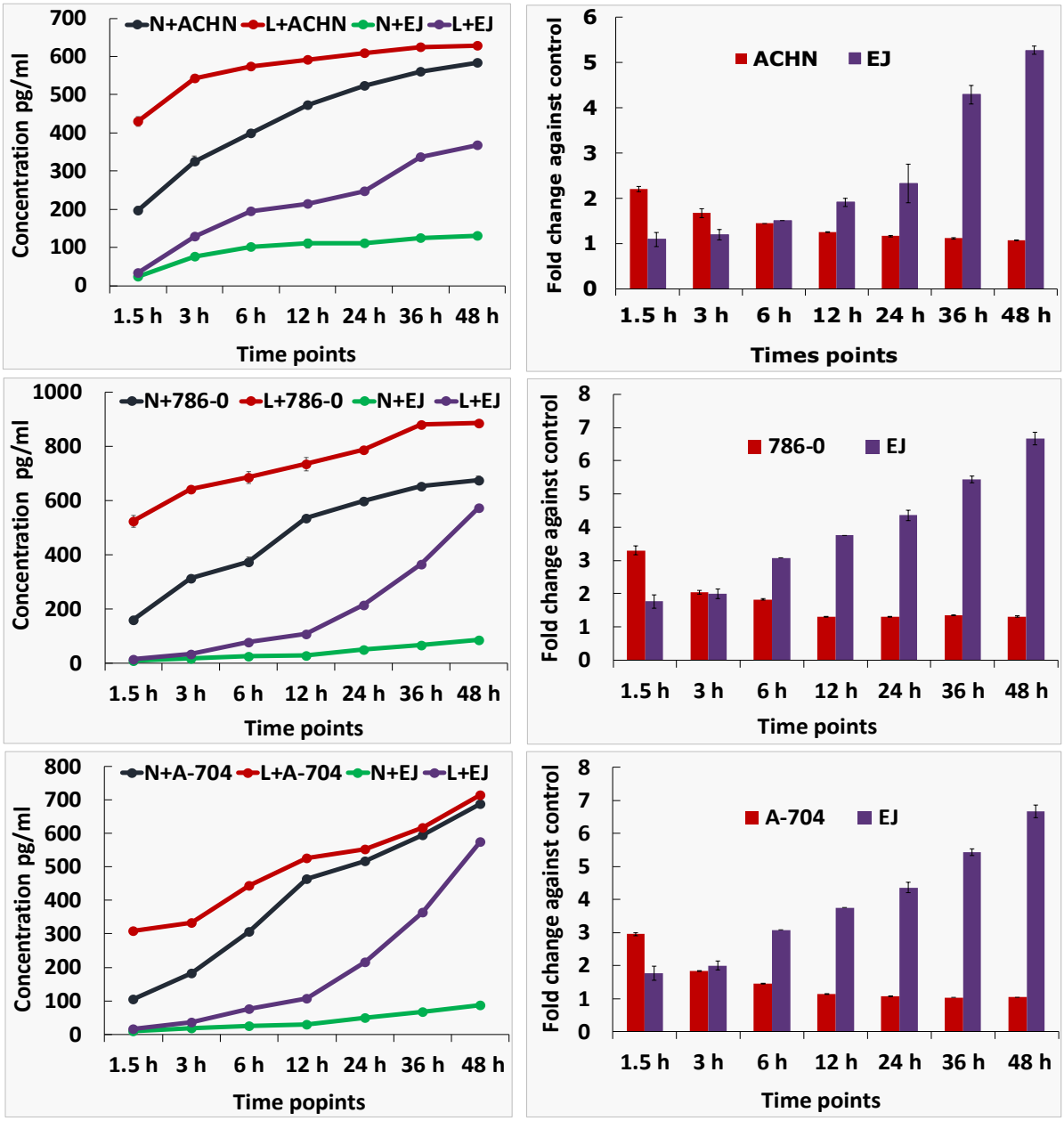

Figure 4.2 mCD40L-mediated IL-8 secretion in RCC cells

RCC cells (ACHN, 786-0 and A-704) were co-cultured at a density of $5x10^4$ with $6x10^4$ of MMC-treated fibroblasts 3T3-CD40L and 3T3-Neo in 24 well plates (as detailed in the Methods) for 1.5-48h) following incubation for the indicated time points, supernatants were taken. Secretion of IL-8 was determined by ELISA assays. Graphs on the left show mean of 2-3 technical replicates of IL-8 concentration, calculated as explained in materials and methods (section 2.12.2) and are representative of 2 independent investigates. Results from these graphs are also presented as fold change (L) relative to control (N) as bar graphs on the right.

Key

N+A-704	: 3T3-Neo co-cultured with A-704	N+786-O	: 3T3-Neo co-cultured with 786-O
L+A-704	: 3T3-CD40L co-cultured with A-704	L+786-O	: 3T3-CD40L co-cultured with 786-O
N+ACHN	: 3T3-Neo co-cultured with ACHN	N+EJ	: 3T3-Neo co-cultured with EJ
L+ACHN	: 3T3-CD40L co-culture with ACHN	L+EJ	: 3T3-CD40L co-cultured with EJ

4.2.2 Detection of IL-6 secretion in RCC cells following CD40 ligation by mCD40L

IL-6 is a multi-functional cytokine the secretion of which is biologically important in various Aspects of immune regulation and in disease. Amongst several functions, IL-6 secretion has important roles in the enhancement of neutrophil production in the bone marrow and IL-6 enhances the response of macrophages to specific microbial molecules (Hirano, 2010, Ara and DeClerck, 2010). IL-6 can interact with two types of receptors, IL-6 receptor (IL-6R) and soluble IL-6 receptor (sIL-6R). Binding of IL-6 to IL-6R leads to formation a complex between IL-6R and IL-6 associates with gp130 and promotes the initiation of intracellular signalling, while binding of sIL-6R to IL-6 strongly sensitizes target cells (Scheller et al., 2006, Imada and Leonard, 2000).

High expression of IL-6 has been detected in most tumours types and caused alteration in the expression of apoptosis regulatory proteins resulted in high resistance of these tumours to chemotherapy (Bellone et al., 2005, Cozen et al., 2004). One of its main functions is to activate JNK signalling and activator of transcription STAT3. IL-6 has also the ability to phosphorylate mitogen activated protein kinases (MAPK) and AKT (Culig and Puhr, 2012). Moreover, a correlation between IL-6 and anti-apoptotic effects in a number of carcinomas, for example in prostate cancer, where IL-6 mediated PI3-K pathway activation, which in turn activates AKT, regulates cell survival (Chung et al., 2000).

Cytokine secretion, including IL-6, has been shown to be regulated by CD40 ligation (Alexandroff et al., 2000, Gallagher et al., 2002a, Cao et al., 2005 Altenburg, 1999 #670, Altenburg et al., 1999). An association between NF-κB and IL-6 secretion has been shown previously, in studies where CD40-negative HeLa cells were transfected with a CD40-expression vector or with a CD40 mutant vector deficient in NF-κB activation; in response to CD40 ligation by either sCD40L or G28.5 mAb, CD40 ligation caused IL-6 secretion in WT receptor-expressing cells, whereas HeLa cells expressing mutant CD40 failed to exhibit IL-6 production following CD40 ligation by either type of agonist (Eliopoulos et al., 1997, Shaw et al., 2005). Findings from our laboratory have

previously demonstrated CD40-mediated IL-6 secretion in UCC EJ cells in response to CD40 ligation by mCD40L (Georgopoulos et al., 2006).

To systematically examine IL-6 secretion in the panel of RCC cells, supernatants from co-cultures of RCC cells with 3T3-CD40L and 3T3-Neo were collected at specific time points (1.5h, 3h, 6h, 12h, 24h, 36h and 48h) and then screened for IL-6 secretion by ELISA assays as above for IL-8. Results showed extensive secretion of IL-6 in response to CD40 ligation in all three RCC lines in a time-dependant manner, consistent with the observations with control EJ cells (Figure 4.3). This induction was observed as early as 1.5h following CD40 ligation. It should be noted that during the course of the experiments the relative increase in IL-6 secretion subsided, which was due to basal IL-6 secretion by all RCC cell lines (Figure 4.3, left panels). This was particularly evident with the A-704 cell line that showed extensive IL-6 secretion. Interestingly also, the rate of IL-6 release in EJ cells was much slower that that observed in the RCC lines.

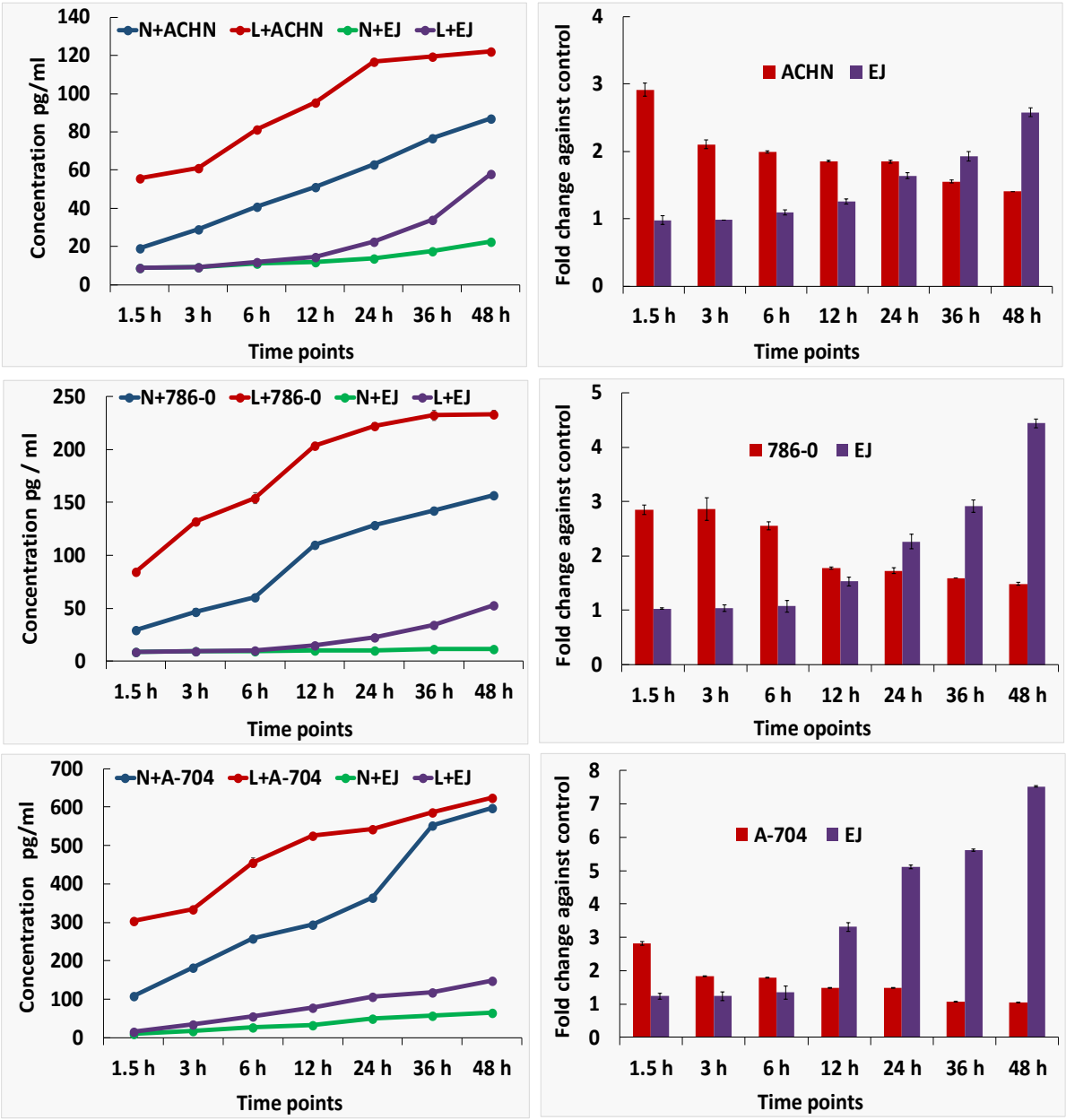

Figure 4.3 mCD40L-mediated IL-6 secretion in RCC cells

RCC cells (ACHN, 786-0 and A-704) were co-cultured at a density of $5x10^4$ with $6x10^4$ of MMC-treated fibroblasts 3T3-CD40L and 3T3-Neo in 24 well plates (as detailed in the Methods) for 1.5-48h) and supernatants were collected at the indicated time points. Secretion of IL-6 was determined by ELISA assays. Graphs on the left show mean of at least 3 technical replicates of IL-6 concentration, calculated as described in materials and methods (section 2.12.2) and are typical of 2 independent experiments. Results from these graphs are also presented as fold change (L) relative to control (N) as bar graphs on the right.

Key

N+A-704	: 3T3-Neo co-cultured with A-704	N+786-O	: 3T3-Neo co-cultured with 786-O
L+A-704	: 3T3-CD40L co-cultured with A-704	L+786-O	: 3T3-CD40L co-cultured with 786-O
N+ACHN	: 3T3-Neo co-cultured with ACHN	N+EJ	: 3T3-Neo co-cultured with EJ
L+ACHN	: 3T3-CD40L co-culture with ACHN	L+EJ	: 3T3-CD40L co-cultured with EJ

4.2.3 Detection of GM-CSF secretion in RCC cells following CD40 ligation by mCD40L

Granulocyte/Macrophage-Colony stimulating factor (GM-CSF) is a strongly pro-inflammatory pleiotropic cytokine that plays essential role in the generation of effective immune responses via its ability to activate monocytes, macrophages and granulocytes at the sites of inflammation (Gasson, 1991).

T cells produce GM-CSF in response to the TCR activation. However, the immunosuppressive drug cyclosporine (CsA) has been shown to inhibit the secretion of GM-CSF via its ability to block the Ca^{2+}/calcineurin pathway (Cockerill et al., 1993, Shannon et al., 1997). The family of transcription factors NFAT have been shown to be induced by the Ca^{2+}/calcineurin pathway (Hernández-Munain and Krangel, 2002, Hogan et al., 2003, Lee et al., 2004, Solymar et al., 2002). Furthermore, it has been observed that NFAT exerts its activity to control GM-CSF gene expression via its synergism with other families of transcription factors including AP-1 (Crabtree and Olson, 2002, Hogan et al., 2003).

It has been reported that GM-CSF secretion in T-cells and B-cells depends on the induction of activator protein-1 (AP-1) transcription factor (Wang et al., 1994, Johnson et al., 2004). Moreover, mCD40L mediates apoptosis via TRAF3-mediated JNK phosphorylation that leads to the induction of AP-1 in carcinoma cells (Georgopoulos et al., 2006, Dunnill et al., 2016), and CD40 ligation by mCD40L triggered GM-CSF secretion in CRC cells (Georgopoulos et al., 2007); thus, it has been hypothesised that CD40 ligation may induce GM-CSF secretion depending on the induction of AP-1 (Georgopoulos et al., 2007). Studies by Shorts et al (2006) demonstrated that stimulation of CD40 in RCC tumours in vivo and in human RCC cell lines in vitro leads to GM-CSF production (Shorts et al., 2006).

Thus, to investigate whether CD40 ligation by mCD40L can induce GM-CSF secretion in human RCC cells, supernatants were collected from co-cultures of RCC cells as above (at time points 1.5h, 3h, 6h, 12h, 24h, 36h and 48h) and GM-CSF concentration determined by ELISA. Results showed significant induction of GM-CSF secretion in all three RCC lines by 3h post CD40 ligation particularly in 786-O cells. More relatively

modest increases were observed in A-704 and ACHN cells, whilst secretion of GM-CSF in EJ cells was more delayed yet particularly marked by 24h (Figure 4.4). As in the case of the other two cytokines (IL-6 and IL-8), during the course of these experiments the relative increase in GM-CSF secretion subsided, which was due to basal secretion by all RCC cell lines (Figure 4.4).

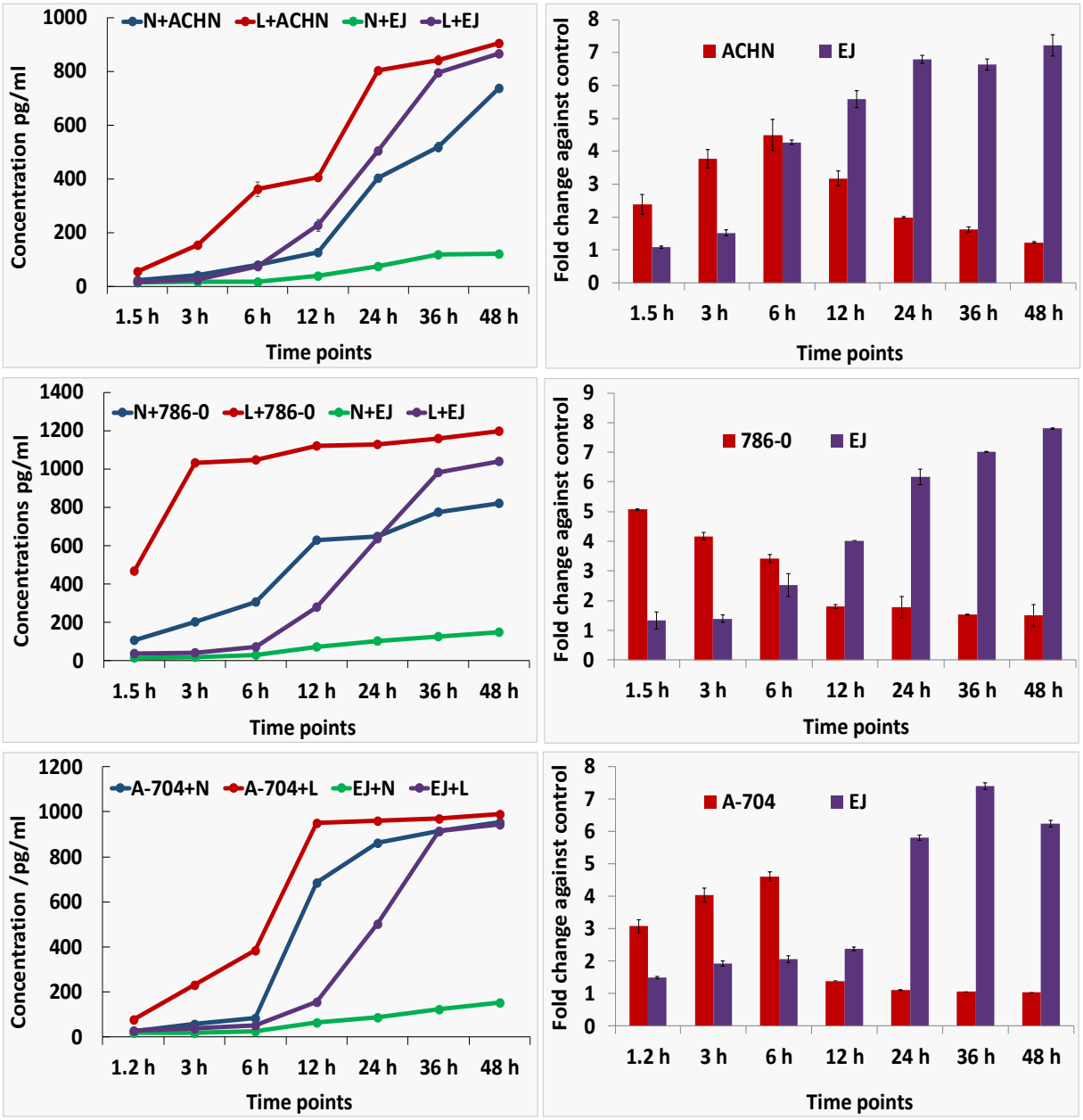

Figure 4.4 mCD40L-mediated GM-CSF secretion in RCC cells

RCC cells (ACHN, 786-0 and A-704) were co-cultured at a density of $5x10^4$ with $6x10^4$ of MMC-treated fibroblasts 3T3-CD40L and 3T3-Neo in 24 well plates (as detailed in the Methods) for 1.5-48h) following incubation at the the indicated time points supernatants were taken at. Secretion of GM-CSF was determined by ELISA assays. Graphs on the left show mean of at least 3 technical replicates of GM-CSF concentration, calculated as explained in materials and methods (section 2.12.2) and are representative of 2 independent investigates. Results from these graphs are also shown as fold change (L) relative to control (N) as bar graphs on the right.

Key

N+A-704	: 3T3-Neo co-cultured with A-704	N+786-O	: 3T3-Neo co-cultured with 786-O
L+A-704	: 3T3-CD40L co-cultured with A-704	L+786-O	: 3T3-CD40L co-cultured with 786-O
N+ACHN	: 3T3-Neo co-cultured with ACHN	N+EJ	: 3T3-Neo co-cultured with EJ
L+ACHN	: 3T3-CD40L co-culture with ACHN	L+EJ	: 3T3-CD40L co-cultured with EJ

4.3 The role of the mode of CD40 ligation in GM-CSF secretion

CD40 ligation by mCD40L triggered apoptosis in UCC cells via TRAF3 recruitment and JNK phosphorylation which then mediated AP-1 induction, while treatment with soluble agonists did not induce JNK activation or detectable apoptosis (Bugajska et al., 2002, Georgopoulos et al., 2006). As shown in this study, the same scenario could be applied in RCC cells, as anti-CD40 agonistic antibody G28-5 did not induce apoptosis while membrane presented CD40L triggered massive apoptotic cell death at 48h following CD40 ligation (Chapter 3).

The degree of receptor cross-linking, however, appears to not only determine functional outcome in terms of apoptosis induction, but it also influences cytokine secretion. Previous studies in B cells (Baccam and Bishop, 1999) and carcinoma cells (Georgopoulos et al., 2007) have shown that the capability of CD40 ligation to mediate cytokine secretion is also reliant on on the 'quality' of the CD40 signal. Particularly in carcinoma cells, soluble agonist can induce IL-6 and IL-8 secretion however that is to a lesser extent that the induction observed with mCD40L. More importantly, GM-CSF secretion induction was only observed following CD40 activation by membrane but not soluble agonist.

To discourse this question in RCC cells, 786-O were treated with 10µg/ml of G28-5 agonists in the presence of 2.5µg/ml of secondary antibody (cross linker), then incubated for 1.5h, 3h, 6h, 12h, 24h, 36h and 48h, alongside mCD40L-treated (by co-culture of 786-O with 3T3-CD40L and 3T3-Neo). Supernatants were collected from both types of cultures in parallel time course experiments and GM-CSF secretion was determined by ELISA assays. Treatment with cross-linked G28-5 mAb caused very small and delayed secretion of GM-CSF in 786-O cells in direct contrast with mCD40L which, as above, caused marked GM-CSF release (Figure 4.5).

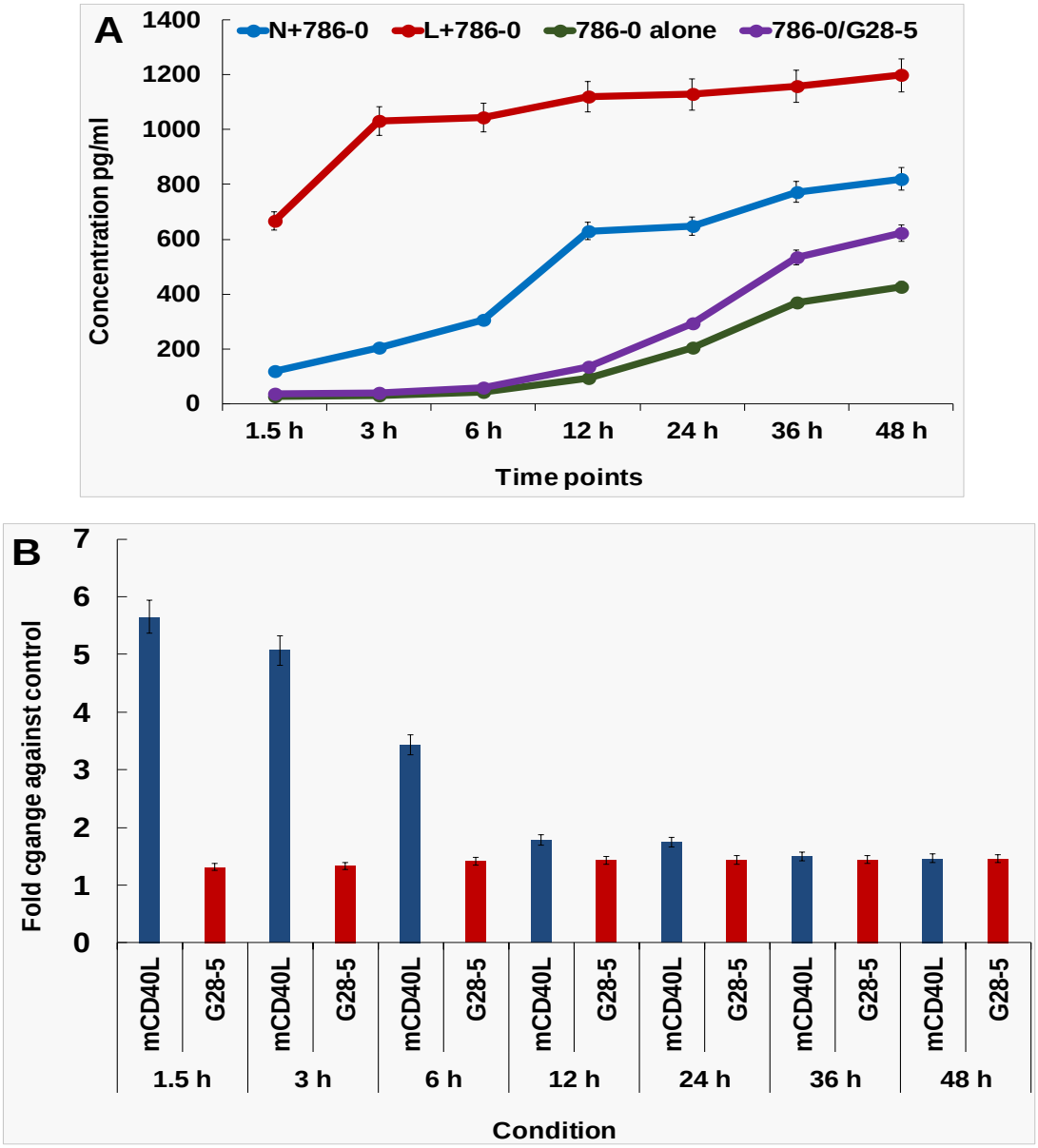

Figure 4.5 GM-CSF secretion in 786-O cells following CD40 activation by soluble versus membrane-presented agonist

RCC cells line 786-O were either cultured at density of $5x10^4$ cell/well in presence of 10µg/ml of cross linked agonistic anti-CD40 antibody G28-5, or co-cultured with $6x10^4$ of MMC-treated fibroblasts 3T3-CD40L and 3T3-Neo in 24 well plates (as detailed in the Methods) for (1.5-48h) and supernatants were collected at the indicated time points. Secretion of GM-CSF was determined by ELISA assay. Graphs on the tope show mean of at least 3 technical replicates of GM-CSF concentration, calculated as described in materials and methods (section 2.12.1) and are typical of 2 independent experiments. Results from this graph is also presented as fold change (L) relative to control (N) as bar graph on the bottom.

Key
N+786-O: 3T3-Neo co-cultured with 786-O
L+786-O: 3T3-CD40L co-cultured with 786-O
786-O/G28-5: 786-O cultured in presence of G28-5

4.4 Summary

- Results in this chapter demonstrated that CD40 ligation by mCD40L induces substantial cytokine secretion in RCC cells
- Initial screening experiments using cytokine filter arrays showed mCD40L-mediated induction of a panel of pro-inflammatory cytokines in RCC cells
- The most highly induced cytokines (previously associated with CD40 signalling) detected in the array experiments were IL-8, IL-6, GM-CSF, GROa, sICAM-1 and MCP-1
- ELISA assay experiments focused on measurement of levels of cytokines IL-6, IL-8 and GM-SCF, due to their previously reported induction by CD40 ligation in our laboratory and based on reports by others
- All RCC lines secreted readily detectable levels of IL-6, IL-8 and GM-CSF, which resulted in progressive accumulation of these cytokines in control supernatants; yet CD40 ligation by mCD40L caused marked induction in cytokine secretion. Control EJ cells did secrete substantial levels of these cytokines
- mCD40L caused marked induction of secretion of IL-8 in all three RCC lines in a time-dependent manner with rapid secretion of IL-8 observed as early as 1.5h following CD40 ligation
- Significant secretion of IL-6 was observed within 6h post CD40 ligation by mCD40L, which was more gradual in the control EJ cells
- Substantial induction of GM-CSF secretion was observed in all RCC lines by 3-6h post CD40 ligation particularly in 786-O cells. More relatively modest increases were observed in A-704 and ACHN cells, whilst secretion of GM-CSF in EJ cells was more delayed yet particularly marked by 24h

- Treatment with cross-linked G28-5 mAb caused little and delayed secretion of GM-CSF in 786-O cells; this was in direct contrast with mCD40L which caused marked and rapid GM-CSF release

- In brief, pro-apoptotic CD40 ligation by mCD40L caused rapid and substantial pro-inflammatory cytokine secretion in RCC cells, while non-apoptotic ligation by soluble agonist triggered little detectable secretion, which confirms the importance of receptor cross-linking in functional outcome.

Chapter 5

Investigations on the intracellular signalling mediators involved in CD40-mediated apoptosis in RCC cells

5 Background

The mechanisms by which CD40 receptor signalling controls homeostatic responses and cell fate, especially in terms of the role of specific TRAF adaptor molecules, have mainly been studied in B cells by elegant work from Gail Bishop's group (Bishop, 2004). Yet comparatively less is known about the precise signalling pathways triggered following activation by CD40L in epithelial cells (Eliopoulos and Young, 2004, Albarbar et al., 2015) and the role of specific TRAFs in CD40 signalling in non-haematopoietic cells remains much less understood. Generally, TRAFs coordinate various Aspects of cellular responses such as proliferation, differentiation or apoptosis (Bishop, 2004).

One common feature, nevertheless, is that cellular responses to CD40 signalling, whether in B cells or epithelial cells, are exquisitely context-specific. The engagement of CD40 with CD40L causes the recruitment of adapter TRAFs to the cytoplasmic tail of the CD40 molecule (Bishop et al., 2007). Cellular relocation of TRAFs and their interaction with CD40 triggers the activation of several signalling pathways, which include NF-κB, the MAPK pathways p38 and JNK/AP-1, and the PI3-K/Akt pathway (Davies et al., 2005, Elgueta et al., 2009). Any intracellular signalling induced by CD40 depends almost exclusively on TRAFs, but can be independent of TRAFs, such as the pathway of STAT5 resulting from the direct association of Janus kinase 3 (JAK3) with CD40 (Säemann et al., 2003, Säemann et al., 2002) (see Figure 1.16).

Previous studies by Eliopoulos and colleagues implied that the isoleucine zipper sCD40L (in the presence of protein synthesis inhibitors) causes paracrine expression of Fas, TRAIL and TNF to induce apoptosis. These classical "death receptors" were shown to induce cell apoptosis via the extrinsic pathway, and inhibition of caspase-8 attenuated CD40-mediated cytotoxicity (Eliopoulos et al., 2000). Yet, CD40 ligation by mCD40L in UCC cells stabilizes and recruits TRAF3, triggers JNK/AP-1 activation and subsequent cell death. However, there is discrepancy over whether this is mediated via extrinsic or intrinsic pathways of apoptosis, or their cross-talk (Georgopoulos et al., 2006, Elmetwali et al., 2010b). At least in part, there has been a consistent implication for Bak and Bax expression and caspase-9 dependency; therefore, it is possible that

intrinsic pathways play a key role in the overall event, due to their ability to create MOMP (Bugajska et al., 2002, Georgopoulos et al., 2006).

Any discrepancies reported might be due to the fact that the response of carcinoma cell lines is highly affected by the type of CD40 agonist and mode of delivery. It is obvious that the “quality‟ of the CD40 signal, reflected by the degree of receptor cross-linking which has a dramatic influence on the functional outcome of CD40 ligation. Yet, although in the case of other TNFRs more cross-linking corresponds to more apoptosis, in the case of CD40 the strength of the signal is often the difference between detectable apoptosis or not: extensive cross-linking corresponds to high level of apoptosis, whilst treatment with weakly cross-linked agonistic anti-CD40 antibodies causes little (in many cases, if any apoptosis) and mainly growth-inhibition without pharmacological intervention (Tong et al., 2001, Hirano et al., 1999).

It has been demonstrated recently that mCD40L, but not soluble agonist, utilises ROS elevation while concurrently down-regulating anti-oxidant responses (Trx) to efficiently kill malignant cells, by operating along a TRAF3-Nox/p40phox-ASK1- MKK4-JNK signalling axis to induce the mitochondrial apoptotic pathway. The ability of mCD40L to induce death is linked with its ability to stabilise TRAF3 and generate ROS via TRAF3-Nox activation of ASK1 (Dunnill et al., 2016).

5.1 Objectives

This chapter aimed to the first time

- Investigate the expression of intracellular proteins that are regulated during CD40-mediated apoptosis in human RCC cell lines; these included:
  - Receptor-proximal events, such as induction or stabilisation of TRAF adaptor proteins
  - Activation (phosphorylation) of early and late MAPKs
  - Induction of expression of pro-apoptotic mediators (e.g. Bak AND Bax)

- To utilize specific pharmacological inhibitors to investigate whether
  - JNK, AP-1, p38, MEK/ERK and NF-κB are involved in CD40-mediated apoptosis in RCC cells
  - Investigate whether JNK/p38 regulate Bak and Bax expression

- To optimise methodologies of the detection of intracellular ROS and examine the ROS level during CD40 ligation either by mCD40L or by agonistic anti-CD40 antibody (G28-5)

- To employ pharmacological inhibitors, death assays and immunoblotting to determine whether the NADPH oxidase complex could be the a crucial mediator for ROS generation and CD40-mediated cell death

- To investigate the expression of intracellular proteins that involved in ROS generation through CD40-CD40L interaction in RCC cells such as ASK-1, Thioredoxin and $p40^{phox}$

5.2 Regulation of TRAF -1, -2, -3 and -6 expression

Previous work in our laboratory has reported that CD40 activation by mCD40L, but not soluble agonists, induces expression of TRAF1, TRAF2 and TRAF3 in urothelial cancer cells (UCC) as well as TRAF6 expression in colorectal cancer cells (CRC) (Georgopoulos et al., 2006, Hill et al., 2008, Mohamed, 2014, Dunnill et al., 2016).

Having shown that mCD40L mediates extensive apoptosis in RCC cells for the first time in this study (Chapter 3) using various death detection assays, the study then focused on the signalling components of the apoptotic CD40 pathway in RCC cells; the work focused on regulation of intracellular mediators following CD40 ligation in RCC cells by mCD40L but not soluble agonist (agonistic anti-CD40 antibody G28-5) due to its inability to induce apoptosis in RCC cells (see chapter 3).

By utilising the already optimised co-culture system, RCC cell lines ACHN, 786-O and A-704 were cultured with mCD40L-expressing effector cells (and control cells) and initially the expression of TRAFs was examined by immunoblotting using human specific antibodies, where possible. To ensure that the antibodies were specifically detecting human (and not effector/fibroblast) proteins, appropriate controls with effector cells alone were included in all experiments.

Results from these studies showed rapid and marked induction in TRAF1, TRAF2, TRAF3 and TRAF6 expression within 1.5h post-CD40 ligation and representative experiments are shown in Figures 5.1, 5.2, 5.3 and 5.4, respectively.

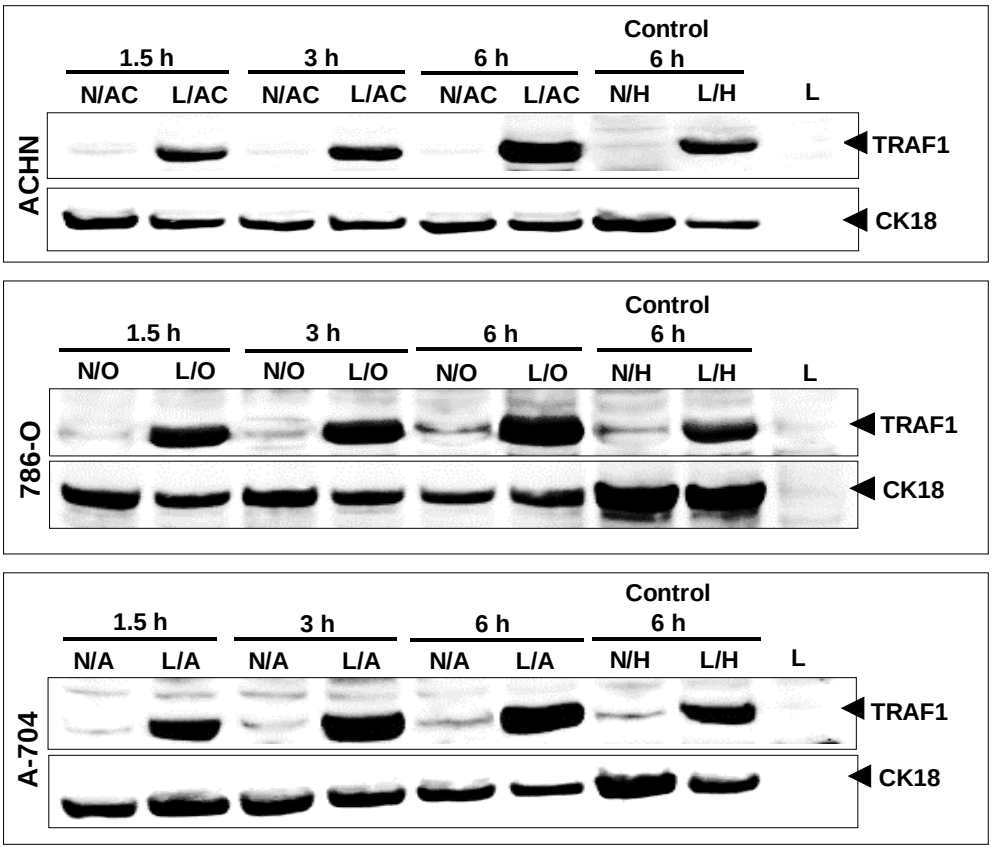

Figure 5.1The regulation of TRAF1 expression by CD40 ligation in RCC cells

RCC cells were co-cultured at $3x10^6$ cells/dish with $3x10^6$ cells/dish of fibroblasts 3T3-Neo and 3T3-CD40L in 10 cm dishes and incubated for 1.5, 3 and 6h. cells were lysis as explained in the Methods (Section 2.9.3) and 40µg of protein/well was analysed by immunoblotting (Section 2.9.5). After normalisation on the basis of CK18 expression (see chapter 3 section 3.10), 40µg of normalised lysates were loaded and analysed by immunoblotting. After overnight incubation at 4ºC by rocking with primary polyclonal antibody (anti-TRAF1) in TBS/Tween 0.1% (1:1000 dilution), secondary antibody goat anti-rabbit IgG IRDye 800 (1:10000 dilution) was added and then incubation in the dark for 1h. For specificity and as a loading control CK18 antibody was used (at 1:1000 dilution), and incubation overnight at 4ºC, then 1h incubation in the dark with secondary antibody goat-anti mouse IgG Alexa 680 (diluted 1:10000). Antibody binding was visualised at 800nm for TRAF1 detection (expected molecular weight 52 kDa) and 700nm for CK18 detection using an Odyssey™ Infra-red Imaging system. Co-cultures for the HCT116 cell line were used as negative (N/H) and positive (L/H) controls, respectively, and 3T3CD40L cell lysate was used for confirmation of antibody specificity for human protein detection.

Key:

N/AC : 3T3Neo co-cultured with ACHN
N/O : 3T3Neo co-cultured with 786-O
N/A : 3T3Neo co-cultured with A-704
L : 3T3CD40L
L/AC : 3T3CD40L co-cultured with ACHN
L/O : 3T3CD40L co-cultured with 786-O
L/A : 3T3CD40L co-cultured with A-704

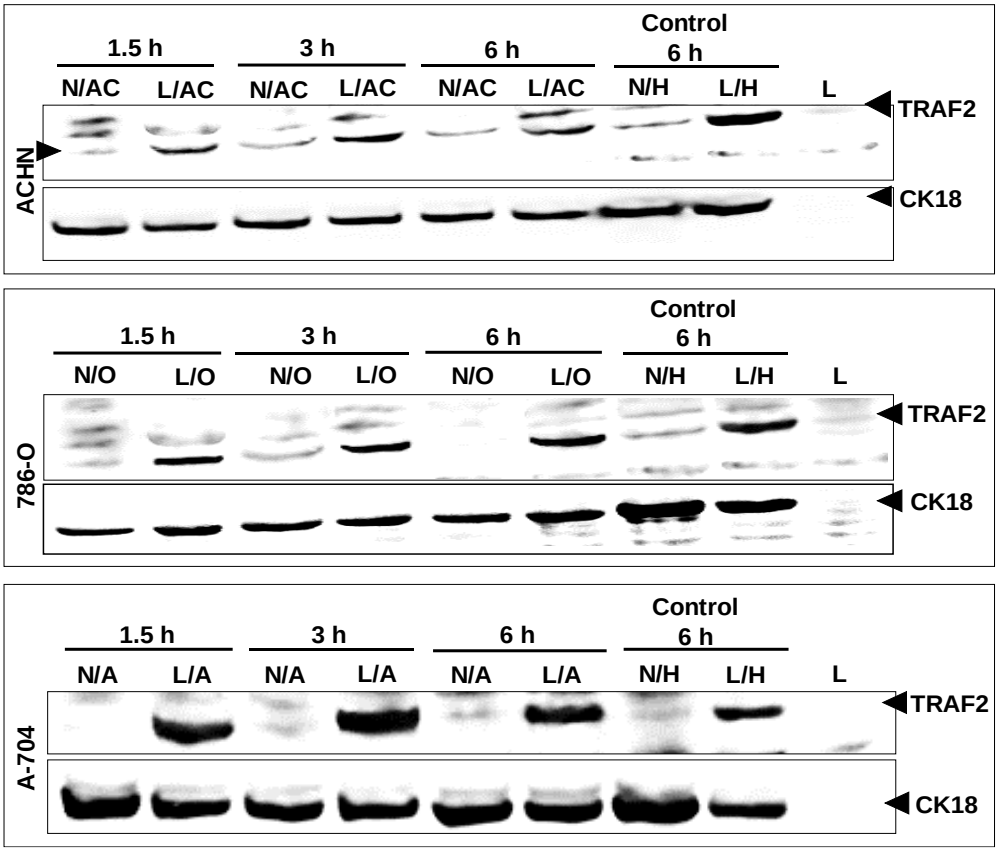

Figure 5.2 The regulation of TRAF2 expression by CD40 ligation in RCC cells

RCC cells were co-cultured at $3x10^6$ cells/dish with $3x10^6$ cells/dish of fibroblasts 3T3-Neo and 3T3-CD40L in 10 cm dishes and incubated for 1.5, 3 and 6h. Whole cell lysates were prepared as described in the Methods (Section 2.9.3) and 40µg of protein/well was analysed by immunoblotting (Section 2.9.5). After normalisation on the basis of CK18 expression (see chapter 3 section 3.10), 40µg of normalised lysates were loaded and analysed by immunoblotting. After overnight incubation at 4ºC by rocking with primary polyclonal antibody (anti-TRAF2) in TBS/Tween 0.1% (1:1000 dilution), secondary antibody goat anti-rabbit IgG IRDye 800 (1:10000 dilution) was added and the membranes were incubated in the dark for 1h. For specificity and as a loading control CK18 antibody was used (at 1:1000 dilution), and incubation overnight at 4ºC, then the membranes were incubated with secondary antibody goat-anti mouse IgG Alexa 680 (diluted 1:10000) in the dark for 1h. Antibody binding was visualised at 800nm for TRAF2 detection (expected molecular weight 50 kDa) and 700nm for CK18 detection using an Odyssey™ Infra-red Imaging system. Co-cultures for the HCT116 cell line were used as negative (N/H) and positive (L/H) controls, respectively, and 3T3CD40L cell lysate was used for confirmation of antibody specificity for human protein detection.

Key:

N/AC : 3T3Neo co-cultured with ACHN
N/O : 3T3Neo co-cultured with 786-O
N/A : 3T3Neo co-cultured with A-704
L : 3T3CD40L
L/AC : 3T3CD40L co-cultured with ACHN
L/O : 3T3CD40L co-cultured with 786-O
L/A : 3T3CD40L co-cultured with A-704

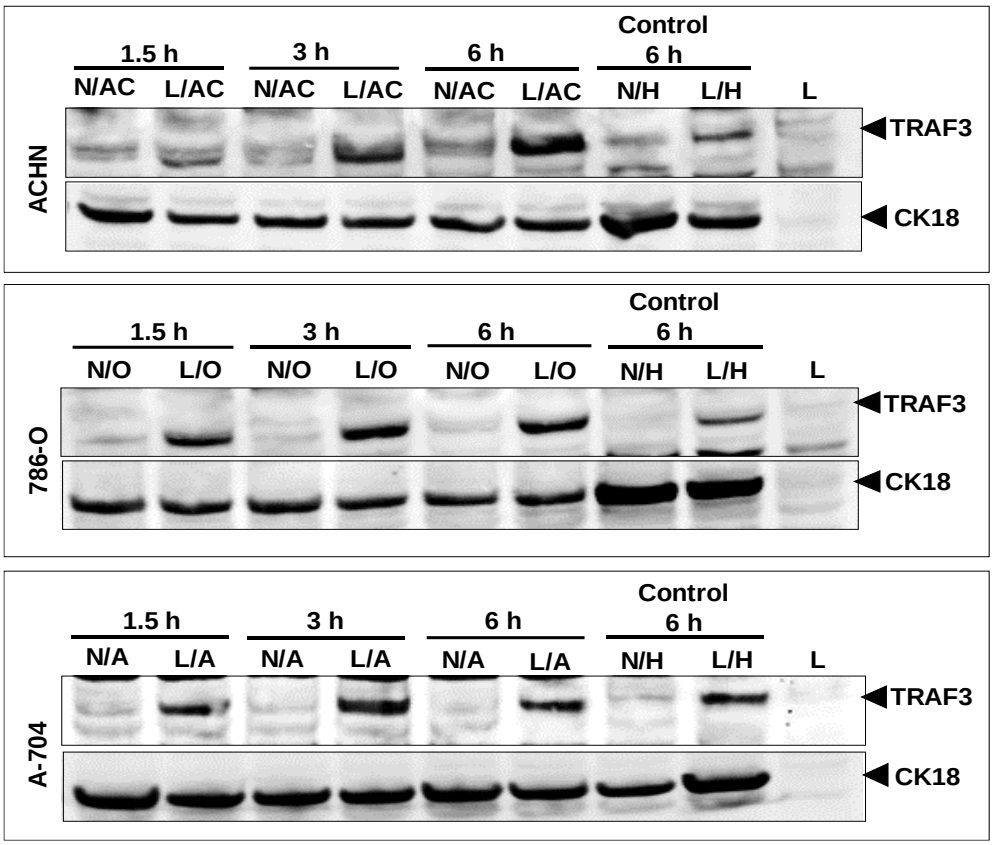

Figure 5.3The regulation of TRAF3 expression by CD40 ligation in RCC cells

RCC cells were co-cultured at $3x10^6$ cells/dish with $3x10^6$ cells/dish of fibroblasts cells 3T3-Neo and 3T3-CD40L in a 10 cm dishes and incubated for (1.5, 3 and 6h). Whole cell lysates were prepared as described in the Methods (Section 2.9.3) and 40µg of protein/well was analysed by immunoblotting (Section 2.9.5). After normalisation on the basis of CK18 expression (see chapter 3 section 3.10), 40µg of normalised lysates were loaded and analysed by immunoblotting. After overnight incubation at 4ºC by rocking with primary polyclonal antibody (anti-TRAF3) in TBS/Tween 0.1% (1:1000 dilution), secondary antibody [goat anti-rabbit IgG IRDye 800nm (1:10000 dilution)] was added and the membranes were incubated in the dark for 1h. For specificity and as a loading control CK18 antibody was used at (1:1000 dilution), and incubation overnight at 4ºC, then the membranes were incubated with secondary antibody goat-anti mouse IgG Alexa 680 (diluted 1:10000) in the dark for 1h.. Antibody binding was visualised at 800nm for TRAF3 detection (expected molecular weight 50 kDa) and 700nm for CK18 detection using an Odyssey™ Infra-red Imaging system. Co-cultures for the HCT116 cell line were used as negative (N/H) and positive (L/H) controls, respectively, and 3T3CD40L cell lysate was used for confirmation of antibody specificity for human protein detection.

Key:

N/AC : 3T3Neo co-cultured with ACHN
N/O : 3T3Neo co-cultured with 786-O
N/A : 3T3Neo co-cultured with A-704
L : 3T3CD40L
L/AC : 3T3CD40L co-cultured with ACHN
L/O : 3T3CD40L co-cultured with 786-O
L/A : 3T3CD40L co-cultured with A-704

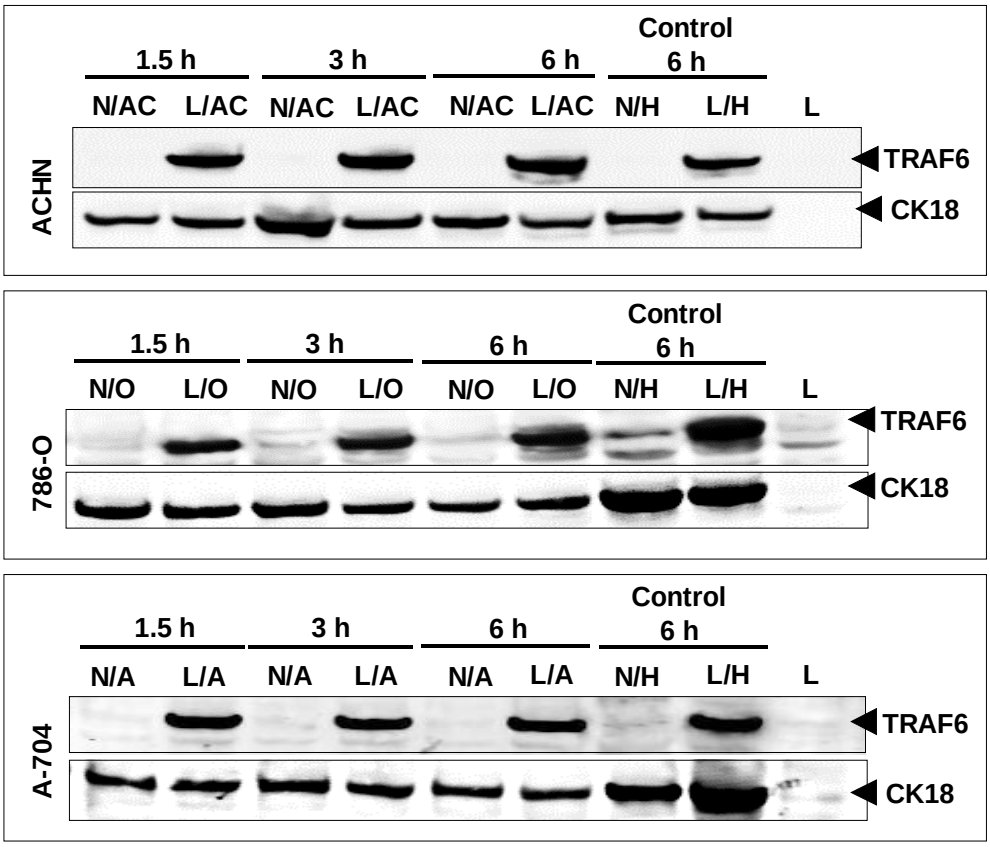

Figure 5.4The regulation of TRAF6 expression by CD40 ligation in RCC cells

RCC cells were co-cultured at $3x10^6$ cells/dish with $3x10^6$ cells/dish of fibroblasts cells 3T3-Neo and 3T3-CD40L in a 10 cm dishes and incubated for (1.5, 3 and 6h). Whole cell lysates were prepared as described in the Methods (Section 2.9.3) and 40µg of protein/well was analysed by immunoblotting (Section 2.9.5). After normalisation on the basis of CK18 expression (see chapter 3 section 3.10), 40µg of normalised lysates were loaded and analysed by immunoblotting. After overnight incubation at 4ºC by rocking with primary monoclonal antibody (anti-TRAF6) in TBS/Tween 0.1% (1:1000 dilution), secondary antibody goat-anti mouse IgG Alexa 680 [(1:10000 dilution)] was added and the membranes were incubated in the dark for 1h. For specificity and as a loading control CK18 antibody was used at (1:1000 dilution), and incubation overnight at 4ºC, then the membranes were incubated with secondary antibody goat-anti mouse IgG Alexa 680 (diluted 1:10000) in the dark for 1h.. Antibody binding was visualised at 800nm for TRAF6 detection (expected molecular weight 52 kDa) and 700nm for CK18 detection using an Odyssey™ Infra-red Imaging system. Co-cultures for the HCT116 cell line were used as negative (N/H) and positive (L/H) controls, respectively, and 3T3CD40L cell lysate was used for confirmation of antibody specificity for human protein detection.

Key:

N/AC : 3T3Neo co-cultured with ACHN
N/O : 3T3Neo co-cultured with 786-O
N/A : 3T3Neo co-cultured with A-704
L : 3T3CD40L
L/AC : 3T3CD40L co-cultured with ACHN
L/O : 3T3CD40L co-cultured with 786-O
L/A : 3T3CD40L co-cultured with A-704

5.3 Detection of activation of MKK4 and MKK7 MAPKs

It has been well-documented that upstream MAPKKs, especially MKK4 and MKK7, in MAPK pathways are often responsible for the up-regulation of pro-apoptotic transcriptional activators, such as JNK and p38 (Wagner and Nebreda, 2009). The MAPK pathway is an important key signal transduction regulating apoptosis, cell proliferation and differentiation. This is a successive complex phosphorylation cascade involving a large number of signalling proteins. These proteins could be sub-divided into three groups: MAPKKK (MAP kinase kinase kinase), MAPKK (MAP kinase kinase) and MAPK (MAP kinase) and are activated by a sequential phosphorylation process in which activated MAPKKKs proteins activate MAPKK via loop phosphorylation of two seryl residues. The MAPKKs in turn trigger MAPK (e.g. JNK and p38) activation by tyrosyl and threonyl phosphorylation. MAPKKs proteins include MKK-3, -4, 6, and -7 as well as MEK1/2. MKK3 activates p38 MAPK alpha and beta (p38-α, and -β) while MKK6 can activate both isoforms equally.

CD40-mediated MKK3/6 and p38 activation have been shown important for IL-6 and IL-10 monocyte secretion during inflammation (Inoue et al., 2004). Activation of MKK4 is mainly mediated by environmental stress and MKK7 by cytokines, both proteins (MKK7 and MKK4 activate JNK in response to external stimuli, whereas other reports showed overexpression of MKK4 and MKK7 in vitro caused phosphorylation of members of p38 family (Davis, 2000). It has been reported previously that complete activation of JNK depends on phosphorylation of both MKK7 and MKK4 in vitro (FLEMING et al., 2000, Kishimoto et al., 2003). Other studies showed that loss of MKK7 causes increase in cell proliferation in fibroblasts indicating the negative role of this kinase in growth regulation (Wada and Penninger, 2004). JNK and AP-1 activation during CD40-mediated apoptosis has been demonstrated previously by our laboratory and others (Georgopoulos et al., 2006, Elmetwali et al., 2010b). Recent work in our group demonstrated that mCD40L triggers rapid phosphorylation of MKK4 and MKK7 in CRCs (Mohamed, 2014), while MKK4 was phosphorylated and played an important functional role in mCD40L-mediated death in UCC cells (Dunnill et al., 2016).

Having demonstrated for the first time induction of TRAF expression, this study then sought to investigate the involvement of MKK4 and/or MKK7 in CD40 signalling in RCC cells. Human specific anti-phospho-MKK7 antibody was used in immunoblotting experiments that showed rapid activation of MKK7 within 1.5 hours in response to CD40 ligation by mCD40L, which is further increased at 6h post-ligation in all three cell lines (ACHN, 786-O and A-704) (Figure 5.5). Similarly to MKK7, phosphorylation of MKK4 was detected within 1.5h after CD40 ligation and gradually increased over the time period tested (3h and 6h) in all three cell lines (Figure 5.6).

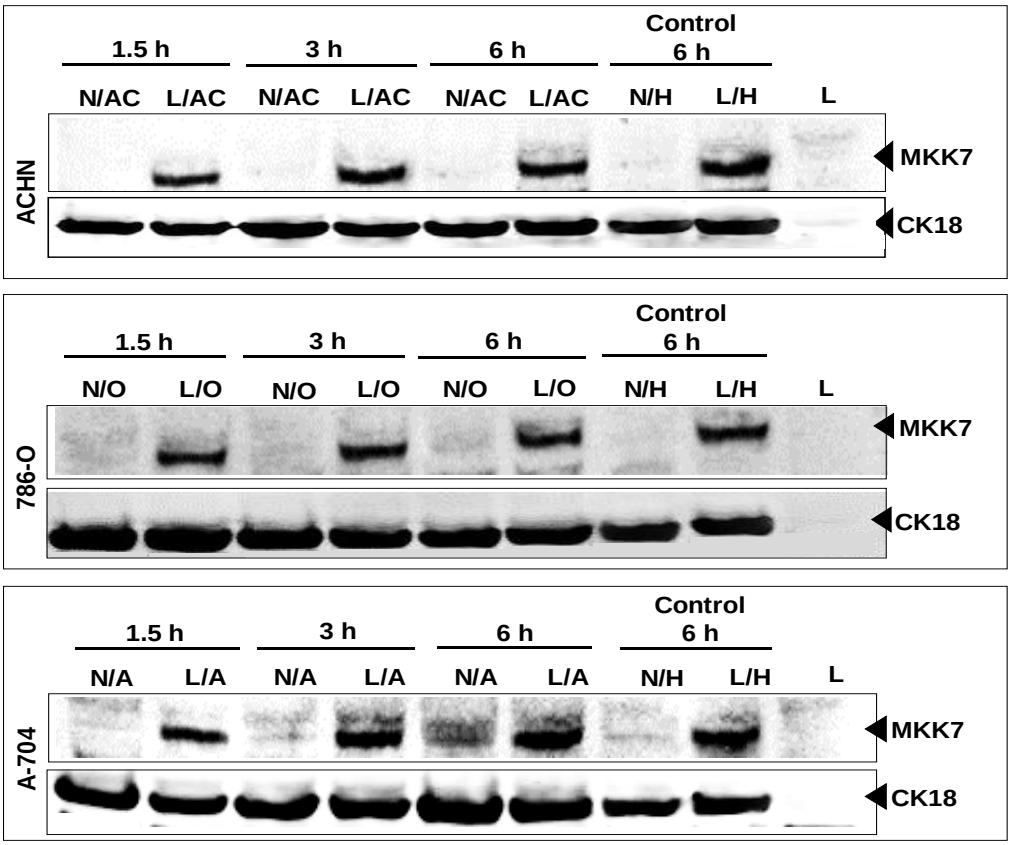

Figure 5.5 CD40 ligation induces MKK7 protein phosphorylation in RCC cells

RCC cells were co-cultured at $3x10^6$ cells/dish with $3x10^6$ cells/dish of fibroblasts cells 3T3-Neo and 3T3-CD40L in a 10 cm dishes and incubated for (1.5, 3 and 6h). Whole cell lysates were prepared as described in the Methods (Section 2.9.3) and 40µg of protein/well was analysed by immunoblotting (Section 2.9.5). After normalisation on the basis of CK18 expression (see chapter 3 section 3.10), 40µg of normalised lysates were loaded and analysed by immunoblotting. After overnight incubation at 4ºC by rocking with primary polyclonal antibody (anti-MKK7) in TBS/Tween 0.1% (1:1000 dilution), secondary antibody [goat anti-rabbit IgG IRDye 800nm (1:10000 dilution)] was added and the membranes were incubated in the dark for 1h. For specificity and as a loading control CK18 antibody was used at (1:1000 dilution), and incubation overnight at 4ºC, then 1h incubation in the dark with secondary antibody goat-anti mouse IgG Alexa 680 (diluted 1:10000). Antibody binding was visualised at 800nm for MKK7 detection (expected molecular weight 48 kDa) and 700nm for CK18 detection using an Odyssey™ Infra-red Imaging system. Co-cultures for the HCT116 cell line were used as negative (N/H) and positive (L/H) controls, respectively, and 3T3CD40L cell lysate was used for confirmation of antibody specificity for human protein detection.

Key:

N/AC : 3T3Neo co-cultured with ACHN
N/O : 3T3Neo co-cultured with 786-O
N/A : 3T3Neo co-cultured with A-704
L : 3T3CD40L
L/AC : 3T3CD40L co-cultured with ACHN
L/O : 3T3CD40L co-cultured with 786-O
L/A : 3T3CD40L co-cultured with A-704

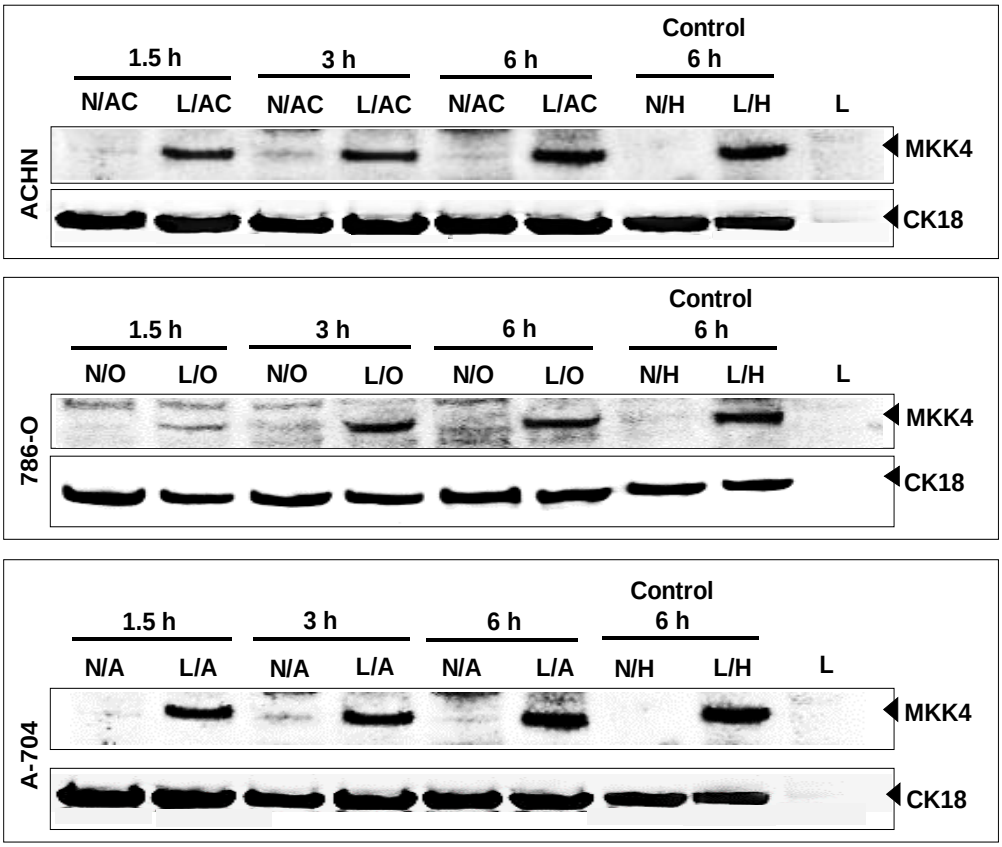

Figure 5.6 CD40 ligation induces MKK4 phosphorylation in RCC cells

RCC cells were co-cultured at $3x10^6$ cells/dish with $3x10^6$ cells/dish of fibroblasts cells 3T3-Neo and 3T3-CD40L in a 10 cm dishes and incubated for (1.5, 3 and 6h). Whole cell lysates were prepared as described in the Methods (Section 2.9.3) and 40µg of protein/well was analysed by immunoblotting (Section 2.9.5). After normalisation on the basis of CK18 expression (see chapter 3 section 3.10), 40µg of normalised lysates were loaded and analysed by immunoblotting. After overnight incubation at 4ºC by rocking with primary polyclonal antibody (anti-MKK4) in TBS/Tween 0.1% (1:1000 dilution), secondary antibody [goat anti-rabbit IgG IRDye 800nm (1:10000 dilution)] was added and the membranes were incubated in the dark for 1h. For specificity and as a loading control CK18 antibody was used at (1:1000 dilution), and incubation overnight at 4ºC, then the membranes were incubated with secondary antibody goat-anti mouse IgG Alexa 680 (diluted 1:10000) in the dark for 1h.. Antibody binding was visualised at 800nm for MKK4 detection (expected molecular weight 44 kDa) and 700nm for CK18 detection using an Odyssey™ Infra-red Imaging system. Co-cultures for the HCT116 cell line were used as negative (N/H) and positive (L/H) controls, respectively, and 3T3CD40L cell lysate was used for confirmation of antibody specificity for human protein detection.

Key:

N/AC : 3T3Neo co-cultured with ACHN
N/O : 3T3Neo co-cultured with 786-O
N/A : 3T3Neo co-cultured with A-704
L : 3T3CD40L
L/AC : 3T3CD40L co-cultured with ACHN
L/O : 3T3CD40L co-cultured with 786-O
L/A : 3T3CD40L co-cultured with A-704

5.4 Activation of JNK and p38 MAPKs

The JNK and p38 MAPK pathways are activated by various extracellular stress and cytokines (Brancho et al., 2003). The protein kinases involved in these pathways are activated through phosphorylation by MAP kinase (MKK or MAPK2K) these in turn are activated by MAPK3K. For instance, MKK4 and MKK7 are primarily able to activate JNK (Dhanasekaran and Reddy, 2008, Kyriakis and Avruch, 2012, Weston and Davis, 2007). Activated JNK induces the transcription factor c-Jun, which has the ability to form transcription factor (TF) complexes of AP-1 (activator protein-1) in most cases by heterodimerization with other family members (JunB/D and Fos/Fra) transcription. AP-1 is a ubiquitous TF and acts as regulator of the expression of a wide variety of proteins, including cell cycle regulators, metalloproteinases (MMP), inflammatory cytokines. The same activation cascades exist for the other two MAPKs: MEK1 and MEK2 activate ERK1 and ERK2 and MKK3/6 activate the p38 MAP kinase. MAPK activation in each cell is tightly controlled (temporally and spatially), and inactivation is dependent on serine / threonine phosphatase, tyrosine phosphatase and dual specificity phosphatases (DUSP) (Bermudez et al., 2010, Shah et al., 2014).

Activation of JNK pathway activation is usually associated with the regulation of cell death (Johnson and Lapadat, 2002, Sabapathy and Wagner, 2004). Moreover, activation of p38 pathway is usually related to the activation of transcription factors and protein kinases involved in the regulation of differentiation and inflammatory response and also cell death (Zhang and Liu, 2002). It has been reported that CD40 ligation by mCD40L mediate JNK activation in UCCs and CRCs (Georgopoulos et al., 2006, Mohamed, 2014, Dunnill et al., 2016) and also p38 activation in CRC cells (Mohamed, 2014).

The expression of the activated (phosphorylated) forms of these stress-activated protein kinases (SAPK) JNK and p38 during CD40-mediated apoptosis in RCC cells was investigated by immunoblotting. Results showed rapid phosphorylation of JNK at 1.5h post CD40 ligation and this was sustained even at 6h in all three RCC cell lines (Figure 5.7); interestingly it was the higher molecular weight isoform (JNK2) that was highly phosphorylated. Similar time-course experiments also permitted detection of

activated p38 in all three cell lines, and p-p38 was detected within 1.5h and its levels continued to rise even at 6h after CD40 ligation in most RCC lines (Figure 5.8).

Of note, for the JNK detection Westerns blot studies a much smaller amount of co-culture lysate was analysed by SDS-PAGE and subsequently immunoblotting, as can be seen in Figure 5.7. During initial optimisation experiments, it became obvious that all the RCC cell lines expressed strikingly high basal levels of phospho-JNK protein (as seen either in lysates from RCC cells alone or in 3T3Neo/RCC cell co-cultures). In order to be able to sensitively detect CD40-specific changes in p-JNK, therefore, a 4-fold reduction in the concentration of total protein loaded (10µg) was used (instead of the routinely used 40µg). Moreover, the dilution of the anti-p-JNK antibody was doubled (1/2000 dilution used instead of 1/1000). Only following these experimental modifications was detection of changes in p-JNK levels by CD40 ligation possible in RCC cells. Finally, because the size of the major JNK band (higher molecular weight band) detected coincided (overlapped) with the molecular weight of CK18 (50-55 kDa), it was also essential that, rather than sequential addition of anti-JNK and anti-CK18 antibodies on the same membranes, loading control CK18 blots were performed separately to avoid overlapping and permit CK18 expression-based confirmation of equal loading.

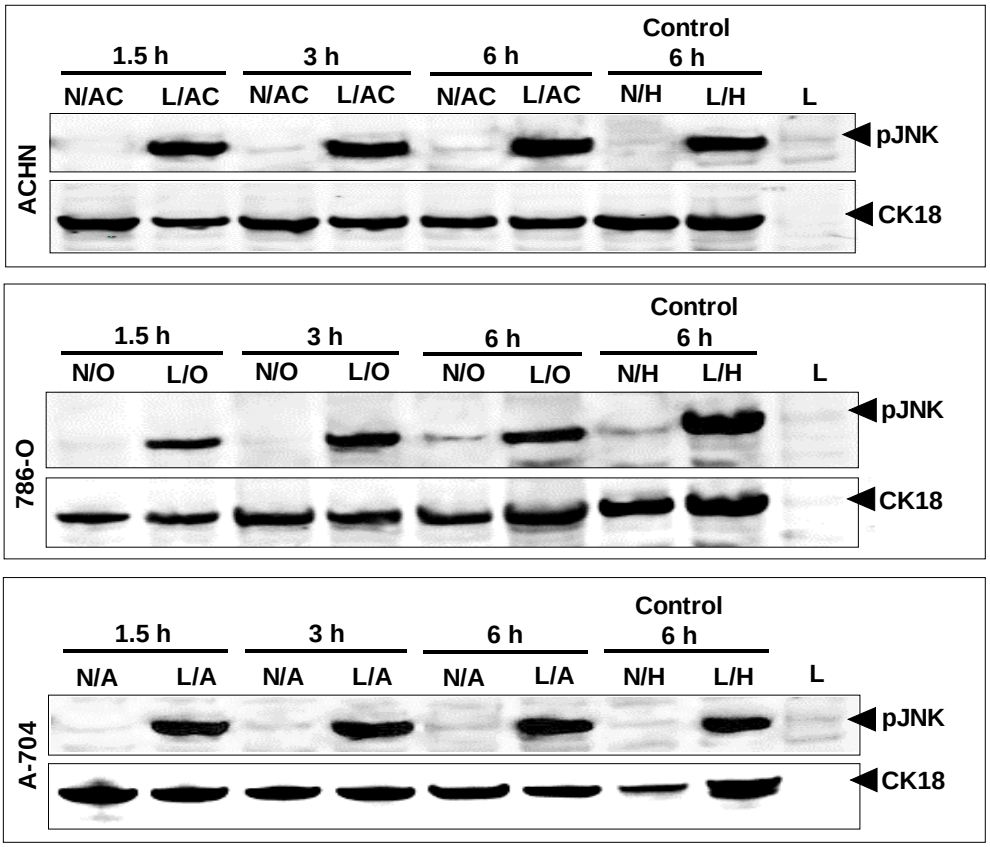

Figure 5.7 JNK activation after CD40 ligation in RCC cells

RCC cells were co-cultured at $3x10^6$ cells/dish with $3x10^6$ cells/dish of fibroblasts cells 3T3-Neo and 3T3-CD40L in a 10 cm dishes and incubated for (1.5, 3 and 6h). Whole cell lysates were prepared as described in the Methods (Section 2.9.3) and 40µg of protein/well was analysed by immunoblotting (Section 2.9.5). After normalisation on the basis of CK18 expression (see chapter 3 section 3.10), 10µg of normalised lysates were loadded and analysed by immunoblotting. The membranes were incubated overnight at 4ºC by rocking with primary monoclonal antibody (anti-p-JNK) in TBS/Tween 0.1% (1:2000 dilution). For specifity and as a loading control, separate gels were blotted alongside and incubated overnight at 4ºC, by rocking with primary monoclonal anti-CK18 antibody (1:1000 dilution), secondary antibody goat-anti mouse IgG Alexa 680 (diluted 1:10000) was added to all membranes and the membranes were incubated in the dark for 1h. Antibody binding was visualised at 700nm for both p-JNK and CK18 detection using an Odyssey™ Infra-red Imaging system, (The JNK-2 band was detected at 50 kDa). Co-cultures for the HCT116 cell line were used as negative (N/H) and positive (L/H) controls, respectively, and 3T3CD40L cell lysate was used for confirmation of antibody specificity for human protein detection.

Key:

N/AC : 3T3Neo co-cultured with ACHN
N/O : 3T3Neo co-cultured with 786-O
N/A : 3T3Neo co-cultured with A-704
L : 3T3CD40L
L/AC : 3T3CD40L co-cultured with ACHN
L/O : 3T3CD40L co-cultured with 786-O
L/A : 3T3CD40L co-cultured with A-704

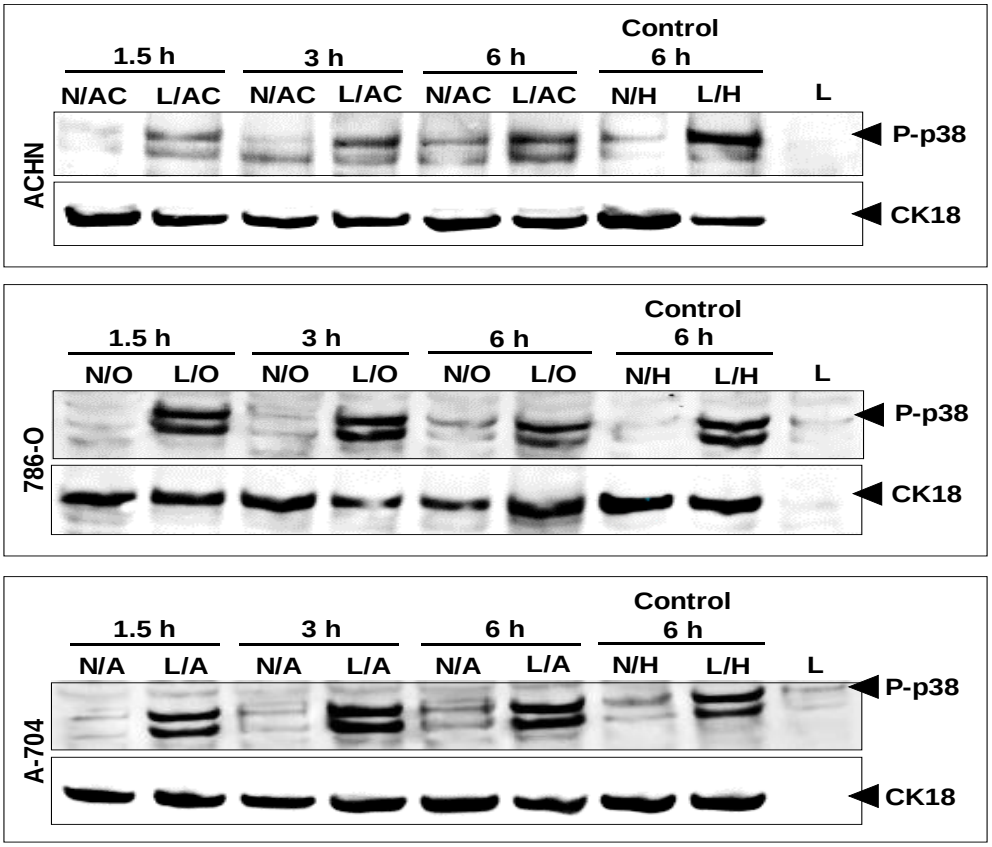

Figure 5.8 p38 activation post CD40 ligation in RCC cells

RCC cells were co-cultured at $3x10^6$ cells/dish with $3x10^6$ cells/dish of fibroblasts cells 3T3-Neo and 3T3-CD40L in a 10 cm dishes and incubated for (1.5, 3 and 6h). Whole cell lysates were prepared as described in the Methods (Section 2.9.3) and 40µg of protein/well was analysed by immunoblotting (Section 2.9.5). After normalisation on the basis of CK18 expression (see chapter 3 section 3.10), 40µg of normalised lysates were loaded and analysed by immunoblotting. After overnight incubation at 4ºC by rocking with primary polyclonal antibody (anti-p-p38) in TBS/Tween 0.1% (1:1000 dilution), secondary antibody [goat anti-rabbit IgG IRDye 800nm (1:10000 dilution)] was added and the membranes were incubated in the dark for 1h. For specificity and as a loading control CK18 antibody was used at (1:1000 dilution), and incubation overnight at 4ºC, then the membranes were incubated with secondary antibody goat-anti mouse IgG Alexa 680 (diluted 1:10000) in the dark for 1h. Antibody binding was visualised at 800nm for p-p38 detection (expected molecular weight 43 kDa) and 700nm for CK18 detection using an Odyssey™ Infra-red Imaging system. Co-cultures for the HCT116 cell line were used as negative (N/H) and positive (L/H) controls, respectively, and 3T3CD40L cell lysate was used for confirmation of antibody specificity for human protein detection.

Key:

N/AC : 3T3Neo co-cultured with ACHN
N/O : 3T3Neo co-cultured with 786-O
N/A : 3T3Neo co-cultured with A-704
L : 3T3CD40L
L/AC : 3T3CD40L co-cultured with ACHN
L/O : 3T3CD40L co-cultured with 786-O
L/A : 3T3CD40L co-cultured with A-704

5.5The functional role of MAPKs and transcription factors in CD40 mediated apoptosis in RCC cells

CD40 ligation in B cells induces stimulation of transcription aspects such as NF-κB and AP-1 (Grammer and Lipsky, 2000) which are able to induce either cell multiplying or apoptotic cell death depending on the signal and cell type (Shaulian and Karin, 2002). In addition to the activation of NF-κB and AP-1, regulation of other components of the CD40 signalling cascade including ERKs, JNK and p38 have been observed to be mediated by TRAFs family recruitment (Grammer and Lipsky, 2000, Hostager et al., 2000). Previous findings in our laboratory indicated that CD40 ligation induce apoptosis in UCC cells via TRAF3-mediated phosphorylation of JNK and activation of AP-1 (Dunnill et al., 2016), whilst in CRC cells CD40-mediated signalling induced both JNK and p38 activation (Georgopoulos et al., 2006, Mohamed, 2014).

Results above showed rapid induction of TRAF3 (Figure 5.3), JNK phosphorylation (Figure 5.7) and p38 phosphorylation (Figure 5.8) within 1.5h post CD40 ligation by mCD40L in RCC cells, Therefore, this study investigated the functional role of MEK/ERK, JNK, p38 MAP kinases, as well as the TFs NF-κB and AP-1 in CD40-mediated apoptosis in RCC cells using specific pharmacological inhibitors U0126, SP600125, SB202190, as well as TF inhibitors PDTC and NDGA, respectively.

Following optimisation experiments to determine the effective doses of the inhibitors (Appendix II), co-cultures of RCC cells with effector cells were carried out (as optimised in Chapter 3) in the existence or lack of JNK, p38 and AP-1 inhibitors and cell death was detected by Cytotox-Glo assays. The presence of all three inhibitors resulted in significant reduction of apoptosis in a dose-dependent manner in all RCC cell lines (ACHN, 786-O and A-704). The most striking and complete inhibition (at the highest concentration used) was observed using the JNK inhibitor SB600125 (Figure 5.9). Interestingly, marked (and near complete) reduction in mCD40L-mediated death was caused by the p38 inhibitor SB202190 (Figure 5.10). Moreover, significant (albeit not complete) attenuation of CD40-mediated apoptosis was caused by the AP-1 inhibitor NDGA (Figure 5.11). By contrast, functional inhibition of ERK signalling using the

MEK1/2 inhibitor U0126 had no or negligible effect on CD40-mediated apoptosis, and neither did the NF-κB inhibitor PDTC (Figures 5.12 and 5.13, respectively).

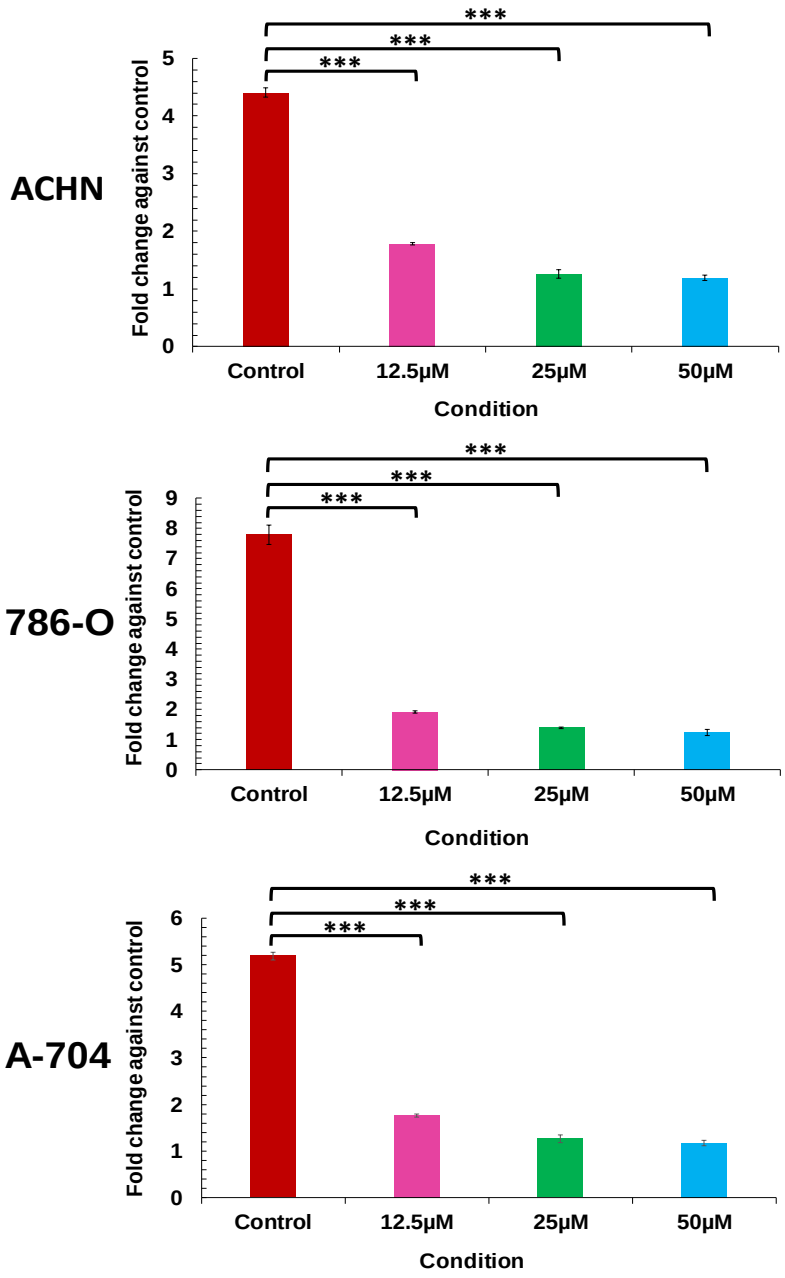

Figure 5.9 Effect of pharmacological inhibition of JNK on CD40-mediated apoptosis in RCC cells

RCC cell lines ACHN, 786-O and A-704 were co-cultured at $0.8x10^4$ cells/well with $1x10^4$ cells/well MMC-treated fibroblasts 3T3-CD40L (mL) and 3T3-Neo (Con) ± JNK inhibitor (SP600125) at the indicated concentrations in white 96-well plates. Plates were incubated for 48 h and apoptosis was assessed by the Cytotox-Glo assay. 50µl of substrate was added to each well followed by 10 min incubation at room temperature. FLUOStar Optima plate reader was used to measure the luminescence and background-corrected relative luminescence units (RLU) were deduced by pair-wise subtraction of mL and Con RLU from the respective co-cultures (as described in the Methods). Bars show mean fold change of RLU of 4-6 technical replicates ± SEM. Stats: ***, $p<0.001$, paired student T-test. “Control” represents Fold change in co-cultures without inhibitor and was statistically compared with Fold change for co-cultures carried out in the presence of the indicated inhibitor concentration. .

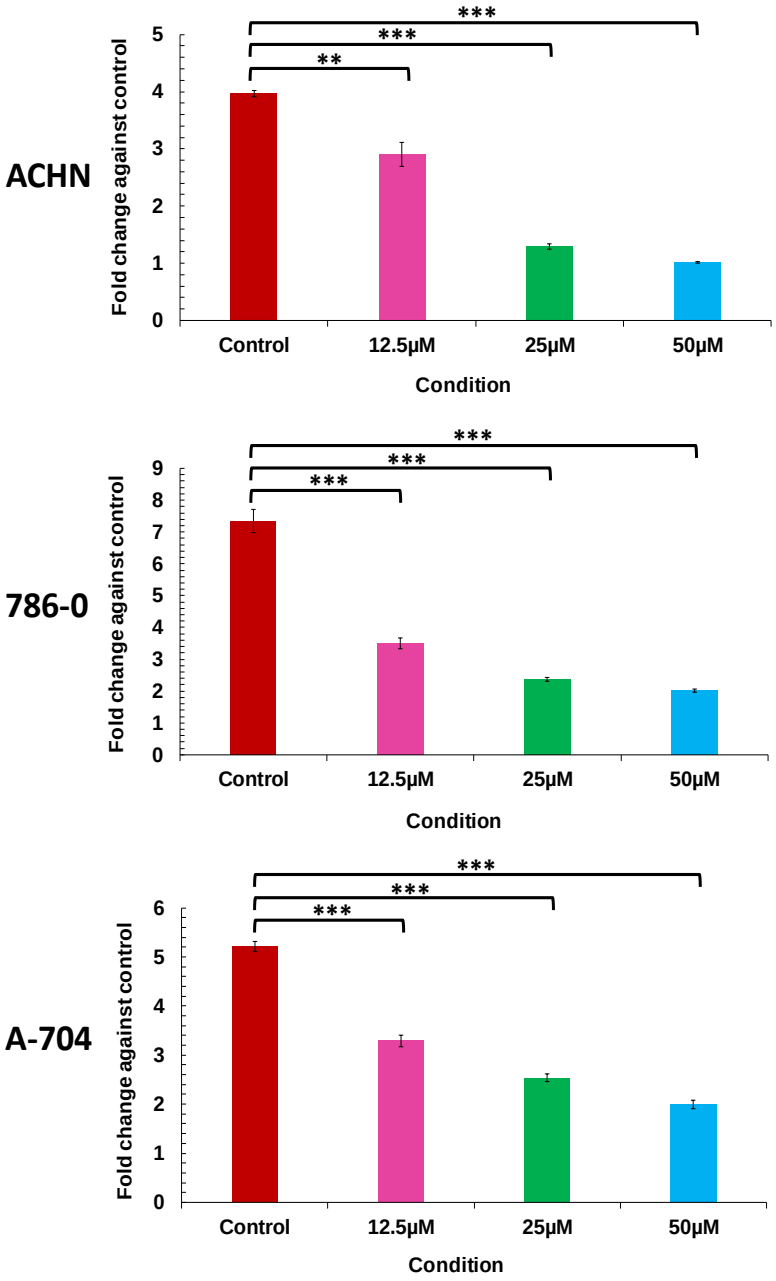

Figure 5.10 Effect of pharmacological inhibition of p38 on CD40-mediated cell death in RCC cells

RCC cell lines ACHN, 786-O and A-704 were co-cultured at $0.8x10^4$ cells/well with $1x10^4$ cells/well MMC-treated fibroblasts 3T3-CD40L (mL) and 3T3-Neo (Con) ± p38 inhibitor (SB202190) at the indicated concentrations in white 96-well plates. Plates were incubated for 48 h and apoptosis was assessed by the Cytotox-Glo assay. 50µl of substrate was added to each well followed by 10 min incubation at room temperature. FLUOStar Optima plate reader was used to measure the luminescence and background-corrected relative luminescence units (RLU) were deduced by pair-wise subtraction of mL and Con RLU from the respective co-cultures (as described in the Methods). Bars show mean fold change of RLU of 4-6 technical replicates ± SEM. Stats: ***, $p<0.001$, paired student T-test. "Control" represents Fold change in co-cultures without inhibitor and was statistically compared with Fold change for co-cultures carried out in the presence of the indicated inhibitor concentration.

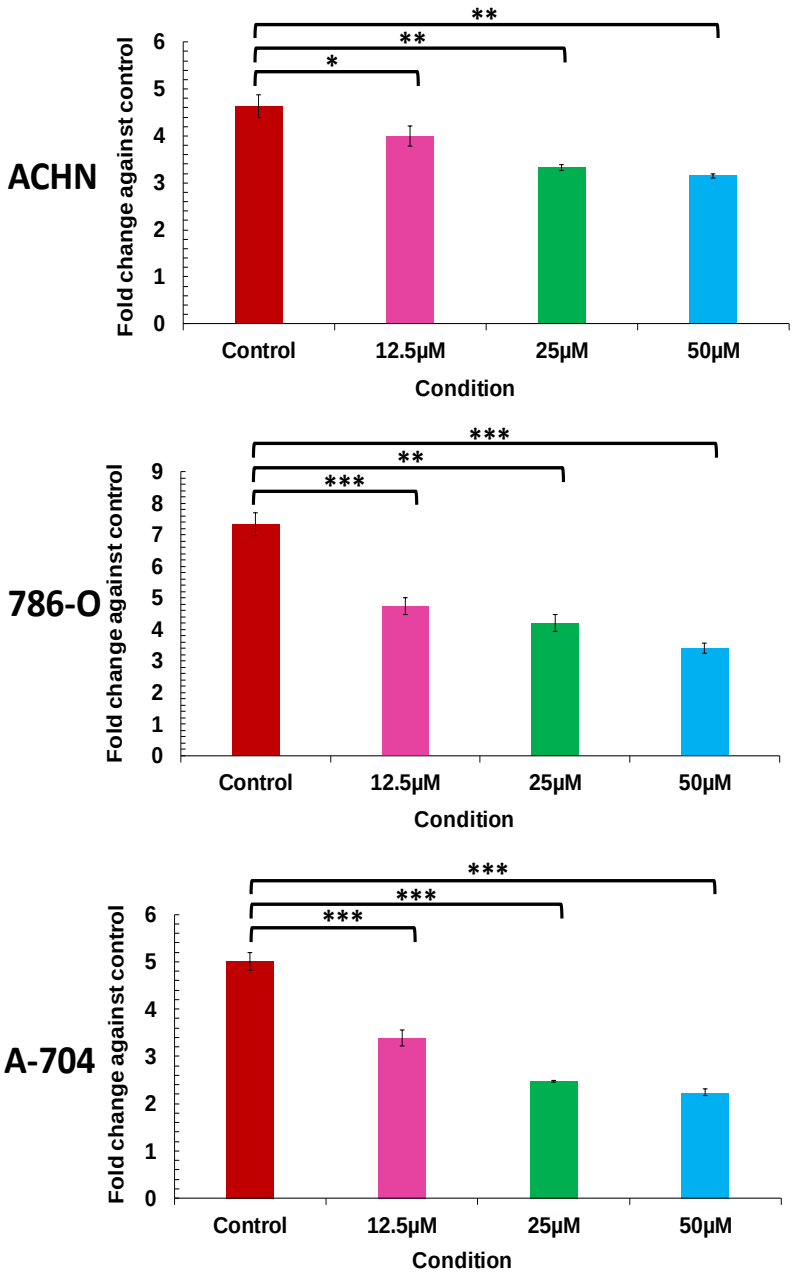

Figure 5.11 Effect of pharmacological inhibition of AP-1 on CD40-mediated cell death in RCC cells

RCC cell lines ACHN, 786-O and A-704 were co-cultured at $0.8x10^4$ cells/well with $1x10^4$ cells/well MMC-treated fibroblasts 3T3-CD40L (mL) and 3T3-Neo (Con) ± AP-1 inhibitor (NDGA) at the indicated concentrations in white 96-well plates. Plates were incubated for 48 h and apoptosis was assessed by the Cytotox-Glo assay. 50µl of substrate was added to each well followed by 10 min incubation at room temperature. FLUOStar Optima plate reader was used to measure the luminescence and background-corrected relative luminescence units (RLU) were deduced by pair-wise subtraction of mL and Con RLU from the respective co-cultures (as described in the Methods). Bars show mean fold change of RLU of 4-6 technical replicates ± SEM. Stats: ***, $p<0.001$; **$p<0.01$; *$p<0.05$ paired student T-test. “Control” represents Fold change in co-cultures without inhibitor and was statistically compared with Fold change for co-cultures carried out in the presence of the indicated inhibitor concentration. .

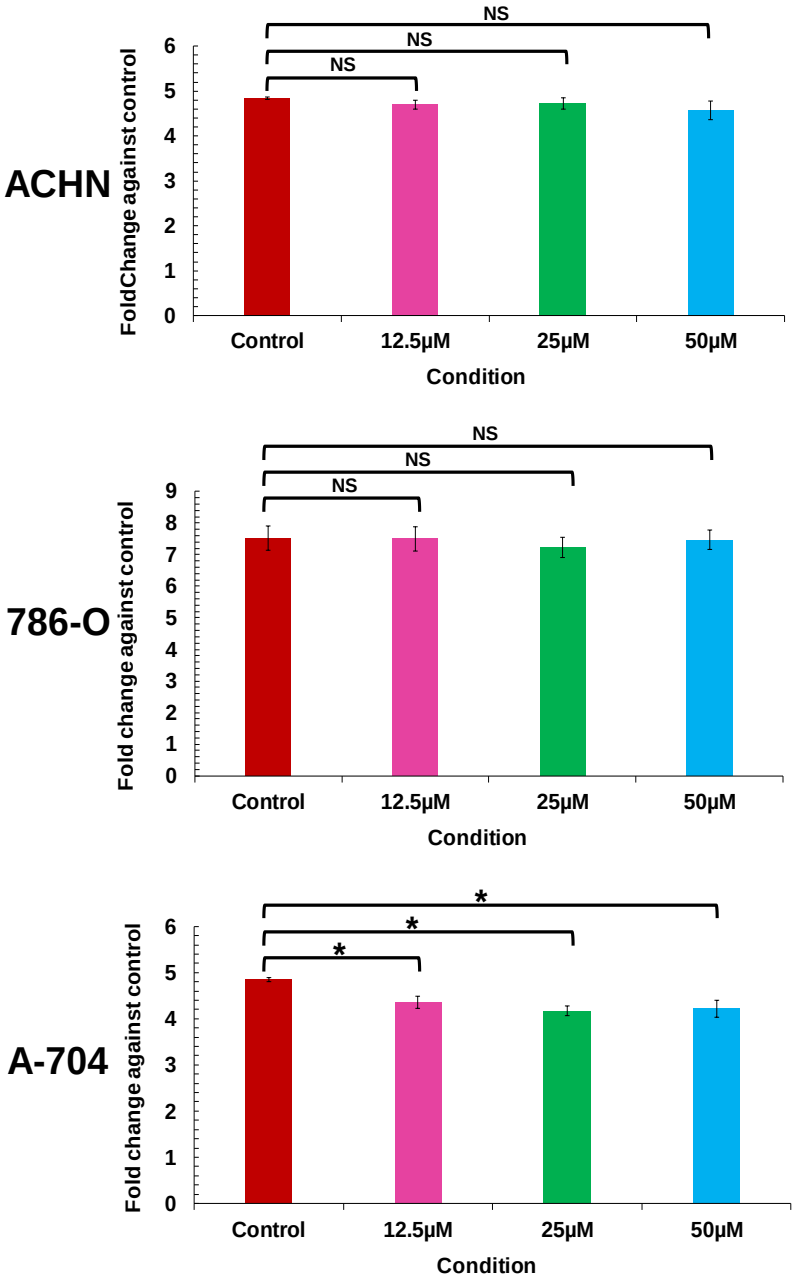

Figure 5.12 Effect of pharmacological inhibition of MEK/ERK on CD40-mediated cell death in RCC cells

RCC cell lines ACHN, 786-O and A-704 were co-cultured at $0.8x10^4$ cells/well with $1x10^4$ cells/well MMC-treated fibroblasts 3T3-CD40L (mL) and 3T3-Neo (Con) ± MEK/ERK inhibitor (u-0126) at the indicated concentrations in white 96-well plates. Plates were incubated for 48 h and apoptosis was assessed by the Cytotox-Glo assay. 50µl of substrate was added to each well followed by 10 min incubation at room temperature. FLUOStar Optima plate reader was used to measure the luminescence and background-corrected relative luminescence units (RLU) were deduced by pair-wise subtraction of mL and Con RLU from the respective co-cultures (as described in the Methods). Bars show mean fold change of RLU of 4-6 technical replicates ± SEM. Stats: NS, non significant; *, $p<0.05$ paired student T-test. “Control” represents Fold change in co-cultures without inhibitor and was statistically compared with Fold change for co-cultures carried out in the presence of the indicated inhibitor concentration. .

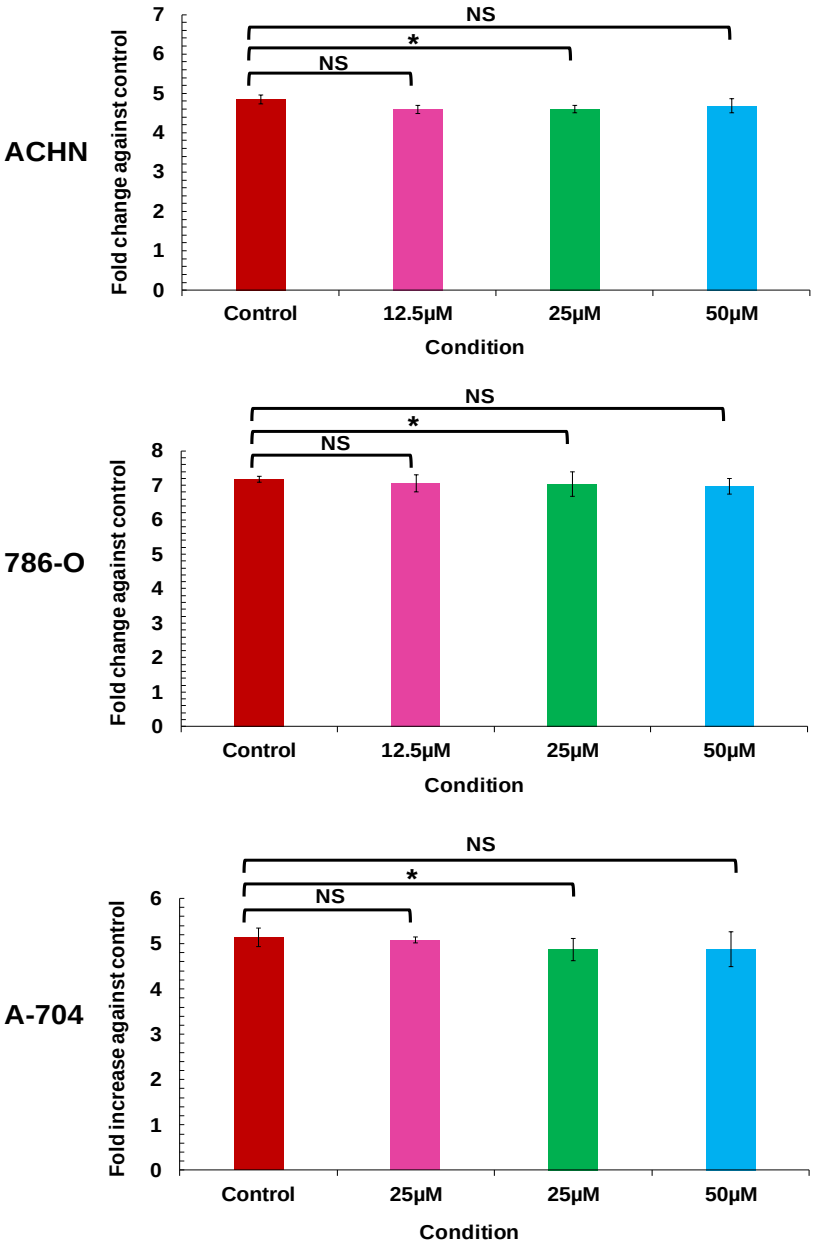

Figure 5.13 Effect of pharmacological inhibition of NF-κB on CD40-mediated cell death in RCC cells

RCC cell lines ACHN, 786-O and A-704 were co-cultured at $0.8x10^4$ cells/well with $1x10^4$ cells/well MMC-treated fibroblasts 3T3-CD40L (mL) and 3T3-Neo (Con) ± NF-κB inhibitor (PDTC) at the indicated concentrations in white 96-well plates. Plates were incubated for 48 h and apoptosis was assessed by the Cytotox-Glo assay. 50µl of substrate was added to each well followed by 10 min incubation at room temperature. FLUOStar Optima plate reader was used to measure the luminescence and background-corrected relative luminescence units (RLU) were deduced by pair-wise subtraction of mL and Con RLU from the respective co-cultures (as described in the Methods). Bars show mean fold change of RLU of 4-6 technical replicates ± SEM. Stats: NS, non significant; *, $p<0.05$ paired student T-test. "Control" represents Fold change in co-cultures without inhibitor and was statistically compared with Fold change for co-cultures carried out in the presence of the indicated inhibitor concentration.

5.6 Activation of the intrinsic (mitochondrial) pathway during mCD40L-mediated apoptosis in RCC cells

It has been shown that mCD40L triggers apoptosis in UCC cells by engaging the intrinsic apoptotic pathway via activation of caspase-9 (Georgopoulos et al., 2006), whilst unpublished work in our laboratory has shown that in CRC cells CD40 ligation induces apoptosis by activation of combination of intrinsic and extrinsic mechanisms (Mohamed, 2014).

To study the contribution of caspases in RCC cell death by mCD40L, biochemical caspase inhibitors were used in functional experiments to determine whether CD40 ligation induces apoptosis via stimulation of inducer caspases associated with the intrinsic (caspase-9) or extrinsic (caspase-8 and caspase-10) pathways in RCC cells. Co-cultures of ACHN, 786-O and A-704 with 3T3-CD40L and 3T3-Neo effectors were carried out in the existence or lack of caspase-8, -9 and -10 inhibitors (z-IETD-FMK, z-LEHD-FMK and z-AEVD-FMK, respectively), as well as the pan-Caspase inhibitor (z-VAD-FMK) and cell death was assessed by Cytotox-Glo assays. Inhibition of caspase-9 caused significant reduction of apoptosis in all three RCC lines, whilst even more marked attenuation of apoptosis was caused by the presence of pan-caspase inhibitor, which confirmed that mCD40L-triggered apoptosis in RCC cells is caspase dependent manner. By contrast, inhibition of caspase-8 and -10 showed little (if any) effect on cell death in all cell lines (Figure 5.14).

The result above that caspase-9 blockade attenuates CD40-mediated apoptosis in RCC cells suggested that cell death may operate via the intrinsic, mitochondrial pathway. Proteins such as Bak and Bax, are critical regulators of MOMP and subsequent cytochrome c release and caspase-9 activation during the intrinsic pathway (Kroemer et al., 2007) and involvement of Bak and Bax in CD40-mediated apoptosis has been previously reported (Georgopoulos et al., 2006, Mohamed, 2014, Dunnill et al., 2016). Expression of Bak and Bax post CD40 ligation in RCC cells was investigated by immunoblotting and it was found that both Bax and Bak were induced by 6h post-CD40 ligation by membrane CD40L in all RCC lines. Induction of Bak expression appeared to increase progressively over time period (6, 12 and 24h)

(Figure 5.15), whereas Bax up-regulation was maximal by 6h and was sustained over the time course tested (Figure 5.16). Of note, no activation of Bak and Bax was observed before the 6h time point (Data not shown).

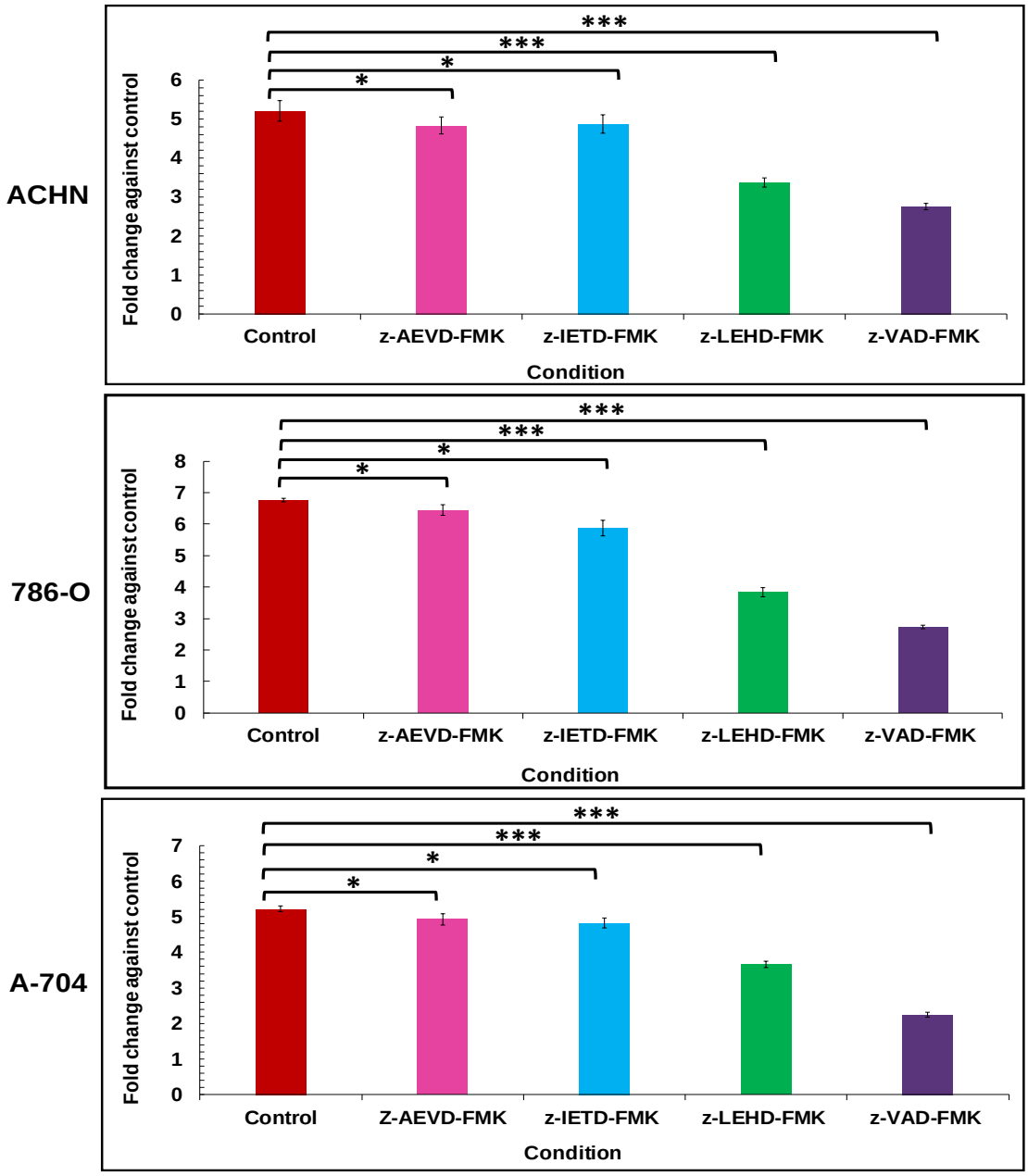

Figure 5.14 Effect of caspase inhibitors on mCD40L-mediated cell death

RCC cell lines ACHN, 786-O and A-704 were co-cultured at $0.8x10^4$ cells/well with $1x10^4$ cells/well MMC-treated fibroblasts 3T3-CD40L (mL) and 3T3-Neo (Con) ± 100μM of caspase-8 (z-IETD-FMK), -9 (Z-LEHD-FMK) and -10 (Z-AEVD-FMK) inhibitors and pan-caspase inhibitor (z-VAD-FMK) in white 96-well plates. Plates were incubated for 48 h and apoptosis was assessed by the Cytotox-Glo assay. 50μl of substrate was added to each well followed by 10 min incubation at room temperature. FLUOStar Optima plate reader was used to measure the luminescence and background-corrected relative luminescence units (RLU) were deduced by pair-wise subtraction of mL and Con RLU from the respective co-cultures (as described in the Methods). Bars show mean fold change of RLU of 4-6 technical replicates ± SEM. Stats: NS, non significant; *, $p<0.05$; ***, $p<0.001$, paired student T-test. "Control" represents Fold change in co-cultures without inhibitor and was statistically compared with Fold change for co-cultures carried out in the presence of the indicated inhibitor concentration.

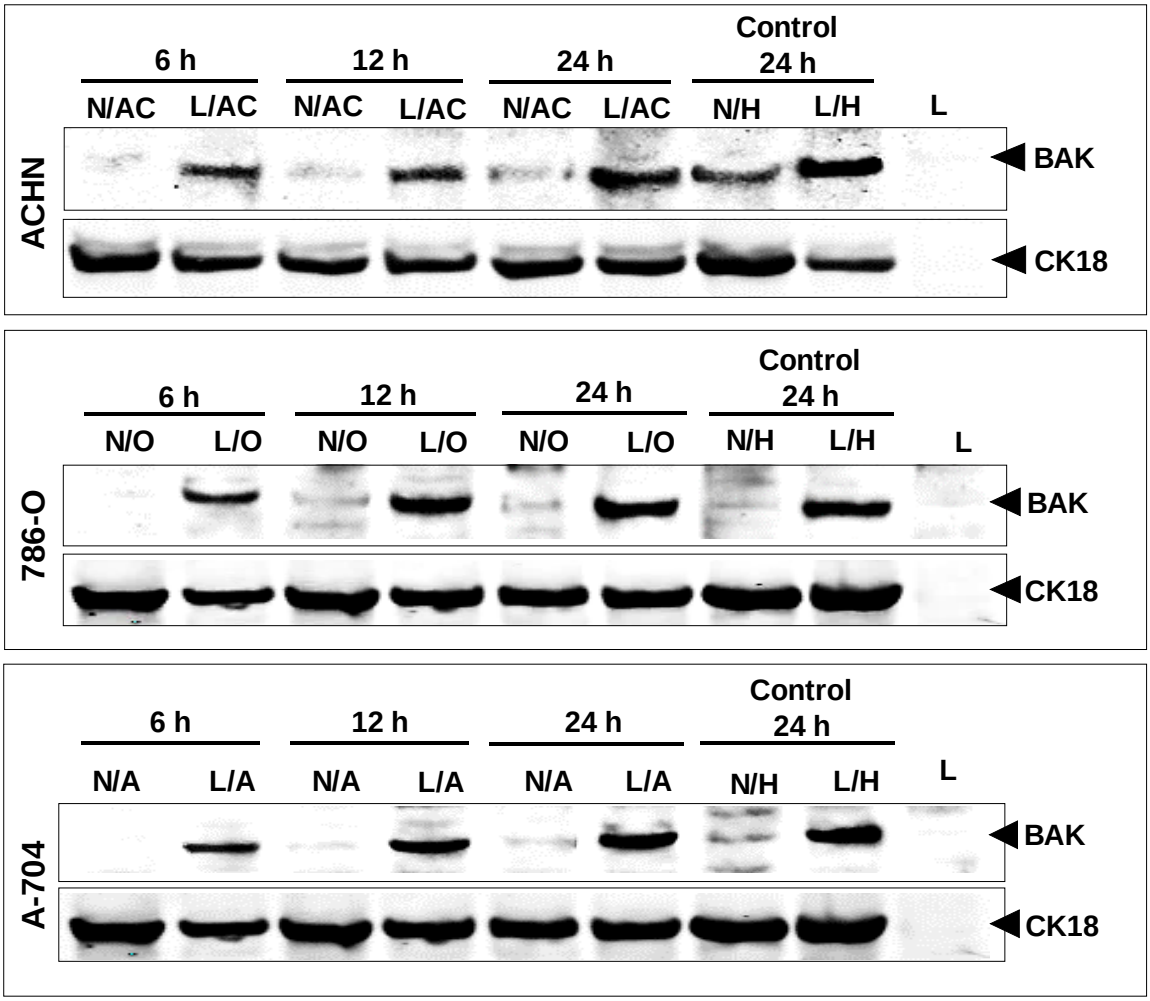

Figure 5.15 Induction of Bak following CD40 ligation by mCD40L

RCC cells were co-cultured at $30x10^5$ cells/dish with $30x10^5$ cells/dish of MMC-treated fibroblasts 3T3-Neo and 3T3-CD40L in a 10 cm dishes and incubated for the specified time points. Cells were lysis as explained in the Methods (Section 2.9.3) and 40µg of protein/well was analysed by immunoblotting (Section 2.9.5). After normalisation on the basis of CK18 expression (see chapter 3 section 3.10), 40µg of normalised lysates were loaded and analysed by immunoblotting. After overnight incubation at 4ºC by rocking with primary polyclonal antibody (anti-Bak) in TBS/Tween 0.1% (1:500 dilution), secondary antibody goat anti-rabbit IgG IRDye 800 (1:10000 dilution) was added and the membranes were incubated in the dark for 1h. For specificity and as a loading control CK18 antibody was used (at 1:1000 dilution), and incubation overnight at 4ºC, then the membranes were incubated with secondary antibody goat-anti mouse IgG Alexa 680 (diluted 1:10000) in the dark for 1h. Antibody binding was visualised at 800nm for Bak detection (expected molecular weight 26 kDa) and 700nm for CK18 detection using an Odyssey™ Infra-red Imaging system. Co-cultures for the HCT116 cell line were used as negative (N/H) and positive (L/H) controls, respectively, and 3T3CD40L cell lysate was used for confirmation of antibody specificity for human protein detection.

Key:

N/AC : 3T3Neo co-cultured with ACHN
N/O : 3T3Neo co-cultured with 786-O
N/A : 3T3Neo co-cultured with A-704
L : 3T3CD40L
L/AC : 3T3CD40L co-cultured with ACHN
L/O : 3T3CD40L co-cultured with 786-O
L/A : 3T3CD40L co-cultured with A-704

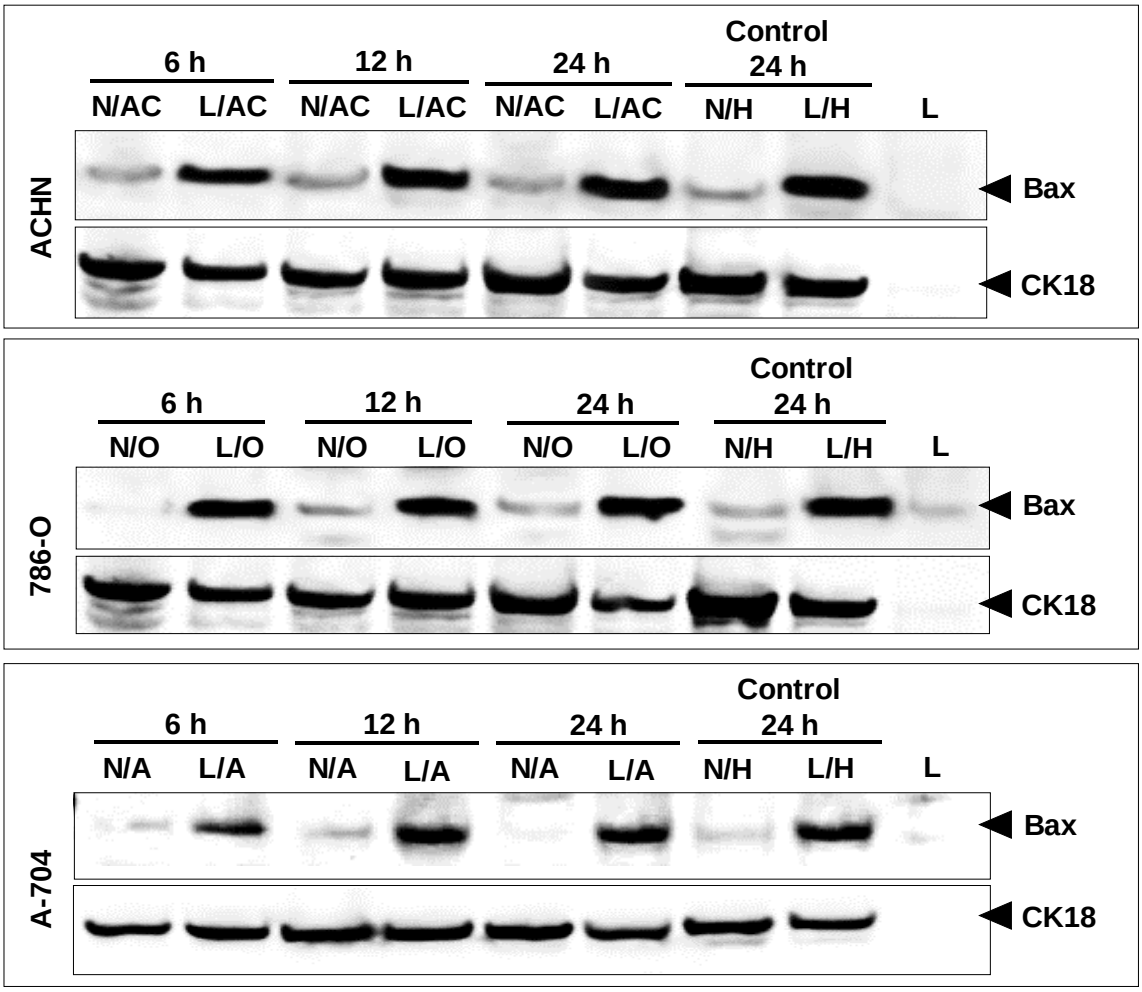

Figure 5.16 Induction of Bax following CD40 ligation by mCD40L

RCC cells were co-cultured at $30x10^5$ cells/dish with $30x10^5$ cells/dish of MMC-treated fibroblasts 3T3-Neo and 3T3-CD40L in a 10 cm dishes and incubated for the indicated time points. Whole cell lysates were prepared as described in the Methods (Section 2.9.3) and 40µg of protein/well was analysed by immunoblotting (Section 2.9.5). After normalisation on the basis of CK18 expression (see chapter 3 section 3.10), 40µg of normalised lysates were loaded and analysed by immunoblotting. After overnight incubation at 4ºC by rocking with primary monoclonal antibody (anti-Bax) in TBS/Tween 0.1% (1:1000 dilution), secondary antibody goat-anti mouse IgG Alexa 680 (diluted 1:10000) was added and the membranes were incubated in the dark for 1h. For specificity and as a loading control CK18 antibody was used (at 1:1000 dilution), and incubation overnight at 4ºC, then the membranes were incubated with secondary antibody goat-anti mouse IgG Alexa 680 (diluted 1:10000) in the dark for 1h. Antibody binding was visualised at 700nm for both Bax and CK18 detection (expected Bax molecular weight 26 kDa) using an OdysseyTM Infra-red Imaging system. Co-cultures for the HCT116 cell line were used as negative (N/H) and positive (L/H) controls, respectively, and 3T3CD40L cell lysate was used for confirmation of antibody specificity for human protein detection.

Key:

N/AC : 3T3Neo co-cultured with ACHN
N/O : 3T3Neo co-cultured with 786-O
N/A : 3T3Neo co-cultured with A-704
L : 3T3CD40L
L/AC : 3T3CD40L co-cultured with ACHN
L/O : 3T3CD40L co-cultured with 786-O
L/A : 3T3CD40L co-cultured with A-704

5.7 Expression of JNK and p38 in RCC cells in the presence of JNK and p38 inhibitors

The results above suggested that mCD40L induces activation (phosphorylation) of both JNK and p38 and that both kinases are functionally important in CD40-mediated apoptosis, as blockade of p38 significantly attenuated apoptosis and inhibition of JNK completely blocked apoptosis (see Figures 5.9 and 5.10). Therefore, it was of interest to better understand how these two kinases regulate CD40-mediated death.

First, the effect of the JNK (SP600125) and p38 (SB202190) inhibitors on the phosphorylation of JNK and p38 was examined by immunoblotting. The outcomes exposed in Figure 5.17 clearly demonstrate that, in all three RCC lines (ACHN, 786-O and A-704), the JNK inhibitor (SP600125) fully blocked activation of JNK (at 3 and 6h after CD40 ligation by mCD40L) and the p38 inhibitor (SB202190) down-regulated p-p38 expression. Interestingly, however, although the p38 inhibitor (SB202190) did not affect JNK activation, treatment with JNK inhibitor (SP600125) not only blocked JNK activation but it also appeared to suppress p-p38, in comparison with the positive controls (non-treated cells) (Figure 5.17). These experiments not only confirmed the functionality of the pharmacological inhibitors but they also provided evidence that activation of p38 is dependent on JNK activity suggesting JNK as a p38 activator.

5.8 The effect of JNK and p38 inhibition on the expression Bak and Bax (Anti-apoptotic proteins)

Use of the JNK and p38 inhibitors stopped CD40-mediated apoptosis in RCC cells. To confirm apoptosis blockade, the expression of Bak and Bax in the presence of JNK and p38 inhibitors during CD40 activation was examined. Induction of Bak and Bax was completely blocked by both JNK and p38 inhibitors in A-704 cells at 3 and 6h post CD40 ligation while little Bak and Bax was detected in ACHN cells by using both JNK and p38 inhibitors and only faint bands of Bak were observed in 786-O by using JNK inhibitor (Figure 5.18). These results confirmed direct functional roles for JNK and p38 in Bak and Bax activation and subsequently CD40-mediated apoptosis.

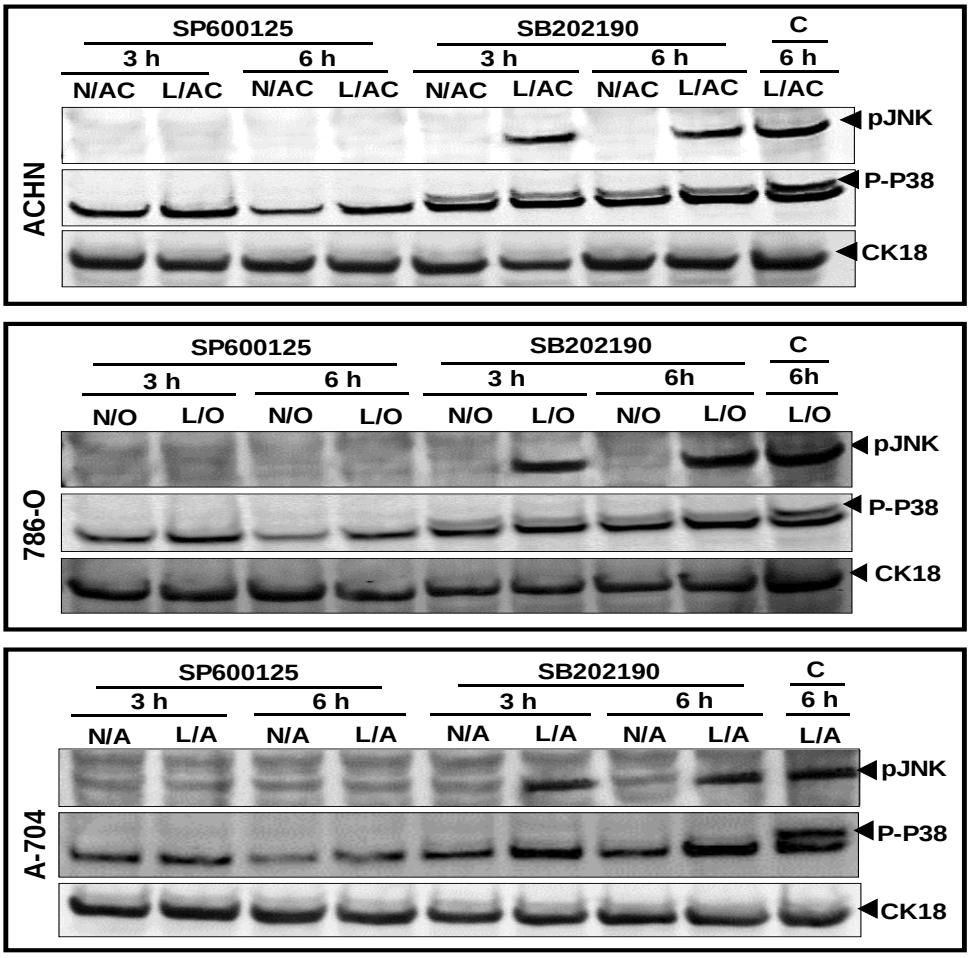

Figure 5.17 Effect of JNK and p38 pharmacological inhibitors on JNK and p38 phosphorylation post CD40 ligation

RCC cells were co-cultured at $30x10^5$ cells/dish with $30x10^5$ cells/dish of fibroblasts 3T3-Neo and 3T3-CD40L ± 25µM of JNK inhibitor SP600125 or 25µM of p38 inhibitor SB202190 in 10 cm dishes and incubated for the indicated time points. Whole cell lysates were prepared as described in the Methods (Section 2.9.3) and 40µg of protein/well was analysed by immunoblotting (Section 2.9.5). After normalisation on the basis of CK18 expression (see chapter 3 section 3.10), 40µg of normalised lysates were loaded and analysed by immunoblotting. After overnight incubation at 4ºC by rocking with primary monoclonal antibody (anti-p-JNK) in TBS/Tween 0.1% (1:1000 dilution), secondary antibody goat-anti mouse IgG Alexa 680 (diluted 1:10000) was added and the membranes were incubated in the dark for 1h. The membranes were incubated again overnight at 4ºC by rocking with primary polyclonal anti-p38 antibody (1:1000 dilution), then secondary antibody goat anti-rabbit IgG IRDye 800 (1:10000 dilution) was added and membranes were incubated in the dark for 1h. For specificity and as a loading control, separate gels were blotted alongside and incubated with anti CK18 antibody in TBS/Tween 0.1% (1:1000 dilution), then secondary antibody goat-anti mouse IgG Alexa 680 (diluted 1:10000) was added and the membranes were incubated in the dark for 1h. Antibody binding was visualised at 700nm for JNK and CK18 detection and 800nm for p38 detection using an Odyssey™ Infra-red Imaging system. "C" indicates untreated co-cultures.

Key:

N/AC : 3T3Neo co-cultured with ACHN	L/AC : 3T3CD40L co-cultured with ACHN
N/O : 3T3Neo co-cultured with 786-O	L/O : 3T3CD40L co-cultured with 786-O
N/A : 3T3Neo co-cultured with A-704	L/A : 3T3CD40L co-cultured with A-704

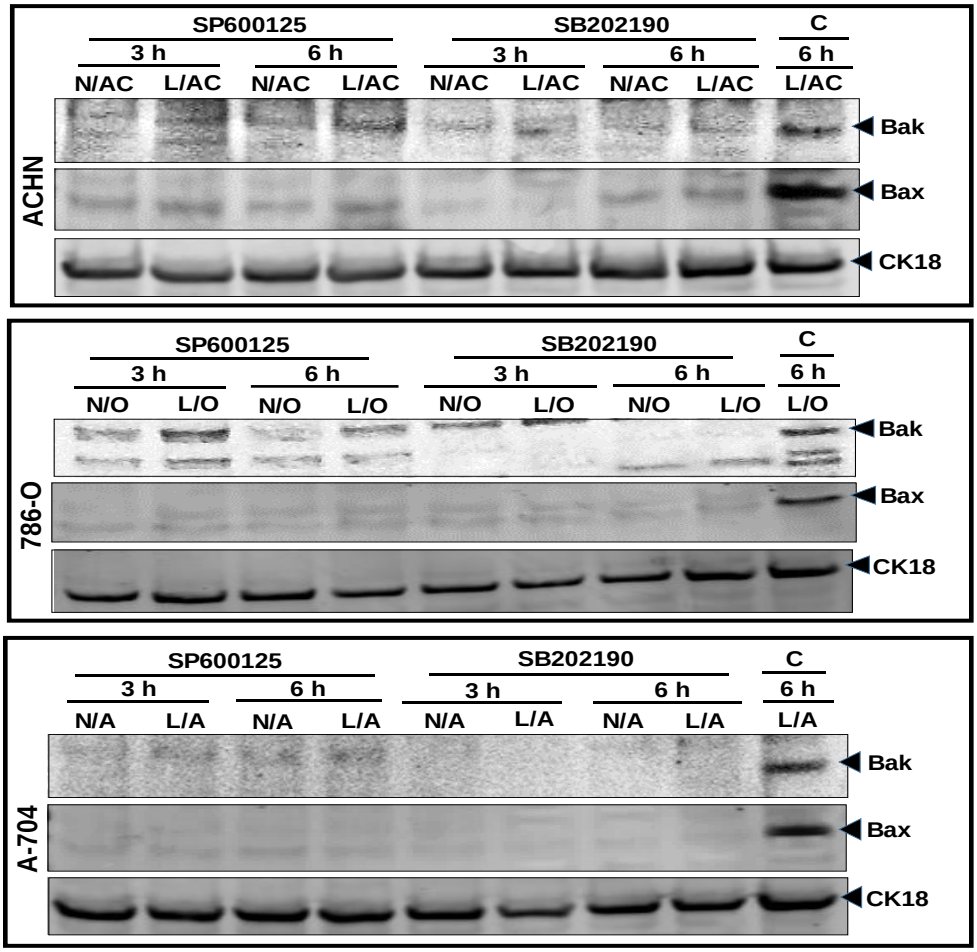

Figure 5.18 Effect of JNK and p38 pharmacological inhibitors on Bak and Bax expression post CD40 ligation

RCC cells were co-cultured at $30x10^5$ cells/dish with $30x10^5$ cells/dish fibroblasts cells 3T3-Neo and 3T3-CD40L ± 25µM of JNK inhibitor (SP600125) or 25µM of p38 inhibitor (SB202190) in 10 cm dishes and incubated for the indicated time points. Whole cell lysates were prepared as described in the Methods (Section 2.9.3) and 40µg of protein/well was analysed by immunoblotting (Section 2.9.5). After normalisation on the basis of CK18 expression (see chapter 3 section 3.10). 40µg of normalised lysates were loaded and analysed by immunoblotting. After overnight incubation at 4ºC by rocking with primary monoclonal antibody (anti-Bax) in TBS/Tween 0.1% (1:1000 dilution), secondary antibody goat-anti mouse IgG Alexa 680 (diluted 1:10000) was added and the membranes were incubated in the dark for 1h. The membranes were incubated again for overnight at 4ºC by rocking with primary polyclonal antibody (anti-Bak) (1:500 dilution), then secondary antibody goat anti-rabbit IgG IRDye 800nm (1:10000 dilution) was added and the membranes were incubated in the dark for 1h. For specificityty and as a loading control CK18 antibody was used (at 1:1000 dilution), and incubation overnight at 4ºC, then the membranes were incubated with secondary antibody goat-anti mouse IgG Alexa 680 (diluted 1:10000) in the dark for 1h. Antibody binding was visualised at 700nm for Bax and CK18 detection and 800nm for Bak detection using an Odyssey™ Infra-red Imaging system. "C" indicates untreated co-cultures.

Key:

N/AC : 3T3Neo co-cultured with ACHN	L/AC : 3T3CD40L co-cultured with ACHN
N/O : 3T3Neo co-cultured with 786-O	L/O : 3T3CD40L co-cultured with 786-O
N/A : 3T3Neo co-cultured with A-704	L/A : 3T3CD40L co-cultured with A-704

5.9 Investigations on the role of reactive oxygen species (ROS) and NADPH Oxidase (Nox) in CD40-mediated apoptosis in RCC cells

5.9.1 Rationale

Elevation of intracellular ROS can be induced by TNFR superfamily members to control cell survival and apoptosis via initiation of oxidative stress-responsive MAPK signalling pathways (Shen and Pervaiz, 2006). Receptor-TRAF interactions may lead to ROS induction, with NADPH oxidase (Nox) being a possible source of ROS generation (Chandel et al., 2001, Ha and Lee, 2004, Li et al., 2005). There is some evidence that CD40 ligation produces ROS via the 5-lipoxygenase pathway and TRAF3-Nox association (Ha and Lee, 2004, Ha et al., 2011) and research performed in B cell lines indicated that low level of ROS can be produced following weak CD40 cross-linking, which can promote activation of the NF-κB pathway; more extensive receptor cross-linking induces stronger oxidative stress and enhances JNK activation (Ha et al., 2011).

Oxidative stress is directly associated with the regulation of apoptotic pathways (Circu and Aw, 2010) because ROS generation can lead to activation of the MAP3K ASK-1 which is facilitated by the auto-phosphorylation and subsequent release of Thioredoxin (Liu and Min, 2002) from the Trx-ASK1 sensor complex and MAPK pathway initiation through release from dual-specificity MAPK phosphatases (DS-MKPs) (Bermudez et al., 2010). Oxidative stress also allows JNK activation through GSTP release (Simic et al., 2005) and promotes AP-1 activity (Biswas et al., 2006), Moreover, oxidative stress also control the expression of other members of the Bcl-2 family, such as pro-apoptotic Bax and Bak (Steckley et al., 2007, Tomiyama et al., 2006).

Recent work in our laboratory has demonstrated for the first time that mCD40L-mediated apoptosis is redox state-reliant, ROS generation in carcinoma cells (UCC and CRC) is critical for apoptosis and that mCD40L down-regulates anti-oxidant responses (Trx) to efficiently kill malignant cells by operating along a TRAF3-Nox/p40phox-ASK1-MKK4-JNK signalling axis to induce the mitochondrial apoptotic pathway (Dunnill et al., 2016).

5.9.2 Induction of ROS generation in RCC cells by mCD40L

The above findings have raised the possibility that CD40-mediated apoptosis in RCC cells could be triggered by ROS. To investigate whether CD40 signalling raises intracellular ROS levels in RCC cells, the ROS detection fluorescent marker 6-carboxy-2', 7'-dichlorodihydrofluorescein diacetate (H_2DCFDA) was used at different concentrations (0.5, 1.0, 2.0, 3.0 and 4.0µM) in co-cultures of RCC cells with 3T3-CD40L or 3T3-Neo effectors cells. ROS levels in such co-cultures were determined at different time points (0.5, 1, 2 and 3h). Furthermore, to account for any auto-fluorescence-related background, co-cultures for each cell line without addition of H_2DCFDA were used as background controls, whilst effector 3T3s cells and RCC cells were also cultured alone with and without addition of H_2DCFDA alongside all conditions tested (concentrations and time points). Then, the relative fluorescence units (RFU) for non-treated cultures of 3T3s alone and non-treated co-cultures were pairwise-subtracted from the RFU for those treated with H_2DCFDA.

This process allowed us to first background correct all relative fluorescence values that for all treatments with H_2DCFDA. Following this initial subtraction of auto-fluorescence, the values underwent a second round of pairwise-subtraction which was to exclude fluorescence background created from the 3T3-CD40L and 3T3-Neo cells in the co-cultures: i.e. we subtracted the RFU for 3T3-CD40L alone or RFU for 3T3-Neo alone from the RFU values for each respective co-culture. After this, the values obtained were a) general background-corrected and b) co-culture-corrected relative fluorescence that was emitted only from the target (RCC) cells.

Results from such extensive optimisation experiments for all three RCC cells ACHN, 786-O and A-704 are presented in Figures 5.19, 5.20 and 5.21, respectively. Of note, these experiments indicated that the optimal concentration of H_2DCFDA that resulted in maximal detection of ROS induction was 1µM for all time points tested. Results for all other concentrations tested are presented in the Appendix III. These experiments demonstrated that mCD40L induced ROS elevation in RCC cells and the highest ROS level was detected at 1h post-CD40 ligation; following that, although a decrease in

ROS was detectable, some level of ROS remained and was sustained over the time-course tested (Figures 5.19, 5.20 and 5.21).

It has been reported both in B cells and carcinoma cells that CD40 signalling is highly dependent on signal quality i.e. the extent of its cross-liking defined by the mode of its ligand presentation (Bugajska et al., 2002, Baccam and Bishop, 1999, Georgopoulos et al., 2006). Results in this study (chapter 3) revealed that agonistic anti-CD40 mAb G28-5 did not induce apoptosis in RCC cells, whilst recent findings in our laboratory showed that soluble agonist has little ability to induce ROS in UCC and CRC (Dunnill et al., 2016). Therefore, RCC cells ACHN were treated with 10µg/ml of G28-5 agonistic anti-CD40 mAb (cross linked with 2.5µg/ml of secondary antibody), and intracellular ROS level was determined (at 0.5, 1, 2 and 3h) by using 1µM H_2DCFDA. Little ROS induction was observed over the time-course following treatment with cross-linked G28-5 mAb, in comparison with mCD40L which caused extensive ROS generation (Figure 5.22).

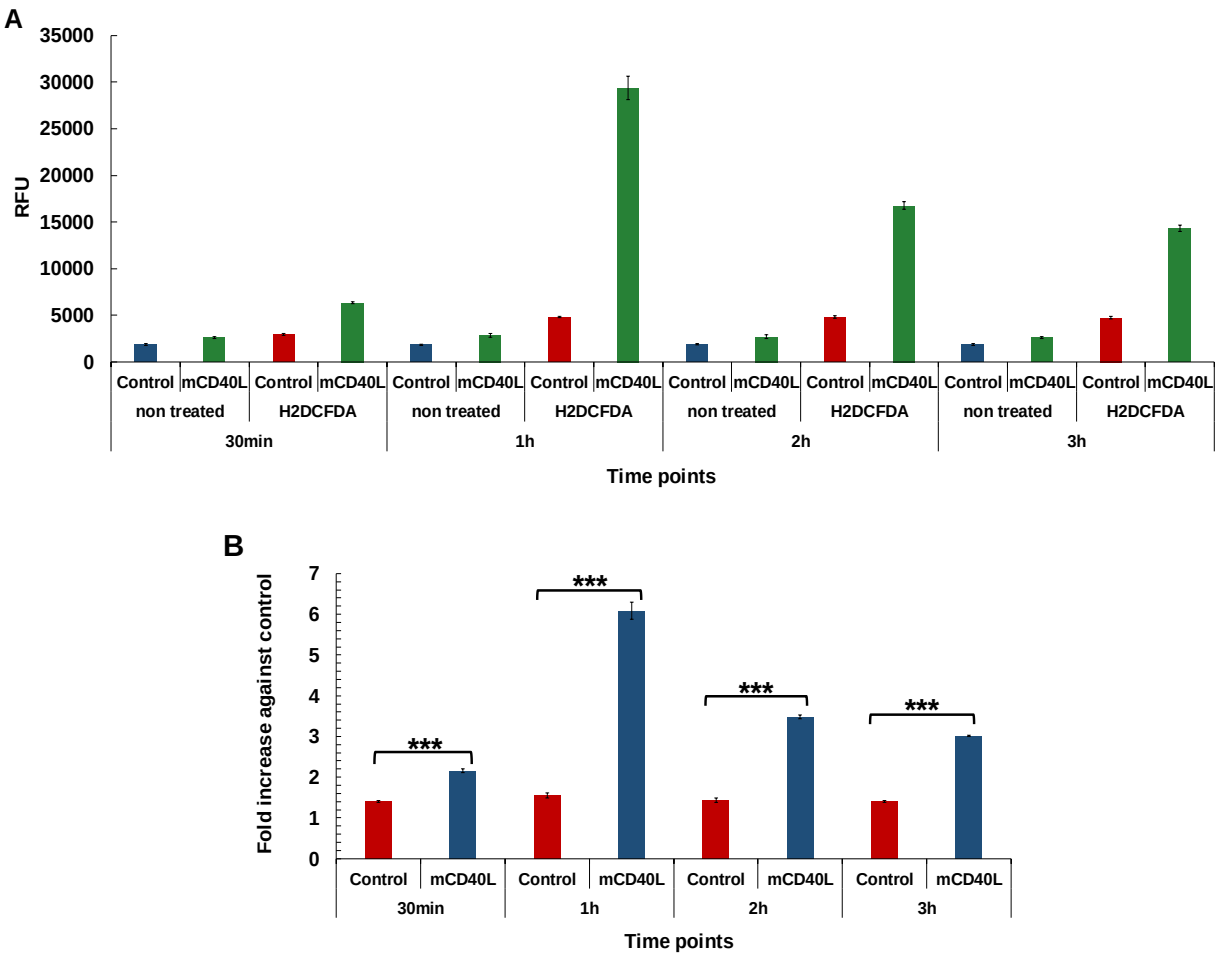

Figure 5.19 mCD40L-mediated ROS generation in ACHN cells

ACHN cells were co-cultured at $0.8x10^4$ cells/well with $1x10^4$ cells/well fibroblasts 3T3-CD40L and 3T3-Neo in white 96-well plates. Plates were incubated for the indicated time points. Then cells were first washed with PBS (see section 2.8.6) and 1µM of H_2DCFDA in pre-warmed (37ºC) PBS was added. The plates then incubated for 30min at 37ºC and 5% CO_2, FLUOStar Optima plate reader was used at Excitation 485nm/Emission 520nm to measure the fluorescence and background-corrected relative fluorescence units (RFU) were deduced by pair-wise subtraction of mL and Control RFU from the respective co-cultures (as described in the text). **A)** Background corrected RFU readings for co-cultures ACHN/3T3-CD40L (mCD40L) and respective 3T3-Neo co-cultures (Control). Bars represent mean RLU. **B)** Results from graph in A are also presented as fold change [H2DCFDA treated co-cultures (mCD40L) relative to non-treated co-cultures (Control)]. Bars show mean values of 4-6 technical replicates ± SEM. Stats: ***, $p<0.001$, paired student T-test.

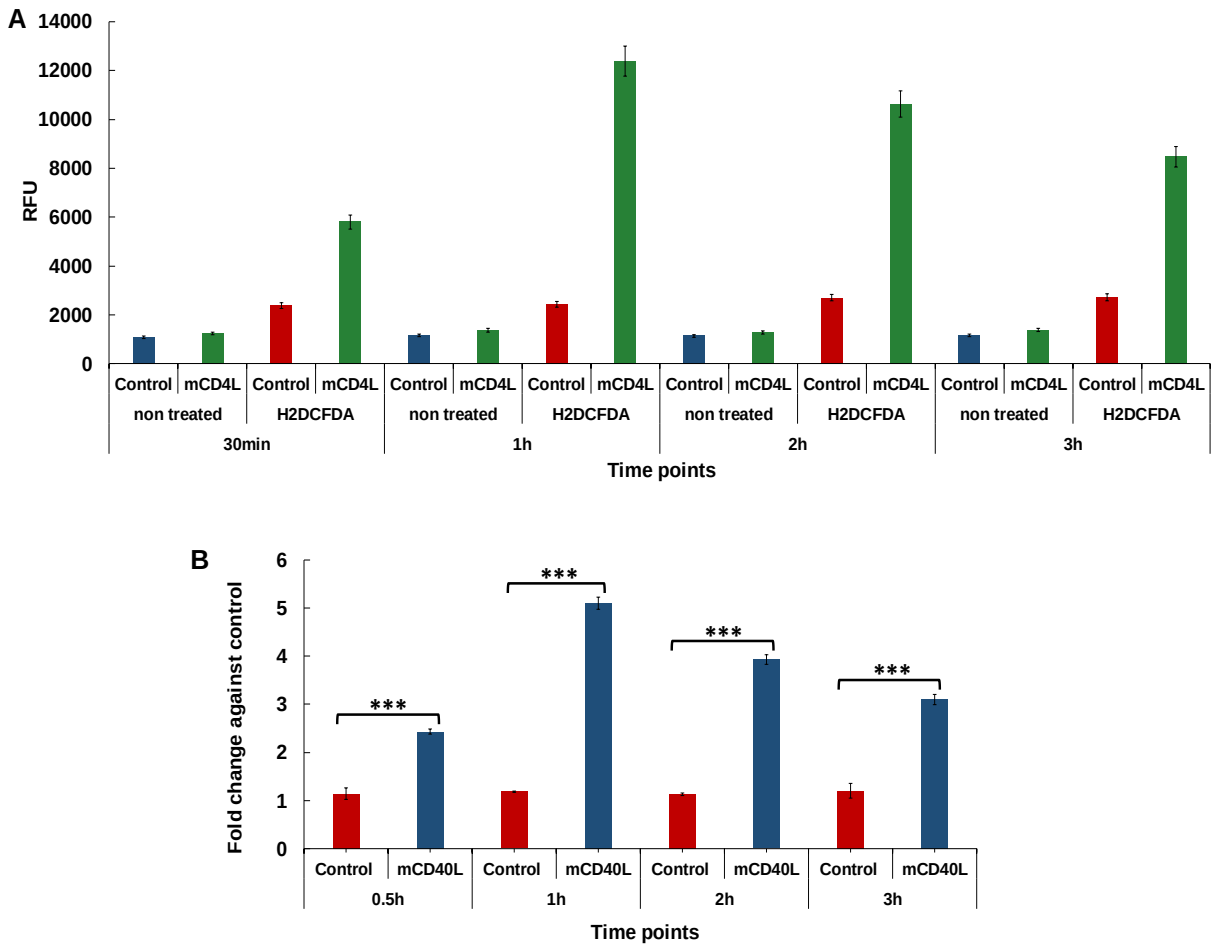

Figure 5.20 mCD40L-mediated ROS generation in 786-O cells

786-O cells were co-cultured at $0.8x10^4$ cells/well with $1x10^4$ cells/well fibroblasts 3T3-CD40L and 3T3-Neo in white 96-well plates. Plates were incubated for the indicated time points. Then cells were first washed with PBS (see section 2.8.6) and 1µM of H_2DCFDA in pre-warmed (37ºC) PBS was added. The plates then incubated for 30min at 37ºC and 5% CO_2. FLUOStar Optima plate reader was used at Excitation 485nm/Emission 520nm to measure the fluorescence and background-corrected relative fluorescence units (RFU) were deduced by pair-wise subtraction of mL and Control RFU from the respective co-cultures (as described in the text). **A)** Background corrected RFU readings for co-cultures 786-O/3T3-CD40L (mCD40L) and respective 3T3-Neo co-cultures (Control). Bars represent mean RLU. **B)** Results from graph in A are also presented as fold change [H2DCFDA treated co-cultures (mCD40L) relative to non-treated co-cultures (Control)]. Bars show mean values of 4-6 technical replicates ± SEM. Stats: ***, $p<0.001$, paired student T-test.

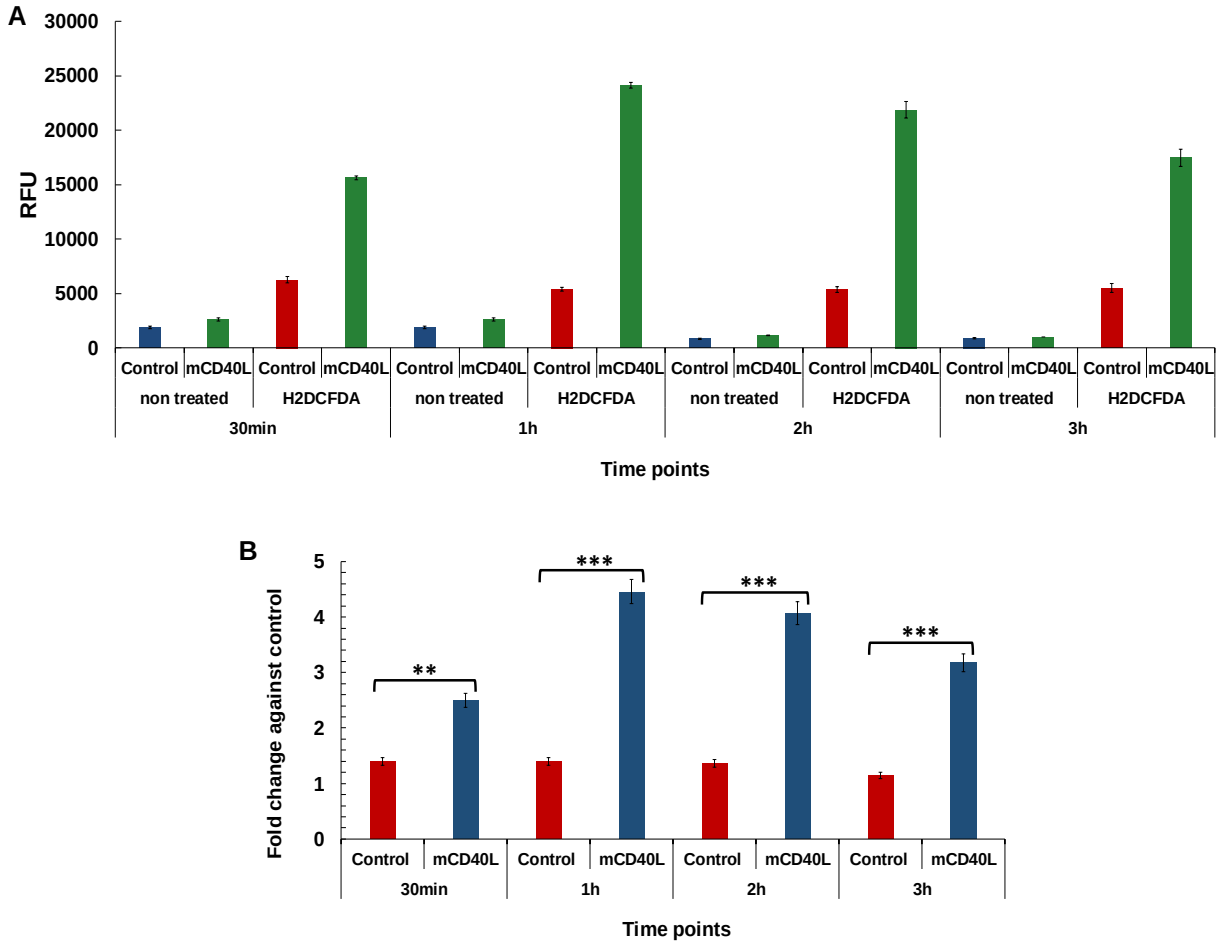

Figure 5.21 mCD40L-mediated ROS generation in A-704 cells

A-704 cells were co-cultured at $0.8x10^4$ cells/well with $1x10^4$ cells/well fibroblasts 3T3-CD40L and 3T3-Neo in white 96-well plates. Plates were incubated for the indicated time points. Then cells were first washed with PBS (see section 2.8.6) and 1µM of H_2DCFDA in pre-warmed (37ºC) PBS was added. The plates then incubated for 30min at 37ºC and 5% CO_2. FLUOStar Optima plate reader was used at Excitation 485nm/Emission 520nm to measure the fluorescence and background-corrected relative fluorescence units (RFU) were deduced by pair-wise subtraction of mL and Control RFU from the respective co-cultures (as described in the text). **A)** Background corrected RFU readings for co-cultures A-704/3T3-CD40L (mCD40L) and respective 3T3-Neo co-cultures (Control). Bars represent mean RLU. **B)** Results from graph in A are also presented as fold change [H2DCFDA treated co-cultures (mCD40L) relative to non-treated co-cultures (Control)]. Bars show mean values of 4-6 technical replicates ± SEM. Stats: ***, $p<0.001$; $p<0.01$, paired student T-test.

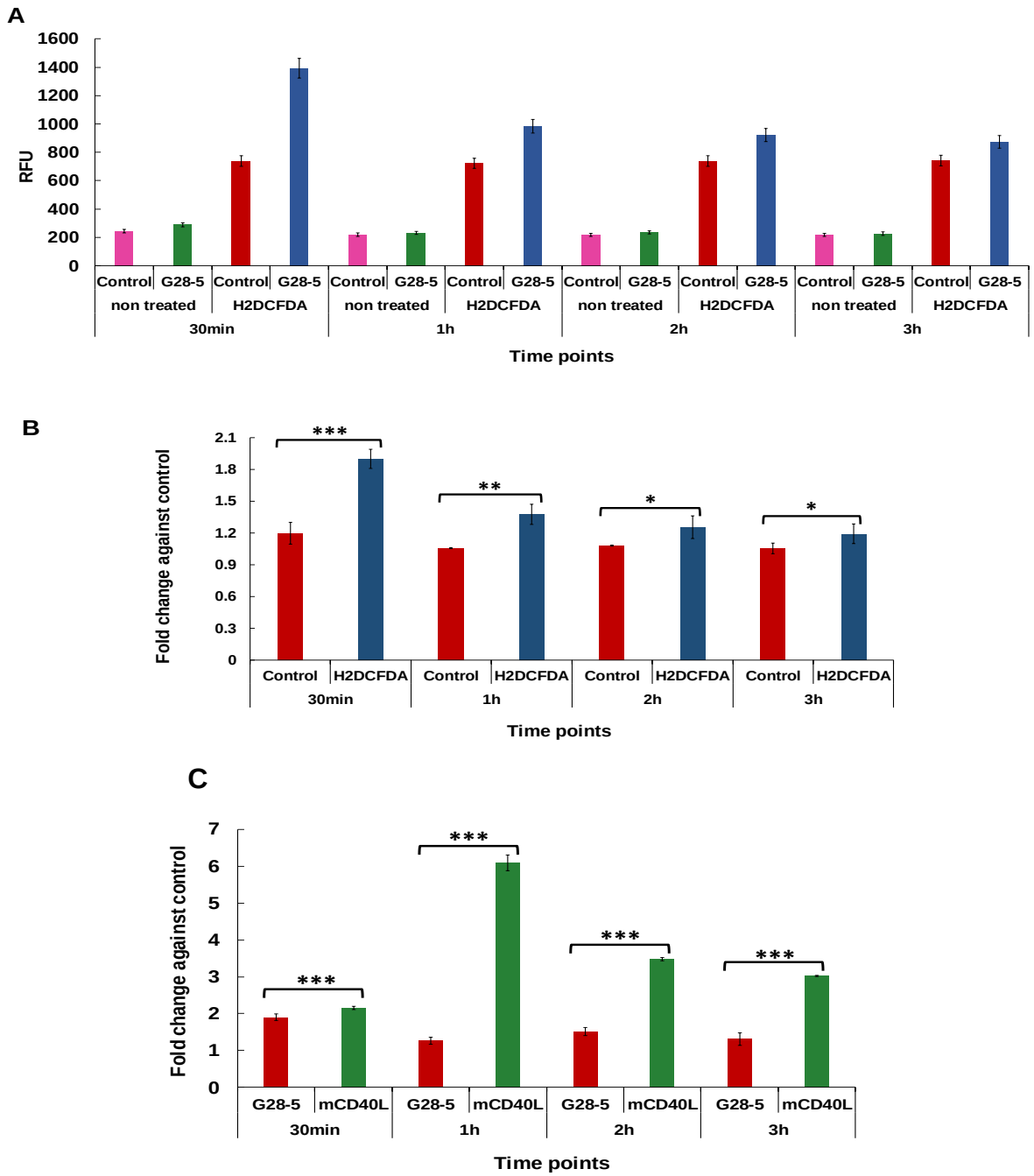

Figure 5.22 ROS generation in ACHN cells treated with soluble agonist

$8x10^3$ cells/well of ACHN cells were seeded in white 96-well plates and treated with 10µg/ml of G28-5 mAb cross-linked with 2.5µg/ml goat anti-mouse (untreated cells served as non-treated Controls). The plates were incubated for 30min, 1h, 2h and 3h. Then 1µM of H_2CDFAD in pre-warmed (37ºC) PBS was added. The plates then incubated for 30min at 37ºC and 5% CO_2. FLUOStar Optima plate reader was used at Excitation 485nm/Emission 520nm to measure the fluorescence. **A)** Raw data. **B)** Results from graphs A also presented as fold change (Cells treated with both G28-5 and H2DCFDA (H2DCFDA) relative to cells treated with only G28-5 (Control). Bars show mean values of 4-5 technical replicates ± SEM. **C)** Comparison of fold changes for co-culture experiments versus fold changes from treatments with cross-linked G28-5 agonist. Bars show mean of 4-5 technical replicates (RLU) ± SEM. Stats: ***, $p<0.001$; **, $p<0.01$; *, $p<0.05$, paired student T-test.

5.9.3 CD40-mediated apoptosis in RCC cells was ROS dependent

Having shown above that CD40 ligation by mCD40L triggered ROS generation in RCC cells, the functional role of ROS in CD40-mediated apoptosis in RCC cells was investigated using the anti-oxidant and ROS scavenger N-acetyl L-cysteine (NAC).

Pre-titration experiments were performed for both target (RCC cells) and effector (3T3-CD40L and 3T3-Neo) cells to assess cell viability (using CellTiter 96® AQueous One Solution Cell Proliferation assays) to ensure that the concentration of NAC used did not interfere with cell viability particularly of the effector cells (Figure 5.23). Both RCC and 3T3 cells tolerated concentrations up to 2mM well, while concentrations >4mM appeared toxic to both cell types. Following these pre-titration experiments, cell death assays demonstrated that NAC significantly attenuated mCD40L-mediated in a dose-dependent manner at 48h post CD40 ligation in all RCC cells although the inhibition was not complete (Figure 5.24, 5.25 and 5.26).

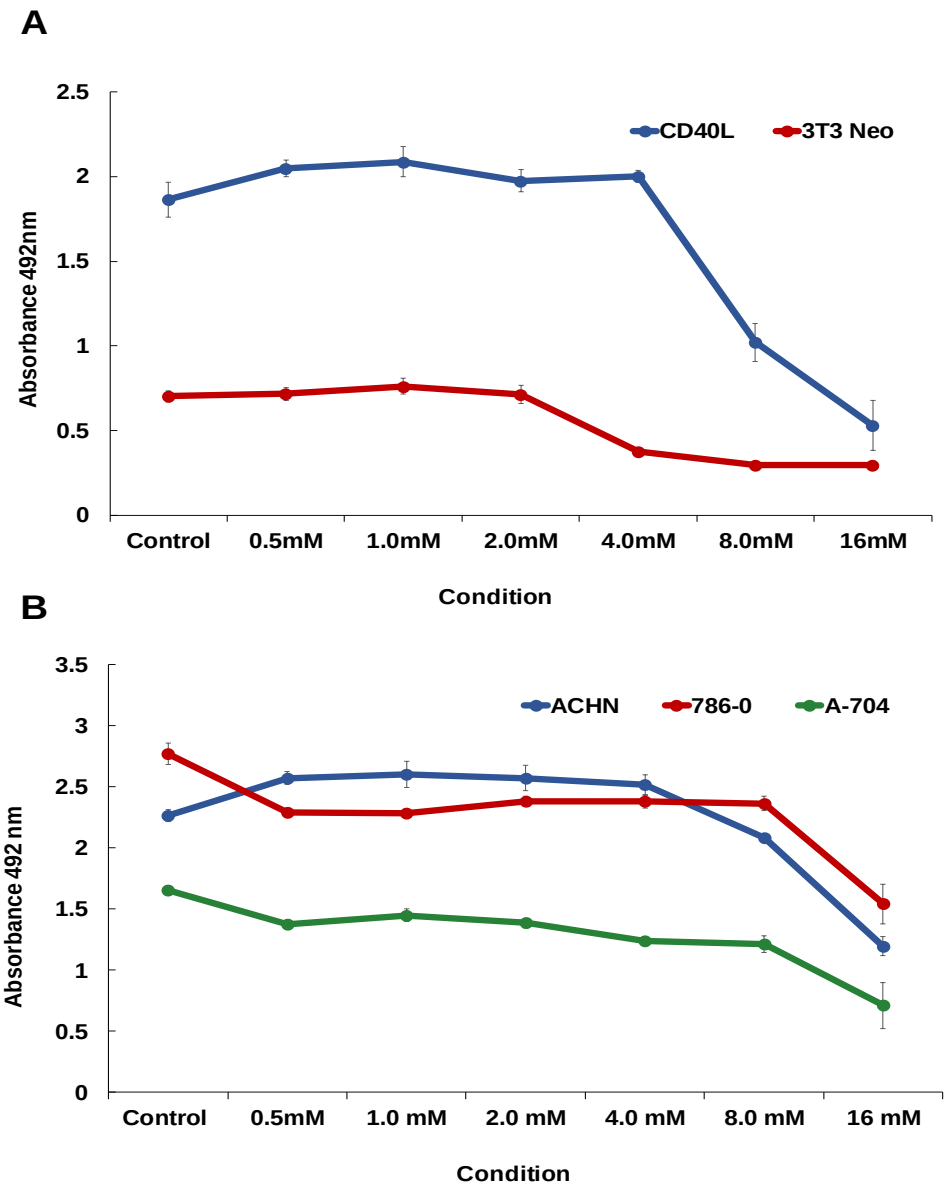

Figure 5.23 NAC titration experiments

Target (ACHN, 786-O and A-704) and effector (MMC-treated 3T3-CD40L and 3T3-Neo) cells were seeded at $0.8x10^4$ cells/well and $1x10^5$ cells/well respectively, in clear 96-well plates. Effector cells (A) were incubated for overnight and target cells (B) incubated for 1h. Then different concentrations of NAC was added to all cells. Plates were incubated for 48 h and cell viability was assessed by the CellTiter assay. 20µl of CellTiter Solution was added followed by 4h incubation at 37ºC. FLUOStar Optima plate reader at wavelength 492nm was used to measure the absorbance. Curves correspond to mean absorbance values of 5-6 technical repeats and results typical of three independent experiments.

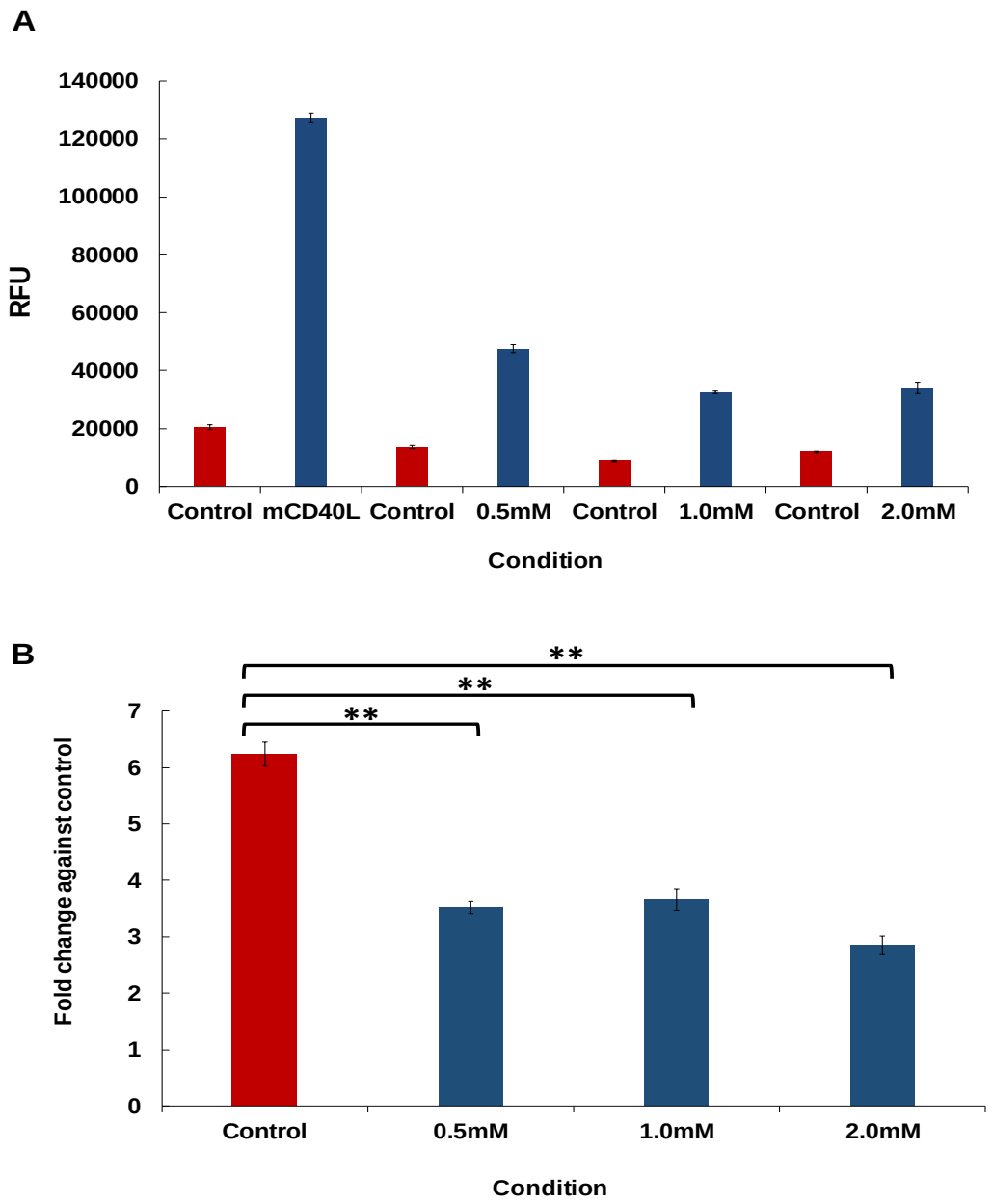

Figure 5.24 Effect of NAC on CD40-mediated apoptosis in ACHN cells

RCC cell lines ACHN were co-cultured at $0.8x10^4$ cells/well with $1x10^4$ cells/well MMC-treated fibroblasts 3T3-CD40L (mL) and 3T3-Neo (Con) ± NAC at the indicated concentrations in white 96-well plates. Plates were incubated for 48 h and apoptosis was assessed by the Cytotox-Glo assay. 50µl of substrate was added to each well followed by 10 min incubation at room temperature. Luminescence was measured on a FLUOStar Optima plate reader and background-corrected relative luminescence units (RLU) were deduced by pair-wise subtraction of mL and Con RLU from the respective co-cultures (as described in the Methods). **A)** Background corrected RLU readings for co-cultures of ACHN/3T3-CD40L ± NAC and respective 3T3-Neo co-culture (Controls) ± NAC. **B)** Results from graphs in A are also presented as fold change of mCD40L treatment (mCD40L) relative to Control). Bars show mean fold change of RLU of 4-6 technical replicates ± SEM. Stats: **, $p<0.01$, paired student T-test. "Control" represents Fold change in co-cultures without NAC and was statistically compared with Fold change for co-cultures carried out in the presence of the indicated NAC concentrations.

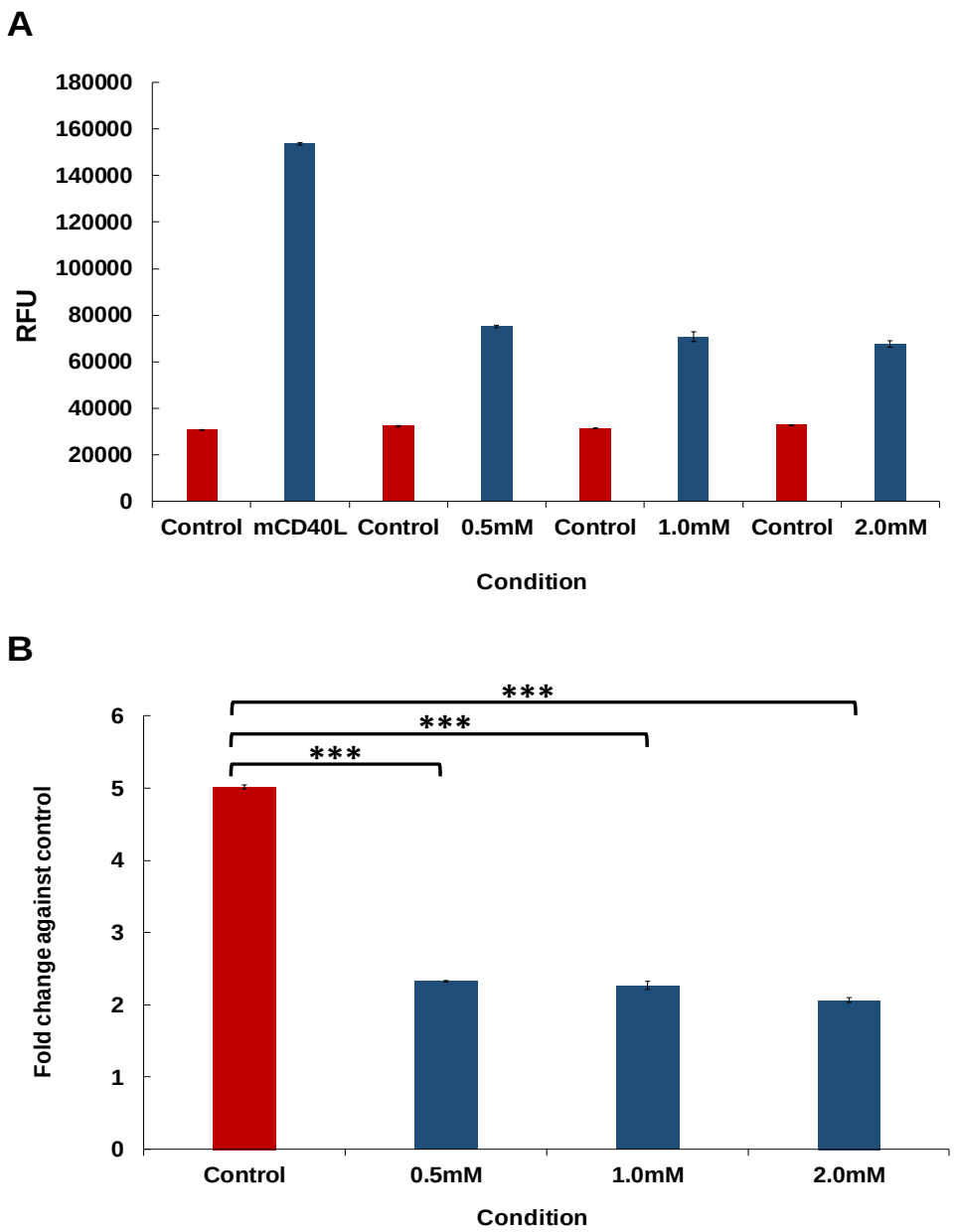

Figure 5.25 Effect of NAC on CD40-mediated apoptosis in 786-O cells

RCC cell lines 786-O were co-cultured at $0.8x10^4$ cells/well with $1x10^4$ cells/well MMC-treated fibroblasts 3T3-CD40L (mL) and 3T3-Neo (Con) ± NAC at the indicated concentrations in white 96-well plates. Plates were incubated for 48 h and apoptosis was assessed by the Cytotox-Glo assay. 50µl of substrate was added to each well followed by 10 min incubation at room temperature. Luminescence was measured on a FLUOStar Optima plate reader and background-corrected relative luminescence units (RLU) were deduced by pair-wise subtraction of mL and Con RLU from the respective co-cultures (as described in the Methods). **A)** Background corrected RLU readings for co-cultures of 786-O/3T3-CD40L ± NAC and respective 3T3-Neo co-culture (Controls) ± NAC. **B)** Results from graphs in A are also presented as fold change of mCD40L treatment (mCD40L) relative to Control). Bars show mean fold change of RLU of 4-6 technical replicates ± SEM. Stats: **, $p<0.01$, paired student T-test. "Control" represents Fold change in co-cultures without NAC and was statistically compared with Fold change for co-cultures carried out in the presence of the indicated NAC concentrations.

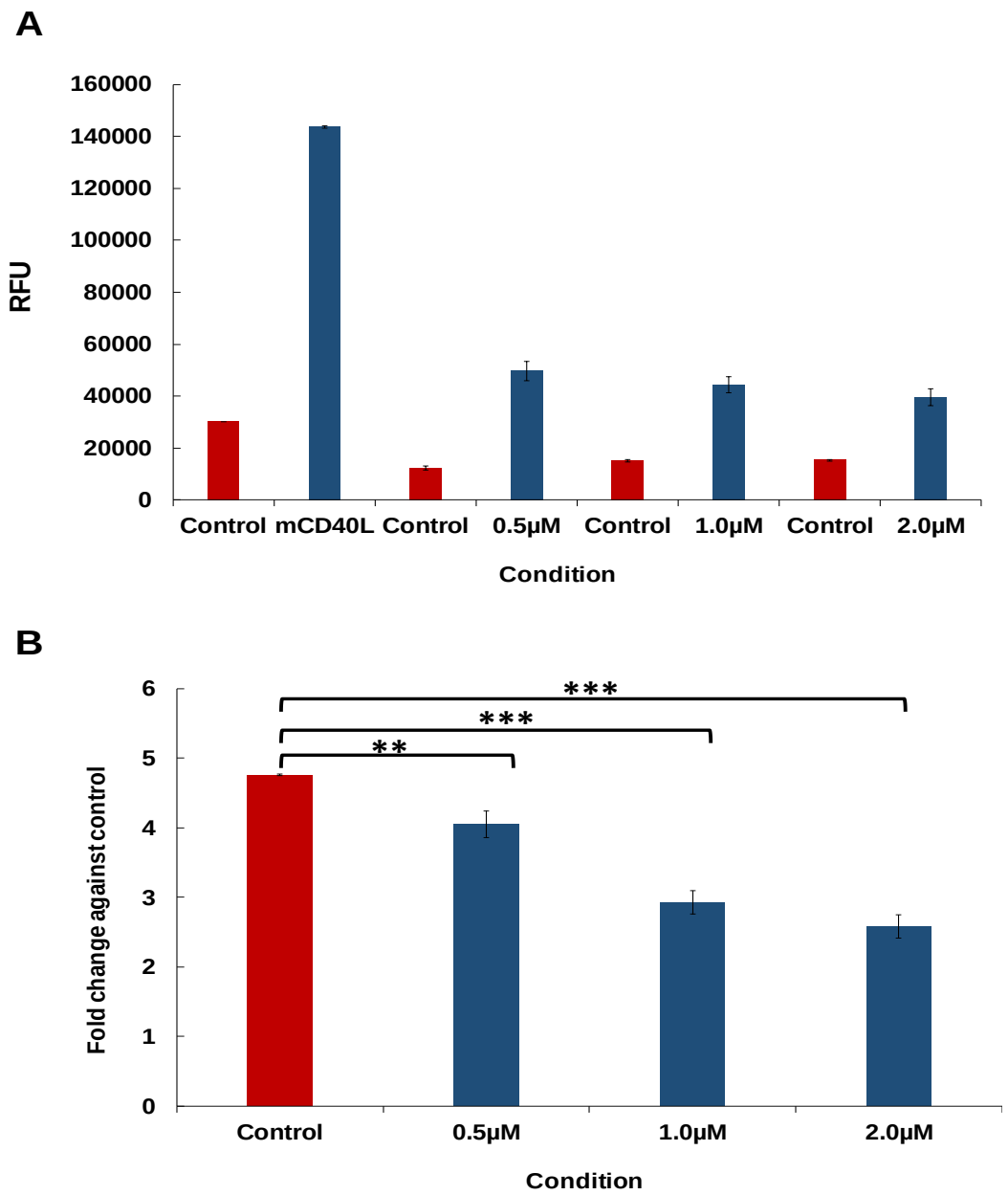

Figure 5.26 Effect of NAC on CD40-mediated apoptosis in A-704 cells

RCC cell lines A-704 were co-cultured at $0.8x10^4$ cells/well with $1x10^4$ cells/well MMC-treated fibroblasts 3T3-CD40L (mL) and 3T3-Neo (Con) ± NAC at the indicated concentrations in white 96-well plates. Plates were incubated for 48 h and apoptosis was assessed by the Cytotox-Glo assay. 50μl of substrate was added to each well followed by 10 min incubation at room temperature. Luminescence was measured on a FLUOStar Optima plate reader and background-corrected relative luminescence units (RLU) were deduced by pair-wise subtraction of mL and Con RLU from the respective co-cultures (as described in the Methods). **A)** Background corrected RLU readings for co-cultures of A-704/3T3-CD40L ± NAC and respective 3T3-Neo co-culture (Controls) ± NAC. **B)** Results from graphs in A are also presented as fold change of mCD40L treatment (mCD40L) relative to Control). Bars show mean fold change of RLU of 4-6 technical replicates ± SEM. Stats: **, $p<0.01$, paired student T-test. "Control" represents Fold change in co-cultures without NAC and was statistically compared with Fold change for co-cultures carried out in the presence of the indicated NAC concentrations.

5.9.4 The role of NADPH in CD40-mediated apoptosis in RCC cells

Previous studies in our laboratory provided evidence for a role for the Nox complex in mCD40L-mediated apoptosis, as apoptosis was not only inhibited by the ROS scavenger NAC but it was also affected by the Nox inhibitor diphenyleneiodonium (DPI) (Mohamed, 2014, Dunnill et al., 2016). Interestingly, there is evidence for translocation of p67phox from the cytosol to the cell membrane in renal epithelial cells via excessive treatment with zinc which resulted in the generation of ROS within 3 hours and was blocked by Nox inhibitor (DPI) (Matsunaga et al., 2005). A possible functional role for Nox in mCD40L-mediated RCC cell apoptosis was therefore examined.

First, as in the case of NAC above, early pre-titration tests were carried out to estimate the optimal concentrations of DPI that not interfere with the cell viability for both target and effector cells (as shown in Figure 5.27). The non-toxic concentrations of Nox inhibitor DPI (0.0157µM, 0.0313µM and 0.0625µM) were tested in RCC ACHN, 786-O and A-704 co-cultures with 3T3-CD40L/3T3-Neo cells and apoptosis was assessed (by CytoTox-Glo death detection assays) at 48h post CD40 ligation (Figure 5.28, 5.29 and 5.30) respectively. Results showed marked reduction in CD40-mediated apoptosis in all three RCC cells.

It has been reported that p^{40phox} is a catalytic subunit of Nox and CD40 engagement in B cells resulted in the activation of NADPH oxidase via p^{40phox} phosphorylation (Babior, 1999, Ha and Lee, 2004) and it has been recently shown in our laboratory that mCD40L in UCC and CRC cells induced p^{40phox} phosphorylation via TRAF3 recruitment (Dunnill et al., 2016). Therefore, this work investigated the expression of phosphorylated p^{40phox} in RCC cells post CD40 ligation by immunoblotting assays. Results showed rapid and marked phosphorylation of p^{40phox} at 1.5, 3 and 6h post CD40 ligation in all three RCC cell lines (Figure 5.31).

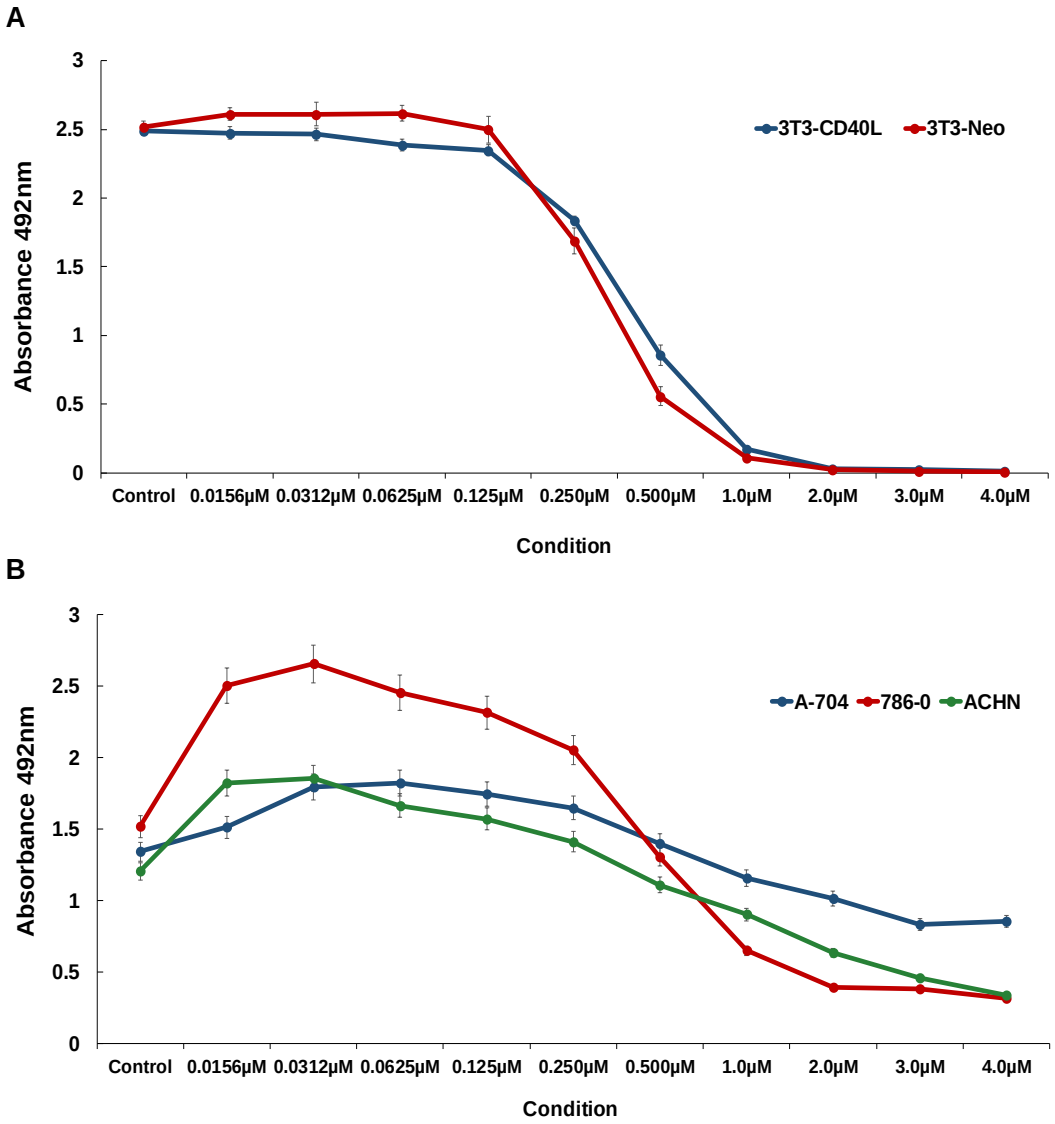

Figure 5.27 DPI titration experiments

Target cells (ACHN, 786-O and A-704) and effector cells (MMC treated 3T3-CD40L and 3T3-Neo) were seeded at $0.8x10^4$ cells/well and $1x10^5$ cells/well respectively, in clear 96-well plates. Effector cells (A) were incubated for overnight and target cells (B) incubated for 1h. Then all cells were treated with different concentrations of DPI. Plates were incubated for 48 h and cell viability was assessed by CellTiter assay. 20μl of CellTiter Solution was added to each well followed by 4h incubation at 37ºC / 5% Co_2. FLUOStar Optima plate reader at wavelength 492nm was used to measure the absorbance. Chart lines correspond to mean absorbance values of 5-6 technical repeats and results typical of three independent experiments.

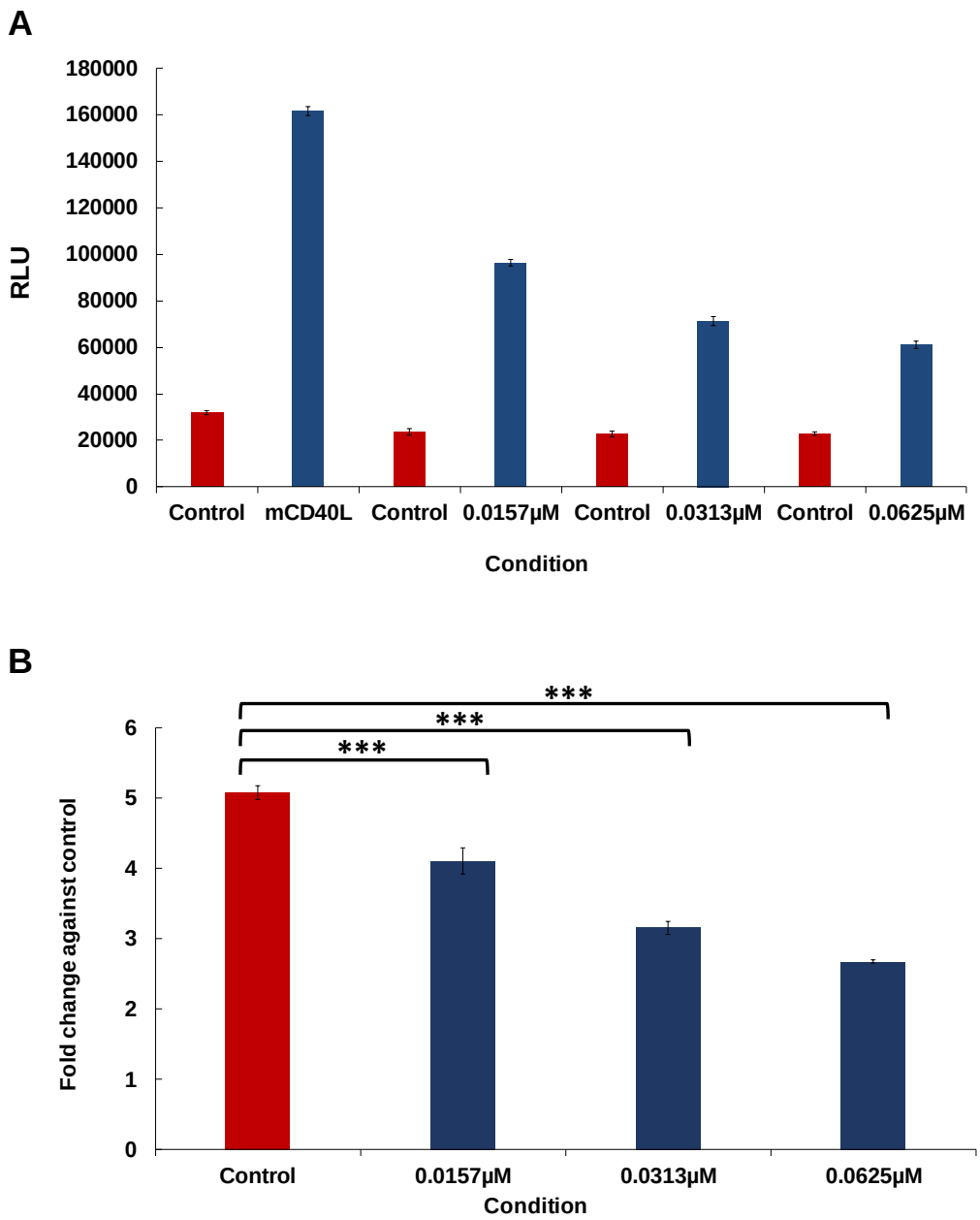

Figure 5.28 Effect of Nox inhibitor DPI on CD40-mediated death in ACHN cells

RCC cells line ACHN were co-cultured at $0.8x10^4$ cells/well with $1x10^4$ cells/well MMC-treated fibroblasts 3T3-CD40L (mL) and 3T3-Neo (Con) ± DPI at the indicated concentrations in white 96-well plates. Plates were incubated for 48 h and apoptosis was assessed by the Cytotox-Glo assay. 50µl of substrate was added to each well followed by 10 min incubation at room temperature. Luminescence was measured on a FLUOStar Optima plate reader and background-corrected relative luminescence units (RLU) were deduced by pair-wise subtraction of mCD40L and Control RLU from the respective co-cultures (as described in the Methods). **A)** Background corrected RLU readings for co-cultures of ACHN/3T3-CD40L ± DPI and respective 3T3-Neo co-culture (Controls) ± DPI. **B)** Results from graphs in A are also presented as fold change of mCD40L treatment (mCD40L) relative to Control). Bars show mean fold change of RLU of 4-6 technical replicates ± SEM. Stats: ***, $p<0.001$ paired student T-test. Control" represents Fold change in co-cultures without DPI and was statistically compared with Fold change for co-cultures carried out in the presence of the indicated DPI concentrations.

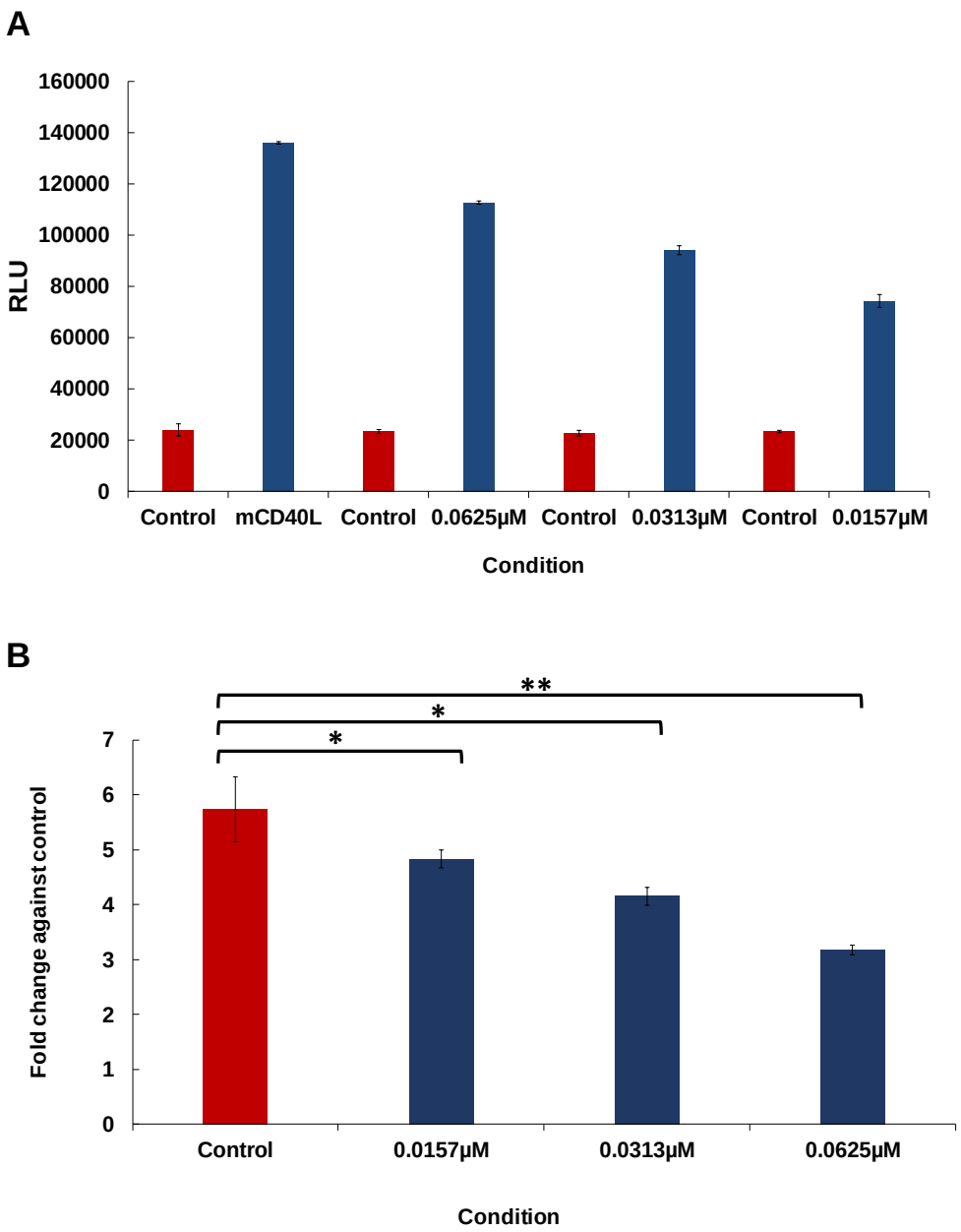

Figure 5.29 Effect of Nox inhibitor DPI on CD40-mediated death in 786-O cells

RCC cells line 786-O were co-cultured at $0.8x10^4$ cells/well with $1x10^4$ cells/well MMC-treated fibroblasts 3T3-CD40L (mL) and 3T3-Neo (Con) ± DPI at the indicated concentrations in white 96-well plates. Plates were incubated for 48 h and apoptosis was assessed by the Cytotox-Glo assay. 50µl of substrate was added to each well followed by 10 min incubation at room temperature. Luminescence was measured on a FLUOStar Optima plate reader and background-corrected relative luminescence units (RLU) were deduced by pair-wise subtraction of mL and Con RLU from the respective co-cultures (as described in the Methods). **A)** Background corrected RLU readings for co-cultures of 786-O/3T3-CD40L ± DPI and respective 3T3-Neo co-culture (Controls) ± DPI. **B)** Results from graphs in A are also presented as fold change of mCD40L treatment (mCD40L) relative to Control). Bars show mean fold change of RLU of 4-6 technical replicates ± SEM. Stats: **, $p<0.01$; *, $p<0.05$, paired student T-test. "Control" represents Fold change in co-cultures without DPI and was statistically compared with Fold change for co-cultures carried out in the presence of the indicated DPI concentrations.

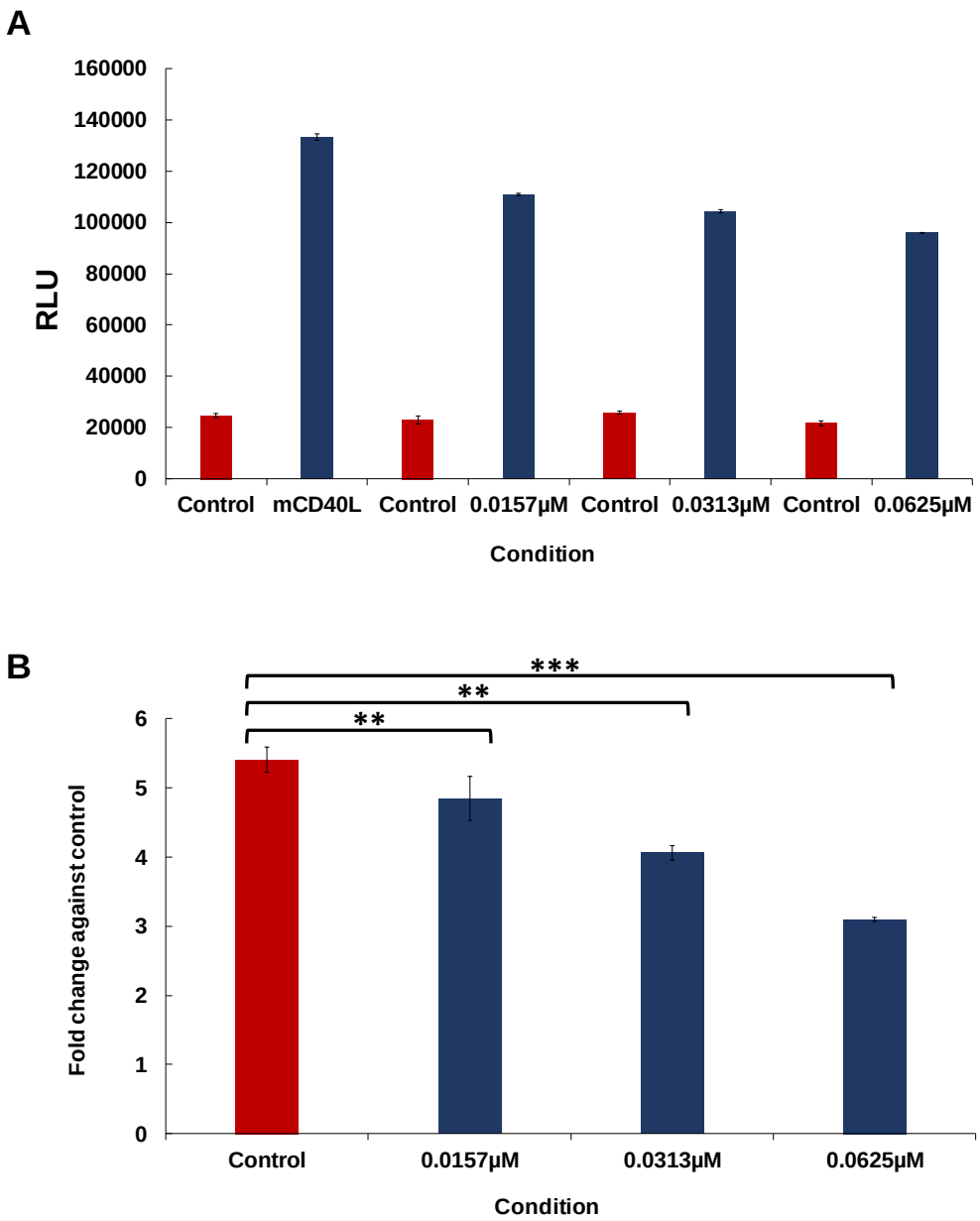

Figure 5.30 Effect of Nox inhibitor DPI on CD40-mediated death in A-704 cells

RCC cells line A-704 were co-cultured at $0.8x10^4$ cells/well with $1x10^4$ cells/well MMC-treated fibroblasts 3T3-CD40L (mL) and 3T3-Neo (Con) ± DPI at the indicated concentrations in white 96-well plates. Plates were incubated for 48 h and apoptosis was assessed by the Cytotox-Glo assay. 50µl of substrate was added to each well followed by 10 min incubation at room temperature. Luminescence was measured on a FLUOStar Optima plate reader and background-corrected relative luminescence units (RLU) were deduced by pair-wise subtraction of mL and Con RLU from the respective co-cultures (as described in the Methods). **A)** Background corrected RLU readings for co-cultures of A-704/3T3-CD40L ± DPI and respective 3T3-Neo co-culture (Controls) ± DPI. **B)** Results from graphs in A are also presented as fold change of mCD40L treatment (mCD40L) relative to Control). Bars show mean fold change of RLU of 4-6 technical replicates ± SEM. Stats: ***, $p<0.001$; **, $p<0.01$, paired student T-test. "Control" represents Fold change in co-cultures without DPI and was statistically compared with Fold change for co-cultures carried out in the presence of the indicated DPI concentrations.

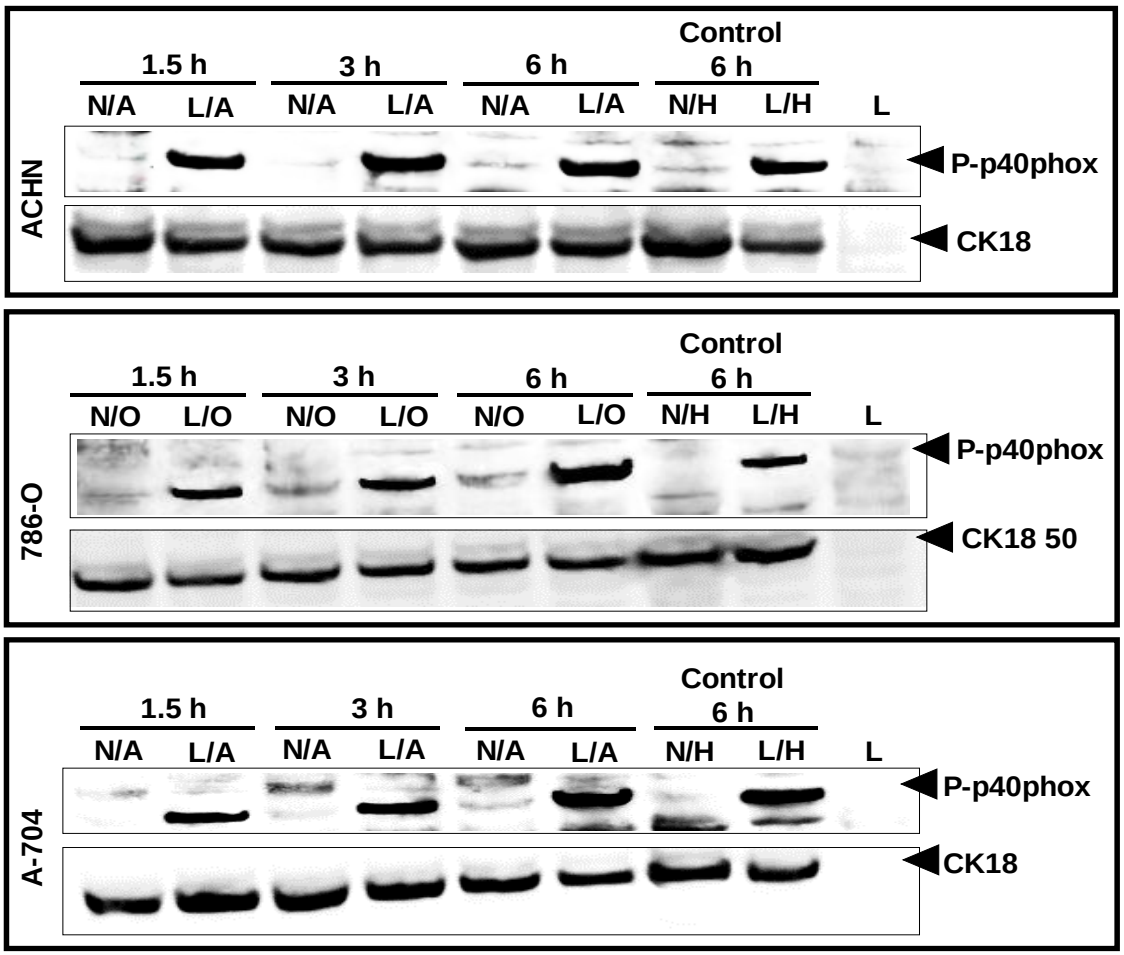

Figure 5.31 Induction of p^{40phox} phosphorylation following CD40 ligation in RCC cells

RCC cells were co-cultured at $30x10^5$ cells/dish with $30x10^5$ cells/dish of fibroblasts 3T3-Neo and 3T3-CD40L in a 10 cm dishes and incubated for the indicated time points. Whole cell lysates were prepared as described in the Methods (Section 2.9.3) and 40µg of protein/well was analysed by immunoblotting (Section 2.9.5). After normalisation on the basis of CK18 expression (see chapter 3 section 3.10), 40µg of normalised lysates were loaded and analysed by immunoblotting. After overnight incubation at 4ºC by rocking with primary polyclonal antibody (anti-p^{40phox}) in TBS/Tween 0.1% (1:1000 dilution), secondary antibody goat anti-rabbit IgG IRDye 800 (1:10000 dilution) was added and the membranes were incubated in the dark for 1h. For specificity and as a loading control CK18 antibody was used (at 1:1000 dilution), and incubation overnight at 4ºC, then the membranes were incubated with secondary antibody goat-anti mouse IgG Alexa 680 (diluted 1:10000) in the dark for 1h. Antibody binding was visualised at 800nm for p^{40phox} detection (expected molecular weight 40 kDa) and 700nm for CK18 detection using an Odyssey™ Infra-red Imaging system. Co-cultures for the HCT116 cell line were used as negative (N/H) and positive (L/H) controls, respectively, and 3T3CD40L cell lysate was used for confirmation of antibody specificity for human protein detection.

Key:

N/AC : 3T3Neo co-cultured with ACHN
N/O : 3T3Neo co-cultured with 786-O
N/A : 3T3Neo co-cultured with A-704
L : 3T3CD40L
L/AC : 3T3CD40L co-cultured with ACHN
L/O : 3T3CD40L co-cultured with 786-O
L/A : 3T3CD40L co-cultured with A-704

5.9.5 ASK-1 regulation during CD40-mediated apoptosis

ASK-1 (Apoptosis signal-regulating kinase one) is a member of the MAP3K family, which has the responsibility to activate MAPKK family members including MKK4, MKK7 and MAPKs such as p38 and JNK (Takeda et al., 2011, Ichijo et al., 1997). ASK-1 can be activated in response to several types of stress and has fundamental roles in many cellular responses including apoptosis, differentiation and inflammation (Ichijo et al., 1997, Nishitoh et al., 2002). It has been reported that CD40 ligation in B cells triggered ROS generation (Ha and Lee, 2004). Moreover, mCD40L in UCC and CRC cells mediated apoptosis via p^{40phox}/Nox-generated ROS which in turn could activate ASK-1 and treatment with Nox inhibitor DPI blocked the phosphorylation of ASK-1 (Mohamed, 2014, Dunnill et al., 2016). This study examined the expression of phosphorylated ASK-1 in RCC cells post CD40 ligation. As shown clearly in Figure 5.32, mCD40L induced ASK-1 phosphorylation within 1.5h post CD40 ligation and this was sustained.

5.9.6 Thioredoxin-1 (Trx) expression following CD40 ligation

It has been well characterised that Trx is responsible for the control of ASK-1 phosphorylation. In the presence of low or now ROS, Trx physically binds to ASK-1 and prevents its auto-phosphorylation and activation. When ROS level rise, Trx acts as a ROS scavenger which results in its release from the complex with ASK-1 and this release of ASK-permits it to be activated by auto-phosphorylation at Thr845 (Soga et al., 2012). Previous findings in our laboratory provided the very interesting observation of down-regulation in Trx-1 expression following CD40 ligation in UCC and CRC (Mohamed, 2014, Dunnill et al., 2016). Therefore, expression of Trx-1 in RCC cells treated with mCD40L was examined at 1.5, 3 and 6h by immunoblotting. Interestingly, although all RCC lines expressed significant basal levels of Trx (evident in control co-cultures of RCC with 3T3-Neo), mCD40L induced rapid and dramatic down-regulation of Trx-1 particularly in ACHN and A-704 cells (Figure 5.33).

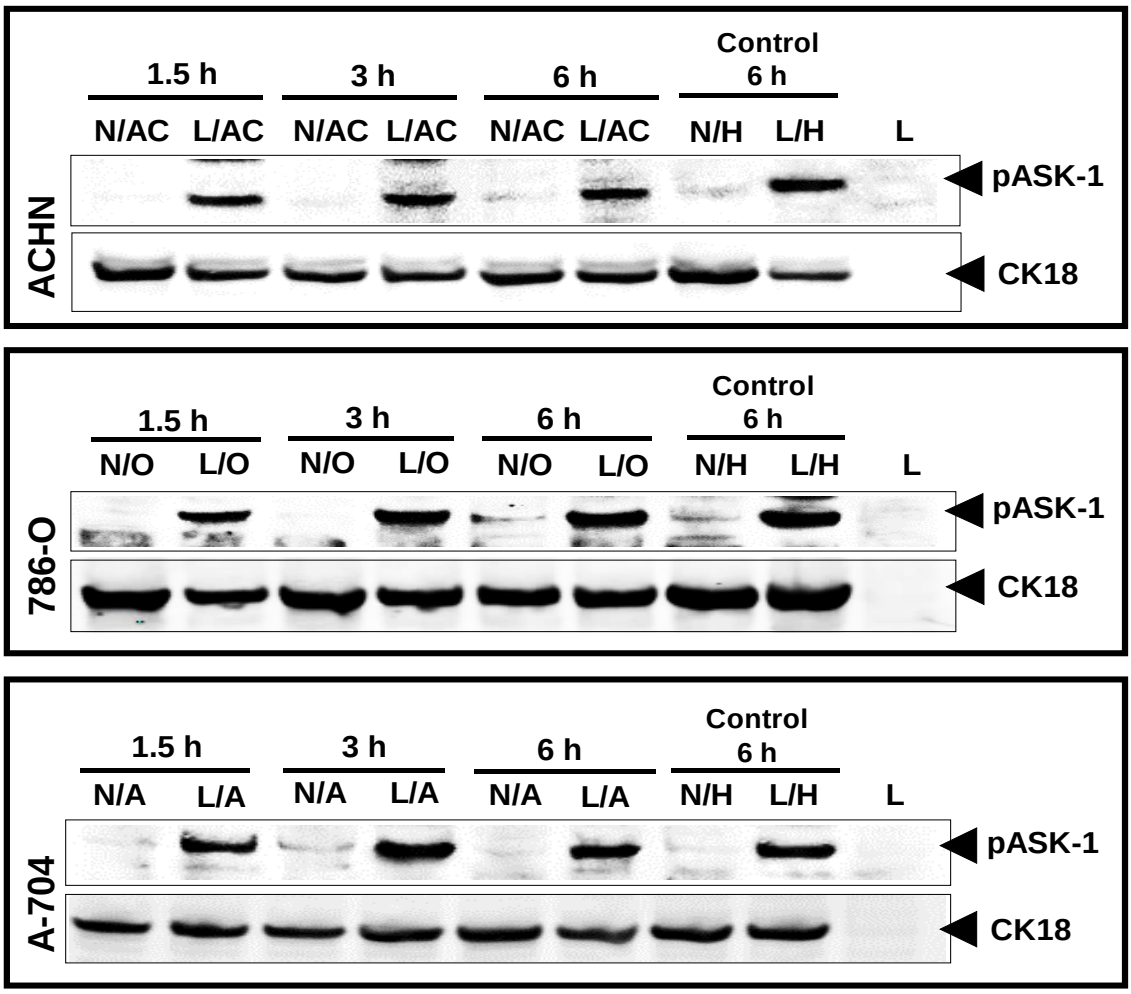

Figure 5.32 Induction of ASK-1 phosphorylation following CD40 ligation

RCC cells were co-cultured at $30x10^5$ cells/dish with $30x10^5$ cells/dish of fibroblasts 3T3-Neo and 3T3-CD40L in 10 cm dishes and incubated for the indicated time points. Whole cell lysates were prepared as described in the Methods (Section 2.9.3) and 40µg of protein/well was analysed by immunoblotting (Section 2.9.5). After normalisation on the basis of CK18 expression (see chapter 3 section 3.10), 40µg of normalised lysates were loaded and analysed by immunoblotting. After overnight incubation at 4ºC by rocking with primary polyclonal antibody (anti-ASK-1) in TBS/Tween 0.1% (1:1000 dilution), secondary antibody goat anti-rabbit IgG IRDye 800 (1:10000 dilution) was added and the membranes were incubated in the dark for 1h. For specificity and as a loading control CK18 antibody was used (at 1:1000 dilution), and incubation overnight at 4ºC, then the membranes were incubated with secondary antibody goat-anti mouse IgG Alexa 680 (diluted 1:10000) in the dark for 1h. Antibody binding was visualised at 800nm for pASK-1 detection (expected molecular weight 39 kDa) and 700nm for CK18 detection using an Odyssey™ Infra-red Imaging system. Co-cultures for the HCT116 cell line were used as negative (N/H) and positive (L/H) controls, respectively, and 3T3CD40L cell lysate was used for confirmation of antibody specificity for human protein detection

Key:

N/AC : 3T3Neo co-cultured with ACHN
N/O : 3T3Neo co-cultured with 786-O
N/A : 3T3Neo co-cultured with A-704
L : 3T3CD40L
L/AC : 3T3CD40L co-cultured with ACHN
L/O : 3T3CD40L co-cultured with 786-O
L/A : 3T3CD40L co-cultured with A-704

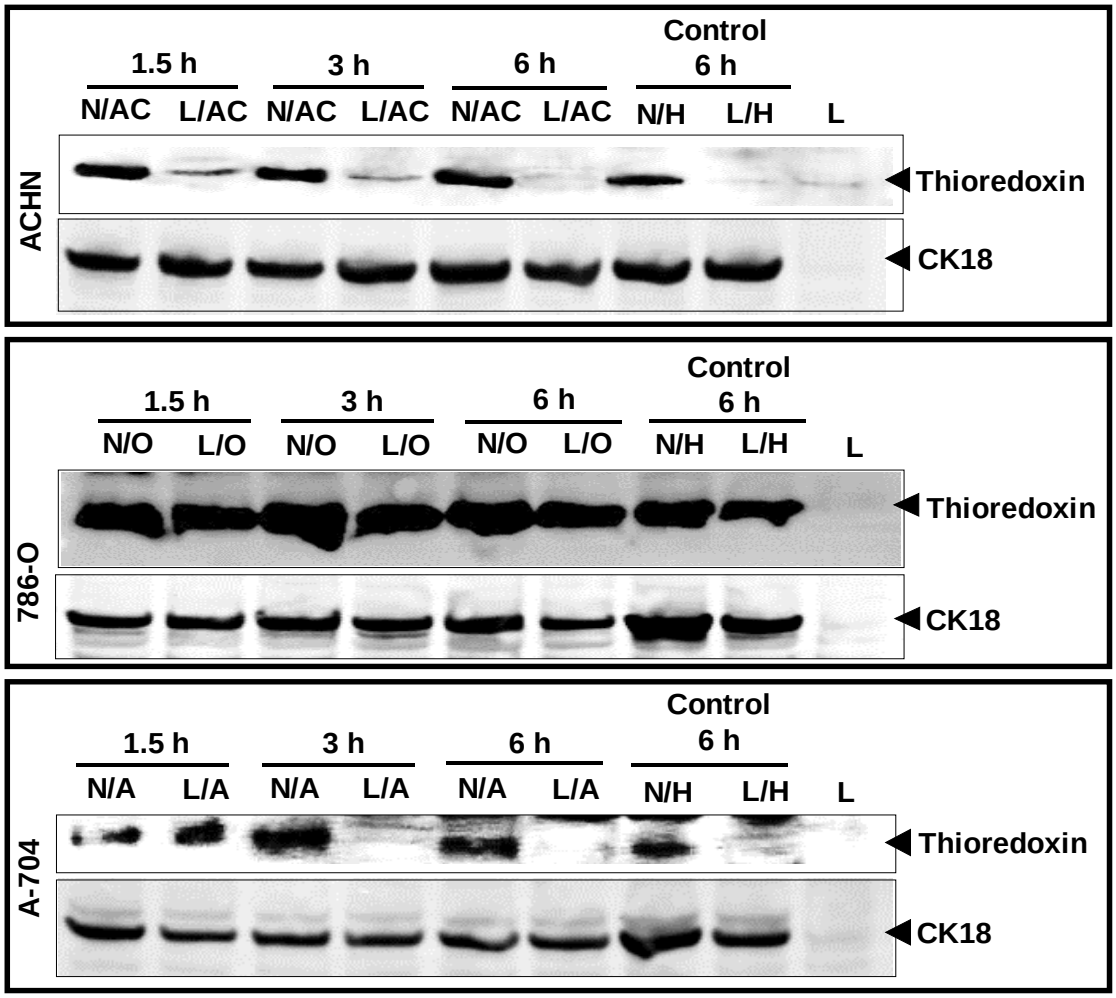

Figure 5.33 Thioredoxin-1 expression in RCC cells following CD40 ligation

RCC cells were co-cultured at $30x10^5$ cells/dish with $30x10^5$ cells/dish of fibroblasts 3T3-Neo and 3T3-CD40L in 10 cm dishes and incubated for the indicated time points. Whole cell lysates were prepared as described in the Methods (Section 2.9.3) and 40µg of protein/well was analysed by immunoblotting (Section 2.9.5). After normalisation on the basis of CK18 expression (see chapter 3 section 3.10), 40µg of normalised lysates were loaded and analysed by immunoblotting. After overnight incubation at 4ºC by rocking with primary polyclonal antibody (anti-Trx-1) in TBS/Tween 0.1% (1:1000 dilution), secondary antibody goat anti-rabbit IgG IRDye 800 (1:10000 dilution) was added and the membranes were incubated in the dark for 1h. For specificity and as a loading control CK18 antibody was used (at 1:1000 dilution), and incubation overnight at 4ºC, then the membranes were incubated with secondary antibody goat-anti mouse IgG Alexa 680 (diluted 1:10000) in the dark for 1h. Antibody binding was visualised at 800nm for Trx-1 detection (expected molecular weight 12 kDa) and 700nm for CK18 detection using an Odyssey™ Infra-red Imaging system. Co-cultures for the HCT116 cell line were used as negative (N/H) and positive (L/H) controls, respectively, and 3T3CD40L cell lysate was used for confirmation of antibody specificity for human protein detection

Key:

N/AC : 3T3Neo co-cultured with ACHN
N/O : 3T3Neo co-cultured with 786-O
N/A : 3T3Neo co-cultured with A-704
L : 3T3CD40L
L/AC : 3T3CD40L co-cultured with ACHN
L/O : 3T3CD40L co-cultured with 786-O
L/A : 3T3CD40L co-cultured with A-704

5.10 Summary

- Immunoblotting results showed that mCD40L mediated marked and sustained induction of TRAF1, TRAF3 and TRAF6 expression in RCC cells at 1.5, 3 and 6h post ligation

- Induction of TRAF2 at 1.5, 3 and 6h was moderate in ACHN and 786-O unlike A-704 that showed high TRAF2 expression

- Pro-apoptotic MAP kinases MKK4 and MKK7 were activated (phosphorylated) in response to mCD40L in RCC cells

- Rapid and sustained phosphorylation of JNK was observed at 1.5h post CD40 ligation and the same observation was made for p38

- CD40 ligation in RCC cells also induced the expression of the pro-apoptotic proteins Bak and Bax at 6h (but not before) post CD40 ligation

- The effect of the pan-caspase inhibitor z-VAD which completely abrogated cell death, indicated that CD40-mediated apoptosis in RCC cells is caspase-dependent. Also by using specific cAspse-9, -8 and -10 inhibitors, results provided indication that CD40-triggered cell death in RCC cells is via caspase-9 activation, and in light of the stimulation of Bak and Bax, it appears to engage the intrinsic pathway

- By using specific pharmacological inhibitors, it was shown that JNK and p38 MAPK are essential for CD40-mediated apoptosis in RCC cells, whilst more detailed investigations suggested a functional hierarchy in the activation of these two pathways, with JNK being ‘upstream’ of p38

- CD40-CD40L interactions in RCC cells induced rapid ROS generation which peaked as early as 1h post CD40 ligation. By contrast, non-apoptotic CD40 agonist G28-5 mAb did not

- The NADPH oxidase (Nox) inhibitor DPI and the ROS scavenger NAC were able to down-regulate (although not fully block) mCD40L-induced apoptosis

- mCD40L induced rapid phosphorylation of Nox enzyme subunit p^{40phox}., providing a possible role for p^{40phox} induction in Nox-mediated ROS generation and ROS-mediated apoptosis

- Phosphorylation of ASK-1 in response to CD40 ligation was also observed within 1.5h which interestingly coincided with the point when maximal level of ROS was detected

- Western blot results demonstrated that RCC cells express substantial basal Thioredoxin-1 (Trx-1) expression which was rapidly down-modulated by CD40 ligation starting at 1.5h and further decreasing gradually over 6h

- These results indicated that CD40-mediated apoptosis in RCC cells may involve induction of TRAFs such as TRAF3 and TRAF6, activation of kinase pathways MKK4/7 and downstream JNK/p38 activation, whilst concurrently engaging a ROS-triggered pathway where p^{40phox} phosphorylation and Nox activation, ROS generation, ASK-1 phosphorylation occurs to induce an apoptotic pathway that involves Bak/Bax and triggers caspase-9 and caspase-3/7 mitochondria-mediated death

Chapter 6

The effect of CD40 ligation in normal human renal proximal tubule (HRPT) cells

6. Background

Human renal proximal tubular (HRPT) epithelial cells were isolated for the first time in 1984. Primary HRPT cells are able to conserve and display their in vivo features during their culture in vitro, thus HRPT cells were used to study the human renal cellular physiology and pathology (Baer et al., 2006). However, all primary cells can be maintained in only short-term culture for a limited number of passages, thus HRPT cells have been transformed using human papilloma virus (HPV) without affecting their functions or their morphological features. HPV-mediated transformation enabled culture of HRPT cells for longer term, with a passaging range of 8-15 passages (Ryan et al., 1994). Previous studies have revealed the important role for renal tubular epithelial cells in the regulation of interstitial inflammation (Healy et al., 1999, van Kooten et al., 1999a, Abbate et al., 1998), which leads to the recruitment of inflammatory cells to the inflammation site.

HRPT cells have been reported to express CD40 (van Kooten et al., 2000). The expression of CD40 on HRPT has been reported to be prominent in the inflammation process (van Kooten et al., 1999a, Kairaitis et al., 2003). Infiltrating of T cells which are expressing CD40L to the inflamed area during the interstitial inflammation, enable the direct contact of T-cells (CD40L) and HRPT cells (CD40) which provides the possibility to enhance an inflammatory cascade (Van Kooten et al., 1999b, van Kooten et al., 2000, Kairaitis et al., 2003, Kuroiwa et al., 2000, Van Kooten et al., 1997). Interstitial infiltration of leukocytes has been demonstrated to be regulated by CD40 ligation on HRPT cells, and activated T cells infiltrated via their secretion of IL-8, monocyte chemoattractant protein-1 (MCP-1) (Van Kooten et al., 1997).

CD40 ligation in other cells like endothelial cells induces ROS generation and promotes apoptosis (Urbich et al., 2002, Longo et al., 2003). Furthermore, CD40-CD40L interaction promotes growth inhibition and apoptosis in some normal primary epithelial cells (Davies et al., 2004) but not in others such as normal human urothelial (NHU) cells (Dunnill et al., 2016). CD40 ligation enhance the activation of NF-κB through the expression of cytoprotective genes (Zazzeroni et al., 2003, Choudhury et al., 2003). More recent studies have reported that CD40 engagement on HRPT cells

did not induce apoptosis despite its ability to promote ROS generation, but such ligation simultaneously mediated activation of cytoprotective genes (such as heme oxygenase-1, HO-1) that prevent the effect of ROS generation and stop cell death (Laxmanan et al., 2005).

This work described in this chapter studied for the first time the outcome of CD40 ligation on normal HRPT cells versus their malignant counterparts by comparing the effects of mCD40L (by adapting the use of the co-culture system for HRPT cells) versus soluble agonist (agonistic anti-CD40 antibody G28-5).

6.1 Objectives

The main aim of this chapter was to investigate the tumour specificity of CD40 by examining the outcome of CD40 ligation in normal renal (HRPT) cells and compare to their malignant counterparts. Primary normal HRPT cells were commercially available and were obtained and cultured as described in the Methods (section 2.6.4).

Precisely, this chapter aimed for:

- To examine the expression of CD40 on normal HRPT cells by
  - immunoblotting
  - flow-cytometry
- To determine whether CD40 stimulation by either mCD40L or by treatment with agonistic anti-CD40 antibody G28-5, trigger cell death in normal HRPT by using
  - CytoTox-Glo assays
  - DNA fragmentation tests
- To investigate cytokine secretion following CD40 ligation on normal HRPT by both mCD40L and G28-5 agonists (including IL-8, IL-6 and GM-CSF)
- To investigate the activation of cell signalling pathways in HRPT cells by studying the expression of key TRAF proteins following treatment of HRPT cells with mCD40L – using the previously optimised co-culture system.

6.2 CD40 expression by primary HRPT cells

In order to for the first time systematically investigate and compare the functional consequences of CD40 ligation in normal *versus* malignant renal cells, the expression of CD40 on HRPT cells was initially determined by immunoblotting and flow cytometry. In addtion to the panel of RCC lines, CRC cells HCT116 were used as an additional positive control for CD40 expression (Georgopoulos et al., 2007) for both experimental techniques, whlist 3T3-Neo fibroblasts and the CRC line SW480 served as negative controls for westren blot and flow cytometry, respectively.

The total expression of CD40 in HRPT cells and RCC cells appeared to be comparable when immunoblotting was used (Figure 6.1), whereas flow cytometry results showed a lower, yet clearly detectable surface expression of CD40 on HRPT cells in comparison with the carcinoma cells (Figure 6.2).

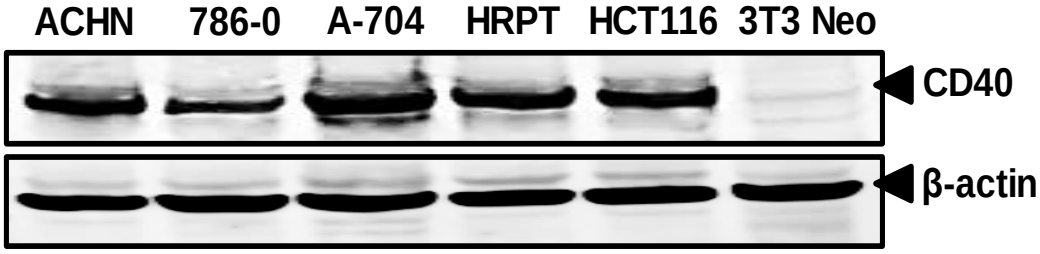

Figure 6.1 Detection of CD40 expression in HRPT cells by Western blotting

Normal HRPT cells and RCC lines ACHN, 786-O and A-704 were cultured until approximately 90% confluent. Whole cell lysates were prepared as described in the Methods (Section 2.9.3) and 20µg of protein/well was analysed by immunoblotting (Section 2.9.5). After overnight incubation at 4ºC by rocking with primary antibody (CD40 H-10 mouse monoclonal IgG diluted 1:500), secondary antibody (goat-anti mouse IgG Alexa 680 dilution 1:10000) was added and the membrane was incubated in the dark for 1h. For specifity and as a loading control, β-actin antibody was used (at 1:10,000 dilution) and incubation overnight at 4ºC, then the membrane was incubated with secondary antibody goat-anti mouse IgG Alexa 680 (diluted 1:10000) in the dark for 1h. Antibody binding was visualised at 700nm using a LI-COR Odyssey Infra-Red Imaging System and the image is shown in black and white. Lysates from HCT116 cell cultures were used as positive controls and from 3T3 Neo cell cultures as negative controls.

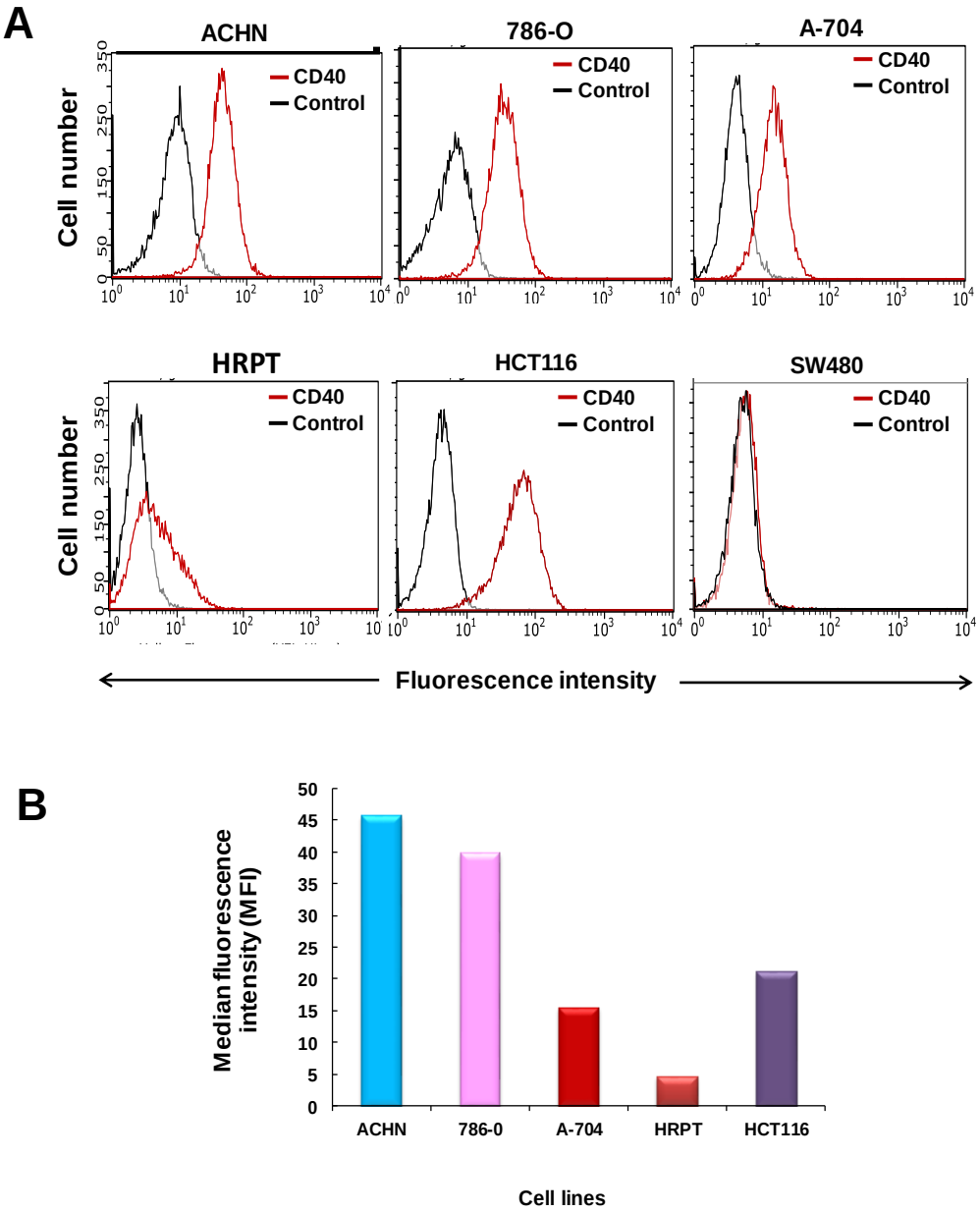

Figure 6.2 Detection of CD40 expression on HRPT cells by flow cytometry

Surface expression of CD40 on normal HRPT cells, RCC cells (ACHN, 786-O and A-704), CRC HCT116 (positive control), SW480 (negative control) was detected by flow cytometry (section 2.10.2). Cells were cultured until approximately 80% confluent, lifted, counted, washed and re-suspended in FACS buffer ($0.25x10^5$ cells/100µl), then incubated for 30 min at 4ºC with PE-conjugated mouse anti-human CD40 Ab (CD40 PE), and a control PE-conjugated isotype-matched control Ab (Control PE). Cells were acquired on a Guava EasyCyte flow cytometer and results analysed using GuavaSoft software. **A)** Representative overlay histograms show surface CD40 expression on normal HRPT cells in comparison with RCCs (ACHN, 786-O and A-704) the positive control (HCT116) and the negative control (SW480). **B)** Median fluorescence intensity (MFI) values are also presented as bar graphs. Bars show mean values of 2-3 technical replicates and results represent 2 independent experiments.

6.3 Detection of cell death in normal HRPT following CD40 ligation by mCD40L

Most previous studies focused on the inflammation process and cytokine secretion in primary HRPT cells following CD40 stimulation by soluble agonists. This work aimed to investigate for the first time the role of CD40 ligation in normal HRPT cells by using two well-characterised death detection assays, CytoTox-Glo and DNA fragmentation ELISA.

6.3.1 Determination of cell death by the CytoTox-Glo assay

Results in chapter 3 demonstrated that mCD40L triggered massive apoptosis in RCC cells, similarly to previous findings in our laboratory in UCC and CRC cells (Bugajska et al., 2002, Georgopoulos et al., 2006, Georgopoulos et al., 2007, Mohamed, 2014, Dunnill et al., 2016). By contrast, recently published studies by our group have shown that ligation of CD40 by mCD40L provides a cyto-protective signal in normal human urothelial (NHU) cells (Dunnill et al., 2016).

The effect of mCD40L in primary HRPT cells, was therefore investigated using the CytoTox-Glo assay and by adapting the co-culture system for the delivery of mCD40L (as described in section 2.8.4). Different cell densities of HRPT (0.6x104, 0.8x104 and 1x104 cells/well) were co-cultured with 1x104 of MMC treated 3T3-CD40L and 3T3-Neo and cell death was determined at 24, 48 and 72h .Results show that mCD40L did not induce cell death in normal HRPT cells in comparison with their malignant counterparts 786-0 at all cell densities and all indicated time points (Figures 6.3, 6.4 and 6.5).

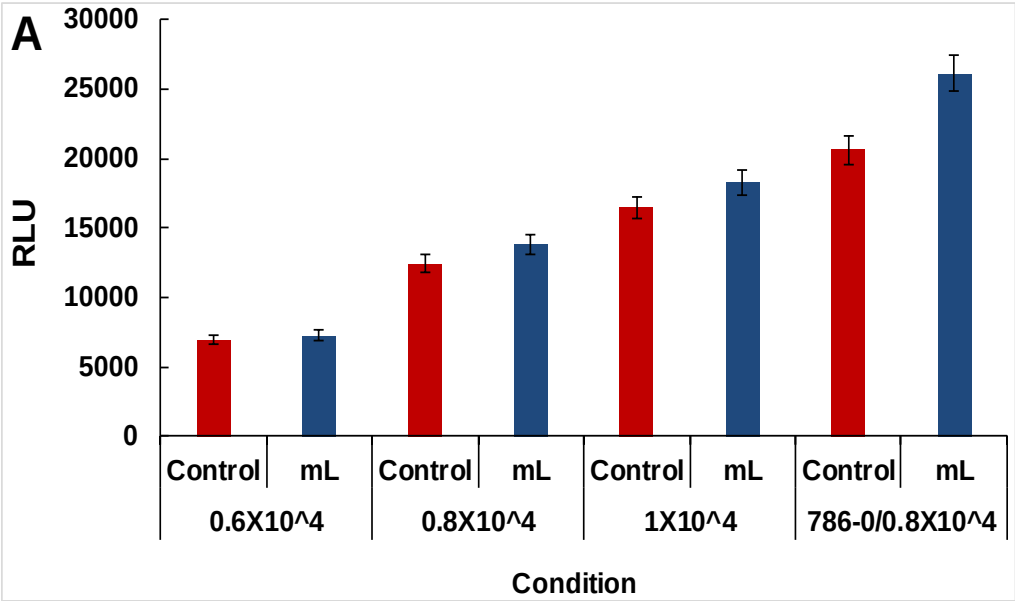

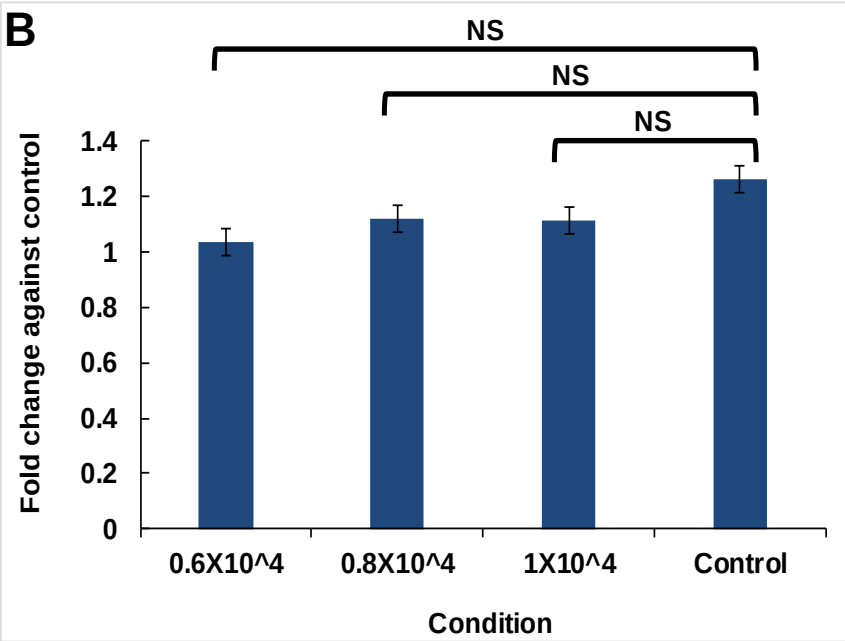

Figure 6.3 Detection of cell death in HRPT cells following 24h of CD40 ligation by mCD40L

Normal HRPT cells were co-cultured at $0.6x10^4$, $0.8x10^4$ and $1x10^4$ cells/well with $1x10^4$ cells/well MMC-treated fibroblasts 3T3-CD40L and 3T3-Neo in white 96-well plates (as detailed in the Methods). Plates were incubated for 24h and apoptosis was assessed by the Cytotox-Glo assay. 50µl of substrate was added to each well followed by 10 min incubation at room temperature. Luminescence was measured on a FLUOStar Optima plate reader and background-corrected relative luminescence units (RLU) were deduced by pair-wise subtraction of mCD40L and Control RLU from the respective co-cultures as described in Materials and Methods. **A)** Background corrected RLU readings for HRPT/3T3-CD40L (mL) and HRPT/3T3-Neo (Control). Bars show mean of 4-6 technical replicates (RLU) ± SEM. **B)** Results from graphs in A are also presented as fold change (mCD40L relative to control). Stats: NS, non-significant ($p>0.05$) paired student T-test

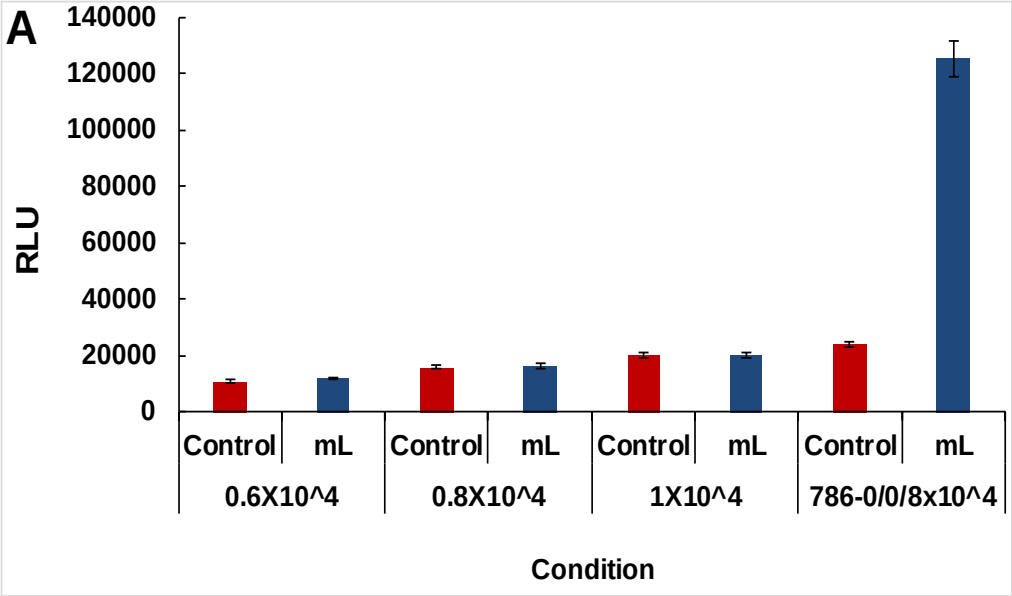

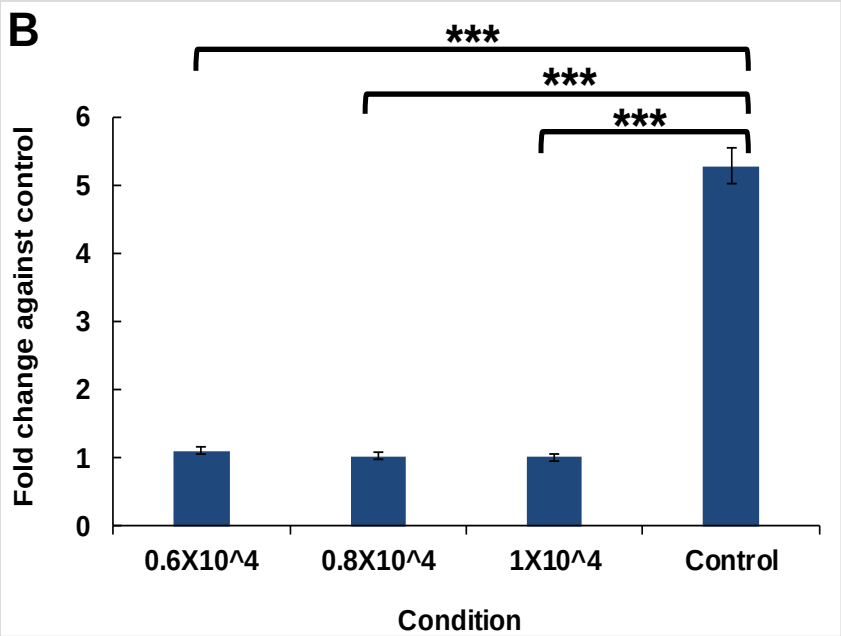

Figure 6.4 Detection of cell death in HRPT cells following 48h of CD40 ligation by mCD40L

Normal HRPT cells were co-cultured at $0.6x10^4$, $0.8x10^4$ and $1x10^4$ cells/well with $1x10^4$ cells/well MMC-treated fibroblasts 3T3-CD40L and 3T3-Neo in white 96-well plates (as detailed in the Methods). Plates were incubated for 48h and apoptosis was assessed by the Cytotox-Glo assay. 50µl of substrate was added to each well followed by 10 min incubation at room temperature. Luminescence was measured on a FLUOStar Optima plate reader and background-corrected relative luminescence units (RLU) were deduced by pair-wise subtraction of mCD40L and Control RLU from the respective co-cultures as described in Materials and Methods. **A)** Background corrected RLU readings for HRPT/3T3-CD40L (mL) and HRPT/3T3-Neo (Control). Bars show mean of 4-6 technical replicates (RLU) ± SEM. **B)** Results from graphs in A are also presented as fold change (mCD40L relative to control). Stats: ***, $p<0.001$ paired student T-test

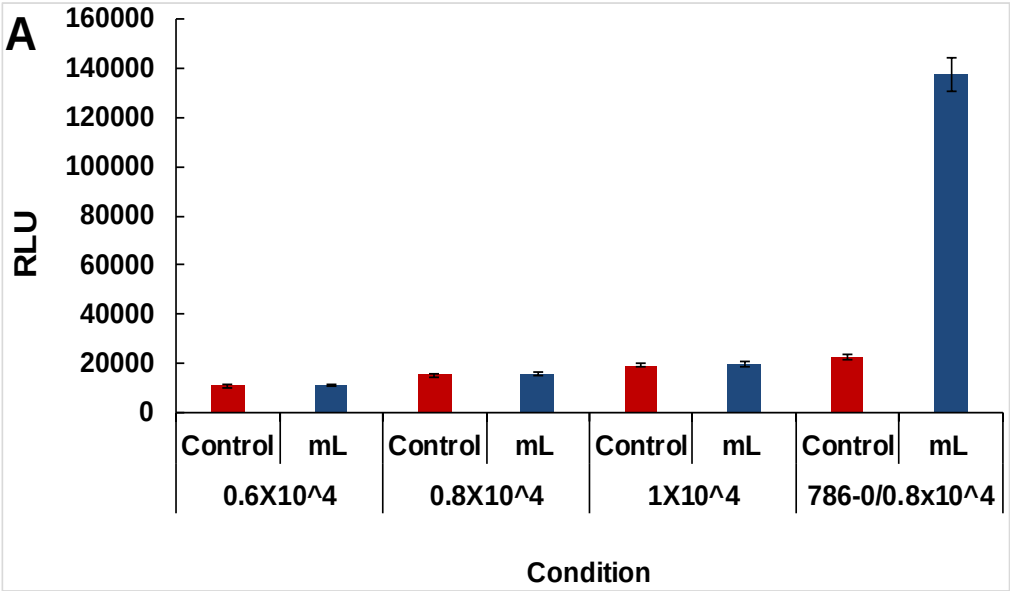

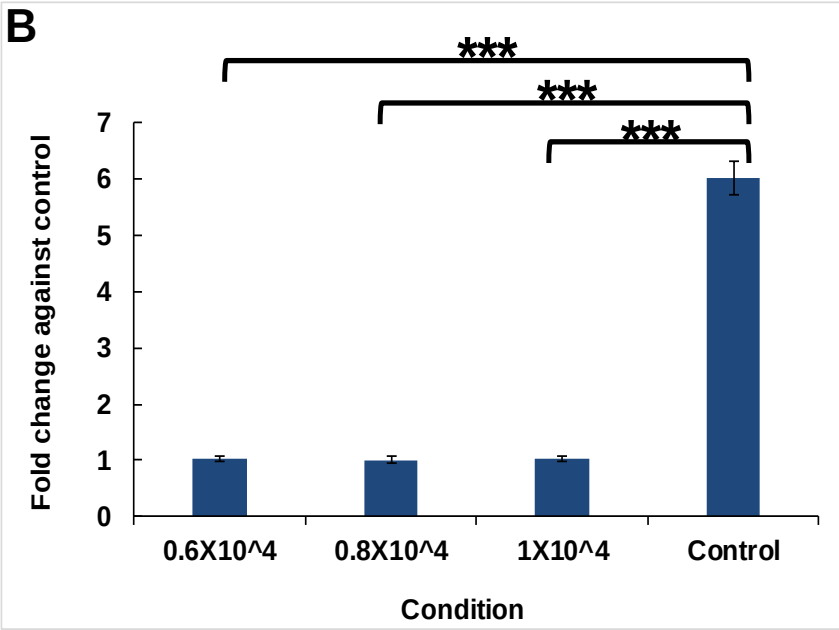

Figure 6.5 Detection of cell death in HRPT cells following 72h of CD40 ligation by mCD40L

Normal HRPT cells were co-cultured at $0.6x10^4$, $0.8x10^4$ and $1x10^4$ cells/well with $1x10^4$ cells/well MMC-treated fibroblasts 3T3-CD40L and 3T3-Neo in white 96-well plates (as detailed in the Methods). Plates were incubated for 72h and apoptosis was assessed by the Cytotox-Glo assay. 50µl of substrate was added to each well followed by 10 min incubation at room temperature. Luminescence was measured on a FLUOStar Optima plate reader and background-corrected relative luminescence units (RLU) were deduced by pair-wise subtraction of mCD40L and Control RLU from the respective co-cultures as described in Materials and Methods. **A)** Background corrected RLU readings for HRPT/3T3-CD40L (mL) and HRPT/3T3-Neo (Control). Bars show mean of 4-6 technical replicates (RLU) ± SEM. **B)** Results from graphs in A are also presented as fold change (mCD40L relative to control). Stats: ***, $p<0.001$ paired student T-test.

6.3.2 Determination of cell death by the DNA fragmentation assay

Previous work has demonstrated that CD40-CD40L interactions did not trigger DNA fragmentation in normal NHU cells, whereas their malignant counterpart such as EJ cells were highly susceptible to CD40 mediated apoptosis, with 60-70% DNA fragmentation shown using the JAM test (Bugajska et al., 2002, Georgopoulos et al., 2006). This study (chapter 3) demonstrated extensive apoptosis in RCC cells (~80%) by using an ELISA-based DNA fragmentation assay, whereas. treatment with agonistic anti-CD40 antibody G28-5 showed non-significant cell death by CytoTox-Glo assay.

To confirm the CytoTox-Glo results in the above section, DNA fragmentation ELISA tests were used to ensure that mCD40L did not induce apoptosis in normal HRPT cells and also to compare the ability of G28-5 agonist to induce apoptosis in normal HRPT cells. As part of the methodology detailed in the Methods (section 2.7), normal HRPT cells were labelled with the DNA labelling agent BrdU for 2h at a concentration of 10µM according to the manufacturer's instructions and either co-cultured with growth-arrested 3T3-CD40L and 3T3-Neo or treated with agonistic anti-CD40 antibody and then incubated for different time points (24,48 and 72h). Supernatants were collected at the indicated time points and then examined for DNA fragmentation (ELISA assay were performed and % of cell death calculated as described in chapter 2 section 2.8.5).

Results from these experiments confirmed that neither mCD40L nor G28-5 mAb had the ability to induce apoptosis in normal HRPT cells as indicated by the low level of DNA fragment in such supernatants and low percentage of cell death at all indicated time points (Figure 6.6. 6.7 and 6.8).

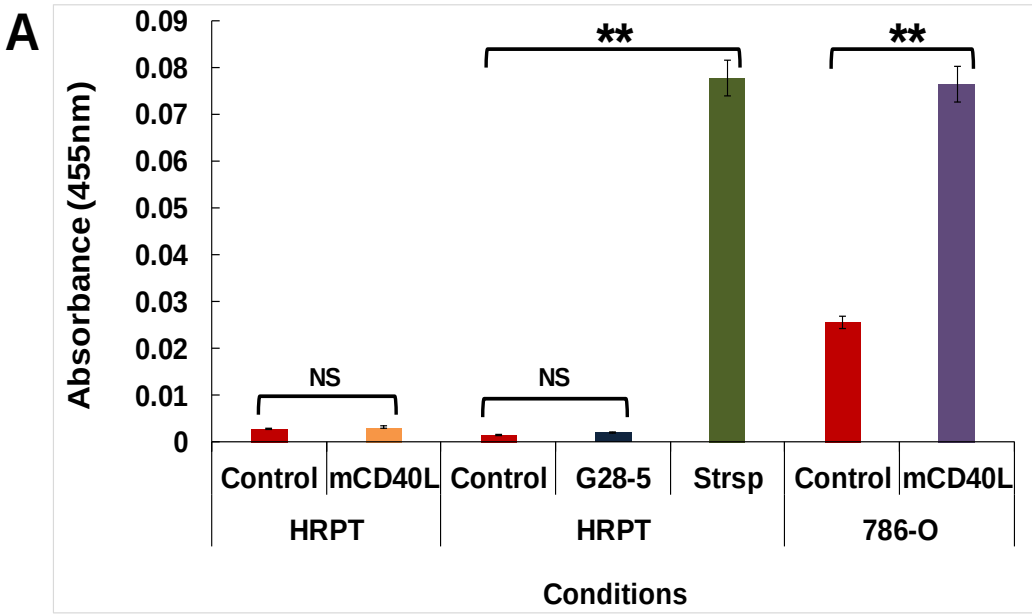

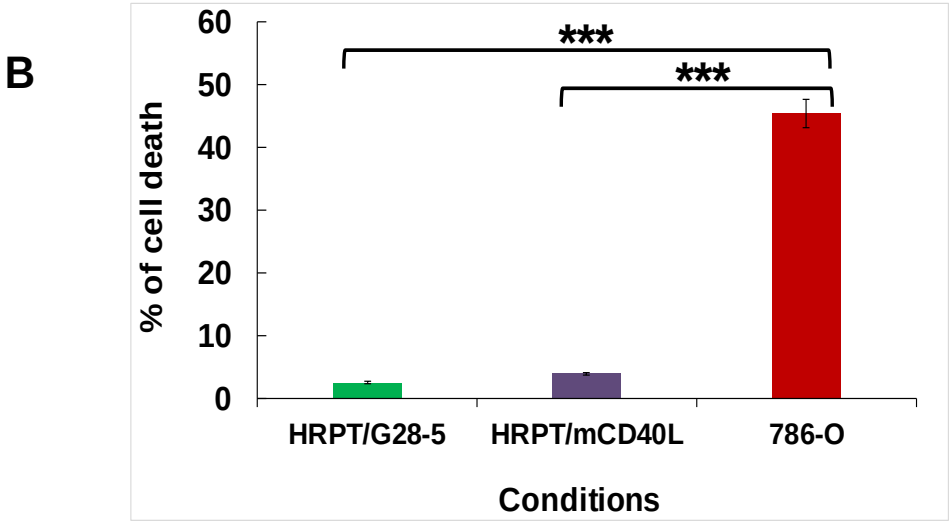

Figure 6.6 Detection of DNA fragmentation in normal HRPT cells following 24h of CD40 ligation by membrane-presented ligand and soluble agonist

Normal HRPT cells were pre-labelled with 10µM of DNA labelling agent BrdU for 2h. Then cells were either co-cultured at a density of $0.8x10^4$cells/well with $1x10^4$ cells/well MMC-treated fibroblasts 3T3-CD40L (mCD40L) and 3T3-Neo (Control) or treated with 10µg/ml of G28-5 mAb cross-linked with 2.5µg/ml goat anti-mouse Ig in 96-well plates. Treatment with 5µM of staurosporine (Strsp) was used as positive control and untreated cells were also included (HRPT). The plates were then incubated for 24h and supernatants were collected. Supernatants (150µl) from each of 6 replicate wells were collected and used to determine DNA fragmentation by ELISA. Absorbance (at 455nm) was measured on a FLUOStar Optima plate reader and % cell death calculated as described in the Methods. **A)** Bars represent mean Absorbance units of 6 technical replicates ± SEM and results are representative of two experiments. **B)** Results from A are also presented as % cell death. Stats: ***, $p<0.001$; **$p<0.01$; NS. Non-significant paired student T-test.

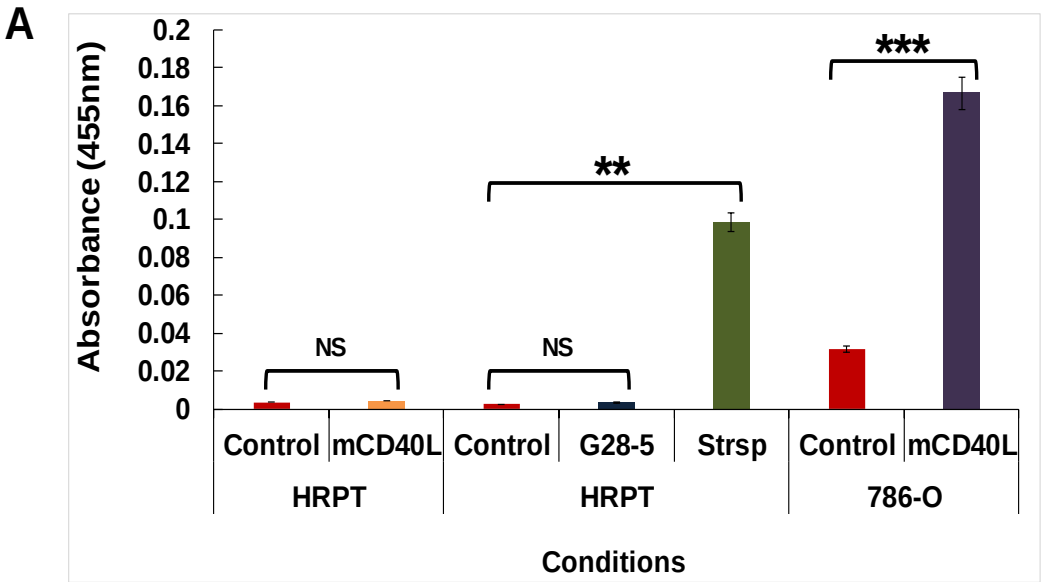

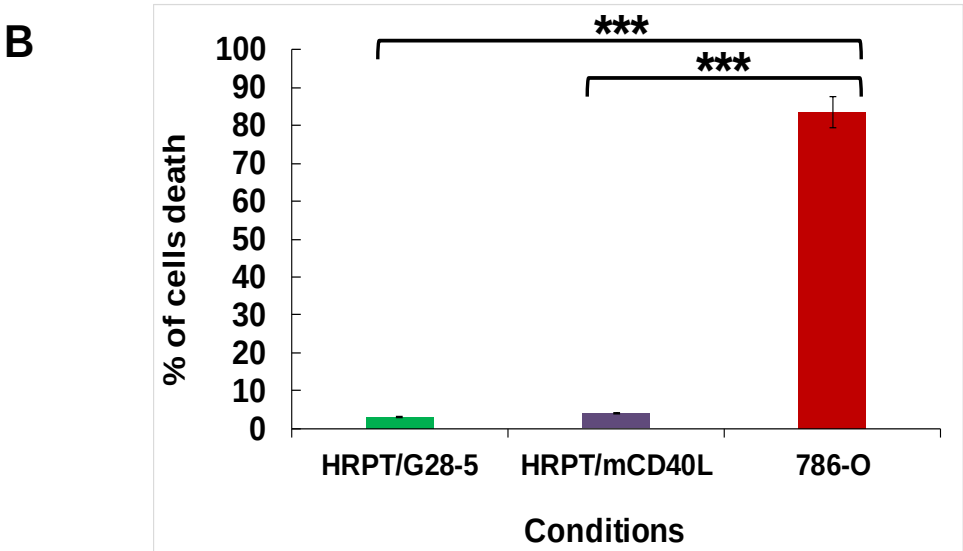

Figure 6.7 Detection of DNA fragmentation in normal HRPT cells following 48h of CD40 ligation by membrane-presented ligand and soluble agonist

Normal HRPT cells were pre-labelled with 10µM of DNA labelling agent BrdU for 2h. Then cells were either co-cultured at a density of $0.8x10^4$cells/well with $1x10^4$ cells/well MMC-treated fibroblasts 3T3-CD40L (mCD40L) and 3T3-Neo (Control) or treated with 10µg/ml of G28-5 mAb cross-linked with 2.5µg/ml goat anti-mouse Ig in 96-well plates. Treatment with 5µM of staurosporine (Strsp) was used as positive control and untreated cells were also included (HRPT). The plates were then incubated for 48h and supernatants were collected. Supernatants (150µl) from each of 6 replicate wells were collected and used to determine DNA fragmentation by ELISA. Absorbance (at 455nm) was measured on a FLUOStar Optima plate reader and % cell death calculated as described in the Methods. **A)** Bars represent mean Absorbance units of 6 technical replicates ± SEM and results are representative of two experiments. **B)** Results from A are also presented as % cell death. Stats: ***, $p<0.001$; **$p<0.01$; NS. Non-significant paired student T-test.

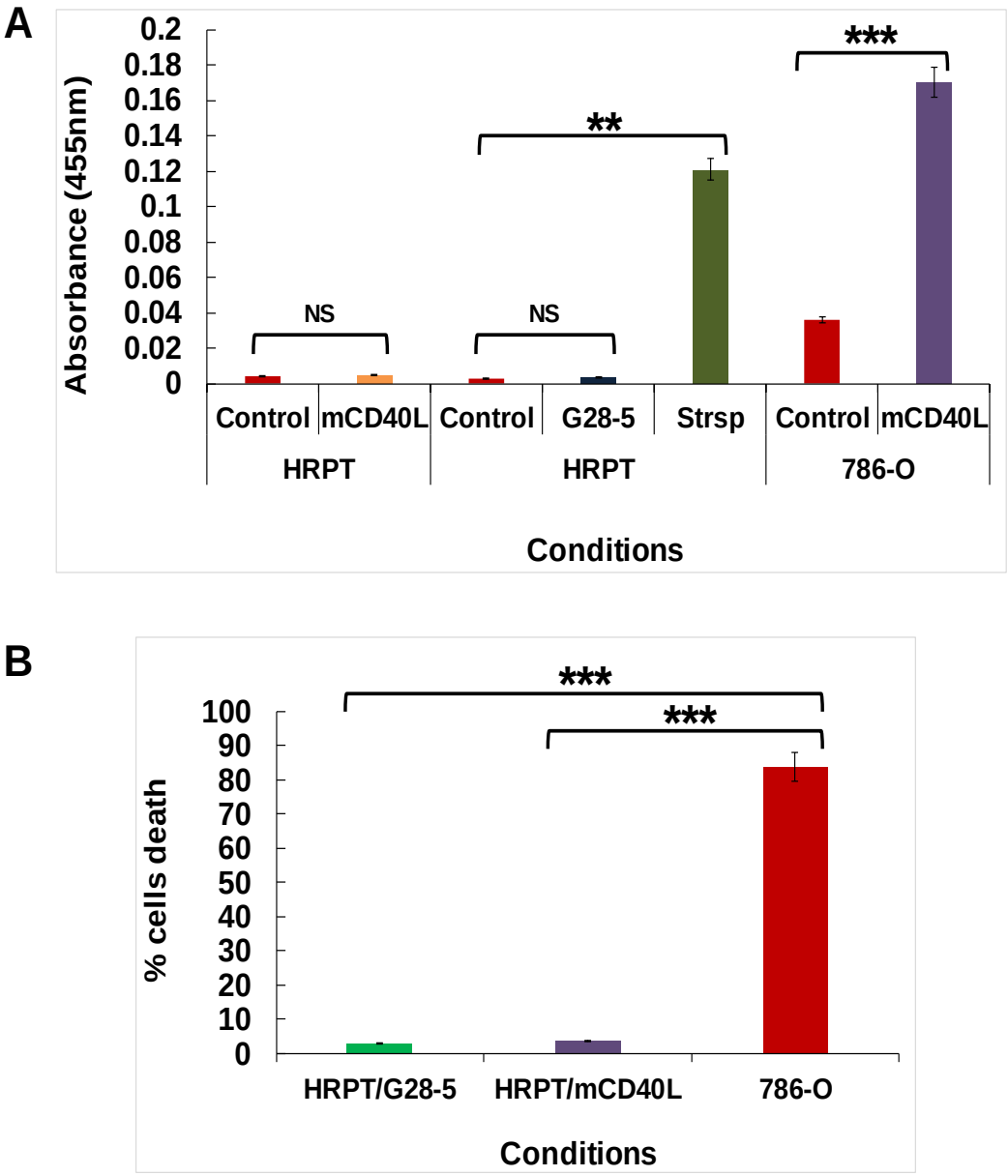

Figure 6.8 Detection of DNA fragmentation in normal HRPT cells following 72h of CD40 ligation by membrane-presented ligand and soluble agonist

Normal HRPT cells were pre-labelled with 10µM of DNA labelling agent BrdU for 2h. Then cells were either co-cultured at a density of $0.8x10^4$cells/well with $1x10^4$ cells/well MMC-treated fibroblasts 3T3-CD40L (mCD40L) and 3T3-Neo (Control) or treated with 10µg/ml of G28-5 mAb cross-linked with 2.5µg/ml goat anti-mouse Ig in 96-well plates. Treatment with 5µM of staurosporine (Strsp) was used as positive control and untreated cells were also included (HRPT). The plates were then incubated for 72h and supernatants were collected. Supernatants (150µl) from each of 6 replicate wells were collected and used to determine DNA fragmentation by ELISA. Absorbance (at 455nm) was measured on a FLUOStar Optima plate reader and % cell death calculated as described in the Methods. **A)** Bars represent mean Absorbance units of 6 technical replicates ± SEM and results are representative of two experiments. **B)** Results from A are also presented as % cell death. Stats: ***, $p<0.001$; **$p<0.01$; NS. Non-significant paired student T-test.

6.4 Detection of cytokine secretion following CD40 ligation in normal HRPT cells

The main feature of human kidney disease is the progressive loss of renal function as a result of interstitial infiltration via inflammatory mononuclear such as macrophages and T-cells. Local expression of adhesion and chemoattractant molecules regulates the recruitment of circulating leukocytes to the inflammatory sites which subsequently induce cytokine secretion by stimulated leukocytes and renal cells (Kuroiwa et al., 2000, Boucher et al., 1986).

It has been demonstrated that normal renal tubular cells secrete inflammatory mediators such as MCP-1 and RANTES (Van Kooten et al., 1999b, Prodjosudjadi et al., 1995). Moreover, previous suggestion for CD40 stimulation on renal tubular cells could be via direct cell-to-cell contact with T-cells or by soluble factors, and mediated cytokines secretion (Lacraz et al., 1994, Rezzonico et al., 1998, McInnes et al., 1997). It is known that renal cells express CD40 and CD40L has been observed to be expressed on infiltrating T-cells in renal biopsy specimens. Furthermore, a blocking antibody for CD40L reduced the production of cytokines by renal tubular cells following their contact with T-cells (Kuroiwa et al., 2000).

Other studies have reported that direct contact of CD40-expressing tubular epithelial cells with CD40L-expressing cells caused increase in IL-15 secretion by tubular epithelial cells which was inhibited by the addition of blocking anti-CD40L antibody; the induction of IL-15 secretion coincided with IL-15 mRNA levels which increased following such direct contact (Weiler et al., 2001). CD40 activation in HRPT cells by membrane-presented CD40 ligand induced the production of RANTES (Deckers et al., 1998), and activated HRPT to produce IL-8 and MCP-1 (Gerritsma et al., 1996). IL-8 production mediates ICAM-1 expression through p38-MAPK pathway (Li and Nord, 2009). On the other hand, stimulation of CD40 by mCD40L mediated TRAF6 recruitment and MAPK activation that induced IL-8 and MCP-1 secretion (Li and Nord, 2002).

In this study, secretion of IL-8, IL-6 and GM-CSF by HRPT cells was determined following CD40 ligation either by mCD40L or by agonistic anti-CD40 antibody G28-5 at different time points (3, 6, 12, 24h).

mCD40L induced rapid IL-8 secretion in a time-dependent manner, with nearly 4.5-fold induction by 24h (Figure 6.9). By contrast, soluble agonist G28-5 mAb caused a less pronounced induction of IL-8 secretion both in terms of absolute amount (less than 700pg/mL were detected with G28-5 at 24h in comparison to nearly 1,400pg/mL with mCD40L) and also in fold-induction (lower than 2.5-fold at 12h in comparison to 4.5-fold observed with mCD40L) (Figure 6.9).

Secretion of IL-6 was observed following ligation of CD40 by both membrane-presented and soluble agonist. Notably, however, although the absolute amount of IL-6 detected was similar, the fold induction of IL-6 secretion appeared to be higher following CD40 ligation by mCD40L (Figure 6.10).

Finally, secretion of GM-CSF in response to CD40 ligation showed a similar pattern to that observed with IL-8. In particular, mCD40L caused a more pronounced secretion of GM-CSF both in absolute concentration detected (~160 pg/mL versus ~110 pg/mL) and in terms of fold-induction (nearly 2.5-fold versus <2-fold) when it was compared to the soluble agonist G28-5 mAb at 24h post CD40 ligation (Figure 6.11).

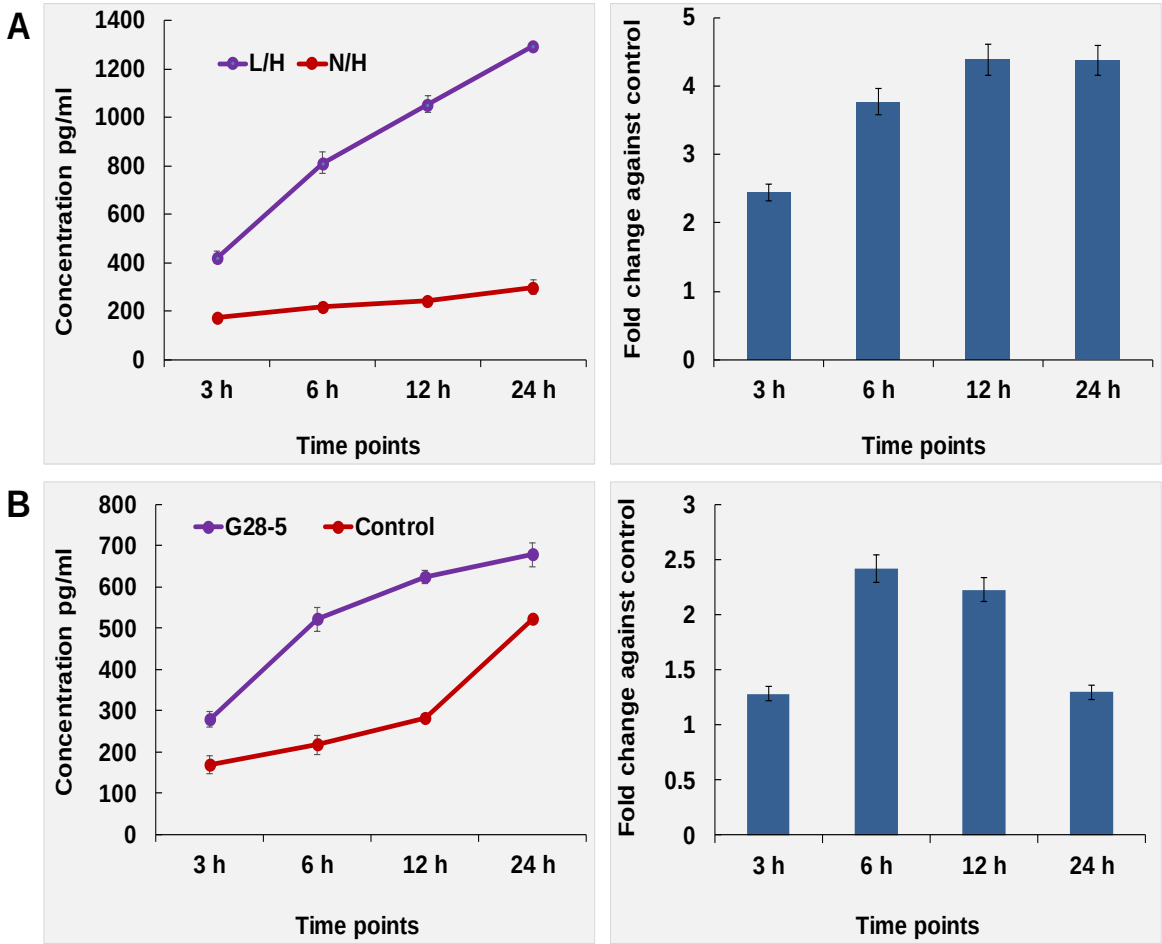

Figure 6.9 Detection of IL-8 secretion by HRPT following CD40 ligation

Normal HRPT were either co-cultured at a density of $5x10^4$ with $6x10^4$ of MMC-treated fibroblasts 3T3-CD40L and 3T3-Neo or treated with 10µg/ml of G28-5 mAb cross-linked with 2.5µg/ml goat anti-mouse Ig (untreated cells served as non-treated Controls) in 24 well plates (as detailed in the Methods). Plates were incubated for different time points (3-24h). Supernatants were collected at the indicated time points. Secretion of IL-8 was determined by an ELISA assay kit. Graphs on the left show means of IL-8 concentration for 2-3 technical replicates, calculated as described in materials and methods (section 2.12.2) and are typical of 2 independent experiments. **A)** IL-8 secreted in co-culture supernatant and **B)** IL-8 secretion after treatment with G28-5 mAb. Bar graphs on the right show the results from graphs on the left also presented as fold change (mCD40L (L) or G28-5) relative to control ((N) or control).

Key:

N/H	:	3T3-Neo co-cultured with HRPT
L/H	:	3T3-CD40L co-cultured with HRPT
Control	:	HRPT alone without treatment
G28-5	:	HRPT treated with G28-5

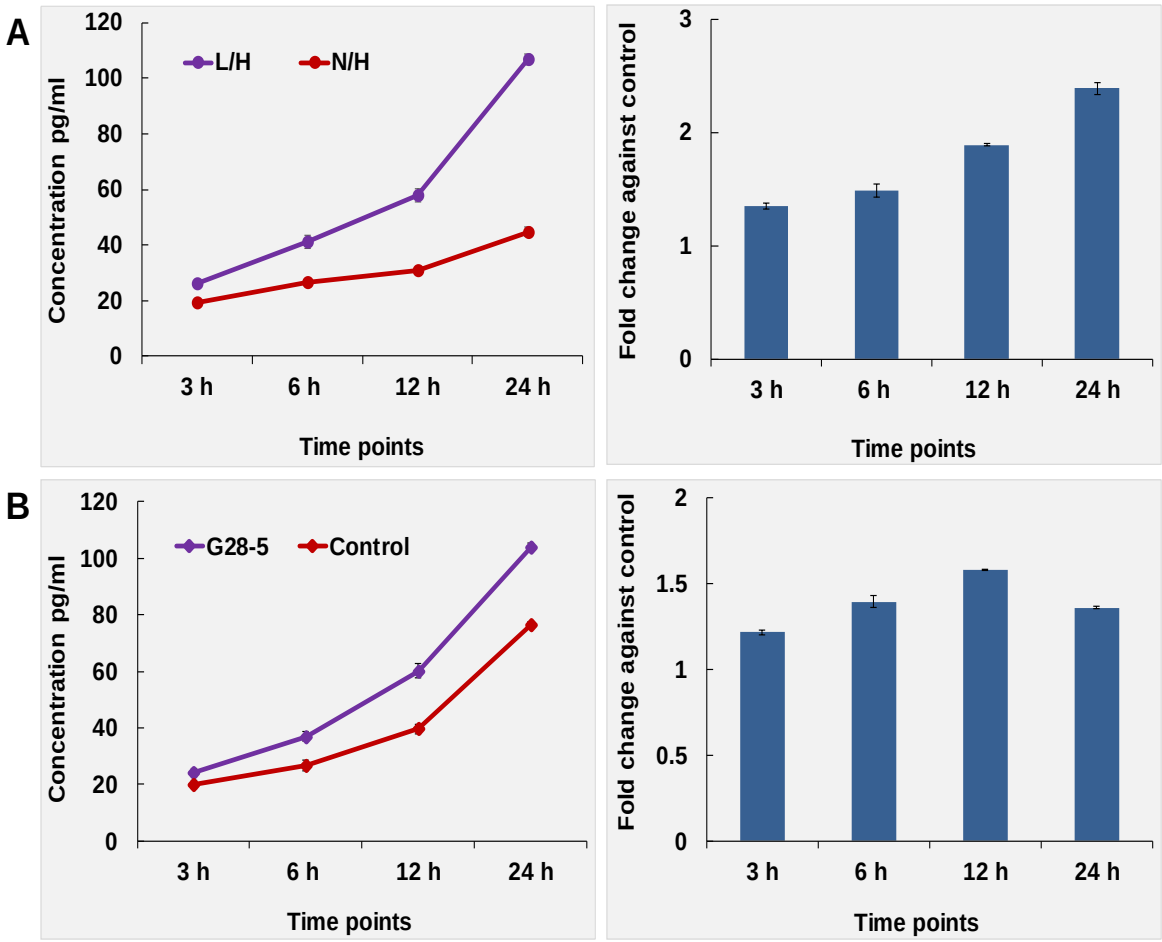

Figure 6.10 Detection of IL-6 secretion by HRPT following CD40 ligation

Normal HRPT were either co-cultured at a density of $5x10^4$ with $6x10^4$ of MMC-treated fibroblasts 3T3-CD40L and 3T3-Neo or treated with 10µg/ml of G28-5 mAb cross-linked with 2.5µg/ml goat anti-mouse Ig (untreated cells served as non-treated Controls) in 24 well plates (as detailed in the Methods). Plates were incubated for different time points (3-24h). Supernatants were collected at the indicated time points. Secretion of IL-6 was determined by an ELISA assay kit. Graphs on the left show means of IL-6 concentration for 2-3 technical replicates, calculated as described in materials and methods (section 2.12.2) and are typical of 2 independent experiments. **A)** IL-6 secreted in co-culture supernatant and **B)** IL-6 secretion after treatment with G28-5 mAb. Bar graphs on the right show the results from graphs on the left also presented as fold change (mCD40L (L) or G28-5) relative to control ((N) or control).

Key:
N/H : 3T3-Neo co-cultured with HRPT
L/H : 3T3-CD40L co-cultured with HRPT
Control : HRPT alone without treatment
G28-5 : HRPT treated with G28-5

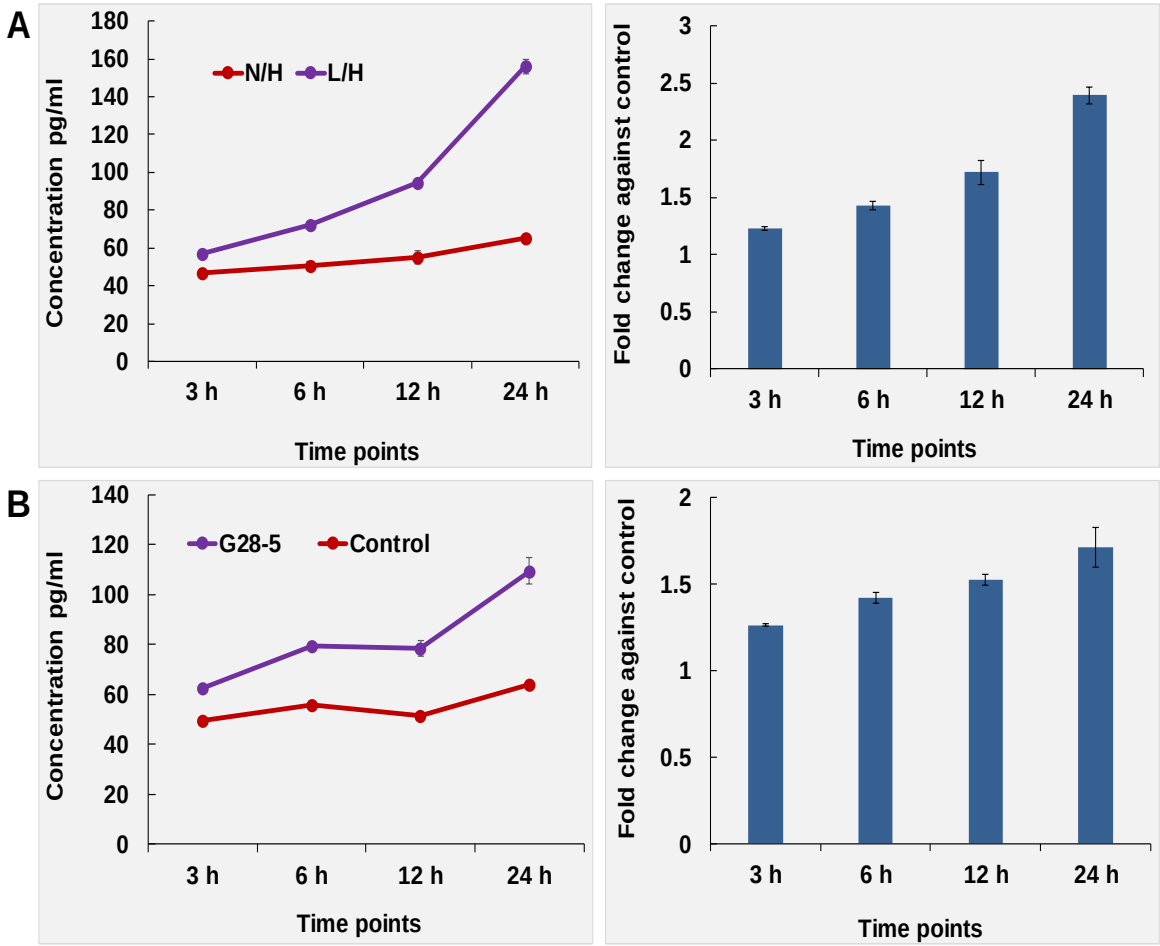

Figure 6.11 Detection of GM-CSF secretion by HRPT following CD40 ligation

Normal HRPT were either co-cultured at a density of $5x10^4$ with $6x10^4$ of MMC-treated fibroblasts 3T3-CD40L and 3T3-Neo or treated with 10µg/ml of G28-5 mAb cross-linked with 2.5µg/ml goat anti-mouse Ig (untreated cells served as non-treated Controls) in 24 well plates (as detailed in the Methods). Plates were incubated for different time points (3-24h). Supernatants were collected at the indicated time points. Secretion of GM-CSF was determined by an ELISA assay kit. Graphs on the left show means of GM-CSF concentration for 2-3 technical replicates, calculated as described in materials and methods (section 2.12.2) and are typical of 2 independent experiments. **A)** GM-CSF secreted in co-culture supernatant and **B)** GM-CSF secretion after treatment with G28-5 mAb. Bar graphs on the right show the results from graphs on the left also presented as fold change (mCD40L (L) or G28-5) relative to control ((N) or control).

Key:

N/H	:	3T3-Neo co-cultured with HRPT
L/H	:	3T3-CD40L co-cultured with HRPT
Control	:	HRPT alone without treatment
G28-5	:	HRPT treated with G28-5

6.5 Regulation of TRAF proteins in normal primary HRPT following CD40 ligation

TRAF protein regulation by CD40 has been well characterised in B-cells (Hostager and Bishop, 1999) and CD40 ligation by mCD40L triggers differential TRAF protein regulation in carcinoma cells particularly UCC cells and CRC cells (Georgopoulos et al., 2006, Mohamed, 2014, Dunnill et al., 2016). Results in chapter 5 in this study showed that TRAF proteins were regulated in response to CD40 ligation on RCC cells. With regards to normal cells, our laboratory has previously reported that CD40-CD40L interaction in NHU cells induced TRAF1 expression but down-regulated the expression of TRAF3 and TRAF2 (Georgopoulos et al., 2006).

Thus, in order to investigate the effect of CD40 ligation on the expression of CD40-associated TRAF proteins in normal HRPT cells, immunoblotting experiments were performed. HRPT cells were co-cultured with 3T3-CD40L (mCD40L) and 3T3-Neo (Control) effectors for 1.5, 3, and 6 h, and cell lysates were prepared to detect the expression of TRAF1, 2 and 3. Induction of TRAF1 expression was observed by 6h post CD40 ligation as shown in Figure 6.12, which is similar to the observations made with the RCC line ACHN. By contrast, mCD40L caused marked TRAF2 down-regulation in HRPT cells as seen by 3h post ligation, with little if any detectable TRAF2 expression at 6h following CD40 ligation (Figure 6.13), whilst in tumour cells (ACHN) there was an induction in TRAF2 expression. Interestingly, no basal TRAF3 expression was observed in HRPT cells and mCD40L did not induce TRAF3 expression in HRPT cells in contrast to the RCC line where, as previously, TRAF3 induction was observed (Figure 6.14).

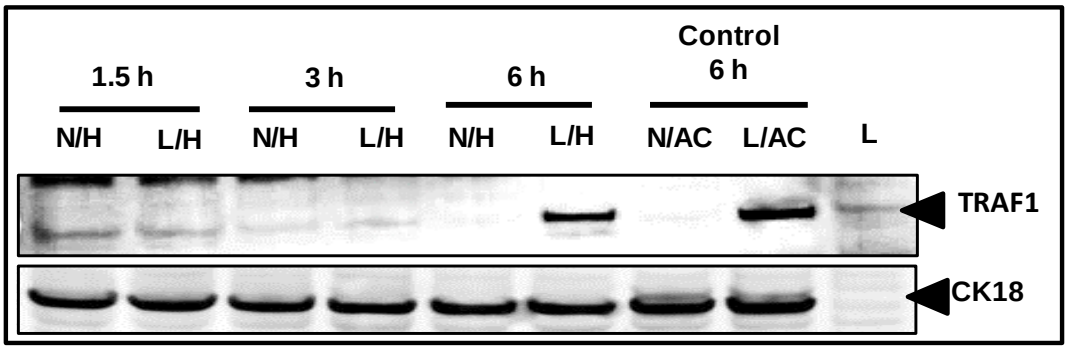

Figure 6.12 TRAF1 protein expression by HRPT cells following CD40 ligation by mCD40L

Normal HRPT cells were co-cultured at $30x10^5$ cells/dish with $30x10^5$ cells/dish of MMC treated fibroblast cells 3T3-Neo and 3T3-CD40L in a 10 cm dishes and incubated for (1.5, 3 and 6h). Whole cell lysate were prepared as described in the Methods (Section 2.9.3) and 40µg of protein/well was analysed by immunoblotting (Section 2.9.5). After normalisation on the basis of CK18 expression (see chapter 3 section 3.10). 40µg of normalised lysates were loaded and analysed by immunoblotting. After overnight incubation at 4ºC by rocking with primary polyclonal antibody (anti-TRAF1) in TBS/Tween 0.1% (1:1000 dilution), secondary antibody [goat anti-rabbit IgG IRDye 800nm (1:10000 dilution)] was added and the membranes were incubated in dark for 1h. For specifity and as a loading control CK18 antibody was used at (1:1000 dilution), and incubation overnight at 4ºC, then the membranes were incubated with secondary antibody goat-anti mouse IgG Alexa 680 (diluted 1:10000) in the dark for 1h. Antibody binding was visualised at 800nm for TRAF1 detection (expected molecular weight 52 kDa) and 700nm for CK18 detection using an Odyssey™ Infra-red Imaging system. Co-cultures for ACHN cell line were used as negative and positive control (N/AC) and (L/AC) respectively.

Key:

N/AC	: 3T3Neo co-cultured with ACHN	L/AC	: 3T3CD40L co-cultured with ACHN
N/H	: 3T3Neo co-cultured with HRPT	L/H	: 3T3CD40L co-cultured with HRPT
L	: 3T3CD40L		

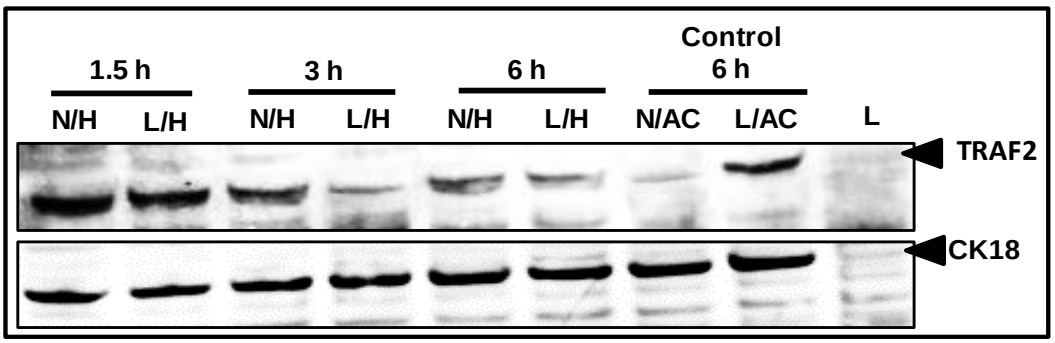

Figure 6.13 TRAF2 protein expression by HRPT cells following CD40 ligation by mCD40L

Normal HRPT cells were co-cultured at $30x10^5$ cells/dish with $30x10^5$ cells/dish of MMC treated fibroblast cells 3T3-Neo and 3T3-CD40L in a 10 cm dishes and incubated for (1.5, 3 and 6h). Whole cell lysate were prepared as described in the Methods (Section 2.9.3) and 40µg of protein/well was analysed by immunoblotting (Section 2.9.5). After normalisation on the basis of CK18 expression (see chapter 3 section 3.10). 40µg of normalised lysates were loaded and analysed by immunoblotting. After overnight incubation at 4ºC by rocking with primary polyclonal antibody (anti-TRAF2) in TBS/Tween 0.1% (1:1000 dilution), secondary antibody [goat anti-rabbit IgG IRDye 800nm (1:10000 dilution)] was added and the membranes were incubated in dark for 1h. For specifity and as a loading control CK18 antibody was used at (1:1000 dilution), and incubation overnight at 4ºC, then the membranes were incubated with secondary antibody goat-anti mouse IgG Alexa 680 (diluted 1:10000) in the dark for 1h. Antibody binding was visualised at 800nm for TRAF2 detection (expected molecular weight 52 kDa) and 700nm for CK18 detection using an OdysseyTM Infra-red Imaging system. Co-cultures for ACHN cell line were used as negative and positive control (N/AC) and (L/AC) respectively.

Key:

N/AC	: 3T3Neo co-cultured with ACHN	L/AC	: 3T3CD40L co-cultured with ACHN
N/H	: 3T3Neo co-cultured with HRPT	L/H	: 3T3CD40L co-cultured with HRPT
L	: 3T3CD40L		

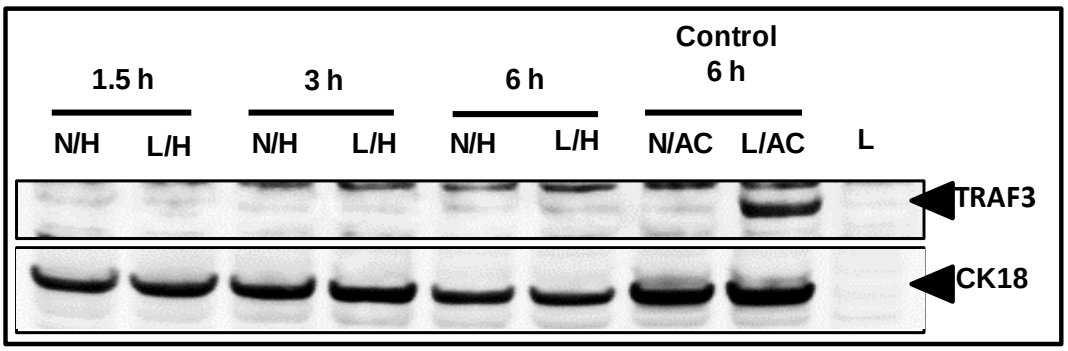

Figure 6.14 TRAF3 protein expression by HRPT cells following CD40 ligation by mCD40L

Normal HRPT cells were co-cultured at $30x10^5$ cells/dish with $30x10^5$ cells/dish of MMC treated fibroblast cells 3T3-Neo and 3T3-CD40L in a 10 cm dishes and incubated for (1.5, 3 and 6h). Whole cell lysate were prepared as described in the Methods (Section 2.9.3) and 40µg of protein/well was analysed by immunoblotting (Section 2.9.5). After normalisation on the basis of CK18 expression (see chapter 3 section 3.10). 40µg of normalised lysates were loaded and analysed by immunoblotting. After overnight incubation at 4ºC by rocking with primary polyclonal antibody (anti-TRAF3) in TBS/Tween 0.1% (1:1000 dilution), secondary antibody [goat anti-rabbit IgG IRDye 800nm (1:10000 dilution)] was added and the membranes were incubated in dark for 1h. For specifity and as a loading control CK18 antibody was used at (1:1000 dilution), and incubation overnight at 4ºC, then the membranes were incubated with secondary antibody goat-anti mouse IgG Alexa 680 (diluted 1:10000) in the dark for 1h. Antibody binding was visualised at 800nm for TRAF3 detection (expected molecular weight 52 kDa) and 700nm for CK18 detection using an OdysseyTM Infra-red Imaging system. Co-cultures for ACHN cell line were used as negative and positive control (N/AC) and (L/AC) respectively.

Key:

N/AC	: 3T3Neo co-cultured with ACHN	L/AC	: 3T3CD40L co-cultured with ACHN
N/H	: 3T3Neo co-cultured with HRPT	L/H	: 3T3CD40L co-cultured with HRPT
L	: 3T3CD40L		

6.6 Summary

- The work described in this chapter has for the first time provided evidence for the cancer cell specificity of CD40 in renal cells

- CD40 expression was detected both by immunoblotting (total expression) and flow cytometry (surface expression) in HRPT cells in comparison to their malignant counterparts (RCC cells)

- CD40 stimulation either by mCD40L or soluble G28-5 agonist did not induce any detectable apoptosis in normal HRPT cells (compared with their malignant counterparts) as shown using both CytoTox-Glo and by DNA fragmentation detection assays

- CD40 expression by HRPT cells was functional as CD40 ligation induced cytokine secretion. mCD40L induced marked IL-8 and GM-CSF secretion in contrast to soluble agonist which caused a less pronounced induction of IL-8 and GM-CSF secretion both in terms of absolute amount and fold-induction. Secretion of IL-6 was induced following CD40 ligation by both membrane-presented and soluble agonist, however, the absolute amount of IL-6 detected was similar, and only the fold induction of IL-6 secretion appeared higher following CD40 ligation by mCD40Lin comparison to G28-5 mAb.

- mCD40L mediated TRAF1 upregulation, which was similar to the observations made with the RCC line ACHN. By contrast, mCD40L caused marked TRAF2 down-regulation in HRPT cells, in comparison to tumour cells (ACHN) where there was an induction in TRAF2 expression. Interestingly, mCD40L did not induce any TRAF3 expression in normal HRPT cells in contrast to RCC cells where, as previously, marked TRAF3 induction was observed

- Thus, collectively, these experimental observations a) provide evidence for differences in the extent of cytokine secretion depending on the ‘quality’ of

the CD40 signal, as well as b) constitute evidence for differential TRAF protein regulation in normal HRPT versus malignant RCC cells.

Chapter 7

General discussion

7.1 General concept

The widespread expression of CD40 on a multiplicity of cell types including tumour cells has suggested a promising role for CD40 in the pathogenesis of cancer. CD40 stimulation has demonstrated pro-apoptotic effects on some CD40-expressing neoplasms (Eliopoulos and Young, 2004). Yet, there is evidence that CD40 ligation in malignant B-cells and some carcinoma cells may play both pro- and anti-apoptotic roles, a capability that is intriguingly dependent not only on the cell type but also on the 'level' of CD40 ligation (Dallman et al., 2003). Equally intriguingly, the effect of CD40 ligation appears to differ in normal and malignant B lymphocytes and epithelial cells, which has led to the observation of an interesting "paradox", since cells appear to become gradually more susceptible to CD40 ligation as they progress through malignant transformation as elegantly discussed by Young and Eliopoulos in (Eliopoulos and Young, 2004). Research in the last 10-15 years has provided further supportive evidence for this fascinating cell type- and context-specificity of CD40 ligation (Albarbar et al., 2015) which will be discussed further below.

Although some studies have previously focused on the role of CD40-CD40L interactions in inflammatory conditions and autoimmune diseases (Maerten et al., 2003), the main interest has revolved around the ability of the CD40-CD40L dyad to induce death in malignant cells. A significant amount of excellent work by Young and colleagues has reported that CD40 agonists have the ability to regulate tumour epithelial cell fate (Eliopoulos and Young, 2004, Tong and Stone, 2003). Yet, despite significant and consistent growth-inhibitory capacity in a variety of tumour cells, the functional outcome of CD40 ligation appears to be highly-dependent on the modality ('quality') of the CD40 signal. Indeed, although growth inhibition in various carcinoma cells can achieved by using soluble CD40 agonists (Vonderheide, 2007, Tong and Stone, 2003), these agonists trigger weak pro-apoptotic signals but can be rendered pro-apoptotic only upon co-treatment with pharmacological inhibitors or in combination with other TNFR agonists (Bugajska et al., 2002, Eliopoulos et al., 2000, Afford et al., 2001, Choudhury et al., 2003, Hess and Engelmann, 1996a). This has implied that the soluble agonist associated signal is not 'strong' enough to trigger adequate cell death. A significant observation that shed light to the unique features of CD40 relates to the

discovery by Georgopoulos and colleagues that membrane-presented CD40L (mCD40L) and cell surface-presented agonists can prompt extensive apoptosis in carcinoma cells but not in their normal counterparts (Bugajska et al., 2002, Georgopoulos et al., 2006, Georgopoulos et al., 2007, Hill et al., 2008, Shaw et al., 2005). Later studies by Young and colleagues provided further support for these observations by demonstrating that a) membrane-presented CD40L delivers an efficient pro-apoptotic CD40 signal in tumour cells (Elmetwali et al., 2010b), and b) the concurrent presence of soluble CD40L can attenuate the strong pro-apoptotic signal of mCD40L, as shown by the observation that engineered CD40L that cannot be cleaved by tumour cell-secreted metalloproteinases shows enhanced anti-tumour cytotoxicity (Elmetwali et al., 2010a). More recent studies have provided for the first time evidence for the tumour-specificity of mCD40L-mediated CD40 ligation (Dunnill et al., 2016).

7.2 Expression of CD40 on human RCC cells and their normal counterparts (HRPT cells) and its cytokine-mediated regulation

CD40 expression has been demonstrated previously in mouse and human RCC cells in vitro (Shorts et al., 2006, Lee et al., 2005), as well as in RCC tumours in vivo (Weiss et al., 2014). Receptor expression has also been detected in primary human tubular epithelial cells (TECs) (van Kooten et al., 2000).

Expression of CD40 by RCC cells was detected in this study not only in RCC lines (chapter 3) but also in cultured HRPT cells, their normal counterparts (chapter 6). According to previous demonstrations for the expression of CD40 on some carcinoma cells such as UCCs and CRCs can be controlled by treatment with pro-inflammatory cytokines (IFN-ɣ and TNF-α) (Bugajska et al., 2002, Georgopoulos et al., 2007). It was of interest to investigate whether the expression of CD40 on RCC cells could be regulated by pro-inflammatory cytokines.

It has been reported that the pro-inflammatory cytokine IFN-ɣ displays dual actions, either as a growth factor or growth inhibitor (Schroder et al., 2004). IFN-ɣ is strong inducer for the expression of STAT-1, under these conditions, subsequently, IFN-ɣ plays crucial role as a growth inhibitor (Schroder et al., 2004, Bromberg et al., 1996).

TNF-α belong to the TNFLs, and binding of TNF-α to either death receptor (TNFR-1) or to non-death receptor (TNFR-2), exerts its biological activity effects on cell signalling whether cell death or cell proliferation and survival (Cabal-Hierro and Lazo, 2012). TNF-α can act as apoptotic mediator throughout the development of mice thymocytes (Giroir et al., 1992, Hernandez-Caselles and Stutman, 1993). In vitro, the effects of TNF-α on normal cells and human cancer cells could be either cytotoxic or growth inhibitory, but in general, it is cytotoxic to cancer cells specially when CHX is used to inhibit the protein synthesis (Porter, 1990, Ruggiero et al., 1987, Meager, 1991). Moreover, a study on mouse fibroblast has reported that both types of cell death (apoptosis and necrosis) can be induced by TNF-α (Kamata et al., 2005), Other study provided evidence of TNF-α has the ability to induce distinctive type of cell death (necroptosis) in some conditions, and particularly when caspase activity is blocked (Vandenabeele et al., 2010). Exactly because of its ability to bind to multiple receptors (including the Lymphotoxin family), it can trigger different signals (Cabal-Hierro and Lazo, 2012), with engagement of TNF-α with TNFR1 leading to proliferation, apoptosis or necrosis (Andera, 2009, Gommerman and Summers deLuca, 2011, Micheau and Tschopp, 2003, Nagata, 1997), while its binding to TNFR2 triggers an anti-apoptotic signal via localization and degradation of TRAF2, but it can also mediate delayed apoptosis (Grell et al., 1999, Rauert et al., 2010, Rodríguez et al., 2011).

The present study investigated the effect of pro-inflammatory cytokines IFN-ɣ and TNF-α on CD40 expression in RCC cells. Clearly, treatment with IFN-ɣ up-regulated CD40 expression in RCC cells. This was in consistent with previous studies on UCCs and CRCs in our laboratory (Bugajska et al., 2002, Georgopoulos et al., 2007). By contrast, when the influence of TNF-α on CD40 expression in RCC cells was examined, treatment with TNF-α caused either no or little up-regulation in CD40 expression in RCC cells. Therefore, IFN-ɣ was a much stronger inducer of CD40 expression in covenant with previous observations (Bugajska et al., 2002, Georgopoulos et al., 2007).

7.3 The influence of CD40 ligation on RCC cells

CD40 engagement on RCC cells by either CD40L or by agonistic anti-CD40 antibody induced ICAM-1 and Fas expression at the transcriptional level and also induced surface protein expression. Moreover, combination of CD40L with IFN-ɣ caused further up-regulation in the expression of Fas which mediated augmentation in Fas-mediated cell death in RCC cells (Lee et al., 2005). CD40 stimulation by agonistic anti-CD40 antibody in vivo showed some anti-tumour effects via its ability to cause recruitment of monocytes and T-cells into the tumour site and subsequently induction of cytokines secretion, such as IL-8, MCP-1 and GM-CSF (Shorts et al., 2006).

Despite these previous studies, however, the influence of direct CD40 ligation in human RCC cells has not been previously described and there are no reports regarding the possibility of capability of human RCC cells to CD40-mediated killing.

7.3.1 Soluble CD40 agonist is a not a pro-apoptotic signal in RCC cells

Agonistic anti-CD40 antibodies and soluble recombinant CD40L are the CD40 agonists used in the majority of previous studies. CD40 signalling in normal and malignant B cells stimulates either apoptosis or survival (van Kooten and Banchereau, 2000, Costello et al., 1999, Van Kooten et al., 1997, Gordon, 1995, Gruss et al., 1997, Klaus et al., 1997) . The subsequent events post CD40 ligation depend on many factors, such as degree of cross linking and antibody epitope specificity (Challa et al., 1999, Pound et al., 1999), with the most pro-apoptotic signal being membrane-presented CD40L on the surface of transfected fibroblasts (using an appropriate co-culture system), indicating that the exact consequence of CD40 ligation rest on on the mode of ligation (‘signal tone’) (Gordon and Pound, 2000, Stewart et al., 2007).

Agonistic anti-CD40 antibody and soluble CD40L (sCD40L) can induce growth inhibition in B lymphoma cells (Dallman et al., 2003). Other studies demonstrated that growth inhibition was detected in Epstein-Barr Virus (EBV)-transformed human B lymphoblastoid cell lines and human diffuse large B-cell lines after treatment with either anti-CD40 mAbs or soluble CD40L (Funakoshi et al., 1994). Cross linking of mAbs

caused stronger inhibition of proliferation and also converted the response of the Burkitt's lymphoma cell line Raji from resistance to growth inhibition (Dallman et al., 2003). On the other hand, stimulation of CD40 by sCD40L in vitro resulted in growth inhibition in normal keratinocytes (Eliopoulos et al., 1997, Eliopoulos et al., 1996, Peguet-Navarro et al., 1997) and in carcinoma cells (Ghamande et al., 2001, Hirano et al., 1999, Tong et al., 2001). Moreover, previous studies performed by our laboratory and others showed that agonistic anti-CD40 antibody and soluble CD40L are growth inhibitory, but it can be pro-apoptotic only if protein synthesis is inhibited by pharmacological intervention (Eliopoulos et al., 2000, Hill et al., 2008, Hassan et al., 2014, Gallagher et al., 2002a, Bugajska et al., 2002, Georgopoulos et al., 2006, Afford et al., 1999, Hill et al., 2005). Furthermore, our laboratory has shown that although unable to induce apoptosis in UCC (Bugajska et al., 2002, Dunnill et al., 2016). and CRC (Georgopoulos et al., 2007) cells, agonistic anti-CD40 antibody G28-5 mAb can induce direct killing effect in UCC cells when presented on the surface of Ig Fcɣ (CD32)-expressing third party cells (Bugajska et al., 2002).

This study demonstrated that the monoclonal antibody G28-5 did not induce detectable death in RCC cells as shown in chapter 3. IFN-ɣ is a pleiotropic cytokine and it has been shown to play double function, it can induce or prevent cell growth (Asao and Fu, 2000). The ability of IFN-ɣ to induce cell death has been stated to be triggered via stimulation of many proteins that up-regulate the expression of Fas and TNF-α, and also through ROS generation (Schroder et al., 2004, Cassatella et al., 1990, Spanaus et al., 1998, Spets et al., 1998, Tsujimoto et al., 1986, Xu et al., 1998, Zheng et al., 2002)**.** However, and despite the observed induction in CD40 expression when RCC cells were treated with IFN-ɣ, combination of IFN-ɣ with cross-linked G28-5 antibody did not render the G28-5 antibody significantly pro-apoptotic(Chapter 3), suggesting that the G28-5 agonist even when cross-linked and in combination with IFN-ɣ, induces a weak signal which is unable to trigger adequate receptor cross-linking and subsequently death in RCC cells, in agreement with previous observations in other carcinoma cells types, such as UCC and CRC (Bugajska et al., 2002, Georgopoulos et al., 2006).

7.3.2 Membrane CD40L induces extensive apoptosis in RCC cells

Cytotoxicity investigations in this study indicated for the first time that mCD40L induces massive apoptosis in human RCC cells (Figure 3.8), whereas it caused no cytotoxic effect in their normal counterparts (HRPT cells) (Figure 6.4). Moreover, the presence of IFN-ɣ during treatment with mCD40L caused further increase in mCD40L-mediated cell death in two of the three RCC cell lines tested.

Collectively the present study for the first time systematically investigated the hypothesis that CD40 may transmit a death signal in RCC cells and provided evidence that CD40 ligation by mCD40L efficiently triggered death in human RCC lines, in agreement with previous findings by our laboratory in UCC and CRC (Georgopoulos et al., 2007, Dunnill et al., 2016); these observations have important therapeutic implications. Equally importantly, in addition to the novelty of the findings concerning CD40-mediated death in RCC cells, it is equally noteworthy that the ability of CD40 to kill is cancer cell-specific, as it did not kill normal human renal proximal tubular (HRPT) cells. This study has therefore extended previous work conducted by our laboratory using the urothelial model (Bugajska et al., 2002, Georgopoulos et al., 2006) and therefore has shown for the first time that not only NHU but also HRPT cells are refractory to CD40-mediated apoptosis.

A number of investigations presented in Chapter 3 demonstrated that stimulation of cell death by mCD40L was accompanied by caspase-3/7 activation in RCC cells and this effector caspase activity was essential, as apoptosis was fully blocked by the universal caspase inhibitor z-VAD (Chapter 5). In combination, Cytotox-Glo (membrane integrity loss) and AnAspec (effector caspase activation) assays allowed measurement of different component of cell death, and full confirmation that the death triggered by mCD40L was apoptotic was provided by experiments demonstrating that mCD40L triggered extensive DNA fragmentation in RCC cells. By contrast, mCD40L did not induce any loss of membrane integrity or detectable DNA fragmentation in normal HRPT cells, observations providing further confirmation that mCD40L is a cancer cell-specific death mediator. Therefore, mCD40L triggered “apoptotic” cell death in renal cells in a tumour cell-specific fashion in agreement with previous findings

in our laboratory in the bladder and colorectal models (Bugajska et al., 2002, Georgopoulos et al., 2007).

7.3.3 Regulation of cytokine secretion by CD40

Stimulation of CD40 has been shown to induce cytokines production such as IL-1, IL-6, IL-8, IL-10, IL-12 and TNF-α (van Kooten and Banchereau, 2000, Grammer and Lipsky, 2000), which are strongly correlated with the activation of Th1 and Th2 responses. A previous study demonstrated that stimulation of CD40 by CD40 agonists triggered secretion of GM-CSF, MCP-1 and IL-8 in mouse RCC cells (Shorts et al., 2006). It has been reported that CD40 stimulation in some carcinoma cells induces secretion of IL-1α, TNF and GM-CSF (Alexandroff et al., 2000) whilst specifically in UCC and RCC cells CD40 ligation by both soluble and membrane-presented agonist caused IL-6 and IL-8 secretion, however only mCD40L induced GM-CSF release (Georgopoulos et al., 2007). In this study, cytokine array experiments showed mCD40L triggered marked secretion of several cytokines, including GM-CSF, GR0a, sICAM-1, IL-8, IL-6 and MCP-1 which are related to CD40 signalling. All RCC lines secreted readily detectable levels of IL-6, IL-8 and GM-CSF by ELISA assays. This basal cytokine release resulted in progressive accumulation of these cytokines in control supernatants; yet CD40 ligation by mCD40L caused marked induction in cytokine secretion.

Detailed investigation by ELISA assays showed that mCD40L induced marked and rapid secretion of IL-8 in RCC cell lines ACHN, 786-O and A-704 within 1.5h and in a time-dependent manner. Furthermore, results in chapter 6 showed mCD40L also induced IL-8 secretion in normal HRPT cells, but treatment of HRPT cells with G28-5 antibody induced low level of IL-8 secretion.

IL-6 was initially recognised as a B-cell differentiation influence, but is known as a pleiotropic cytokine that plays critical roles in inflammation, haematopoiesis and bone metabolism (Cozen et al., 2004, Culig and Puhr, 2012, Mansell and Jenkins, 2013). mCD40L triggered significant secretion of IL-6 in human RCC cells at 6h post ligation as previously in UCC cells EJ (Georgopoulos et al., 2006). However, IL-6 secretion in normal renal proximal tubular epithelial cells has been shown in vitro in response to

several stimulation factors including TNF-α and LPS (Leonard et al., 1999, Boswell et al., 1994). Significant secretion of IL-6 was observed within 6h post CD40 ligation by mCD40L in RCC cells. Secretion of IL-6 was induced following CD40 ligation by both membrane-presented and soluble agonist in normal HRPT cells, however, the absolute amount of IL-6 detected was similar, and only the fold induction of IL-6 secretion appeared higher following CD40 ligation by mCD40Lin comparison to G28-5 mAb.

It is well documented that GM-CSF is a pleiotropic cytokine that is fundamentally involved in immune responses. Moreover, secretion of GM-CSF has been observed to enhance the recruitment of neutrophils and macrophages towards tumour cells, which assists in tumour cell lysis via direct contact with macrophages. GM-CSF is also able to promote recruitment, maturation and activation of dendritic cells and then enhance their antigen presentation activity (Shinohara et al., 2000, Kielian et al., 1999). This study showed mCD40L induced GM-CSF secretion in RCC cells, but soluble agonists caused very little secretion of GM-CSF in 786-O cells. In normal HRPT cells, secretion of GM-CSF in response to CD40 ligation showed a similar pattern to that observed with IL-8. In particular, mCD40L caused a more pronounced secretion of GM-CSF both in absolute concentration detected and in terms of fold-induction when it was compared to soluble agonist (G28-5 mAb).

Collectively, these results in agreement with previous findings in our laboratory reporting that although soluble CD40 agonists could induce some IL-8 and IL-6 secretion in tumour cells, only mCD40L caused GM-CSF secretion in CRC cells and UCC cells (Georgopoulos et al., 2007). Moreover, despite the inability of CD40 ligation to induce apoptosis in normal (HRPT) cells, receptor expression was functional as it caused cytokine secretion – which was signal quality-dependent.

It has been reported that IL-8 secretion in normal and malignant epithelial cells is an NF-κB dependant (Li and Nord, 2002, Schwabe et al., 2001, Gallagher et al., 2002a, Cagnoni et al., 2004), whilst GM-CSF secretion requires AP-1 activation (Wang et al., 1994, Johnson et al., 2004). Of note, although NF-κB is activated by both mCD40L and soluble agonists, AP-1 is exclusively activated by mCD40L. It is therefore tempting to speculate that not only does AP-1 drive apoptosis (see below) but also its activation

may define the repertoire of cytokines released, however additional experimental work would be required to address these hypotheses.

7.4 Regulation of TRAF proteins and MAPKs by mCD40L in RCC cells

TNF ligands can induce activation of TRAFs protein via interaction of receptor cytoplasmic domains. Several studies have reported that CD40 ligation leads to rapid recruitment of TRAFs molecules, however, most of these studies are reports on CD40 stimulation in B cells by elegant studies from Gail Bishop's research group (Bishop et al., 2007, Bishop, 2004, Bishop et al., 2002). It has been reported that TRAF1 regulates transcriptional activation (Schwenzer et al., 1999, Cha et al., 2003) and it does so by being indirectly recruited to the cytoplasmic tail of CD40 via interaction with TRAF2 (Bishop et al., 2007, Pullen et al., 1999, Pullen et al., 1998). In contrast, TRAF2 acts as NF-κB inducer, whereas TRAF3 opposes TRAF2 and functions as an NF-κB inhibitor (Hostager et al., 2003), as over-expression of TRAF3 can efficiently inhibit NF-κB activation (Qian et al., 2002).

A more limited number of reports exist (mainly from our laboratory) on CD40-mediated regulation of TRAF expression (and localisation) in normal and malignant epithelial cells (Georgopoulos et al., 2006, Mohamed, 2014, Dunnill et al., 2016). This study investigated for the first time the intracellular signalling events triggered by CD40 ligation both in RCC cells and their normal counterparts. It was shown that mCD40L triggered rapid induction of TRAF1, 2, 3 and 6 as early as 1.5h post CD40 ligation in RCC cells, whilst it caused up-regulation of only TRAF1 at 6h post CD40 ligation in normal HRPT cells but it down regulated TRAF2 expression and cause no induction in TRAF3 expression. The induction of TRAF1 and TRAF3 expression is in agreement with previous observations in UCC and CRC cells (Georgopoulos et al., 2006). More strikingly, the observations on TRAF regulation in normal HRPT cells are in close agreement with previous findings in normal urothelial (NHU) cells (Georgopoulos et al., 2006). It appears therefore that the regulation of TRAFs in NHU and HRPT cells is more reminiscent of the regulation of TRAFs in normal B lymphocytes where TRAFs 2 and 3 are either down-regulated or not activated, whilst in malignant epithelial cells TRAF3 is prominently activated discussed in (Bugajska et al., 2002).

TRAF3 is a CD40-associated adaptor protein which relays signals for the activation of MAPKs. In general, such signals can generate multifaceted cell responses ranging from epithelial cell death to cell growth and survival (Häcker et al., 2011). TRAF3 has been shown in some instances to trigger growth inhibition or apoptotic signals in epithelial based models, although the mechanistic explanations for this were until recently not fully understood (Dunnill et al., 2016). TRAF3 seems to mediate apoptotic signals via lipid raft formation (Dadgostar et al., 2002).

The current study investigated the ability of mCD40L to regulate TRAF signalling, as soluble agonists did not induce apoptosis in RCC cells. Moreover, previous reports have demonstrated that soluble CD40 agonists did not stabilise TRAF3 as efficiently as mCD40L did (Georgopoulos et al., 2006), and rapid and sustained induction of TRAF3 expression was mediated only by mCD40L (Georgopoulos et al., 2006, Elmetwali et al., 2010b). Our laboratory previously provided evidence of the functional role of TRAF3 in CD40 signalling in UCC cells and CRC cells, as RNAi-mediated stable TRAF3 knock-down not only stopped mCD40L-mediated apoptosis but also specifically abrogated p38 and JNK phosphorylation, Bak/Bax induction and caspase 3/7 activation (Mohamed, 2014, Dunnill et al., 2016).

CD40 ligation in malignant cells can also induce expression of anti-apoptotic proteins by the stimulation of PI3-K and ERK (Davies et al., 2004). However, in this study, inhibition of MEK1/2 did not alter CD40-mediated apoptosis in RCC cells in agreement with previous studies where it was shown that ERK is not involved in the regulation of mCD40L-mediated apoptosis in UCC cells (Georgopoulos et al., 2006). Moreover, it has been reported that ERK-1 stimulated cell survival in renal cell lines (Kim et al., 2005). Our data in chapter 5 also showed that NF-κB inhibition did not affect CD40-mediated apoptosis.

The MAPK signalling pathways, specifically those driven by p38 and JNK can play critical role in the control of cell death. CD40 triggered JNK activation in carcinoma cells as response to mCD40L (Georgopoulos et al., 2007, Dunnill et al., 2016, Elmetwali et al., 2010a). JNK kinases are stimulated by phosphorylation of threonine and tyrosine remains of their activation loop by MAPKK kinases such as ASK-1

(Kyriakis and Avruch, 2012). However, p38 kinase isoforms can be activated by phosphorylation of threonine and tyrosine residues of their activation loop by MAPK kinases MKK3, 4 and 6 (Brancho et al., 2003). The MAPKKKs involved in the p38 and JNK pathway are mainly ASK-1 and MLK3 (Zarubin and Jiahuai, 2005).

It has been shown previously that JNK activation has important function in cell death via the directive of pro-apoptotic proteins of Bcl-2 resulting in intrinsic cell death (mitochondrial pathway) following CD40 stimulation via mCD40L (Mohamed, 2014, Dunnill et al., 2016, Georgopoulos et al., 2006). Furthermore, unpublished work by our laboratory has confirmed that CD40-mediated apoptosis initiated p38 and inhibition of p38 role reduced the ability of CD40-mediated cell death in CRC cells (Mohamed, 2014). Regular with the function of JNK and p38 in cell death, this study revealed for the first time that CD40-mCD40L interactions in RCC cells caused phosphorylation of both JNK and p38 and functional inhibition experiments using pharmacological inhibitors demonstrated that JNK and p38 phosphorylation was essential, as inhibition of JNK or p38 significantly abrogated CD40-mediated apoptosis in RCC cells. Interestingly, our data showed that the JNK inhibitor stopped p38 activation, while the p38 inhibitor did not block JNK activation (Figure 5.17), therefore these experiments not only confirmed the functionality of the pharmacological inhibitors but they also provided evidence that activation of p38 may be dependent on JNK activity suggesting JNK as a p38 activator; however, further work would be required to fully elucidate this mechanism. By contrast of our observations, the majority of published studies demonstrated that JNK and p38 can be simultaneously activated but independently of each other during apoptosis (Cuadrado and Nebreda, 2010, Geiger et al., 2005, Avisetti et al., 2014). The current study also demonstrated that mCD40L triggered MKK7 and MKK4 activation, which may be upstream of p38 and JNK along the signalling pathway. Although these results are in agreement with recent findings by our laboratory in UCC cells where CD40 induced activation of MKK7 and MKK4 in a TRAF3-dependent manner (Dunnill et al., 2016), they have provided the unique observation that both JNK and p38 are required for CD40-mediated apoptosis in RCC cells.

7.5 CD40-mediated apoptosis via the intrinsic pathway in RCC cells

It is well established that the Bcl-2 family of proteins, and particularly pro-apoptotic Bak and Bax can form oligomers and insert themselves stably into the mitochondrial outer membrane permeabilisation to induce MOMP and subsequently apoptosis (Chipuk and Green, 2008). Previous studies have suggested that mCD40L can induce the expression of Bak and Bax proteins (Bugajska et al., 2002, Georgopoulos et al., 2006). Moreover, our lab have recently investigated the precise regulation and functional role of Bax and Bak in mCD40L-mediated apoptosis in UCC cells and CRC cells (Mohamed, 2014, Dunnill et al., 2016). As shown by these studies, in UCC cells Bak and Bax are activated by 12-24h post CD40 ligation but in CRC cells Bak and Bax activation occurred within less than 6h of CD40 ligation. Both studies showed Bak and Bax are critical in the induction of MOMP, cytochrome release and CD40-mediated apoptosis, as demonstrated by RNAi-mediated knock-down. Results in this study demonstrated that induction of Bak and Bax occurred by 6h post CD40 ligation in RCC cells. On the other hand, inhibition of caspase-9 significantly attenuated CD40-mediated apoptosis in RCC cells, while caspase-8 and 10 inhibition caused non-significant alteration in cell death, suggesting overall that CD40-induced apoptosis in RCC cells occurs through the intrinsic apoptotic pathway. The functional role of the pro-apoptotic proteins Bak and Bax in CD40-mediated apoptosis in RCC cells needs to be further investigated. Previous studies have reported that CD40-mediated apoptosis in hepatocytes requires induction of the Fas pathway (Afford et al., 2001, Afford et al., 1999), while in carcinoma cells CD40 ligation has been shown to induce up-regulation of death ligands, specifically FasL and TRAIL, thus suggesting a cross-talk with other TNFRs to indirectly initiate cell death (Eliopoulos et al., 2000). Earlier performance in our laboratory has demonstrated that in UCC cells CD40 triggers a direct signalling pathway that does not involve other TNFRs (Dunnill et al., 2016), whereas in CRC cells it appears that CD40 mediated apoptosis involves induction of TRAIL (but not FasL) expression and partial functional cross-talk with TRAIL-mediated extrinsic apoptosis (manuscript in preparation) (Mohamed, 2014). Ligation of CD40 in the Renca RCC (adeno-carcinoma) cells induced Fas expression and either CD40

agonist or combination of anti-CD40 agonist with IFN-ɣ up-regulated the expression of Fas and

sensitised cells to Fas-mediated killing (Lee et al., 2005). However, in this study, immunoblotting studies that investigated possible induction of FasL and TRAIL expression, showed no detectable expression of either TRAIL or FasL in human RCC cells even at 6h post CD40 ligation by mCD40L (data not shown). Collectively, these findings suggest that CD40-mediated apoptosis in RCC cells does not involve cross-talk with the extrinsic pathway, but appears to trigger a direct JNK/p38-dependent pathway.

7.6 The role of ROS and NOX in CD40-mediated apoptosis in RCC cells

It has been well known that ROS are natural secondary products of mitochondrial oxidative metabolism (see section 1.6) but also play a role to control cell proliferation and survival (Terada, 2006, Ray et al., 2012). When ROS are not efficiently controlled by antioxidants, eventually this will cause “oxidative stress” that leads to macromolecular damage (Sharma et al., 2012). Prolonged elevation of ROS can enhance malignant transformation due to DNA damage and subsequent oncogene and tumour suppressor mutations (Valko et al., 2004). The importance of controlling the oxidative stress is demonstrated by mutations in the cellular antioxidants GSH and Trx caused elevation in cancer risks. By contrast, Over-expression of antioxidants by advanced cancer serves to protect from oxidative stress elevated due to excessive demand for energy generation (Halliwell, 2007). Therefore, it has been hypothesised that continuous oxidative stress may be exploited by tumour cells to initiate pathway for malignant transformation. Yet, ROS can drive the initiation and execution of pro-apoptotic and necrotic responses that mostly involve mitochondrial pathways (Circu and Aw, 2010, Biswas et al., 2006). Therefore, ROS generation represents proliferation at a cost and what has been described a “double edged sword” for tumour cells (Pan et al., 2009). At early stage of malignant transformation ROS assist to increase the ability of proliferation, whereas oxidative stress causes increase in the sensitivity of the cells to pro-apoptotic signals and pushes cells past a ‘pro-apoptotic threshold’. Low

level of ROS are important in normal homeostasis but high level of ROS induce stress-responsive, cell signalling pathways like JNK that push cells to apoptosis (Terada, 2006, D'Autréaux and Toledano, 2007).

One of the mechanisms of ROS generation is via the action of the NADPH oxidase (NOX) family, which are proteins often referred to as the ‘professional’ ROS producers (Jiang et al., 2011). In humans, the family of NADPH oxidases include NOX1 to NOX5, DUOX1 and DUOX2 (De Deken et al., 2000). Although the structures of the various isoforms of NOX are highly homologous, their tissue distributions, cellular and subcellular and their activation mechanisms, and therefore their physiological functions, are very different (Bedard and Krause, 2007)..

Results in chapter 5 showed for the first time that mCD40L triggered ROS production in RCC cells within 1h post CD40 ligation. ROS production is critical in the induction of cell death, as CD40-mediated apoptosis in RCC cells was repressed by the antioxidant NAC. Earlier effort in our laboratory has revealed that CD40 ligation triggered phosphorylation of the catalytic NOX subunit p40phox in a TRAF3-dependent manner in both UCC cells and CRC cells (Mohamed, 2014, Dunnill et al., 2016) whilst apoptosis was attenuated by the NOX inhibitor DPI, therefore the initial ROS ‘wave’ appears to be mediated by the activity of the NOX complex. Results in chapter 5 demonstrated that mCD40L triggered TRAF 3 induction and p40phox phosphorylation within 1.5h post CD40 ligation in RCC cells, and the NOX inhibitor DPI attenuated apoptosis suggesting that a ROS-dependent Nox-triggered pathway may occur in RCC cells. Importantly, non-apoptotic CD40 agonist (G28-5 mAb) did not induce ROS production in RCC cells thus providing molecular evidence for the inability of soluble agonist to induce apoptosis and further supporting the importance of ROS in the induction of cell death. It appears that the ability of CD40 to kill RCC cells may push these cells past a similar pro-apoptotic threshold, but more specific studies that can compare normal (HRPT) cells and their malignant counterparts would be necessary to address these hypotheses.

7.7 The role of ASK-1 and Trx in mCD40L-mediated apoptosis in RCC cells

Phosphorylation of ASK-1 in response to CD40 ligation was observed within 1.5h which interestingly coincided with the point when maximal level of ROS was detected. This indicates that CD40 ligation in RCC cells most probably engages the ASK-1 pathway to subsequently activate JNK/p38.

To understand the mechanism of ASK-1 activation further, this study investigated the expression of Trx-1 in RCC cells with the first 6h post CD40 ligation and strikingly it was shown that mCD40L rapidly down-regulated the expression of Trx-1, in agreement with previous findings showing that mCD40L down-regulated expression of Trx-1 in UCC cells and CRC cells (Mohamed, 2014, Dunnill et al., 2016).

Collectively, results in this study demonstrated that CD40 ligation induced TRAF3 induction (stabilisation), p40phox activation, active Trx-1 down-regulation and ASK-1 phosphorylation. Previous findings in our laboratory showed that knockdown of ASK-1 completely blocked CD40-mediated apoptosis and TRAF3-knockdown attenuated p40phox activation, suggesting that TRAF3 dependent p40phox activation leads to Trx-1 down-regulation and mediated ASK-1 phosphorylation, (Mohamed, 2014, Dunnill et al., 2016). It would be important that similar studies are performed to investigate whether this is the case in RCC cells.

Overall, CD40 ligation by mCD40L in human RCC cells triggered cytokine secretion, ROS generation, expression of key intracellular proteins such as TRAF3, p^{40phox}, ASK-1, MKK4 and MKK7, p-JNK, p-p38 as well as the pro-apoptotic proteins Bak and Bax, and subsequently caspase-9 activation and efficiently mediated an intrinsic apoptotic signalling pathway. By contrast CD40 ligation in normal HRPT cells did not cause apoptosis although CD40 expression by normal cells was functional, as evident by CD40-mediated cytokine secretion. The tumour-cell specificity of CD40 is reflected by the differential regulation of TRAFs and particularly TRAF3, as this TRAF protein appears to be central in CD40 mediated apoptosis (Mohamed, 2014, Dunnill et al., 2016),

7.8 Future directions

The great capacity of CD40 to activate the immune response permits the possibility of using agonistic CD40-targeting humanised mAbs for the treatment of cancer. Such mAb preparations can enhance the immune response against tumours via activating dendritic cells and supporting an effective cytotoxic T-cell response (Khong et al., 2012). In phase I and II clinical trials for cancer treatment, the anti-CD40 CP-870,893 humanised mAb showed improvement in the response of T-cells against tumour antigen (Fonsatti et al., 2010). However, limited efficacy overall has been a limiting factors in the success of CD40-targeting approaches.

The ability of CD40 ligation to mediate apoptosis in carcinoma cells (of bladder and colorectal origins) has been under detailed investigations in our laboratory and has provided clear therapeutic promise. Since mCD40L represents a strong apoptotic signal contrary to soluble agonists, our laboratory has been bright to reward for the failure of soluble agonist to kill proficiently by linking soluble CD40 agonists with a Trx-1 inhibitor, which extracted the soluble agonist effectively equal to mCD40L (Dunnill et al., 2016) and provided a novel and patented combinatorial therapeutic approach. The soluble-agonist/Trx inhibitor combinatorial treatment was functionally equivalent to mCD40L-induced CD40 ligation and it would be of interest to investigate the efficacy of such combination in RCC cells. However, before this, further functional experimental work would be required to understand the precise mechanisms and signalling pathways specifically involved in CD40-mediated apoptosis in RCC cells. This would require functional inhibition experiments (by RNAi or CRISPR/Cas9) to investigate the role of key proteins such as $p40^{phox}$, ASK-1, and particularly TRAF3 in CD40-mediated apoptosis. Understanding the nature of the pro-apoptotic signals triggered by CD40 is significant, as recent studies in our laboratory have demonstrated

that the precise mechanisms of CD40 killing might different in different tumour cell types (e.g. prostate – Ateeg and Georgopoulos unpublished observations). Other important areas of investigation would focus on understanding the mechanisms of TRAF up-regulation as well as the involvement of the pro-apoptotic Bak and Bax, which would involve cell fractionation and immunofluorescence microscopy. Finally, the

ability to culture primary normal HRPT cells represents as additional area of investigation that could permit further studies on the tumour-specificity of CD40 ligation.

7.9 Concluding remarks

Expression of CD40 in RCC appears to be strongly associated with prolonged patient survival, although no relation was observed between CD40 expression and tumour stage (Weiss et al., 2014). Furthermore, activation of CD40 in vivo resulted in recruitment of monocytes and T cells into the tumour and increased the number of DC and caused reduction in tumour size (Shorts et al., 2006).

This study has for the first time reported that mCD40L induced extensive apoptosis in RCC cells while sparing their normal cell counterparts. However, agonistic anti-CD40 antibody G28-5 did not cause cell death in RCC cells. Although additional functional experiments would be necessary, it appears that CD40 mediated apoptosis in RCC cells via a TRAF3-p40phox-ROS-ASK-1-MKK-p38/JNK pathway leading to caspase-9 and effector caspase-3/7 activation and intrinsic apoptosis.

These findings provide novel observations on the role of CD40 in human RCC cells cell fate, and have also reinforced the significance of the superiority of CD40 signal in defining practical consequence. Equally importantly, the findings have also assisted in the formulation of novel therapeutic avenues that may exploit CD40 for anticancer therapy and specifically renal cell carcinoma.

Appendix

Appendix I

Reagents

1. EDTA

Reagents	Mass or volume
Ethylenediaminetetraacetic acid (EDTA)	1g
Phosphate-buffered saline (PBS) (1x)	1000mL

The solution was mixed well and then autoclaved.

2. Preparation of SDS lysis buffer for cell lysate preparation

Reagents	Mass or volume
SDS	1g
Glycerol	10mL
Tris-HCl	6.25mL (stock 1M) (pH 6.8)
Sodium orthovandate	0.0184 g
Sodium fluoride (NaF)	0.42g
Sodium pyrophosphate tetrabasic	0.446g

The volume was complete up to 50mL with deionised water (dH_2O) and magnetic heat stirrer and magnetic flea were used to thaw all substances. SDS lysis buffer was then divided into 50 Eppendorf tubes at 1mL each and stored at -20°C.

3. Tris Buffered Saline (TBS)

Reagent	Mass or volume
Tris (Hydroxy methyl amino methan)	1.21g
Sodium hydrochloride (NaCl)	8.18g

The reagent dissolved in 1 L deionised water using magnetic flea and magnetic stirrer and buffered to pH 7.4.

4. TBS-Tween

Reagent	Mass or volume
Tris (Hydroxy methyl amino methan)	1.21g
Sodium chloride (NaCl)	8.18g
Deionised water	1L and pH 7.4 as above
Tween-20	1 mL

The solution was mixed well using magnetic flea and magnetic stirrer.

5. Transfer Buffer

Reagents	Mass or volume
Tris (Hydroxy methyl amino methan) (12mM)	1.45g
Glycine (96mM)	7.2g
Methanol (20%)	200mL

Topped up with deionised water to total of 1 L (*prepared fresh on day of use*)

6. Preparation of samples for SDS-PAGE and Western blotting based on the concentration of protein in cell lysates

A	Control	mCD40L	Control	mCD40L	Control	mCD40L	Control -ve	Control +ve	3T3-CD40L
µg/ml	5432.981	4036.142	4422.205	6126.114	6055.568	7867.231	3484.139	6363.265	1237.405
µg/µl	5.432981	4.036142	4.422205	6.126114	6.055568	7.867231	3.484139	6.363265	1.237405
Volume with 20µg	3.681221	4.955227	4.522631	3.264713	3.302746	2.542191	5.740299	3.143041	3.190381
dH2O	9.318779	8.044773	8.477369	9.735287	9.697254	10.45781	7.259701	9.856959	9.809619
Sample volume	13	13	13	13	13	13	13	13	13
Reducing agent	2	2	2	2	2	2	2	2	2
LDS sample buffer	5	5	5	5	5	5	5	5	5
Total volume (µl)	20	20	20	20	20	20	20	20	20

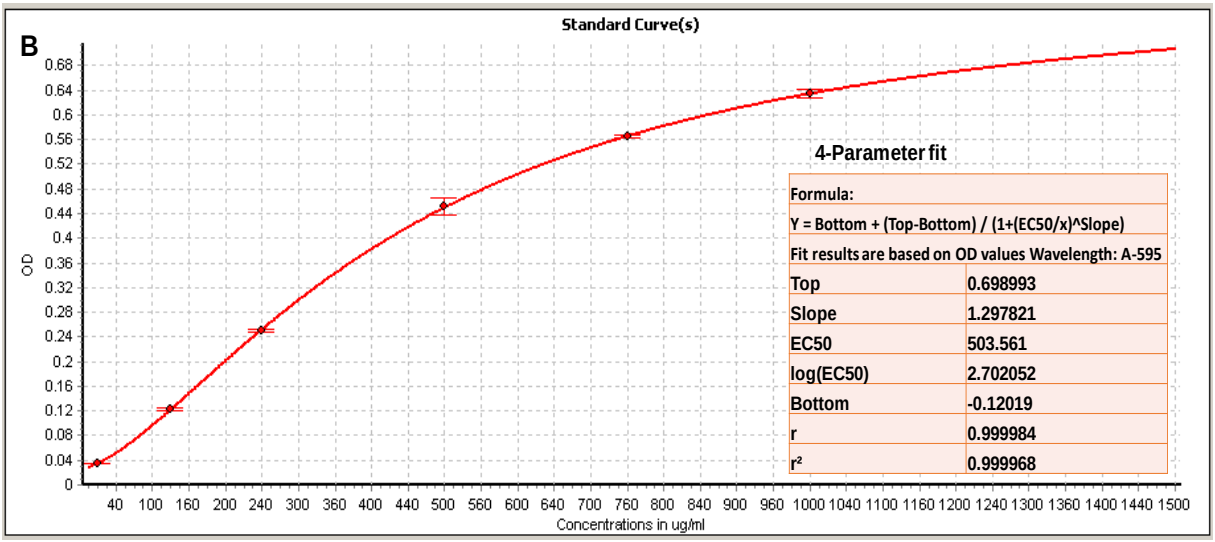

A) Protein amount in cell lysates, table also shows the quantity of other components added to the lysates preparation for immunoblotting assay.

B) Standard curve (4-parameter-fit to measure protein amount in cell lysate.

Appendix II

Titrations of MAPK inhibitors

1. JNK inhibitor (SP600125)

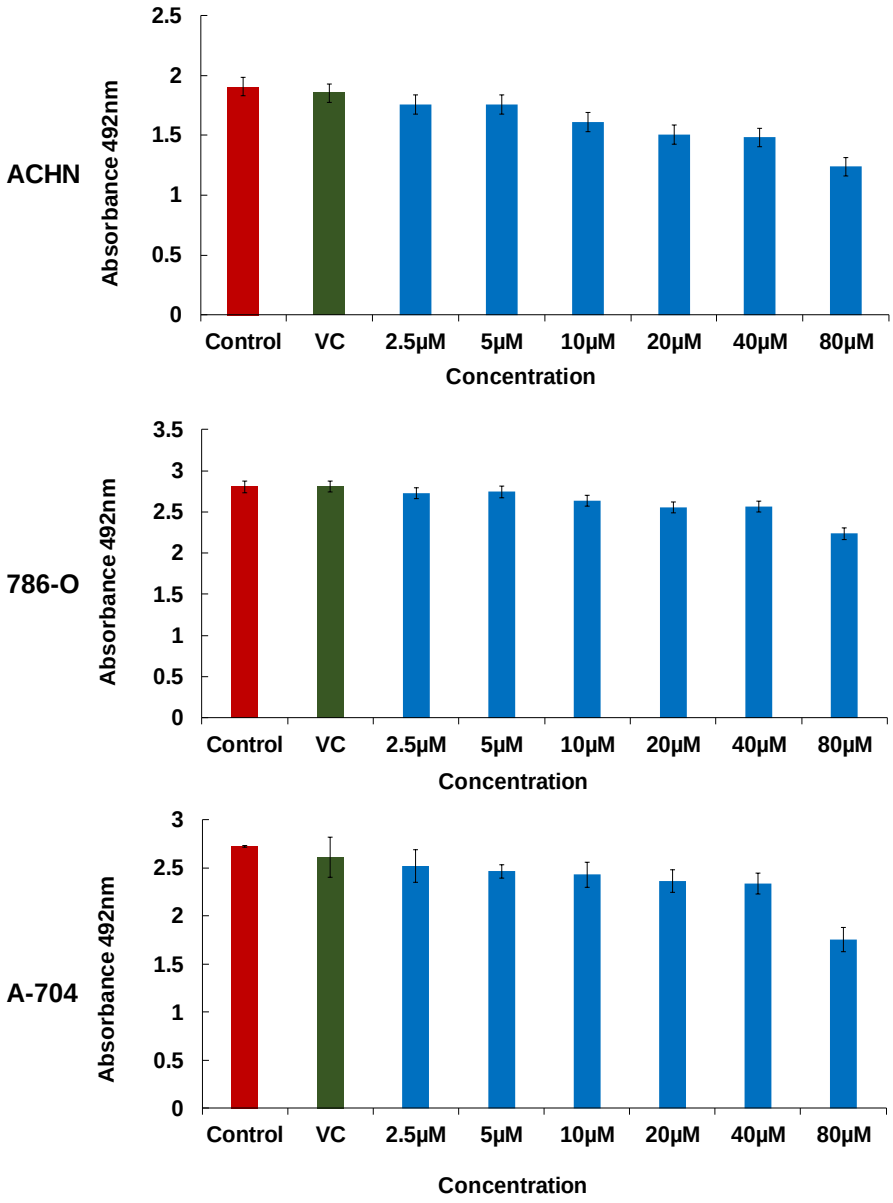

Effects of the JNK inhibitor (SP600125) on RCC cell viability

RCC cells (ACHN, 786-O and A-704) were seeded at $0.8x10^4$ cells/well in clear 96-well plates and incubated for 1h. Then cells were treated with JNK inhibitor (SP600125) as indicated, non-treated cells were served as (control) and vehicle control (VC) was also included. Then plates were incubated for 48 h and cell viability was assessed by CellTiter assay. 20µl of CellTiter Solution was added to each well followed by 4h incubation at 37ºC / 5% CO_2. Absorbance was measured on a FLUOStar Optima plate reader at wavelength 492nm. Data presented as mean absorbance values of 4-5 technical replicates ± SEM.

2. p38 inhibitor (SB202190)

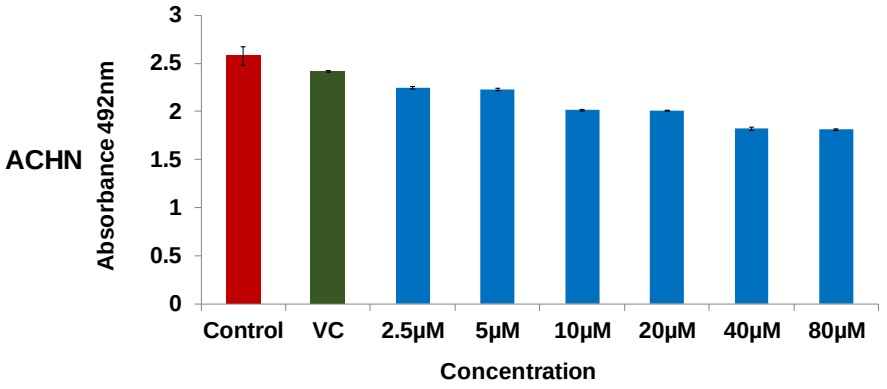

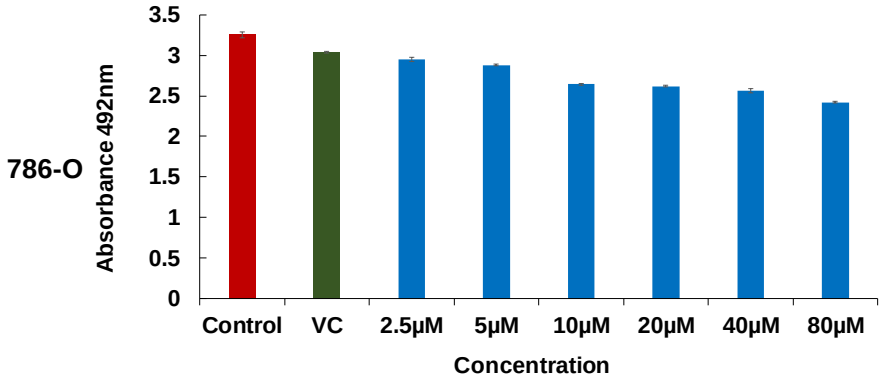

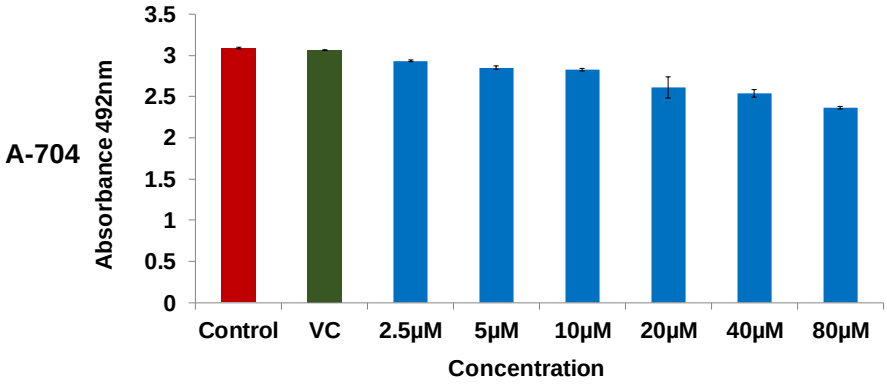

Effects of the p38 inhibitor (SB202190) on RCC cell viability

RCC cells (ACHN, 786-O and A-704) were seeded at $0.8x10^4$ cells/well in clear 96-well plates and incubated for 1h. Then cells were treated with p38 inhibitor (SB202190) as indicated, non-treated cells were served as control and vehicle control (VC) was also included. Then plates were incubated for 48 h and cell viability was assessed by CellTiter assay. 20µl of CellTiter Solution was added to each well followed by 4h incubation at 37ºC / 5% Co_2. Absorbance was measured on a FLUOStar Optima plate reader at wavelength 492nm. Data presented as mean absorbance values of 4-5 technical replicates ± SEM.

3. AP-1 inhibitor (NDGA)

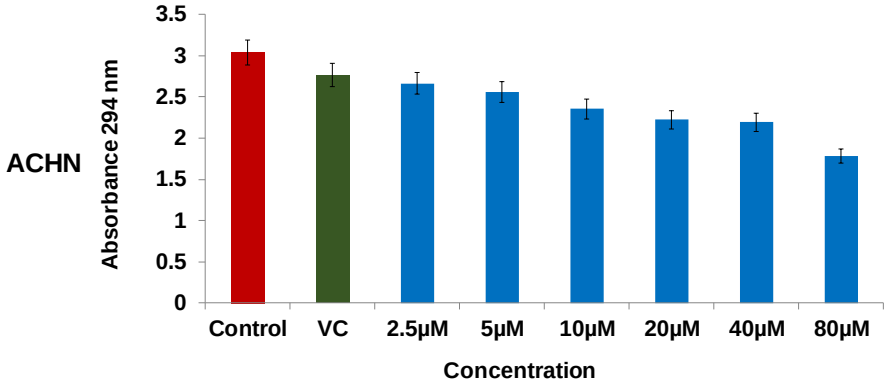

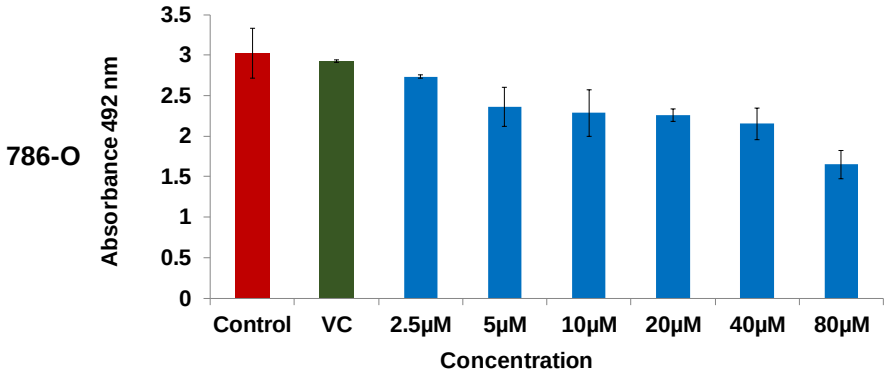

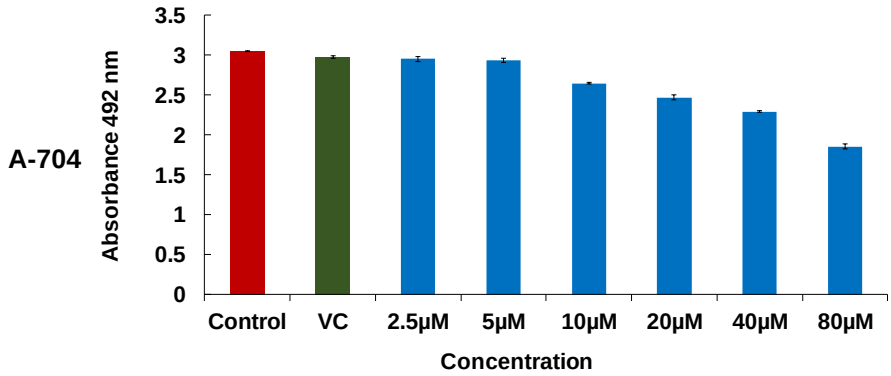

Effects of the AP-1 inhibitor NDGA on RCC cell viability

RCC cells (ACHN, 786-O and A-704) were seeded at $0.8x10^4$ cells/well in clear 96-well plates and incubated for 1h. Then cells were treated with AP-1 inhibitor (NDGA) as indicated, non-treated cells were served as control and vehicle control (VC) was also included. Then plates were incubated for 48 h and cell viability was assessed by CellTiter assay. 20µl of CellTiter Solution was added to each well followed by 4h incubation at 37ºC / 5% Co_2. Absorbance was measured on a FLUOStar Optima plate reader at wavelength 492nm. Data presented as mean absorbance values of 4-5 technical replicates ± SEM.

4. MEK-1 inhibitor (U0126)

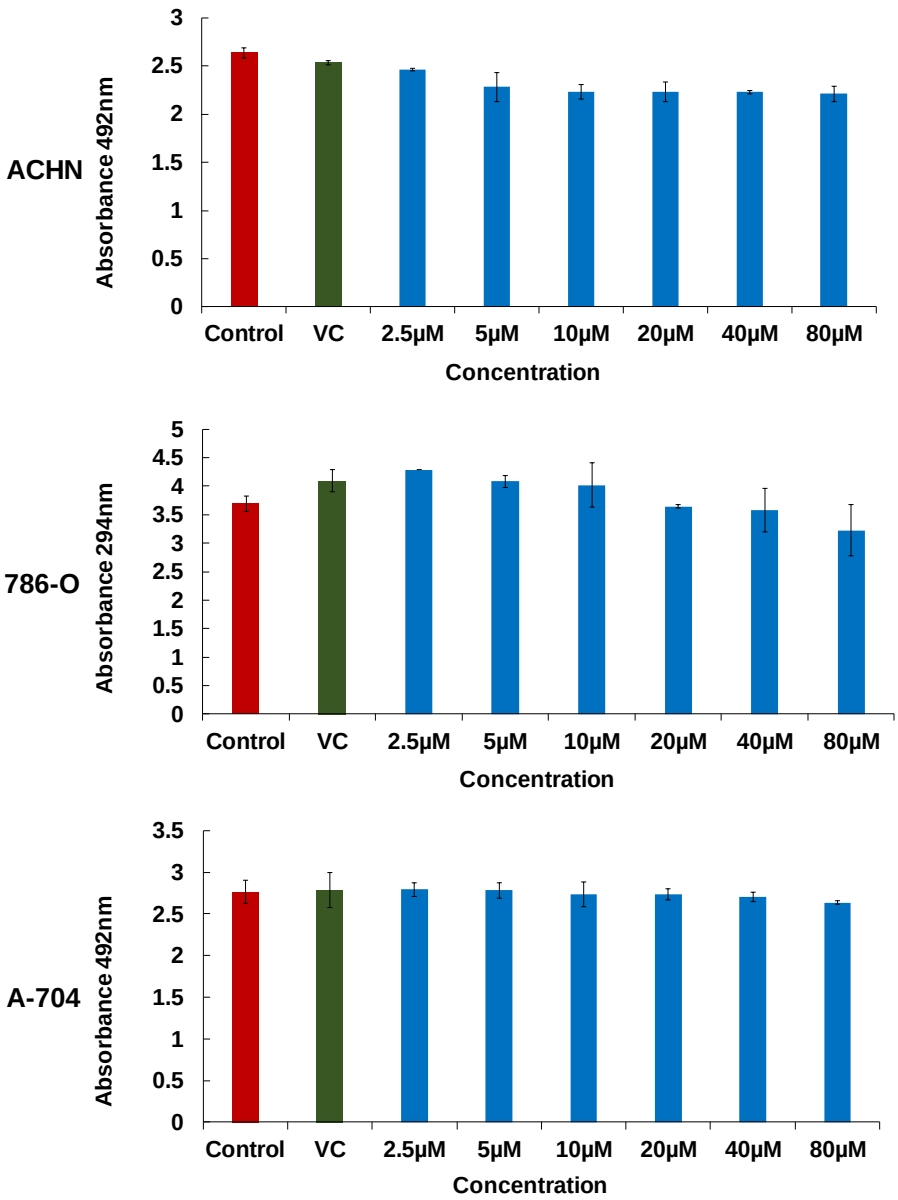

Effects of the MEK-1 inhibitor U0126 on RCC cell viability

RCC cells (ACHN, 786-O and A-704) were seeded at $0.8x10^4$ cells/well in clear 96-well plates and incubated for 1h. Then cells were treated with MEK-1 inhibitor (u-0126) as indicated, non-treated cells were served as control and vehicle control (VC) was also included. Then plates were incubated for 48 h and cell viability was assessed by CellTiter assay. 20µl of CellTiter Solution was added to each well followed by 4h incubation at 37ºC / 5% Co_2. Absorbance was measured on a FLUOStar Optima plate reader at wavelength 492nm. Data presented as mean absorbance values of 4-5 technical replicates ± SEM

5. NF-κB Inhibitor (PDTC)

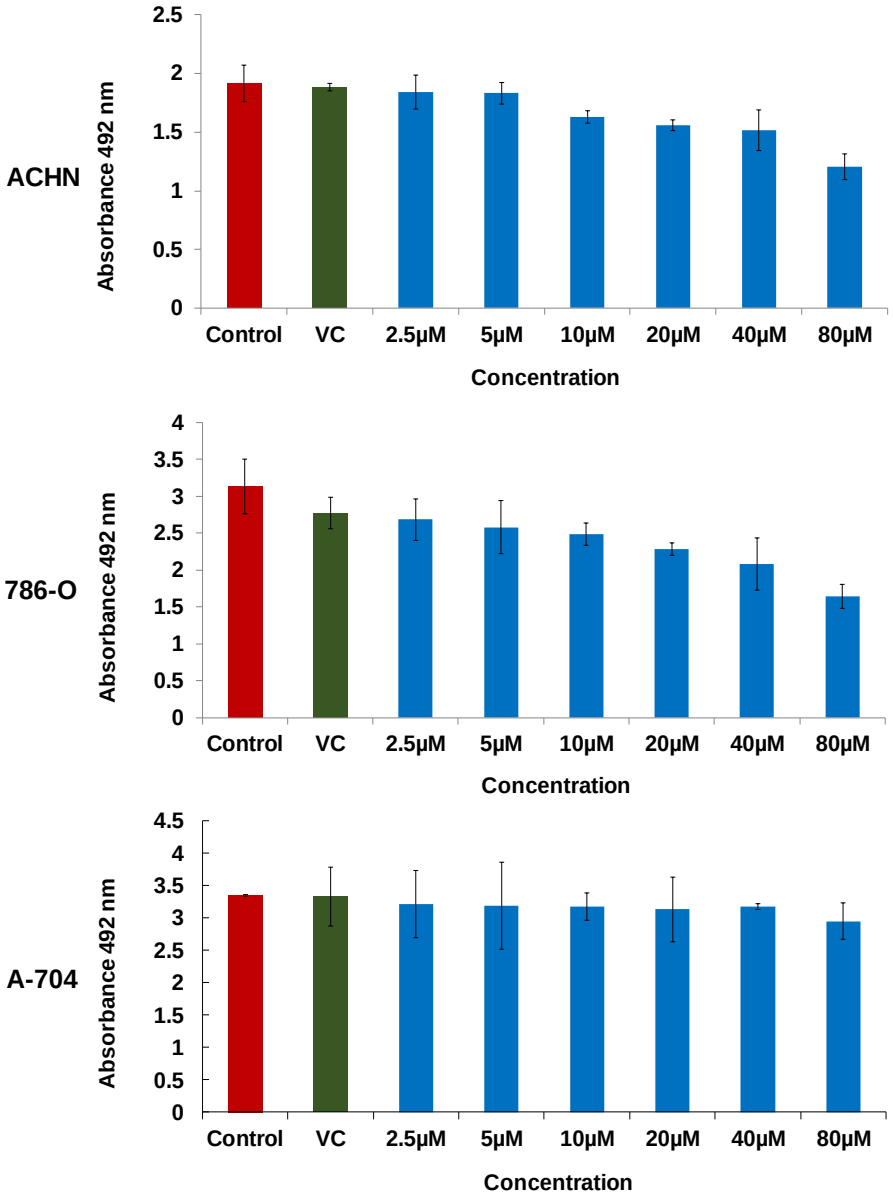

Effects of the NF-κB Inhibitor PDTC on RCC cell viability

RCC cells (ACHN, 786-O and A-704) were seeded at $0.8x10^4$ cells/well in clear 96-well plates and incubated for 1h. Then cells were treated with NF-κB Inhibitor (PDTC) as indicated, non-treated cells were served as control and vehicle control (VC) was also included. Then plates were incubated for 48 h and cell viability was assessed by CellTiter assay. 20μl of CellTiter Solution was added to each well followed by 4h incubation at 37ºC / 5% Co_2. Absorbance was measured on a FLUOStar Optima plate reader at wavelength 492nm. Data presented as mean absorbance values of 4-5 technical replicates ± SEM

Appendix III

H_2DCFDA optimisation for ROS detection

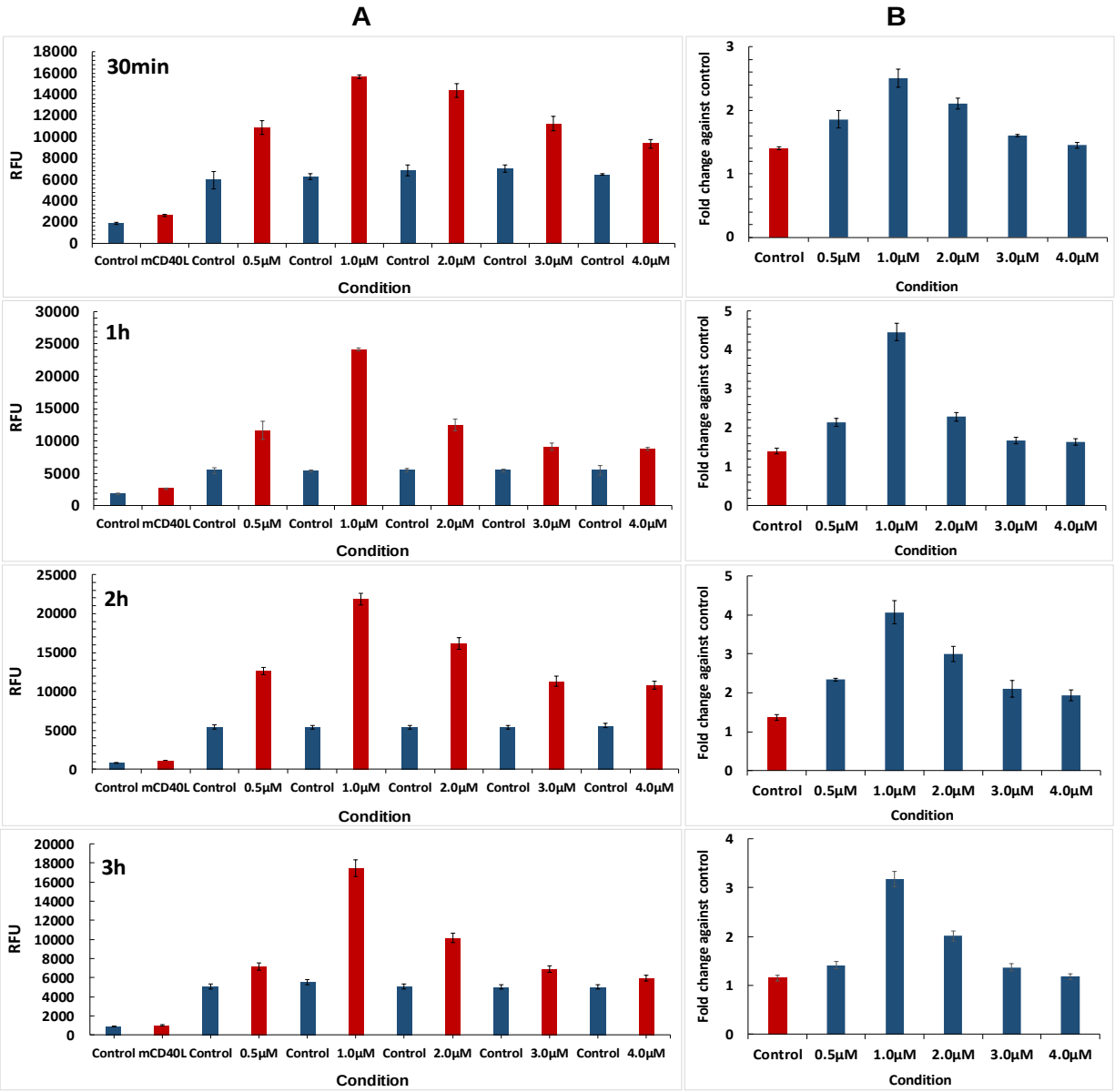

mCD40L-mediated ROS generation in RCC (ACHN) cells

RCC cells line ACHN were co-cultured at $0.8x10^4$ cells/well with $1x10^4$ cells/well of MMC-treated fibroblasts 3T3-CD40L and 3T3-Neo in white 96-well plates. Plates were incubated for (30min, 1h, 2h and 3h). Then cells were first washed with PBS (see section 2.8.6), and H_2CDFAD in pre-warmed (37ºC) PBS was added at concentrations of (0.5µM, 1µM, 2µM, 3µM and 4µM). The plates then incubated for 30min at 37ºC and 5% CO_2. Fluorescence was measured on a FLUOStar Optima plate reader and background-corrected relative fluorescence units (RFU) were deduced by pair-wise subtraction of mL and Control RFU from the respective co-cultures (as described in µM the Methods). **A)** Background corrected RFU readings for co-cultures ACHN/3T3-CD4OL (mCD40L) and respective 3T3-Neo co-culturs (Control). **B)** Results from graph in A are also presented as fold change (mCD40L relative to control). Bars show mean RFU of 4-6 technical replicates ± SEM.

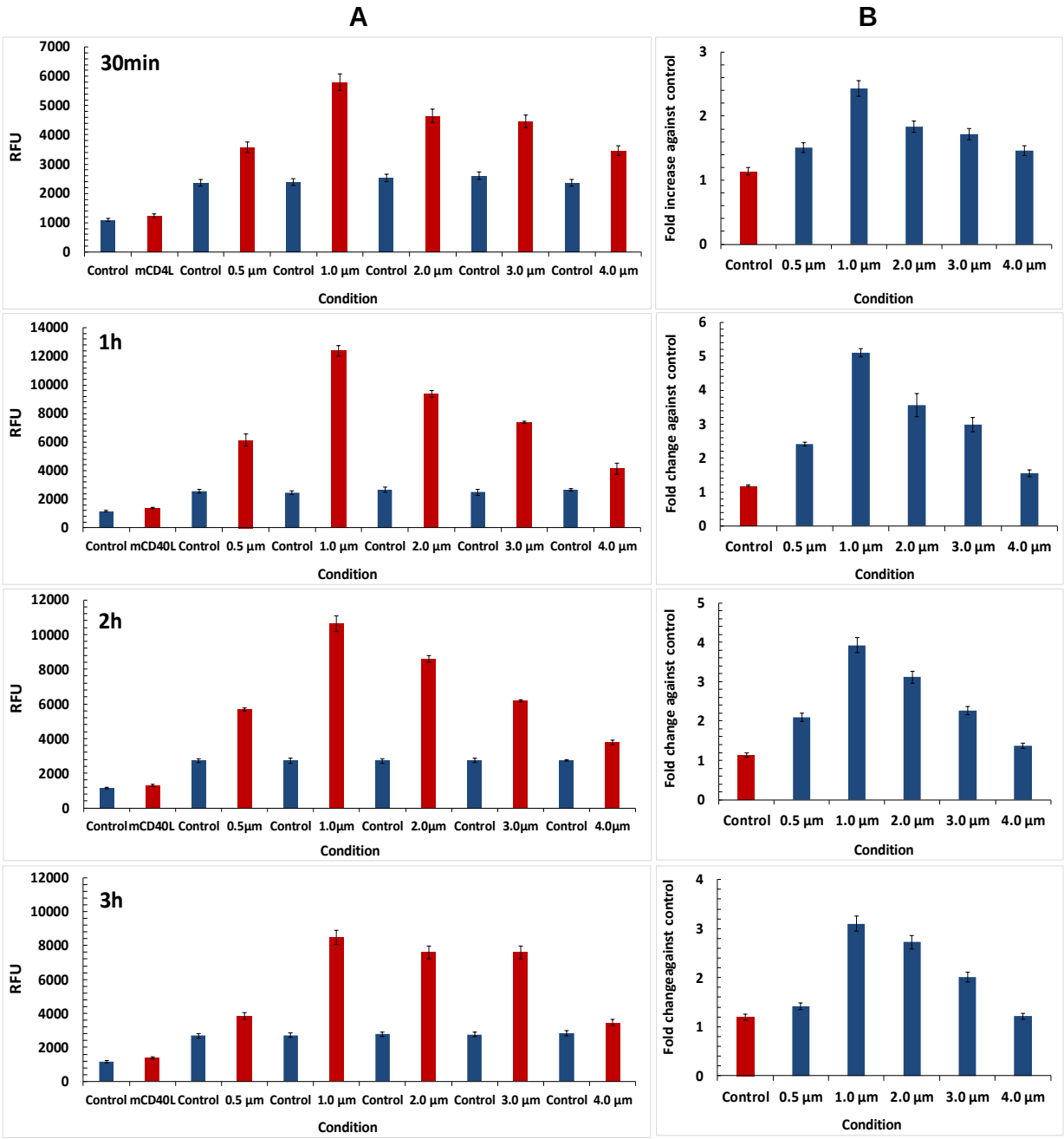

mCD40L-mediated ROS generation in RCC (786-O) cells

RCC cells line 786-O were co-cultured at $0.8x10^4$ cells/well with $1x10^4$ cells/well of MMC-treated fibroblasts 3T3-CD40L and 3T3-Neo in white 96-well plates. Plates were incubated for (30min, 1h, 2h and 3h). Then cells were first washed with PBS (see section 2.8.6), and H_2CDFAD in pre-warmed (37ºC) PBS was added at concentrations of (0.5µM, 1µM, 2µM, 3µM and 4µM). The plates then incubated for 30min at 37ºC and 5% CO_2. Fluorescence was measured on a FLUOStar Optima plate reader and background-corrected relative fluorescence units (RFU) were deduced by pair-wise subtraction of mL and Control RFU from the respective co-cultures (as described in µM the Methods). **A)** Background corrected RFU readings for co-cultures 786-O/3T3-CD4OL (mCD40L) and respective 3T3-Neo co-culturs (Control). **B)** Results from graph in A are also presented as fold change (mCD40L relative to control). Bars show mean RFU of 4-6 technical replicates ± SEM.

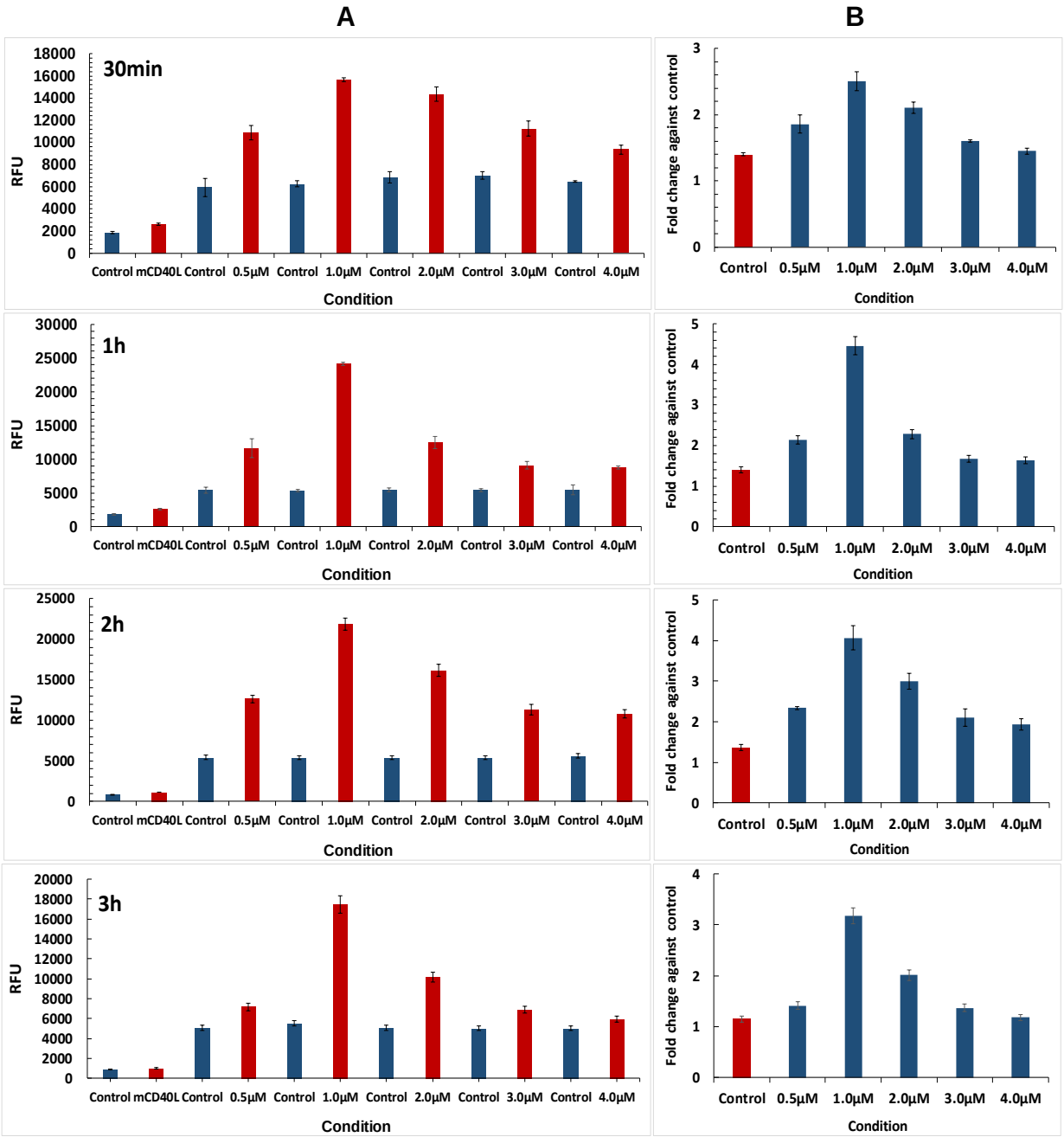

mCD40L-mediated ROS generation in RCC (A-704) cells

RCC cells line A-704 were co-cultured at $0.8x10^4$ cells/well with $1x10^4$ cells/well of MMC-treated fibroblasts 3T3-CD40L and 3T3-Neo in white 96-well plates. Plates were incubated for (30min, 1h, 2h and 3h). Then cells were first washed with PBS (see section 2.8.6), and H_2CDFAD in pre-warmed (37ºC) PBS was added at concentrations of (0.5µM, 1µM, 2µM, 3µM and 4µM). The plates then incubated for 30min at 37ºC and 5% CO_2. Fluorescence was measured on a FLUOStar Optima plate reader and background-corrected relative fluorescence units (RFU) were deduced by pair-wise subtraction of mL and Control RFU from the respective co-cultures (as described in µM the Methods). **A)** Background corrected RFU readings for co-cultures A-704/3T3-CD4OL (mCD40L) and respective 3T3-Neo co-culturs (Control). **B)** Results from graph in A are also presented as fold change (mCD40L relative to control). Bars show mean RFU of 4-6 technical replicates ± SEM.

Appendix IIII

Human Cytokine Array coordinates

Coordinate	Target/Control	Entrez Gene ID	Alternate Nomenclature
A1, A2	Reference Spots	N/A	
A3, A4	CCL1/I-309	6346	P500, SCYA1, SCYA2, TCA-3
A5, A6	CCL2/MCP-1	6347	MCAF
A7, A8	MIP-1α/MIP-1β	6348/6351	CCL3/CCL4
A9, A10	CCL5/RANTES	6352	
A11, A12	CD40 Ligand/TNFSF5	959	CD154, CD40LG, gp39, TRAP
A13, A14	Complement Component C5/C5a	727	C5/C5a
A15, A16	CXCL1/GROα	2919	CINC-1, KC
A17, A18	CXCL10/IP-10	3627	CRG-2
A19, A20	Reference Spots	N/A	
B3, B4	CXCL11/I-TAC	6373	β-R1, H174
B5, B6	CXCL12/SDF-1	6387	PBSF
B7, B8	G-CSF	1440	CSFβ, CSF-3
B9, B10	GM-CSF	1437	CSFα, CSF-2
B11, B12	ICAM-1/CD54	3383	
B13, B14	IFN-γ	3458	Type II IFN
B15, B16	IL-1α/IL-1F1	3552	
B17, B18	IL-1β/IL-1F2	3553	
C3, C4	IL-1ra/IL-1F3	3557	
C5, C6	IL-2	3558	TCGF
C7, C8	IL-4	3565	BCDF, BSF1
C9, C10	IL-5	3567	———
C11, C12	IL-6	3569	BSF-2
C13, C14	IL-8	3576	CXCL8, GCP1, NAP1
C15, C16	IL-10	3586	CSIF
C17, C18	IL-12 p70	3592/3593	CLMF p35
D3, D4	IL-13	3596	———
D5, D6	IL-16	3603	LCF
D7, D8	IL-17A	3605	CTLA-8
D9, D10	IL-17E	64806	IL-25
D11, D12	IL-18/IL-1F4	3606	IGIF
D13, D14	IL-21	59067	———
D15, D16	IL-27	246778	IL-27 A
D17, D18	IL-32α	9235	

E1, E2	Reference Spots	N/A	
E3, E4	MIF	4282	GIF, DER6
E5, E6	Serpin E1/PAI-1	5054	Nexin, PLANH1
E7, E8	TNF-α	7124	TNFSF1A
E9, E10	TREM-1	54210	CD354
	Negative Control	N/A	

List of cytokines that can detected by this kit with their number of spot and their alternative name

Cytokine measurement standard curves (ELISA)

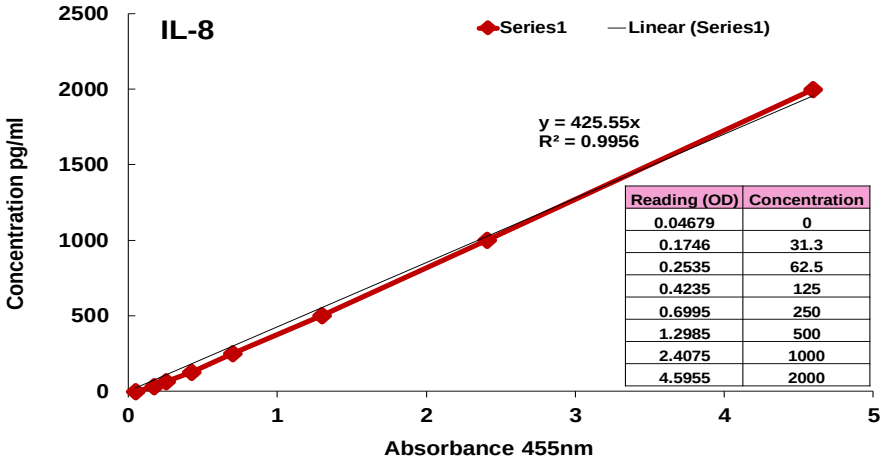

Reading (OD)	Concentration
0.04679	0
0.1746	31.3
0.2535	62.5
0.4235	125
0.6995	250
1.2985	500
2.4075	1000
4.5955	2000

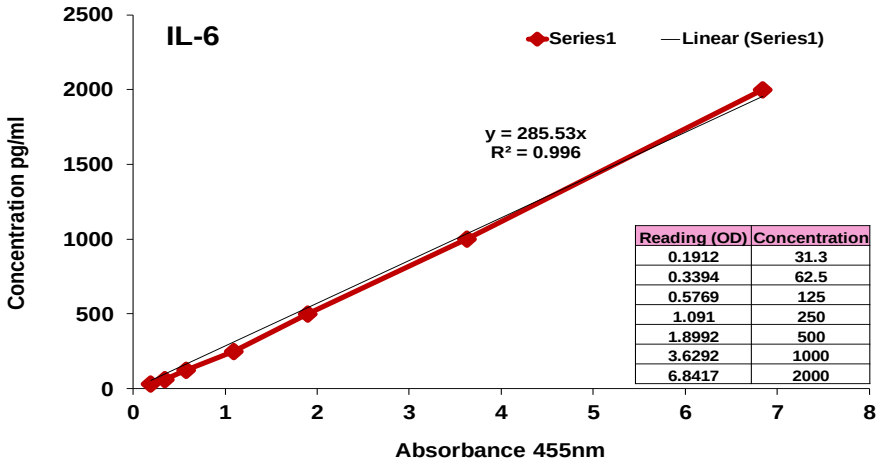

Reading (OD)	Concentration
0.1912	31.3
0.3394	62.5
0.5769	125
1.091	250
1.8992	500
3.6292	1000
6.8417	2000

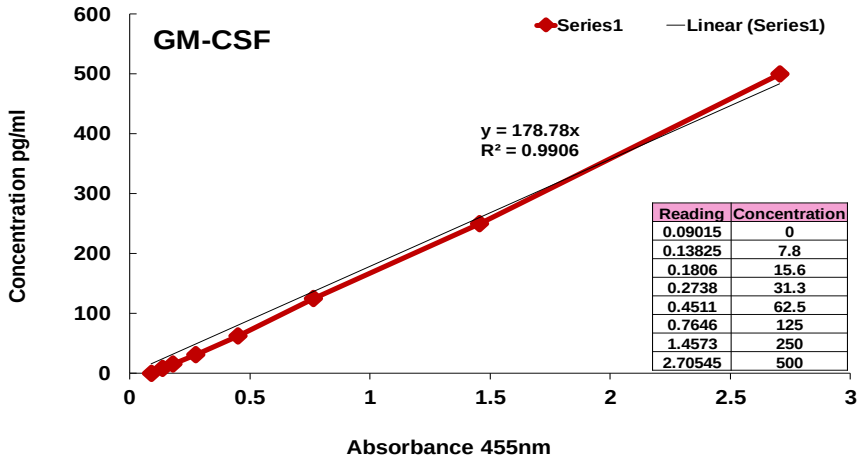

Reading	Concentration
0.09015	0
0.13825	7.8
0.1806	15.6
0.2738	31.3
0.4511	62.5
0.7646	125
1.4573	250
2.70545	500

Standard curves (4-parameter-fit to measure cytokines concentrations (IL-8. IL-6 and GM-CSF) in cell cultures supernatants by ELISA assay.

References

ABBATE, M., ZOJA, C., CORNA, D., CAPITANIO, M., BERTANI, T. & REMUZZI, G. 1998. In progressive nephropathies, overload of tubular cells with filtered proteins translates glomerular permeability dysfunction into cellular signals of interstitial inflammation. *Journal of the American Society of Nephrology,* 9**,** 1213-1224.

ABREU-MARTIN, M. T., VIDRICH, A., LYNCH, D. H. & TARGAN, S. R. 1995. Divergent induction of apoptosis and IL-8 secretion in HT-29 cells in response to TNF-alpha and ligation of Fas antigen. *The Journal of Immunology,* 155**,** 4147-4154.

ACEHAN, D., JIANG, X., MORGAN, D. G., HEUSER, J. E., WANG, X. & AKEY, C. W. 2002. Three-dimensional structure of the apoptosome: implications for assembly, procaspase-9 binding, and activation. *Molecular cell,* 9**,** 423-432.

ADAMS, J. & CORY, S. 2007. The Bcl-2 apoptotic switch in cancer development and therapy. *Oncogene,* 26**,** 1324-1337.

ADAMS, J. M. 2003. Ways of dying: multiple pathways to apoptosis. *Genes & development,* 17**,** 2481-2495.

ADRAIN, C., CREAGH, E. M. & MARTIN, S. J. 2002. Caspase cascades in apoptosis. *Caspases: their role in cell death and cell survival. Kluwer Academic/Plenum Publishers, New York, NY***,** 41-51.

AFFORD, S. C., AHMED-CHOUDHURY, J., RANDHAWA, S., RUSSELL, C., YOUSTER, J., CROSBY, H. A., ELIOPOULOS, A., HUBSCHER, S. G., YOUNG, L. S. & ADAMS, D. H. 2001. CD40 activation-induced, Fas-dependent apoptosis and NF-κB/AP-1 signaling in human intrahepatic biliary epithelial cells. *The FASEB Journal,* 15**,** 2345-2354.

AFFORD, S. C., RANDHAWA, S., ELIOPOULOS, A. G., HUBSCHER, S. G., YOUNG, L. S. & ADAMS, D. H. 1999. CD40 activation induces apoptosis in cultured human hepatocytes via induction of cell surface fas ligand expression and amplifies fas-mediated hepatocyte death during allograft rejection. *The Journal of experimental medicine,* 189**,** 441-446.

ALBARBAR, B., DUNNILL, C. & GEORGOPOULOS, N. T. 2015. Regulation of cell fate by lymphotoxin (LT) receptor signalling: Functional differences and similarities of the LT system to other TNF superfamily (TNFSF) members. *Cytokine & growth factor reviews,* 26**,** 659-671.

ALEXANDROFF, A. B., JACKSON, A. M., PATERSON, T., HALEY, J. L., ROSS, J. A., LONGO, D., MURPHY, W., JAMES, K. & TAUB, D. D. 2000. Role for CD40–CD40 ligand interactions in the immune response to solid tumours. *Molecular immunology,* 37**,** 515-526.

ALTENBURG, A., BALDUS, S. E., SMOLA, H., PFISTER, H. & HESS, S. 1999. CD40 ligand-CD40 interaction induces chemokines in cervical carcinoma cells in synergism with IFN-γ. *The Journal of Immunology,* 162**,** 4140-4147.

ANAND, S. X., VILES-GONZALEZ, J. F., BADIMON, J. J., CAVUSOGLU, E. & MARMUR, J. D. 2003. Membrane-associated CD40L and sCD40L in atherothrombotic disease. *THROMBOSIS AND HAEMOSTASIS-STUTTGART-,* 90**,** 377-384.

ANDERA, L. 2009. Signaling activated by the death receptors of the TNFR family. *Biomedical papers,* 153**,** 173-180.

ANTONIADES, C., BAKOGIANNIS, C., TOUSOULIS, D., ANTONOPOULOS, A. S. & STEFANADIS, C. 2009. The CD40/CD40 Ligand SystemLinking Inflammation With Atherothrombosis. *Journal of the American College of Cardiology,* 54**,** 669-677.

ANTONSSON, B. & MARTINOU, J.-C. 2000. The Bcl-2 protein family. *Experimental cell research,* 256**,** 50-57.

ARA, T. & DECLERCK, Y. A. 2010. Interleukin-6 in bone metastasis and cancer progression. *European journal of cancer,* 46**,** 1223-1231.

ARCH, R. H., GEDRICH, R. W. & THOMPSON, C. B. 1998. Tumor necrosis factor receptor-associated factors (TRAFs)—a family of adapter proteins that regulates life and death. *Genes & development,* 12**,** 2821-2830.

ARDESTANI, S., DESKINS, D. & YOUNG, P. 2013. Membrane TNF-alpha-activated programmed necrosis is mediated by Ceramide-induced reactive oxygen species. *Journal of molecular signaling,* 8.

ARMITAGE, R. J., FANSLOW, W. C., STROCKBINE, L., SATO, T. A., CLIFFORD, K. N., MACDUFF, B. M., ANDERSON, D. M., GIMPEL, S. D., DAVIS-SMITH, T. & MALISZEWSKI, C. R. 1992. Molecular and biological characterization of a murine ligand for CD40. *Nature,* 357**,** 80-82.

ARMITAGE, R. J., TOUGH, T. W., MACDUFF, B. M., FANSLOW, W. C., SPRIGGS, M. K., RAMSDELL, F. & ALDERSON, M. R. 1993. CD40 ligand is a T cell growth factor. *European journal of immunology,* 23**,** 2326-2331.

ARRON, J. R., PEWZNER-JUNG, Y., WALSH, M. C., KOBAYASHI, T. & CHOI, Y. 2002. Regulation of the subcellular localization of tumor necrosis factor receptor–associated factor (TRAF) 2 by TRAF1 reveals mechanisms of TRAF2 signaling. *The Journal of experimental medicine,* 196**,** 923-934.

ARUFFO, A., FARRINGTON, M., HOLLENBAUGH, D., LI, X., MILATOVICH, A., NONOYAMA, S., BAJORATH, J., GROSMAIRE, L. S., STENKAMP, R. & NEUBAUER, M. 1993. The CD40 ligand, gp39, is defective in activated T cells from patients with X-linked hyper-IgM syndrome. *Cell,* 72**,** 291-300.

ASAO, H. & FU, X.-Y. 2000. Interferon-γ has dual potentials in inhibiting or promoting cell proliferation. *Journal of Biological Chemistry,* 275**,** 867-874.

ASHKENAZI, A. 2002. Targeting death and decoy receptors of the tumour-necrosis factor superfamily. *Nature Reviews Cancer,* 2**,** 420-430.

AVISETTI, D. R., BABU, K. S. & KALIVENDI, S. V. 2014. Activation of p38/JNK pathway is responsible for embelin induced apoptosis in lung cancer cells: transitional role of reactive oxygen species. *PloS one,* 9**,** e87050.

BABIOR, B. M. 1999. NADPH oxidase: an update. *Blood,* 93**,** 1464-1476.

BACCAM, M. & BISHOP, G. A. 1999. Membrane-bound CD154, but not CD40-specific antibody, mediates NF-κB-independent IL-6 production in B cells. *European journal of immunology,* 29**,** 3855-3866.

BAER, P. C., BEREITER-HAHN, J., SCHUBERT, R. & GEIGER, H. 2006. Differentiation status of human renal proximal and distal tubular epithelial cells in vitro: differential expression of characteristic markers. *Cells Tissues Organs,* 184**,** 16-22.

BAKER, A. F., DRAGOVICH, T., TATE, W. R., RAMANATHAN, R. K., ROE, D., HSU, C.-H., KIRKPATRICK, D. L. & POWIS, G. 2006. The antitumor thioredoxin-1 inhibitor PX-12 (1-methylpropyl 2-imidazolyl disulfide) decreases thioredoxin-1 and VEGF levels in cancer patient plasma. *Journal of Laboratory and Clinical Medicine,* 147**,** 83-90.

BAKER, M. P., ELIOPOULOS, A. G., YOUNG, L. S., ARMITAGE, R. J., GREGORY, C. D. & GORDON, J. 1998. Prolonged phenotypic, functional, and molecular change in group I Burkitt lymphoma cells on short-term exposure to CD40 ligand. *Blood,* 92**,** 2830-2843.

BANCHEREAU, J., BRIERE, F., CAUX, C., DAVOUST, J., LEBECQUE, S., LIU, Y.-J., PULENDRAN, B. & PALUCKA, K. 2000. Immunobiology of dendritic cells. *Annual review of immunology,* 18**,** 767-811.

BAXENDALE, A. J., DAWSON, C. W., STEWART, S. E., MUDALIAR, V., REYNOLDS, G., GORDON, J., MURRAY, P. G., YOUNG, L. S. & ELIOPOULOS, A. G. 2005. Constitutive activation of the CD40 pathway promotes cell transformation and neoplastic growth. *Oncogene,* 24**,** 7913-7923.

BEDARD, K. & KRAUSE, K.-H. 2007. The NOX family of ROS-generating NADPH oxidases: physiology and pathophysiology. *Physiological reviews,* 87**,** 245-313.

BELLONE, S., WATTS, K., PALMIERI, M., CANNON, M. J., BURNETT, A., ROMAN, J. J., PECORELLI, S. & SANTIN, A. D. 2005. High serum levels of interleukin-6 in endometrial carcinoma are associated with uterine serous papillary histology, a highly aggressive and chemotherapy-resistant variant of endometrial cancer. *Gynecologic oncology,* 98**,** 92-98.

BELPERIO, J. A., KEANE, M. P., ARENBERG, D. A., ADDISON, C. L., EHLERT, J. E., BURDICK, M. D. & STRIETER, R. M. 2000. CXC chemokines in angiogenesis. *Journal of leukocyte biology,* 68**,** 1-8.

BENHAR, M., DALYOT, I., ENGELBERG, D. & LEVITZKI, A. 2001. Enhanced ROS production in oncogenically transformed cells potentiates c-Jun N-terminal kinase and p38 mitogen-activated protein kinase activation and sensitization to genotoxic stress. *Molecular and cellular biology,* 21**,** 6913-6926.

BENSON, R. J., HOSTAGER, B. S. & BISHOP, G. A. 2006. Rapid CD40-mediated rescue from CD95-induced apoptosis requires TNFR-associated factor-6 and PI3K. *European journal of immunology,* 36**,** 2535-2543.

BERG, T., HASBOLD, J., LAVALETTE, C. R., DÖPP, E., DIJKSTRA, C. & KLAUS, G. 1996. Properties of mouse CD40: differential expression of CD40 epitopes on dendritic cells and epithelial cells. *Immunology,* 88**,** 294-300.

BERGTOLD, A., DESAI, D. D., GAVHANE, A. & CLYNES, R. 2005. Cell surface recycling of internalized antigen permits dendritic cell priming of B cells. *Immunity,* 23**,** 503-514.

BERMUDEZ, O., PAGÈS, G. & GIMOND, C. 2010. The dual-specificity MAP kinase phosphatases: critical roles in development and cancer. *American Journal of Physiology-Cell Physiology,* 299**,** C189-C202.

BHOGAL, R. H., WESTON, C. J., CURBISHLEY, S. M., ADAMS, D. H. & AFFORD, S. C. 2012. Activation of CD40 with platelet derived CD154 promotes reactive oxygen species dependent death of human hepatocytes during hypoxia and reoxygenation. *PloS one,* 7**,** e30867.

BISHOP, D. & GAIL, A. The many faces of CD40: multiple roles in normal immunity and disease. Seminars in immunology, 2009. Academic Press, 255-256.

BISHOP, G. A. 2004. The multifaceted roles of TRAFs in the regulation of B-cell function. *Nature Reviews Immunology,* 4**,** 775-786.

BISHOP, G. A. & HOSTAGER, B. S. 2001. Signaling by CD40 and its mimics in B cell activation. *Immunologic research,* 24**,** 97-109.

BISHOP, G. A., HOSTAGER, B. S. & BROWN, K. D. 2002. Mechanisms of TNF receptor-associated factor (TRAF) regulation in B lymphocytes. *Journal of leukocyte biology,* 72**,** 19-23.

BISHOP, G. A., MOORE, C. R., XIE, P., STUNZ, L. L. & KRAUS, Z. J. 2007. TRAF proteins in CD40 signaling. *TNF Receptor Associated Factors (TRAFs).* Springer.

BISWAS, S., CHIDA, A. S. & RAHMAN, I. 2006. Redox modifications of protein–thiols: emerging roles in cell signaling. *Biochemical pharmacology,* 71**,** 551-564.

BLOSSOM, S., CHU, E. B., WEIGLE, W. O. & GILBERT, K. M. 1997. CD40 ligand expressed on B cells in the BXSB mouse model of systemic lupus erythematosus. *The Journal of Immunology,* 159**,** 4580-4586.

BOLDIN, M. P., GONCHAROV, T. M., GOLTSEVE, Y. V. & WALLACH, D. 1996. Involvement of MACH, a novel MORT1/FADD-interacting protease, in Fas/APO-1-and TNF receptor–induced cell death. *Cell,* 85**,** 803-815.

BOSSY-WETZEL, E., NEWMEYER, D. D. & GREEN, D. R. 1998. Mitochondrial cytochrome c release in apoptosis occurs upstream of DEVD-specific caspase activation and independently of mitochondrial transmembrane depolarization. *The EMBO journal,* 17**,** 37-49.

BOSWELL, R., YARD, B., SCHRAMA, E., VAN ES, L., DAHA, M. & VAN DER WOUDE, F. 1994. Interleukin 6 production by human proximal tubular epithelial cells in vitro: analysis of the effects of interleukin-1α (IL-1α) and other cytokines. *Nephrology Dialysis Transplantation,* 9**,** 599-606.

BOUCHER, A., DROZ, D., ADAFER, E. & NOËL, L.-H. 1986. Characterization of mononuclear cell subsets in renal cellular interstitial infiltrates. *Kidney international,* 29**,** 1043-1049.

BOUSSIOTIS, V. A., NADLER, L. M., STROMINGER, J. L. & GOLDFELD, A. E. 1994. Tumor necrosis factor alpha is an autocrine growth factor for normal human B cells. *Proceedings of the National Academy of Sciences,* 91**,** 7007-7011.

BRAESCH-ANDERSEN, S., PAULIE, S., KOHO, H., NIKA, H., ASPENSTRÖM, P. & PERLMANN, P. 1989. Biochemical characteristics and partial amino acid sequence of the receptor-like human B cell and carcinoma antigen CDw40. *The Journal of Immunology,* 142**,** 562-567.

BRANCHO, D., TANAKA, N., JAESCHKE, A., VENTURA, J.-J., KELKAR, N., TANAKA, Y., KYUUMA, M., TAKESHITA, T., FLAVELL, R. A. & DAVIS, R. J. 2003. Mechanism of p38 MAP kinase activation in vivo. *Genes & development,* 17**,** 1969-1978.

BRAT, D. J., BELLAIL, A. C. & VAN MEIR, E. G. 2005. The role of interleukin-8 and its receptors in gliomagenesis and tumoral angiogenesis. *Neuro-oncology,* 7**,** 122-133.

BRISCOE, D. M., ALEXANDER, S. I. & LICHTMAN, A. H. 1998. Interactions between T lymphocytes and endothelial cells in allograft rejection. *Current opinion in immunology,* 10**,** 525-531.

BRODACZEWSKA, K. K., SZCZYLIK, C., FIEDOROWICZ, M., PORTA, C. & CZARNECKA, A. M. 2016. Choosing the right cell line for renal cell cancer research. *Molecular Cancer,* 15**,** 83.

BROMBERG, J. F., HORVATH, C. M., WEN, Z., SCHREIBER, R. D. & DARNELL, J. E. 1996. Transcriptionally active Stat1 is required for the antiproliferative effects of both interferon alpha and interferon gamma. *Proceedings of the national academy of sciences,* 93**,** 7673-7678.

BROWN, D. I. & GRIENDLING, K. K. 2009. Nox proteins in signal transduction. *Free Radical Biology and Medicine,* 47**,** 1239-1253.

BROWN, K. D., HOSTAGER, B. S. & BISHOP, G. A. 2002. Regulation of TRAF2 signaling by self-induced degradation. *Journal of Biological Chemistry,* 277**,** 19433-19438.

BRUEY, J.-M., DUCASSE, C., BONNIAUD, P., RAVAGNAN, L., SUSIN, S. A., DIAZ-LATOUD, C., GURBUXANI, S., ARRIGO, A.-P., KROEMER, G. & SOLARY, E. 2000. Hsp27 negatively regulates cell death by interacting with cytochrome c. *Nature cell biology,* 2**,** 645-652.

BUGAJSKA, U., GEORGOPOULOS, N. T., SOUTHGATE, J., JOHNSON, P. W., GRABER, P., GORDON, J., SELBY, P. J. & TREJDOSIEWICZ, L. K. 2002. The effects of malignant transformation on susceptibility of human urothelial cells to CD40-mediated apoptosis. *Journal of the National Cancer Institute,* 94**,** 1381-95.

BUHTOIAROV, I. N., LUM, H., BERKE, G., PAULNOCK, D. M., SONDEL, P. M. & RAKHMILEVICH, A. L. 2005. CD40 ligation activates murine macrophages via an IFN-γ-dependent mechanism resulting in tumor cell destruction in vitro. *The Journal of Immunology,* 174**,** 6013-6022.

CABAL-HIERRO, L. & LAZO, P. S. 2012. Signal transduction by tumor necrosis factor receptors. *Cellular signalling,* 24**,** 1297-1305.

CAGNONI, F., ODDERA, S., GIRON-MICHEL, J., RICCIO, A. M., OLSSON, S., DELLACASA, P., MELIOLI, G., CANONICA, G. W. & AZZARONE, B. 2004. CD40 on adult human airway epithelial cells: expression and proinflammatory effects. *The Journal of Immunology,* 172**,** 3205-3214.

CAIN, K., BRATTON, S. B. & COHEN, G. M. 2002. The Apaf-1 apoptosome: a large caspase-activating complex. *Biochimie,* 84**,** 203-214.

CANDÉ, C., COHEN, I., DAUGAS, E., RAVAGNAN, L., LAROCHETTE, N., ZAMZAMI, N. & KROEMER, G. 2002. Apoptosis-inducing factor (AIF): a novel caspase-independent death effector released from mitochondria. *Biochimie,* 84**,** 215-222.

CAO, W., CAVACINI, L. A., TILLMAN, K. C. & POSNER, M. R. 2005. CD40 function in squamous cell cancer of the head and neck. *Oral oncology,* 41**,** 462-469.

CAPES-DAVIS, A., THEODOSOPOULOS, G., ATKIN, I., DREXLER, H. G., KOHARA, A., MACLEOD, R. A., MASTERS, J. R., NAKAMURA, Y., REID, Y. A. & REDDEL, R. R. 2010. Check your cultures! A list of cross-contaminated or misidentified cell lines. *International journal of cancer,* 127**,** 1-8.

CARBONE, E., RUGGIERO, G., TERRAZZANO, G., PALOMBA, C., MANZO, C., FONTANA, S., SPITS, H., KÄRRE, K. & ZAPPACOSTA, S. 1997. A new mechanism of NK cell cytotoxicity activation: the CD40–CD40 ligand interaction. *The Journal of experimental medicine,* 185**,** 2053-2060.

CARDONE, M. H., SALVESEN, G. S., WIDMANN, C., JOHNSON, G. & FRISCH, S. M. 1997. The regulation of anoikis: MEKK-1 activation requires cleavage by caspases. *Cell,* 90**,** 315-323.

CARGNELLO, M. & ROUX, P. P. 2011. Activation and function of the MAPKs and their substrates, the MAPK-activated protein kinases. *Microbiology and Molecular Biology Reviews,* 75**,** 50-83.

CASSATELLA, M., BAZZONI, F., FLYNN, R. M., DUSI, S., TRINCHIERI, G. & ROSSI, F. 1990. Molecular basis of interferon-gamma and lipopolysaccharide enhancement of phagocyte respiratory burst capability. Studies on the gene expression of several NADPH oxidase components. *Journal of Biological Chemistry,* 265**,** 20241-20246.

CASTIGLI, E., ALT, F. W., DAVIDSON, L., BOTTARO, A., MIZOGUCHI, E., BHAN, A. K. & GEHA, R. S. 1994. CD40-deficient mice generated by recombination-activating gene-2-deficient blastocyst complementation. *Proceedings of the National Academy of Sciences,* 91**,** 12135-12139.

CHA, G.-H., CHO, K. S., LEE, J. H., KIM, M., KIM, E., PARK, J., LEE, S. B. & CHUNG, J. 2003. Discrete functions of TRAF1 and TRAF2 in Drosophila melanogaster mediated by c-Jun N-terminal kinase and NF-κB-dependent signaling pathways. *Molecular and cellular biology,* 23**,** 7982-7991.

CHAI, J., DU, C., WU, J.-W., KYIN, S., WANG, X. & SHI, Y. 2000. Structural and biochemical basis of apoptotic activation by Smac/DIABLO. *Nature,* 406**,** 855-862.

CHAKRABARTI, S., VARGHESE, S., VITSEVA, O., TANRIVERDI, K. & FREEDMAN, J. E. 2005. CD40 ligand influences platelet release of reactive oxygen intermediates. *Arteriosclerosis, thrombosis, and vascular biology,* 25**,** 2428-2434.

CHALLA, A., POUND, J., GORDON, J. & ARMITAGE, R. 1999. Epitope-dependent synergism and antagonism between CD40 antibodies and soluble CD40 ligand for the regulation of CD23 expression and IgE synthesis in human B cells. *Allergy,* 54**,** 576-583.

CHAN, F. K.-M., CHUN, H. J., ZHENG, L., SIEGEL, R. M., BUI, K. L. & LENARDO, M. J. 2000. A domain in TNF receptors that mediates ligand-independent receptor assembly and signaling. *Science,* 288**,** 2351-2354.

CHANDEL, N. S., SCHUMACKER, P. T. & ARCH, R. H. 2001. Reactive oxygen species are downstream products of TRAF-mediated signal transduction. *Journal of Biological Chemistry,* 276**,** 42728-42736.

CHANG, B. S., MINN, A. J., MUCHMORE, S. W., FESIK, S. W. & THOMPSON, C. B. 1997. Identification of a novel regulatory domain in Bcl-xL and Bcl-2. *The EMBO journal,* 16**,** 968-977.

CHEN, Y., CHEN, J., XIONG, Y., DA, Q., XU, Y., JIANG, X. & TANG, H. 2006. Internalization of CD40 regulates its signal transduction in vascular endothelial cells. *Biochemical and biophysical research communications,* 345**,** 106-117.

CHENG, G., CLEARY, A. M., YE, Z.-S. & HONG, D. I. 1995. Involvement of CRAF1, a relative of TRAF, in CD40 signaling. *Science,* 267**,** 1494.

CHIN, Y. E., KITAGAWA, M., KUIDA, K., FLAVELL, R. A. & FU, X.-Y. 1997. Activation of the STAT signaling pathway can cause expression of caspase 1 and apoptosis. *Molecular and cellular biology,* 17**,** 5328-5337.

CHIPUK, J. E. & GREEN, D. R. 2008. How do BCL-2 proteins induce mitochondrial outer membrane permeabilization? *Trends in cell biology,* 18**,** 157-164.

CHOI, K.-S., SONG, E.-K. & YIM, C.-Y. 2008. Cytokines secreted by IL-2-activated lymphocytes induce endogenous nitric oxide synthesis and apoptosis in macrophages. *Journal of leukocyte biology,* 83**,** 1440-1450.

CHONGHAILE, T. N., SAROSIEK, K. A., VO, T.-T., RYAN, J. A., TAMMAREDDI, A., MOORE, V. D. G., DENG, J., ANDERSON, K. C., RICHARDSON, P. & TAI, Y.-T. 2011. Pretreatment mitochondrial priming correlates with clinical response to cytotoxic chemotherapy. *Science,* 334**,** 1129-1133.

CHOPRA, B., GEORGOPOULOS, N. T., NICHOLL, A., HINLEY, J., OLEKSIEWICZ, M. & SOUTHGATE, J. 2009. Structurally diverse peroxisome proliferator-activated receptor agonists induce apoptosis in human uro-epithelial cells by a receptor-independent mechanism involving store-operated calcium channels. *Cell proliferation,* 42**,** 688-700.

CHOUDHURY, J. A., RUSSELL, C. L., RANDHAWA, S., YOUNG, L. S., ADAMS, D. H. & AFFORD, S. C. 2003. Differential induction of nuclear factor-κB and activator protein-1 activity after CD40 ligation is associated with primary human hepatocyte apoptosis or intrahepatic endothelial cell proliferation. *Molecular biology of the cell,* 14**,** 1334-1345.

CHOWDHURY, F., JOHNSON, P. W., GLENNIE, M. J. & WILLIAMS, A. P. 2014. Ex vivo assays of dendritic cell activation and cytokine profiles as predictors of in vivo effects in an anti-human CD40 monoclonal antibody ChiLob 7/4 phase I trial. *Cancer immunology research,* 2**,** 229-240.

CHUNG, T. D., YU, J. J., KONG, T. A., SPIOTTO, M. T. & LIN, J. M. 2000. Interleukin-6 activates phosphatidylinositol-3 kinase, which inhibits apoptosis in human prostate cancer cell lines. *The Prostate,* 42**,** 1-7.

CIRCU, M. L. & AW, T. Y. 2010. Reactive oxygen species, cellular redox systems, and apoptosis. *Free Radical Biology and Medicine,* 48**,** 749-762.

CLARK, E. A. & LEDBETTER, J. A. 1986. Activation of human B cells mediated through two distinct cell surface differentiation antigens, Bp35 and Bp50. *Proceedings of the National Academy of Sciences,* 83**,** 4494-4498.

CLODI, K., ASGARY, Z., ZHAO, S., KLICHE, K. O., CABANILLAS, F., ANDREEFF, M. & YOUNES, A. 1998. Coexpression of CD40 and CD40 ligand in B-cell lymphoma cells. *British journal of haematology,* 103**,** 270-275.

COCKERILL, P. N., SHANNON, M. F., BERT, A. G., RYAN, G. R. & VADAS, M. A. 1993. The granulocyte-macrophage colony-stimulating factor/interleukin 3 locus is regulated by an inducible cyclosporin A-sensitive enhancer. *Proceedings of the National Academy of Sciences,* 90**,** 2466-2470.

COSTELLO, R. T., GASTAUT, J.-A. & OLIVE, D. 1999. What is the real role of CD40 in cancer immunotherapy? *Immunology today,* 20**,** 488-493.

COULOMBE, P. & MELOCHE, S. 2007. Atypical mitogen-activated protein kinases: structure, regulation and functions. *Biochimica et Biophysica Acta (BBA)-Molecular Cell Research,* 1773**,** 1376-1387.

COZEN, W., GILL, P. S., INGLES, S. A., MASOOD, R., MARTÍNEZ-MAZA, O., COCKBURN, M. G., GAUDERMAN, W. J., PIKE, M. C., BERNSTEIN, L. & NATHWANI, B. N. 2004. IL-6 levels and genotype are associated with risk of young adult Hodgkin lymphoma. *Blood,* 103**,** 3216-3221.

CRABTREE, G. R. & OLSON, E. N. 2002. NFAT signaling: choreographing the social lives of cells. *Cell,* 109**,** S67-S79.

CRALLAN, R., GEORGOPOULOS, N. T. & SOUTHGATE, J. 2006. Experimental models of human bladder carcinogenesis. *Carcinogenesis,* 27**,** 374-381.

CROMPTON, M. 1999. The mitochondrial permeability transition pore and its role in cell death. *Biochemical Journal,* 341**,** 233-249.

CROSS, C. E., HALLIWELL, B., BORISH, E. T., PRYOR, W. A., AMES, B. N., SAUL, R. L., MCCORD, J. M. & HARMAN, D. 1987. Oxygen radicals and human disease. *Annals of internal medicine,* 107**,** 526-545.

CUADRADO, A. & NEBREDA, A. 2010. Mechanisms and functions of p38 MAPK signalling. *Biochem. J,* 429**,** 403-417.

CULIG, Z. & PUHR, M. 2012. Interleukin-6: a multifunctional targetable cytokine in human prostate cancer. *Molecular and cellular endocrinology,* 360**,** 52-58.

CULLEN, S. & MARTIN, S. 2009. Caspase activation pathways: some recent progress. Nature Publishing Group.

D'AUTRÉAUX, B. & TOLEDANO, M. B. 2007. ROS as signalling molecules: mechanisms that generate specificity in ROS homeostasis. *Nature reviews Molecular cell biology,* 8**,** 813-824.

DADGOSTAR, H., ZARNEGAR, B., HOFFMANN, A., QIN, X.-F., TRUONG, U., RAO, G., BALTIMORE, D. & CHENG, G. 2002. Cooperation of multiple signaling pathways in CD40-regulated gene expression in B lymphocytes. *Proceedings of the National Academy of Sciences,* 99**,** 1497-1502.

DALLMAN, C., JOHNSON, P. & PACKHAM, G. 2003. Differential regulation of cell survival by CD40. *Apoptosis,* 8**,** 45-53.

DAVIES, C. C., MAK, T. W., YOUNG, L. S. & ELIOPOULOS, A. G. 2005. TRAF6 is required for TRAF2-dependent CD40 signal transduction in nonhemopoietic cells. *Molecular and cellular biology,* 25**,** 9806-9819.

DAVIES, C. C., MASON, J., WAKELAM, M. J., YOUNG, L. S. & ELIOPOULOS, A. G. 2004. Inhibition of phosphatidylinositol 3-kinase-and ERK MAPK-regulated protein synthesis reveals the pro-apoptotic properties of CD40 ligation in carcinoma cells. *Journal of Biological Chemistry,* 279**,** 1010-1019.

DAVIS, R. J. 2000. Signal transduction by the JNK group of MAP kinases. *Cell,* 103**,** 239-252.

DE DEKEN, X., WANG, D., MANY, M.-C., COSTAGLIOLA, S., LIBERT, F., VASSART, G., DUMONT, J. E. & MIOT, F. 2000. Cloning of two human thyroid cDNAs encoding new members of the NADPH oxidase family. *Journal of Biological Chemistry,* 275**,** 23227-23233.

DE MOOR, J. S., MARIOTTO, A. B., PARRY, C., ALFANO, C. M., PADGETT, L., KENT, E. E., FORSYTHE, L., SCOPPA, S., HACHEY, M. & ROWLAND, J. H. 2013. Cancer survivors in the United States: prevalence across the survivorship trajectory and implications for care. *Cancer Epidemiology Biomarkers & Prevention,* 22**,** 561-570.

DEBATIN, K.-M. & KRAMMER, P. H. 2004. Death receptors in chemotherapy and cancer. *Oncogene,* 23**,** 2950-2966.

DECKERS, J., DE HAIJ, S., VAN DER WOUDE, F., VAN DER KOOIJ, S., DAHA, M. R. & VAN KOOTEN, C. 1998. IL-4 and IL-13 augment cytokine-and CD40-induced RANTES production by human renal tubular epithelial cells in vitro. *Journal of the American Society of Nephrology,* 9**,** 1187-1193.

DECLERCQ, W., DENECKER, G., FIERS, W. & VANDENABEELE, P. 1998. Cooperation of both TNF receptors in inducing apoptosis: involvement of the TNF receptor-associated factor binding domain of the TNF receptor 75. *The Journal of Immunology,* 161**,** 390-399.

DEGLI-ESPOSTI, M. A., DAVIS-SMITH, T., DIN, W. S., SMOLAK, P. J., GOODWIN, R. G. & SMITH, C. A. 1997. Activation of the lymphotoxin beta receptor by cross-linking induces chemokine production and growth arrest in A375 melanoma cells. *The Journal of Immunology,* 158**,** 1756-1762.

DELIVORIA-PAPADOPOULOS, M., GORN, M., ASHRAF, Q. M. & MISHRA, O. P. 2007. ATP and cytochrome c-dependent activation of caspase-9 during hypoxia in the cerebral cortex of newborn piglets. *Neuroscience letters,* 429**,** 115-119.

DEMPSEY, P. W., DOYLE, S. E., HE, J. Q. & CHENG, G. 2003. The signaling adaptors and pathways activated by TNF superfamily. *Cytokine & growth factor reviews,* 14**,** 193-209.

DENAULT, J.-B. & SALVESEN, G. S. 2002. Caspases: keys in the ignition of cell death. *Chemical reviews,* 102**,** 4489-4500.

DERIJARD, B., RAINGEAUD, J., BARRETT, T. & WU, I.-H. 1995. Independent human MAP kinase signal transduction pathways defined by MEK and MKK isoforms. *Science,* 267**,** 682.

DEVERAUX, Q. L., LEO, E., STENNICKE, H. R., WELSH, K., SALVESEN, G. S. & REED, J. C. 1999. Cleavage of human inhibitor of apoptosis protein XIAP results in fragments with distinct specificities for caspases. *The EMBO journal,* 18**,** 5242-5251.

DHANASEKARAN, D. N. & REDDY, E. P. 2008. JNK signaling in apoptosis. *Oncogene,* 27**,** 6245-6251.

DIEHL, L., DEN BOER, A. T., SCHOENBERGER, S. P., VAN DER VOORT, E. I., SCHUMACHER, T. N., MELIEF, C. J., OFFRINGA, R. & TOES, R. E. 1999. CD40 activation in vivo overcomes peptide-induced peripheral cytotoxic T-lymphocyte tolerance and augments anti-tumor vaccine efficacy. *Nature medicine,* 5**,** 774-779.

DU, C., FANG, M., LI, Y., LI, L. & WANG, X. 2000. Smac, a mitochondrial protein that promotes cytochrome c–dependent caspase activation by eliminating IAP inhibition. *Cell,* 102**,** 33-42.

DUNNILL, C., IBRAHEEM, K., MOHAMED, A., SOUTHGATE, J. & GEORGOPOULOS, N. T. 2016. A redox state-dictated signalling pathway deciphers the malignant cell specificity of CD40-mediated apoptosis. *Oncogene*.

DUNNILL, C. J. 2013. *The role of CD40 in epithelial cell fate.* University of Huddersfield.

DUQUE-PARRA, J. E. 2005. Note on the origin and history of the term “apoptosis”. *The Anatomical Record Part B: The New Anatomist,* 283**,** 2-4.

EDLICH, F., BANERJEE, S., SUZUKI, M., CLELAND, M. M., ARNOULT, D., WANG, C., NEUTZNER, A., TJANDRA, N. & YOULE, R. J. 2011. Bcl-x L retrotranslocates Bax from the mitochondria into the cytosol. *Cell,* 145**,** 104-116.

EKERT, P. G., SILKE, J., HAWKINS, C. J., VERHAGEN, A. M. & VAUX, D. L. 2001. DIABLO promotes apoptosis by removing MIHA/XIAP from processed caspase 9. *The Journal of cell biology,* 152**,** 483-490.

ELGUETA, R., BENSON, M. J., DE VRIES, V. C., WASIUK, A., GUO, Y. & NOELLE, R. J. 2009. Molecular mechanism and function of CD40/CD40L engagement in the immune system. *Immunological reviews,* 229**,** 152-172.

ELIOPOULOS, A. G., DAVIES, C., KNOX, P. G., GALLAGHER, N. J., AFFORD, S. C., ADAMS, D. H. & YOUNG, L. S. 2000. CD40 induces apoptosis in carcinoma cells

through activation of cytotoxic ligands of the tumor necrosis factor superfamily. *Molecular and cellular biology,* 20**,** 5503-5515.

ELIOPOULOS, A. G., DAWSON, C. W., MOSIALOS, G., FLOETTMANN, J. E., ROWE, M., ARMITAGE, R. J., DAWSON, J., ZAPATA, J., KERR, D. J. & WAKELAM, M. 1996. CD40-induced growth inhibition in epithelial cells is mimicked by Epstein-Barr Virus-encoded LMP1: involvement of TRAF3 as a common mediator. *Oncogene,* 13**,** 2243-2254.

ELIOPOULOS, A. G., STACK, M., DAWSON, C. W., KAYE, K. M., HODGKIN, L., SIHOTA, S., ROWE, M. & YOUNG, L. S. 1997. Epstein-Barr virus-encoded LMP1 and CD40 mediate IL-6 production in epithelial cells via an NF-kB pathway involving TNF receptor-associated factors. *Oncogene,* 14**,** 2899-2916.

ELIOPOULOS, A. G. & YOUNG, L. S. 2004. The role of the CD40 pathway in the pathogenesis and treatment of cancer. *Current opinion in pharmacology,* 4**,** 360-367.

ELLMARK, P. 2002. *The CD40 Receptor-Target, Tool and Technology*, Lund University.

ELMETWALI, T., SEARLE, P. F., MCNEISH, I., YOUNG, L. S. & PALMER, D. H. 2010a. CD40 ligand induced cytotoxicity in carcinoma cells is enhanced by inhibition of metalloproteinase cleavage and delivery via a conditionally-replicating adenovirus. *Mol Cancer,* 9**,** 52.

ELMETWALI, T., YOUNG, L. S. & PALMER, D. H. 2010b. CD40 ligand-induced carcinoma cell death: a balance between activation of TNFR-associated factor (TRAF) 3-dependent death signals and suppression of TRAF6-dependent survival signals. *The Journal of Immunology,* 184**,** 1111-1120.

ELMORE, S. 2007. Apoptosis: a review of programmed cell death. *Toxicologic pathology,* 35**,** 495-516.

ENGELS, I. H., TOTZKE, G., FISCHER, U., SCHULZE-OSTHOFF, K. & JÄNICKE, R. U. 2005. Caspase-10 sensitizes breast carcinoma cells to TRAIL-induced but not tumor necrosis factor-induced apoptosis in a caspase-3-dependent manner. *Molecular and cellular biology,* 25**,** 2808-2818.

ERMOLAEVA, M. A. 2008. *Analysis of the physiological function of TNF Receptor I Associated Death Domain Protein (TRADD) and Familial Cylindromatosis Protein (CYLD) by using conditional gene targeting in mice.*

FERNANDES, M. T., DEJARDIN, E. & DOS SANTOS, N. R. 2016. Context-dependent roles for lymphotoxin-β receptor signaling in cancer development. *Biochimica et Biophysica Acta (BBA)-Reviews on Cancer,* 1865**,** 204-219.

FERRI, K. F. & KROEMER, G. 2001. Organelle-specific initiation of cell death pathways. *Nature cell biology,* 3**,** E255-E263.

FESIK, S. W. & SHI, Y. 2001. Controlling the caspases. *Science,* 294**,** 1477-1478.

FINKEL, T. 1998. Oxygen radicals and signaling. *Current opinion in cell biology,* 10**,** 248-253.

FLECKENSTEIN, D. S., DIRKS, W. G., DREXLER, H. G. & QUENTMEIER, H. 2003. Tumor necrosis factor receptor-associated factor (TRAF) 4 is a new binding partner for the p70S6 serine/threonine kinase. *Leukemia research,* 27**,** 687-694.

FLEMING, Y., ARMSTRONG, C. G., MORRICE, N., PATERSON, A., GOEDERT, M. & COHEN, P. 2000. Synergistic activation of stress-activated protein kinase 1/c-Jun N-terminal kinase (SAPK1/JNK) isoforms by mitogen-activated protein kinase kinase 4 (MKK4) and MKK7. *Biochemical Journal,* 352**,** 145-154.

FONSATTI, E., MAIO, M., ALTOMONTE, M. & HERSEY, P. Biology and clinical applications of CD40 in cancer treatment. Seminars in oncology, 2010. Elsevier, 517-523.

FRENCH, R. R., CHAN, H. C., TUTT, A. L. & GLENNIE, M. J. 1999. CD40 antibody evokes a cytotoxic T-cell response that eradicates lymphoma and bypasses T-cell help. *Nature medicine,* 5**,** 548-553.

FUJINO, G., NOGUCHI, T., TAKEDA, K. & ICHIJO, H. Thioredoxin and protein kinases in redox signaling. Seminars in cancer biology, 2006. Elsevier, 427-435.

FUNAKOSHI, S., LONGO, D. L., BECKWITH, M., CONLEY, D. K., TSARFATY, G., TSARFATY, I., ARMITAGE, R. J., FANSLOW, W. C., SPRIGGS, M. K. & MURPHY, W. J. 1994. Inhibition of human B-cell lymphoma growth by CD40 stimulation. *Blood,* 83**,** 2787-2794.

GAIL A BISHOP, C. R. M., PING XIE, LAURA L. STUNZ & KRAUS, A. Z. J. 2007. TRAF Proteins in CD40 Signaling. *TNF Receptor Associated Factors (TRAFs)***,** 131-151.

GALLAGHER, E., ENZLER, T., MATSUZAWA, A., ANZELON-MILLS, A., OTERO, D., HOLZER, R., JANSSEN, E., GAO, M. & KARIN, M. 2007. Kinase MEKK1 is required for CD40-dependent activation of the kinases Jnk and p38, germinal center formation, B cell proliferation and antibody production. *Nature immunology,* 8**,** 57-63.

GALLAGHER, N., ELIOPOULOS, A., AGATHANGELO, A. & OATES, J. 2002a. CD40 activation in epithelial ovarian carcinoma cells modulates growth, apoptosis, and cytokine secretion. *Journal of Clinical Pathology,* 55**,** 110.

GALLAGHER, N., ELIOPOULOS, A., AGATHANGELO, A., OATES, J., CROCKER, J. & YOUNG, L. 2002b. CD40 activation in epithelial ovarian carcinoma cells modulates growth, apoptosis, and cytokine secretion. *Molecular Pathology,* 55**,** 110.

GALLUZZI, L., AARONSON, S., ABRAMS, J., ALNEMRI, E., ANDREWS, D., BAEHRECKE, E., BAZAN, N., BLAGOSKLONNY, M., BLOMGREN, K. & BORNER, C. 2009a. Guidelines for the use and interpretation of assays for monitoring cell death in higher eukaryotes. *Cell Death & Differentiation,* 16**,** 1093-1107.

GALLUZZI, L., BRAVO-SAN PEDRO, J. M. & KROEMER, G. 2014. Organelle-specific initiation of cell death. *Nature cell biology,* 16**,** 728-736.

GALLUZZI, L., GIORDANETTO, F. & KROEMER, G. 2009b. Targeting HSP70 for cancer therapy. *Molecular cell,* 36**,** 176-177.

GALLUZZI, L., VITALE, I., ABRAMS, J., ALNEMRI, E., BAEHRECKE, E., BLAGOSKLONNY, M., DAWSON, T., DAWSON, V., EL-DEIRY, W. & FULDA, S. 2011. Molecular definitions of cell death subroutines: recommendations of the Nomenclature Committee on Cell Death 2012. *Cell Death & Differentiation,* 19**,** 107-120.

GARDAM, S., SIERRO, F., BASTEN, A., MACKAY, F. & BRINK, R. 2008. TRAF2 and TRAF3 signal adapters act cooperatively to control the maturation and survival signals delivered to B cells by the BAFF receptor. *Immunity,* 28**,** 391-401.

GASSON, J. C. 1991. Molecular physiology of granulocyte-macrophage colony-stimulating factor. *Blood,* 77**,** 1131-1145.

GEIGER, P. C., WRIGHT, D. C., HAN, D.-H. & HOLLOSZY, J. O. 2005. Activation of p38 MAP kinase enhances sensitivity of muscle glucose transport to insulin. *American Journal of Physiology-Endocrinology and Metabolism,* 288**,** E782-E788.

GELBMANN, C., LEEB, S., VOGL, D., MAENDEL, M., HERFARTH, H., SCHÖLMERICH, J., FALK, W. & ROGLER, G. 2003. Inducible CD40 expression mediates NFκB activation and cytokine secretion in human colonic fibroblasts. *Gut,* 52**,** 1448-1456.

GELDART, T., HARVEY, M., CARR, N., GLENNIE, M. & JOHNSON, P. Cancer immunotherapy with a chimeric anti-CD40 monoclonal antibody: Evidence of preclinical efficacy. ASCO Annual Meeting Proceedings, 2004. 2577.

GEORGOPOULOS, N. T., MERRICK, A., SCOTT, N., SELBY, P. J., MELCHER, A. & TREJDOSIEWICZ, L. K. 2007. CD40-mediated death and cytokine secretion in colorectal cancer: A potential target for inflammatory tumour cell killing. *International journal of cancer,* 121**,** 1373-1381.

GEORGOPOULOS, N. T., STEELE, L. P., THOMSON, M., SELBY, P. J., SOUTHGATE, J. & TREJDOSIEWICZ, L. K. 2006. A novel mechanism of CD40-induced apoptosis of carcinoma cells involving TRAF3 and JNK/AP-1 activation. *Cell Death & Differentiation,* 13**,** 1789-1801.

GERRITSMA, J., HIEMSTRA, P., GERRITSEN, A., PRODJOSUDJADI, W., VERWEIJ, C., VAN ES, L. & DAHA, M. 1996. Regulation and production of IL-8 by human proximal tubular epithelial cells in vitro. *Clinical & Experimental Immunology,* 103**,** 289-294.

GERRITSMA, J. S., VAN KOOTEN, C., GERRITSEN, A. F., VAN ES, L. A. & DAHA, M. R. 1998. Transforming growth factor-β1 regulates chemokine and complement production by human proximal tubular epithelial cells. *Kidney international,* 53**,** 609-616.

GEWIES, A. 2003. ApoReview-Introduction to Apoptosis. *2003***,** 1-26.

GHAMANDE, S., HYLANDER, B. L., OFLAZOGLU, E., LELE, S., FANSLOW, W. & REPASKY, E. A. 2001. Recombinant CD40 ligand therapy has significant antitumor effects on CD40-positive ovarian tumor xenografts grown in SCID mice and demonstrates an augmented effect with cisplatin. *Cancer research,* 61**,** 7556-7562.

GIROIR, B. P., BROWN, T. & BEUTLER, B. 1992. Constitutive synthesis of tumor necrosis factor in the thymus. *Proceedings of the National Academy of Sciences,* 89**,** 4864-4868.

GLAND, P. 2012. General Human Physiology for the Sleep. *Fundamentals of Sleep Technology***,** 78.

GLAUNER, H., SIEGMUND, D., MOTEJADDED, H., SCHEURICH, P., HENKLER, F., JANSSEN, O. & WAJANT, H. 2002. Intracellular localization and transcriptional regulation of tumor necrosis factor (TNF) receptor-associated factor 4 (TRAF4). *European journal of biochemistry,* 269**,** 4819-4829.

GOGVADZE, V., ORRENIUS, S. & ZHIVOTOVSKY, B. 2008. Mitochondria in cancer cells: what is so special about them? *Trends in cell biology,* 18**,** 165-173.

GOLDSTEIN, J. C., WATERHOUSE, N. J., JUIN, P., EVAN, G. I. & GREEN, D. R. 2000. The coordinate release of cytochrome c during apoptosis is rapid, complete and kinetically invariant. *Nature cell biology,* 2**,** 156-162.

GOMMERMAN, J. L. & SUMMERS DELUCA, L. 2011. LTβR and CD40: working together in dendritic cells to optimize immune responses. *Immunological reviews,* 244**,** 85-98.

GORDON, J. 1995. CD40 and its ligand: central players in B lymphocyte survival, growth, and differentiation. *Blood reviews,* 9**,** 53-56.

GORDON, J. & POUND, J. 2000. Fortifying B cells with CD154: an engaging tale of many hues. *Immunology,* 100**,** 269-280.

GORMAND, F., BRIERE, F., PEYROL, S., RACCURT, M., DURAND, I., AIT-YAHIA, S., LEBECQUE, S., BANCHEREAU, J. & PACHECO, Y. 1999. CD40 expression by human bronchial epithelial cells. *Scandinavian journal of immunology,* 49**,** 355-361.

GRAMMER, A. C. & LIPSKY, P. E. 2000. CD40-mediated regulation of immune responses by TRAF-dependent and TRAF-independent signaling mechanisms. *Advances in immunology,* 76**,** 61-178.

GRAMMER, A. C. & LIPSKY, P. E. 2001. CD40-mediated regulation of immune responses by TRAF-dependent and TRAF-independent signaling mechanisms. *Advances in immunology,* 76**,** 61-178.

GREEN, D. R. & KROEMER, G. 2004. The pathophysiology of mitochondrial cell death. *Science,* 305**,** 626-629.

GRELL, M., ZIMMERMANN, G., GOTTFRIED, E., CHEN, C. M., GRÜNWALD, U., HUANG, D., LEE, Y. H. W., DÜRKOP, H., ENGELMANN, H. & SCHEURICH, P. 1999. Induction of cell death by tumour necrosis factor (TNF) receptor 2, CD40 and CD30: a role for TNF-R1 activation by endogenous membrane-anchored TNF. *The EMBO journal,* 18**,** 3034-3043.

GROSS, A., MCDONNELL, J. M. & KORSMEYER, S. J. 1999. BCL-2 family members and the mitochondria in apoptosis. *Genes & development,* 13**,** 1899-1911.

GRUSS, H.-J., HERRMANN, F., GATTEI, V., GLOGHINI, A., PINTO, A. & CARBONE, A. 1997. CD40/CD40 ligand interactions in normal, reactive and malignant lympho-hematopoietic tissues. *Leukemia & lymphoma,* 24**,** 393-422.

GRÜTTER, M. G. 2000. Caspases: key players in programmed cell death. *Current opinion in structural biology,* 10**,** 649-655.

GUO, Y., XU, F., LU, T., DUAN, Z. & ZHANG, Z. 2012. Interleukin-6 signaling pathway in targeted therapy for cancer. *Cancer treatment reviews,* 38**,** 904-910.

GUPTA, S. C., HEVIA, D., PATCHVA, S., PARK, B., KOH, W. & AGGARWAL, B. B. 2012. Upsides and downsides of reactive oxygen species for cancer: the roles of reactive oxygen species in tumorigenesis, prevention, and therapy. *Antioxidants & redox signaling,* 16**,** 1295-1322.

HA, Y. J. & LEE, J. R. 2004. Role of TNF receptor-associated factor 3 in the CD40 signaling by production of reactive oxygen species through association with p40phox, a cytosolic

subunit of nicotinamide adenine dinucleotide phosphate oxidase. *The Journal of Immunology,* 172**,** 231-239.

HA, Y. J., SEUL, H. J. & LEE, J. R. 2011. Ligation of CD40 receptor in human B lymphocytes triggers the 5-lipoxygenase pathway to produce reactive oxygen species and activate p38 MAPK. *Experimental & molecular medicine,* 43**,** 101-110.

HÄCKER, H., TSENG, P.-H. & KARIN, M. 2011. Expanding TRAF function: TRAF3 as a tri-faced immune regulator. *Nature Reviews Immunology,* 11**,** 457-468.

HALLIWELL, B. 2007. Oxidative stress and cancer: have we moved forward? *Biochemical Journal,* 401**,** 1-11.

HANAHAN, D. & WEINBERG, R. A. 2000. The hallmarks of cancer. *Cell,* 100**,** 57-70.

HANAHAN, D. & WEINBERG, R. A. 2011. Hallmarks of cancer: the next generation. *Cell,* 144**,** 646-74.

HANCOCK, J., DESIKAN, R. & NEILL, S. 2001. Role of reactive oxygen species in cell signalling pathways. *Biochemical Society Transactions,* 29**,** 345-349.

HARADA, H., BECKNELL, B., WILM, M., MANN, M., HUANG, L. J.-S., TAYLOR, S. S., SCOTT, J. D. & KORSMEYER, S. J. 1999. Phosphorylation and inactivation of BAD by mitochondria-anchored protein kinase A. *Molecular cell,* 3**,** 413-422.

HARRIS, I. S., TRELOAR, A. E., INOUE, S., SASAKI, M., GORRINI, C., LEE, K. C., YUNG, K. Y., BRENNER, D., KNOBBE-THOMSEN, C. B. & COX, M. A. 2015. Glutathione and thioredoxin antioxidant pathways synergize to drive cancer initiation and progression. *Cancer cell,* 27**,** 211-222.

HASSAN, S. B., SØRENSEN, J. F., OLSEN, B. N. & PEDERSEN, A. E. 2014. Anti-CD40-mediated cancer immunotherapy: an update of recent and ongoing clinical trials. *Immunopharmacology and immunotoxicology,* 36**,** 96-104.

HAUER, J., PÜSCHNER, S., RAMAKRISHNAN, P., SIMON, U., BONGERS, M., FEDERLE, C. & ENGELMANN, H. 2005. TNF receptor (TNFR)-associated factor (TRAF) 3 serves as an inhibitor of TRAF2/5-mediated activation of the noncanonical NF-κB pathway by TRAF-binding TNFRs. *Proceedings of the National Academy of Sciences of the United States of America,* 102**,** 2874-2879.

HAYAKAWA, J., MITTAL, S., WANG, Y., KORKMAZ, K. S., ADAMSON, E., ENGLISH, C., OHMICHI, M., MCCLELLAND, M. & MERCOLA, D. 2005. Identification of promoters bound by c-Jun/ATF2 during rapid large-scale gene activation following genotoxic stress. *Molecular Cell,* 17**,** 161.

HE, L., GRAMMER, A. C., WU, X. & LIPSKY, P. E. 2004. TRAF3 forms heterotrimers with TRAF2 and modulates its ability to mediate NF-κB activation. *Journal of Biological Chemistry,* 279**,** 55855-55865.

HE, L., WU, X., SIEGEL, R. & LIPSKY, P. E. 2006. TRAF6 regulates cell fate decisions by inducing caspase 8-dependent apoptosis and the activation of NF-κB. *Journal of biological chemistry,* 281**,** 11235-11249.

HEALY, E., LEONARD, M., MADRIGAL-ESTEBAS, L., O'FARRELLY, C., WATSON, A. J. & RYAN, M. P. 1999. Factors produced by activated leukocytes alter renal epithelial cell differentiation. *Kidney international,* 56**,** 1266-1269.

HEGDE, R., SRINIVASULA, S. M., ZHANG, Z., WASSELL, R., MUKATTASH, R., CILENTI, L., DUBOIS, G., LAZEBNIK, Y., ZERVOS, A. S. & FERNANDES-ALNEMRI, T. 2002. Identification of Omi/HtrA2 as a mitochondrial apoptotic serine protease that disrupts inhibitor of apoptosis protein-caspase interaction. *Journal of Biological Chemistry,* 277**,** 432-438.

HEHLGANS, T. & PFEFFER, K. 2005. The intriguing biology of the tumour necrosis factor/tumour necrosis factor receptor superfamily: players, rules and the games. *Immunology,* 115**,** 1-20.

HEISKANEN, K. M., BHAT, M. B., WANG, H.-W., MA, J. & NIEMINEN, A.-L. 1999. Mitochondrial Depolarization Accompanies Cytochrome cRelease During Apoptosis in PC6 Cells. *Journal of Biological Chemistry,* 274**,** 5654-5658.

HENGARTNER, M. O. 2000. The biochemistry of apoptosis. *Nature,* 407**,** 770-776.

HERNANDEZ-CASELLES, T. & STUTMAN, O. 1993. Immune functions of tumor necrosis factor. I. Tumor necrosis factor induces apoptosis of mouse thymocytes and can also stimulate or inhibit IL-6-induced proliferation depending on the concentration of mitogenic costimulation. *The Journal of Immunology,* 151**,** 3999-4012.

HERNÁNDEZ-MUNAIN, C. & KRANGEL, M. S. 2002. Distinct roles for c-Myb and core binding factor/polyoma enhancer-binding protein 2 in the assembly and function of a multiprotein complex on the TCR δ enhancer in vivo. *The Journal of Immunology,* 169**,** 4362-4369.

HESS, S. & ENGELMANN, H. 1996a. A novel function of CD40: induction of cell death in transformed cells. *Journal of Experimental Medicine,* 183**,** 159-167.

HESS, S. & ENGELMANN, H. 1996b. A novel function of CD40: induction of cell death in transformed cells. *The Journal of experimental medicine,* 183**,** 159-167.

HILL, A. & CHAPEL, H. 1993. X-linked immunodeficiency. The fruits of cooperation.

HILL, K. S., ERRINGTON, F., STEELE, L. P., MERRICK, A., MORGAN, R., SELBY, P. J., GEORGOPOULOS, N. T., O'DONNELL, D. M. & MELCHER, A. A. 2008. OK432-activated human dendritic cells kill tumor cells via CD40/CD40 ligand interactions. *The Journal of Immunology,* 181**,** 3108-3115.

HILL, S. C., YOUDE, S. J., MAN, S., TEALE, G. R., BAXENDALE, A. J., HISLOP, A., DAVIES, C. C., LUESLEY, D. M., BLOM, A. M. & RICKINSON, A. B. 2005. Activation of CD40 in cervical carcinoma cells facilitates CTL responses and augments chemotherapy-induced apoptosis. *The Journal of Immunology,* 174**,** 41-50.

HIRANO, A., LONGO, D. L., TAUB, D. D., FERRIS, D. K., YOUNG, L. S., ELIOPOULOS, A. G., AGATHANGGELOU, A., CULLEN, N., MACARTNEY, J. & FANSLOW, W. C. 1999. Inhibition of human breast carcinoma growth by a soluble recombinant human CD40 ligand. *Blood,* 93**,** 2999-3007.

HIRANO, T. 2010. Interleukin 6 in autoimmune and inflammatory diseases: a personal memoir. *Proceedings of the Japan Academy. Series B, Physical and biological sciences,* 86**,** 717.

HITOSHI, Y., LORENS, J., KITADA, S.-I., FISHER, J., LABARGE, M., RING, H. Z., FRANCKE, U., REED, J. C., KINOSHITA, S. & NOLAN, G. P. 1998. Toso, a cell surface, specific regulator of Fas-induced apoptosis in T cells. *Immunity,* 8**,** 461-471.

HOFFMAN, A., SPETNER, L. & BURKE, M. 2008. Ramifications of a redox switch within a normal cell: its absence in a cancer cell. *Free Radical Biology and Medicine,* 45**,** 265-268.

HOGAN, P. G., CHEN, L., NARDONE, J. & RAO, A. 2003. Transcriptional regulation by calcium, calcineurin, and NFAT. *Genes & development,* 17**,** 2205-2232.

HÖLL, M., KOZIEL, R., SCHÄFER, G., PIRCHER, H., PAUCK, A., HERMANN, M., KLOCKER, H., JANSEN-DÜRR, P. & SAMPSON, N. 2014. ROS signaling by NADPH oxidase 5 modulates the proliferation and survival of prostate carcinoma cells. *Molecular carcinogenesis*.

HOSTAGER, B. S. & BISHOP, G. A. 1999. Cutting edge: contrasting roles of TNF receptor-associated factor 2 (TRAF2) and TRAF3 in CD40-activated B lymphocyte differentiation. *The Journal of Immunology,* 162**,** 6307-6311.

HOSTAGER, B. S., CATLETT, I. M. & BISHOP, G. A. 2000. Recruitment of CD40 and tumor necrosis factor receptor-associated factors 2 and 3 to membrane microdomains during CD40 signaling. *Journal of Biological Chemistry,* 275**,** 15392-15398.

HOSTAGER, B. S., HAXHINASTO, S. A., ROWLAND, S. L. & BISHOP, G. A. 2003. Tumor necrosis factor receptor-associated factor 2 (TRAF2)-deficient B lymphocytes reveal novel roles for TRAF2 in CD40 signaling. *Journal of Biological Chemistry,* 278**,** 45382-45390.

HSING, Y., HOSTAGER, B. S. & BISHOP, G. A. 1997. Characterization of CD40 signaling determinants regulating nuclear factor-kappa B activation in B lymphocytes. *The Journal of Immunology,* 159**,** 4898-4906.

HU, B. T., LEE, S. C., MARIN, E., RYAN, D. H. & INSEL, R. A. 1997. Telomerase is up-regulated in human germinal center B cells in vivo and can be re-expressed in memory B cells activated in vitro. *The Journal of Immunology,* 159**,** 1068-1071.

HU, Y., DING, L., SPENCER, D. M. & NÚÑEZ, G. 1998. WD-40 repeat region regulates Apaf-1 self-association and procaspase-9 activation. *Journal of Biological Chemistry,* 273**,** 33489-33494.

HÜBNER, A., BARRETT, T., FLAVELL, R. A. & DAVIS, R. J. 2008. Multisite phosphorylation regulates Bim stability and apoptotic activity. *Molecular cell,* 30**,** 415-425.

HWANG, J.-H., KIM, S.-W., LEE, H.-J., YUN, H.-J., KIM, S. & JO, D.-Y. 2006. Interferon γ has dual potential in inhibiting or promoting survival and growth of hematopoietic progenitors: interactions with stromal cell-derived factor 1. *International journal of hematology,* 84**,** 143-150.

ICHIJO, H., NISHIDA, E., IRIE, K., TEN DIJKE, P., SAITOH, M., MORIGUCHI, T., TAKAGI, M., MATSUMOTO, K., MIYAZONO, K. & GOTOH, Y. 1997. Induction of apoptosis by

ASK1, a mammalian MAPKKK that activates SAPK/JNK and p38 signaling pathways. *Science,* 275**,** 90-94.

IMADA, K. & LEONARD, W. J. 2000. The jak-STAT pathway. *Molecular immunology,* 37**,** 1-11.

INOUE, J.-I., ISHIDA, T., TSUKAMOTO, N., KOBAYASHI, N., NAITO, A., AZUMA, S. & YAMAMOTO, T. 2000. Tumor necrosis factor receptor-associated factor (TRAF) family: adapter proteins that mediate cytokine signaling. *Experimental cell research,* 254**,** 14-24.

INOUE, M., SATO, E. F., NISHIKAWA, M., PARK, A.-M., KIRA, Y., IMADA, I. & UTSUMI, K. 2003. Mitochondrial generation of reactive oxygen species and its role in aerobic life. *Current medicinal chemistry,* 10**,** 2495-2505.

INOUE, Y., OTSUKA, T., NIIRO, H., NAGANO, S., ARINOBU, Y., OGAMI, E., AKAHOSHI, M., MIYAKE, K., NINOMIYA, I. & SHIMIZU, S. 2004. Novel regulatory mechanisms of CD40-induced prostanoid synthesis by IL-4 and IL-10 in human monocytes. *The Journal of Immunology,* 172**,** 2147-2154.

INUI, S., KAISHO, T., KIKUTANI, H., STAMENKOVIC, I., SEED, B., CLARK, E. A. & KISHIMOTO, T. 1990. Identification of the intracytoplasmic region essential for signal transduction through a B cell activation molecule, CD40. *European journal of immunology,* 20**,** 1747-1753.

IP, W.-K. & LAU, Y.-L. 2004. Distinct maturation of, but not migration between, human monocyte-derived dendritic cells upon ingestion of apoptotic cells of early or late phases. *The Journal of Immunology,* 173**,** 189-196.

JACKSON, A. L. & LOEB, L. A. 2001. The contribution of endogenous sources of DNA damage to the multiple mutations in cancer. *Mutation Research/Fundamental and Molecular Mechanisms of Mutagenesis,* 477**,** 7-21.

JANEWAY JR, C. A., TRAVERS, P., WALPORT, M. & SHLOMCHIK, M. J. 2001. Macrophage activation by armed CD4 TH1 cells.

JEMAL, A., SIEGEL, R., WARD, E., MURRAY, T., XU, J., SMIGAL, C. & THUN, M. J. 2006. Cancer statistics, 2006. *CA: a cancer journal for clinicians,* 56**,** 106-130.

JEMAL, A., SIEGEL, R., XU, J. & WARD, E. 2010. Cancer statistics, 2010. *CA: a cancer journal for clinicians,* 60**,** 277-300.

JIANG, F., ZHANG, Y. & DUSTING, G. J. 2011. NADPH oxidase-mediated redox signaling: roles in cellular stress response, stress tolerance, and tissue repair. *Pharmacological reviews,* 63**,** 218-242.

JIJON, H. B., PANENKA, W. J., MADSEN, K. L. & PARSONS, H. G. 2002. MAP kinases contribute to IL-8 secretion by intestinal epithelial cells via a posttranscriptional mechanism. *American Journal of Physiology-Cell Physiology,* 283**,** C31-C41.

JIN, C., CHEN, J., MENG, Q., CARREIRA, V., TAM, N. N., GEH, E., KARYALA, S., HO, S.-M., ZHOU, X. & MEDVEDOVIC, M. 2013. Deciphering gene expression program of MAP3K1 in mouse eyelid morphogenesis. *Developmental biology,* 374**,** 96-107.

JOHNSON, B. V., BERT, A. G., RYAN, G. R., CONDINA, A. & COCKERILL, P. N. 2004. Granulocyte-macrophage colony-stimulating factor enhancer activation requires cooperation between NFAT and AP-1 elements and is associated with extensive nucleosome reorganization. *Molecular and Cellular Biology,* 24**,** 7914-7930.

JOHNSON, G. L. & LAPADAT, R. 2002. Mitogen-activated protein kinase pathways mediated by ERK, JNK, and p38 protein kinases. *Science,* 298**,** 1911-1912.

JUO, P., KUO, C. J., REYNOLDS, S. E., KONZ, R. F., RAINGEAUD, J., DAVIS, R. J., BIEMANN, H.-P. & BLENIS, J. 1997. Fas activation of the p38 mitogen-activated protein kinase signalling pathway requires ICE/CED-3 family proteases. *Molecular and cellular biology,* 17**,** 24-35.

KAIRAITIS, L., WANG, Y., ZHENG, L., TAY, Y.-C., WANG, Y. & HARRIS, D. C. 2003. Blockade of CD40-CD40 ligand protects against renal injury in chronic proteinuric renal disease. *Kidney international,* 64**,** 1265-1272.

KAMATA, H., HONDA, S.-I., MAEDA, S., CHANG, L., HIRATA, H. & KARIN, M. 2005. Reactive oxygen species promote TNFα-induced death and sustained JNK activation by inhibiting MAP kinase phosphatases. *Cell,* 120**,** 649-661.

KANG, J.-O. & SUCOV, H. M. 2005. Convergent proliferative response and divergent morphogenic pathways induced by epicardial and endocardial signaling in fetal heart development. *Mechanisms of development,* 122**,** 57-65.

KARIN, M. & LIN, A. 2002. NF-κB at the crossroads of life and death. *Nature immunology,* 3**,** 221-227.

KATOH, I., TOMIMORI, Y., IKAWA, Y. & KURATA, S.-I. 2004. Dimerization and processing of procaspase-9 by redox stress in mitochondria. *Journal of Biological Chemistry,* 279**,** 15515-15523.

KATZ, M., AMIT, I. & YARDEN, Y. 2007. Regulation of MAPKs by growth factors and receptor tyrosine kinases. *Biochimica et Biophysica Acta (BBA)-Molecular Cell Research,* 1773**,** 1161-1176.

KAWAI, T. & AKIRA, S. 2007. Signaling to NF-κB by Toll-like receptors. *Trends in molecular medicine,* 13**,** 460-469.

KAYKAS, A., WORRINGER, K. & SUGDEN, B. 2001. CD40 and LMP-1 both signal from lipid rafts but LMP-1 assembles a distinct, more efficient signaling complex. *The EMBO Journal,* 20**,** 2641-2654.

KENNY, D. T. K. C. V. D. T. K. P. R. D. B. 2012. Cancer - A General Overview.

KHALIL, M. & VONDERHEIDE, R. H. 2007. Anti-CD40 agonist antibodies: preclinical and clinical experience. *Update on cancer therapeutics,* 2**,** 61-65.

KHANNA, R., COOPER, L., KIENZLE, N., MOSS, D. J., BURROWS, S. R. & KHANNA, K. K. 1997. Engagement of CD40 antigen with soluble CD40 ligand up-regulates peptide transporter expression and restores endogenous processing function in Burkitt's lymphoma cells. *The Journal of Immunology,* 159**,** 5782-5785.

KHONG, A., NELSON, D. J., NOWAK, A. K., LAKE, R. A. & ROBINSON, B. W. 2012. The use of agonistic anti-CD40 therapy in treatments for cancer. *International reviews of immunology,* 31**,** 246-266.

KIELIAN, T., NAGAI, E., IKUBO, A., RASMUSSEN, C. A. & SUZUKI, T. 1999. Granulocyte/macrophage-colony-stimulating factor released by adenovirally transduced CT26 cells leads to the local expression of macrophage inflammatory protein 1α and accumulation of dendritic cells at vaccination sites in vivo. *Cancer Immunology, Immunotherapy,* 48**,** 123-131.

KIM, H., RAFIUDDIN-SHAH, M., TU, H.-C., JEFFERS, J. R., ZAMBETTI, G. P., HSIEH, J. J.-D. & CHENG, E. H.-Y. 2006. Hierarchical regulation of mitochondrion-dependent apoptosis by BCL-2 subfamilies. *Nature cell biology,* 8**,** 1348-1358.

KIM, H. S., CHO, J. W., HIDAKA, K. & MORISAKI, T. 2007. Activation of MEK–ERK by heregulin-β1 promotes the development of cardiomyocytes derived from ES cells. *Biochemical and biophysical research communications,* 361**,** 732-738.

KIM, Y. K., KIM, H. J., KWON, C. H., KIM, J. H., WOO, J. S., JUNG, J. S. & KIM, J. M. 2005. Role of ERK activation in cisplatin-induced apoptosis in OK renal epithelial cells. *Journal of Applied Toxicology,* 25**,** 374-382.

KISHIMOTO, H., NAKAGAWA, K., WATANABE, T., KITAGAWA, D., MOMOSE, H., SEO, J., NISHITAI, G., SHIMIZU, N., OHATA, S. & TANEMURA, S. 2003. Different properties of SEK1 and MKK7 in dual phosphorylation of stress-induced activated protein kinase SAPK/JNK in embryonic stem cells. *Journal of Biological Chemistry,* 278**,** 16595-16601.

KLAUS, G. G., CHOI, M. S., LAM, E. W.-F., JOHNSON-LEGER, C. & CLIFF, J. 1997. CD40: a pivotal receptor in the determination of life/death decisions in B lymphocytes. *International reviews of immunology,* 15**,** 5-31.

KLUCK, R. M., BOSSY-WETZEL, E., GREEN, D. R. & NEWMEYER, D. D. 1997. The release of cytochrome c from mitochondria: a primary site for Bcl-2 regulation of apoptosis. *Science,* 275**,** 1132-1136.

KNALL, C., WORTHEN, G. S. & JOHNSON, G. L. 1997. Interleukin 8-stimulated phosphatidylinositol-3-kinase activity regulates the migration of human neutrophils independent of extracellular signal-regulated kinase and p38 mitogen-activated protein kinases. *Proceedings of the National Academy of Sciences,* 94**,** 3052-3057.

KNALL, C., YOUNG, S., NICK, J. A., BUHL, A. M., WORTHEN, G. S. & JOHNSON, G. L. 1996. Interleukin-8 regulation of the Ras/Raf/mitogen-activated protein kinase pathway in human neutrophils. *Journal of Biological Chemistry,* 271**,** 2832-2838.

KONTOYIANNIS, D., KOTLYAROV, A., CARBALLO, E., ALEXOPOULOU, L., BLACKSHEAR, P. J., GAESTEL, M., DAVIS, R., FLAVELL, R. & KOLLIAS, G. 2001. Interleukin-10 targets p38 MAPK to modulate ARE-dependent TNF mRNA translation and limit intestinal pathology. *The EMBO journal,* 20**,** 3760-3770.

KOOTEN, C. V. & BANCHEREAU, J. 1997. Functions of CD40 on B cells, dendritic cells and other cells. *Current opinion in immunology,* 9**,** 330-337.

KRAJEWSKI, S., TANAKA, S., TAKAYAMA, S., SCHIBLER, M. J., FENTON, W. & REED, J. C. 1993. Investigation of the subcellular distribution of the bcl-2 oncoprotein: residence in the nuclear envelope, endoplasmic reticulum, and outer mitochondrial membranes. *Cancer research,* 53**,** 4701-4714.

KROEMER, G., GALLUZZI, L. & BRENNER, C. 2007. Mitochondrial membrane permeabilization in cell death. *Physiological reviews,* 87**,** 99-163.

KROEMER, G., ZAMZAMI, N. & SUSIN, S. A. 1997. Mitochondrial control of apoptosis. *Immunology today,* 18**,** 44-51.

KUROIWA, T., SCHLIMGEN, R., ILLEI, G. G., MCINNES, I. B. & BOUMPAS, D. T. 2000. Distinct T cell/renal tubular epithelial cell interactions define differential chemokine production: implications for tubulointerstitial injury in chronic glomerulonephritides. *The Journal of Immunology,* 164**,** 3323-3329.

KUWANA, T., BOUCHIER-HAYES, L., CHIPUK, J. E., BONZON, C., SULLIVAN, B. A., GREEN, D. R. & NEWMEYER, D. D. 2005. BH3 domains of BH3-only proteins differentially regulate Bax-mediated mitochondrial membrane permeabilization both directly and indirectly. *Molecular cell,* 17**,** 525-535.

KYRIAKIS, J. M. & AVRUCH, J. 2012. Mammalian MAPK signal transduction pathways activated by stress and inflammation: a 10-year update. *Physiological reviews,* 92**,** 689-737.

L'ALLEMAIN, G. 1994. Deciphering the MAP kinase pathway. *Progress in growth factor research,* 5**,** 291-334.

LACRAZ, S., ISLER, P., VEY, E., WELGUS, H. G. & DAYER, J.-M. 1994. Direct contact between T lymphocytes and monocytes is a major pathway for induction of metalloproteinase expression. *Journal of Biological Chemistry,* 269**,** 22027-22033.

LAKHANI, S. A., MASUD, A., KUIDA, K., PORTER, G. A., BOOTH, C. J., MEHAL, W. Z., INAYAT, I. & FLAVELL, R. A. 2006. Caspases 3 and 7: key mediators of mitochondrial events of apoptosis. *Science,* 311**,** 847-851.

LAXMANAN, S., DATTA, D., GEEHAN, C., BRISCOE, D. M. & PAL, S. 2005. CD40: a mediator of pro-and anti-inflammatory signals in renal tubular epithelial cells. *Journal of the American Society of Nephrology,* 16**,** 2714-2723.

LEE, D. U., AVNI, O., CHEN, L. & RAO, A. 2004. A distal enhancer in the interferon-γ (IFN-γ) locus revealed by genome sequence comparison. *Journal of Biological Chemistry,* 279**,** 4802-4810.

LEE, J.-K., SEKI, N., SAYERS, T., SUBLESKI, J., GRUYS, E., MURPHY, W. & WILTROUT, R. 2005. Constitutive expression of functional CD40 on mouse renal cancer cells: induction of Fas and Fas-mediated killing by CD40L. *Cellular immunology,* 235**,** 145-152.

LEONARD, M., RYAN, M. P., WATSON, A. J., SCHRAMEK, H. & HEALY, E. 1999. Role of MAP kinase pathways in mediating IL-6 production in human primary mesangial and proximal tubular cells. *Kidney international,* 56**,** 1366-1377.

LEY, R., BALMANNO, K., HADFIELD, K., WESTON, C. & COOK, S. J. 2003. Activation of the ERK1/2 signaling pathway promotes phosphorylation and proteasome-dependent

degradation of the BH3-only protein, Bim. *Journal of Biological Chemistry,* 278**,** 18811-18816.

LEY, R., EWINGS, K. E., HADFIELD, K., HOWES, E., BALMANNO, K. & COOK, S. J. 2004. Extracellular signal-regulated kinases 1/2 are serum-stimulated "BimEL kinases" that bind to the BH3-only protein BimEL causing its phosphorylation and turnover. *Journal of Biological Chemistry,* 279**,** 8837-8847.

LI, G., SANDERS, J. M., BEVARD, M. H., SUN, Z., CHUMLEY, J. W., GALKINA, E. V., LEY, K. & SAREMBOCK, I. J. 2008. CD40 ligand promotes Mac-1 expression, leukocyte recruitment, and neointima formation after vascular injury. *The American journal of pathology,* 172**,** 1141-1152.

LI, H. & NORD, E. P. 2002. CD40 ligation stimulates MCP-1 and IL-8 production, TRAF6 recruitment, and MAPK activation in proximal tubule cells. *American Journal of Physiology-Renal Physiology,* 282**,** F1020-F1033.

LI, H. & NORD, E. P. 2009. IL-8 amplifies CD40/CD154-mediated ICAM-1 production via the CXCR-1 receptor and p38-MAPK pathway in human renal proximal tubule cells. *American Journal of Physiology-Renal Physiology,* 296**,** F438-F445.

LI, J.-M., FAN, L. M., CHRISTIE, M. R. & SHAH, A. M. 2005. Acute tumor necrosis factor alpha signaling via NADPH oxidase in microvascular endothelial cells: role of p47phox phosphorylation and binding to TRAF4. *Molecular and Cellular Biology,* 25**,** 2320-2330.

LI, J. & YUAN, J. 2008. Caspases in apoptosis and beyond. *Oncogene,* 27**,** 6194-6206.

LI, K., LI, Y., SHELTON, J. M., RICHARDSON, J. A., SPENCER, E., CHEN, Z. J., WANG, X. & WILLIAMS, R. S. 2000. Cytochrome c deficiency causes embryonic lethality and attenuates stress-induced apoptosis. *Cell,* 101**,** 389-399.

LI, L. Y., LUO, X. & WANG, X. 2001. Endonuclease G is an apoptotic DNase when released from mitochondria. *Nature,* 412**,** 95-99.

LIOU, G.-Y. & STORZ, P. 2010. Reactive oxygen species in cancer. *Free radical research,* 44**,** 479-496.

LIU, X., KIM, C. N., YANG, J., JEMMERSON, R. & WANG, X. 1996. Induction of apoptotic program in cell-free extracts: requirement for dATP and cytochrome c. *Cell,* 86**,** 147-157.

LIU, Y. & MIN, W. 2002. Thioredoxin promotes ASK1 ubiquitination and degradation to inhibit ASK1-mediated apoptosis in a redox activity-independent manner. *Circulation research,* 90**,** 1259-1266.

LIU, Z., SUN, C., OLEJNICZAK, E. T., MEADOWS, R. P., BETZ, S. F., OOST, T., HERRMANN, J., WU, J. C. & FESIK, S. W. 2000. Structural basis for binding of Smac/DIABLO to the XIAP BIR3 domain. *Nature,* 408**,** 1004-1008.

LONGO, C. R., ARVELO, M. B., PATEL, V. I., DANIEL, S., MAHIOU, J., GREY, S. T. & FERRAN, C. 2003. A20 protects from CD40-CD40 ligand-mediated endothelial cell activation and apoptosis. *Circulation,* 108**,** 1113-1118.

LU, Z. & XU, S. 2006. ERK1/2 MAP kinases in cell survival and apoptosis. *IUBMB life,* 58**,** 621-631.

LUIS, A., SANDALIO, L. M., PALMA, J., BUENO, P. & CORPAS, F. J. 1992. Metabolism of oxygen radicals in peroxisomes and cellular implications. *Free Radical Biology and Medicine,* 13**,** 557-580.

LUM, H. D., BUHTOIAROV, I. N., SCHMIDT, B. E., BERKE, G., PAULNOCK, D. M., SONDEL, P. M. & RAKHMILEVICH, A. L. 2006. In vivo CD40 ligation can induce T cell-independent antitumor effects that involve macrophages. *Journal of leukocyte biology,* 79**,** 1181-1192.

LUO, X., BUDIHARDJO, I., ZOU, H., SLAUGHTER, C. & WANG, X. 1998. Bid, a Bcl2 interacting protein, mediates cytochrome c release from mitochondria in response to activation of cell surface death receptors. *Cell,* 94**,** 481-490.

LUPPI, F., LONGO, A., DE BOER, W., RABE, K. & HIEMSTRA, P. 2007. Interleukin-8 stimulates cell proliferation in non-small cell lung cancer through epidermal growth factor receptor transactivation. *Lung cancer,* 56**,** 25-33.

MA, D. Y. & CLARK, E. A. The role of CD40 and CD154/CD40L in dendritic cells. Seminars in immunology, 2009. Elsevier, 265-272.

MACH, F., SCHÖNBECK, U., BONNEFOY, J.-Y., POBER, J. S. & LIBBY, P. 1997. Activation of monocyte/macrophage functions related to acute atheroma complication by ligation of CD40. *Circulation,* 96**,** 396-399.

MACMANUS, C. F., PETTIGREW, J., SEATON, A., WILSON, C., MAXWELL, P. J., BERLINGERI, S., PURCELL, C., MCGURK, M., JOHNSTON, P. G. & WAUGH, D. J. 2007. Interleukin-8 signaling promotes translational regulation of cyclin D in androgen-independent prostate cancer cells. *Molecular Cancer Research,* 5**,** 737-748.

MAERTEN, P., LIU, Z. & CEUPPENS, J. L. 2003. Targeting of costimulatory molecules as a therapeutic approach in inflammatory bowel disease. *Biodrugs,* 17**,** 395-411.

MANSELL, A. & JENKINS, B. J. 2013. Dangerous liaisons between interleukin-6 cytokine and toll-like receptor families: a potent combination in inflammation and cancer. *Cytokine & growth factor reviews,* 24**,** 249-256.

MARTINOU, J.-C., DESAGHER, S. & ANTONSSON, B. 2000. Cytochrome c release from mitochondria: all or nothing. *Nature cell biology,* 2**,** E41-E43.

MASSON, R., RÉGNIER, C. H., CHENARD, M.-P., WENDLING, C., MATTEI, M.-G., TOMASETTO, C. & RIO, M.-C. 1998. Tumor necrosis factor receptor associated factor 4 (TRAF4) expression pattern during mouse development. *Mechanisms of development,* 71**,** 187-191.

MATSUNAGA, Y., KAWAI, Y., KOHDA, Y. & GEMBA, M. 2005. Involvement of activation of NADPH oxidase and extracellular signal-regulated kinase (ERK) in renal cell injury induced by zinc. *The Journal of toxicological sciences,* 30**,** 135-144.

MCINNES, I. B., LEUNG, B. P., STURROCK, R., FIELD, M. & LIEW, F. Y. 1997. Interleukin-15 mediates T cell-dependent regulation of tumor necrosis factor- production in rheumatoid arthritis. *Nature medicine,* 3**,** 189-195.

MCWHIRTER, S. M., PULLEN, S. S., HOLTON, J. M., CRUTE, J. J., KEHRY, M. R. & ALBER, T. 1999. Crystallographic analysis of CD40 recognition and signaling by human TRAF2. *Proceedings of the National Academy of Sciences,* 96**,** 8408-8413.

MEAGER, A. 1991. A cytotoxicity assay for tumour necrosis using a human rhabdomyosarcoma cell line. *Journal of immunological methods,* 144**,** 141-143.

MICHEAU, O. & TSCHOPP, J. 2003. Induction of TNF receptor I-mediated apoptosis via two sequential signaling complexes. *Cell,* 114**,** 181-190.

MILHAS, D., CUVILLIER, O., THERVILLE, N., CLAVÉ, P., THOMSEN, M., LEVADE, T., BENOIST, H. & SÉGUI, B. 2005. Caspase-10 triggers Bid cleavage and caspase cascade activation in FasL-induced apoptosis. *Journal of Biological Chemistry,* 280**,** 19836-19842.

MISHINA, N. M., TYURIN-KUZMIN, P. A., MARKVICHEVA, K. N., VOROTNIKOV, A. V., TKACHUK, V. A., LAKETA, V., SCHULTZ, C., LUKYANOV, S. & BELOUSOV, V. V. 2011. Does cellular hydrogen peroxide diffuse or act locally? *Antioxidants & redox signaling,* 14**,** 1-7.

MOHAMED, A. 2014. *Identification of the biochemical signalling mechanisms underlying CD40 killing in colorectal cancer cells.* University of Huddersfield.

MORIMOTO, S., KANNO, Y., TANAKA, Y., TOKANO, Y., HASHIMOTO, H., JACQUOT, S., MORIMOTO, C., SCHLOSSMAN, S. F., YAGITA, H. & OKUMURA, K. 2000. CD134L engagement enhances human B cell Ig production: CD154/CD40, CD70/CD27, and CD134/CD134L interactions coordinately regulate T cell-dependent B cell responses. *The Journal of Immunology,* 164**,** 4097-4104.

MORRIS, A. E., REMMELE, R. L., KLINKE, R., MACDUFF, B. M., FANSLOW, W. C. & ARMITAGE, R. J. 1999. Incorporation of an isoleucine zipper motif enhances the biological activity of soluble CD40L (CD154). *Journal of Biological Chemistry,* 274**,** 418-423.

MOSIALOS, G., BIRKENBACHT, M., YALAMANCHILL, R., VAN ARSDALE, T., WARE, C. & KLEFF, E. 1995. The Epstein-Barr virus transforming protein LMP1 engages signaling proteins for the tumor necrosis factor receptor family. *Cell,* 80**,** 389-399.

MUKUNDAN, L., BISHOP, G. A., HEAD, K. Z., ZHANG, L., WAHL, L. M. & SUTTLES, J. 2005. TNF receptor-associated factor 6 is an essential mediator of CD40-activated proinflammatory pathways in monocytes and macrophages. *The Journal of Immunology,* 174**,** 1081-1090.

MURPHY, M. P. 2009. How mitochondria produce reactive oxygen species. *Biochemical Journal,* 417**,** 1-13.

NADEAU, P. J., CHARETTE, S. J., TOLEDANO, M. B. & LANDRY, J. 2007. Disulfide bond-mediated multimerization of Ask1 and its reduction by thioredoxin-1 regulate H2O2-induced c-Jun NH2-terminal kinase activation and apoptosis. *Molecular biology of the cell,* 18**,** 3903-3913.

NAGATA, S. 1997. Apoptosis by death factor. *cell,* 88**,** 355-365.

NAKANO, H., SAKON, S., KOSEKI, H., TAKEMORI, T., TADA, K., MATSUMOTO, M., MUNECHIKA, E., SAKAI, T., SHIRASAWA, T. & AKIBA, H. 1999. Targeted disruption of Traf5 gene causes defects in CD40-and CD27-mediated lymphocyte activation. *Proceedings of the National Academy of Sciences,* 96**,** 9803-9808.

NAPOLITANO, G. & KARIN, M. 2010. Sphingolipids: the oil on the TRAFire that promotes inflammation. *Sci. Signal.,* 3**,** pe34-pe34.

NGUYEN, V. T., WALKER, W. S. & BENVENISTE, E. N. 1998. Post-transcriptional inhibition of CD40 gene expression in microglia by transforming growth factor-b. *European journal of immunology,* 28**,** 2537-2548.

NI, C.-Z., WELSH, K., LEO, E., CHIOU, C.-K., WU, H., REED, J. C. & ELY, K. R. 2000. Molecular basis for CD40 signaling mediated by TRAF3. *Proceedings of the National Academy of Sciences,* 97**,** 10395-10399.

NISHITOH, H., MATSUZAWA, A., TOBIUME, K., SAEGUSA, K., TAKEDA, K., INOUE, K., HORI, S., KAKIZUKA, A. & ICHIJO, H. 2002. ASK1 is essential for endoplasmic reticulum stress-induced neuronal cell death triggered by expanded polyglutamine repeats. *Genes & development,* 16**,** 1345-1355.

NISHIYAMA, A., OHNO, T., IWATA, S., MATSUI, M., HIROTA, K., MASUTANI, H., NAKAMURA, H. & YODOI, J. 1999. Demonstration of the interaction of thioredoxin with p40phox, a phagocyte oxidase component, using a yeast two-hybrid system. *Immunology letters,* 68**,** 155-159.

PAI, S., LIN, Y., MACAES, B., MENESHIAN, A., HUNG, C. & WU, T. 2006. Prospects of RNA interference therapy for cancer. *Gene therapy,* 13**,** 464-477.

PAN, J.-S., HONG, M.-Z. & REN, J.-L. 2009. Reactive oxygen species: a double-edged sword in oncogenesis. *World J Gastroenterol,* 15**,** 1702-1707.

PANDEY, P., SALEH, A., NAKAZAWA, A., KUMAR, S., SRINIVASULA, S. M., KUMAR, V., WEICHSELBAUM, R., NALIN, C., ALNEMRI, E. S. & KUFE, D. 2000. Negative regulation of cytochrome c-mediated oligomerization of Apaf-1 and activation of procaspase-9 by heat shock protein 90. *The EMBO journal,* 19**,** 4310-4322.

PARRISH, A. B., FREEL, C. D. & KORNBLUTH, S. 2013. Cellular mechanisms controlling caspase activation and function. *Cold Spring Harbor perspectives in biology,* 5**,** a008672.

PATEL, D. D., WHICHARD, L. P., RADCLIFF, G., DENNING, S. M. & HAYNES, B. F. 1995. Characterization of human thymic epithelial cell surface antigens: phenotypic similarity of thymic epithelial cells to epidermal keratinocytes. *Journal of clinical immunology,* 15**,** 80-92.

PAULIE, S., EHLIN-HENRIKSSON, B., MELLSTEDT, H., KOHO, H., BEN-AISSA, H. & PERLMANN, P. 1985. A p50 surface antigen restricted to human urinary bladder carcinomas and B lymphocytes. *Cancer Immunology, Immunotherapy,* 20**,** 23-28.

PEGUET-NAVARRO, J., DALBIEZ-GAUTHIER, C., MOULON, C., BERTHIER, O., RÉANO, A., GAUCHERAND, M., BANCHEREAU, J., ROUSSET, F. & SCHMITT, D. 1997. CD40 ligation of human keratinocytes inhibits their proliferation and induces their differentiation. *The Journal of Immunology,* 158**,** 144-152.

PETER, M. E. & KRAMMER, P. 2003. The CD95 (APO-1/Fas) DISC and beyond. *Cell Death & Differentiation,* 10**,** 26-35.

PETROS, A. M., OLEJNICZAK, E. T. & FESIK, S. W. 2004. Structural biology of the Bcl-2 family of proteins. *Biochimica et Biophysica Acta (BBA)-Molecular Cell Research,* 1644**,** 83-94.

PHAM, L. V., TAMAYO, A. T., YOSHIMURA, L. C., LO, P., TERRY, N., REID, P. S. & FORD, R. J. 2002. A CD40 signalosome anchored in lipid rafts leads to constitutive activation of NF-κB and autonomous cell growth in B cell lymphomas. *Immunity,* 16**,** 37-50.

PISKOUNOVA, E., AGATHOCLEOUS, M., MURPHY, M. M., HU, Z., HUDDLESTUN, S. E., ZHAO, Z., LEITCH, A. M., JOHNSON, T. M., DEBERARDINIS, R. J. & MORRISON, S. J. 2015. Oxidative stress inhibits distant metastasis by human melanoma cells. *Nature*.

POP, C. & SALVESEN, G. S. 2009. Human caspases: activation, specificity, and regulation. *Journal of biological Chemistry,* 284**,** 21777-21781.

PORTER, A. G. 1990. Human tumour necrosis factors-α and-β: Differences in their structure, expression and biological properties. *FEMS microbiology immunology,* 2**,** 193-199.

POTAPOVA, O., BASU, S., MERCOLA, D. & HOLBROOK, N. J. 2001. Protective role for c-Jun in the cellular response to DNA damage. *Journal of biological chemistry,* 276**,** 28546-28553.

POUND, J. D., CHALLA, A., HOLDER, M. J., ARMITAGE, R. J., DOWER, S. K., FANSLOW, W. C., KIKUTANI, H., PAULIE, S., GREGORY, C. D. & GORDON, J. 1999. Minimal cross-linking and epitope requirements for CD40-dependent suppression of apoptosis contrast with those for promotion of the cell cycle and homotypic adhesions in human B cells. *International immunology,* 11**,** 11-20.

PRODJOSUDJADI, W., GERRITSMA, J. S., KLAR-MOHAMAD, N., GERRITSEN, A. F., BRUIJN, J. A. & DAHA, M. R. 1995. Production and cytokine-mediated regulation of monocyte chemoattractant protein-1 by human proximal tubular epithelial cells. *Kidney international,* 48**,** 1477-1486.

PROPST, S. M., ESTELL, K. & SCHWIEBERT, L. M. 2002. CD40-mediated activation of NF-κB in airway epithelial cells. *Journal of Biological Chemistry,* 277**,** 37054-37063.

PULLEN, S. S., LABADIA, M. E., INGRAHAM, R. H., MCWHIRTER, S. M., EVERDEEN, D. S., ALBER, T., CRUTE, J. J. & KEHRY, M. R. 1999. High-affinity interactions of tumor necrosis factor receptor-associated factors (TRAFs) and CD40 require TRAF trimerization and CD40 multimerization. *Biochemistry,* 38**,** 10168-10177.

PULLEN, S. S., MILLER, H. G., EVERDEEN, D. S., DANG, T. T., CRUTE, J. J. & KEHRY, M. R. 1998. CD40-tumor necrosis factor receptor-associated factor (TRAF) interactions: regulation of CD40 signaling through multiple TRAF binding sites and TRAF hetero-oligomerization. *Biochemistry,* 37**,** 11836-11845.

PUTHALAKATH, H., HUANG, D. C., O'REILLY, L. A., KING, S. M. & STRASSER, A. 1999. The proapoptotic activity of the Bcl-2 family member Bim is regulated by interaction with the dynein motor complex. *Molecular cell,* 3**,** 287-296.

QI, C.-J., ZHENG, L., ZHOU, X., TAO, Y., GE, Y., ZHUANG, Y.-M., XU, Y., YU, G. & ZHANG, X.-G. 2004. Cross-linking of CD40 using anti-CD40 antibody, 5C11, has different effects on XG2 multiple myeloma cells. *Immunology letters,* 93**,** 151-158.

QIAN, Y., ZHAO, Z., JIANG, Z. & LI, X. 2002. Role of NFκB activator Act1 in CD40-mediated signaling in epithelial cells. *Proceedings of the National Academy of Sciences,* 99**,** 9386-9391.

RAMESH, N., RAMESH, V., GUSELLA, J. F. & GEHA, R. 1993. Chromosomal localization of the gene for human B-cell antigen CD40. *Somatic cell and molecular genetics,* 19**,** 295-298.

RASOLA, A. & BERNARDI, P. 2007. The mitochondrial permeability transition pore and its involvement in cell death and in disease pathogenesis. *Apoptosis,* 12**,** 815-833.

RATH, P. C. & AGGARWAL, B. B. 1999. TNF-induced signaling in apoptosis. *Journal of clinical immunology,* 19**,** 350-364.

RAUERT, H., WICOVSKY, A., MÜLLER, N., SIEGMUND, D., SPINDLER, V., WASCHKE, J., KNEITZ, C. & WAJANT, H. 2010. Membrane tumor necrosis factor (TNF) induces p100 processing via TNF receptor-2 (TNFR2). *Journal of Biological Chemistry,* 285**,** 7394-7404.

RAVAGNAN, L., GURBUXANI, S., SUSIN, S. A., MAISSE, C., DAUGAS, E., ZAMZAMI, N., MAK, T., JÄÄTTELÄ, M., PENNINGER, J. M. & GARRIDO, C. 2001. Heat-shock protein 70 antagonizes apoptosis-inducing factor. *Nature cell biology,* 3**,** 839-843.

RAY, P. D., HUANG, B.-W. & TSUJI, Y. 2012. Reactive oxygen species (ROS) homeostasis and redox regulation in cellular signaling. *Cellular signalling,* 24**,** 981-990.

REED, J. C. 2000. Mechanisms of apoptosis. *The American journal of pathology,* 157**,** 1415-1430.

RÉGNIER, C. H., TOMASETTO, C., MOOG-LUTZ, C., CHENARD, M.-P., WENDLING, C., BASSET, P. & RIO, M.-C. 1995. Presence of a new conserved domain in CART1, a novel member of the tumor necrosis factor receptor-associated protein family, which is expressed in breast carcinoma. *Journal of Biological Chemistry,* 270**,** 25715-25721.

REMUZZI, G., RUGGENENTI, P. & BENIGNI, A. 1997. Understanding the nature of renal disease progression. *Kidney international,* 51**,** 2-15.

REYES-MORENO, C., GIROUARD, J., LAPOINTE, R., DARVEAU, A. & MOURAD, W. 2004. CD40/CD40 homodimers are required for CD40-induced phosphatidylinositol 3-kinase-dependent expression of B7. 2 by human B lymphocytes. *Journal of Biological Chemistry,* 279**,** 7799-7806.

REZZONICO, R., BURGER, D. & DAYER, J.-M. 1998. Direct contact between T lymphocytes and human dermal fibroblasts or synoviocytes down-regulates types I and III collagen production via cell-associated cytokines. *Journal of Biological Chemistry,* 273**,** 18720-18728.

RICHARDSON, H. & KUMAR, S. 2002. Death to flies: Drosophila as a model system to study programmed cell death. *Journal of immunological methods,* 265**,** 21-38.

RODRIGUEZ, J. & LAZEBNIK, Y. 1999. Caspase-9 and APAF-1 form an active holoenzyme. *Genes & development,* 13**,** 3179-3184.

RODRÍGUEZ, M., CABAL-HIERRO, L., CARCEDO, M. T., IGLESIAS, J. M., ARTIME, N., DARNAY, B. G. & LAZO, P. S. 2011. NF-κB signal triggering and termination by tumor necrosis factor receptor 2. *Journal of Biological Chemistry,* 286**,** 22814-22824.

ROTHE, M., PAN, M.-G., HENZEL, W. J., AYRES, T. M. & GOEDDEL, D. V. 1995. The TNFR2-TRAF signaling complex contains two novel proteins related to baculoviral inhibitor of apoptosis proteins. *Cell,* 83**,** 1243-1252.

ROUSSEAU, A., RIO, M.-C. & ALPY, F. 2011. TRAF4, at the crossroad between morphogenesis and cancer. *Cancers,* 3**,** 2734-2749.

ROUSSET, F., GARCIA, E. & BANCHEREAU, J. 1991. Cytokine-induced proliferation and immunoglobulin production of human B lymphocytes triggered through their CD40 antigen. *The Journal of experimental medicine,* 173**,** 705-710.

ROWLAND, S. L., TREMBLAY, M. M., ELLISON, J. M., STUNZ, L. L., BISHOP, G. A. & HOSTAGER, B. S. 2007. A novel mechanism for TNFR-associated factor 6-dependent CD40 signaling. *The Journal of Immunology,* 179**,** 4645-4653.

RUGGIERO, V., LATHAM, K. & BAGLIONI, C. 1987. Cytostatic and cytotoxic activity of tumor necrosis factor on human cancer cells. *The Journal of Immunology,* 138**,** 2711-2717.

RYAN, M. J., JOHNSON, G., KIRK, J., FUERSTENBERG, S. M., ZAGER, R. A. & TOROK-STORB, B. 1994. HK-2: an immortalized proximal tubule epithelial cell line from normal adult human kidney. *Kidney international,* 45**,** 48-57.

SABAPATHY, K. & WAGNER, E. F. 2004. JNK2: a negative regulator of cellular proliferation. *Cell Cycle,* 3**,** 1520-1523.

SÄEMANN, M., KELEMEN, P., ZEYDA, M., BÖHMIG, G., STAFFLER, G. & ZLABINGER, G. CD40 triggered human monocyte-derived dendritic cells convert to tolerogenic dendritic cells when JAK3 activity is inhibited. Transplantation proceedings, 2002. Elsevier, 1407-1408.

SÄEMANN, M. D., DIAKOS, C., KELEMEN, P., KRIEHUBER, E., ZEYDA, M., BÖHMIG, G. A., HÖRL, W. H., BAUMRUKER, T. & ZLABINGER, G. J. 2003. Prevention of CD40-Triggered Dendritic Cell Maturation and Induction of T-Cell Hyporeactivity by Targeting of Janus Kinase 3. *American Journal of Transplantation,* 3**,** 1341-1349.

SALEH, A., SRINIVASULA, S. M., BALKIR, L., ROBBINS, P. D. & ALNEMRI, E. S. 2000. Negative regulation of the Apaf-1 apoptosome by Hsp70. *Nature cell biology,* 2**,** 476-483.

SAMEJIMA, K., TONE, S. & EARNSHAW, W. C. 2001. CAD/DFF40 nuclease is dispensable for high molecular weight DNA cleavage and stage I chromatin condensation in apoptosis. *Journal of Biological Chemistry,* 276**,** 45427-45432.

SAQUIB A. LAKHANI, A. M., KEISUKE KUIDA, GEORGE A. PORTER JR, CARMEN J. & BOOTH, W. Z. M., IRTEZA INAYAT, AND RICHARD A. FLAVELL1, 2006. Caspases 3 and 7: Key Mediators of Mitochondrial Events of

Apoptosis. *National institute of health*.

SARASTE, A. & PULKKI, K. 2000. Morphologic and biochemical hallmarks of apoptosis. *Cardiovascular research,* 45**,** 528-537.

SAROSIEK, K. A., CHI, X., BACHMAN, J. A., SIMS, J. J., MONTERO, J., PATEL, L., FLANAGAN, A., ANDREWS, D. W., SORGER, P. & LETAI, A. 2013. BID preferentially activates BAK while BIM preferentially activates BAX, affecting chemotherapy response. *Molecular cell,* 51**,** 751-765.

SATO, M., HATA, N., ASAGIRI, M., NAKAYA, T., TANIGUCHI, T. & TANAKA, N. 1998. Positive feedback regulation of type I IFN genes by the IFN-inducible transcription factor IRF-7. *FEBS letters,* 441**,** 106-110.

SAX, J. K. & EL-DEIRY, W. S. 2003. Identification and characterization of the cytoplasmic protein TRAF4 as a p53-regulated proapoptotic gene. *Journal of Biological Chemistry,* 278**,** 36435-36444.

SCARLETT, U. K., CUBILLOS-RUIZ, J. R., NESBETH, Y. C., MARTINEZ, D. G., ENGLE, X., GEWIRTZ, A. T., AHONEN, C. L. & CONEJO-GARCIA, J. R. 2009. In situ stimulation of CD40 and toll-like receptor 3 transforms ovarian cancer–infiltrating dendritic cells from immunosuppressive to immunostimulatory cells. *Cancer research,* 69**,** 7329-7337.

SCHELLENBERG, B., WANG, P., KEEBLE, J. A., RODRIGUEZ-ENRIQUEZ, R., WALKER, S., OWENS, T. W., FOSTER, F., TANIANIS-HUGHES, J., BRENNAN, K. & STREULI, C. H. 2013. Bax exists in a dynamic equilibrium between the cytosol and mitochondria to control apoptotic priming. *Molecular cell,* 49**,** 959-971.

SCHELLER, J., OHNESORGE, N. & ROSE-JOHN, S. 2006. Interleukin-6 trans-signalling in chronic inflammation and cancer. *Scandinavian journal of immunology,* 63**,** 321-329.

SCHENDEL, S. L., MONTAL, M. & REED, J. C. 1998. Bcl-2 family proteins as ion-channels. *Cell Death & Differentiation,* 5.

SCHLESINGER, P. H., GROSS, A., YIN, X.-M., YAMAMOTO, K., SAITO, M., WAKSMAN, G. & KORSMEYER, S. J. 1997. Comparison of the ion channel characteristics of proapoptotic BAX and antiapoptotic BCL-2. *Proceedings of the National Academy of Sciences,* 94**,** 11357-11362.

SCHNEIDER, P., HOLLER, N., BODMER, J.-L., HAHNE, M., FREI, K., FONTANA, A. & TSCHOPP, J. 1998. Conversion of membrane-bound Fas (CD95) ligand to its soluble form is associated with downregulation of its proapoptotic activity and loss of liver toxicity. *Journal of Experimental Medicine,* 187**,** 1205-1213.

SCHÖNBECK, U., GERDES, N., VARO, N., REYNOLDS, R. S., HORTON, D. B., BAVENDIEK, U., ROBBIE, L., GANZ, P., KINLAY, S. & LIBBY, P. 2002. Oxidized low-density lipoprotein augments and 3-hydroxy-3-methylglutaryl coenzyme A reductase inhibitors limit CD40 and CD40L expression in human vascular cells. *Circulation,* 106**,** 2888-2893.

SCHÖNBECK, U. & LIBBY, P. 2001. The CD40/CD154 receptor/ligand dyadRID="†" ID="†" Review. *Cellular and Molecular Life Sciences CMLS,* 58**,** 4-43.

SCHRODER, K., HERTZOG, P. J., RAVASI, T. & HUME, D. A. 2004. Interferon-γ: an overview of signals, mechanisms and functions. *Journal of leukocyte biology,* 75**,** 163-189.

SCHWABE, R. F., SCHNABL, B., KWEON, Y. O. & BRENNER, D. A. 2001. CD40 activates NF-κB and c-Jun N-terminal kinase and enhances chemokine secretion on activated human hepatic stellate cells. *The Journal of Immunology,* 166**,** 6812-6819.

SCHWENZER, R., SIEMIENSKI, K., LIPTAY, S., SCHUBERT, G., PETERS, N., SCHEURICH, P., SCHMID, R. M. & WAJANT, H. 1999. The human tumor necrosis factor (TNF) receptor-associated factor 1 gene (TRAF1) is up-regulated by cytokines of the TNF ligand family and modulates TNF-induced activation of NF-κB and c-Jun N-terminal kinase. *Journal of Biological Chemistry,* 274**,** 19368-19374.

SHAH, S., KING, E. M., CHANDRASEKHAR, A. & NEWTON, R. 2014. Roles for the mitogen-activated protein kinase (MAPK) phosphatase, DUSP1, in feedback control of inflammatory gene expression and repression by dexamethasone. *Journal of Biological Chemistry,* 289**,** 13667-13679.

SHANNON, M. F., COLES, L. S., VADAS, M. A. & COCKERILL, P. N. 1997. Signals for activation of the GM-CSF promoter and enhancer in T cells. *Critical Reviews™ in Immunology,* 17.

SHARMA, P., JHA, A. B., DUBEY, R. S. & PESSARAKLI, M. 2012. Reactive oxygen species, oxidative damage, and antioxidative defense mechanism in plants under stressful conditions. *Journal of Botany,* 2012.

SHARMA, S. A., TUMMURU, M. K., BLASER, M. J. & KERR, L. D. 1998. Activation of IL-8 gene expression by Helicobacter pylori is regulated by transcription factor nuclear factor-κB in gastric epithelial cells. *The Journal of Immunology,* 160**,** 2401-2407.

SHAULIAN, E. & KARIN, M. 2002. AP-1 as a regulator of cell life and death. *Nature cell biology,* 4**,** E131-E136.

SHAW, N. J., GEORGOPOULOS, N. T., SOUTHGATE, J. & TREJDOSIEWICZ, L. K. 2005. Effects of loss of p53 and p16 function on life span and survival of human urothelial cells. *International journal of cancer,* 116**,** 634-639.

SHEN, H.-M. & LIU, Z.-G. 2006. JNK signaling pathway is a key modulator in cell death mediated by reactive oxygen and nitrogen species. *Free Radical Biology and Medicine,* 40**,** 928-939.

SHEN, H.-M. & PERVAIZ, S. 2006. TNF receptor superfamily-induced cell death: redox-dependent execution. *The FASEB Journal,* 20**,** 1589-1598.

SHI, Y. 2002a. Apoptosome: the cellular engine for the activation of caspase-9. *Structure,* 10**,** 285-288.

SHI, Y. 2002b. Mechanisms of caspase activation and inhibition during apoptosis. *Molecular cell,* 9**,** 459-470.

SHIBASAKI, F., KONDO, E., AKAGI, T. & MCKEON, F. 1997. Suppression of signalling through transcription factor NF-AT by interactions between calcineurin and Bcl-2.

SHIMIZU, S., EGUCHI, Y., KAMIIKE, W., FUNAHASHI, Y., MIGNON, A., LACRONIQUE, V., MATSUDA, H. & TSUJIMOTO, Y. 1998. Bcl-2 prevents apoptotic mitochondrial dysfunction by regulating proton flux. *Proceedings of the National Academy of Sciences,* 95**,** 1455-1459.

SHINOHARA, H., YANO, S., BUCANA, C. D. & FIDLER, I. J. 2000. Induction of chemokine secretion and enhancement of contact-dependent macrophage cytotoxicity by engineered expression of granulocyte-macrophage colony-stimulating factor in human colon cancer cells. *The Journal of Immunology,* 164**,** 2728-2737.

SHORTS, L., WEISS, J. M., LEE, J. K., WELNIAK, L. A., SUBLESKI, J., BACK, T., MURPHY, W. J. & WILTROUT, R. H. 2006. Stimulation through CD40 on mouse and human renal cell carcinomas triggers cytokine production, leukocyte recruitment, and antitumor responses that can be independent of host CD40 expression. *Journal of Immunology,* 176**,** 6543-6552.

SHOSHAN-BARMATZ, V. & GINCEL, D. 2003. The voltage-dependent anion channel. *Cell biochemistry and biophysics,* 39**,** 279-292.

SIGRUENER, A., BUECHLER, C., BARED, S. M., GRANDL, M., ASLANIDIS, C., UGOCSAI, P., GEHRMANN, M. & SCHMITZ, G. 2007. E-LDL upregulates TOSO expression and enhances the survival of human macrophages. *Biochemical and biophysical research communications,* 359**,** 723-728.

SIMIC, T., MIMIC-OKA, J., SAVIC-RADOJEVIC, A., OPACIC, M., PLJESA, M., DRAGICEVIC, D., DJOKIC, M. & RADOSAVLJEVIC, R. 2005. Glutathione S-transferase T1-1 activity upregulated in transitional cell carcinoma of urinary bladder. *Urology,* 65**,** 1035-1040.

SINGH, J., GARBER, E., VLIJMEN, H. V., KARPUSAS, M., HSU, Y. M., ZHENG, Z., THOMAS, D. & NAISMITH, J. H. 1998. The role of polar interactions in the molecular recognition of CD40L with its receptor CD40. *Protein science,* 7**,** 1124-1135.

SOGA, M., MATSUZAWA, A. & ICHIJO, H. 2012. Oxidative stress-induced diseases via the ASK1 signaling pathway. *International journal of cell biology,* 2012.

SOLYMAR, D. C., AGARWAL, S., BASSING, C. H., ALT, F. W. & RAO, A. 2002. A 3′ enhancer in the IL-4 gene regulates cytokine production by Th2 cells and mast cells. *Immunity,* 17**,** 41-50.

SOTOMAYOR EM1, B. I., TUBB E, RATTIS FM, BIEN H, LU Z, FEIN S, SCHOENBERGER S, LEVITSKY HI. 1999. Conversion of tumor-specific CD4+ T-cell tolerance to T-cell priming through in vivo ligation of CD40. *Nature,* 780**,** 7.

SPANAUS, K. S., SCHLAPBACH, R. & FONTANA, A. 1998. TNF-α and IFN-γ render microglia sensitive to Fas ligand-induced apoptosis by induction of Fas expression and down-regulation of Bcl-2 and Bcl-xL. *European journal of immunology,* 28**,** 4398-4408.

SPETS, H., GEORGII-HEMMING, P., SILJASON, J., NILSSON, K. & JERNBERG-WIKLUND, H. 1998. Fas/APO-1 (CD95)–Mediated Apoptosis Is Activated by Interferon-γ and Interferon-・ in Interleukin-6 (IL-6)–Dependent and IL-6–Independent Multiple Myeloma Cell Lines. *Blood,* 92**,** 2914-2923.

SRINIVASULA, S. M., HEGDE, R., SALEH, A., DATTA, P., SHIOZAKI, E., CHAI, J., LEE, R.-A., ROBBINS, P. D., FERNANDES-ALNEMRI, T. & SHI, Y. 2001. A conserved XIAP-interaction motif in caspase-9 and Smac/DIABLO regulates caspase activity and apoptosis. *Nature,* 410**,** 112-116.

STAMENKOVIC, I., CLARK, E. & SEED, B. 1989. A B-lymphocyte activation molecule related to the nerve growth factor receptor and induced by cytokines in carcinomas. *The EMBO Journal,* 8**,** 1403.

STECKLEY, D., KARAJGIKAR, M., DALE, L. B., FUERTH, B., SWAN, P., DRUMMOND-MAIN, C., POULTER, M. O., FERGUSON, S. S., STRASSER, A. & CREGAN, S. P.

2007. Puma is a dominant regulator of oxidative stress induced Bax activation and neuronal apoptosis. *Journal of Neuroscience,* 27**,** 12989-12999.

STEELE, L. P., GEORGOPOULOS, N. T., SOUTHGATE, J., SELBY, P. J. & TREJDOSIEWICZ, L. K. 2006. Differential susceptibility to TRAIL of normal versus malignant human urothelial cells. *Cell Death & Differentiation,* 13**,** 1564-1576.

STEWART, R., WEI, W., CHALLA, A., ARMITAGE, R. J., ARRAND, J. R., ROWE, M., YOUNG, L. S., ELIOPOULOS, A. & GORDON, J. 2007. CD154 tone sets the signaling pathways and transcriptome generated in model CD40-pluricompetent L3055 Burkitt's lymphoma cells. *The Journal of Immunology,* 179**,** 2705-2712.

SUDA, T., HASHIMOTO, H., TANAKA, M., OCHI, T. & NAGATA, S. 1997. Membrane Fas ligand kills human peripheral blood T lymphocytes, and soluble Fas ligand blocks the killing. *Journal of Experimental Medicine,* 186**,** 2045-2050.

SUNDARESAN, M., YU, Z.-X., FERRANS, V. J., IRANI, K. & FINKEL, T. 1995. Requirement for generation of H2O2 for platelet-derived growth factor signal transduction. *Science,* 270**,** 296.

SUSIN, S. A., LORENZO, H. K., ZAMZAMI, N., MARZO, I., SNOW, B. E., BROTHERS, G. M., MANGION, J., JACOTOT, E., COSTANTINI, P. & LOEFFLER, M. 1999. Molecular characterization of mitochondrial apoptosis-inducing factor. *Nature,* 397**,** 441-446.

SUTTLES, J. & STOUT, R. D. Macrophage CD40 signaling: a pivotal regulator of disease protection and pathogenesis. Seminars in immunology, 2009. Elsevier, 257-264.

SUZUKI, Y., IMAI, Y., NAKAYAMA, H., TAKAHASHI, K., TAKIO, K. & TAKAHASHI, R. 2001. A serine protease, HtrA2, is released from the mitochondria and interacts with XIAP, inducing cell death. *Molecular cell,* 8**,** 613-621.

SZABÓ, C., ISCHIROPOULOS, H. & RADI, R. 2007. Peroxynitrite: biochemistry, pathophysiology and development of therapeutics. *Nature reviews Drug discovery,* 6**,** 662-680.

TAIT, S. W., PARSONS, M. J., LLAMBI, F., BOUCHIER-HAYES, L., CONNELL, S., MUÑOZ-PINEDO, C. & GREEN, D. R. 2010. Resistance to caspase-independent cell death requires persistence of intact mitochondria. *Developmental cell,* 18**,** 802-813.

TAKEDA, K., NAGURO, I., NISHITOH, H., MATSUZAWA, A. & ICHIJO, H. 2011. Apoptosis signaling kinases: from stress response to health outcomes. *Antioxidants & redox signaling,* 15**,** 719-761.

TERADA, L. S. 2006. Specificity in reactive oxidant signaling: think globally, act locally. *The Journal of cell biology,* 174**,** 615-623.

THORNBERRY, N. A. 1998. Caspases: key mediators of apoptosis. *Chemistry & biology,* 5**,** R97-R103.

THORNBERRY, N. A., CHAPMAN, K. T. & NICHOLSON, D. W. 2000. Determination of caspase specificities using a peptide combinatorial library. *Methods in enzymology,* 322**,** 100.

TODT, F., CAKIR, Z., REICHENBACH, F., EMSCHERMANN, F., LAUTERWASSER, J., KAISER, A., ICHIM, G., TAIT, S. W., FRANK, S. & LANGER, H. F. 2015. Differential retrotranslocation of mitochondrial Bax and Bak. *The EMBO journal,* 34**,** 67-80.

TODT, F., CAKIR, Z., REICHENBACH, F., YOULE, R. & EDLICH, F. 2013. The C-terminal helix of Bcl-xL mediates Bax retrotranslocation from the mitochondria. *Cell Death & Differentiation,* 20**,** 333-342.

TOMIYAMA, A., SERIZAWA, S., TACHIBANA, K., SAKURADA, K., SAMEJIMA, H., KUCHINO, Y. & KITANAKA, C. 2006. Critical role for mitochondrial oxidative phosphorylation in the activation of tumor suppressors Bax and Bak. *Journal of the National Cancer Institute,* 98**,** 1462-1473.

TONG, A. W., PAPAYOTI, M. H., NETTO, G., ARMSTRONG, D. T., ORDONEZ, G., LAWSON, J. M. & STONE, M. J. 2001. Growth-inhibitory effects of CD40 ligand (CD154) and its endogenous expression in human breast cancer. *Clinical cancer research,* 7**,** 691-703.

TONG, A. W. & STONE, M. J. 2003. Prospects for CD40-directed experimental therapy of human cancer. *Cancer gene therapy,* 10**,** 1-13.

TOUTIRAIS, O., GERVAIS, A., CABILLIC, F., LE GALLO, M., COUDRAIS, A., LEVEQUE, J., CATROS-QUEMENER, V. & GENETET, N. 2007. Effects of CD40 binding on ovarian carcinoma cell growth and cytokine production in vitro. *Clinical & Experimental Immunology,* 149**,** 372-377.

TRACHOOTHAM, D., ALEXANDRE, J. & HUANG, P. 2009. Targeting cancer cells by ROS-mediated mechanisms: a radical therapeutic approach? *Nature reviews Drug discovery,* 8**,** 579-591.

TRACHOOTHAM, D., ZHOU, Y., ZHANG, H., DEMIZU, Y., CHEN, Z., PELICANO, H., CHIAO, P. J., ACHANTA, G., ARLINGHAUS, R. B. & LIU, J. 2006. Selective killing of oncogenically transformed cells through a ROS-mediated mechanism by β-phenylethyl isothiocyanate. *Cancer cell,* 10**,** 241-252.

TSUJIMOTO, M., YIP, Y. & VILCEK, J. 1986. Interferon-gamma enhances expression of cellular receptors for tumor necrosis factor. *The Journal of Immunology,* 136**,** 2441-2444.

URBICH, C., DERNBACH, E., AICHER, A., ZEIHER, A. M. & DIMMELER, S. 2002. CD40 ligand inhibits endothelial cell migration by increasing production of endothelial reactive oxygen species. *Circulation,* 106**,** 981-986.

URBICH, C., MALLAT, Z., TEDGUI, A., CLAUSS, M., ZEIHER, A. M. & DIMMELER, S. 2001. Upregulation of TRAF-3 by shear stress blocks CD40-mediated endothelial activation. *The Journal of clinical investigation,* 108**,** 1451-1458.

VALKO, M., IZAKOVIC, M., MAZUR, M., RHODES, C. J. & TELSER, J. 2004. Role of oxygen radicals in DNA damage and cancer incidence. *Molecular and cellular biochemistry,* 266**,** 37-56.

VALKO, M., RHODES, C., MONCOL, J., IZAKOVIC, M. & MAZUR, M. 2006. Free radicals, metals and antioxidants in oxidative stress-induced cancer. *Chemico-biological interactions,* 160**,** 1-40.

VALLABHAPURAPU, S., MATSUZAWA, A., ZHANG, W., TSENG, P.-H., KEATS, J. J., WANG, H., VIGNALI, D. A., BERGSAGEL, P. L. & KARIN, M. 2008. Non-redundant and complementary functions of adaptor proteins TRAF2 and TRAF3 in a ubiquitination cascade that activates NIK-dependent alternative NF-κB signaling. *Nature immunology,* 9**,** 1364.

VAN KOOTEN, C. & BANCHEREAU, J. 2000. CD40-CD40 ligand. *Journal of leukocyte biology,* 67**,** 2-17.

VAN KOOTEN, C., DAHA, M. R. & VAN ES, L. A. 1999a. Tubular epithelial cells: A critical cell type in the regulation of renal inflammatory processes. *Nephron Experimental Nephrology,* 7**,** 429-437.

VAN KOOTEN, C., GERRITSMA, J. S., PAAPE, M. E., VAN ES, L. A., BANCHEREAU, J. & DAHA, M. R. 1997. Possible role for CD40-CD40L in the regulation of interstitial infiltration in the kidney. *Kidney international,* 51**,** 711-721.

VAN KOOTEN, C., VAN DER LINDE, X., WOLTMAN, A. M., VAN ES, L. A. & DAHA, M. R. 1999b. Synergistic effect of interleukin-1 and CD40L on the activation of human renal tubular epithelial cells. *Kidney international,* 56**,** 41-51.

VAN KOOTEN, C., WOLTMAN, A. M. & DAHA, M. R. 2000. Immunological function of tubular epithelial cells: the functional implications of CD40 expression. *Nephron Experimental Nephrology,* 8**,** 203-207.

VANDENABEELE, P., GALLUZZI, L., BERGHE, T. V. & KROEMER, G. 2010. Molecular mechanisms of necroptosis: an ordered cellular explosion. *Nature reviews Molecular cell biology,* 11**,** 700-714.

VANDER HEIDEN, M. G., CHANDEL, N. S., SCHUMACKER, P. T. & THOMPSON, C. B. 1999. Bcl-x L prevents cell death following growth factor withdrawal by facilitating mitochondrial ATP/ADP exchange. *Molecular cell,* 3**,** 159-167.

VARDOULI, L., LINDQVIST, C., VLAHOU, K., LOSKOG, A. & ELIOPOULOS, A. 2009. Adenovirus delivery of human CD40 ligand gene confers direct therapeutic effects on carcinomas. *Cancer gene therapy,* 16**,** 848-860.

VEMPATI, U. D., DIAZ, F., BARRIENTOS, A., NARISAWA, S., MIAN, A. M., MILLÁN, J. L., BOISE, L. H. & MORAES, C. T. 2007. Role of cytochrome C in apoptosis: increased sensitivity to tumor necrosis factor alpha is associated with respiratory defects but not with lack of cytochrome C release. *Molecular and cellular biology,* 27**,** 1771-1783.

VENKATAKRISHNAN, G., SALGIA, R. & GROOPMAN, J. E. 2000. Chemokine receptors CXCR-1/2 activate mitogen-activated protein kinase via the epidermal growth factor receptor in ovarian cancer cells. *Journal of Biological Chemistry,* 275**,** 6868-6875.

VERHAGEN, A. M., COULSON, E. J. & VAUX, D. L. 2001. Inhibitor of apoptosis proteins and their relatives: IAPs and other BIRPs. *Genome biology,* 2**,** 1.

VIEIRA, H. & KROEMER, G. 1999. Pathophysiology of mitochondrial cell death control. *Cellular and Molecular Life Sciences CMLS,* 56**,** 971-976.

VOGELZANG, N. J. & STADLER, W. M. 1998. Kidney cancer. *The Lancet,* 352**,** 1691-1696.

VON LEOPRECHTING, A., VAN DER BRUGGEN, P., PAHL, H. L., ARUFFO, A. & SIMON, J. C. 1999. Stimulation of CD40 on immunogenic human malignant melanomas augments their cytotoxic T lymphocyte-mediated lysis and induces apoptosis. *Cancer research,* 59**,** 1287-1294.

VONDERHEIDE, R., FLAHERTY, K., KHALIL, M., STUMACHER, M., BAJOR, D., GALLAGHER, M., SULLIVAN, P., MAHANEY, J., O'DWYER, P. & HUHN, R. Clinical activity and immune modulation in cancer patients treated with CP-870,893, a novel CD40 agonist monoclonal antibody. ASCO Annual Meeting Proceedings, 2006. 2507.

VONDERHEIDE, R. H. 2007. Prospect of targeting the CD40 pathway for cancer therapy. *Clinical cancer research,* 13**,** 1083-1088.

VONDERHEIDE, R. H. & GLENNIE, M. J. 2013. Agonistic CD40 antibodies and cancer therapy. AACR.

WADA, T. & PENNINGER, J. M. 2004. Stress Kinase MKK7: Saviour of Cell Cycle Arrest and Cellular Senescence. *Cell cycle,* 3**,** 575-577.

WAGNER, D. H., VAITAITIS, G., SANDERSON, R., POULIN, M., DOBBS, C. & HASKINS, K. 2002. Expression of CD40 identifies a unique pathogenic T cell population in type 1 diabetes. *Proceedings of the National Academy of Sciences,* 99**,** 3782-3787.

WAGNER, E. F. & NEBREDA, Á. R. 2009. Signal integration by JNK and p38 MAPK pathways in cancer development. *Nature Reviews Cancer,* 9**,** 537-549.

WAJANT, H., HENKLER, F. & SCHEURICH, P. 2001. The TNF-receptor-associated factor family: scaffold molecules for cytokine receptors, kinases and their regulators. *Cellular signalling,* 13**,** 389-400.

WANG, C.-Y., BASSUK, A. G., BOISE, L. H., THOMPSON, C. B., BRAVO, R. & LEIDEN, J. M. 1994. Activation of the granulocyte-macrophage colony-stimulating factor promoter in T cells requires cooperative binding of Elf-1 and AP-1 transcription factors. *Molecular and Cellular Biology,* 14**,** 1153-1159.

WANG, J., CHUN, H. J., WONG, W., SPENCER, D. M. & LENARDO, M. J. 2001. Caspase-10 is an initiator caspase in death receptor signaling. *Proceedings of the National Academy of Sciences,* 98**,** 13884-13888.

WANG, J. & YI, J. 2008. Cancer cell killing via ROS: to increase or decrease, that is the question. *Cancer biology & therapy,* 7**,** 1875-1884.

WANG, X., SON, Y.-O., CHANG, Q., SUN, L., HITRON, J. A., BUDHRAJA, A., ZHANG, Z., KE, Z., CHEN, F. & LUO, J. 2011. NADPH oxidase activation is required in reactive oxygen species generation and cell transformation induced by hexavalent chromium. *Toxicological Sciences,* 123**,** 399-410.

WAUGH, D. J. & WILSON, C. 2008. The interleukin-8 pathway in cancer. *Clinical cancer research,* 14**,** 6735-6741.

WEI, Y., FAN, T. & YU, M. 2008. Inhibitor of apoptosis proteins and apoptosis. *Acta biochimica et biophysica Sinica,* 40**,** 278-288.

WEILER, M., KACHKO, L., CHAIMOVITZ, C., VAN KOOTEN, C. & DOUVDEVANI, A. 2001. CD40 ligation enhances IL-15 production by tubular epithelial cells. *Journal of the American Society of Nephrology,* 12**,** 80-87.

WEISS, J. M., GREGORY ALVORD, W., QUIÑONES, O. A., STAUFFER, J. K. & WILTROUT, R. H. 2014. CD40 expression in renal cell carcinoma is associated with tumor apoptosis, CD8< sup>+</sup> T cell frequency and patient survival. *Human immunology*.

WESTON, C. R. & DAVIS, R. J. 2007. The JNK signal transduction pathway. *Current opinion in cell biology,* 19**,** 142-149.

WHEELER, M. L. & DEFRANCO, A. L. 2012. Prolonged production of reactive oxygen species in response to B cell receptor stimulation promotes B cell activation and proliferation. *The Journal of Immunology,* 189**,** 4405-4416.

WHITMARSH, A. J. 2007. Regulation of gene transcription by mitogen-activated protein kinase signaling pathways. *Biochimica et Biophysica Acta (BBA)-Molecular Cell Research,* 1773**,** 1285-1298.

WIDLAK, P. & GARRARD, W. 2009. Roles of the major apoptotic nuclease-DNA fragmentation factor-in biology and disease. *Cellular and Molecular Life Sciences,* 66**,** 263-274.

WILSON, K. P., BLACK, J.-A. F., THOMSON, J. A., KIM, E. E., GRIFFITH, J. P., NAVIA, M. A., MURCKO, M. A., CHAMBERS, S. P., ALDAPE, R. A. & RAYBUCK, S. A. 1994. Structure and mechanism of interleukin-lβ converting enzyme.

WYZGOL, A., MÜLLER, N., FICK, A., MUNKEL, S., GRIGOLEIT, G. U., PFIZENMAIER, K. & WAJANT, H. 2009. Trimer stabilization, oligomerization, and antibody-mediated cell surface immobilization improve the activity of soluble trimers of CD27L, CD40L, 41BBL, and glucocorticoid-induced TNF receptor ligand. *The Journal of Immunology,* 183**,** 1851-1861.

XIA, M., LI, G., MA, J. & LING, W. 2010. Phosphoinositide 3-kinase mediates CD40 ligand-induced oxidative stress and endothelial dysfunction via Rac1 and NADPH oxidase 2. *Journal of Thrombosis and Haemostasis,* 8**,** 397-406.

XIA, Z., DICKENS, M., RAINGEAUD, J., DAVIS, R. J. & GREENBERG, M. E. 1995. Opposing effects of ERK and JNK-p38 MAP kinases on apoptosis. *Science,* 270**,** 1326.

XIE, P., HOSTAGER, B. S. & BISHOP, G. A. 2004. Requirement for TRAF3 in signaling by LMP1 but not CD40 in B lymphocytes. *The Journal of experimental medicine,* 199**,** 661-671.

XIE, P., HOSTAGER, B. S., MUNROE, M. E., MOORE, C. R. & BISHOP, G. A. 2006. Cooperation between TNF receptor-associated factors 1 and 2 in CD40 signaling. *The Journal of Immunology,* 176**,** 5388-5400.

XU, J., FOY, T. M., LAMAN, J. D., ELLIOTT, E. A., DUNN, J. J., WALDSCHMIDT, T. J., ELSEMORE, J., NOELLE, R. J. & FLAVELL, R. A. 1994. Mice deficient for the CD40 ligand. *Immunity,* 1**,** 423-431.

XU, L.-G. & SHU, H.-B. 2002. TNFR-associated factor-3 is associated with BAFF-R and negatively regulates BAFF-R-mediated NF-κB activation and IL-10 production. *The Journal of Immunology,* 169**,** 6883-6889.

XU, X., FU, X.-Y., PLATE, J. & CHONG, A. S. 1998. IFN-γ induces cell growth inhibition by Fas-mediated apoptosis: requirement of STAT1 protein for up-regulation of Fas and FasL expression. *Cancer research,* 58**,** 2832-2837.

YANG, J., LIU, X., BHALLA, K., KIM, C. N., IBRADO, A. M., CAI, J., PENG, T.-I., JONES, D. P. & WANG, X. 1997. Prevention of apoptosis by Bcl-2: release of cytochrome c from mitochondria blocked. *Science,* 275**,** 1129-1132.

YE, H., CANDE, C., STEPHANOU, N. C., JIANG, S., GURBUXANI, S., LAROCHETTE, N., DAUGAS, E., GARRIDO, C., KROEMER, G. & WU, H. 2002. DNA binding is required for the apoptogenic action of apoptosis inducing factor. *Nature Structural & Molecular Biology,* 9**,** 680-684.

YEH, W.-C., SHAHINIAN, A., SPEISER, D., KRAUNUS, J., BILLIA, F., WAKEHAM, A., DE LA POMPA, J. L., FERRICK, D., HUM, B. & ISCOVE, N. 1997. Early lethality, functional NF-κB activation, and increased sensitivity to TNF-induced cell death in TRAF2-deficient mice. *Immunity,* 7**,** 715-725.

YELLIN, M. J., WINIKOFF, S., FORTUNE, S. M., BAUM, D., CROW, M. K., LEDERMAN, S. & CHESS, L. 1995. Ligation of CD40 on fibroblasts induces CD54 (ICAM-1) and CD106 (VCAM-1) up-regulation and IL-6 production and proliferation. *Journal of Leukocyte Biology,* 58**,** 209-216.

YODOI, J., MASUTANI, H. & NAKAMURA, H. 2001. Redox regulation by the human thioredoxin system. *Biofactors,* 15**,** 107-111.

YOU, R.-I., CHEN, M.-C., WANG, H.-W., CHOU, Y.-C., LIN, C.-H. & HSIEH, S.-L. 2006. Inhibition of Lymphotoxin-β Receptor–Mediated Cell Death by Survivin-ΔEx3. *Cancer research,* 66**,** 3051-3061.

YOUNG, L. S., ELIOPOULOS, A. G., GALLAGHER, N. J. & DAWSON, C. W. 1998. CD40 and epithelial cells: across the great divide. *Immunology today,* 19**,** 502-506.

YOUNG, T. W., MEI, F. C., YANG, G., THOMPSON-LANZA, J. A., LIU, J. & CHENG, X. 2004. Activation of antioxidant pathways in ras-mediated oncogenic transformation of human surface ovarian epithelial cells revealed by functional proteomics and mass spectrometry. *Cancer research,* 64**,** 4577-4584.

YUAN, S., YU, X., TOPF, M., LUDTKE, S. J., WANG, X. & AKEY, C. W. 2010. Structure of an apoptosome-procaspase-9 CARD complex. *Structure,* 18**,** 571-583.

ZAPATA, J. M., PAWLOWSKI, K., HAAS, E., WARE, C. F., GODZIK, A. & REED, J. C. 2001. A diverse family of proteins containing tumor necrosis factor receptor-associated factor domains. *Journal of Biological Chemistry,* 276**,** 24242-24252.

ZARNEGAR, B. J., WANG, Y., MAHONEY, D. J., DEMPSEY, P. W., CHEUNG, H. H., HE, J., SHIBA, T., YANG, X., YEH, W.-C. & MAK, T. W. 2008. Noncanonical NF-κB activation requires coordinated assembly of a regulatory complex of the adaptors cIAP1, cIAP2, TRAF2 and TRAF3 and the kinase NIK. *Nature immunology,* 9**,** 1371-1378.

ZARUBIN, T. & JIAHUAI, H. 2005. Activation and signaling of the p38 MAP kinase pathway. *Cell research,* 15**,** 11-18.

ZAZZERONI, F., PAPA, S., ALGECIRAS-SCHIMNICH, A., ALVAREZ, K., MELIS, T., BUBICI, C., MAJEWSKI, N., HAY, N., DE SMAELE, E. & PETER, M. E. 2003. Gadd45β

mediates the protective effects of CD40 costimulation against Fas-induced apoptosis. *Blood,* 102**,** 3270-3279.

ZHA, J., HARADA, H., YANG, E., JOCKEL, J. & KORSMEYER, S. J. 1996. Serine phosphorylation of death agonist BAD in response to survival factor results in binding to 14-3-3 not BCL-X L. *Cell,* 87**,** 619-628.

ZHANG, A. Y., YI, F., JIN, S., XIA, M., CHEN, Q. Z., GULBINS, E. & LI, P. L. 2007. Acid sphingomyelinase and its redox amplification in formation of lipid raft redox signaling platforms in endothelial cells. *Antioxidants & redox signaling,* 9**,** 817-828.

ZHANG, A. Y., YI, F., ZHANG, G., GULBINS, E. & LI, P.-L. 2006. Lipid raft clustering and redox signaling platform formation in coronary arterial endothelial cells. *Hypertension,* 47**,** 74-80.

ZHANG, W. & LIU, H. T. 2002. MAPK signal pathways in the regulation of cell proliferation in mammalian cells. *Cell research,* 12**,** 9-18.

ZHANG, X., LI, L., CHOE, J., KRAJEWSKI, S., REED, J. C., THOMPSON, C. & CHOI, Y. S. 1996. Up-Regulation of Bcl-xLExpression Protects CD40-Activated Human B Cells from Fas-Mediated Apoptosis. *Cellular immunology,* 173**,** 149-154.

ZHANG, X. D., GILLESPIE, S. K. & HERSEY, P. 2004. Staurosporine induces apoptosis of melanoma by both caspase-dependent and-independent apoptotic pathways. *Molecular cancer therapeutics,* 3**,** 187-197.

ZHENG, H., LUO, R., ZHANG, L. & MAI, G. 2002. Interferon-gamma up-regulates Fas expression and increases Fas-mediated apoptosis in tumor cell lines. *Di 1 jun yi da xue xue bao= Academic journal of the first medical college of PLA,* 22**,** 1090-1092.

ZHENG, L., SCHICKLING, O., PETER, M. E. & LENARDO, M. J. 2001. The death effector domain-associated factor plays distinct regulatory roles in the nucleus and cytoplasm. *Journal of Biological Chemistry,* 276**,** 31945-31952.

ZHU, Y. M. & WOLL, P. J. 2005. Mitogenic effects of interleukin-8/CXCL8 on cancer cells.

ZIRLIK, A., MAIER, C., GERDES, N., MACFARLANE, L., SOOSAIRAJAH, J., BAVENDIEK, U., AHRENS, I., ERNST, S., BASSLER, N. & MISSIOU, A. 2007. CD40 ligand mediates inflammation independently of CD40 by interaction with Mac-1. *Circulation,* 115**,** 1571-1580.

ZORATTI, M. & SZABÒ, I. 1995. The mitochondrial permeability transition. *Biochimica et Biophysica Acta (BBA)-Reviews on Biomembranes,* 1241**,** 139-176.